CHEM 3110: DESCRIPTIVE INORGANIC CHEMISTRY



Catherine McCusker
East Tennessee State University

LibreTexts™

CHEM 3110 - Descriptive Inorganic Chemistry

This text is disseminated via the Open Education Resource (OER) LibreTexts Project (https://LibreTexts.org) and like the thousands of other texts available within this powerful platform, it is freely available for reading, printing, and "consuming."

The LibreTexts mission is to bring together students, faculty, and scholars in a collaborative effort to provide an accessible, and comprehensive platform that empowers our community to develop, curate, adapt, and adopt openly licensed resources and technologies; through these efforts we can reduce the financial burden born from traditional educational resource costs, ensuring education is more accessible for students and communities worldwide.

Most, but not all, pages in the library have licenses that may allow individuals to make changes, save, and print this book. Carefully consult the applicable license(s) before pursuing such effects. Instructors can adopt existing LibreTexts texts or Remix them to quickly build course-specific resources to meet the needs of their students. Unlike traditional textbooks, LibreTexts' web based origins allow powerful integration of advanced features and new technologies to support learning.



LibreTexts is the adaptable, user-friendly non-profit open education resource platform that educators trust for creating, customizing, and sharing accessible, interactive textbooks, adaptive homework, and ancillary materials. We collaborate with individuals and organizations to champion open education initiatives, support institutional publishing programs, drive curriculum development projects, and more.

The LibreTexts libraries are Powered by NICE CXone Expert and was supported by the Department of Education Open Textbook Pilot Project, the California Education Learning Lab, the UC Davis Office of the Provost, the UC Davis Library, the California State University Affordable Learning Solutions Program, and Merlot. This material is based upon work supported by the National Science Foundation under Grant No. 1246120, 1525057, and 1413739.

Any opinions, findings, and conclusions or recommendations expressed in this material are those of the author(s) and do not necessarily reflect the views of the National Science Foundation nor the US Department of Education.

Have questions or comments? For information about adoptions or adaptions contact info@LibreTexts.org or visit our main website at https://LibreTexts.org.

This text was compiled on 01/11/2026

TABLE OF CONTENTS

Licensing

1: Introduction to Inorganic Chemistry

- 1.1: What is Inorganic Chemistry?
- 1.2: Inorganic vs Organic Chemistry
- 1.3: History of Inorganic Chemistry

2: Atomic Theory

- 2.1: Quantum Numbers and Atomic Wavefunctions
- 2.2: Shielding
- 2.3: Aufbau Principle
- 2.4: Periodic Properties of Atoms

3: Bonding Theories

- 3.1: Types of Bonding
- 3.2: Electronegativity Values
  - 3.2A: Pauling Electronegativity Values
  - 3.2B: Mulliken Electronegativity Values
  - 3.2C: Allred-Rochow Electronegativity Values
- 3.3: Lewis Electron-Dot Diagrams
  - 3.3A: Formal Charge
  - 3.3B: Resonance
  - 3.3C: Expanded Octets
  - 3.3D: Limitation of Lewis Theory
- 3.4: Valence-Shell Electron-Repulsion Theory
- 3.5: Molecular Polarity
- 3.6: Valence Bond Theory
- 3.7: Molecular Orbital Theory
  - 3.7A: Orbital Overlap
  - 3.7B: Homonuclear Diatomic Molecules
  - 3.7C: Heteronuclear Diatomic Molecules

4: Molecular Symmetry and Point Groups

- 4.1: Symmetry Operations and Elements
- 4.2: Point Groups
- 4.3: Introduction to Character Tables
- 4.4: Applications of Symmetry in Chemistry

5: Structure and Energetics of Solids

- 5.1: Crystal Structures and Unit Cells
- 5.2: Energetics of Ionic Solids- Lattice Energy
- 5.3: Lattice Enthalpies and Born Haber Cycles
- 5.4: Lattice Energy and Solubility

- 5.5: Bonding in Metals and Semicondoctors
- 5.6: Nanomaterials

6: Acid-Base and Donor-Acceptor Chemistry

- 6.1: Arrhenius Model
- 6.2: Brønsted-Lowry Model
- 6.3: Lewis Concept and Frontier Orbitals
- 6.4: Hard and Soft Acids and Bases

7: Reduction and Oxidation Chemistry

- 7.1: Balancing Redox Reactions
- 7.2: Electrochemical Potentials
- 7.3: Latimer Diagrams
- 7.4: Frost Diagrams
- 7.5: Pourbaix Diagrams

8: Coordination Chemistry- Structure and Isomers

- 8.1: History
- 8.2: Nomenclature and Ligands
- 8.3: Coordination Numbers and Structures
- 8.4: Isomerism

9: Coordination Chemistry- Bonding

- 9.1: Crystal Field Theory
- 9.2: Crystal Field Stabilization Energy
- 9.3: Jahn-Teller Distortions
- 9.4: Factors That Affect Crystal Field Splitting
- 9.5: Ligand Field Theory

10: Coordination Chemistry- Reactions and Mechanisms

- 10.1: Thermodynamic Stability of Metal Complexes
- 10.2: Trends in Kinetic Lability
- 10.3: Ligand Substitution Mechanisms
- 10.4: The Trans Effect
- 10.5: Electron Transfer Reactions

11: Organometallic Chemistry

- 11.1: Organometallic Ligands
- 11.2: The 18 Electron Rule
- 11.3: Oxidative Addition
- 11.4: Reductive Elimination
- 11.5: Migratory Insertion- 1,2-Insertions
- 11.6: β-Elimination Reactions
- 11.7: Organometallic Catalysts

12: Bioinorganic Chemistry

- 12.1: Biological Significance of Metals
- 12.2: Introduction to Amino Acids and Proteins
- 12.3: Biological Dioxygen Transport and Storage
- 12.4: Biological Metal Storage
- 12.5: Zinc as Lewis Acid and Template
- 12.6: Electron Transfer

Index

Glossary

Detailed Licensing

Licensing

*A detailed breakdown of this resource's licensing can be found in **Back Matter/Detailed Licensing**.*

CHAPTER OVERVIEW

1: Introduction to Inorganic Chemistry

This chapter will introduce the breadth of the field of inorganic chemistry

Learning Objectives

- Identify different subfields of inorganic chemistry
- Recognize the historical and modern distinction between the fields of inorganic and organic chemistry

1.1: What is Inorganic Chemistry?
1.2: Inorganic vs Organic Chemistry
1.3: History of Inorganic Chemistry

1: Introduction to Inorganic Chemistry is shared under a CC BY-NC-SA 4.0 license and was authored, remixed, and/or curated by LibreTexts.

1.1: What is Inorganic Chemistry?

Where did the name "Inorganic Chemistry" come from? Well, the term "Organic Chemistry" literally means the *chemistry of life*. Organic chemistry is the study of carbon-based molecules because the first molecules that were isolated from living organisms contained carbon. On the other hand, minerals and other non-living things seemed to be made of other elements. For some time in our history, scientists believed that the chemical difference between living and non-living things was carbon. So, if "organic" molecules are the molecules of life, then is "inorganic chemistry" the "chemistry of death"? Almost? "Inorganic" chemistry historically meant the chemistry of "non-living" things; and these were non-carbon based molecules and ions.

The names "organic" and "inorganic" come from science history, and still today a generally-accepted definition of *Inorganic Chemistry is the study of non-carbon molecules, or all the elements on the periodic table except carbon (*Figure **1.1.1**. But, this definition is not completely correct because the field of Inorganic Chemistry also includes organometallic compounds and the study of some carbon-based molecules that have properties that are familiar to metals (like conduction of electricity). This makes the field of inorganic chemistry very broad, and practically limitless. A great way to understand the breadth of the field is to take a look at the abstracts in the latest article of Inorganic Chemistry. Or, check out the 20 most-read articles from this past year using the links below.

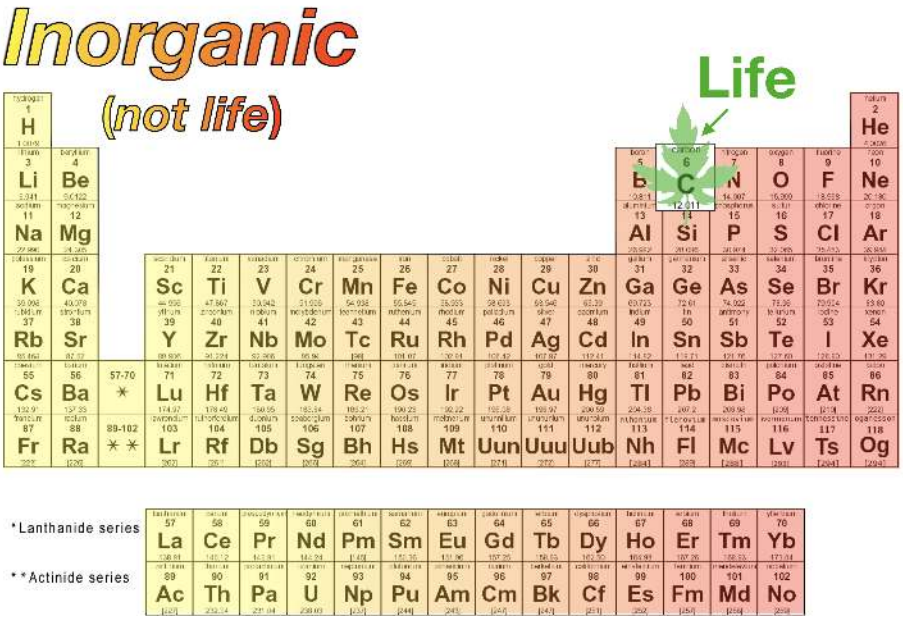


Figure **1.1.1**. An illustration of the historic meaning of "organic" and "inorganic". The modern understanding of organic and inorganic chemistry is not consistent with these historical meanings. (Kathryn Haas; CC-NC-BY-SA)

External links:

- The journal, Inorganic Chemistry: https://pubs.acs.org/journal/inocaj
- The latest issue of Inorganic chemistry: https://pubs.acs.org/toc/inocaj/current
- The most popular Inorganic Chemistry articles from the past month and the past year: https://pubs.acs.org/action/showMostReadArticles?journalCode=inocaj

Practice

? What are the Sub-Fields of Inorganic Chemistry?

To appreciate the breadth of Inorganic Chemistry, go to the most recent issue of Inorganic Chemistry and look at the titles and visual abstracts. Identify at least 4 sub-fields of Inorganic Chemistry.

Answer

There are a lot of correct answers here! The point here is that you notice that Inorganic Chemistry is a very broad field. It has something for almost everyone because many other fields overlap with Inorganic Chemistry. You might notice that some of the sub-fields you identified are also interdisciplinary fields between inorganic chemistry and another discipline. For a list of some of the subfields of Inorganic Chemistry, check this Wikipedia article.

1.1: What is Inorganic Chemistry? is shared under a CC BY-NC-SA 4.0 license and was authored, remixed, and/or curated by LibreTexts.

- **1.1: What is Inorganic Chemistry?** by Kathryn Haas is licensed CC BY-NC-SA 4.0.

1.2: Inorganic vs Organic Chemistry

The division between the fields of Inorganic and Organic chemistry has become blurred. For example, let's look at one of the major classes of catalysts used for organic synthesis reactions: organometalic catalysts (Figure **1.2.1**). Organometallic catalysts like these, and all organometallic compounds, contain metals that are bonded to carbon or carbon-containing molecules. So, are they "inorganic" because they contain metals, or "organic" because they contain carbon? These illustrate that clear divisions between organic and inorganic chemistry do not exist. Further, metal ions are common in biology and so the idea that metals are "inorganic" and thus classed as "non-living or non-biological" is incorrect. A canonical example is the organometallic catalyst adenosylcobalbumin, which is an important biological cofactor containing a cobalt (Co) ion (Figure **1.2.1**, right) and a cobalt-carbon bond.

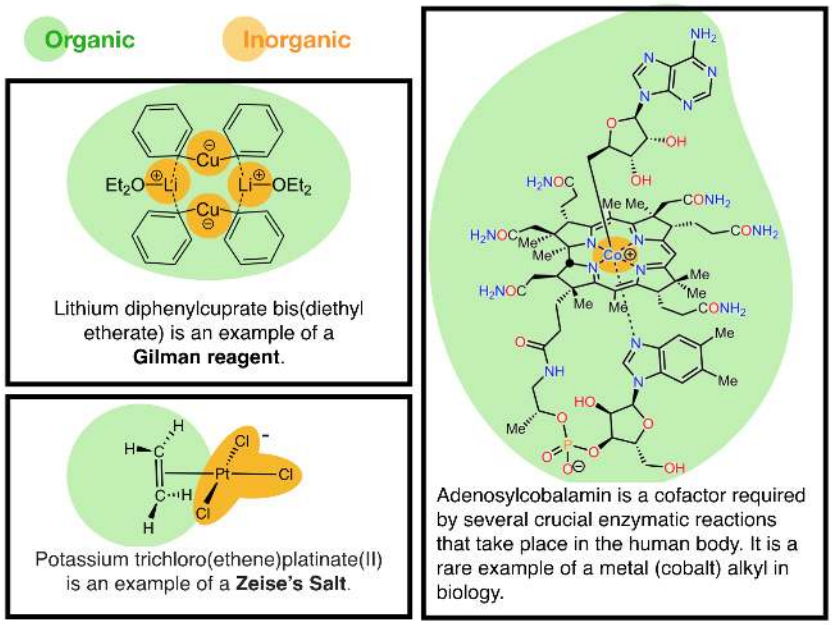


Figure **1.2.1**: Some examples of organometallic catalysts. These compounds catalyze organic reactions or biochemical reactions and they are compounds that contain both carbon and metals. These compounds are examples of molecules that cannot be defined only as organic molecules or only as inorganic molecules. Adenosylcobalbumin is an example of an organometallic catalyst that is present in biology, further illustrating that "inorganic" metals are important cofactors in biology. This image is based on information on the Wikipedia article on Organometallic Chemistry and is created from images found there; attribution to images created by Alsosaid1987, AdoCbl-ColorCoded, CC BY-SA 4.0 and Smokefoot, Zeise'sSalt, CC BY-SA 3.0. (Kathryn Haas; CC-BY-SA)

Some of the subfields of Inorganic Chemistry focus on electrical conductivity of inorganic materials (i.e., conduction, superconduction, and semiconduction) and on the study of optical and electronic properties of inorganic nanomaterials. Electrical conductivity is a canonical property of metals, but carbon-based materials also demonstrate electrical conductivity. For example, carbon nanotubes conduct electricity through their extended conjugated π systems. Fullerenes, of which the most famous is Buckminsterfullerene, or Buckeyball (C_{60}), demonstrate interesting properties that are similar to nanoparticles, and when combined with metals and crystallized can demonstrate superconductivity.

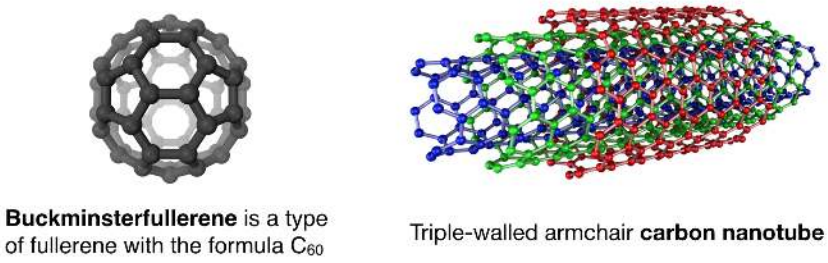


Figure 1.2.2: This figure is created from information found on the Wikipedia articles for Buckmisterfullerene and carbon nanotubes. Attribution Eric Wieser, Multi-walled Carbon Nanotube, CC BY-SA 3.0. (Kathryn Haas; CC-BY-SA)

Although carbon nanotubes and fullerenes are allotropes of carbon, their material properties are somewhat foreign to many organic chemists, who traditionally have focused on smaller organic molecules having very different properties. However, these properties are familiar to inorganic chemists. Thus, inorganic chemists have embraced these molecules as "inorganic" due to the fact that they behave more like inorganic materials than smaller organic molecules. This class of carbon-based molecules serves as another example of molecules that are not perfectly matched to the traditional definitions of "organic" and "inorganic" chemistry. Certainly, the future will hold more and more examples of molecules that do not fit into the traditional disciplines of chemistry.

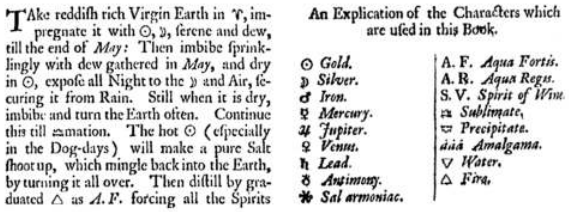
This page titled 1.2: Inorganic vs Organic Chemistry is shared under a CC BY-NC-SA 4.0 license and was authored, remixed, and/or curated by Kathryn Haas.

- **1.2: Inorganic vs Organic Chemistry** by Kathryn Haas is licensed CC BY-NC-SA 4.0.

1.3: History of Inorganic Chemistry

Metals serve an essential role in many aspects of human civilization and have defined Ages of human history. The period of time from about 3300 BC to 1200 BC is often referred to as the Bronze Age. During this period our ancestors first started using metal and learned to mix various elements with copper to make a strong alloy, called bronze. This Age yielded significant advancement in crafting of sharper knives and stronger weapons out of metal instead of rock, wood and bone. Around 1200 BC the human race found an even harder metal and discovered a much stronger alloy called steel. This period is known as the Iron Age. More recently, periods of time known as Gold Rushes have caused huge changes in population distributions and wealth in some countries. Metal has obvious importance in our modern way of life. Today, iron and steel are used for making buildings, machines, automobiles, jewelry, cooking pots, tools, weapons, vehicles, electronics, surgical instruments and symbolic structures like the Eiffel Tower. Gold, silver, and copper still serve as currency for trade and exchange of goods and services.

The existence of Chemistry as a field of study owes much to the fact that gold was a valuable commodity throughout our history. In both the ancient Egyptian society and during the Roman Empire, the gold mines were the property of the state, not an individual or group. So there were few ways for most people to legally get any gold for themselves. The Alchemists were a varied group of scholars and charlatans who aimed to solve this problem by creating the **Philosopher's Stone** (which caused the transmutation of lead into gold). Three major streams of alchemy are known, Chinese, Indian, and European, with all three streams having some factors in common. Techniques developed in the European stream ultimately influenced the development of the science of chemistry.



TAke reddiſh rich Virgin Earth in ♈, impregnate it with ☉, ☽, ſerene and dew, till the end of *May*: Then imbibe ſprinklingly with dew gathered in *May*, and dry in ☉, expoſe all Night to the ☽ and Air, ſecuring it from Rain. Still when it is dry, imbibe and turn the Earth often. Continue this till ſ. mation. The hot ☉ (eſpecially in the Dog-days) will make a pure Salt ſhoot up, which mingle back into the Earth, by turning it all over. Then diſtill by graduated △ as *A. F.* forcing all the Spirits

An Explication of the Characters which are uſed in this Book.

☉ *Gold.*
☽ *Silver.*
♂ *Iron.*
☿ *Mercury.*
♃ *Jupiter.*
♀ *Venus.*
♄ *Lead.*
♁ *Antimony.*
✻ *Sal armoniac.*

A. F. *Aqua Fortis.*
A. R. *Aqua Regis.*
S. V. *Spirit of Wine.*
♎ *Sublimate.*
♍ *Precipitate.*
ääā *Amalgama.*
▽ *Water.*
△ *Fire.*

Figure **1.3.1**. Alchemist recipe. Many of the specific approaches that alchemists used when they tried changing lead into gold are vague and unclear. Each alchemist had his own code for recording his data. The processes were kept secret so others could not profit from them. Different scholars developed their own set of symbols as they recorded the information they came up with. Many alchemists were not very honest, taking money from a nobleman by claiming to be able to make gold from lead, then leaving town in the middle of the night. Sometimes the nobleman would detect the fraud and have the alchemist hung. By the 1300's, several European rulers had declared alchemy to be illegal and set out strict punishments for those practicing the alchemical arts.

Although alchemists were never successful in changing lead into gold, they made several contributions to modern-day chemistry. Strong acids and bases were discovered, including nitric acid (H_2NO_3), sulfuric acid (H_3SO_4), and hydrochloric acid (HCl), and sodium hydroxide (NaOH). Glassware for running chemical reactions were developed, as well as methods for distillation, crystallization, sublimation. Alchemy helped improve the study of metallurgy and the extraction of metals from ores. More systematic approaches to research were developed that allowed the discovery of atoms and laid the groundwork for development of the periodic table. For more about the History of Chemistry in general, try the LibreText page History of Chemistry.

Inorganic compounds have been known and used since antiquity; probably the oldest is the deep blue pigment called Prussian blue, $Fe_4[Fe(CN)_6]$. However, the chemical nature of these substances was unknown until the late nineteenth and early twentieth century when the modern field of Coordination Chemistry emerged. Much of what we know about inorganic chemistry is based largely on the work of and debates between of Alfred Werner (1866–1919; Nobel Prize in Chemistry in 1913) and Sophus Mads Jørgensen (1837 –1914). After Werner succeeded in these debates, the field of Inorganic Chemistry declined in popularity until the mid twentieth century when the second world war stimulated renewed interest. During the post-war era, several important discoveries and theories were developed. For example, important theories of bonding in coordination compounds were developed. Soon after World War II, Crystal Field Theory (CFT) and Ligand Field Theory (LFT) were developed. These are two critical and complimentary theories that provide explanation of spectroscopic, chemical, and structural properties of inorganic coordination compounds; CFT being more simple, and LFT more accurate. In the 1950's, organometallic catalysts were discovered that catalyzed important organic reactions.

$$\mathrm{N_2\,(g) + 3\,H_2\,(g) \rightleftharpoons 2\,NH_3\,(g)} \tag{1.3.1}$$

The Haber-Bosch Process is catalyzed by an inorganic oxide catalyst and is one of the world's most important industrial reactions. It provides for the synthesis of ammonia directly from elemental nitrogen, N_2, and hydrogen, H_2. Since its development in the early twentieth century, it has led to the production of an enormous quantity of fertilizer, vastly increasing global food production. As a result, it is estimated that a significant fraction of the nitrogen content in the typical human body is ultimately derived from this process. Yet while the reaction must be run at high temperatures and pressures in the industrial setting, the nitrogenase enzyme on the roots of plants can carry out this reaction at the mild conditions within soil. Intense investigations were then aimed to improve inorganic catalysts through understanding the metal cofactors in enzymes. The link between the Haber-Bosch industrial process and the nitrogenase enzyme was an early bridge between the fields of organometallic chemistry and biochemistry.

Contributions

Part of this page is adapted from K.Haas Ph.D. dissertation

Part of this page is adapted from the following LibreTexts pages

- Alchemy contributed by CK-12 Foundation by Sharon Bewick, Richard Parsons, Therese Forsythe, Shonna Robinson, and Jean Dupon.
- Werner's Theory of Coordination Compounds
- The Haber-Bosch Process Worksheet

1.3: History of Inorganic Chemistry is shared under a CC BY-NC-SA 4.0 license and was authored, remixed, and/or curated by LibreTexts.

- **1.3: History of Inorganic Chemistry** by Kathryn Haas is licensed CC BY-NC-SA 4.0.
- **Current page** is licensed CC BY-NC-SA 4.0.

CHAPTER OVERVIEW

2: Atomic Theory

This chapter reviews atomic orbitals and the periodic properties of atoms.

Learning Objectives

- Understand the sizes, shapes, and relative energies of atomic orbitals and how they depend on quantum numbers
- Identify the number of radial and angular nodes in an atomic orbital
- Determine the ground state electron configuration and number of unpaired electrons for a given atom
- Explain periodic trends and their physical origins

Thumbnail illustrates the electron density of a 3d orbital, generated with the Orbitron

2.1: Quantum Numbers and Atomic Wavefunctions

2.2: Shielding

2.3: Aufbau Principle

2.4: Periodic Properties of Atoms

2: Atomic Theory is shared under a CC BY-NC-SA 4.0 license and was authored, remixed, and/or curated by LibreTexts.

2.1: Quantum Numbers and Atomic Wavefunctions

Considering the failures of the Bohr model in systems with more than one electron, Erwin Schrödinger and Werner Heisenberg proposed a major change in the paradigm regarding the electron. In several breakthrough papers (1925-1927) they attributed wave properties to electrons and they each received Nobel prizes for developing the theories of Wave Mechanics (or the "New Quantum Mechanics"). This approach treated electrons as having "dual" nature: posessing properties of *both* waves and particles.

Schrödinger's Equation describes the behavior of the electron (in a hydrogen atom) in three dimensions. It is a mathematical equation that defines the electron's position, mass, total energy, and potential energy. The simplest form of the Schrödinger Equation is as follows:

$$\hat{H}\psi = E\psi \tag{2.1.1}$$

where $\hat{H}$ is the Hamiltonian operator, **E** is the energy of the electron, and ψ is the wavefunction.

The Hamiltonian, $\hat{H}$

The Hamiltonian operator is like a set of instructions that tells us what to do with the function that follows it. A Hamiltonian operator is a function over three-dimensional space that corresponds to the sum of kinetic energies and potential energies of the particles in a system, one electron and its nucleus in this case. The Hamiltonian operator for a one-electron system is:

$$\hat{H} = \frac{-h^2}{8\pi^2 m_e}\left(\frac{\partial^2}{\partial x^2} + \frac{\partial^2}{\partial y^2} + \frac{\partial^2}{\partial z^2}\right) - \frac{Ze^2}{4\pi\epsilon_0 r} \tag{2.1.2}$$

Where h is Planc's constant, m_e is the mass of the electron, e is the charge of the electron, r is the distance from the nucleus ($r = \sqrt{x^2+y^2+z^2}$), Z is the charge of the nucleus, and $4\pi\epsilon_0$ is permittivity of a vacuum.

Kinetic Energy

The first part of the Hamiltonian written above, $\frac{-h^2}{8\pi^2 m_e}\left(\frac{\partial^2}{\partial x^2} + \frac{\partial^2}{\partial y^2} + \frac{\partial^2}{\partial z^2}\right)$ describes the kinetic energy of the electron. This is the energy due to motion of the electron.

Potential energy

The second part written above, $\frac{-Ze^2}{4\pi\epsilon_0 r}$ describes the potential energy of the electron, and is commonly written as $V(r)$ or $V(x,y,z)$.

$$V(x,y,x) = \frac{-Ze^2}{4\pi\epsilon_0 r} = \frac{-Ze^2}{4\pi\epsilon_0\sqrt{x^2+y^2+z^2}} \tag{2.1.3}$$

The potential energy depends on the attractive electrostatic force between the electron and the nucleus. You might notice that this attraction is essentially the same as the electrostatic force defined by Coulomb's law. And, just as in Coulomb's law, when two opposite charges are attracted to one another, the potential energy of the force is negative. Thus, when an electron is close to the nucleus, the potential energy is a large negative number corresponding to a strong attractive force. When an electron is farther from the nucleus, the potential energy is still negative but with a smaller magnitude, corresponding to a weaker attractive force. If the electron is very far from the nucleus ($r = \infty$) then the attractive force, and the potential energy, is zero.

The Wavefunction, ψ

In simple terms, the wavefunction (ψ) of an electron describes the electron's position in space, relative to the nucleus. The square of the ψ describes an atomic orbital. We can't define the position too exactly because we would violate the Heisenberg Uncertainty principle, but we can define its wave. Here, we will describe the ψ in general terms. Generally, in a one-electron atom, the electron ψ is defined by the wave's distance from the nucleus and its angle with respect to x, y, and z axes of the atom's Cartesian coordinates (nucleus is at the origin). The general form of the (ψ) for an electron in a hydrogen atom can be written as follows:

$$\psi_{n,l,m_l} = R_{n,l}(r) + Y_{l,m_l}(\theta,\phi) \tag{2.1.4}$$

Quantum numbers

In one dimension, the wavefunction requires only one quantum number, n. A full explanation of the three-dimensional wavefunction for an electron is outside of the scope of this course. Instead, we will focus on gaining a conceptual understanding by extending knowledge of the one-dimensional wavefunction to a three-dimensional space. Extending the wavefunction to three dimensions requires a total of three quantum numbers. In addition to n, which we saw in the one-dimensional case, we also need l and m_l to express the wavefunction in three dimensions. A complete solution to the Schrödinger equation, both the three-dimensional wavefunction and energy, includes a set of three quantum numbers (n, l, m_l). The wavefunction describes what we know as an atomic orbital; it defines the region in space where the electron is located. Additionally, there is a fourth quantum number, m_s. The m_s quantum number accounts for the observed interaction of electrons with an applied magnetic field; it is an additional postulate that is not part of the wavefunction. These four quantum numbers are described below.

The quantum number, n: This is the principle quantum number. This number represents the shell, including both the overall energy of the electron in that shell and the size of that shell. An allowed value for n is any non-zero, positive integer (1, 2, 3, 4, ... etc are allowed, but 4.1 is not allowed).

The quantum number, l: This is the angular momentum quantum number that corresponds to the subshell and its shape. It represents the angular dependence of the subshell, or the "shape" of the orbitals within a subshell. The allowed values of$l$ depends on n. The allowed values of l for an electron in shell n are integer values between 0 to $(n-1)$, or $l = 0 \rightarrow (n-1)$. These values correspond to the orbital shape where $l = 0$ is an s-orbital, $l = 1$ is a p-orbital, $l = 2$ is a d-orbital, $l = 3$ is an f-orbital.

The quantum number m_l: This is the magnetic quantum number. Its possible values give the the number of orbitals within a subshell and its specific value gives the orbital's orientation in space. The allowed values of m_l depend on the value of l. The value of m_l is allowed to be any positive or negative integer between $+l$ and $-l$. In other terms, $m_l = (0, \pm 1 ... \pm l)$. For example, if the electron is in a 3-p-orbital, then $n = 3, l = 1$, and the possible values of m_l are $-1, 0$, and $+1$. Since there are three possible values of m_l there are three orbitals in the p subshell. The specific m_l value defines in which of the three possible p-orbitals (p_x, p_y, or p_z) the electron exists. In the case of the s subshell, there is only one value, $m_l = 0$ because $l = 0$. The one value corresponds to the fact that there is only one s orbital in any shell.

The quantum number m_s: This quantum number accounts for the electron's "spin". In short, electrons interact with magnetic fields in a way that is similar to how a tiny bar magnet would interact with a magnetic field. The allowed values for m_s are $+\frac{1}{2}$ and $-\frac{1}{2}$.

Table 2.1.1. Quantum Numbers

SYMBOL	NAME	VALUES	MEANING
n	principle	$1, 2, 3$...(any integer)	energy level, orbital size
l	angular momentum	$0 \rightarrow (n-1)$	subshell, $0 = s, 1 = p, 2 = d, 3 = f$... this is the angular dependence of the orbital, shape of the orbital *letters have historical meaning, sharp, principle, diffuse, fundamental
m_l	magnetic	$0, \pm 1 ... \pm l$	orientation of angular momentum in space, orbital orientation
m_s	spin	$+\frac{1}{2}, -\frac{1}{2}$	orientation of the electron's magnetic field "spin up" or "spin down"

Atomic orbitals (one electron wavefunctions)

One simplified representation of the three-dimensional wavefunction is shown below. This representation breaks the wavefunction into two parts: the **radial contribution** ($R_{n,l}(r)$) and the **angular contribution** ($Y_{l,m_l}(\theta,\phi)$).

$$\psi_{(n,l,m_l)} = R_{n,l}(r) \times Y_{l,m_l}(\theta,\phi) \tag{2.1.5}$$

Radial contribution, $R_{n,l}(r)$

The radial part of the wavefunction, $R_{n,l}(r)$ gives the radial variation of ψ. In other words, $R_{n,l}(r)$ defines how the wavefunction depends on the distance of the electron from the nucleus (the radius). The principle quantum number n is derived from the radial part of the wavefunction, and determines the size (radial extent) of an orbital. The $R_{n,l}(r)$ parts of the wavefunction for a hydrogenic atom are plotted in Figure **2.1.1**. Notice that the $R_{n,l}(r)$ of all s-orbitals (solid lines) reaches a maximum at $r = 0$. This is unique to the s-orbitals' $R_{n,l}(r)$. The $R_{n,l}(r)$ of p- and d-orbitals orbitals approaches zero as r approaches zero. This has important consequences for how closely an electron in these orbitals can approach the nucleus.

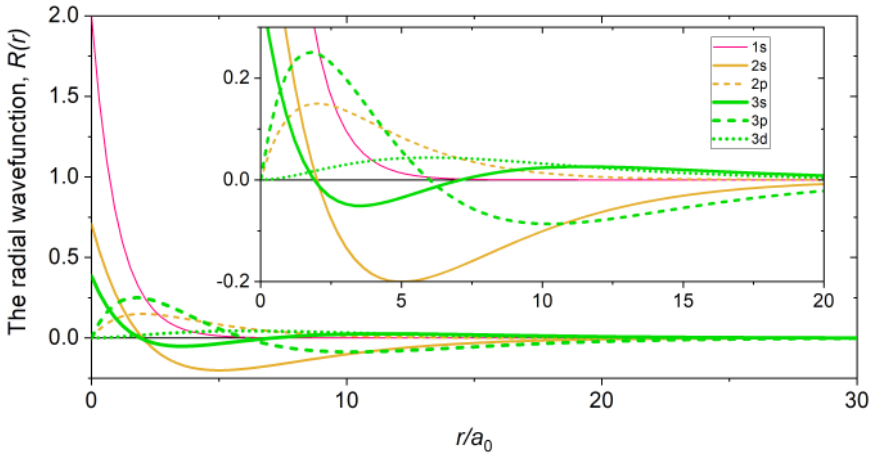


Figure **2.1.1**: Plots of the radial wavefunction, $R_{n,l}(r)$, for the first three shells. The wavefunctions are plotted relative to $\frac{r}{a_0}$, where $a_0 = 52.9pm = 0.529\mathring{A}$ is the Bohr Radius (the radius of a hydrogen 1s orbital). The expressions for these radial wavefunctions ($R_{n,l}(r)$) are shown in Table **2.1.2**.

Radial probability function, $4\pi r^2(R_{n,l}(r))^2$

The square of the wavefunction is proportional to the probability of finding a particle (electron) at some point in space. The square of the radial part of the wavefuction is called the radial distribution function $4\pi r^2(R_{n,l}(r))^2$, and it describes the probability of locating the electron at some distance r away from the nucleus. When we normalize the probability functions by dividing the function by its integral over all space, we get the plots shown in Figure **2.1.2**. The normalized probability functions are compared to the original radial part of the wavefunctions in Figure **2.1.3**. The most probable distance for finding an electron is shown by the maximum value of the function. For an electron in the 1s orbital of H, the most probable distance from the nucleus occurs at $r = 1a_0$. This is the Bohr Radius, and it has a value of ($a_0 = 52.9pm = 0.529\mathring{A}$). It is convenient to plot the functions of the hydrogen atomic orbitals relative to the size of its smallest orbital, the 1s orbital; this is the reason we plot $R_{n,l}(r)$ and $4\pi r^2(R_{n,l}(r))^2$ relative to $\frac{r}{a_0}$.

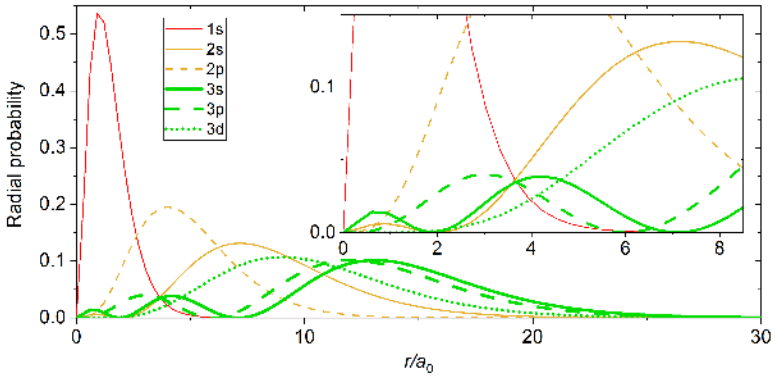


Figure **2.1.2**: Plots of the normalized radial probability functions for the first three shells.

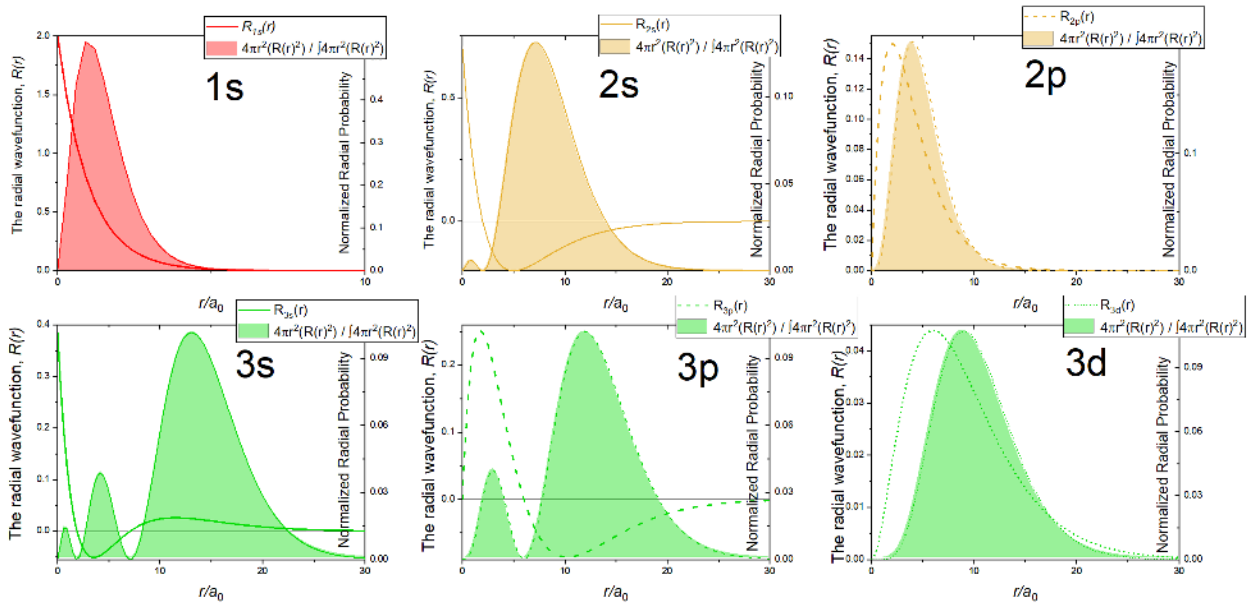


Figure **2.1.3**. Plots of the normalized radial probability function for each orbital in the first three shells (shaded curves). The y-axis on the left of each plot corresponds to the radial wavefunction (line); the y-axis on the right of each plot corresponds to radial probability function (shaded).

Radial nodes

In the case of the 3-dimensional wavefunction, there are two different types of nodes: radial nodes and angular nodes. **Radial nodes occur where the radial part of the wavefunction is zero ($R(x) = 0$)**. These are easy to see by plotting the radial part of the wavefunction and finding where the radial part of the wavefunction (and the radial probability function) is zero as seen in Figures **2.1.2** and **2.1.3**. These nodes are spherical in shape and depend on the energy level and subshell (the values of n and l). **The number of radial nodes is $n - l - 1$**. An example of a radial node is the single node that occurs in the **2*s*** orbital ($2 - 0 - 1 = 1$ node). In contrast, the 1s orbital has zero radial nodes ($1 - 0 - 1 = 0$ nodes). Where there is a node, there is zero probability of finding an electron.

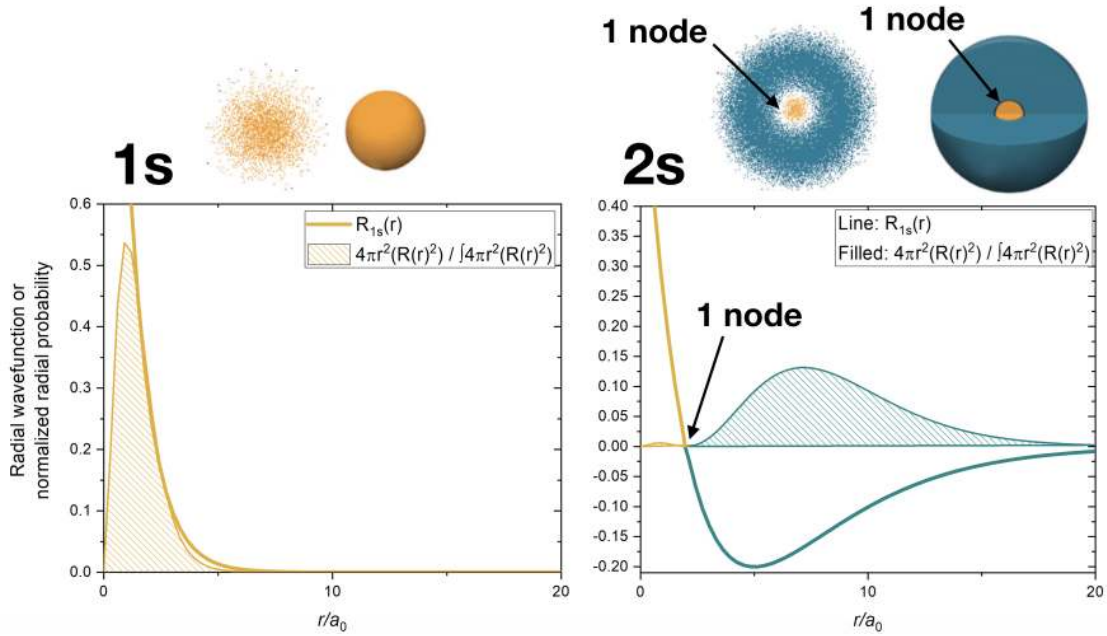


Figure **2.1.4**: Visualization of the 1s and 2s atomic orbitals. Each orbital is shown as both an electron probability density plot and a contour plot above its wavefunction and probability density function. The 1s orbital has zero radial nodes. The 2s orbital has one radial node where its wavefunction changes sign and its radial probability function is zero. Modified by K. Haas (CC-BY-NC-SA; Libretexts)

Boundary surfaces

A true node occurs where the probability of finding an electron is zero. Nodes occur where $\psi = \psi^2 = 0$. Far from the nucleus, the probability of finding the electron rapidly approaches zero, but is never *exactly* zero. What this means is that it is rather improbable to find the electron at far distances from the nucleus, but its not impossible. The rapid fall of probability creates a boundary surface rather than a node. The boundary surface represents the area around the nucleus where the electron exists most of the time.

Exercise 2.1.1

How many radial nodes are in the s, p, d, and f orbitals in the first four shells? $n = 1, 2, 3, 4$?

Answer

You can approach this answer by using the mathematical relationship between the number of radial nodes and the values of n and l: **number of radial nodes is $n - 1 - l$**. You could also notice the pattern that the first orbital of any type (1s, 2p, 3d...) has zero radial nodes, the second orbital of a type (2s, 3p, 4d...) has one radial node, the third orbital of a type has two radial nodes (3s, 4p, 5d...)...etc.

A full list of all of the orbitals in the first four shells and their number of radial nodes is below. Its a good idea to prove to yourself that the numbers given below are consistent with the plots of the orbitals wavefunctions for those orbitals in the first three shells:

s-orbitals:

1s: $n - 1 - l = 1 - 1 - 0 = 0$, zero radial nodes

2s: $n - 1 - l = 2 - 1 - 0 = 1$, one radial node

3s: $n - 1 - l = 3 - 1 - 0 = 2$, two radial nodes

4s: $n - 1 - l = 4 - 1 - 0 = 3$, three radial nodes

p-orbitals

2p: $n - 1 - l = 2 - 1 - 1 = 0$, zero radial nodes

3p: $n-1-l=3-1-1=1$, one radial node

4p: $n-1-l=4-1-1=2$, two radial nodes

d-orbitals

3d: $n-1-l=3-1-2=0$, zero radial nodes

4d: $n-1-l=4-1-2=1$, one radial nodes

f-orbital

4f: $n-1-l=4-1-3=0$, zero radial nodes

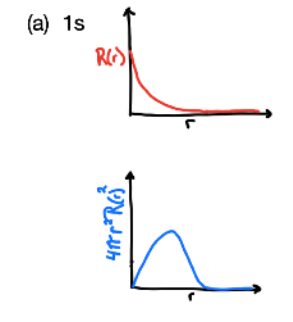
Exercise 2.1.2

Draw a rough plot of the following:

a. The radial wavefunction, $R_{n,l}(r)$ and the probability density function, $4\pi r^2(R_{n,l}(r))^2$, for the 1s orbital.
b. The radial wavefunction, $R_{n,l}(r)$ and the probability density function, $4\pi r^2(R_{n,l}(r))^2$, for the 4s orbital.

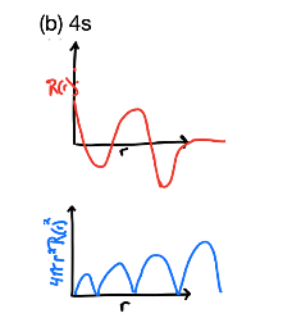
Answer, 1s

The 1s orbital's $R_{n,l}(r)$ reaches a maximum near the origin and approaches zero far from the nucleus. The $4\pi r^2(R_{n,l}(r))^2$ approaches zero at the origin, has a maximum intensity at the Bohr radius, and approaches zero far from the nucleus (its boundary surface).



Answer, 4s

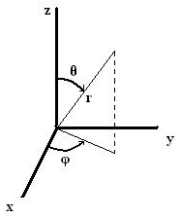
Like all s orbitals, the 4s orbital's $R_{n,l}(r)$ reaches a maximum near X=0, but it would be less intense than the function of the 1s, 2s, and 3s orbitals. It should have three radial nodes and so its wavefunction would change sign three times. This would give four regions of electron density in the probability function while the function would approach zero (boundary surface) far from the nucleus.



Angular contribution, $Y_{l,m_l}(\theta,\phi)$, and angular probability function, $(Y_{l,m_l}(\theta,\phi))^2$

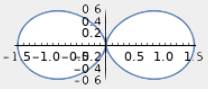
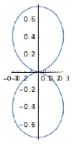
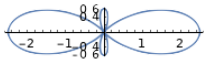
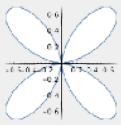
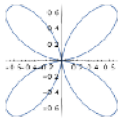
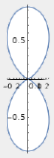
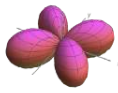
The angular contribution to the wavefunction, $Y_{l,m_l}(\theta,\phi)$, describes the wavefunction's shape, or the angle with respect to a coordinate system. To describe the direction in space, we use spherical coordinates that tell us distance *and* orientation in 3-

dimensional space. There are three spherical coordinates: r, ϕ, and θ. r is the radius, or the actual distance from the origin. ϕ and θ are angles. ϕ is measured from the positive x axis in the xy plane and may be between 0 and 2π. θ is measured from the positive z axis towards the xy plane and may be between 0 and π. $Y_{l,m_l}(\theta,\phi)$, is slightly more difficult to describe than the radial contribution was. This is partly because $Y_{l,m_l}(\theta,\phi)$ contains imaginary numbers, which have no real, physical meaning. However, the angular part of the wavefunction becomes more "real" when you square it to get angular probability density, a more tangible concept described as the **shapes of orbitals**.



The values of θ, ϕ, and $y(\theta,\phi)$ for orbitals in the hydrogen atom are listed in Table **2.1.2**, but $Y_{l,m_l}(\theta,\phi)$ is only a mathematical function and has not real physical meaning. The square of the radial wavefunction, $Y_{l,m_l}(\theta,\phi)^2$ gives the probability of finding the electron at a point in space on a ray described by (ϕ,θ). Thus $Y_{l,m_l}(\theta,\phi)^2$ describes the shape of the orbital.

Table 2.1.2. Components of the angular wavefunction and the resulting orbital shapes. The plots in the two right hand columns were created using Desmos and Mathematica: specifically "Spherical Harmonics" from the Wolfram Demonstrations Project, http://demonstrations.wolfram.com/SphericalHarmonics/ and "Visualizing Atomic Orbitals", https://demonstrations.wolfram.com/VisualizingAtomicOrbitals/.

subshell	m_l (orbital)	θ	ϕ	Plots of θ^2	orbital shapes
$l = 0$, s	$m_l = 0$	$\frac{1}{\sqrt{2}}$	$\frac{1}{\sqrt{2\pi}}$		
$l = 1$, p	$m_l = 0$	$\frac{\sqrt{6}}{2}\cos\theta$	$\frac{1}{\sqrt{2\pi}}$		
$l = 1$, p	$m_l = +1$	$\frac{\sqrt{3}}{2}\sin\theta$	$\frac{1}{\sqrt{2\pi}}e^{i\phi}$		
$l = 1$, p	$m_l = -1$	$\frac{\sqrt{3}}{2}\sin\theta$	$\frac{1}{\sqrt{2\pi}}e^{-i\phi}$		
$l = 2$, d	0	$\frac{\sqrt{10}}{4}\left(3\cos^2\theta - 1\right)$	$\frac{1}{\sqrt{2\pi}}$		
$l = 2$, d	$m_l = +1$	$\frac{\sqrt{15}}{2}\sin\theta\cos\theta$	$\frac{1}{\sqrt{2\pi}}e^{i\phi}$		
$l = 2$, d	$m_l = -1$	$\frac{\sqrt{15}}{2}\sin\theta\cos\theta$	$\frac{1}{\sqrt{2\pi}}e^{-i\phi}$		
$l = 2$, d	$m_l = +2$	$\frac{\sqrt{15}}{4}\sin^2\theta$	$\frac{1}{\sqrt{2\pi}}e^{i2\phi}$		
$l = 2$, d	$m_l = -2$	$\frac{\sqrt{15}}{4}\sin^2\theta$	$\frac{1}{\sqrt{2\pi}}e^{-i2\phi}$		

https://chem.libretexts.org/@go/page/328838

Angular nodes

Angular nodes exist where $(Y_{l,m_l}(\theta,\phi))^2 = 0$. These nodes are planar in shape, and they depend on the value of l. The number of angular nodes in any orbital is equal to l. This means that s-orbitals ($l = 0$) have zero angular nodes, p-orbitals ($l = 1$) have one angular node, d-orbitals ($l = 2$) have two angular nodes, and so on. Planar nodes can be flat planes (like the nodes in all p orbitals) or they can have a conical shape, like the two angular nodes in the d_{z^2} orbital. Angular nodes in some p and d orbitals are shown in Figure 2.1.5.

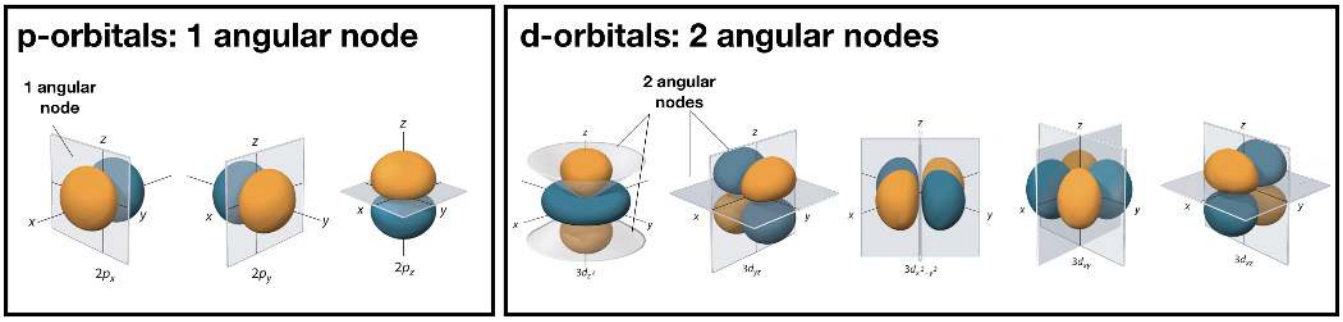
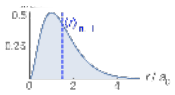
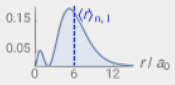
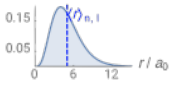
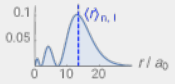
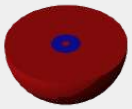
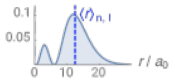
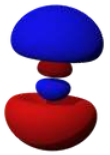
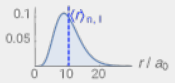
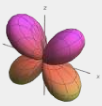


Figure 2.1.5: The angular nodes in p-orbitals and d-orbitals are shown. Every p orbital has one angular node, and every d orbital has two angular nodes. The number of angular nodes in any orbital is equal to the value of the quantum number, l. (CC BY-NC-SA; anonymous by request)

Atomic Orbitals

Atomic orbitals result from a combination of both the radial and angular contributions of the wavefunction. Atomic orbitals can have both angular nodes and radial nodes, depending on the values of n and l.

The chart below compares the radial variation, angular variation, and their combinations (orbitals).

Orbital	Radial Probability	Radial Nodes	Angular Probability	Angular Nodes	Combination (Orbital)	Total Nodes
1s		0		0		0
2s		1		0		1
2p		0		1		1
3s		2		0		2
3p		1		1		2
3d		0		2		2

This page titled 2.1: Quantum Numbers and Atomic Wavefunctions is shared under a CC BY-NC-SA 4.0 license and was authored, remixed, and/or curated by Kathryn Haas.

- **2.2: The Schrödinger equation, particle in a box, and atomic wavefunctions** by Kathryn Haas is licensed CC BY-NC-SA 4.0.
- **Current page** by Kathryn Haas is licensed CC BY-NC-SA 4.0.
- **2.2.2: Quantum Numbers and Atomic Wave Functions** by Kathryn Haas is licensed CC BY-NC-SA 4.0.

2.2: Shielding

Introduction

Coulomb's Law is from classical physics; it tells us that particles with opposite electrostatic charge are attracted to each other; and the larger the charge on either particle or the closer the distance between them, the stronger the attraction. Coulomb's law explains why atomic size decreases as the charge on the nucleus increases, but it can't explain the nuances and variations in size as we go across the periodic table. Coulomb's Law also explains why electrons in different shells (*n*), at different distances from the nucleus, have different energies. But on its own, Coulomb's law doesn't quite explain why electron subshells within a shell (like 2s vs 2p) would have different energies. To explain these things, we need to consider how both electron **shielding** and **penetration** result in variations in effective nuclear charge (Z*) that depend on shell and subshell.

Effective Nuclear Charge (Z*)

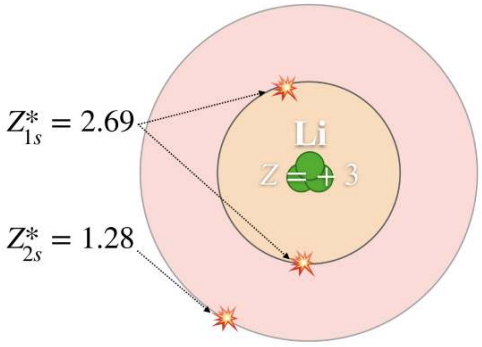


Figure **2.2.1**. In a lithium atom, the nuclear charge (Z) is +3. 1s electrons experience an effective nuclear charge (Z*) of +2.69, and 2s electrons experience an Z* of +1.28. (CC-BY-NC-SA; Kathryn Haas)

Coulombs' law works well for predicting the energy of an electron in a hydrogen atom (because H has only one electron). It also works for hydrogen-like atoms: any nucleus with exactly one electron (a He^+ ion, for example, has one electron). However, Coulomb's law is insufficient for predicting the energies of electrons in multi-electron atoms and ions.

Electrons within a multi-electron atom interact with the nucleus and with all other electrons. Each electron in a multi-electron atom experiences both attraction to the nucleus and repulsion from interactions with other electrons. The presence of multiple electrons decreases the nuclear attraction to some extent. Each electron in a multi-electron atom experiences a different magnitude of (and attraction to) the nuclear charge depending on what specific shell and subshell the electron occupies. The amount of positive nuclear charge experienced by any individual electron is the **effective nuclear charge (Z*)**.

For example, in lithium (Li), none of the three electrons "feel" the full +3 charge from the nucleus (see Figure **2.2.1**). Rather, each electron "feels" a Z* that is less than the actual Z and that depends on the electron's orbital. The actual nuclear charge in Li is $Z = +3$; the 1s electrons experience a $Z^* = +2.69$, and the 2s electron experiences a $Z^* = +1.28$. In general, core electrons (or the electrons closest to the nucleus), "feel" a Z* that is close to, but less than, Z. On the other hand, outer valence electrons experience a Z* that is much less than Z.

In summary:

- Core electrons: $Z^* \lessapprox Z$
- Valence electrons: $Z^* \ll Z$

Shielding:

Shielding is the reduction of true nuclear charge (Z) to the effective nuclear charge (Z*) by other electrons in a multi-electron atom or ion. Shielding occurs in all atoms and ions that have more than one electron. H is the only atom in which shielding does not occur.

Explanation of shielding: Electrons in a multi-electron atom interact with the nucleus and all other electrons in the atom. To describe shielding, we can use a simplified model of the atom: we will choose an electron-of-interest in a multi-electron atom and treat all the "other" electrons as a group of spherically-distributed negative charge. Classical electrostatics allows us to treat spherical distribution of charge as a point of charge at the center of the distribution. Thus, we consider all the "other" electrons in our atom as a point of negative charge in the center of the atom. While the positive charge of the nucleus provides an attractive force toward our electron, the negative charge distribution at the center of the atom would provide a repulsive force. The attractive and repulsive forces would partially cancel each other; but since there are less "other" electrons than there are protons in our atom, the nuclear charge is never completely canceled. The "other" electrons partially block, or shield, part of the nuclear charge so that our electron-of-interest experiences a partially-reduced nuclear charge, the Z*.

In reality, there is not a one-for-one "canceling" of the nuclear charge by each electron. Partly due to *penetration*, no single electron can completely shield a full unit of positive charge. Core electrons shield valence electrons, but valence electrons have little effect on the Z* of core electrons. The ability to shield, and be shielded by, other electrons strongly depends the electron orbital's average distance from the nucleus and its *penetration*; thus shielding depends on both shell (n) and subshell (l).

Shielding depends on electron penetration

Coulomb's law shows us that distance of an electron from its nucleus is important in determining the electron's energy (its attraction to the nucleus). The shell number (n) determines approximately how far an electron is from the nucleus *on average*. Thus, all orbitals in the same shell (s,p,d) have similar sizes and similar average distance of their electrons from the nucleus. But there is another distance-related factor that plays a critical role in determining orbital energy levels: *penetration*. **Penetration** describes the ability of an electron in a given subshell to penetrate into other shells and subshells to get close to the nucleus. Penetration is the **extent to which an electron can approach the nucleus**. Penetration depends on both the shell (n) and subshell (l).

The penetration of individual orbitals can be visualized using the radial probability functions. For example, Figure **2.2.2** below shows plots of the radial probability function of the 1s, 2s, and 2p orbitals. From these plots, we can see that the 1s orbital is able to approach the closest to the nucleus; thus it is the most penetrating. While the 2s and 2p have most of their probability at a farther distance from the nucleus (compared to 1s), the 2s orbital and the 2p orbital have different extents of penetration. Notice that the 2s orbital is able to penetrate the 1s orbital because of the central 2s lobe. The 2p orbital penetrates somewhat into the 1s, but it cannot approach the nucleus as closely as the 2s orbital can. While the 2s orbital penetrates more than 2p (2s orbital can approach closer to the nucleus), the 2p is slightly *closer on average* than 2s. The order of Z* in 2s and 2p subshells depends on which factor (average distance or penetration) is more important. In the first two rows of the periodic table, penetration is the dominant factor that results in 2s having a lower energy compared to 2p (see Figure **2.2.4** for values).

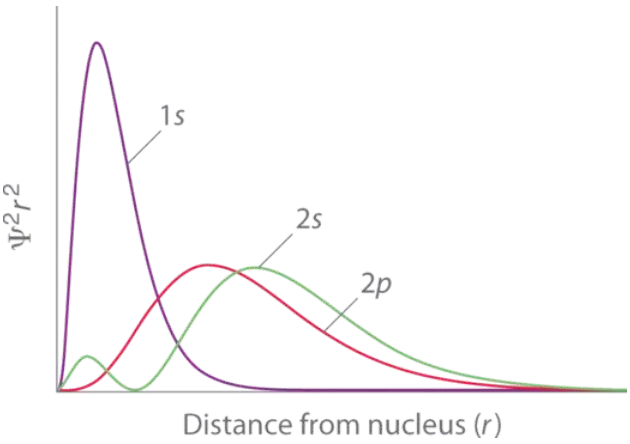


Figure 2.2.2. Orbital Penetration. A comparison of the radial probability distribution of the 2s and 2p orbitals for various states of the hydrogen atom shows that the 2s orbital penetrates inside the 1s orbital more than the 2p orbital does. Consequently, when an electron is in the small inner lobe of the 2s orbital, it experiences a relatively large value of Z*, which causes the energy of the 2s orbital to be lower than the energy of the 2p orbital.

An electron orbital's penetration effects its ability to shield other electrons and effects the extent to which it is shielded by other electrons. In general, electron orbitals that have greater penetration experience stronger attraction to the nucleus and less shielding by other electrons; these electrons thus experience a larger (Z*). Electrons in orbitals that have greater penetration also shield other electrons to a greater extent.

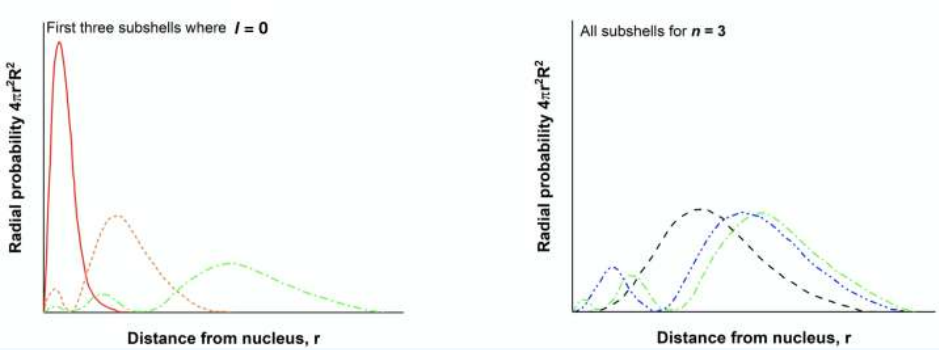
Within the same shell value (n), the penetrating power of an electron follows this trend in subshells ($\boldsymbol{l}$):

$$s>p>d>f$$

Exercises

Exercises

1. Compare the 2s and 2p orbitals:
   (a) Which is closer to the nucleus on average?
   (b) Which is more penetrating?
   (c) Which orbital experiences a stronger Z* and is thus lower in energy (consider your experience, but also inspect Figure **2.2.5**)? Please explain.
2. Visit the Orbitron and peruse the radial distribution functions for different orbitals. Compare the 2p and 3s orbitals:
   (a) Which is farther from the nucleus on average?
   (b) Which is more penetrating?
   (c) Which orbital is lower in energy?
3. Which atom, Li, or N, has a stronger valence Z*? Explain why.
4. Explain why 2s and 2p subshells are completely degenerate in a hydrogen atom.
5. Which atom has a smaller radii: Be or F? Explain.
6. Which electrons shield others more effectively: 3p or 3d?
7. Use the clues given in the figures below to label the radial distribution functions shown.



8. Explain why the ground state (most energetically favorable) electron configuration of Be is $1s^2 2s^2$ rather than alternative configurations like $1s^2 2s^1 2p^1$ or $1s^2 2p^2$.

Answer 1

(a) The 2s orbital is closer to the nucleus on average.

(b) The 2s orbital is more penetrating than 2p.

(c) You might "know" that the 2s orbital is lower in energy than 2p because 2s fills first. But a close inspection of Figures 1.1.2.3 and 1.1.2.4 from the previous page indicates that while the 2s and 2p elements are degenerate in Ne (element 10), for elements with atomic number 11 and greater 2p has a higher Z* than 2s! This example illustrates that both average distance and penetration are factors in determining Z*, and the factor that is more important may change as we increase in atomic number.

Answer 2

(a) The 3s orbital reaches farther away from the nucleus and is on average farther from the nucleus than 2p.

(b) The 3s orbital is more penetrating than 2p, even though 3s is farther on average!

(c) The 2p orbital is lower in energy than 3s; this is because 2p is still significantly closer to the nucleus on average and experiences a stronger Z*. (Penetration is not the only consideration!)

Answer 3

A nitrogen atom has a stronger effective nuclear charge (Z*) than lithium due to its greater number of protons; even though N also has more electrons that would shield the nuclear charge, each electron only partially shields each proton. This means that atoms with greater atomic number always have greater Z* for any given electron.

Answer 4

The hydrogen atom has only one electron; thus there is no shielding to consider. When there are not other electrons to shield the nucleus, penetration and shielding are irrelevant, and subshells within a shell are degenerate.

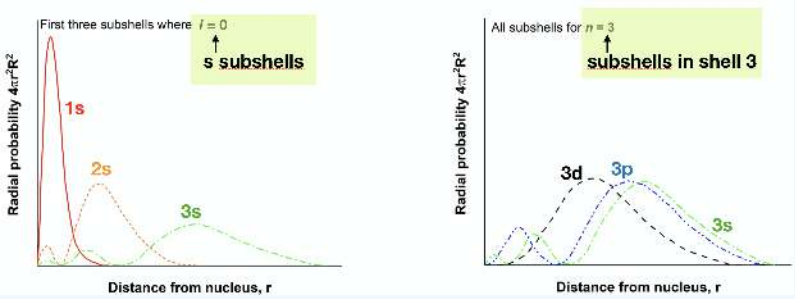
Answer 5

Fluorine has a smaller radii than Beryllium due to F having a greater valence Z* and therefore pulling the valence electrons close to the nucleus and providing a smaller atomic radii.

Answer 6

3p shields better than 3d because p orbitals penetrate more than d orbitals within the same shell.

Answer 7

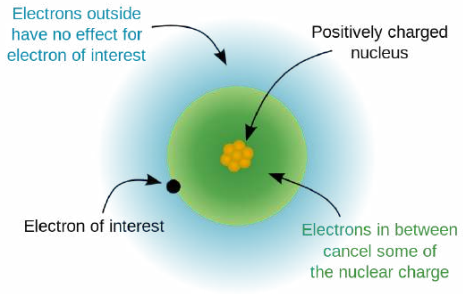


Answer 8

This question is asking why the 2s orbital fills in Be before 2p is occupied. This is a multi-electron atom, therefore core electrons shield the 2s and 2p orbitals to different extents. In Be we expect the 2s orbital to fill before 2p because 2s penetrates more and experiences a higher Z*.

Slater's rules for estimating Z*

Figure 2.2.3. Diagram illustrating effective nuclear charge according to Slater's rules.



The Z* can be estimated using a number of different methods; probably the best known and most commonly used method is known as **Slater's Rules**. Slater developed a set of rules to estimate Z* based on how many other electrons exist in the atom and on the orbital location of the electron-of-interest. These two factors are important determinants in shielding, and they are used to calculate a **shielding constant (S)** used in Slater's formula:

$$Z* = Z - S \tag{2.2.1}$$

where Z is the actual nuclear charge (the atomic number) and Z* is the effective nuclear charge.

In the calculation of S, it is assumed that electrons closer to the nucleus than our electron-of-interest cancel some of the nuclear charge; those farther from the nucleus have no effect. To calculate S, all the relevant orbitals in an atom are written out in order of increasing energy, separating them into in "groups". Each change in shell number is a new group; s and p subshells are in the same group but d and f orbitals are their own group. You write out all the orbitals using parentheses until you get to the group of the electron-of-interest, like this:

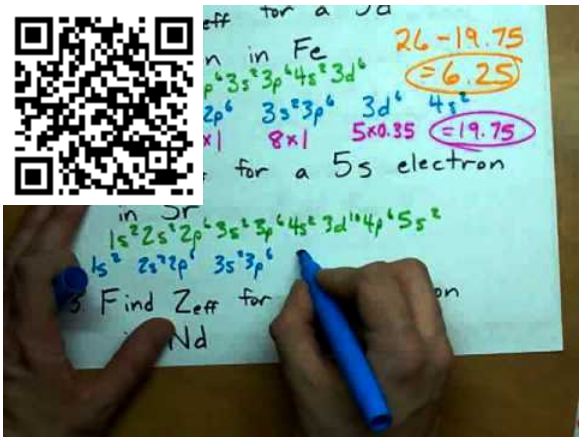
(1s)(2s,2p)(3s,3p)(3d)(4s,4p)(4d)(4f)(5s,5p) etc.

**Critical: The orbitals must be written in order of increasing energy!

1. **Electrons in the same Group():**
   - Each other electron (not counting the electron-of-interest) in the same group () as the chosen electron, contributes 0.35 to S.
   - Each 1s electron contributes 0.30 to S.
     Conceptually, this means electrons in the same group shield each other 30-35%.
2. **Electrons in Groups() to the left:**
   - If the electron-of-interest is in a d or f subshell, every electron in groups () to the left contributes 1.00 to S.
     Conceptually, this means that d and f electrons are shielded 100% by all electrons in the same shell with a smaller value of l, as well as all electrons in lower shells (n).
   - If the electron-of-interest is in an s or p subshell, all electrons in the next lower shell (n - 1) contribute 0.85 to S. And all the electrons in even lower shells contribute 1.00 to S.
     Conceptually, this means that s and p electrons are shielded 85% by the electrons one shell lower, and 100% by all electrons in shells n - 2 or lower.
3. **Electrons in Groups() to the right:**
   - Electrons to the right contribute 0 to S.
     Conceptually, this means electrons in higher energy groups don't contribute to shielding.

A video explaining how to use Slater's Rules





Example 2.2.1: Fluorine, Neon, and Sodium

What is the Z* experienced by the valence electrons in the three isoelectronic species: fluorine anion (F^-), neutral neon atom (Ne), and sodium cation (Na^+)?

Solution

Each species has 10 electrons, and the number of core electrons is 2 (10 total electrons - 8 valence), but the effective nuclear charge varies because each has a different atomic number (Z). The approximate Z* can be found with Slater's Rules. For all of these species, we would calculate the same sigma value:

Calculating S: (1s)(2s,2p), $S = 2(0.85) + 7(0.35) = 1.7 + 2.45 = 4.15$

Fluorine anion: $Z* = 9 - S = 9 - 4.15 = 4.85$

Neon atom: $Z* = 10 - S = 10 - 4.15 = 5.85$

Sodium Cation: $Z* = 11 - S = 11 - 4.15 = 6.85$

So, the sodium cation has the greatest effective nuclear charge.

Exercise 2.2.1

Calculate Z* for a 3d-electron in a zinc (Zn) atom.

Answer

Write out the relevant orbitals: (1s)(2s,2p)(3s,3p)(3d) ~~(4s)~~

Notice that although 4s is fully occupied, we don't include it because in Zn, 4s is higher in energy than 3d. Therefore, 4s is to the right of the d electrons we are considering. The electron-of-interest is in 3d, so the other nine electrons in 3d each contribute 0.35 to the value of S. The other 18 electrons each contribute 1 to the value of S.

$S = 18(1) + 9(0.35) = 21.15$

$Z* = 30 - 21.15 = 8.85$

So, although the nuclear charge of Zn is 30, the 3d electrons only experience a $Z* \approx 8.85$!

"Best" values for Z*

Slater's rules are a set of simple rules for predicting S and Z* based on empirical evidence from quantum mechanical calculations. In other words, the Z* calculated from Slater's rules are approximate values. The values considered to be the most accurate are derived from quantum mechanical calculations directly. You can find these values in a nice chart on the Wikipedia article of Effective Nuclear Charge. The chart is recreated here in Figure 2.2.4 for convenience:

Z or Z_{eff}	H																	He
Z	1.00																	2.00
1s	1.00																	1.69
	Li	Be											B	C	N	O	F	Ne
Z	3.00	4.00											5.00	6.00	7.00	8.00	9.00	10.00
1s	2.69	3.69											4.68	5.67	6.67	7.66	8.65	9.64
2s	1.28	1.91											2.58	3.22	3.85	4.49	5.13	5.76
2p													2.42	3.14	3.83	4.45	5.10	5.76
	Na	Mg											Al	Si	P	S	Cl	Ar
Z	11.00	12.00											13.00	14.00	15.00	16.00	17.00	18.00
1s	10.63	11.61											12.59	13.58	14.56	15.54	16.52	17.51
2s	6.57	7.39											8.21	9.02	9.83	10.63	11.43	12.23
2p	6.80	7.83											8.96	9.95	10.96	11.98	12.99	14.01
3s	2.51	3.31											4.12	4.90	5.64	6.37	7.07	7.76
3p													4.07	4.29	4.89	5.48	6.12	6.76
	K	Ca	Sc	Ti	V	Cr	Mn	Fe	Co	Ni	Cu	Zn	Ga	Ge	As	Se	Br	Kr
Z	19.00	20.00	21.00	22.00	23.00	24.00	25.00	26.00	27.00	28.00	29.00	30.00	31.00	32.00	33.00	34.00	35.00	36.00
1s	18.49	19.47	20.46	21.44	22.43	23.41	24.40	25.38	26.37	27.35	28.34	29.33	30.31	31.29	32.28	33.26	34.25	35.23
2s	13.01	13.78	14.57	15.38	16.18	16.98	17.79	18.60	19.41	20.21	21.02	21.83	22.60	23.37	24.13	24.89	25.64	26.40
2p	15.03	16.04	17.06	18.07	19.07	20.08	21.08	22.09	23.09	24.10	25.10	26.10	27.09	28.08	29.07	30.07	31.06	32.05
3s	8.68	9.60	10.34	11.03	11.71	12.37	13.02	13.68	14.32	14.96	15.59	16.22	17.00	17.79	18.60	19.40	20.22	21.03
3p	7.73	8.66	9.41	10.10	10.79	11.47	12.11	12.78	13.44	14.09	14.73	15.37	16.20	17.01	17.85	18.71	19.57	20.43
4s	3.50	4.40	4.63	4.82	4.98	5.13	5.28	5.43	5.58	5.71	5.84	5.97	7.07	8.04	8.94	9.76	10.55	11.32
3d			7.12	8.14	8.98	9.76	10.53	11.18	11.86	12.53	13.20	13.88	15.09	16.25	17.38	18.48	19.56	20.63
4p													6.22	6.78	7.45	8.29	9.03	9.34
	Rb	Sr	Y	Zr	Nb	Mo	Tc	Ru	Rh	Pd	Ag	Cd	In	Sn	Sb	Te	I	Xe
Z	37.00	38.00	39.00	40.00	41.00	42.00	43.00	44.00	45.00	46.00	47.00	48.00	49.00	50.00	51.00	52.00	53.00	54.00
1s	36.21	37.19	38.18	39.16	40.14	41.13	42.11	43.09	44.08	45.06	46.04	47.03	48.01	48.99	49.97	50.96	51.94	52.92
2s	27.16	27.90	28.62	29.37	30.13	30.88	31.63	32.38	33.16	33.88	34.63	35.39	36.12	36.86	37.60	38.33	39.07	39.80
2p	33.04	34.03	35.00	35.99	36.98	37.97	38.94	39.95	40.94	41.93	42.92	43.91	44.90	45.89	46.87	47.86	48.85	49.84
3s	21.84	22.66	23.55	24.36	25.17	25.98	26.79	27.60	28.44	29.22	30.03	30.84	31.63	32.42	33.21	34.00	34.79	35.58
3p	21.30	22.17	23.09	23.85	24.62	25.47	26.38	27.22	28.15	29.02	29.81	30.69	31.52	32.35	33.18	34.01	34.84	35.67
4s	12.39	13.44	14.26	14.90	15.28	16.10	17.20	17.66	18.58	18.99	19.87	20.87	21.76	22.66	23.54	24.41	25.30	26.17
3d	21.68	22.73	25.40	25.57	26.25	27.23	28.35	29.36	30.41	31.45	32.54	33.61	34.68	35.74	36.80	37.84	38.90	39.95
4p	10.88	11.93	12.75	13.46	14.08	14.98	15.81	16.44	17.14	17.72	18.56	19.41	20.37	21.27	22.18	23.12	24.03	24.96
5s	4.99	6.07	6.26	6.45	5.92	6.11	7.23	6.49	6.64	(empty)	6.76	8.19	9.51	10.63	11.62	12.54	13.40	14.22
4d			15.96	13.07	11.24	11.39	12.88	12.81	13.44	13.62	14.76	15.88	16.94	17.97	18.97	19.96	20.93	21.89
5p													8.47	9.10	10.00	10.81	11.61	12.43

Figure 2.2.4. This chart shows Z* values calculated by Clementi et. al. in 1963 and 1967 that are consistent with SCF Calculations. This chart was created using data from the Wikipedia article on Effective Nuclear Charge.

Z* modulates attraction

When valence electrons experience less nuclear charge than core electrons, different electrons experience different magnitudes of attraction to the nucleus. A modified form of Coulomb's Law is written below, where e is the charge of an electron, Z* is the effective nuclear charge experienced by that electron, and r is the radius (distance of the electron from the nucleus).

$$F_{eff} = k\frac{Z * e^2}{r^2} \tag{2.2.2}$$

This formula suggests that if we can estimate Z*, then we can predict the attractive force experienced by, and the energy of, an electron in a multi-electron atom (ex. Li).

The attraction of the nucleus to valence electrons determines the atomic or ionic size, ionization energy, electron affinity, and electronegativity. The stronger the attraction, and the stronger Z*, the closer the electrons are pulled toward the nucleus. This in turn results in a smaller size, higher ionization energy, higher electron affinity, and stronger electronegativity.

General Periodic Trends in Z*

Close inspection of Figure **2.2.4** and analysis of Slater's rules indicate that there are some predictable trends in Z*. The data from Figure **2.2.4** is plotted below in Figure **2.2.5** to provide a visual aid to the discussion below.

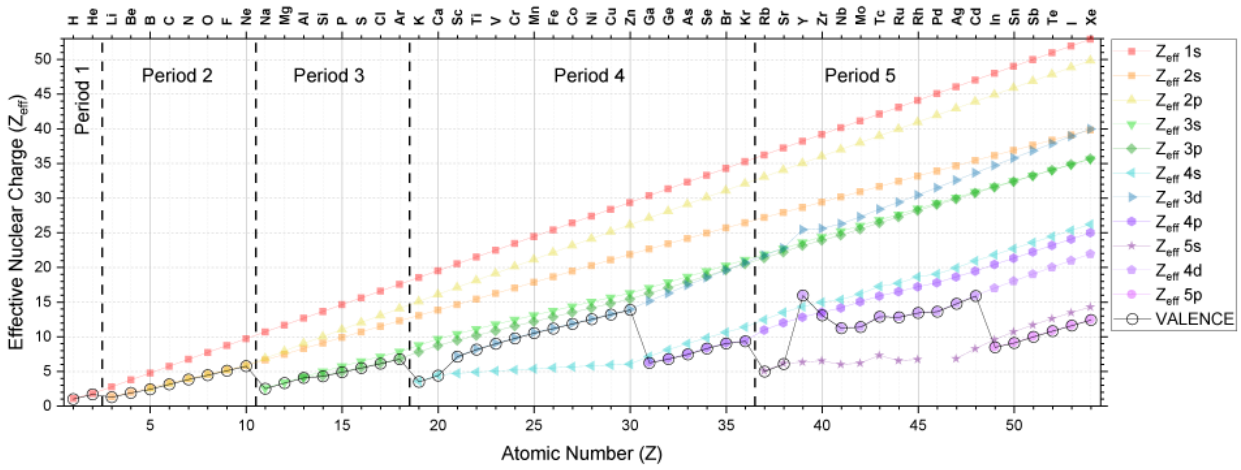


Figure 2.2.5: The Z* values for electrons in each subshell of the first 54 elements (H to Xe) are plotted. Each subshell is plotted as a different series (see legend) and the valence shell is highlighted by a solid black line with open circles. (CC-BY-NC-SA; Kathryn Haas)

Trends in Z* for electrons in a specific shell and subshell

The Z* for electrons in a given shell and subshell generally increases as atomic number increases; this trend holds true going across the periodic table and down the periodic table. Convince yourself that this is true for any subshell by examining Figure 2.2.5.

Do you notice any exceptions to this general trend?

Inspection of Figure 2.2.5 should confirm for you that the Z* increases as Z increases for electrons in any subshell (like the 1s subshell for example, which is plotted above as a red line with square points). You can see this trend as the positive slope in each series. There is one obvious exception in Period 5 in elements 39 (Y) to 41 (Nb; the Z* of 4s actually decreases across these three elements as atomic number increases. There is also an exception between Y and Zr in the 3d subshell, and between Tc and Ru in the 5s subshell.

For valence electrons:

It is useful to understand trends in valence Z* because the valence Z* determines atomic/ionic properties and chemical reactivity. The trends in the valence Z* are not simple because as atomic number increases, the valence shell and/or subshell also changes. The valence Z* is indicated in Figure 2.2.5 as a black line with open circles.

Down the table: As we go down a column of the periodic table, the valence Z* increases. This is a simple trend because type of subshell is consistent and there is an increase only in shell and in atomic number, Z. This trend is best illustrated by inspection of Figure 2.2.4.

Across the table: the trend depends on shell and subshell, but generally Z* increases across a period.

Periods 1-3 (s and p only): As we go across the table in periods 1-3, the shell stays constant as Z increases and the subshell changes from s to p. In these periods, there is a gradual increase in valence Z* as we move across any of the first three periods.

Periods 4 and 5 (s, p, and d): Now we have some more complex trends because valence subshell and shell are changing as we increase in atomic number. Notice that the valence Z* generally increases going across a period as long as subshell isn't changing; the exception is within the 4d subshell (elements 39-44 or Y-Ru). In general, going from $(n)s$ subshell to $(n-1)d$ subshell, there a relatively large increase in valence Z*. And in going from $(n-1$d\) subshell to $(n)p$ subshell, there is a relatively large decrease in Z*.

From one period to another: From Figure 2.2.5, we can see that as we increase Z by one proton, going from one period to the next, there is a relatively large decrease in Z* (from Ne to Na, for example). This is because as Z increases by a small

interval, the shell number increases, and so the electrons in the valence shell are much farther from the nucleus and are more shielded by all the electrons in the lower shell numbers.

Exercises

Exercise 2.2.2

1. Compare trends in Z* and atomic size. Explain how and why atomic size depends on Z*.
2. Compare trends in Z* and ionization energy. Explain how and why ionization energy depends on Z*.

Answer

1. On the periodic table, atomic radius generally decreases across the periods (left to right) and increases down the groups. As atomic number increases across the periodic table, nuclear charge (Z) increases and Z* increases. In turn, the atomic radius decreases because the higher nuclear charge (and thus higher Z*) pulls electrons closer to the nucleus. Atomic radius increases down the periodic table because the shell number increases. Despite an increase in Z* going down the periodic table, larger atomic radii results from electrons occupying higher shells.

2. Ionization energies (IE) are inversely related to atomic radius; IE increases across the periods and decreases down the groups. Since the nucleus holds valence electrons more strongly (due to higher Z*) across the periods, IE increases because valence electrons are harder to remove. Down the periodic table, larger atomic radius causes electrons in valence orbitals to be shielded by core electrons. Recall that shielding reduces the nuclear charge available to electrons in higher orbital levels, resulting in a lower Z*. With more shielding and lower Z*, the valence electrons are held less tightly by the nucleus such that ionization energy decreases (i.e. valence electrons are easier to remove).

References

1. Petrucci, Ralph H., William S. Harwood, F. Geoffrey Herring, and Jeffry D. Madura. General Chemistry: Principles and Modern Applications, Ninth Edition. Pearson Education Inc. Upper Saddle River, New Jersey: 2007.
2. Raymond Chang. Physical Chemistry for Biological Sciences. Sausalito, California: University Science Books, 2005
3. R. S. Mulliken, Electronic Structures of Molecules and Valence. II General Considerations, Physical Review, vol. 41, pp. 49-71 (1932)
4. Anastopoulos, Charis (2008). *Particle Or Wave: The Evolution of the Concept of Matter in Modern Physics*. Princeton University Press. pp. 236–237. ISBN 0691135126. http://books.google.com/?id=rDEvQZhpltEC&pg=PA236.

Contributors and Attributions

- Sidra Ayub (UCD), Alan Chu (UCD)
- Emily V Eames (City College of San Francisco)
- Curated or created by Kathryn Haas

2.2: Shielding is shared under a CC BY-NC-SA 4.0 license and was authored, remixed, and/or curated by LibreTexts.

- **2.2.4: Shielding** by Kathryn Haas is licensed CC BY-NC-SA 4.0.
- **Current page** is licensed CC BY-NC-SA 4.0.

2.3: Aufbau Principle

Introduction

The **Aufbau Principle** (also called the **building-up principle** or the **Aufbau rule**) states that, in the ground state of an atom or ion, electrons fill atomic orbitals of the lowest available energy level before occupying higher-energy levels. In general, an electron will occupy an atomic orbital with the lowest value of n, l, m_l, in that order of priority. The value of m_s for an unpaired electron is conventionally assigned a value of $+\frac{1}{2}$. Each electron in an atom/ion must have a unique set of values for all four quantum numbers.

The Ground State of Hydrogenic Atoms/Ions

In a hydrogenic atom/ion, there is only one electron. In this case, the *only factor determining energy is the value of* n. The ground state will always be the 1s orbital ($n = 1, l = 0, m_l = 0, m_s = +\frac{1}{2}$).

The Ground State of Multi-electron Atoms/Ions

In atoms/ions with two or more electrons, the ground state electron configuration (1) minimizes the total energy of the electrons, (2) obeys the Pauli exclusion principle, (3) obeys Hunds rule of maximum multiplicity, and (4) considers the exchange interaction. These "rules" are described below.

(1) Electrons will occupy the lowest energy orbitals in order to minimize the total energy. The two quantum numbers that are related to energy in multi-electron atoms are n, and l. Thus, orbitals with the lowest values of n and l will fill first.

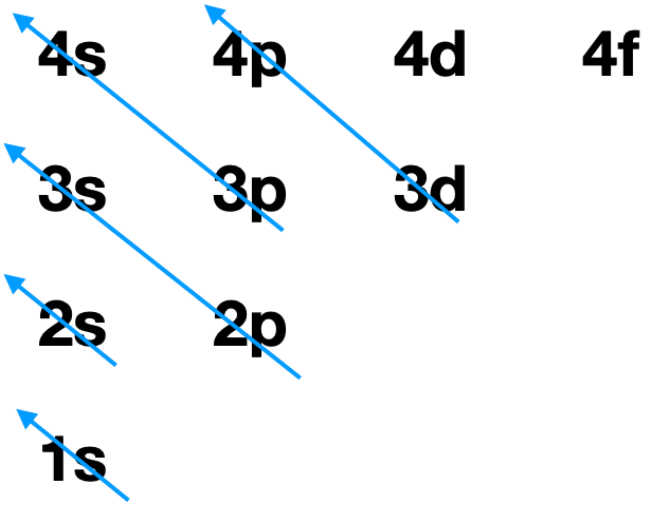


Figure 2.3.1. The order of filling of ground state electron orbitals is 1s, 2s, 2p, 3s, 3p, 4s, 3d, 4p, etc... (CC-BY-NC-SA; Kathryn Haas)

(2) Hund's rule of maximum multiplicity states that for a given electron configuration, the lowest energy arrangement of electrons in degenerate orbitals is the one with the greatest "multiplicity," where multiplicity is the number of unpaired electrons (n) plus 1 (multiplicity = n + 1). This rule is used to predict the ground state of an atom or molecule with one or more open electronic shells.

Hund's rule is based on empirical observation of atomic spectra, and it is a consequence of the energy required to pair two electrons in the same orbital. This energy of repulsion between two electrons in the same orbitals is a Coulombic energy of repulsion, Π_c, caused by two electrons with like charge sharing the same area of space (an orbital). When more than one electron occupies a set of degenerate orbitals, the most favorable arrangement is one where the number of paired electrons is minimized.

A simplified definition of Hund's rule is that **the lowest energy arrangement is the one with the greatest number of unpaired electrons**. This implies that if two or more orbitals of equal energy are available, electrons will occupy them singly before filling them in pairs. Examples of ground

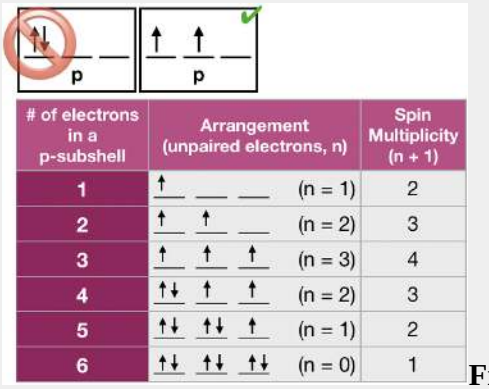


Figure 2.3.2. Hund's rule is that spin multiplicity must be maximized in the ground state. (CC-BY-NC-SA; Libretexts)

state arrangements of electrons in three degenerate p-orbitals is given in the figure shown here.

(3) The Pauli exclusion principle states that it is impossible for two electrons of a multi-electron atom to have the same set of values for the four quantum numbers. Two electrons in different orbitals will have a different set of n, l, and m_l values. When two electrons reside in the same orbital, they posses the same n, l, and m_l values, therefore their m_s must be different. Thus, two electrons in the same orbital must have opposite half-integer spin projections of $+\frac{1}{2}$ and $-\frac{1}{2}$.

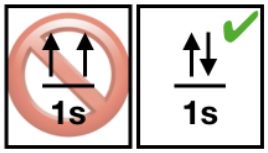


Figure 2.3.3. Pauli's principle tells us that paired electrons must have opposite spin. CC-BY-NC-SA; Libretexts)

(4) The exchange interaction is sometimes called the *exchange energy* or *exchange force*, however it is not a true energy or force. Rather, it is a quantum mechanical effect that takes place between identical particles. The exchange interaction results in a ground state electron configuration with unpaired electrons all being of the same spin. Unpaired electrons are conventionally written in the "spin up" direction.

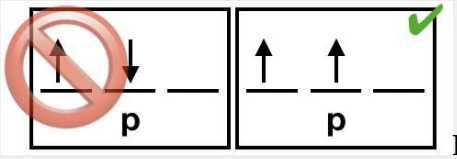


Figure 2.3.4. Unpaired electrons should have identical spins according due to the exchange interaction. CC-BY-NC-SA; Libretexts)

Trends in Expected Electron Configuration

The four "rules" above can be used as guidelines to predict the ground state electron configuration of atoms, the filling of subshells, and the configuration of electrons in degenerate orbitals. However, the utility of these guidelines for predicting actual electron configurations requires more nuanced knowledge of the relative energy levels of orbitals.

Generally, orbital energy levels directly correspond to their shell number. Additionally, orbitals within a shell generally follow the energetic trend where s<p<d<f. Although these general trends for relative orbital energy levels hold true for most of the main block elements (the s - and p-blocks), there are important exceptions in the orbital energy levels of transition metal atoms and ions of the d- and f-blocks.

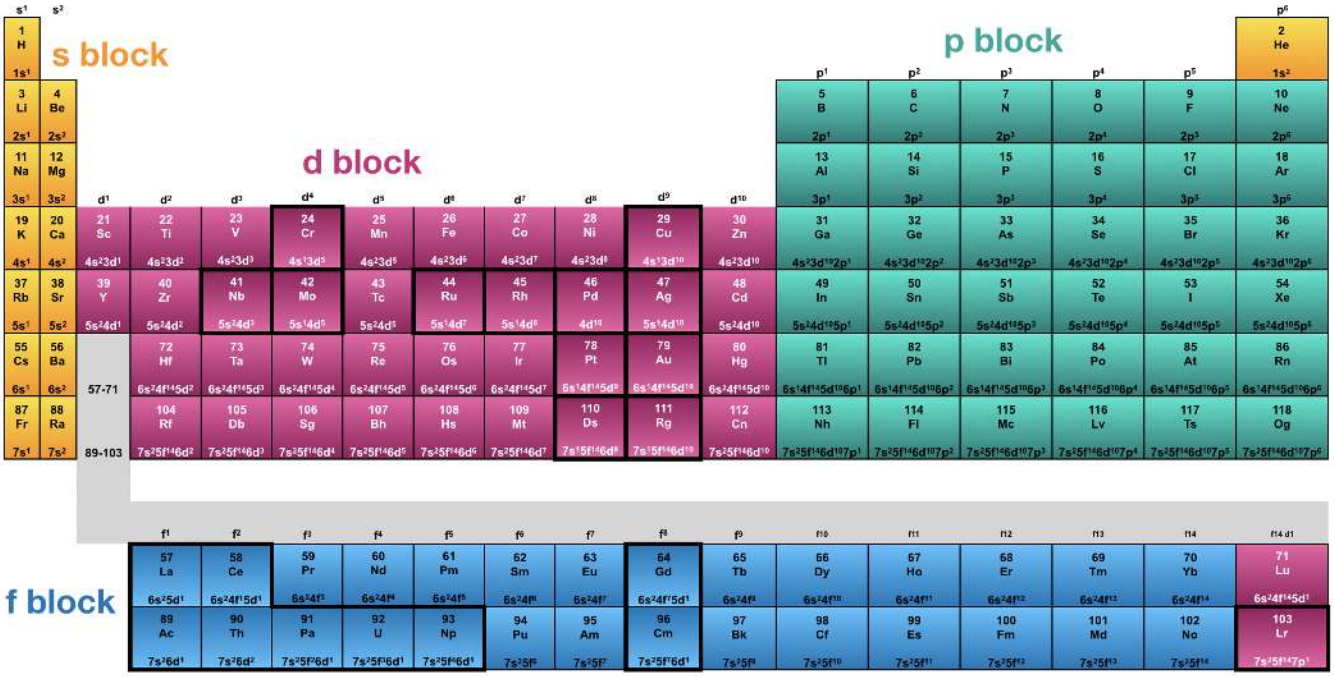


Figure **2.3.5**. This is a depiction of the periodic table that highlights the s-, p-, d-, and f- blocks in different colors. Violations of the expected trend in electron configurations are outlined in a heavy black line. Several elements of the d block and f block violate the general trends in electron configuration because their orbital energy levels do not follow *general* trends. (CC-BY-NC-SA; Kathryn Haas)

Elements that violate general trends in electron configuration are outlined with a dark line in Figure **2.3.5**. All of the exceptions are within the d- and f- blocks, and the violations are caused by an unexpected order of the orbital energy levels.

In the next section you will learn why the orbital energy levels correlate with shell number and why subshells within a shell usually follow the trend that s<p<d<f. You will also learn why there are occasional exceptions to this trend and how these exceptions influence elemental properties.

References

1. Miessler, Gary L., and Donald A. Tarr. *Inorganic Chemistry*. Upper Saddle River, NJ: Pearson Prentice Hall, 2010. Print.
2. Brown, Ian David. *The Chemical Bond in Inorganic Chemistry the Bond Valence Model*. Oxford: Oxford UP, 2006. Print.

This page titled 2.3: Aufbau Principle is shared under a CC BY-NC-SA 4.0 license and was authored, remixed, and/or curated by Kathryn Haas.

- **2.2.3: Aufbau Principle** by Kathryn Haas is licensed CC BY-NC-SA 4.0.
- **Current page** by Kathryn Haas is licensed CC BY-NC-SA 4.0.

2.4: Periodic Properties of Atoms

Introduction

General periodic trends are specific patterns that are present within the periodic table; these are patterns in properties like electronegativity, ionization energy, electron affinity, atomic radius, melting point, and metallic character. General periodic trends provide chemists with an invaluable tool to quickly predict an element's properties. These trends exist because of the similar atomic structure of the elements within their respective group families or periods, and because of the periodic nature of the elements. Some of the general periodic trends are described in this section.

Ionization Energy

Ionization energy (IE) is the energy required to **remove an electron from a neutral atom or cation in its gaseous phase**. IE is also known as *ionization potential*.

$$A^{n+}_{(g)} \longrightarrow A^{(n+1)+}_{(g)} + e^- \qquad IE = \Delta U \tag{2.4.1}$$

Conceptually, ionization energy is the affinity of an element for its outermost electron (an electron it already has in its valence shell).

1st, 2nd, and 3rd Ionization Energies

The symbol IE_1 stands for the ***first ionization energy*** (energy required to take away an electron from a neutral atom, where $n = 0$). The symbol IE_2 stands for the ***second ionization energy*** (energy required to take away an electron from an atom with a +1 charge, $n = 2$.)

First Ionization Energy, IE_1 (general element, A): $A_{(g)} \rightarrow A^{1+}_{(g)} + e^-$

Second Ionization Energy, IE_2 (general element, A): $A^{1+}_{(g)} \rightarrow A^{2+}_{(g)} + e^-$

Third Ionization Energy, IE_3 (general element, A): $A^{2+}_{(g)} \rightarrow A^{3+}_{(g)} + e^-$

Each succeeding ionization energy is larger than the preceding energy. This means that $IE_1 < IE_2 < IE_3 < ... < IE_n$ will always be true. For example, ionization energy increases as succeeding electrons are taken away from Mg.

$$Mg_{(g)} \rightarrow Mg^+_{(g)} + e^- \quad IE_1 = 738\,kJ/mol \tag{2.4.2}$$

$$Mg^+_{(g)} \rightarrow Mg^{2+}_{(g)} + e^- \quad IE_2 = 1451\,kJ/mol \tag{2.4.3}$$

Ionization energy is correlated with the strength of attraction between the positively-charged nucleus and the negatively-charged valence electrons, and therefore the effective nuclear charge Z_eff. The higher the ionization energy, the stronger the attractive force between nucleus and valence electrons, and the more energy is required to remove a valence electron. The lower the ionization energy, the weaker the attractive force between nucleus and valence electrons, and the less energy required to remove a valence electron.

General periodic trends in ionization energy

In general, ionization energies increase from left to right and decrease down a group; however there are variations in these trends that would be expected from the effects of penetration and shielding. The trends in **first ionization energy** are shown in Figure **2.4.1** and are summarized below.

- **Across a period:** As Z* increases across a period, the ionization energy of the elements generally increases from left to right. However there are breaks or variation in the trends in the following cases:
  - IE is especially low when removal of an electron creates a newly empty p subshell (examples include IE_1 of B, Al, Sc)
  - IE energy is especially low where removal of an electron results in a half-filled p or d subshell (examples include IE_1 of O, S)

- IE increases more gradually across the d- and f-subshells compared to s- and p- subshells. This is because d- and f-electrons are weakly penetrating and experience especially low Z*.

- **From one period to the next:** There is an especially large decrease in IE with the start of every new period (from He to Li or from Ne to Na for example). This is consistent with the idea that IE is especially low when removal of an electron creates a newly empty s-subshell.
- **Nobel gases:** The noble gases posses very high ionization energies. Note that helium has the highest ionization energy of all the elements.
- **Down a group:** Although Z* increases going down a group, there is no reliable trend in IE going down any group; in some cases IE increases going down a group, while in other cases IE decreases going down a group.

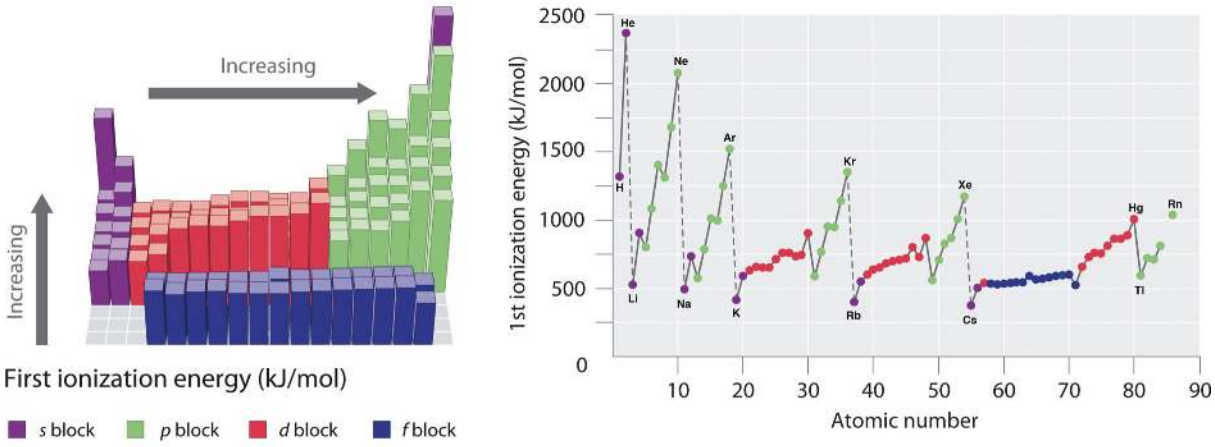


Figure 2.4.1: Graph showing the First Ionization Energy of the Elements. Left: ionization energies are mapped onto the periodic table, where the magnitude of ionization energy is depicted as a bar graph. Right: the first ionization energy is plotted against atomic number. In both panels the elements of the s-block are shown in purple, p-block are shown in green, d-block are shown in red, and f-block are shown in blue.

Plots of the IE_1, IE_2, and IE_3 of elements from hydrogen to krypton (first four periods) are shown in Figure 2.4.2. Notice that $IE_3 > IE_2 > IE_1$. Also notice that trends mentioned above for IE_1 hold true for subsequent ionizations when electron configurations are considered!

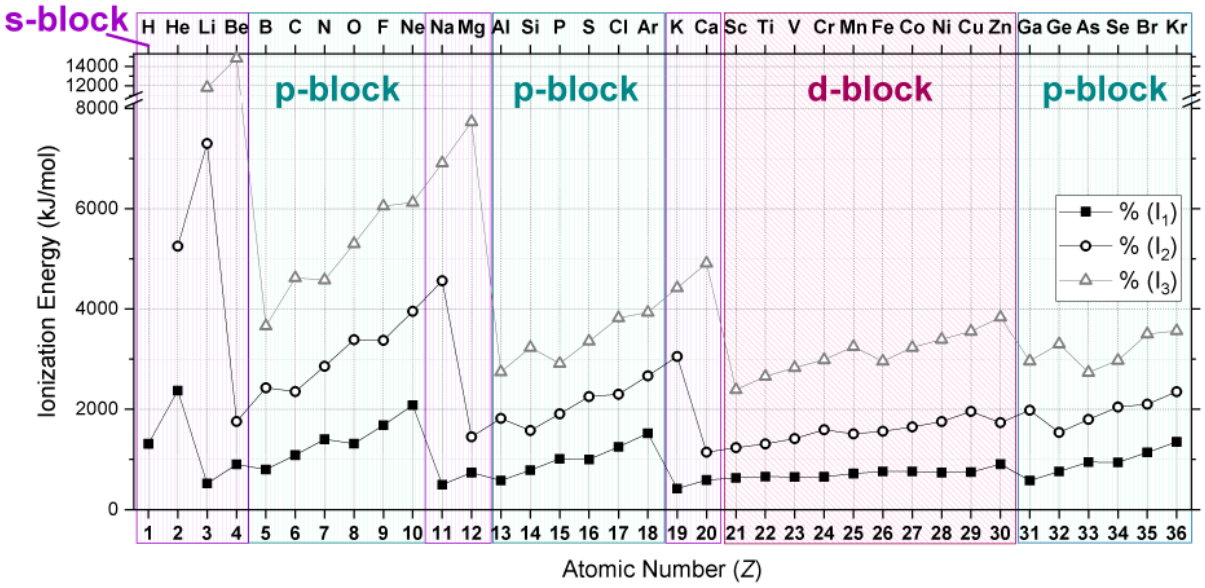


Figure 2.4.2. The first (I_1), second (I_2), and third (I_3) ionization energies are plotted for elements with Z = 1 to 36 (H to Kr). The position of each element in its atomic form is indicated as s- p- or d-block. (CC-BY-NC-SA; Kathryn Haas)

Electron Affinity

According to IUPAC, there are two different, but equivalent, definitions of **electron affinity (EA)**.[6]

EA defined as removal of an electron

Electron affinity can be defined as the energy *required* when an electron is removed from a gaseous anion. The reaction as shown in equation 2.4.4 is *endothermic* (positive ΔU) for elements except noble gases and alkaline earth metals. Under this definition, the more positive the EA value, the higher an atom's affinity for electrons.

$$A^-_{(g)} \longrightarrow A_{(g)} + e^- \qquad EA = \Delta U \tag{2.4.4}$$

The reaction shown in equation 2.4.4 is similar those that define ionization energy. For this reason, the EA is also described as the *zeroth ionization energy*.

EA defined as addition of an electron

An alternate and more common definition is the microscopic reverse of equation 2.4.4. This more common definition states that electron affinity is the energy *released* when an electron is added to a gaseous atom, as shown in equation 2.4.5. The reaction as shown in equation 2.4.5 is *exothermic* (negative ΔU) for elements except noble gases and alkaline earth metals. The more negative this EA value, the higher an atom's affinity for electrons.

$$A_{(g)} + e^- \longrightarrow A^-_{(g)} \qquad EA = \Delta U \tag{2.4.5}$$

Conceptually, this second definition is quite similar to the concept of electronegativity; but unlike electronegativity, EA is a well-defined quantitative measurement.

Trends in Electron Affinity

For this discussion, we will use the first definition of EA: a more positive (larger) value means that the EA is higher (meaning stronger affinity toward an electron).

Across a period: Similar to ionization energy, EA generally increases across a row of the periodic table; this observation is consistent with the increase in effective nuclear charge (Z*) from left to right across a period. However, there are variations across

a period that are similar to variations in ionization energy and that can be explained by shielding, penetration, and electron configuration.

Down a group: Like the case of ionization energy trends, EA does not consistently decrease going down a column of the periodic table despite the fact that Z^* increases down a group.

The trend in EA follows a similar zig-zag pattern as the one seen with ionization energies, except that it is displaced by one unit from the trend in IE_1, two units from IE_2, and so on. For example, EA peaks at F, while IE_1 peaks at Ne, IE_2 peaks at Na, and IE_3 peaks at Mg. A plot of EA for the first 13 elements is shown overlaid on plots of IE_1, IE_2 and IE_3 in Figure **2.4.3**., where the shifts in the peaks and valleys within each zig-zag trend are indicated.

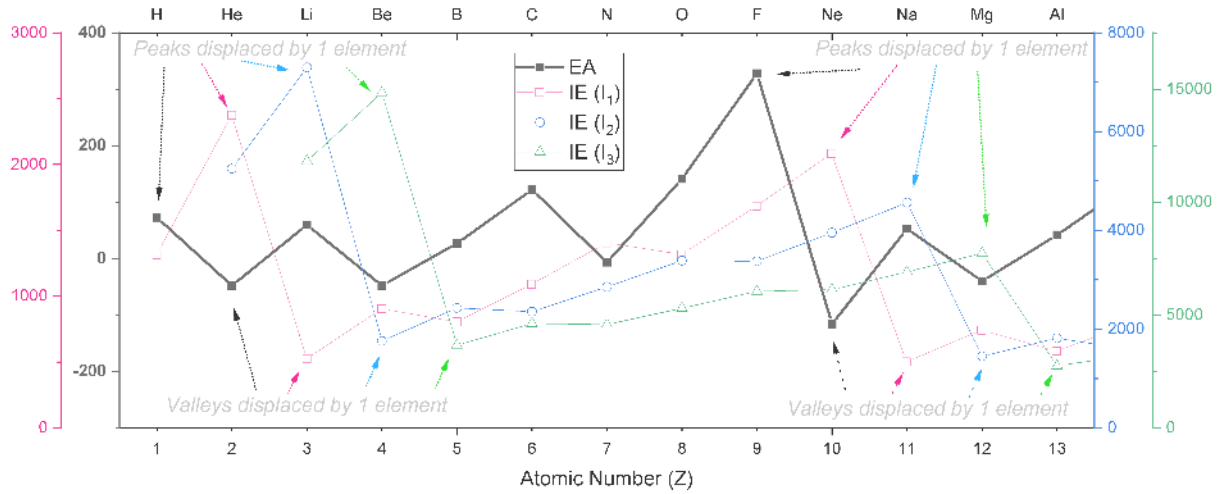


Figure **2.4.3**. A plot of electron affinity (the zeroth ionization energy) is overlaid on plots of the first (I_1), second (I_2), and third (I_3) ionization energies. Each plot is shown using separate y-axes. Trends in EA are similar to those in ionization energies, except the peaks and valleys of the trends are shifted by one unit, as indicated. These plots are shown in units of kJ/mole. (CC-BY-NC-SA; Kathryn Haas)

Atomic and Ionic Radii

There are several methods that can be used to determine radii of atoms and ions:

- **Nonpolar atomic radii:** The radius of an atom is derived from the bond lengths within nonpolar molecules; one-half the distance between the nuclei of two atoms within a covalent bond.
- **van der Waals radius:** The radius of an atom is determined by collision with other atoms.
- **Crystal Radii**: The atomic or ionic radius is determined using electron density maps from X-ray data.

The measurement of atomic or ionic size will depend on a number of factors, including the covalent character of bonding in any particular molecule, coordination number, physical state (liquid, solid, gas), the identity of nearby atoms/ions, variation in crystal structure, and distortions within regular crystal structures. You should keep in mind that the size of an atom or ion is a "fuzzy" measure, and the radius under a different set of conditions will probably change slightly.

Regardless, measured atomic and ionic radii reveal obvious trends across the periodic table and between atoms and ions. The relative atomic sizes shown in Figure **2.4.4** were derived from crystallographic data.[9]

Trends in Atomic Radius

Atomic size generally decreases gradually from left to right across a period of elements. As nuclear charge (Z) increases, we expect the effective nuclear charge (Z*) of the valence electrons to also increase. Increasing Z pulls electrons closer to the nucleus. However, with each additional unit of Z, there is also an additional electron. The change in size is a balance of a compression caused by increasing Z and an expansion in the number of electrons. As a result, the atomic radius decreases *gradually* across a period.

Atomic size generally increases going down a group. As valence electrons occupying higher level shells due to the increasing quantum number (n), size increases despite the fact that Z and Z* are increasing going down the group.

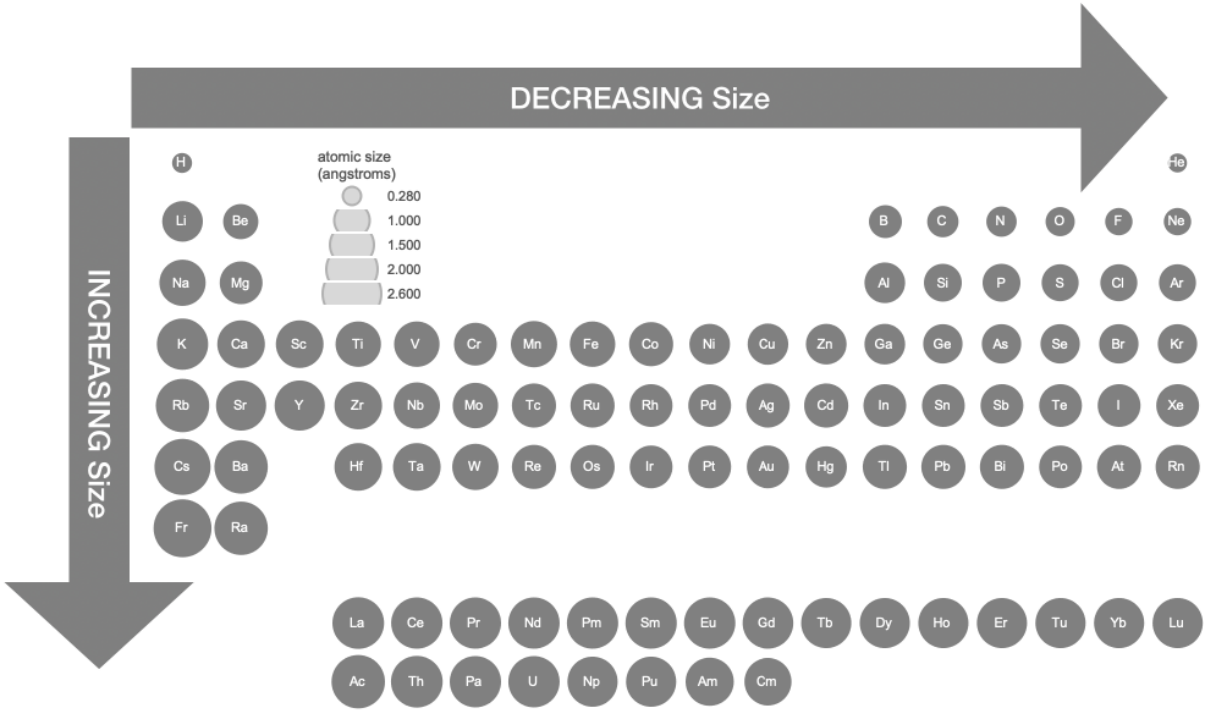


Figure 2.4.4. *Atomic Radii Calculated from Crystalographic Data. Data from Cordero, Beatriz, Veronica Gomez, Ana E. Platero-Prats, Marc Reves, Jorge Echeverria, Eduard Cremades, Flavia Barragan, and Santiago Alvarez. "Covalent Radii Revisited." Dalton Transactions, no. 21 (2008): 2832–38. doi:10.1039/b801115j.*

Trends in Ionic Radius

Trends in ionic radius follow general trends in atomic radius for ions of the same charge. Ionic radius varies with charge of the ion (and number of electrons) and the electron configuration (e.g. high spin or low spin).

Cations

Compared to their atoms, cations have the same Z but fewer electrons. Removal of electrons from an atom to form a cation results in a significant increase in effective nuclear charge, resulting in all other electrons being more strongly attracted to the nucleus, and having a lower energy level. The result is a contraction in size from the atom to cation. Figure **2.4.5** visually illustrates the relative size of atoms and some cations of the first four periods; the data is available in tabular format in Figure **2.4.6**.

Anions

Compared to their atoms, anions have the same Z but more electrons. Addition of electrons to an atom to form an anion results in a decrease in effective nuclear charge, which corresponds to a decrease in attractive force between the nucleus and electrons. Lower attractive force leads to expansion, where the size of the atom becomes larger in the formation of an anion. Figure **2.4.5** visually illustrates the relative size of atoms and some anions of the first four periods, while the data is available in tabular format in Figure **2.4.6**.

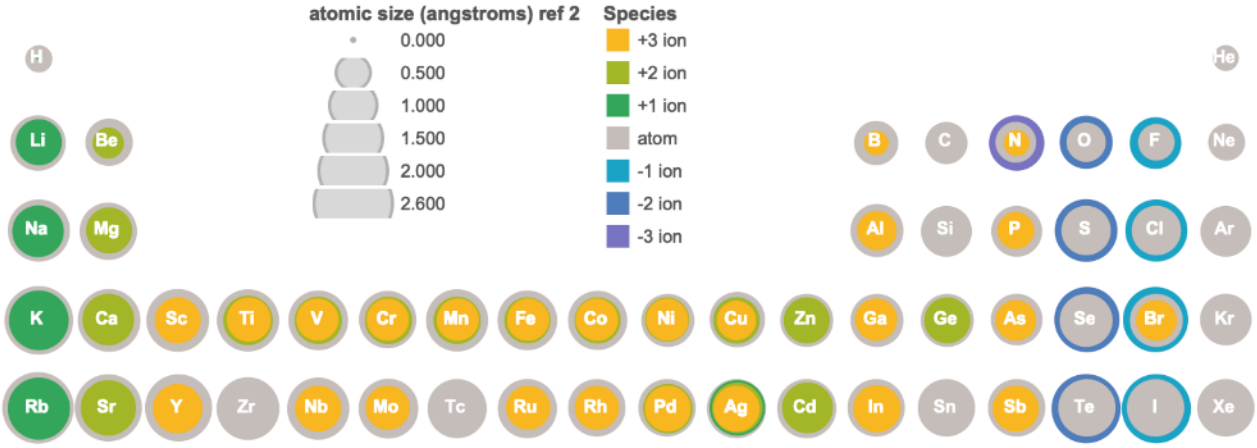


Figure **2.4.5**. This figure illustrates relative size of atoms and ions of the first four periods of the periodic table. Atomic radius is indicated by grey circles. Radius of cations is shown in green (+1), lime (+2), and yellow (+3) circles. Radius of anions are shown as aqua (-1), blue (-2), and purple (-3) circles. Data from sources 1-3

H 0.31 (atom) 0 (+1)																	He 0.28 (atom)
Li 1.28 (atom) 0.9 (+1) - -	Be 0.96 (atom) 0.41 (+2) - -												B 0.84 (atom) 0.25 (+1)	C 0.76 (atom) 0.29 (+4)	N 1.32 (-3) 0.71 (atom) 0.3 (+3) 0.27 (+5)	O 1.21 (-2) 0.66 (atom)	F 1.145 (-1) 0.57 (atom)	Ne 0.58 (atom)
Na 1.66 (atom) 1.16 (+1)	Mg 1.41 (atom) 0.86 (+2)												Al 1.21 (atom) 0.675 (+3)	Si 1.11 (atom) 0.4 (+4)	P 1.07 (atom) 0.58 (+3) 0.31 (+5)	S 1.7 (-2) 1.05 (atom) 0.51 (+4) 0.26 (+6)	Cl 1.67 (-1) 1.02 (atom)	Ar 1.06 (atom)
K 2.03 (atom) 1.52 (+1)	Ca 1.76 (atom) 1.14 (+2)	Sc 1.7 (atom) 0.885 (+3)	Ti 1.6 (atom) 1 (+2) 0.81 (+3) 0.745 (+4)	V 1.53 (atom) 0.93 (+2) 0.78 (+3) 0.72 (+4)	Cr 1.39 (atom) 0.94 (+2 hs) 0.87 (+2 ls) 0.7555 (+3) 0.69 (+4) 0.63 (+5) 0.58 (+6)	Mn 1.61 (atom) 0.97 (+2 hs) 0.81 (+2 ls) 0.785 (+3 hs) 0.72 (+3 ls) 0.67 (+4) 0.47 (+5) 0.395 (+6) 0.39 (+7)	Fe 1.52 (atom) 0.92 (+2 hs) 0.765 (+3 hs) 0.75 (+2 ls) 0.725 (+4) 0.69 (+3 ls) 0.39 (+6)	Co 1.5 (atom) 0.885 (+2 hs) 0.79 (+2 ls) 0.75 (+3 hs) 0.685 (+3 ls) 0.67 (+4 hs)	Ni 1.24 (atom) 0.83 (+2) 0.74 (+3 hs) 0.7 (+3 ls) 0.62 (+4)	Cu 1.32 (atom) 0.91 (+1, cn6) 0.87 (+2, cn6) 0.68 (+3, cn6)	Zn 1.22 (atom) 0.88 (+2)	Ga 1.22 (atom) 0.76 (+3)	Ge 1.2 (atom) 0.87 (+2) 0.67 (+4)	As 1.19 (atom) 0.72 (+3) 0.6 (+5)	Se 1.84 (-2) 1.2 (atom) 0.64 (+4) 0.56 (+6)	Br 1.82 (-1) 1.2 (atom) 0.73 (+3) 0.53 (+7) 0.45 (+5)	Kr 1.16 (atom)
Rb 2.2 (atom) 1.66 (+1)	Sr 1.95 (atom) 1.32 (+2)	Y 1.9 (atom) 1.04 (+3)	Zr 1.75 (atom) 0.86 (+4)	Nb 1.64 (atom) 0.86 (+3) 0.82 (+4) 0.78 (+5)	Mo 1.54 (atom) 0.83 (+3) 0.79 (+4) 0.75 (+5) 0.73 (+6)	Tc 1.47 (atom) 0.785 (+4) 0.74 (+5) 0.7 (+7)	Ru 1.46 (atom) 0.82 (+3) 0.76 (+4) 0.705 (+5) 0.52 (+7) 0.5 (+8)	Rh 1.42 (atom) 0.805 (+3) 0.74 (+4) 0.69 (+5)	Pd 1.39 (atom) 0.73 (+1) 1 (+2) 0.9 (+3) 0.755 (+4)	Ag 1.45 (atom) 1.29 (+1) 1.08 (+2) 0.89 (+3)	Cd 1.44 (atom) 1.09 (+2)	In 1.42 (atom) 0.94 (+3)	Sn 1.39 (atom) 0.83 (+4)	Sb 1.39 (atom) 0.9 (+3) 0.74 (+5)	Te 2.07 (-2) 1.38 (atom) 1.1 (+4) 0.7 (+6)	I 2.06 (-1) 1.39 (atom) 1.09 (+5) 0.67 (+7)	Xe 1.4 (atom) 0.62 (+8)

Figure 2.4.6.

This figure shows radii (in Angstroms) of atoms and ions of the first four periods of the periodic table. Radii from each element are listed from largest to smallest, ionic charge indicated in parentheses (); hs = high spin, ls = low spin, cn6 = coordination number is 6. Data from sources 9-11.

Contributors and Attributions

- Swetha Ramireddy (UCD), Bingyao Zheng (UCD), Emily Nguyen (UCD)
- Curated or created by Kathryn Haas

References

1. Russo, Steve, and Mike Silver. Introductory Chemistry. San Francisco: Pearson, 2007.
2. Petrucci, Ralph H, et al. General Chemistry: Principles and Modern Applications. 9th Ed. New Jersey: Pearson, 2007.
3. Atkins, Peter et. al, *Physical Chemistry*, 7th Edition, 2002, W.H Freeman and Company, New York, pg. 390.
4. Alberty, Robert A. et. al, *Physical Chemistry*, 3rd Edition, 2001, John Wiley & Sons, Inc, pg. 380.
5. Kots, John C. et. al, *Chemistry & Chemical Reactivity*, 5th Edition, 2003, Thomson Learning Inc, pg. 305-309.
6. *IUPAC. Compendium of Chemical Terminology, 2nd ed. (the "Gold Book"). Compiled by A. D. McNaught and A. Wilkinson. Blackwell Scientific Publications, Oxford (1997). Online version (2019-) created by S. J. Chalk. ISBN 0-9678550-9-8. doi.org/10.1351/goldbook.*
7. *Electron Affinity (data page), Wikipedia. en.Wikipedia.org/wiki/Electron_affinity_(data_page) Accessed 12/3/19.*

8. Cordero, Beatriz, Veronica Gomez, Ana E. Platero-Prats, Marc Reves, Jorge Echeverria, Eduard Cremades, Flavia Barragan, and Santiago Alvarez. *"Covalent Radii Revisited." Dalton Transactions, no. 21 (2008): 2832–38. doi:10.1039/b801115j.*
9. R. D. Shannon (1976). "Revised effective ionic radii and systematic studies of interatomic distances in halides and chalcogenides". *Acta Crystallogr A.* **32** (5): 751–767. Bibcode:1976AcCrA..32..751S. doi:10.1107/S0567739476001551.
10. *Atomic Radius, Wikipedia.* https://en.Wikipedia.org/wiki/Atomic_radius
11. *Ionic Radius, Wikipedia.* https://en.Wikipedia.org/wiki/Ionic_radius

---

2.4: Periodic Properties of Atoms is shared under a CC BY-NC-SA 4.0 license and was authored, remixed, and/or curated by LibreTexts.

- **2.3: Periodic Properties of Atoms** by Kathryn Haas is licensed CC BY-NC-SA 4.0.
- **Current page** is licensed CC BY-NC-SA 4.0.
- **2.3.1: Ionization energy** by Bingyao Zheng, Emily Nguyen, Kathryn Haas, Swetha Ramireddy is licensed CC BY-NC-SA 3.0.
- **2.3.2: Electron Affinity** by Kathryn Haas is licensed CC BY-NC-SA 4.0.
- **2.3.3: Covalent and Ionic Radii** by Bingyao Zheng, Emily Nguyen, Kathryn Haas, Swetha Ramireddy is licensed CC BY-NC-SA 4.0.

CHAPTER OVERVIEW

3: Bonding Theories

This chapter discusses the different theories which can be used to describe bonding in molecules. Some of these theories should be familiar from general or organic chemistry and some may be new to you this semester. Not every theory is applicable in every situation so, so we will look at cases where these theories are successful and cases where they fail (can't explain or reproduce experimental observations).

Learning Objectives

- Apply Lewis and VSEPR theories to determine molecular geometry and bond angles
- Identify polar and non-polar molecules
- Model bonding and orbital hybridization with s and p atomic orbitals
- Illustrate how atomic orbitals can overlap to form sigma, pi, delta, or non-bonding interactions
- Construct a qualitative molecular orbital diagram for a homo or heteronuclear diatomic molecule

The thumbnail image compares the Lewis dot structure with the sigma antibonding molecular orbital in HCl. The molecular orbital was calculated and rendered with WebMO.

3.1: Types of Bonding
3.2: Electronegativity Values
3.2A: Pauling Electronegativity Values
3.2B: Mulliken Electronegativity Values
3.2C: Allred-Rochow Electronegativity Values
3.3: Lewis Electron-Dot Diagrams
3.3A: Formal Charge
3.3B: Resonance
3.3C: Expanded Octets
3.3D: Limitation of Lewis Theory
3.4: Valence-Shell Electron-Repulsion Theory
3.5: Molecular Polarity
3.6: Valence Bond Theory
3.7: Molecular Orbital Theory
3.7A: Orbital Overlap
3.7B: Homonuclear Diatomic Molecules
3.7C: Heteronuclear Diatomic Molecules

3: Bonding Theories is shared under a CC BY-NC-SA 4.0 license and was authored, remixed, and/or curated by LibreTexts.

3.1: Types of Bonding

In general chemistry we learned that bonding between atoms can classified as range of possible bonding between **ionic bonds** (fully charge transfer) and **covalent bonds** (fully shared electrons). When two atoms of slightly differing electronegativities come together to form a covalent bond, one atom attracts the electrons more than the other; this is called a polar covalent bond. However, simple “ionic” and “covalent” bonding are idealized concepts and most bonds exist on a two-dimensional continuum described by the van Arkel-Ketelaar Triangle (Figure **3.1.1**).

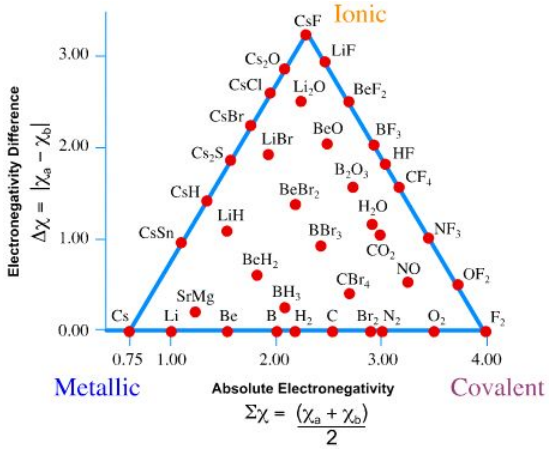


Figure **3.1.1**: van Arkel-Ketelaar Triangle plots the difference in electronegativity ($\Delta\chi$) and the average electronegativity in a bond ($\sum\chi$). the top region is where bonds are mostly ionic, the lower left region is where bonding is metallic, and the lower right region is where the bonding is covalent.

Bond triangles or **van Arkel–Ketelaar** triangles (named after Anton Eduard van Arkel and J. A. A. Ketelaar) are triangles used for showing different compounds in varying degrees of ionic, metallic and covalent bonding. In 1941 van Arkel recognized three extreme materials and associated bonding types. Using 36 main group elements, such as metals, metalloids and non-metals, he placed ionic, metallic and covalent bonds on the corners of an equilateral triangle, as well as suggested intermediate species. The bond triangle shows that chemical bonds are not just particular bonds of a specific type. Rather, bond types are interconnected and different compounds have varying degrees of different bonding character (for example, polar covalent bonds).



Video **3.1.1**: What is the van Arkel-Ketelaar Triangle of Bonding?

Using electronegativity - two compound average electronegativity on x-axis of Figure **3.1.1**.

$$\sum\chi = \frac{\chi_A + \chi_B}{2} \tag{3.1.1}$$

and electronegativity difference on y-axis,

$$\Delta\chi = |\chi_A - \chi_B| \tag{3.1.2}$$

we can rate the dominant bond between the compounds. On the right side of Figure **3.1.1** (from ionic to covalent) should be compounds with varying difference in electronegativity. The compounds with equal electronegativity, such as Cl_2 (chlorine) are placed in the covalent corner, while the ionic corner has compounds with large electronegativity difference, such as NaCl (table salt). The bottom side (from metallic to covalent) contains compounds with varying degree of directionality in the bond. At one extreme is metallic bonds with delocalized bonding and at the other are covalent bonds in which the orbitals overlap in a particular direction. The left side (from ionic to metallic) is meant for delocalized bonds with varying electronegativity difference.

The Three Extremes in bonding

In general:

- Metallic bonds have low $\Delta\chi$ **and** low average $\sum\chi$.
- Ionic bonds have moderate-to-high $\Delta\chi$ and moderate values of average $\sum\chi$.
- Covalent bonds have moderate to high average $\sum\chi$ and can exist with moderately low $\Delta\chi$.

Example 3.1.1

Use the tables of electronegativities and Figure **3.1.1** to estimate the following values

- difference in electronegativity ($\Delta\chi$)
- average electronegativity in a bond ($\sum\chi$)
- percent ionic character
- likely bond type

for the selected compounds:

a. AsH (e.g., in arsine AsH)
b. SrLi
c. KF.

Solution

a: AsH

- The electronegativity of As is 2.18
- The electronegativity of H is 2.22

Using Equations 3.1.1 and 3.1.2:

$$\begin{aligned}\sum\chi &= \frac{\chi_A + \chi_B}{2} \\ &= \frac{2.18 + 2.22}{2} \\ &= 2.2\end{aligned}$$

$$\begin{aligned}\Delta\chi &= \chi_A - \chi_B \\ &= 2.18 - 2.22 \\ &= 0.04\end{aligned}$$

- From Figure **3.1.1**, the bond is fairly nonpolar and has a low ionic character (10% or less)
- The bonding is in the middle of a covalent bond and a metallic bond

b: SrLi

- The electronegativity of Sr is 0.95
- The electronegativity of Li is 0.98

Using Equations 3.1.1 and 3.1.2:

$$\sum \chi = \frac{\chi_A + \chi_B}{2}$$
$$= \frac{0.95 + 0.98}{2}$$
$$= 0.965$$

$$\Delta\chi = \chi_A - \chi_B$$
$$= 0.98 - 0.95$$
$$= 0.025$$

- From Figure 3.1.1, the bond is fairly nonpolar and has a low ionic character (~3% or less)
- The bonding is likely metallic.

c: **KF**

- The electronegativity of **K** is 0.82
- The electronegativity of **F** is 3.98

Using Equations 3.1.1 and 3.1.2:

$$\sum \chi = \frac{\chi_A + \chi_B}{2}$$
$$= \frac{0.82 + 3.98}{2}$$
$$= 2.4$$

$$\Delta\chi = \chi_A - \chi_B$$
$$= |0.82 - 3.98|$$
$$= 3.16$$

- From Figure 3.1.1, the bond is fairly polar and has a high ionic character (~75%)
- The bonding is likely ionic.

Exercise 3.1.1

Contrast the bonding of **NaCl** and silicon tetrafluoride.

Answer

NaCl is an ionic crystal structure, and an electrolyte when dissolved in water; $\Delta\chi = 1.58$, average $\sum\chi = 1.79$, while silicon tetrafluoride is covalent (molecular, non-polar gas; $\Delta\chi = 2.08$, average $\sum\chi = 2.94$.

Contributors and Attributions

- Jim Clark (Chemguide.co.uk)
- Daniel James Berger
- Wikipedia
- Ed Vitz (Kutztown University), John W. Moore (UW-Madison), Justin Shorb (Hope College), Xavier Prat-Resina (University of Minnesota Rochester), Tim Wendorff, and Adam Hahn.

This page titled 3.1: Types of Bonding is shared under a CC BY-NC-SA 4.0 license and was authored, remixed, and/or curated by Delmar Larsen.

SECTION OVERVIEW

3.2: Electronegativity Values

There are a few different 'types' of electronegativity which differ only in their definitions and the system by which they assign values for electronegativity. For example, there is Mulliken electronegativity which is defined as "the average of the ionization energy and electron affinity of an atom"[3], which as we will see, differs slightly from Pauling's definition of electronegativity.

Topic hierarchy

3.2A: Pauling Electronegativity Values

3.2B: Mulliken Electronegativity Values

3.2C: Allred-Rochow Electronegativity Values

3.2: Electronegativity Values is shared under a CC BY-NC-SA 4.0 license and was authored, remixed, and/or curated by LibreTexts.

3.2A: Pauling Electronegativity Values

Linus Pauling described electronegativity as “the power of an atom in a molecule to attract electrons to itself.”[1] Basically, the electronegativity of an atom is a relative value of that atom's ability to attract election density toward itself when it bonds to another atom. The higher the electronegativity of an element, the more that atom will attempt to pull electrons towards itself and away from any atom it bonds to. The main properties of an atom dictate it's electronegativity are it's atomic number as well as its atomic radius. The trend for electronegativity is to increase as you move from left to right and bottom to top across the periodic table. This means that the most electronegative atom is Fluorine and the least electronegative is Francium.

There are a few different 'types' of electronegativity which differ only in their definitions and the system by which they assign values for electronegativity. For example, Mulliken electronegativity defines electronegativity as the "the average of the ionization energy and electron affinity of an atom."[3] As we will see, this definition differs slightly from Pauling's definition of electronegativity.

Pauling Electronegativity

Linus Pauling was the original scientist to describe the phenomena of electronegativity. The best way to describe his method is to look at a hypothetical molecule that we will call XY. By comparing the measured X-Y bond energy with the theoretical X-Y bond energy (computed as the average of the X-X bond energy and the Y-Y bond energy), we can describe the relative affinities of these two atoms with respect to each other.

$$\Delta\text{Bond Energies} = (X-Y)_{measured} - (X-Y)_{expected}$$

If the electonegativities of X and Y are the same, then we would expect the measured bond energy to equal the theoretical (expected) bond energy and therefore the Δ bond energies would be zero. If the electronegativities of these atoms are not the same, we would see a polar molecule where one atom would start to pull electron density toward itself, causing it to become partially negative.

By doing some careful experiments and calculations, Pauling came up with a slightly more sophisticated equation for the relative electronegativities of two atoms in a molecule:

$$EN(X) - EN(Y) = 0.102\sqrt{\Delta}.$$

In that equation, the factor 0.102 is simply a conversion factor between kJ and eV to keep the units consistent with bond energies.

By assigning a value of 4.0 to Fluorine (the most electronegative element), Pauling was able to set up relative values for all of the elements. This was when he first noticed the trend that the electronegativity of an atom was determined by it's position on the periodic table and that the electronegativity tended to increase as you moved left to right and bottom to top along the table. The range of values for Pauling's scale of electronegativity ranges from Fluorine (most electronegative = 4.0) to Francium (least electronegative = 0.7). [2] Furthermore, if the electronegativity difference between two atoms is very large, then the bond type tends to be more ionic, however if the difference in electronegativity is small then it is a nonpolar covalent bond.

? Exercise 3.2A.1

Explain the difference between Electronegativity and Electron Affinity

? Exercise 3.2A.2

Predict the order or increasing electronegativity from the following elements

a. F, Li, C, O
b. Te, Cl, S, Se
c. Cs, At, Tl, I

References

1. Zumdahl, Steven S. "Chemical Principles" 5th Edition. Houghton Mifflin Company 2005. Chapter 13.2 "Electronegativity" pgs. 587-590.
2. Housecroft, Catherine E. et. al. "Inorganic Chemistry" 3rd Edition. Pearson Education Limited 2008. Chapter 2.5 "Electronegativity Values" pgs. 42-44
3. International Union of Pure and Applied Chemistry. "Electronegativity". goldbook.iupac.org/E01990.html.

3.2A: Pauling Electronegativity Values is shared under a CC BY-NC-SA 4.0 license and was authored, remixed, and/or curated by LibreTexts.

- **Pauling Electronegativity** by Matthew Salem is licensed CC BY 4.0.

3.2B: Mulliken Electronegativity Values

A method for estimating electronegativity was developed by Robert Mulliken (1896–1986; Nobel Prize in Chemistry 1966) who noticed that elements with large first ionization energies tend to have very negative electron affinities and gain electrons in chemical reactions. Conversely, elements with small first ionization energies tend to have slightly negative (or even positive) electron affinities and lose electrons in chemical reactions. Mulliken recognized that an atom's tendency to gain or lose electrons could therefore be described quantitatively by the average of the values of its first ionization energy and the absolute value of its electron affinity.

Robert S. Mulliken proposed that the arithmetic mean of the first ionization energy (E_{I_1}) and the electron affinity (E_{ea}) should be a measure of the tendency of an atom to attract electrons. As this definition is not dependent on an arbitrary relative scale, it has also been termed *absolute electronegativity.* Using our definition of electron affinity, we can write Mulliken's original expression for electronegativity as follows:Mulliken's definition used the magnitude of the ionization energy and the electron affinity. By definition, the magnitude of a quantity is a positive number. Our definition of electron affinity produces negative values for the electron affinity for most elements, so vertical lines indicating absolute value are needed in Equation 3.2B.1 to make sure that we are adding two positive numbers in the numerator.

$$\chi = \frac{|E_{I_1} + E_{ea}|}{2} \tag{3.2B.1}$$

Elements with a large first ionization energy and a very negative electron affinity have a large positive value in the numerator of Equation 3.2B.1, so their electronegativity is high. Elements with a small first ionization energy and a small electron affinity have a small positive value for the numerator in Equation 3.2B.1, so they have a low electronegativity. Inserting the appropriate data into Equation 3.2B.1 gives a Mulliken electronegativity value for fluorine of 1004.6 kJ/mol. To compare Mulliken's electronegativity values with those obtained by Pauling, Mulliken's values are divided by 252.4 kJ/mol, which gives Pauling's value (3.98).

However, it is more usual to use a linear transformation to transform these absolute values into values that resemble the more familiar Pauling values. For ionization energies and electron affinities in electronvolts:

$$\chi_{Mulliken} = 0.187(E_{I_1} + E_{ea}) + 0.17 \tag{3.2B.2}$$

and for energies in kJ/mol,

$$\chi_{Mulliken} = (1.97 \times 10^{-3})(E_{I_1} + E_{ea}) + 0.19 \tag{3.2B.3}$$

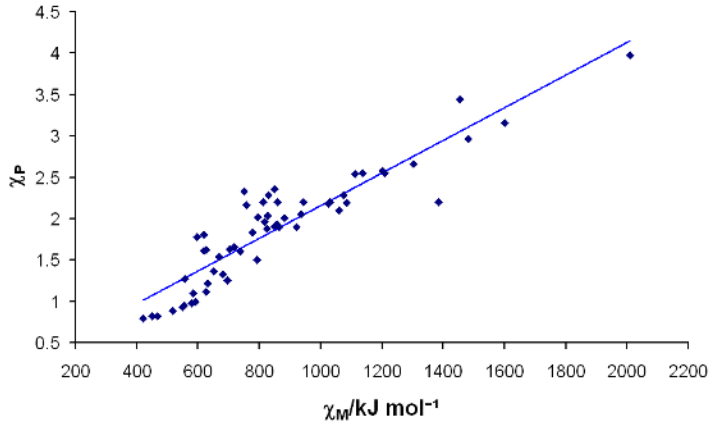
The Mulliken electronegativity can only be calculated for an element for which the electron affinity is known, fifty-seven elements as of 2006. The Mulliken electronegativity of an atom is sometimes said to be the negative of the chemical potential. By inserting the energetic definitions of the ionization potential and electron affinity into the Mulliken electronegativity, it is possible to show that the Mulliken chemical potential is a finite difference approximation of the electronic energy with respect to the number of electrons., i.e.,

$$\mu_{Mulliken} = -\chi_{Mulliken} = -\frac{E_{I_1} + E_{ea}}{2} \tag{3.2B.4}$$

All electronegativity scales give essentially the same results for one element relative to another. Even though the Mulliken scale is based on the properties of individual *atoms* and the Pauling scale is based on the properties of atoms in *molecules*, they both apparently measure the same basic property of an element. In the following discussion, we will focus on the relationship between electronegativity and the tendency of *atoms* to form positive or negative ions. We will therefore be implicitly using the Mulliken definition of electronegativity. Because of the parallels between the Mulliken and Pauling definitions, however, the conclusions are likely to apply to atoms in molecules as well.

Significance

Despite being developed from a very different set of principles than Pauling Electronegativity, which is based on bond dissociation energies, there is a good correlation between Mullikin and Pauling Electronegativities for the atoms, as shown in the plot below.



Although Pauling electronegativities are usually what are found in textbooks, the Mullikin electronegativity more intuitively corresponds to the "ability of an atom to draw electrons toward itself in bonding," and is probably a better indicator of that property. However, because of the good correlation between the two scales, using the Pauling scale is sufficient for most purposes.

References

1. Mulliken, R. S. (1934). "A New Electroaffinity Scale; Together with Data on Valence States and on Valence Ionization Potentials and Electron Affinities". Journal of Chemical Physics 2 (11): 782–793.
2. Mulliken, R. S. (1935). "Electronic Structures of Molecules XI. Electroaffinity, Molecular Orbitals and Dipole Moments". J. Chem. Phys.3 (9): 573–585.
3. Pearson, R. G. (1985). "Absolute electronegativity and absolute hardness of Lewis acids and bases". J. Am. Chem. Soc. 107 (24): 6801.
4. Huheey, J. E. (1978). Inorganic Chemistry (2nd Edn.). New York: Harper & Row. p. 167.
5. This second relation has been recalculated using the best values of the first ionization energies and electron affinities available in 2006.

3.2B: Mulliken Electronegativity Values is shared under a CC BY-NC-SA 4.0 license and was authored, remixed, and/or curated by LibreTexts.

- **Mulliken Electronegativity** is licensed CC BY-NC-SA 4.0.

3.2C: Allred-Rochow Electronegativity Values

Allred-Rochow Electronegativity

Allred-Rochow Electronegativity is a measure that determines the values of the electrostatic force exerted by the effective nuclear charge on the valence electrons. The value of the effective nuclear charges is estimated from Slater's rules. The higher charge, the more likely it will attract electrons. Although, Slater's rule are partly empirical. So the Allred-Rochow electronegativity is no more rigid than the Pauling Electronegativity. Allred and Rochow were two chemists who came up with the Allred-Rochow Electronegativity values by taking the electrostatic force exerted by effective nuclear charge, Z_{eff}, on the valence electron. To do so, they came up with an equation:

$$\chi^{AR} = \left(\frac{3590 \times Z_{eff}}{r_{cov}^2}\right) + 0.744 \tag{3.2C.1}$$

At the time, the values for the covalent radius, r_{cov}, were inaccurate. Allred and Rochow added certain perimeters so that it would more closely correspond to Pauling's electronegativity scale.

Table 1: Allred-Rochow Electronegativity Values

H **2.20**																
Li **0.97**	Be **1.47**											B **2.01**	C **2.50**	N **3.07**	O **3.50**	F **4.10**
Na **1.01**	Mg **1.23**											Al **1.47**	Si **1.74**	P **2.06**	S **2.44**	Cl **2.83**
K **0.91**	Ca **1.04**	Sc **1.20**	Ti **1.32**	V **1.45**	Cr **1.56**	Mn **1.60**	Fe **1.64**	Co **1.70**	Ni **1.75**	Cu **1.75**	Zn **1.66**	Ga **1.82**	Ge **2.02**	As **2.20**	Se **2.48**	Br **2.74**
Rb **0.89**	Sr **0.99**	Y **1.11**	Zr **1.22**	Nb **1.23**	Mo **1.30**	Te **1.36**	Ru **1.42**	Rh **1.45**	Pd **1.35**	Ag **1.42**	Cd **1.46**	In **1.49**	Sn **1.72**	Sb **1.82**	Te **2.01**	I **2.21**
Cs **0.86**	Ba **0.97**	La **1.08**	Hf **1.23**	Ta **1.33**	W **1.40**	Re **1.46**	Os **1.52**	Ir **1.55**	Pt **1.44**	Au **1.42**	Hg **1.44**	Tl **1.44**	Pb **1.55**	Bi **1.67**	Po **1.76**	At **1.90**

In this table, the electronegativities increases from left to right just like Pauling's scale because the Z is increasing. As we go down the group, it decreases because of the larger atomic size that increases the distance between the electrons and nucleus.

References

1. Gary Wulfsberg. *Inorganic Chemistry*. University Science Books, February 2000.
2. Housecroft, Catherine E., and Alan G. Sharpe. *Inorganic Chemistry*. 3rd ed. Harlow: Pearson Education, 2008. Print. (Pg. 43-44)
3. Sarah Anderson. *Intro to Inorganic Chemistry*. University Science Books, September 2004.
4. Linus Pauling. *General Chemistry*. University Science Books, March 2002.
5. Leroy G. Wade. *Organic Chemistry. 7th ed. Harlow: Pearson Education, 2006.*
6. *John E. McMurry. General Chemistry: Atoms. 1st ed. Harlow: Pearson Education, 2000.*

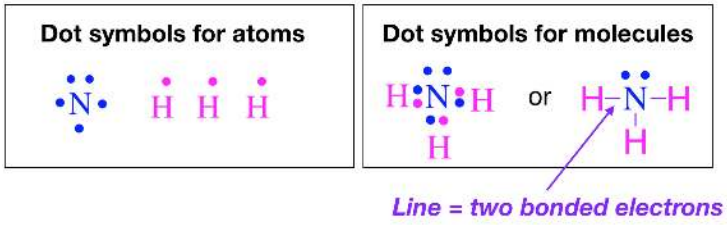
Contributors and Attributions

- Mark Vu

3.2C: Allred-Rochow Electronegativity Values is shared under a CC BY-NC-SA 4.0 license and was authored, remixed, and/or curated by LibreTexts.

3.3: Lewis Electron-Dot Diagrams

In 1916, Gilbert Lewis Newton introduced a simple way to show the bonding between atoms in a molecule though Lewis electron dot diagrams. Creating Lewis diagrams is rather simple and requires only a few steps and some accounting of the valence electrons on each atom. Valence electrons are represented as dots. When two electrons are paired (lone pairs), they are represented by two adjacent dots located on an atom, and when two paired electrons are shared between atoms (bonds), they are shown as lines. For example, below are the electron dot structures of atoms and the Lewis electron dot structures of the molecules. These diagrams are helpful because they allow us to show how atoms are connected, and when coupled with Valence Shell Electron Repulsion Theory (VSEPR), we can use Lewis structures to predict the shape of the molecule.



The drawing of Lewis electron-dot structures is guided largely by the **octet rule**: that atoms form bonds to achieve eight electrons in their valence shell. For many elements, a full valence shell has an electron configuration of s^2p^6, or eight electrons. A common exception to this rule is the first row elements, H and He. These two elements have $n = 1$ as their valence shell, and so they have only two electrons in a full valence shell ($1s^2$ electron configuration). Although H and He are exceptions to the "octet rule", they still form bonds to achieve a full valence shell. It may be better to think of this as the "full valence" rule of bonding. We will see many more violations to the "octet" rule as we progress through this course. In the case of metals and metalloids, breaking of the rules is particularly common. (CC-BY-NC-SA; Kathryn Haas)

Common Volations of the Octet Rule

- **Less than eight electrons (hypovalency)**: H and He are examples of elements that cannot have more than two electrons in their full valence shell. Additionally, there are cases where a valid Lewis structure contains atoms with ***hypovalency:*** *partially-filled valence shells*. This is common in atoms with few valence electrons, such as berillium and boron
- **More than eight electrons (hypervalency)**: This is a case where an element has more than eight electrons in its valence shell. It is common for larger atoms ($n \geq 3$, and it is discussed further in Section 3.3.3.

There are different rules for counting electrons depending on the purpose of the counting. These are the rules for counting for "octets". The rules for calculation of an atom's formal charge are !!different!! and are described in Section 3.3.1. When an atom is part of a molecule, all electrons that are associated with the atom are counted as contributing to the atom's valence. This includes electrons that are lone pairs on the atoms, and *all* electrons that are shared in bonds. If four electrons are shared between two atoms, it is a double bond. If six electrons are shared between atoms, it is a triple bond.

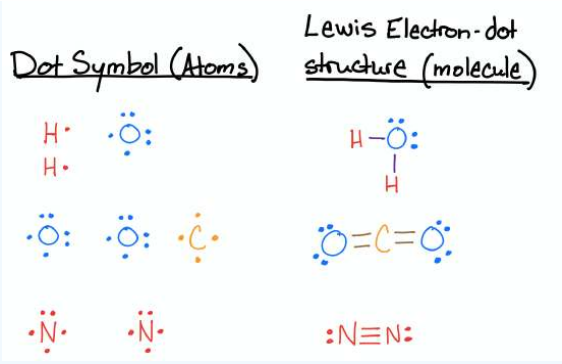
Electrons in valence (octet) = total unbonded electrons on the atom + total bonded electrons (2 electrons per bond)

Even if you're an old pro at drawing Lewis structures, it's a good idea to polish up. Please complete the practice exercises below. You should get out an actual piece of paper (I know...just do it. It's good for you.) and a writing tool and try to complete each problem before checking the answer.

Exercise 3.3.1

Draw the Lewis structures for H_2O, CO_2, and N_2.

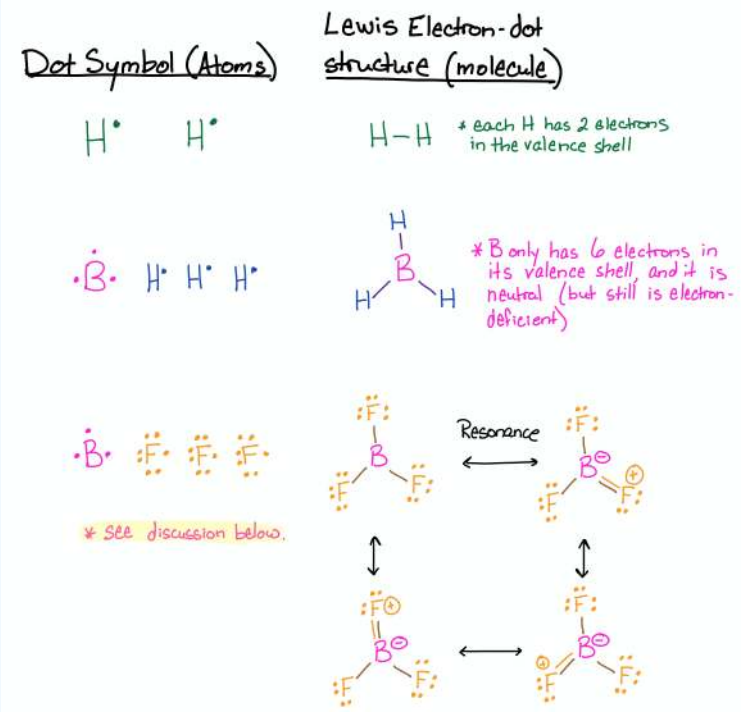
Answer



Exercise 3.3.2

Draw the Lewis structures for H_2, BH_3 and BF_3.

Answer



These three examples include atoms that have less than eight electrons in their valence shell. In the case of H, it is satisfied with only two electrons in its valence, as was discussed earlier in this section. The case of BH_3 was also discussed above. In the Lewis structure of BH_3, the boron can only have six electrons in its octet and it is neutral in charge. The boron is electron deficient even though it has neutral charge.

The case of BF_3 deserves a discussion: If you are unfamiliar with resonance and formal charge, see Sections 3.3.1 (Formal Charge) and 3.3.2 (Resonance) first and come back to this afterward. You might have drawn the BF_3 structure similar to the one that is drawn for BH_3, where boron has three bonds and only six electrons in its valence shell. If you did that, then you are correct; but if you only gave this structure, then your answer is not complete. There are three other correct ways to draw structure. Since F has lone pairs of electrons, other valid Lewis structures would each have a double bond to one of the fluorines (three total). All of these structures are called resonance structures, and based on the four of them, we could predict that BF_3 would have B-F bonds that have some double-bond character. If fact, this is the case for BF_3; it has bond

lengths that are shorter than single bonds, but longer than double bonds. Read more about it on its Wikipedia page here (click).

Outside Resources

- en.Wikipedia.org/wiki/Lewis_structures

Contributors and Attributions

- Modified from Lewis Structures by Andrew Iskandar, University of California, Davis
- Curated or created by Kathryn Haas

This page titled 3.3: Lewis Electron-Dot Diagrams is shared under a CC BY-NC-SA 4.0 license and was authored, remixed, and/or curated by Kathryn Haas.

- **3.1: Lewis Electron-Dot Diagrams** by Kathryn Haas is licensed CC BY-NC-SA 4.0.
- **Current page** by Kathryn Haas is licensed CC BY-NC-SA 4.0.

3.3A: Formal Charge

The formal charge of an atom in a molecule is the *hypothetical* charge the atom would have if we could redistribute the electrons in the bonds evenly between the atoms. Another way of saying this is that formal charge results when we take the number of valence electrons of a neutral atom, subtract the nonbonding electrons, and then subtract the number of bonds connected to that atom in the Lewis structure.

Calculating Formal Charges

We calculate the formal charge of an atom in a molecule or polyatomic ions as follows:

Formal Charge = (valence electrons of the "free" element) - (unshared electrons) - (bonds).

We can double-check formal charge calculations by determining the sum of the formal charges for the whole structure. The sum of the formal charges of all atoms in a molecule must be zero; the sum of the formal charges in an ion should equal the charge of the ion.

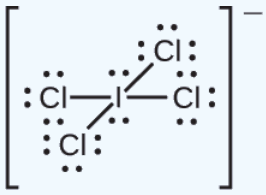
We must remember that the formal charge calculated for an atom is not the *actual* charge of the atom in the molecule. Formal charge is only a useful bookkeeping procedure; it does not indicate the presence of actual charges.

Calculating Formal Charge from Lewis Structures

Assign formal charges to each atom in the interhalogen ion ICl_4^-.

Solution

We divide the bonding electron pairs equally for all I–Cl bonds:



We assign lone pairs of electrons to their atoms. Each Cl atom now has seven electrons assigned to it, and the I atom has eight.

Subtract this number from the number of valence electrons for the neutral atom:

- I: 7 – 8 = –1
- Cl: 7 – 7 = 0

The sum of the formal charges of all the atoms equals –1, which is identical to the charge of the ion (–1).

Exercise 3.3A.1

Calculate the formal charge for each atom in the carbon monoxide molecule:



Answer

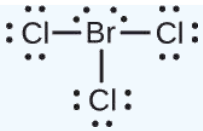
C −1, O +1

Example: Calculating Formal Charge from Lewis Structures

Assign formal charges to each atom in the interhalogen molecule $BrCl_3$.

Solution

Assign one of the electrons in each Br–Cl bond to the Br atom and one to the Cl atom in that bond:



Assign the lone pairs to their atom. Now each Cl atom has seven electrons and the Br atom has seven electrons.

Subtract this number from the number of valence electrons for the neutral atom. This gives the formal charge:

- Br: 7 – 7 = 0
- Cl: 7 – 7 = 0

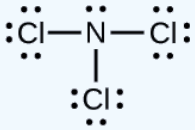
All atoms in $\mathbf{BrCl_3}$ have a formal charge of zero, and the sum of the formal charges totals zero, as it must in a neutral molecule.

? Exercise 3.3A.2

Determine the formal charge for each atom in $\mathbf{NCl_3}$.

Answer

N: 0; all three Cl atoms: 0



3.3A: Formal Charge is shared under a CC BY-NC-SA 4.0 license and was authored, remixed, and/or curated by LibreTexts.

- **7.5: Formal Charges and Resonance** by OpenStax is licensed CC BY 4.0. Original source: https://openstax.org/details/books/chemistry-2e.

3.3B: Resonance

Resonance structures are a set of two or more Lewis Structures that collectively describe the electronic bonding a single polyatomic species including fractional bonds and fractional charges. Resonance structures are capable of describing delocalized electrons that cannot be expressed by a single Lewis formula with an integer number of covalent bonds.

Sometimes One Lewis Structure Is Not Enough

Sometimes, even when formal charges are considered, the bonding in some molecules or ions cannot be described by a single Lewis structure. Resonance is a way of describing delocalized electrons within certain molecules or polyatomic ions where the bonding cannot be expressed by a single Lewis formula. A molecule or ion with such delocalized electrons is represented by several contributing structures (also called resonance structures or canonical forms). Such is the case for ozone ($\mathbf{O_3}$), an allotrope of oxygen with a V-shaped structure and an O–O–O angle of 117.5°.

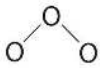
Ozone (O_3)

1. We know that ozone has a V-shaped structure, so one O atom is central:



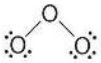
2. Each O atom has 6 valence electrons, for a total of 18 valence electrons.

3. Assigning one bonding pair of electrons to each oxygen–oxygen bond gives



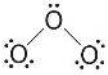
with 14 electrons left over.

4. If we place three lone pairs of electrons on each terminal oxygen, we obtain

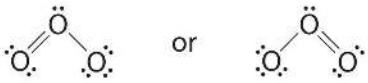


and have 2 electrons left over.

5. At this point, both terminal oxygen atoms have octets of electrons. We therefore place the last 2 electrons on the central atom:

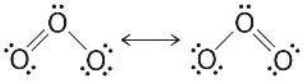


6. The central oxygen has only 6 electrons. We must convert one lone pair on a terminal oxygen atom to a bonding pair of electrons —but which one? Depending on which one we choose, we obtain either



Which is correct? In fact, neither is correct. Both predict one O–O single bond and one O=O double bond. As you will learn, if the bonds were of different types (one single and one double, for example), they would have different lengths. It turns out, however, that both O–O bond distances are identical, 127.2 pm, which is shorter than a typical O–O single bond (148 pm) and longer than the O=O double bond in O_2 (120.7 pm).

Equivalent Lewis dot structures, such as those of ozone, are called **resonance structures**. The position of the *atoms* is the same in the various resonance structures of a compound, but the position of the *electrons* is different. Double-headed arrows link the different resonance structures of a compound:



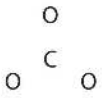
The double-headed arrow indicates that the actual electronic structure is an *average* of those shown, not that the molecule oscillates between the two structures.

> *When it is possible to write more than one equivalent resonance structure for a molecule or ion, the actual structure is the average of the resonance structures.*

The Carbonate (CO_3^{2-}) Ion

Like ozone, the electronic structure of the carbonate ion cannot be described by a single Lewis electron structure. Unlike O_3, though, the actual structure of CO_3^{2-} is an average of *three* resonance structures.

1. Because carbon is the least electronegative element, we place it in the central position:

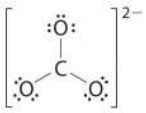


2. Carbon has 4 valence electrons, each oxygen has 6 valence electrons, and there are 2 more for the −2 charge. This gives 4 + (3 × 6) + 2 = 24 valence electrons.

3. Six electrons are used to form three bonding pairs between the oxygen atoms and the carbon:

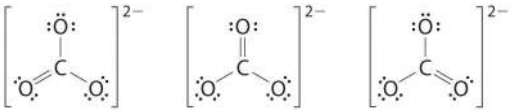


4. We divide the remaining 18 electrons equally among the three oxygen atoms by placing three lone pairs on each and indicating the −2 charge:

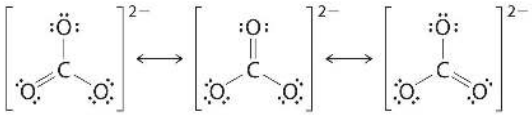


5. No electrons are left for the central atom.

6. At this point, the carbon atom has only 6 valence electrons, so we must take one lone pair from an oxygen and use it to form a carbon–oxygen double bond. In this case, however, there are *three* possible choices:



As with ozone, none of these structures describes the bonding exactly. Each predicts one carbon–oxygen double bond and two carbon–oxygen single bonds, but experimentally all C–O bond lengths are identical. We can write resonance structures (in this case, three of them) for the carbonate ion:



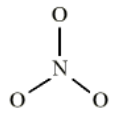
The actual structure is an average of these three resonance structures.

https://chem.libretexts.org/@go/page/326152

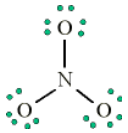
The Nitrate (NO_3^-) ion

1. Count up the valence electrons: (1*5) + (3*6) + 1(ion) = **24** electrons

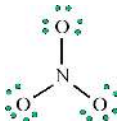
2. Draw the bond connectivities:



3. Add octet electrons to the atoms bonded to the center atom:

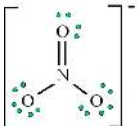


4. Place any leftover electrons (24-24 = **0**) on the center atom:



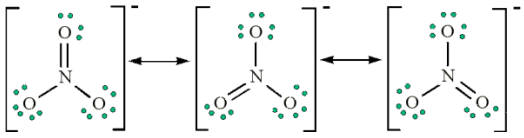
5. Does the central atom have an octet?

- **NO**, it has 6 electrons
- Add a multiple bond (first try a double bond) to see if the central atom can achieve an octet:



6. Does the central atom have an octet?

- YES
- Are there possible resonance structures? YES



Note: We would expect that the bond lengths in the $\mathbf{NO_3^-}$ ion to be somewhat shorter than a single bond.

Warning

For second period elements you cannot exced the octet, even if additional double or triple bonds would reduce the formal charges in the structure.

Example 3.3B.1: Benzene

Benzene is a common organic solvent that was previously used in gasoline; it is no longer used for this purpose, however, because it is now known to be a carcinogen. The benzene molecule ($\mathbf{C_6H_6}$) consists of a regular hexagon of carbon atoms, each of which is also bonded to a hydrogen atom. Use resonance structures to describe the bonding in benzene.

Given: molecular formula and molecular geometry

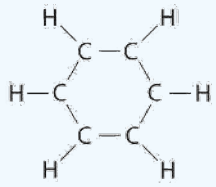
Asked for: resonance structures

Strategy:

A. Draw a structure for benzene illustrating the bonded atoms. Then calculate the number of valence electrons used in this drawing.
B. Subtract this number from the total number of valence electrons in benzene and then locate the remaining electrons such that each atom in the structure reaches an octet.
C. Draw the resonance structures for benzene.

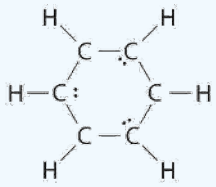
Solution:

A Each hydrogen atom contributes 1 valence electron, and each carbon atom contributes 4 valence electrons, for a total of (6 × 1) + (6 × 4) = 30 valence electrons. If we place a single bonding electron pair between each pair of carbon atoms and between each carbon and a hydrogen atom, we obtain the following:



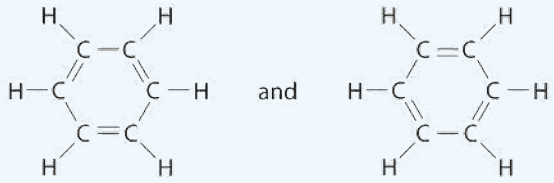
Each carbon atom in this structure has only 6 electrons and has a formal charge of +1, but we have used only 24 of the 30 valence electrons.

B If the 6 remaining electrons are uniformly distributed pairwise on alternate carbon atoms, we obtain the following:

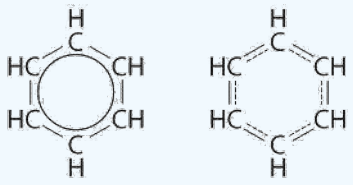


Three carbon atoms now have an octet configuration and a formal charge of −1, while three carbon atoms have only 6 electrons and a formal charge of +1. We can convert each lone pair to a bonding electron pair, which gives each atom an octet of electrons and a formal charge of 0, by making three C=C double bonds.

C There are, however, two ways to do this:



Each structure has alternating double and single bonds, but experimentation shows that each carbon–carbon bond in benzene is identical, with bond lengths (139.9 pm) intermediate between those typically found for a C–C single bond (154 pm) and a C=C double bond (134 pm). We can describe the bonding in benzene using the two resonance structures, but the actual electronic structure is an average of the two. The existence of multiple resonance structures for aromatic hydrocarbons like benzene is often indicated by drawing either a circle or dashed lines inside the hexagon:



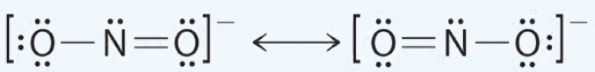
Benzene

https://chem.libretexts.org/@go/page/326152

Exercise 3.3*B*.1: Nitrate Ion

The sodium salt of nitrite is used to relieve muscle spasms. Draw two resonance structures for the nitrite ion (NO_2^-).

Answer



Resonance structures are particularly common in oxoanions of the *p*-block elements, such as sulfate and phosphate, and in aromatic hydrocarbons, such as benzene and naphthalene.

How do resonance structures represent the true structure?

If several reasonable resonance forms for a molecule exists, the "actual electronic structure" of the molecule will probably be intermediate between all the forms that you can draw. The classic example is benzene in Example **3.3*B*.1**. One would expect the double bonds to be shorter than the single bonds, but if once overlays the two structures, you see that one structure has a single bond where the other structure has a double bond. The best measurements that we can make of benzene do not show two bond lengths - instead, they show that the bond length is intermediate between the two resonance structures.

Resonance structures is a mechanism that allows us to use all of the possible resonance structures to try to predict what the actual form of the molecule would be. Single bonds, double bonds, triple bonds, +1 charges, -1 charges, these are our limitations in explaining the structures, and the true forms can be in between - a carbon-carbon bond could be mostly single bond with a little bit of double bond character and a partial negative charge, for example.

Summary

Some molecules have two or more chemically equivalent Lewis electron structures, called resonance structures. Resonance is a mental exercise and method within the Valence Bond Theory of bonding that describes the delocalization of electrons within molecules. These structures are written with a **double-headed arrow** between them, indicating that none of the Lewis structures accurately describes the bonding but that the actual structure is an average of the individual resonance structures. Resonance structures are used when one Lewis structure for a single molecule cannot fully describe the bonding that takes place between neighboring atoms relative to the empirical data for the actual bond lengths between those atoms. The net sum of valid resonance structures is defined as a resonance hybrid, which represents the overall delocalization of electrons within the molecule. A molecule that has several resonance structures is more stable than one with fewer. Some resonance structures are more favorable than others.

3.3B: Resonance is shared under a CC BY-NC-SA 4.0 license and was authored, remixed, and/or curated by LibreTexts.

- **Current page** is licensed CC BY-NC-SA 4.0.
- **8.6: Resonance Structures** is licensed CC BY-NC-SA 3.0.

3.3C: Expanded Octets

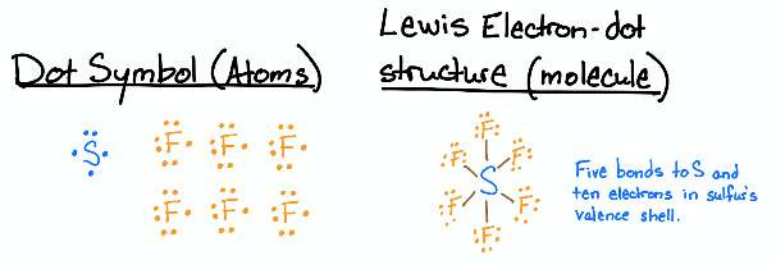
Hypervalency

The octet rule applies well to atoms in the second row of the periodic table, where a full valence shell includes eight electrons with an electron configuration of s^2p^6. Even elements in the third and fourth row are known to follow this rule *sometimes*, but not always. In larger atoms, where $n \geq 3$ the valence shell contains additional subshells: the $d, f, g...$ subshells. Therefore, atoms with $n \geq 3$ can have higher valence shell counts by "expanding" into these additional subshells. When atoms contain more than eight electrons in their valence shell, they are said to be **hypervalent**. Hypervalency allows atoms with $n \geq 3$ to break the octet rule by having more than eight electrons. This also means they can have five or more bonds; something that is nearly unheard of for atoms with $n \leq 2$. Complete the exercises below to see examples of molecules containing hypervalent atoms.

Exercise 3.3C.1

Draw the Lewis structures for SF_6.

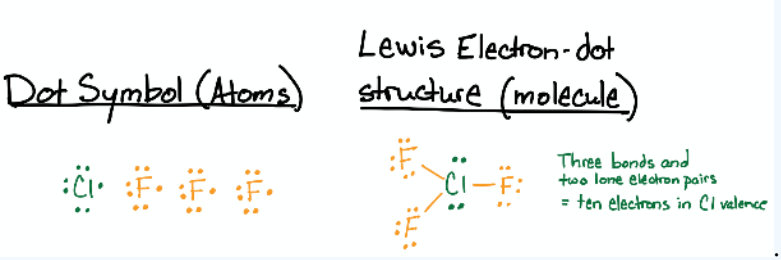
Answer



Exercise 3.3C.2

Draw the Lewis structure for ClF_3.

Answer



Is hypervalency real? Not exactly. Hypervalency is a concept associated with hybrid orbital theory and Lewis theory. It's useful for some simple things, like predicting how atoms are connected and predicting molecular shape. But the idea that the d-orbitals are involved in bonding isn't accurate according to wave mechanics.

For main group molecules, chemists (like Pauling) thought a long time ago that hypervalence is due to expanded s^2p^6 octets. The consensus is now clear that d orbitals are **NOT** involved in bonding in molecules like SF_6 any more than they are in SF_4 and SF_2. In all three cases, there is a small and roughly identical participation of d-orbitals in the wavefunctions. This has been established in both MO and VB theory. However using hybrid orbitals with d-orbital contributions equips us with a language which can pragmatically describe the geometries of highly coordinated substances.

While hybrid orbitals are a powerful tool to describe the geometries and shape of molecules and metal complexes. However, in "real" molecules, their significance may be debated. Often with a more realistically molecular orbitals approach is needed. However, from an epistemologically simple point of view, bonding theories can only be judged by their predictions. To the extent

that hybridization can explain the shapes of PF_5 and SF_6, valence bond theory is a perfectly good theory. To the extent that if you write out the valence bond wavefunction using hybridized orbitals and calculate energies and other properties à la Pauling (i.e., ionization energy and electron affinities) and find them to be off from experimental results (by tens of kcals/mol), then valence bond theory is not accurate.

> *Bonding theories can only be judged by their predictions.*

An Alternate View of Expanded Octets

Another way to represent main group compounds with more than four bonds is to include ionic bonding character. This allows for compounds with more than 4 bonds to the central atom to not exceed their octets. For example, the Lewis structure of SF_6 can be redrawn with two ionic S-F bonds and four covalent S-F bonds as shown in Figure **3.3*C*.1**. In this picture the central S atom has six F atoms coordinated, but only shares four bonding pairs of electrons and has a complete (non-expanded) octet. Considering all the possible resonance structures for SF_6, each S-F bond is $\frac{2}{3}$ covalent and $\frac{1}{3}$ ionic.

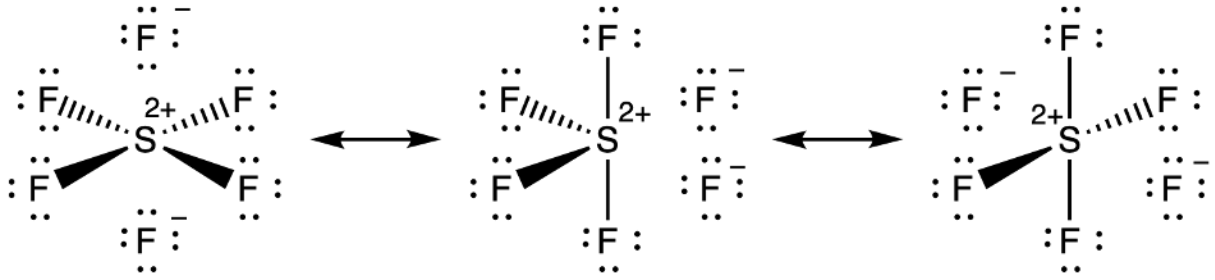


Figure **3.3*C*.1**: Three of the 15 possible resonance structures for sulfur hexafluorophosphate with four covalent and two ionic S-F bonds. (CC BY-NC-SA; Catherine McCusker)

Additional Resources

- Gillespie, R. The Octet Rule and Hypervalence: Two Misunderstood Concepts. *Coord. Chem. Rev.* **2002**, *233–234*, 53–62. https://doi.org/10.1016/S0010-8545(02)00102-9.

Contributors and Attributions

- Modified by Catherine McCusker, ETSU

This page titled 3.3C: Expanded Octets is shared under a CC BY-NC-SA 4.0 license and was authored, remixed, and/or curated by Kathryn Haas.

- **Current page** by Kathryn Haas is licensed CC BY-NC-SA 4.0.
- **3.1.2: Breaking the octet rule with higher electron counts (hypervalent atoms)** by Kathryn Haas is licensed CC BY-NC-SA 4.0.

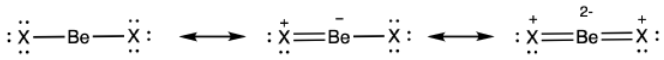
3.3D: Limitation of Lewis Theory

Two notable cases where Lewis theory fails to predict structure is in the cases of beryllium (Be) and boron (B). These two atoms are in period 2 ($n = 2$) of the periodic table and their atoms have the valence electron configurations of $2s^2$ and $2s^2 2p^1$, respectively.

Beryllium

Prediction based on Lewis structure:

The Lewis electron dot structures are shown below for BeX_2, where X is one of the halogens, F or Cl.



Each of the structures above would predict a linear geometry for the BeX_2 molecule. Together the three resonance structures suggest partial double-bond character in the Be-X bond, which results in an intermediate bond length between a single and double bond.

There are issues with each of these resonance structures. The structure on the left would predict only four electrons around Be; thus, the atom does not fulfill the octet rule. The structure on the right suggests multiple bonds for the halogen (X) and high separation of charge with formal charge on each atom. The structure in the middle is a mix of these problems. None of these situations is ideal according to Lewis theory. Further, experimental data is not consistent with any of these structures or their resonance hybrid (except in the case of $BeCl_2$ at very high temperatures).

It turns out that the monomer of BeX_2 (shown above) does exist, but only at very high temperatures and low pressures. Even under extreme conditions, the monomer is not particularly stable due to the electron deficiency around Be.

BeF_2

At ambient temperature and pressure, BeF_2 is a solid that looks similar to quartz (Figure **3.3*D*.1**) The Be is four-coordinate with tetrahedral geometry; each F is two-coordinate and the Be-F bond length is 1.54 Å. This structure is possible due to an extended 3-dimensional network in the solid where adjacent BeF_2 units are bonded to one another, as shown in Figure **3.3*D*.1**.

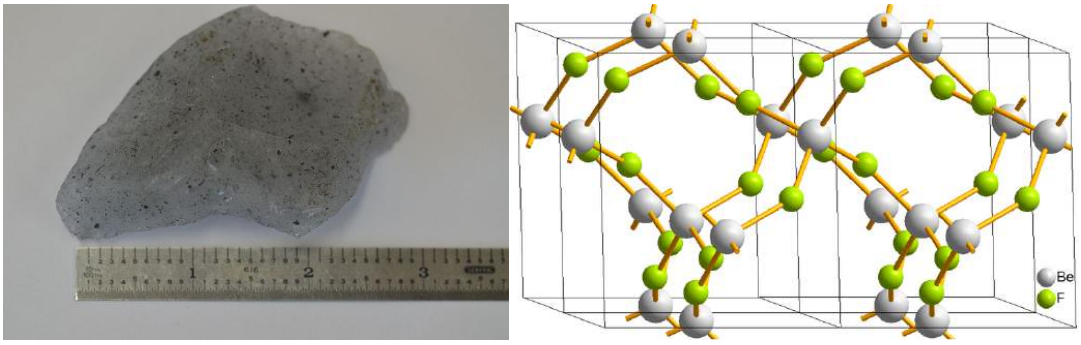


Figure **3.3*D*.1**: (left) A nugget of beryllium fluoride obtained from Materion. Black spots are carbon (CC BY-SA 3.0; Bckelleher via Wikipedia). (right) BeF2 structure (CC BY-SA 3.0 Unported; Materialscientist via Wikipedia)

In the liquid phase, BeF_2 has a fluctuating tetrahedral structure where Be and F ions exchange. The vapor phase is reached at temperatures higher than 1000 °C (at ~ 1 atm). In the vapor phase, BeF_2 exists as a monomer with linear geometry and a bond length of 1.43 Å, consistent with a double bond between Be and F.

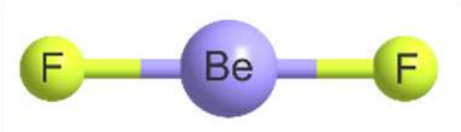


Figure **3.3*D*.2**: Geometries of **BeF_2**. (CC BY; Ibon Alkorta and Anthony C. Legoe via Inorganics)

$BeCl_2$

At ambient temperature and pressure, $BeCl_2$ is a solid. As in BeF_2 described above, $BeCl_2$ has four-coordinate, tetrahedral Be and two-coordinate F. In contrast to BeF_2, solid $BeCl_2$ is a 1-dimensional polymer consisting of edge-shared tetrahedral.

In the gas phase, $BeCl_2$ exists as a dimer with two chlorine atoms bridging two Be atoms. In the dimer, the Be atoms are 3-coordinate. Bridging Cl atoms are two-coordinate, while terminal Cl atoms are one-coordinate. At higher temperatures in the vapor phase, the linear monomer also exists.

Boron ($2s^2 2p^1$)

Prediction based on Lewis structures:

Lewis structures of **BH_3** and **BF_3** were described in Exercise 3.1.2, and are drawn again below for convenience.

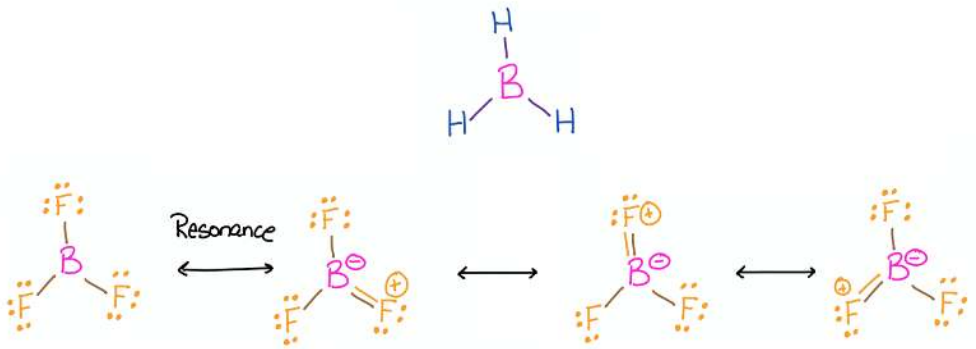


Figure 3.3*D*.3:
Lewis structures of \(\ce{
BH3
}\) and \(\ce{
BF3
}\)

Boron trihalides (ex. BF_3)

Boron trihalides, like BF_3, have properties that are largely predicted by Lewis structures and VSEPR theory. The Lewis structure for BF_3 includes several resonance structures. The structure with only single bonds is the most common representation for this molecule because the charge separation shown in the other structures is considered to be unfavorable. The highly polarized B-F bond has a dipole moment that lies opposite of the indicated formal charges shown in the resonance structures with double bonds between boron and fluorine.

The resonance hybrid of BF_3 predicts partial double bond character between boron and fluorine, thus a bond length shorter than a single bond. Using the Lewis structures and VSEPR theory, we would predict a trigonal planar geometry around boron. In fact, the actual structure of BF_3 is a monomer with trigonal planar geometry and with bond length that is shorter than a single bond. The case is similar to structures of other boron trihalides as well.

Boron trihalides are electron deficient at the boron center and react readily with Lewis bases. In other words they are strong Lewis acids (electrophiles).

Boron trihydride (BH_3 is really B_2H_6)

The properties of boron trihydride (BH_3) are not predicted by the simple predictions made through Lewis structures and VSEPR. The monomer, BH_3, is not stable, but when dissolved in the presence of a Lewis base, BH_3 can form a stable acid-base adduct. In its pure form, the compound actually exists as a dimeric gas with a molecular unit of B_2H_6 (try drawing a valid Lewis structure for that!). Its unexpected structure includes two H's that bridge the two boron atoms in 3-center-2-electron bonds. You can read more about B_2H_6 on the Wikipedia page for Diborane.

This page titled 3.3D: Limitation of Lewis Theory is shared under a CC BY-NC-SA 4.0 license and was authored, remixed, and/or curated by Kathryn Haas.

- **3.1.4: Lewis Fails to Predict Unusual Cases - Boron and Beryllium** by Kathryn Haas is licensed CC BY-NC-SA 4.0.
- **Current page** by Kathryn Haas is licensed CC BY-NC-SA 4.0.

3.4: Valence-Shell Electron-Repulsion Theory

The Lewis electron-pair approach can be used to predict the number and types of bonds between the atoms in a substance, and it indicates which atoms have lone pairs of electrons. This approach gives no information about the actual arrangement of atoms in space, however. We continue our discussion of structure and bonding by introducing the **valence-shell electron-pair repulsion** (VSEPR) model (pronounced "vesper"), which can be used to predict the shapes of many molecules and polyatomic ions. Keep in mind, however, that the VSEPR model, like any model, is a limited representation of reality; the model provides no information about bond lengths or the presence of multiple bonds.

The VSEPR Model

The VSEPR model can predict the structure of nearly any molecule or polyatomic ion in which the central atom is a nonmetal, as well as the structures of many molecules and polyatomic ions with a central metal atom. The premise of the VSEPR theory is that electron pairs located in bonds and lone pairs repel each other and will therefore adopt the geometry that places electron pairs as far apart from each other as possible. This theory is very simplistic and does not account for the subtleties of orbital interactions that influence molecular shapes; however, the simple VSEPR counting procedure accurately predicts the three-dimensional structures of a large number of compounds, which cannot be predicted using the Lewis electron-pair approach.

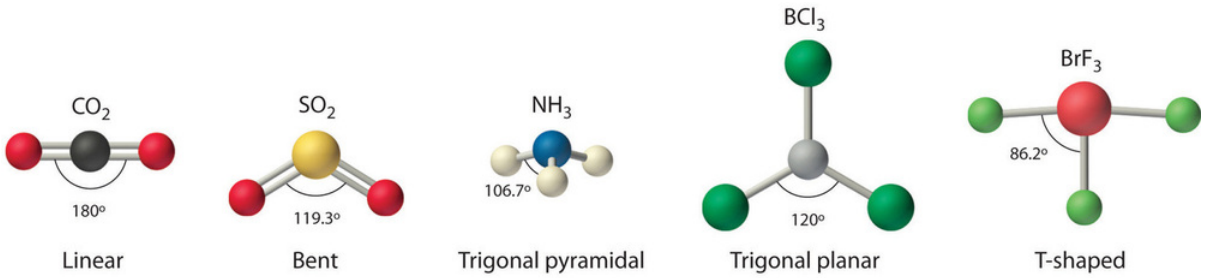


Figure 3.4.1: Common Structures for Molecules and Polyatomic Ions That Consist of a Central Atom Bonded to Two or Three Other Atoms. (CC BY-NC-SA; anonymous)

We can use the VSEPR model to predict the geometry of most polyatomic molecules and ions by focusing only on the number of electron pairs around the *central atom*, ignoring all other valence electrons present. According to this model, valence electrons in the Lewis structure form *groups*, which may consist of a single bond, a double bond, a triple bond, a lone pair of electrons, or even a single unpaired electron, which in the VSEPR model is counted as a lone pair. Because electrons repel each other electrostatically, the most stable arrangement of electron groups (i.e., the one with the lowest energy) is the one that minimizes repulsions. Groups are positioned around the central atom in a way that produces the molecular structure with the lowest energy, as illustrated in Figures 3.4.1 and 3.4.2.

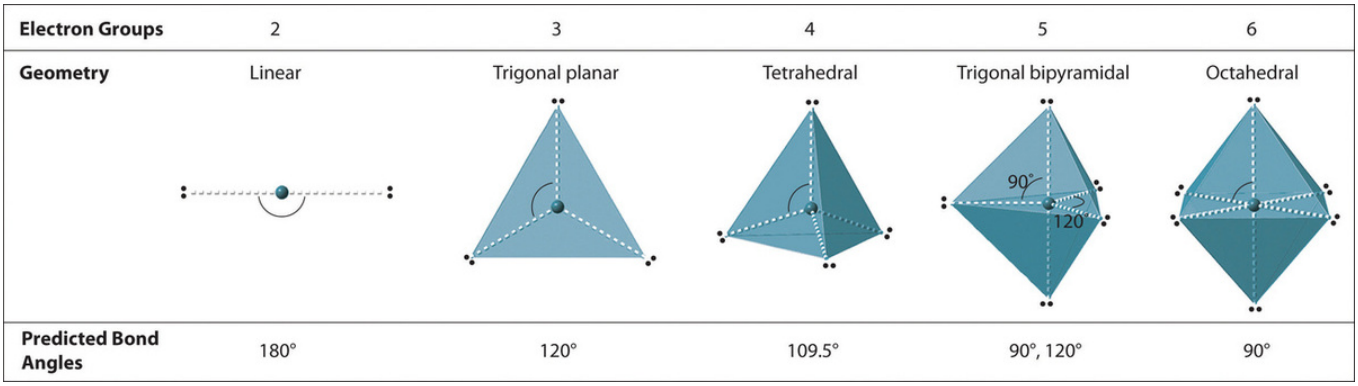


Figure 3.4.2: Electron Geometries for Species with Two to Six Electron Groups. Groups are placed around the central atom in a way that produces a molecular structure with the lowest energy, that is, the one that minimizes repulsions. (CC BY-NC-SA; anonymous)

In the VSEPR model, the molecule or polyatomic ion is given an AX_mE_n designation, where A is the central atom, X is a bonded atom, E is a nonbonding valence electron group (usually a lone pair of electrons), and m and n are integers. Each group around the central atom is designated as a bonding pair (BP) or lone (nonbonding) pair (LP). From the BP and LP interactions we can predict

both the relative positions of the atoms and the angles between the bonds, called the bond angles. Using this information, we can describe the molecular geometry, the arrangement of the *bonded atoms* in a molecule or polyatomic ion.

Using VESPR Theory

This VESPR procedure is summarized as follows:

1. Draw the Lewis electron structure of the molecule or polyatomic ion.
2. Determine the electron group arrangement around the central atom that minimizes repulsions.
3. Assign an AX_mE_n designation; then identify the LP–LP, LP–BP, or BP–BP interactions and predict deviations from ideal bond angles.
4. Describe the molecular geometry.

We will illustrate the use of this procedure with several examples, beginning with atoms with two electron groups. In our discussion we will refer to Figure **3.4.2** and Figure **3.4.3**, which summarize the common molecular geometries and idealized bond angles of molecules and ions with two to six electron groups.

AX_mE_n Notation	AX_2	AX_2E	AX_3	AX_3E
Geometry	Linear	Bent (V-shaped)	Trigonal planar	Trigonal pyramidal
Idealized Bond Angles	180°	<180°	120°	<120°
AX_mE_n Notation	AX_4E_2	AX_4	AX_5	AX_6
Geometry	Square planar	Tetrahedral	Trigonal bipyramidal	Octahedral
Idealized Bond Angles	90°	109.5°	90°, 120°	90°

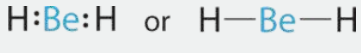
Figure **3.4.3**: Common Molecular Geometries for Species with Two to Six Electron Groups. Lone pairs are shown using a dashed line. (CC BY-NC-SA; anonymous)

Two Electron Groups

Our first example is a molecule with two bonded atoms and no lone pairs of electrons, BeH_2.

AX_2 Molecules: BeH_2

1. The central atom, beryllium, contributes two valence electrons, and each hydrogen atom contributes one. The Lewis electron structure is



Lewis structure

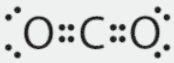
Figure **3.4.2** that the arrangement that minimizes repulsions places the groups 180° apart. (CC BY-NC-SA; anonymous)

3. Both groups around the central atom are bonding pairs (BP). Thus BeH_2 is designated as AX_2.

4. From Figure **3.4.3** we see that with two bonding pairs, the molecular geometry that minimizes repulsions in BeH_2 is *linear*.

AX_2 Molecules: CO_2

1. The central atom, carbon, contributes four valence electrons, and each oxygen atom contributes six. The Lewis electron structure is



2. The carbon atom forms two double bonds. Each double bond is a group, so there are two electron groups around the central atom. Like BeH_2, the arrangement that minimizes repulsions places the groups 180° apart.

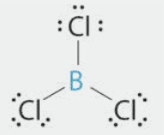
3. Once again, both groups around the central atom are bonding pairs (BP), so CO_2 is designated as AX_2.

4. VSEPR only recognizes groups around the *central* atom. Thus the lone pairs on the oxygen atoms do not influence the molecular geometry. With two bonding pairs on the central atom and no lone pairs, the molecular geometry of CO_2 is linear (Figure **3.4.3**). The structure of CO_2 is shown in Figure **3.4.1**.

Three Electron Groups

AX_3 Molecules: BCl_3

1. The central atom, boron, contributes three valence electrons, and each chlorine atom contributes seven valence electrons. The Lewis electron structure is



Lewis structure

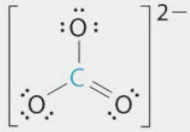
Figure **3.4.2**): (CC BY-NC-SA; anonymous)

3. All electron groups are bonding pairs (BP), so the structure is designated as AX_3.

4. From Figure **3.4.3** we see that with three bonding pairs around the central atom, the molecular geometry of BCl_3 is *trigonal planar*, as shown in Figure **3.4.2**.

AX_3 Molecules: CO_3^{2-}

1. The central atom, carbon, has four valence electrons, and each oxygen atom has six valence electrons. As you learned previously, the Lewis electron structure of one of three resonance forms is represented as

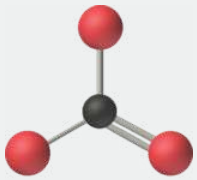


Lewis structure

Figure **3.4.2**).

3. All electron groups are bonding pairs (BP). With three bonding groups around the central atom, the structure is designated as AX_3.

4. We see from Figure **3.4.3** that the molecular geometry of CO_3^{2-} is trigonal planar with bond angles of 120°.



Molecular geometry
(trigonal planar)

In our next example we encounter the effects of lone pairs and multiple bonds on molecular geometry for the first time.

AX_2E Molecules: SO_2

1. The central atom, sulfur, has 6 valence electrons, as does each oxygen atom. With 18 valence electrons, the Lewis electron structure is shown below.

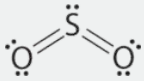


Figure **3.4.2**): (CC BY-NC-SA; anonymous)

3. There are two bonding pairs and one lone pair, so the structure is designated as AX_2E. This designation has a total of three electron pairs, two X and one E. Because a lone pair is not shared by two nuclei, it occupies more space near the central atom than a bonding pair (Figure **3.4.4**). Thus bonding pairs and lone pairs repel each other electrostatically in the order BP–BP < LP–BP < LP–LP. In SO_2, we have one BP–BP interaction and two LP–BP interactions.

4. The molecular geometry is described only by the positions of the nuclei, *not* by the positions of the lone pairs. Thus with two nuclei and one lone pair the shape is *bent*, or *V shaped*, which can be viewed as a trigonal planar arrangement with a missing vertex (Figures **3.4.2** and **3.4.3**). The O-S-O bond angle is expected to be *less than* 120° because of the extra space taken up by the lone pair.

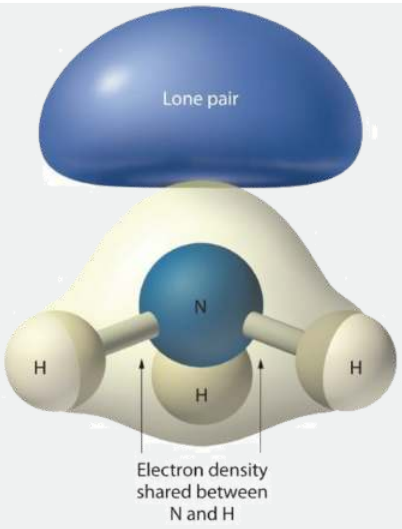
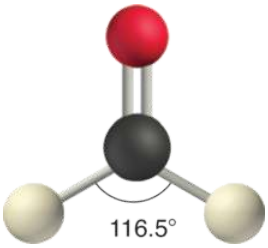


Figure **3.4.4**: The Difference in the Space Occupied by a Lone Pair of Electrons and by a Bonding Pair. (CC BY-NC-SA; anonymous)

As with SO_2, this composite model of electron distribution and negative electrostatic potential in ammonia shows that a lone pair of electrons occupies a larger region of space around the nitrogen atom than does a bonding pair of electrons that is shared with a hydrogen atom.

Like lone pairs of electrons, multiple bonds occupy more space around the central atom than a single bond, which can cause other bond angles to be somewhat smaller than expected. This is because a multiple bond has a higher electron density than a single bond, so its electrons occupy more space than those of a single bond. For example, in a molecule such as CH_2O (AX_3), whose structure is shown below, the double bond repels the single bonds more strongly than the single bonds repel each other. This causes a deviation from ideal geometry (an H–C–H bond angle of 116.5° rather than 120°).

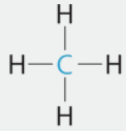


Four Electron Groups

One of the limitations of Lewis structures is that they depict molecules and ions in only two dimensions. With four electron groups, we must learn to show molecules and ions in three dimensions.

AX_4 Molecules: CH_4

1. The central atom, carbon, contributes four valence electrons, and each hydrogen atom has one valence electron, so the full Lewis electron structure is

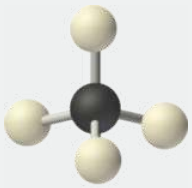


Lewis structure

2. There are four electron groups around the central atom. As shown in Figure **3.4.2**, repulsions are minimized by placing the groups in the corners of a tetrahedron with bond angles of 109.5°.

3. All electron groups are bonding pairs, so the structure is designated as AX_4.

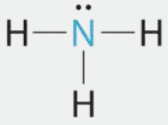
4. With four bonding pairs, the molecular geometry of methane is *tetrahedral* (Figure **3.4.3**).



Molecular geometry
(tetrahedral)

AX_3E Molecules: NH_3

1. In ammonia, the central atom, nitrogen, has five valence electrons and each hydrogen donates one valence electron, producing the Lewis electron structure



Lewis structure

2. There are four electron groups around nitrogen, three bonding pairs and one lone pair. Repulsions are minimized by directing each hydrogen atom and the lone pair to the corners of a tetrahedron.

3. With three bonding pairs and one lone pair, the structure is designated as AX_3E. This designation has a total of four electron pairs, three X and one E. We expect the LP–BP interactions to cause the bonding pair angles to deviate significantly from the angles of a perfect tetrahedron.

4. There are three nuclei and one lone pair, so the molecular geometry is *trigonal pyramidal*. In essence, this is a tetrahedron with a vertex missing (Figure **3.4.3**). However, the H–N–H bond angles are less than the ideal angle of 109.5° because of LP–BP repulsions (Figure **3.4.3** and Figure **3.4.4**).

AX_2E_2 Molecules: H_2O

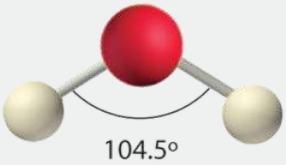
1. Oxygen has six valence electrons and each hydrogen has one valence electron, producing the Lewis electron structure



Figure **3.4.2**: (CC BY-NC-SA; anonymous)

3. With two bonding pairs and two lone pairs, the structure is designated as AX_2E_2 with a total of four electron pairs. Due to LP–LP, LP–BP, and BP–BP interactions, we expect a significant deviation from idealized tetrahedral angles.

4. With two hydrogen atoms and two lone pairs of electrons, the structure has significant lone pair interactions. There are two nuclei about the central atom, so the molecular shape is *bent*, or *V shaped*, with an H–O–H angle that is even less than the H–N–H angles in NH_3, as we would expect because of the presence of two lone pairs of electrons on the central atom rather than one. This molecular shape is essentially a tetrahedron with two missing vertices.



Five Electron Groups

In previous examples it did not matter where we placed the electron groups because all positions were equivalent. In some cases, however, the positions are not equivalent. We encounter this situation for the first time with five electron groups.

AX_5 Molecules: PCl_5

1. Phosphorus has five valence electrons and each chlorine has seven valence electrons, so the Lewis electron structure of PCl_5 is

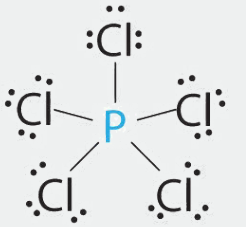
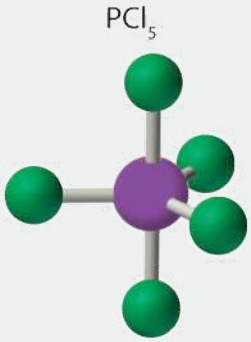


Figure **3.4.2**): (CC BY-NC-SA; anonymous)

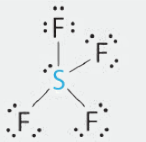
3. All electron groups are bonding pairs, so the structure is designated as AX_5. There are no lone pair interactions.

4. The molecular geometry of PCl_5 is *trigonal bipyramidal*, as shown in Figure **3.4.3**. The molecule has three atoms in a plane in *equatorial* positions and two atoms above and below the plane in *axial* positions. The three equatorial positions are separated by 120° from one another, and the two axial positions are at 90° to the equatorial plane. The axial and equatorial positions are not chemically equivalent, as we will see in our next example.



AX_4E Molecules: SF_4

1. The sulfur atom has six valence electrons and each fluorine has seven valence electrons, so the Lewis electron structure is



Lewis structure

With an expanded valence, this species is an exception to the octet rule.

2. There are five groups around sulfur, four bonding pairs and one lone pair. With five electron groups, the lowest energy arrangement is a trigonal bipyramid, as shown in Figure **3.4.2**.

3. We designate SF_4 as AX_4E; it has a total of five electron pairs. However, because the axial and equatorial positions are not chemically equivalent, where do we place the lone pair? If we place the lone pair in the axial position, we have three LP–BP repulsions at 90°. If we place it in the equatorial position, we have two 90° LP–BP repulsions at 90°. With fewer 90° LP–BP repulsions, we can predict that the structure with the lone pair of electrons in the *equatorial position is more stable than the one with the lone pair in the axial position*. We also expect a deviation from ideal geometry because a lone pair of electrons occupies more space than a bonding pair.

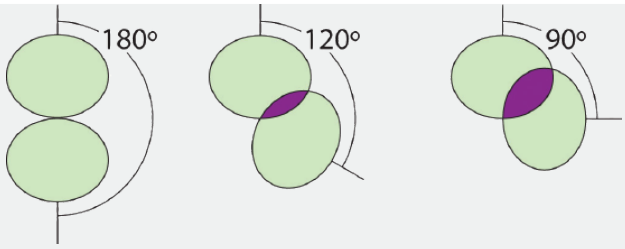
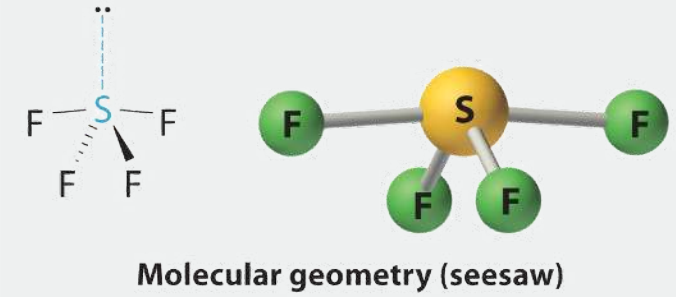


Figure **3.4.5**: Illustration of the Area Shared by Two Electron Pairs versus the Angle between Them

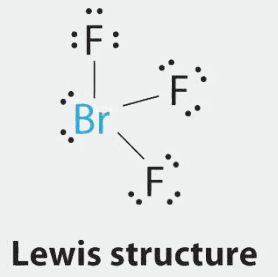
At 90°, the two electron pairs share a relatively large region of space, which leads to strong repulsive electron–electron interactions.

4. With four nuclei and one lone pair of electrons, the molecular structure is based on a trigonal bipyramid with a missing equatorial vertex; it is described as a *seesaw*. The F_{axial}–S–F_{axial} angle is 173° rather than 180° because of the lone pair of electrons in the equatorial plane.



AX_3E_2 Molecules: BrF_3

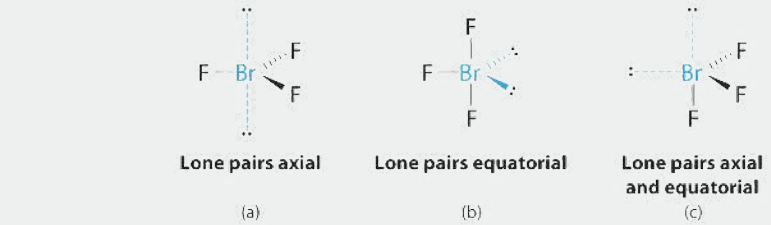
1. The bromine atom has seven valence electrons, and each fluorine has seven valence electrons, so the Lewis electron structure is



Once again, we have a compound that is an exception to the octet rule.

2. There are five groups around the central atom, three bonding pairs and two lone pairs. We again direct the groups toward the vertices of a trigonal bipyramid.

3. With three bonding pairs and two lone pairs, the structural designation is AX_3E_2 with a total of five electron pairs. Because the axial and equatorial positions are not equivalent, we must decide how to arrange the groups to minimize repulsions. If we place both lone pairs in the axial positions, we have six LP–BP repulsions at 90°. If both are in the equatorial positions, we have four LP–BP repulsions at 90°. If one lone pair is axial and the other equatorial, we have one LP–LP repulsion at 90° and three LP–BP repulsions at 90°:



Interactions			
90° LP–LP	0	0	1
90° LP–BP	6	4	3

Structure (c) can be eliminated because it has a LP–LP interaction at 90°. Structure (b), with fewer LP–BP repulsions at 90° than (a), is lower in energy. However, we predict a deviation in bond angles because of the presence of the two lone pairs of electrons.

4. The three nuclei in BrF_3 determine its molecular structure, which is described as *T shaped*. This is essentially a trigonal bipyramid that is missing two equatorial vertices. The F_{axial}–Br–F_{axial} angle is 172°, less than 180° because of LP–BP repulsions (Figure **3.4.2**.1).

Because lone pairs occupy more space around the central atom than bonding pairs, electrostatic repulsions are more important for lone pairs than for bonding pairs.

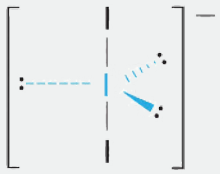
AX_2E_3 Molecules: I_3^-

1. Each iodine atom contributes seven electrons and the negative charge one, so the Lewis electron structure is



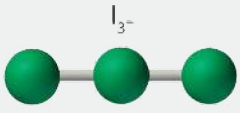
2. There are five electron groups about the central atom in I_3^-, two bonding pairs and three lone pairs. To minimize repulsions, the groups are directed to the corners of a trigonal bipyramid.

3. With two bonding pairs and three lone pairs, I_3^- has a total of five electron pairs and is designated as AX_2E_3. We must now decide how to arrange the lone pairs of electrons in a trigonal bipyramid in a way that minimizes repulsions. Placing them in the axial positions eliminates 90° LP–LP repulsions and minimizes the number of 90° LP–BP repulsions.



The three lone pairs of electrons have equivalent interactions with the three iodine atoms, so we do not expect any deviations in bonding angles.

4. With three nuclei and three lone pairs of electrons, the molecular geometry of I_3^- is linear. This can be described as a trigonal bipyramid with three equatorial vertices missing. The ion has an I–I–I angle of 180°, as expected.

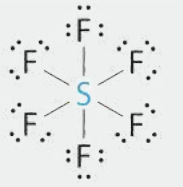


Six Electron Groups

Six electron groups form an *octahedron*, a polyhedron made of identical equilateral triangles and six identical vertices (Figure **3.4.2**.)

AX_6 Molecules: SF_6

1. The central atom, sulfur, contributes six valence electrons, and each fluorine atom has seven valence electrons, so the Lewis electron structure is



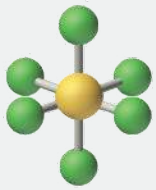
Lewis structure

With an expanded valence, this species is an exception to the octet rule.

2. There are six electron groups around the central atom, each a bonding pair. We see from Figure **3.4.2** that the geometry that minimizes repulsions is *octahedral*.

3. With only bonding pairs, SF_6 is designated as AX_6. All positions are chemically equivalent, so all electronic interactions are equivalent.

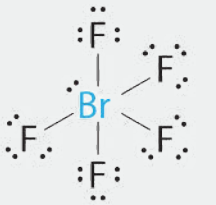
4. There are six nuclei, so the molecular geometry of SF_6 is octahedral.



Molecular geometry
(octahedral)

AX_5E Molecules: BrF_5

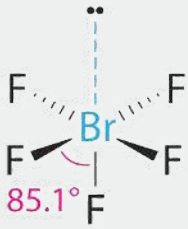
1. The central atom, bromine, has seven valence electrons, as does each fluorine, so the Lewis electron structure is



Lewis structure

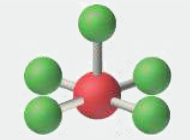
With its expanded valence, this species is an exception to the octet rule.

2. There are six electron groups around the Br, five bonding pairs and one lone pair. Placing five F atoms around Br while minimizing BP–BP and LP–BP repulsions gives the following structure:



3. With five bonding pairs and one lone pair, BrF_5 is designated as AX_5E; it has a total of six electron pairs. The BrF_5 structure has four fluorine atoms in a plane in an equatorial position and one fluorine atom and the lone pair of electrons in the axial positions. We expect all F_{axial}–Br–$F_{equatorial}$ angles to be less than 90° because of the lone pair of electrons, which occupies more space than the bonding electron pairs.

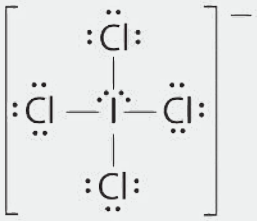
4. With five nuclei surrounding the central atom, the molecular structure is based on an octahedron with a vertex missing. This molecular structure is *square pyramidal*. The F_{axial}–B–$F_{equatorial}$ angles are 85.1°, less than 90° because of LP–BP repulsions.



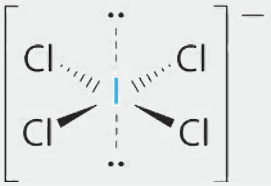
Molecular geometry
(square pyramidal)

AX_4E_2 Molecules: ICl_4^-

1. The central atom, iodine, contributes seven electrons. Each chlorine contributes seven, and there is a single negative charge. The Lewis electron structure is

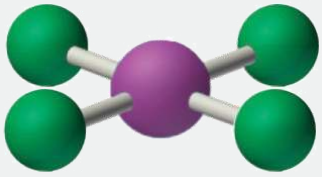


2. There are six electron groups around the central atom, four bonding pairs and two lone pairs. The structure that minimizes LP–LP, LP–BP, and BP–BP repulsions is



3. ICl_4^- is designated as AX_4E_2 and has a total of six electron pairs. Although there are lone pairs of electrons, with four bonding electron pairs in the equatorial plane and the lone pairs of electrons in the axial positions, all LP–BP repulsions are the same. Therefore, we do not expect any deviation in the Cl–I–Cl bond angles.

4. With five nuclei, the ICl4− ion forms a molecular structure that is *square planar*, an octahedron with two opposite vertices missing.



The relationship between the number of electron groups around a central atom, the number of lone pairs of electrons, and the molecular geometry is summarized in Figure **3.4.6**.

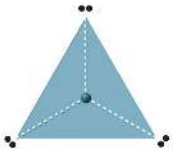
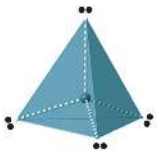
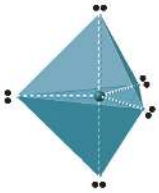
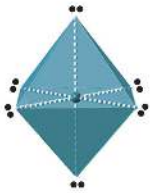
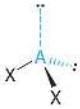
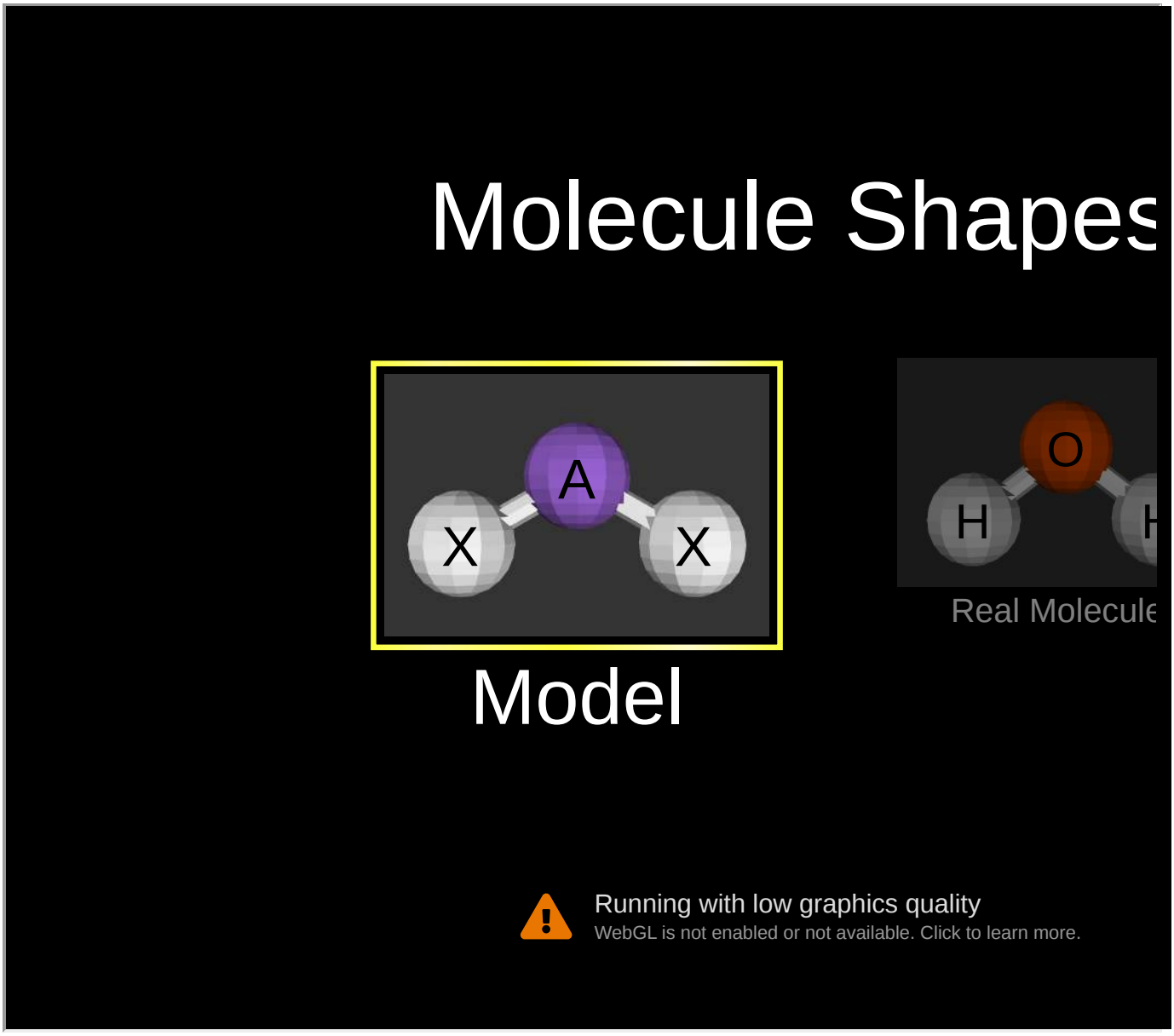
Electron Groups	2	3	4	5	6
Molecular Geometry	 Linear	 Trigonal planar	 Tetrahedral	 Trigonal bipyramidal	 Octahedral
Zero Lone Pairs	 Linear AX_2	 Trigonal planar AX_3	 Tetrahedral AX_4	 Trigonal bipyramidal AX_5	 Octahedral AX_6
One Lone Pair		 Bent (V-shaped) AX_2E	 Trigonal pyramidal AX_3E	 Seesaw AX_4E One axial lone pair	 Square pyramidal AX_5E
Two Lone Pairs			 Bent (V-shaped) AX_2E_2	 T-shaped AX_3E_2 Two axial lone pairs	 Square planar AX_4E_2
Three Lone Pairs				 Linear AX_2E_3 Three axial lone pairs	

Figure **3.4.6**: Overview of Molecular Geometries



Template:HideTOC

Example 3.4.1

Using the VSEPR model, predict the molecular geometry of each molecule or ion.

1. PF_5 (phosphorus pentafluoride, a catalyst used in certain organic reactions)
2. H_3O^+ (hydronium ion)

Given: two chemical species

Asked for: molecular geometry

Strategy:

A. Draw the Lewis electron structure of the molecule or polyatomic ion.
B. Determine the electron group arrangement around the central atom that minimizes repulsions.
C. Assign an AX_mE_n designation; then identify the LP–LP, LP–BP, or BP–BP interactions and predict deviations in bond angles.
D. Describe the molecular geometry.

Solution:

1. **A** The central atom, P, has five valence electrons and each fluorine has seven valence electrons, so the Lewis structure of PF_5 is

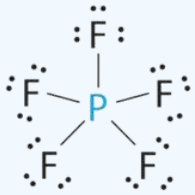


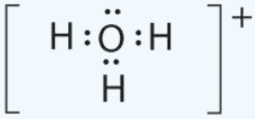
Figure **3.4.6**): (CC BY-NC-SA; anonymous)

C All electron groups are bonding pairs, so PF_5 is designated as AX_5. Notice that this gives a total of five electron pairs. With no lone pair repulsions, we do not expect any bond angles to deviate from the ideal.

D The PF_5 molecule has five nuclei and no lone pairs of electrons, so its molecular geometry is trigonal bipyramidal.



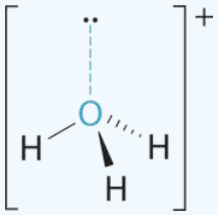
2. **A** The central atom, O, has six valence electrons, and each H atom contributes one valence electron. Subtracting one electron for the positive charge gives a total of eight valence electrons, so the Lewis electron structure is



B There are four electron groups around oxygen, three bonding pairs and one lone pair. Like NH_3, repulsions are minimized by directing each hydrogen atom and the lone pair to the corners of a tetrahedron.

C With three bonding pairs and one lone pair, the structure is designated as AX_3E and has a total of four electron pairs (three X and one E). We expect the LP–BP interactions to cause the bonding pair angles to deviate significantly from the angles of a perfect tetrahedron.

D There are three nuclei and one lone pair, so the molecular geometry is *trigonal pyramidal*, in essence a tetrahedron missing a vertex. However, the H–O–H bond angles are less than the ideal angle of 109.5° because of LP–BP repulsions:



Exercise 3.4.1

Using the VSEPR model, predict the molecular geometry of each molecule or ion.

a. XeO_3
b. PF_6^-
c. NO_2^+

Answer a

trigonal pyramidal

Answer b

octahedral

Answer c

linear

Example 3.4.2

Predict the molecular geometry of each molecule.

1. XeF_2
2. $SnCl_2$

Given: two chemical compounds

Asked for: molecular geometry

Strategy:

Use the strategy given in Example **3.4.1**.

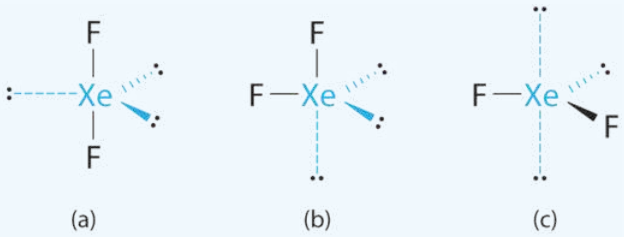
Solution:

1. **A** Xenon contributes eight electrons and each fluorine seven valence electrons, so the Lewis electron structure is



B There are five electron groups around the central atom, two bonding pairs and three lone pairs. Repulsions are minimized by placing the groups in the corners of a trigonal bipyramid.

C From B, XeF_2 is designated as AX_2E_3 and has a total of five electron pairs (two X and three E). With three lone pairs about the central atom, we can arrange the two F atoms in three possible ways: both F atoms can be axial, one can be axial and one equatorial, or both can be equatorial:

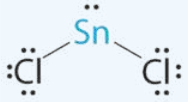


Interactions	(a)	(b)	(c)
90 LP–LP	0	2	2

The structure with the lowest energy is the one that minimizes LP–LP repulsions. Both (b) and (c) have two 90° LP–LP interactions, whereas structure (a) has none. Thus both F atoms are in the axial positions, like the two iodine atoms around the central iodine in I_3^-. All LP–BP interactions are equivalent, so we do not expect a deviation from an ideal 180° in the F–Xe–F bond angle.

D With two nuclei about the central atom, the molecular geometry of XeF_2 is linear. It is a trigonal bipyramid with three missing equatorial vertices.

2. **A** The tin atom donates 4 valence electrons and each chlorine atom donates 7 valence electrons. With 18 valence electrons, the Lewis electron structure is



B There are three electron groups around the central atom, two bonding groups and one lone pair of electrons. To minimize repulsions the three groups are initially placed at 120° angles from each other.

C From B we designate $SnCl_2$ as AX_2E. It has a total of three electron pairs, two X and one E. Because the lone pair of electrons occupies more space than the bonding pairs, we expect a decrease in the Cl–Sn–Cl bond angle due to increased LP–BP repulsions.

D With two nuclei around the central atom and one lone pair of electrons, the molecular geometry of $SnCl_2$ is bent, like SO_2, but with a Cl–Sn–Cl bond angle of 95°. The molecular geometry can be described as a trigonal planar arrangement with one vertex missing.

Exercise 3.4.2

Predict the molecular geometry of each molecule.

a. SO_3
b. XeF_4

Answer a

trigonal planar

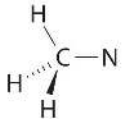
Answer b

square planar

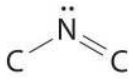
Molecules with No Single Central Atom

The VSEPR model can be used to predict the structure of somewhat more complex molecules with no single central atom by treating them as linked AX_mE_n fragments. We will demonstrate with methyl isocyanate (CH_3–N=C=O), a volatile and highly toxic molecule that is used to produce the pesticide Sevin. In 1984, large quantities of Sevin were accidentally released in Bhopal, India, when water leaked into storage tanks. The resulting highly exothermic reaction caused a rapid increase in pressure that ruptured the tanks, releasing large amounts of methyl isocyanate that killed approximately 3800 people and wholly or partially disabled about 50,000 others. In addition, there was significant damage to livestock and crops.

We can treat methyl isocyanate as linked AX_mE_n fragments beginning with the carbon atom at the left, which is connected to three H atoms and one N atom by single bonds. The four bonds around carbon mean that it must be surrounded by four bonding electron pairs in a configuration similar to AX_4. We can therefore predict the CH_3–N portion of the molecule to be roughly tetrahedral, similar to methane:



The nitrogen atom is connected to one carbon by a single bond and to the other carbon by a double bond, producing a total of three bonds, C–N=C. For nitrogen to have an octet of electrons, it must also have a lone pair:



Because multiple bonds are not shown in the VSEPR model, the nitrogen is effectively surrounded by three electron pairs. Thus according to the VSEPR model, the C–N=C fragment should be bent with an angle less than 120°.

The carbon in the –N=C=O fragment is doubly bonded to both nitrogen and oxygen, which in the VSEPR model gives carbon a total of two electron pairs. The N=C=O angle should therefore be 180°, or linear. The three fragments combine to give the following structure:

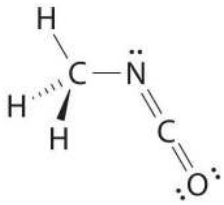


Figure 3.4.7).

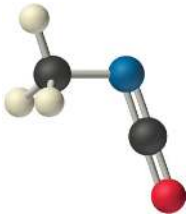


Figure 3.4.7: The Experimentally Determined Structure of Methyl Isocyanate

Certain patterns are seen in the structures of moderately complex molecules. For example, carbon atoms with four bonds (such as the carbon on the left in methyl isocyanate) are generally tetrahedral. Similarly, the carbon atom on the right has two double bonds that are similar to those in CO_2, so its geometry, like that of CO_2, is linear. Recognizing similarities to simpler molecules will help you predict the molecular geometries of more complex molecules.

Example 3.4.3

Use the VSEPR model to predict the molecular geometry of propyne ($H_3C–C≡CH$), a gas with some anesthetic properties.

Given: chemical compound

Asked for: molecular geometry

Strategy:

Count the number of electron groups around each carbon, recognizing that in the VSEPR model, a multiple bond counts as a single group. Use Figure 3.4.3 to determine the molecular geometry around each carbon atom and then deduce the structure of the molecule as a whole.

Solution:

Because the carbon atom on the left is bonded to four other atoms, we know that it is approximately tetrahedral. The next two carbon atoms share a triple bond, and each has an additional single bond. Because a multiple bond is counted as a single bond in the VSEPR model, each carbon atom behaves as if it had two electron groups. This means that both of these carbons are linear, with C–C≡C and C≡C–H angles of 180°.

Exercise 3.4.3

Predict the geometry of allene ($H_2C=C=CH_2$), a compound with narcotic properties that is used to make more complex organic molecules.

Answer

The terminal carbon atoms are trigonal planar, the central carbon is linear, and the C–C–C angle is 180°.

3.4: Valence-Shell Electron-Repulsion Theory is shared under a CC BY-NC-SA 4.0 license and was authored, remixed, and/or curated by LibreTexts.

3.5: Molecular Polarity

Dipole moments occur when there is a separation of charge. They can occur between two ions in an ionic bond or between atoms in a covalent bond; dipole moments arise from differences in electronegativity. The larger the difference in electronegativity, the larger the dipole moment. The distance between the charge separation is also a deciding factor into the size of the dipole moment. The dipole moment is a measure of the polarity of the molecule.

Introduction

When atoms in a molecule share electrons unequally, they create what is called a dipole moment. This occurs when one atom is more electronegative than another, resulting in that atom pulling more tightly on the shared pair of electrons, or when one atom has a lone pair of electrons and the difference of electronegativity vector points in the same way. One of the most common examples is the water molecule, made up of one oxygen atom and two hydrogen atoms. The differences in electronegativity and lone electrons give oxygen a partial negative charge and each hydrogen a partial positive charge.

Dipole Moment

When two electrical charges, of opposite sign and equal magnitude, are separated by a distance, an electric dipole is established. The size of a dipole is measured by its dipole moment (μ). Dipole moment is measured in Debye units, which is equal to the distance between the charges multiplied by the charge (1 Debye equals $3.34 \times 10^{-30}\ C\,m$). The dipole moment of a molecule can be calculated by Equation 3.5.1:

$$\vec{\mu} = \sum_i q_i \vec{r}_i \tag{3.5.1}$$

where

- $\vec{\mu}$ is the dipole moment vector
- q_i is the magnitude of the i^{th} charge, and
- $\vec{r}_i$ is the vector representing the position of i^{th} charge.

The dipole moment acts in the direction of the vector quantity. An example of a polar molecule is H_2O. Because of the lone pair on oxygen, the structure of H_2O is bent (via VEPSR theory), and the vectors representing the bond dipole moments do not cancel each other out. Hence, water is polar.

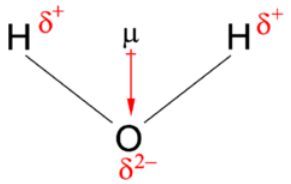


Figure 3.5.1: Dipole moment of water. The convention in chemistry is that the arrow representing the dipole moment goes from positive to negative. Physicist tend to use the opposite orientation.

The vector points from positive to negative, on both the molecular (net) dipole moment and the individual bond dipoles. Table A2 shows the electronegativity of some of the common elements. The larger the difference in electronegativity between the two atoms, the more electronegative that bond is. To be considered a polar bond, the difference in electronegativity must be large. The dipole moment points in the direction of the vector quantity of each of the bond electronegativities added together.

It is relatively easy to measure dipole moments; just place a substance between charged plates (Figure 3.5.2) and polar molecules increase the charge stored on plates and the dipole moment can be obtained (i.e., via the capacitance of the system). Nonpolar CCl_4 is not deflected; moderately polar acetone deflects slightly; highly polar water deflects strongly. In general, polar molecules will align themselves: (1) in an electric field, (2) with respect to one another, or (3) with respect to ions (Figure 3.5.2).

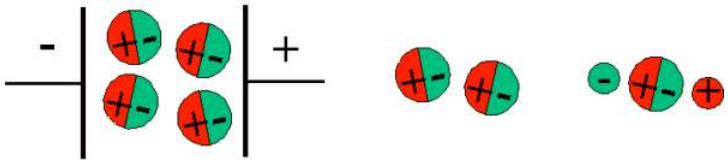


Figure **3.5.2**: *Polar molecules align themselves in an electric field (left), with respect to one another (middle), and with respect to ions (right)*

Polarity and Structure of Molecules

The shape of a molecule and the polarity of its bonds determine the OVERALL POLARITY of that molecule. A molecule that contains polar bonds, might not have any overall polarity, depending upon its shape. The simple definition of whether a complex molecule is polar or not depends upon whether its overall centers of positive and negative charges overlap. If these centers lie at the same point in space, then the molecule has no overall polarity (and is non polar). If a molecule is completely symmetric, then the dipole moment vectors on each molecule will cancel each other out, making the molecule nonpolar. A molecule can only be polar if the structure of that molecule is not symmetric.

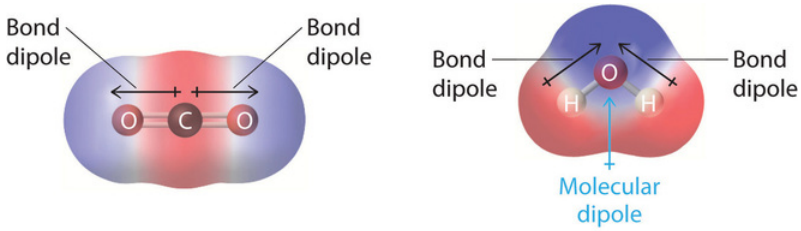


Figure **3.5.3**: Charge distributions of CO_2 and H_2O. Blue and red colored regions are negative and positively signed regions, respectively.

A good example of a nonpolar molecule that contains polar bonds is carbon dioxide (Figure **3.5.3***a*). This is a linear molecule and each C=O bond is, in fact, polar. The central carbon will have a net positive charge, and the two outer oxygen atoms a net negative charge. However, since the molecule is linear, these two bond dipoles cancel each other out (i.e. the vector addition of the dipoles equals zero) and the overall molecule has a zero dipole moment ($\mu = 0$).

For AB_n molecules, where A is the central atom and B are all the same types of atoms, there are certain molecular geometries which are symmetric. Therefore, they will have no dipole even if the bonds are polar. These geometries include linear, trigonal planar, tetrahedral, octahedral and trigonal bipyramidal.

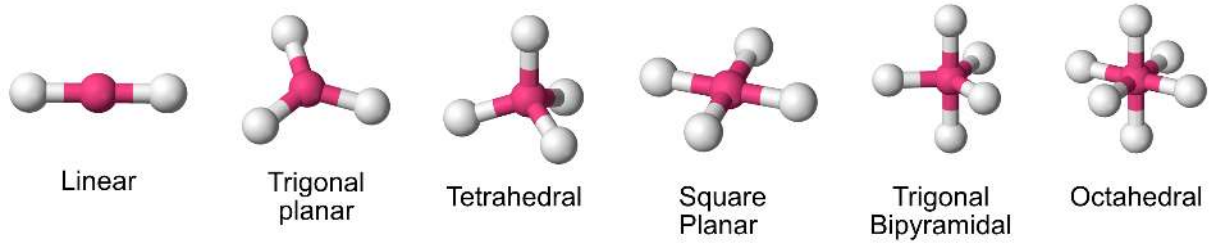
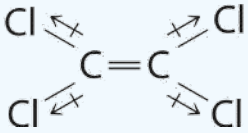


Figure **3.5.4**: *Molecular geometries with exact cancelation of polar bonding to generate a non-polar molecule ($\mu = 0$). (Images adapted from VSEPR theory, Wikipedia)*

Example 3.5.1: C_2Cl_4

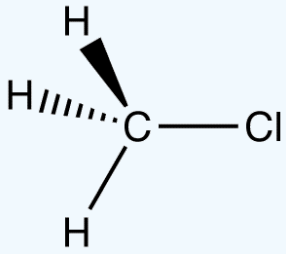
Although the C–Cl bonds are rather polar, the individual bond dipoles cancel one another in this symmetrical structure, and $Cl_2C{=}CCl_2$ does not have a net dipole moment.



Example 3.5.2: CH_3Cl

C-Cl, the key polar bond, is 178 pm. Measurement reveals 1.87 D. From this data, % ionic character can be computed. If this bond were 100% ionic (based on proton & electron),

$$\mu = \frac{178}{100}(4.80\ D)$$
$$= 8.54\ D$$



Although the bond length is ***increasing***, the dipole is ***decreasing*** as you move down the halogen group. The electronegativity decreases as we move down the group. Thus, the greater influence is the electronegativity of the two atoms (which influences the ***charge*** at the ends of the dipole).

Table **3.5.1***: Relationship between Bond length, Electronegativity and Dipole moments in simple Diatomics*

Compound	Bond Length (Å)	Electronegativity Difference	Dipole Moment (D)
HF	0.92	1.9	1.82
HCl	1.27	0.9	1.08
HBr	1.41	0.7	0.82
HI	1.61	0.4	0.44

References

1. *Housecroft, Catherine E. and Alan G. Sharpe. Inorganic Chemistry. 3rd ed. Harlow: Pearson Education, 2008. Print. (Pages 44-46)*
2. *Tro, Nivaldo J. Chemistry: A Molecular Approach. Upper Saddle River: Pearson Education, 2008. Print. (Pages 379-386)*

Contributors and Attributions

- Mike Blaber (Florida State University)

3.5: Molecular Polarity is shared under a CC BY-NC-SA 4.0 license and was authored, remixed, and/or curated by LibreTexts.

3.6: Valence Bond Theory

Introduction

Valence bond (VB) Theory has its roots in Gilbert Newton Lewis's paper *The Atom and The Molecule*. Possibly unaware that Lewis's model existed, Walter Heitler and Fritz London came up with the idea that resonance and wavefunctions contributed to chemical bonds, in which they used dihydrogen as an example. Their theory was equivalent to Lewis's theory, with the difference of quantum mechanics being developed. Nonetheless, Heitler and London's theory proved to be successful, providing Linus Pauling and John C. Slater with an opportunity to assemble a general chemical theory containing all of these ideas. Valence bond theory was the result, which included the ideas of resonance, covalent-ionic superposition, atomic orbital overlap, and hybridization to describe chemical bonds. Valence bond theory looks at the interaction between atoms to explain chemical bonds. It is one of the two common theories that helps describe the bonding between atoms. The other theory is molecular orbital theory, which will be discussed in the next section. Take note that these are theories and should be treated as such; they are not always perfect.

Atomic Orbital Overlap

In VB theory, bonds are formed between atoms because a singly occupied atomic orbital on each atom overlaps to form a two electron bond. Dihydrogen (H_2) is a simple diatomic gas that has been used to illustrate this idea; however, let's look at Cl_2 as a simple example. Cl has seven valence electrons, and has a valence electron configuration of $3s^2 3p^5$. From the electron configuration, one can see that Cl has an unpaired electron in one of its p orbitals. That one unpaired electron indicates that Cl can bond once. As a general rule, in VB theory the number of unpaired electrons denotes how many bonds that atom can make. Since there is only one unpaired electron on each Cl, the 3p orbitals overlap to form a bond as shown in Figure **3.6.1**. Lone pairs can be seen as filled atomic orbitals that don't interact or overlap. The idea of atomic orbitals overlapping works well for simple diatomic molecules, but other bonding geometries (trigonal planar, tetrahedral, etc.) can be created with pure atomic orbitals. For example, the central atom in a trigonal planar geometry has three bonds separated by **120°**, but bonds formed by overlap with the three p orbitals would be separated by **90°**.

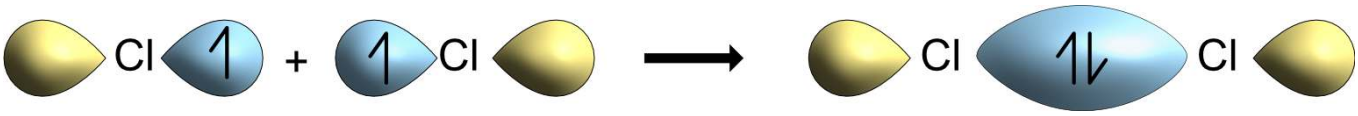


Figure **3.6.1**: Illustration showing the overlap of two singly occupied 3p orbitals on Cl to form a Cl-Cl bond. (CC BY-NC-SA; Catherine McCusker)

Atomic Orbital Hybridization

Atomic orbitals can be combined, or hybridized, to form a set of equivalent hybrid orbitals in the desired geometry.

Forming hybrid orbitals

1. The number of electron pairs (bonds and lone pairs) around the central atom determines the number of hybrid orbitals needed.
2. Orbitals cannot be created or destroyed. The number of atomic orbitals mixed will equal the number of resulting hybrid orbitals.
3. Always start with the s atomic orbital and add additional p and d* orbitals as needed.

Reminder

* As discussed previously, it is now known that d orbitals do not contribute significantly to bonding in main group compounds. As such, this discussion of valence bond theory and orbital hybridization will focus on the s and p orbitals.

Hybridization of *s* and *p* Orbitals

The Lewis structure of BeH_2 shows that it has two bonds and no lone pairs. We can generate two equivalent hybrid orbitals by combining the 2*s* orbital of beryllium and any one of the three degenerate 2*p* orbitals. By taking the sum and the difference of Be

2*s* and 2p_z atomic orbitals, for example, we produce two new orbitals with major and minor lobes oriented along the *z*-axes, as shown in Figure **3.6.2**.

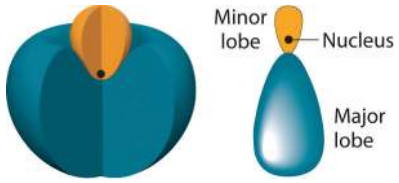


Figure **3.6.2:** The position of the atomic nucleus with respect to an sp hybrid orbital. The nucleus is actually located slightly inside the minor lobe, not at the node separating the major and minor lobes.

Because the difference A − B can also be written as A + (−B), in Figure **3.6.3** and subsequent figures we have reversed the phase(s) of the orbital being subtracted, which is the same as multiplying it by −1 and adding. This gives us Equation **3.6.2**, where the value $\frac{1}{\sqrt{2}}$ is needed mathematically to indicate that the 2*s* and 2*p* orbitals contribute equally to each hybrid orbital.

$$sp = \frac{1}{\sqrt{2}}(2s + 2p_z) \tag{3.6.1}$$

and

$$sp = \frac{1}{\sqrt{2}}(2s - 2p_z) \tag{3.6.2}$$

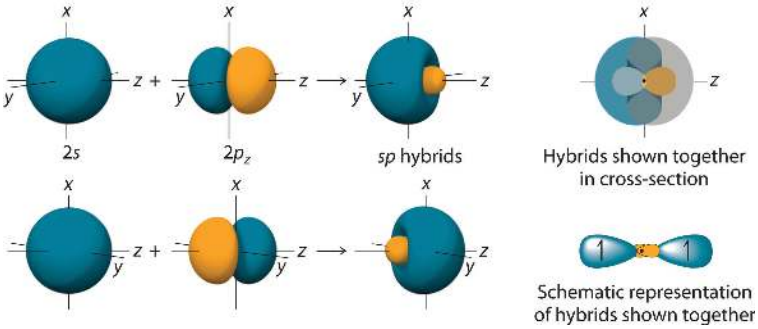


Figure **3.6.3**: The Formation of *sp* Hybrid Orbitals. Taking the sum and difference of an *ns* and an *np* atomic orbital where *n* = 2 gives two equivalent *sp* hybrid orbitals oriented at 180° to each other.

The nucleus resides just inside the minor lobe of each orbital. In this case, the new orbitals are called *sp hybrids* because they are formed from one *s* and one *p* orbital. The two new orbitals are equivalent in energy, and their energy is between the energy values associated with pure *s* and *p* orbitals, as illustrated in Figure **3.6.4**.

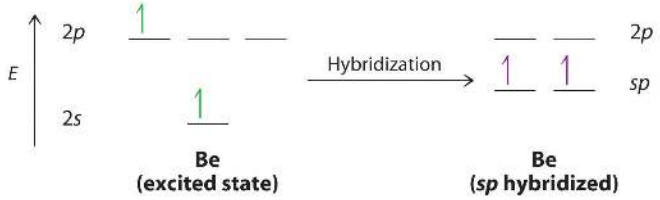


Figure **3.6.4**. each *sp* orbital on Be has the correct orientation for the major lobes to overlap with the 1*s* atomic orbital of an H atom. The formation of two energetically equivalent Be–H bonds produces a linear BeH_2 molecule. Thus valence bond theory does what neither the Lewis electron structure nor the VSEPR model is able to do; it explains why the bonds in BeH_2 are equivalent in energy and why BeH_2 has a linear geometry.

https://chem.libretexts.org/@go/page/326159

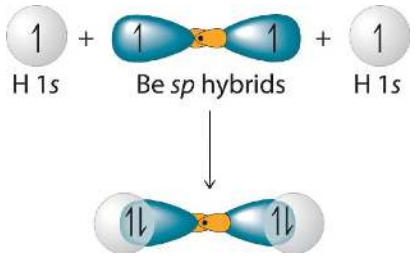


Figure **3.6.5**: Explanation of the Bonding in BeH_2 Using *sp* Hybrid Orbitals. Each singly occupied *sp* hybrid orbital on beryllium can form an electron-pair bond with the singly occupied 1*s* orbital of a hydrogen atom. Because the two *sp* hybrid orbitals are oriented at a 180° angle, the BeH_2 molecule is linear.

Because both promotion and hybridization require an input of energy, the formation of a set of singly occupied hybrid atomic orbitals is energetically uphill. The overall process of forming a compound with hybrid orbitals will be energetically favorable *only* if the amount of energy released by the formation of covalent bonds is greater than the amount of energy used to form the hybrid orbitals (Figure **3.6.6**). As we will see, some compounds are highly unstable or do not exist because the amount of energy required to form hybrid orbitals is greater than the amount of energy that would be released by the formation of additional bonds.

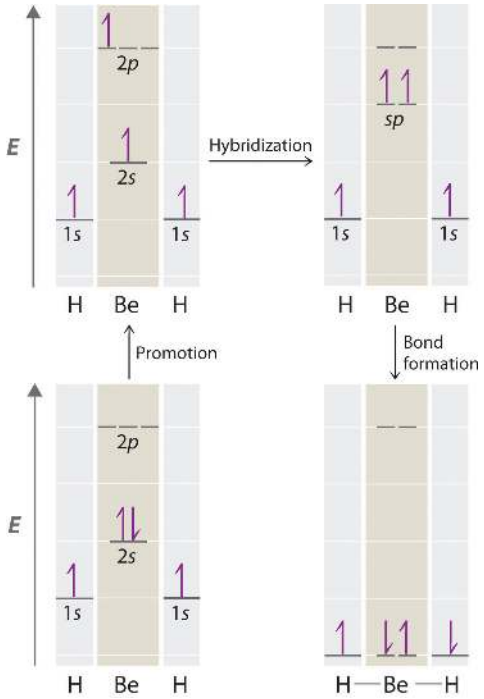


Figure **3.6.6**: A Hypothetical Stepwise Process for the Formation of BeH_2 from a Gaseous Be Atom and Two Gaseous H Atoms. The promotion of an electron from the 2*s* orbital of beryllium to one of the 2*p* orbitals is energetically uphill. The overall process of forming a BeH_2 molecule from a Be atom and two H atoms will therefore be energetically favorable *only* if the amount of energy released by the formation of the two Be–H bonds is greater than the amount of energy required for promotion and hybridization.

The concept of hybridization also explains why boron, with a $2s^2 2p^1$ valence electron configuration, forms three bonds with fluorine to produce BF_3, as predicted by the Lewis and VSEPR approaches. With only a single unpaired electron in its ground state, boron should form only a single covalent bond. By the promotion of one of its 2*s* electrons to an unoccupied 2*p* orbital, however, followed by the hybridization of the three singly occupied orbitals (the 2*s* and two 2*p* orbitals), boron acquires a set of three equivalent hybrid orbitals with one electron each, as shown here:

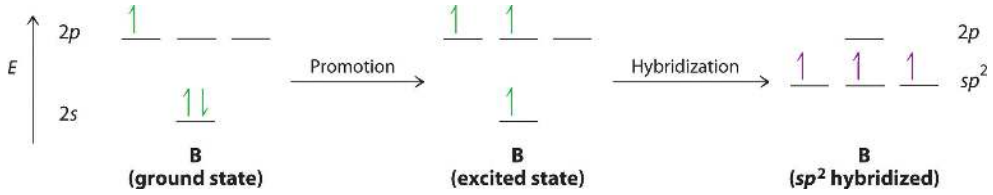


Figure **3.6.7**). Because the hybrid atomic orbitals are formed from one *s* and two *p* orbitals, boron is said to be sp^2 *hybridized* (pronounced "s-p-two" or "s-p-squared"). The singly occupied sp^2 hybrid atomic orbitals can overlap with the singly occupied orbitals on each of the three F atoms to form a trigonal planar structure with three energetically equivalent B–F bonds.

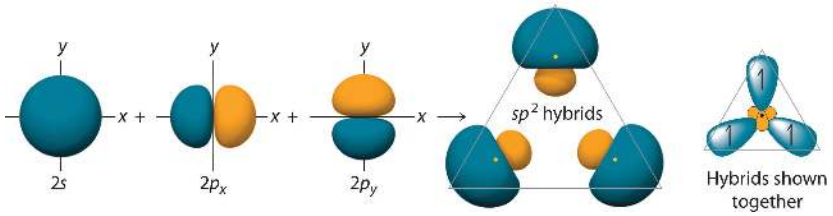


Figure **3.6.8**: Formation of sp^2 Hybrid Orbitals. Combining one *ns* and two *np* atomic orbitals gives three equivalent sp^2 hybrid orbitals in a trigonal planar arrangement; that is, oriented at 120° to one another.

Looking at the $2s^22p^2$ valence electron configuration of carbon, we might expect carbon to use its two unpaired 2*p* electrons to form compounds with only two covalent bonds. We know, however, that carbon typically forms compounds with four covalent bonds. We can explain this apparent discrepancy by the hybridization of the 2*s* orbital and the three 2*p* orbitals on carbon to give a set of four degenerate sp^3 hybrid orbitals, each with a single electron:

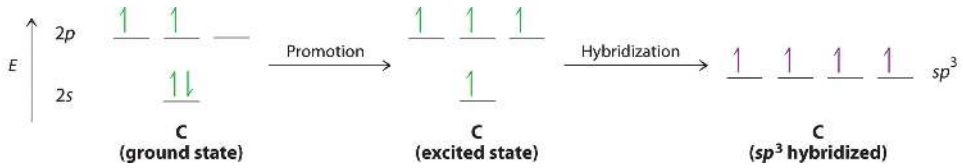


Figure **3.6.9**). Like all the hybridized orbitals discussed earlier, the sp^3 hybrid atomic orbitals are predicted to be equal in energy. Thus, methane (CH_4) is a tetrahedral molecule with four equivalent C-H bonds.

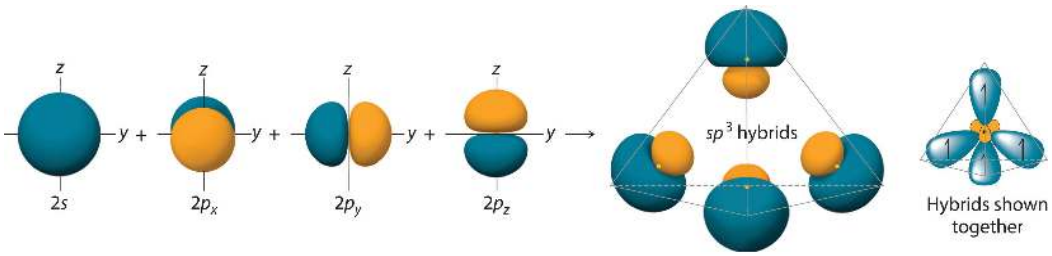


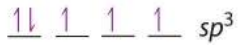
Figure **3.6.10**: Formation of sp^3 Hybrid Orbitals. Combining one *ns* and three *np* atomic orbitals results in four sp^3 hybrid orbitals oriented at 109.5° to one another in a tetrahedral arrangement.

In addition to explaining why some elements form more bonds than would be expected based on their valence electron configurations, and why the bonds formed are equal in energy, valence bond theory explains why these compounds are so stable: the amount of energy released increases with the number of bonds formed. In the case of carbon, for example, much more energy is released in the formation of four bonds than two, so compounds of carbon with four bonds tend to be more stable than those with only two. Carbon does form compounds with only two covalent bonds (such as CH_2 or CF_2), but these species are highly reactive, unstable intermediates that only form in certain chemical reactions.

> *Valence bond theory explains the number of bonds formed in a compound and the relative bond strengths.*

The bonding in molecules such as NH_3 or H_2O, which have lone pairs on the central atom, can also be described in terms of hybrid atomic orbitals. In NH_3, for example, N, with a $2s^22p^3$ valence electron configuration, can hybridize its 2*s* and 2*p* orbitals to produce four sp^3 hybrid orbitals. Placing five valence electrons in the four hybrid orbitals, we obtain three that are singly occupied and one with a pair of electrons:

https://chem.libretexts.org/@go/page/326159



The three singly occupied sp^3 lobes can form bonds with three H atoms, while the fourth orbital accommodates the lone pair of electrons. Similarly, H_2O has an sp^3 hybridized oxygen atom that uses two singly occupied sp^3 lobes to bond to two H atoms, and two to accommodate the two lone pairs predicted by the VSEPR model. Such descriptions explain the approximately tetrahedral distribution of electron pairs on the central atom in NH_3 and H_2O. Unfortunately, however, recent experimental evidence indicates that in NH_3 and H_2O, the hybridized orbitals are *not* entirely equivalent in energy, making this bonding model an active area of research.

Multiple Bonds

In valence bond theory double and triple bonds are formed from unhybridized p orbitals. For example in ethylene (C_2H_4), both C atoms have three bonding pairs and no lone pairs, meaning they are both sp^2 hybridized, similar to the BF_3 example above. However because C has one more valence electron than B, the remaining unhybridized p orbital is occupied by 1 electron (Figure **3.6.11**). The double bond between the two C atoms is formed because the unhybridized p orbitals on each C atom overlap and form a pi bond, the second bond in a double bond. An sp hybridized carbon would have two unhybridized p orbitals available for pi bonding and could form a triple bond.

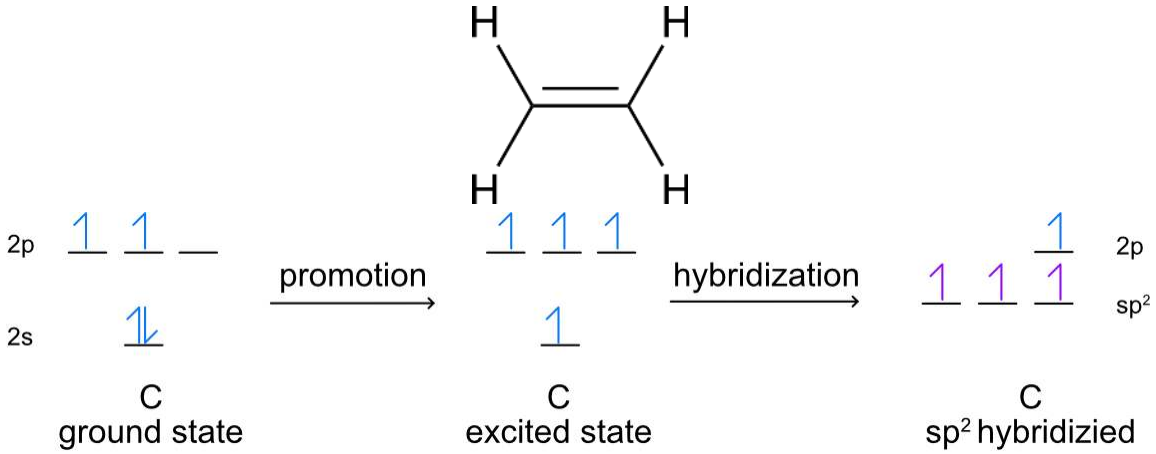


Figure **3.6.11**: Lewis structure of ethylene (left) and the formation of 3 sp^2 hybridized orbitals on C, leaving one unhybridized p orbital available for pi bonding. (CC BY-NC-SA; Catherine McCusker)

Example 3.6.1

Use the VSEPR model to predict the number of electron pairs and molecular geometry in each compound and then describe the hybridization and bonding of all atoms except hydrogen.

a. H_2S
b. $CHCl_3$

Strategy:

1. Using the Lewis structure and VSEPR approach to determine the number of electron pairs and the molecular geometry of the molecule.
2. From the valence electron configuration of the central atom, predict the number and type of hybrid orbitals that can be produced. Fill these hybrid orbitals with the total number of valence electrons around the central atom and describe the hybridization.

Solution

a. H_2S has four electron pairs around the sulfur atom with two bonded atoms, so the VSEPR model predicts a molecular geometry that is bent. Sulfur has a $3s^23p^4$ valence electron configuration with six electrons, but by hybridizing its 3*s* and 3*p* orbitals, it can produce four sp^3 hybrids. If the six valence electrons are placed in these orbitals, two have electron pairs and two are singly occupied. The two sp^3 hybrid orbitals that are singly occupied are used to form S–H bonds, whereas the other

two have lone pairs of electrons. Together, the four sp^3 hybrid orbitals produce an approximately tetrahedral arrangement of electron pairs, which agrees with the molecular geometry predicted by the VSEPR model.

b. The $CHCl_3$ molecule has four valence electrons around the central atom. In the VSEPR model, the carbon atom has four electron pairs, and the molecular geometry is tetrahedral. Carbon has a $2s^2 2p^2$ valence electron configuration. By hybridizing its 2*s* and 2*p* orbitals, it can form four sp^3 hybridized orbitals that are equal in energy. Eight electrons around the central atom (four from C, one from H, and one from each of the three Cl atoms) fill three sp^3 hybrid orbitals to form C–Cl bonds, and one forms a C–H bond. Similarly, the Cl atoms, with seven electrons each in their 3*s* and 3*p* valence subshells, can be viewed as sp^3 hybridized. Each Cl atom uses a singly occupied sp^3 hybrid orbital to form a C–Cl bond and three hybrid orbitals to accommodate lone pairs.

Exercise 3.6.1

Use the VSEPR model to predict the number of electron pairs and molecular geometry in each compound and then describe the hybridization and bonding of all atoms except hydrogen.

a. the BF_4^- ion
b. hydrazine ($H_2N–NH_2$)

Answer

Answer a

B is sp^3 hybridized; F is also sp^3 hybridized so it can accommodate one B–F bond and three lone pairs. The molecular geometry is tetrahedral.

Answer b

Each N atom is sp^3 hybridized and uses one sp^3 hybrid orbital to form the N–N bond, two to form N–H bonds, and one to accommodate a lone pair. The molecular geometry about each N is trigonal pyramidal.

Summary

Hybridization increases the overlap of bonding orbitals and explains the molecular geometries of many species whose geometry cannot be explained using a VSEPR approach. The *localized bonding* model (called **valence bond theory**) assumes that covalent bonds are formed when atomic orbitals overlap and that the strength of a covalent bond is proportional to the amount of overlap. It also assumes that atoms use combinations of atomic orbitals (*hybrids*) to maximize the overlap with adjacent atoms. The formation of **hybrid atomic orbitals** can be viewed as occurring via **promotion** of an electron from a filled ns^2 subshell to an empty *np* valence orbital, followed by **hybridization**, the combination of the orbitals to give a new set of (usually) equivalent orbitals that are oriented properly to form bonds. The combination of an *ns* and an *np* orbital gives rise to two equivalent **sp hybrids** oriented at 180°, whereas the combination of an *ns* and two or three *np* orbitals produces three equivalent $\boldsymbol{sp^2}$ **hybrids** or four equivalent $\boldsymbol{sp^3}$ **hybrids**, respectively. The spatial orientation of the hybrid atomic orbitals is consistent with the geometries predicted using the VSEPR model.

References

1. Kotz, John C., Paul M. Treichel., John R. Townsend. *Chemistry and Chemical Reactivity.* 7th ed. Australia: Thomson Brooks/Cole., 2009. Print.
2. Shaik, Sason S., Hiberty, Philippe C. *A Chemist's Guide to Valence Bond Theory*. Hoboken, New Jersey: Wiley, 2008. Print.
3. Wijesekera, Ramanee D. *Coordination Compounds: Bonding, Structure and Nomenclature*. Oxford, U.K.: Alpha Science International Ltd., 2008. Print.
4. Overlap of Atomic Orbitals to form Molecular Orbitals. http://www.chm.davidson.edu/vce/MolecularOrbitals/overlap/overlap1.html

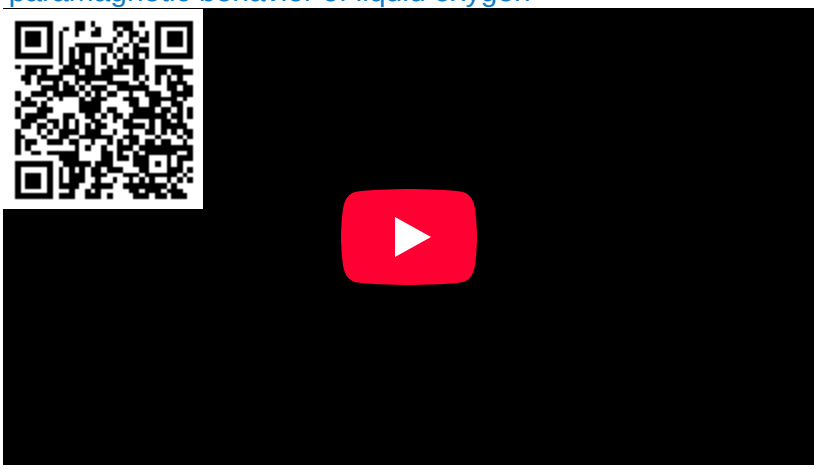
3.6: Valence Bond Theory is shared under a CC BY-NC-SA 4.0 license and was authored, remixed, and/or curated by LibreTexts.

SECTION OVERVIEW

3.7: Molecular Orbital Theory

VSPER and valence bond theory have their advantages. They are easily applied using atomic properties like valence electron configuration and electronegativity. They can easily and accurate predict many molecular properties such as molecular shape and bond angles, bond lengths and strengths, polarity, and chirality. Like any theory, there are disadvantages and places where VSPER and valence bond theory fail to explain experimental data. For example, diatomic oxygen (O_2) is a very simple molecule. Both the Lewis structure and valence bond theory would predict that O_2 has a double bond and each O atom has two lone pairs of electrons, and is a diamagnetic molecule (all the electrons are paired). Experiment shows that O_2 is in fact paramagnetic (has unpaired electrons). VSEPR and valence bond theory are not always useful at predicting reactivity. For example, those theories can predict that CO has a triple bond and one lone pair on both O and C. However those theories can't predict if C or the O of CO would react with a Lewis acid.

A video showing the paramagnetic behavior of liquid oxygen



Molecular orbital theory is another bonding theory that can work in places where VSEPR and valence bond fail. Similar to valence bond theory, molecular orbital theory involves the mixing of atomic orbitals, but rather than mixing multiple atomic orbitals on the central atom to form hybrid orbitals atomic orbitals from multiple atoms are mixed together to form molecular orbitals.

Topic hierarchy

3.7A: Orbital Overlap

3.7B: Homonuclear Diatomic Molecules

3.7C: Heteronuclear Diatomic Molecules

3.7: Molecular Orbital Theory is shared under a CC BY-NC-SA 4.0 license and was authored, remixed, and/or curated by LibreTexts.

3.7A: Orbital Overlap

Molecular orbital theory is based on the overlap of atomic orbitals, linear combinations of atomic orbitals are taken to form atomic orbitals. At a research level this involves computationally solving the overlap integral between the two or more contributing atomic orbital wavefunctions. In this course we will qualitatively assess orbital overlap primarily through visual inspection.

Sigma (σ) Molecular Orbitals

s orbitals

Similar to valence bond theory, the number of atomic orbitals combines is equal to the number of molecular orbitals formed. Therefore there are two types of molecular orbitals that can form from the overlap of two atomic *s* orbitals. The two types are illustrated in Figure **3.7A.1**. The in-phase combination produces a lower energy bonding σ_s molecular orbital in which most of the electron density is directly between the nuclei. The out-of-phase addition (which can also be thought of as subtracting the wave functions) produces a higher energy antibonding σ_s^* molecular orbital in which there is a node between the nuclei. The asterisk signifies that the orbital is an antibonding orbital. Electrons in a σ_s orbital are attracted by both nuclei at the same time and are more stable (of lower energy) than they would be in the isolated atoms. Adding electrons to these orbitals creates a force that holds the two nuclei together, so we call these orbitals bonding orbitals. Electrons in the σ_s^* orbitals are located well away from the region between the two nuclei. The attractive force between the nuclei and these electrons pulls the two nuclei apart. Hence, these orbitals are called antibonding orbitals.

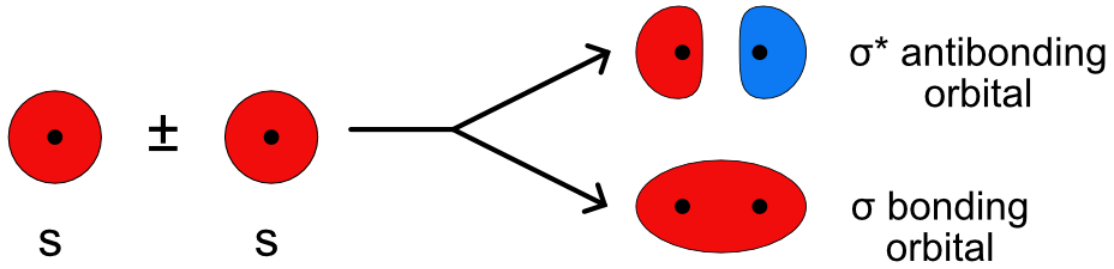


Figure **3.7A.1**: Sigma (σ) and sigma antibonding (σ*) molecular orbitals are formed by the combination of two s atomic orbitals. (CC BY-NC-SA; Catherine McCusker)

p orbitals

Unlike s orbitals, *p* orbitals have two lobes with opposite phases, indicated by shading the orbital lobes different colors. When orbital lobes of the same phase overlap, constructive wave interference increases the electron density between the two nuclei. When regions of opposite phase overlap, the destructive wave interference decreases electron density and creates nodes between the two nucei. When *p* orbitals overlap end to end, they create σ and σ* orbitals. If the two *p* orbitals are located along the bond axis (assumed to be the *z*-axis unless otherwise stated), they overlap end to end and form σ_p (bonding) and σ_p^* (antibonding) as illustrated in (Figure **3.7A.2**. Just as with *s*-orbital overlap, the asterisk indicates the orbital with a node between the nuclei, which is a higher-energy, antibonding orbital.

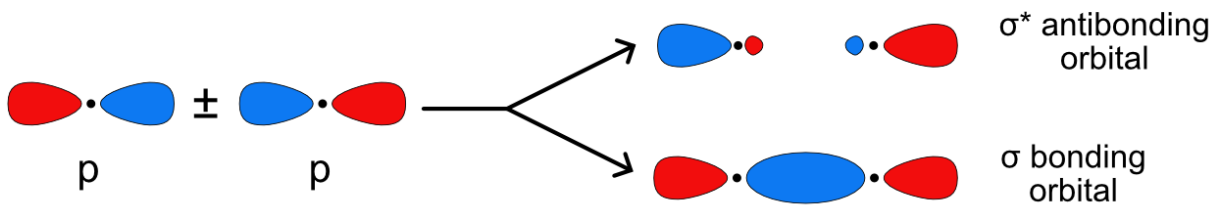


Figure **3.7A.2**: Sigma (σ) and sigma antibonding (σ*) molecular orbitals are formed by the combination of two p atomic orbitals. (CC BY-NC-SA; Catherine McCusker)

d orbitals

Recall the shapes and orientations of the five d orbitals from chapter 2. Three of the d orbitals (d_{xy}, d_{xz}, and d_{yz}) have electron density between the axes and nodes along the axes. Two of the d orbitals (d_{z^2} and $d_{x^2-y^2}$) have electron density along the axes. Only the latter two d orbitals can possibly form sigma bonds. These will be similar to sigma bonds formed from p orbitals, when two lobes of the same phase overlap the electron density between the two nuclei increases and sigma bond is formed as shown in Figure **3.7*A*.3**

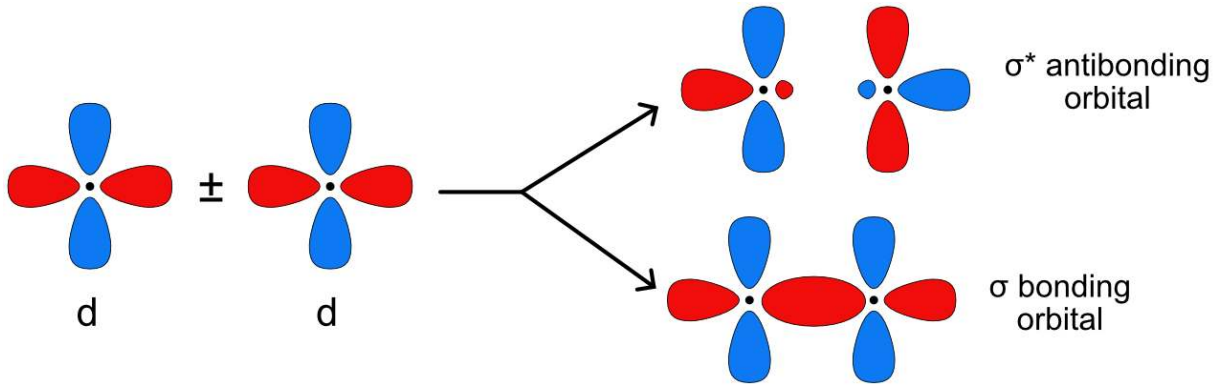


Figure **3.7*A*.3**: Sigma (σ) and sigma antibonding (σ*) molecular orbitals formed from two $d_{x^2-y^2}$ orbitals. (CC BY-NC-SA; Catherine McCusker)

Pi (π) Molecular Orbitals

If two p orbitals are orientated perpendicular to the bond axis they give rise to a pi (π) bonding molecular orbital and a (π^*) antibonding molecular orbital, as shown in Figure **3.7*A*.4**. The in phase overlap forms a pi bonding orbital, which has increased electron density between the nuclei above and below the internuclear bond axis, with a single node along the bond axis. For the out-of-phase combination, an antibonding orbital is formed with two nodal planes created, one along the internuclear axis and a perpendicular one between the nuclei.

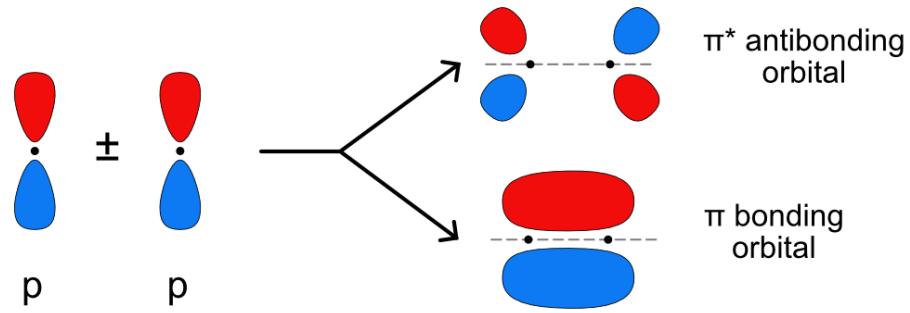


Figure **3.7*A*.4**: Pi (π) and pi antibonding (π*) molecular orbitals are formed by the combination of two perpendicular p atomic orbitals. The grey dashed line indicates the one node containing the internuclear bond axis. (CC BY-NC-SA; Catherine McCusker)

The d orbitals with electron density between the axes (d_{xy}, d_{xz}, and d_{yz}) can also form pi bonds in the same way that p orbitals can, but an s orbital doesn't have the correct geometry to form pi bonds.

Delta (δ) Molecular Orbitals

In main group chemistry only sigma and pi bonds are possible. When two metal atoms are bonded together, a third type of bond, a delta bond, is possible. Two d orbitals orientated face-to-face along the internuclear bond axis ((d_{xy} or $d_{x^2-y^2}$ if the bond is on the z axis) will overlap to form delta bonding and antibonding orbitals as shown in Figure **3.7*A*.5**. The in-phase bonding combination has four areas of electron density above and below the two nuclei, with a vertical and a horizontal node along the internuclear bond axis. In the out-of-phase combination there is a third node bisecting the internuclear axis. With delta bonding it it possible to have quadruple or even quintuple bonds between two metal centers, although in practice quintuple bonds are exceedingly rare and have only been observed in a few chromium and molybdenum dimers.

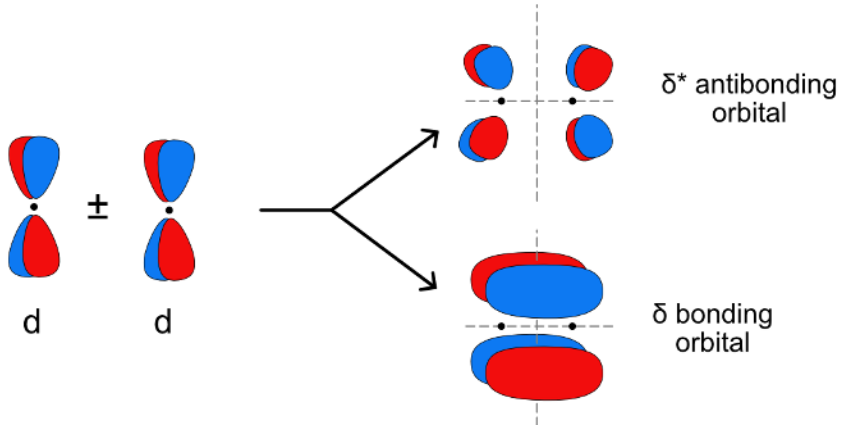


Figure **3.7A.5**: Delta (δ) and delta antibonding (δ*) molecular orbitals are formed by the combination of two face-to-face d atomic orbitals. The grey dashed lines indicate the two nodes containing the internuclear bond axis. (CC BY-NC-SA; Catherine McCusker)

Summary

Bonding orbitals are ones that increase the amount of electron density between the two nuclei relative to the atomic orbitals. Antibonding orbitals are ones that decrease the amount of electron density between the two nuclei relative to the atomic orbitals. Bonding orbitals will have fewer nodes and be lower in energy than antibonding orbitals.A sigma (σ) orbital is one that has **no nodes** along the internuclear bond axis. Any two orbitals (s, p, or d) that are oriented along the bonding axis can form a sigma bond. A pi (π) orbital is one that has **one node** containing the internuclear bond axis. A pi bond can be formed from p or d orbitals orientated perpendicular to the bond axis. A delta (δ) orbital is one that has **two nodes** containing the internuclear bond axis. Only d (or f) orbitals can form delta bonds so they are only possible between two metal atoms.

Multiple Bonds

- Single bonds are formed from **1** sigma bond
- Double bonds are formed from **1** sigma bond and **1** pi bond
- Triple bonds are formed from **1** sigma bond and **2** pi bonds
- Quadruple bonds (only found between two metal atoms) are formed from **1** sigma bond, **2** pi bonds and **1** delta bond
- Quintuple bonds (only found between two metal atoms) are formed from **1** sigma bond, **2** pi bonds and **2** delta bonds

Factors That Influence Covalent Interaction

Now let us refine our understanding of molecular orbitals and molecular orbitals diagrams. Not all atomic orbitals can be combined to form molecular orbitals, and the degree of overlap or covalent interaction between two atomic orbitals can vary lot. What are the criteria according to which we can decide if covalent interaction between two atomic orbitals is possible, and if so how much? There are three criteria to consider; the symmetry criterion, the overlap criterion, and the energy criterion. The symmetry criterion says that If there is a combination of atomic orbitals with bonding and the antibonding interactions that do not cancel out then there is a bonding interaction. The overlap criterion states that the better the atomic orbitals (of appropriate symmetry!) overlap the stronger the covalent interaction. The energy criterion states that the closer the orbitals are in energy the more covalent interaction between them. We will discuss all three criteria in greater detail below.

Criteria for Covalent Interactions

- **Symmetry Criterion:** If there is a combination of atomic orbitals with bonding and the antibonding interactions that do not cancel out then there is a bonding interaction.
- **Overlap Criterion:** The better the atomic orbitals overlap the stronger the covalent interaction.
- **Energy Criterion:** The closer the atomic orbitals in energy the stronger the covalent interaction.

The Overlap Criterion

Let us now look at each criterion in more detail. Let us start with the one we can probably most easily understand, the overlap criterion. The greater the overlap the greater the covalent interaction. The overlap can be estimated according to three rules.

Rule 1: Distance

The first rule says that the overlap is the greater the smaller the distance between the two orbitals. This means that a small distance between the orbital leads to a strongly bonding and a strongly anti-bonding orbital, respectively while a large distance leads to a weakly bonding and a weakly anti-bonding orbital. When the distance is small then there is a large energy difference between the bonding and the anti-bonding molecular orbital, when the distance is large then the energy difference is small (Figure **3.7A.6**).

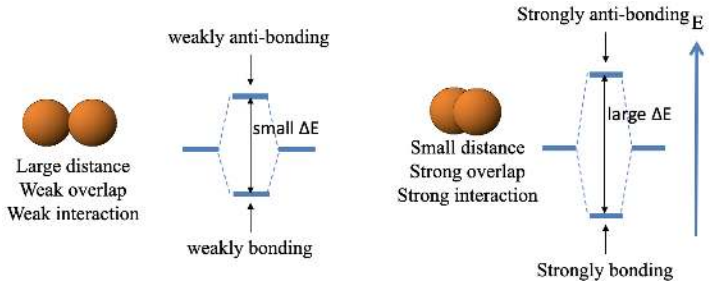


Figure **3.7A.6** The effect of the distance between atomic orbitals on the energy difference of the resulting molecular orbitals.

Rule 2: Size

Rule 2 states that a large diffuse orbital tends to overlap better (interact more strongly) with another orbital when this orbital is also a large diffuse orbital. A small, less diffuse orbital tends to interact more strongly with another small orbital. If we combine a large orbital with a small orbital however, then this typically does not lead to good overlap and thus weak interaction. We can qualitatively understand this by looking at the image below (Figure **3.7A.7**).

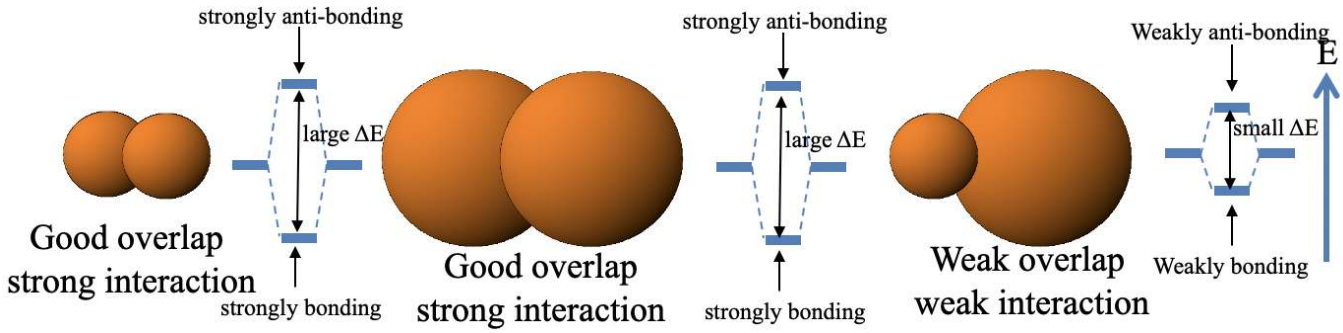


Figure **3.7A.7** Relationships between orbital size and covalent interactions.

Only a small volume fraction of the large orbital can overlap with the small orbital due to the small size of the small orbital. Due that small overlap the bonding orbital is only weakly bonding, and the anti-bonding is only weakly anti-bonding. The energy difference between the bonding and the anti-bonding MO is small. In the other two cases, the bonding orbitals tend to be strongly bonding, and the anti-bonding ones strongly anti-bonding. The energy differences between the MOs tend to be large.

Rule 3: Orientation

Rule 3 says that that orbitals that overlap in σ-fashion tend to interact more strongly than orbitals that overlap in π-fashion, which interact more strongly than overlap in δ-fashion. One can see easily from the image below that two p orbitals that have the same distance *d* from each other overlap much more when they overlap in σ-fashion compared to π-fashion (Figure **3.7A.8**).

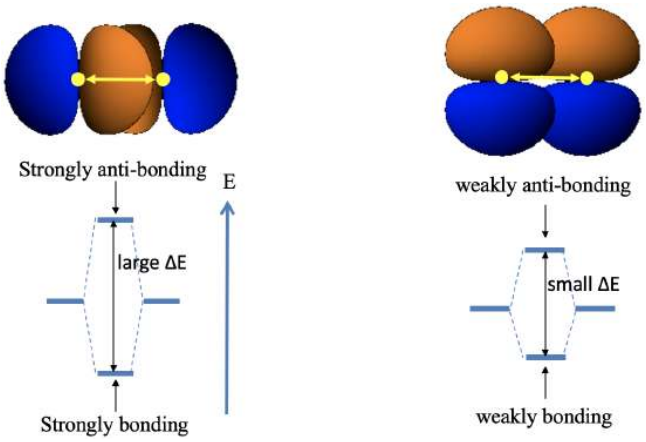


Figure **3.7A.8** Visual representation of orbitals overlapping in σ-fashion vs orbitals overlapping in π-fashion

This is because in the first case they point toward each other, and the orbital overlap is on the bond axis, while in the latter case they are oriented parallel to each other, and the orbital overlap is above and below the bond axis. This implies that σ-overlap leads to more strongly bonding and anti-bonding orbitals with a larger energy gap between them compared to π-overlap and π-overlap leads to more strongly bonding and anti-bonding orbitals compared to δ-overlap.

The Energy Criterion

The energy criterion states that the covalent interaction between atomic orbitals is larger the smaller the energy difference is between the atomic orbitals. We can understand this qualitatively when considering that orbitals are waves, and waves of similar energy interfere more significantly with each other than waves with different energies. Just imagine two waves with very different wavelengths associated with very different energies. Would they interfere effectively? No, they wouldn't. Rather, two waves with very similar wavelengths would interfere better. Because greater energy difference means less interaction, molecular orbitals that result from the interaction of two atomic orbitals with large energy difference are much more similar in shape, size, and location compared to molecular orbitals that result from atomic orbitals with similar energy.

The greatest covalent interaction is expected when the energy between the two orbitals is exactly the same. This is only possible when two, same orbitals A of the two same atoms overlap. In this case we form a perfect covalent bond with electrons exactly equally shared between the orbitals. The maximum of the amplitude of the bonding molecular orbital is exactly in the middle between the two atoms. In the molecular orbital diagram the energy difference between the bonding MO and the atomic orbitals is about the same as the energy difference between the anti-bonding MO and the atomic orbitals. Electrons the bonding (or antibonding) MO are equally shared between the atoms (Figure **3.7A.9**)

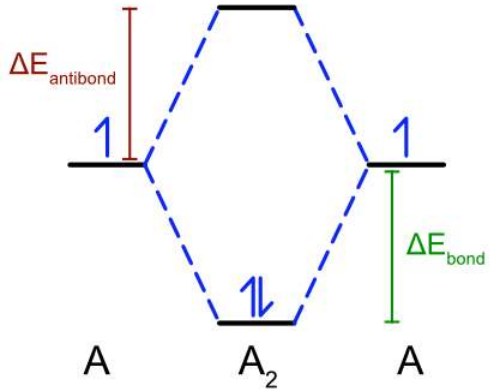


Figure **3.7A.9** Covalent interaction occurring when the energy between the two atomic orbitals is exactly the same.

Now let us make the energy of the two atomic orbitals somewhat different. Because they are different we denote the atomic orbitals A and B now, whereby we choose the energy of orbital A to be somewhat higher than that of orbital B. Overlap between the atomic orbital still produces covalent interaction yielding a bonding and an anti-bonding molecular orbital. However, the energy difference of the molecular orbitals to the two atomic orbitals is no longer the same. The antibonding MO is now closer to the atomic orbital

with the higher energy, and the bonding MO is now closer in energy to the atomic orbital with the lower energy. This has another consequence. The bonding molecular orbital is now localized primarily at atom A, and the anti-bonding orbital is located primarily at atom B. An electron in the bonding MO is now primarily localized at atom B. This means the bond is a polar covalent bond which is polarized toward atom B (Figure **3.7*A*.10**).

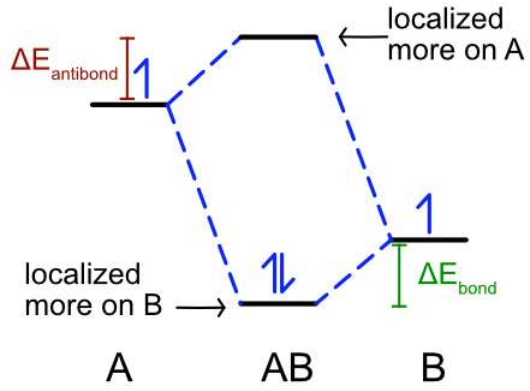


Figure **3.7*A*.10** An example of covalent interaction occurring when the energy between the two atomic orbitals is somewhat different

Now let us make the energy difference between the two atomic orbitals of the atoms A and B very large (Figure **3.7*A*.11**). In this case, the bonding MO is energetically very close to the atomic orbital of atom B, and is localized almost exclusively at atom B. Actually, the bonding MO closely resembles the atomic orbital of atom B in shape, size and localization. In other words, the atomic orbital of B has hardly changed due to the very weak covalent interaction resulting from the large energy difference between the atomic orbitals. Vice versa, the antibonding orbital is energetically very close to the atomic orbital of atom A, and is localized almost completely at atom A. The antibonding MO is very close to the atomic orbital in shape, size, and location. Due to the weak covalent interaction, there is almost no change to the atomic orbital of A.

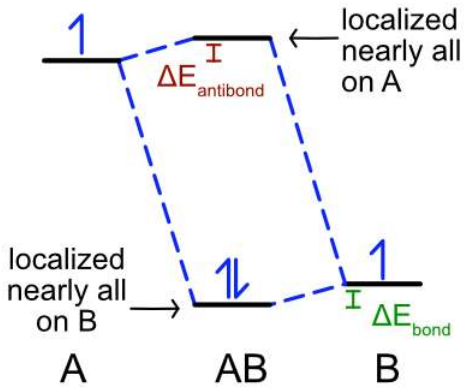


Figure **3.7*A*.11** Covalent interaction occurring when the energy difference between two atomic orbitals is very large.

Another conclusion that we can draw is that bonding electrons are located closer to the atom with the atomic orbital of lower energy, and antibonding electrons are located closer to the atoms with the atomic orbital of higher energy. Orbital energy is correlated with electronegativity. For orbitals of the same type and the same elements, orbitals with higher electronegativity have lower energy. For example, a 2s orbital of fluorine has a lower energy than a 2s orbital of oxygen because the electronegativity of fluorine is higher. Bonding electrons are therefore located primarily at the more electronegative atom, while anti-bonding electrons are located primarily at the less electronegative atom. When there are enough anti-bonding orbitals occupied it is possible that the overall polarity in the molecule is such that the dipole moment points toward the more electro-positive atom. An example is carbon monoxide which is slightly polarized toward the carbon atom. We will discuss the MO diagram of the carbon monoxide in detail later.

The Symmetry Criterion

Lastly, let us look at the symmetry criterion. The symmetry criterion tells us if a covalent interaction between orbitals is possible based on the relative orientation of the orbitals. Only if the bonding and antibonding interactions do not cancel out, a bonding interaction is possible, and we can construct molecular orbitals from atomic orbitals. Bonding and antibonding interactions cancel out when positive and negative interferences due to orbital overlap are exactly equal. This can be determined by inspection of orbital overlap.

For example, let us look at the orbital overlap between the 1s orbitals of hydrogen and the $2p_z$ orbital of oxygen in the water molecule (Figure **3.7*A*.12**).

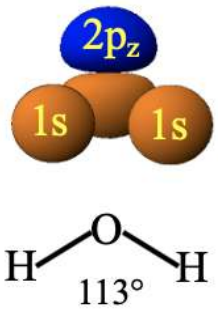


Figure **3.7*A*.12** The orbital overlap between the 1s orbitals of hydrogen and the $2p_z$ orbital of oxygen in the water molecule

In the water molecule the orbitals are oriented to each other in a specific way because of the bent structure of the water molecule. Due to the bent structure of the water molecule the 1s orbitals overlap differently with the two lobes of the $2p_z$ molecule. The lobe that points downward overlaps more strongly than the lobe that points upward and the two lobes have different phases. Now we choose the phases of 1s orbitals so that bonding is maximized. We can see that the overlap of the 1s with the $2p_z$ orbital produces more constructive than destructive interferences. This is equivalent to saying that bonding and anti-bonding interactions do not cancel out. Therefore, the symmetry is “right”, we can construct molecular orbitals from this combination of atomic orbitals.

Can the $2p_x$ orbital of oxygen also combined with the 1s orbitals of the hydrogen atom to form molecular orbitals? The $2p_x$ orbital is oriented differently relative to the 1s orbitals in the H_2O molecule (Figure **3.7*A*.13**).

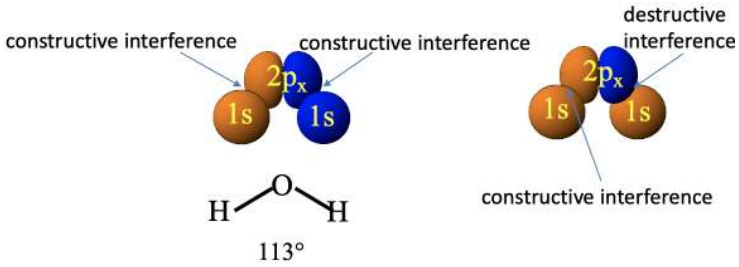


Figure **3.7*A*.13** The orbital overlap between the 1s orbitals of hydrogen and the $2p_x$ orbital of oxygen in the water molecule shown in two different orientations

In this case, we must choose the phases of the two 1s orbitals to be different so that bonding interactions are possible. The bonding and the antibonding interactions only do not cancel out if the left 1s orbital has the same phanse as the left lobe of the $2p_x$ orbital and the right 1s orbital has the same phase as the right lobe of the $2p_x$ orbital. If, for instance, we chose both 1s orbitals to be the same phase then the bonding interactions between the left lobe and the left 1s orbital would be canceled out by the equally strong anti-bonding interactions between the right lobe and the right 1s orbital. Overall, we see however, that if we select the phase of the 1s orbitals appropriately then the symmetry is “right” and we can create molecular orbitals from the atomic orbitals.

What about the interactions between the 1s orbitals and the $2p_y$ orbital (Figure **3.7*A*.14**)?

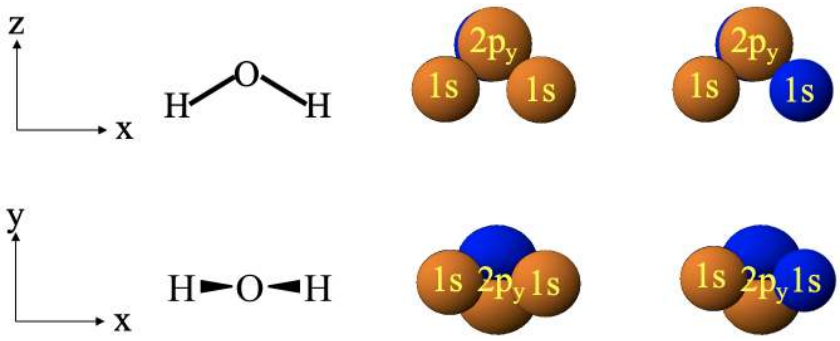


Figure **3.7A.14** The orbital overlap between the 1s orbitals of hydrogen and the $2p_y$ orbital of oxygen in the water molecule shown in two different orientations

In this case, the two 1s orbitals are in the plane of the page and the $2p_y$ orbital stands perpendicular to it. That makes the 1s orbitals overlap equally with both lobes of the $2p_y$ orbital. Because the two lobes of a $2p_y$ orbital must have different phases, the constructive and the destructive interferences will cancel out, no matter how we chose the phases of our 1s orbitals. That means there is no possibility to create orbital overlap in which bonding an anti-bonding interactions do not cancel out. Therefore, we cannot produce molecular orbitals from a combination of 1s and $2p_y$ orbitals. The $2p_y$ must remain non-bonding. You may be able to see the cancelation of the bonding and antibonding orbital overlap better if you choose your coordination system differently. Let us have the y-axis point up, and the x-axis point right (Figure **3.7A.9**, bottom). Now we look at the H_2O molecule from the bird perspective, and the $2p_y$ orbital is oriented vertically. The 1s orbitals are still on the x-axis. You can see the overlap between the 1s orbitals and the $2p_y$ orbital more clearly now. No matter how we choose the phase of our orbitals, the bonding and the anti-bonding interactions cancel out.

We have seen thus far that is is possible to decide about "right" and "wrong" symmetries by inspection, but we have noticed that this is not trivial. Generally, the more complex a molecule gets the more difficult it is to decide about "right" and "wrong" symmetry. In this course we will limit our discussion of molecular orbital theory to cases where we can determine symmetry by visual inspection only. In Advanced Inorganic we will use group theory as a tool to help us decide about "right" and "wrong" symmetry for orbital overlap in more complex molecules.

Example 3.7A.1: Molecular Orbitals

Predict what type (if any) of molecular orbital would result from the overlap of each pair of orbitals shown. The orbitals are all similar in energy. Assume the z axis is the bonding axis in all cases.

a. $s + p_z$
b. $p_x + p_z$
c. $d_{xz} + d_{xz}$
d. (d_{xy} + (d_{xy}

Solution

a. These both have electron density along the bond axis, so they would form a sigma bonding molecular orbital
b. This would be a non-bonding interaction. The p_x orbital has a node at z axis where it would overlap with the p_z orbital. This means there is no net overlap and on bond of any kind is formed.
c. These d orbitals are perpendicular to the bond axis, and would therefore form a pi bond.
d. These d orbitals are oriented face-to-face along the bond axis, so they would form a delta bonding orbital.

Exercise 3.7A.1

Label the molecular orbital shown as σ,π, or δ, bonding or antibonding, and indicate where any nodes occur.



Answer

The orbital is located along the internuclear axis, so it is a σ orbital. There is a node bisecting the internuclear axis, so it is an antibonding orbital.



Contributors and Attributions

- Adapted from

  Dr. Kai Landskron (Lehigh University). If you like this textbook, please consider to make a donation to support the author's research at Lehigh University: Click Here to Donate.

  Paul Flowers (University of North Carolina - Pembroke), Klaus Theopold (University of Delaware) and Richard Langley (Stephen F. Austin State University) with contributing authors. Textbook content produced by OpenStax College is licensed under a Creative Commons Attribution License 4.0 license. Download for free at http://cnx.org/contents/85abf193-2bd...a7ac8df6@9.110).

- Modified by Catherine McCusker (East Tennessee State University)

3.7A: Orbital Overlap is shared under a not declared license and was authored, remixed, and/or curated by LibreTexts.

- **Current page** has no license indicated.
- **8.5: Molecular Orbital Theory** by OpenStax is licensed CC BY 4.0. Original source: https://openstax.org/details/books/chemistry-2e.
- **3.1: Introduction into Molecular Orbital Theory** by Kai Landskron is licensed CC BY 4.0.

3.7B: Homonuclear Diatomic Molecules

Introduction

Using our knowledge of how the different types of atomic orbitals can overlap and form molecular orbitals (MOs), we can now construct molecular orbital diagrams for simple diatomic molecules. In these cases we can draw and visualize all the possible ways the valence atomic orbitals on both atoms can overlap.

Creating molecular orbital diagrams

- Include all the valence atomic orbitals on both atoms, whether they are empty or filled.
- The total number of atomic orbitals **MUST ALWAYS** equal the total number of molecular orbitals.
- Bonding molecular orbitals are more stable than the atomic orbitals and increase the electron density between the nuclei.
- Antibonding molecular orbitals are less stable than the atomic orbitals and decrease the electron density between the nuclei.
- Fill the completed diagram with electrons according to the Aufbau principle.

First Period Diatomic Molecules

Dihydrogen (H_2)

To generate the molecular orbital diagram for H_2, begin with the valence atomic orbitals. In the case of H_2, each H atom has a single 1s valence orbital. As seen previously, then two s orbitals overlap they form a σ bonding combination and a σ* antibonding combination. The σ bonding molecular orbital increases the electron density between the two H atoms and has no nodes, which makes this combination lower in energy than the H 1s atomic orbitals. The σ* antibonding molecular orbital has a node between the two H atoms and decreases the amount of electron density between the two H atoms, which makes this combination higher energy than the H 1s atomic orbitals. This is illustrated in Figure **3.7*B*.1**. Notice that combining **two** 1s atomic orbitals has given **two** MOs. Each H atom has one valence electron, so two electrons are placed in the σ bonding MO.

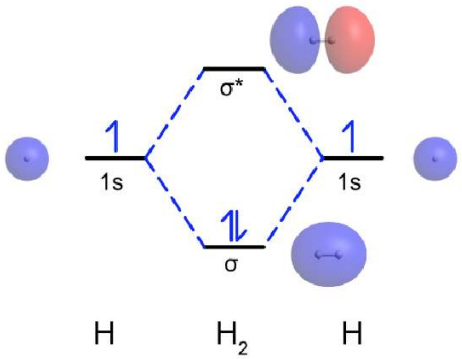


Figure **3.7*B*.1**: Molecular orbital diagram for H_2. Atomic and molecular orbitals calculated and visualized using WebMO. (CC BY-NC-SA; Catherine McCusker)

Bond order

Once filled with electrons, molecular orbital diagrams can be used to determine bond order in a molecule. Bond order is defined as the difference between the number of electron pairs occupying bonding and antibonding orbitals in the molecule. A bond order of 1 is equivalent to a single bond, a bond order of two is equivalent to a double bond, etc.

$$bond\ order = \frac{(bonding\ electrons) - (antibonding\ electrons)}{2} \tag{3.7B.1}$$

Equation 3.7B.1 can be used to calculate the bond order of a molecule from its molecular orbital diagram. In the H_2 example in Figure **3.7*B*.1** There are two electrons in the sigma bonding MO and no electrons in the sigma antibonding MO. Therefore the bond order is $\frac{2-0}{2} = 1$. This agrees with the picture of H_2 from the Lewis structure where the two H atoms are bonded by a single bond.

Other first period diatomics

Qualitatively, the molecular orbital diagrams He_2 and any ions of H_2 and He_2 will be the same because they all will involve the overlap of two 1s atomic orbitals. What will change is the number of electrons in the diagram, and therefore the bond order. Consider the two hydrogen ions, H_2^+ and H_2^- (Figure **3.7*B*.2**). The H_2^+ ion has one fewer electron than H_2, meaning the sigma bonding MO has one single electron in it and the sigma antibonding MO is still unoccupied. This results in H_2^+ having a bond order of 0.5. Non-integer bond order doesn't have a direct equivalent in Lewis theory. A bond order of 0.5 tell you that the molecule is (somewhat) stable relative to the two free atoms, but the bond will be weaker than a single bond. From this we can predict that H_2^+ will have a longer bond and a lower bond dissociation energy than H_2. H_2^- has one more electron than H_2, meaning the sigma bonding MO is filled and the additional electron occupies the sigma antibonding MO. This arrangement of electrons also results in a bond order of 0.5, so H_2^- is expected to have a bond strength and length similar to H_2^+. In the case of He_2, each He atom has two valence electrons so the completed MO diagram has two electrons in the sigma bonding MO and 2 electrons in the sigma antibonding MO. With both the bonding an antibonding MOs completely filled, He_2 has a bond order of 0. This means that He_2 isn't energetically favorable relative to two He atoms, and should not exist. In practice, He_2 can be observed at very low temperatures, but the "bond" between the He atoms is better described as van der Waals forces than a covalent bond.

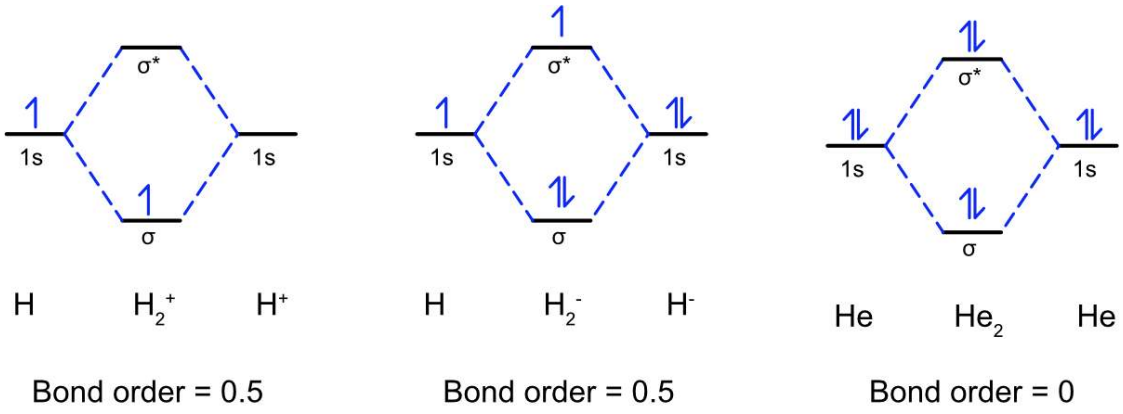
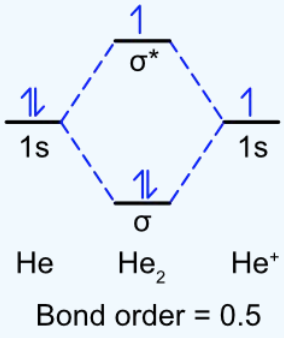


Figure **3.7*B*.2**: Molecular orbital diagrams for H_2^+ (left), H_2^- (center), and He_2 (right). (CC BY-NC-SA; Catherine McCusker)

Exercise 3.7*B*.1

Draw the molecular orbital diagram for He_2^+ and calculate its bond order.

Answer



He_2^+ has three valence electrons, two in the sigma bonding and 1 in the sigma antibonding. This makes the bond order 0.5.

Second Period Diatomic Molecules

The four simplest molecules we have examined so far involve molecular orbitals that derived from two 1*s* atomic orbitals. If we wish to extend our model to larger atoms, we will have to contend with higher atomic orbitals as well. One greatly simplifying principle here is that only the *valence* orbitals need to be considered. Core atomic orbitals such as 1*s* are deep within the atom and

well-shielded from the electric field of a neighboring nucleus, so that these orbitals largely retain their atomic character when bonds are formed. For second period molecules that means we need to consider the overlap of the 2s and the 2p atomic orbitals.

Dioxygen (O_2)

One major failing of Lewis and valence bond theories is their inability to explain why O_2 is paramagnetic. To construct a molecular orbital diagram for O_2 we have to consider the interactions between both the 2s and 2p atomic orbitals on each oxygen atom. Because of oxygen's high effective nuclear charge and the penetration of the 2s orbital there is a large energy difference between the 2s and the 2p atomic orbitals. This means the 2s and 2p atomic orbitals do not meet the energy criterion for overlap and cannot mix together. We will consider the overlap of the 2s and 2p orbitals separately.

The energy of the 2s atomic orbitals in oxygen are lower and the radius is larger when compared to the 1s orbitals of hydrogen, but qualitatively when two 2s orbitals overlap the will also form σ bonding and antibonding molecular orbitals as seen in Figure **3.7*B*.3**. As seen previously, the 2p orbitals can overlap to form both σ and π bonds. If we assume the O-O bond is on the z axis, this means the p_z orbitals on each O atom will lie along the bond axis and overlap to form σ_p bonding and σ_p* antibonding molecular orbitals. The p_x and p_y atomic orbitals both lie parallel to the bond axis and overlap to form a degenerate (same energy) pair of π_p bonding and π_p* antibonding molecular orbitals. As there is less orbital overlap in π bonds compared to σ bonds, the π_p bonding MO is stabilized less than the σ_p bonding MO and the π_p* antibonding MO is destabilized less than the σ_p* antibonding MO as shown in Figure **3.7*B*.3**. Each oxygen atom has six valence electrons, and so the center MO diagram is filled with 12 electrons. This leaves two electrons in the pair of π_p* antibonding MOs, and to maximize spin multiplicity according to Hund's rule one is placed in each of the MOs. Unlike the Lewis structure, the molecular orbital diagram for O_2 shows that oxygen is paramagnetic, having two unpaired electrons, in agreement with experimental observations. The MO diagram also predicts that O_2 has a bond order of 2 ($\frac{8-4}{2} = 2$) which agrees with Lewis and valence bond theories as well as experimental bond length.

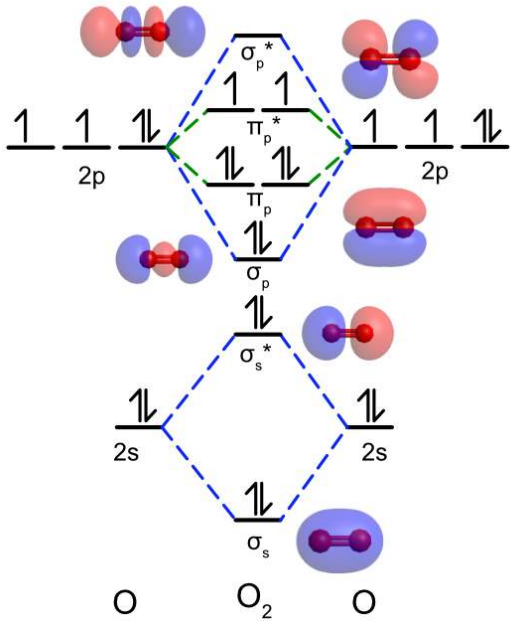


Figure **3.7*B*.3**: Qualitative molecular orbital diagram for O_2. Note that the energies of the atomic orbitals are not drawn to scale. Molecular orbitals calculated and visualized using WebMO. (CC BY-NC-SA; Catherine McCusker)

s-p mixing

In the molecular orbital diagram of O_2 we made the assumption that the 2s orbitals would only interact with other 2s orbitals and that 2p orbitals would only interact with other 2p orbitals because the energy difference between the 2s and 2p is large. However, in less electronegative atoms we can't make that same assumption. As Figure **3.7*B*.4** illustrates, in less electronegative elements, the energies of the 2s and 2p orbitals are closer in energy and meet the energy criterion for overlap. Therefore to construct molecular orbital diagrams for most of the second period elements (except O, F, and Ne) we need to consider how the s and p orbitals can possibly overlap.

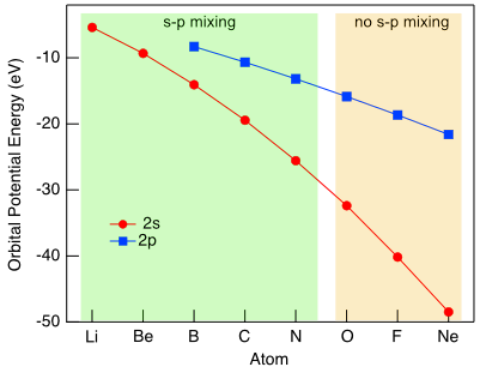


Figure **3.7*B*.4**: Trends in the 2s (red circle) and 2p (blue square) atomic orbital potential energies for second period elements. Energies from Meissler, G. L.; Fischer, P. J.; Tarr, D. A. *Inorganic Chemistry*, 5th Ed. (CC BY-NC-SA; Catherine McCusker)

The p orbital which lies along the bond axis (p_z if we assume z is the bond axis) can overlap with the s orbital and form a sigma bonding (and antibonding) molecular orbital. The remaining two p orbitals are perpendicular to the bond axis, which means the s orbital would overlap with the node of the p orbital resulting in no net overlap and no bonding (or antibonding) MO is formed (Figure **3.7*B*.5**). The s and p orbitals mixing together also means we have to consider what happens when more than two non-degenerate orbitals mix together. Based on the rules for forming molecular orbitals, the number of atomic orbitals that mix together is always equal to the number of molecular orbitals formed, as shown in Figure **3.7*B*.6**. When two atomic orbitals mix they form one bonding and one antibonding MO. When three atomic orbitals mix they form one bonding and one antibonding molecular orbital plus one intermediate molecular orbital that is approximately nonbonding, meaning it is neither stabilized nor destabilized relative to the atomic orbitals. When four atomic orbitals mix two bonding MOs, one strongly stabilized and one weakly stabilized, and two antibonding MOs, one strongly destabilized and one weakly destabilized, are formed.

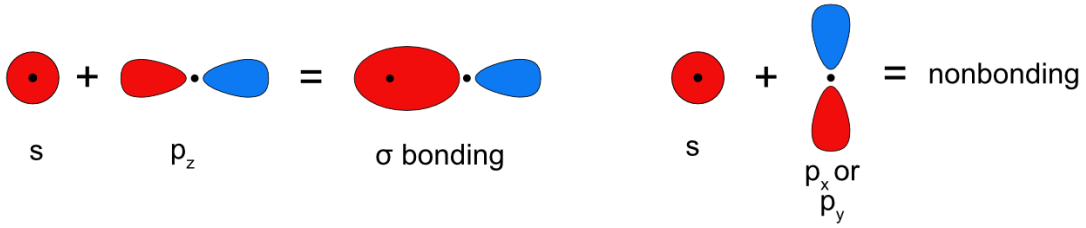


Figure **3.7*B*.5**: Assuming the bond axis is the z axis, the s and p_z will overlap to form a sigma bond (left) and the s and p_x or p_y do not have the correct orientation to overlap (right). (CC BY-NC-SA; Catherine McCusker)

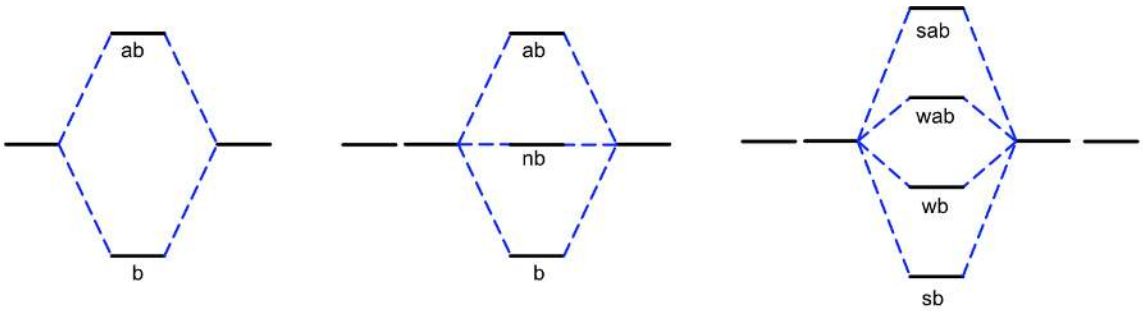


Figure **3.7*B*.6**: Two atomic orbitals (left) will overlap to form bonding (b) and antibonding (ab) molecular orbitals. Three atomic orbitals (center) will overlap to form bonding, nonbonding (nb), and antibonding molecular orbitals. Four atomic orbitals (right) will overlap to form strongly bonding (sb), weakly bonding (wb), weakly antibonding (wab) and strongly antibonding (sab) molecular orbitals. (CC BY-NC-SA; Catherine McCusker)

Dinitrogen (N_2)

Just like in O_2 the valence orbitals used to create the molecular orbital diagram of N_2 are the 2s and 2p orbitals on each N atom. Unlike the O_2 example above we cannot make the assumption that the 2s and 2p orbitals are too far apart in energy to mix together.

In the case of N_2 there are four total atomic orbitals that can overlap in a sigma fashion, the 2s and $2p_z$ orbitals from each N atom. As shown above, when four atomic orbitals overlap the result is two bonding MOs, labeled σ_s and σ_s* in Figure **3.7*B*.7** to be consistent with Figure **3.7*B*.3**, and two antibonding MOs, labeled σ_p and σ_p*. As the $2p_x$ and $2p_y$ cannot overlap with the 2s, they form a degenerate pair of pi bonding and antibonding MOs. Each N atom has 5 valence electrons, so the N_2 molecular orbital diagram is filled with 10 total electrons, giving a bond order of 3 ($\frac{8-2}{2}=3$). The biggest difference between the MO diagram of O_2 above and N_2 is the position of the σ_p MO. In O_2 it is a bonding orbital and is lower in energy than the π_p MOs. In N_2 this MO is weakly antibonding and is now higher than the π_p MOs. This change in molecular orbital ordering is the hallmark experimental observable showing s-p mixing occurs in N_2.

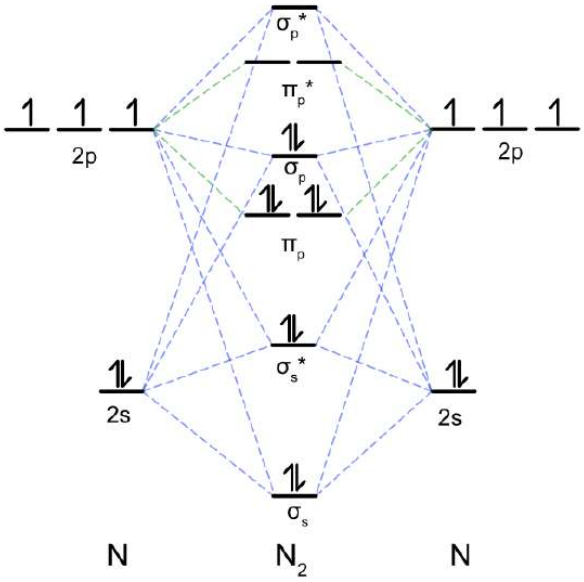


Figure **3.7*B*.7**: Qualitative molecular orbital diagram for N_2. Blue dashed lines indicate the mixing of 2s and $2p_z$ to form sigma bonding and antibonding MO's . The green dashed lines indicate the mixing of $2p_x$ and $2p_y$ to form pi bonding and antibonding MOs. Note that the energies of the atomic orbitals are not drawn to scale. (CC BY-NC-SA; Catherine McCusker)

Exercise 3.7*B*.2

Draw the complete molecular orbital diagram for B_2. Calculate the bond order and indicate whether it is diamagnetic or paramagnetic.

Answer

B_2 is paramagnetic with a bond order of 1. Bond order $=\frac{4-2}{2}=1$

https://chem.libretexts.org/@go/page/332304

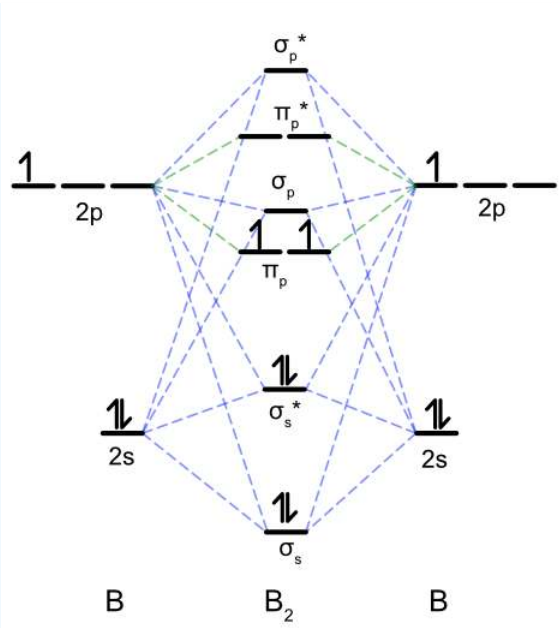
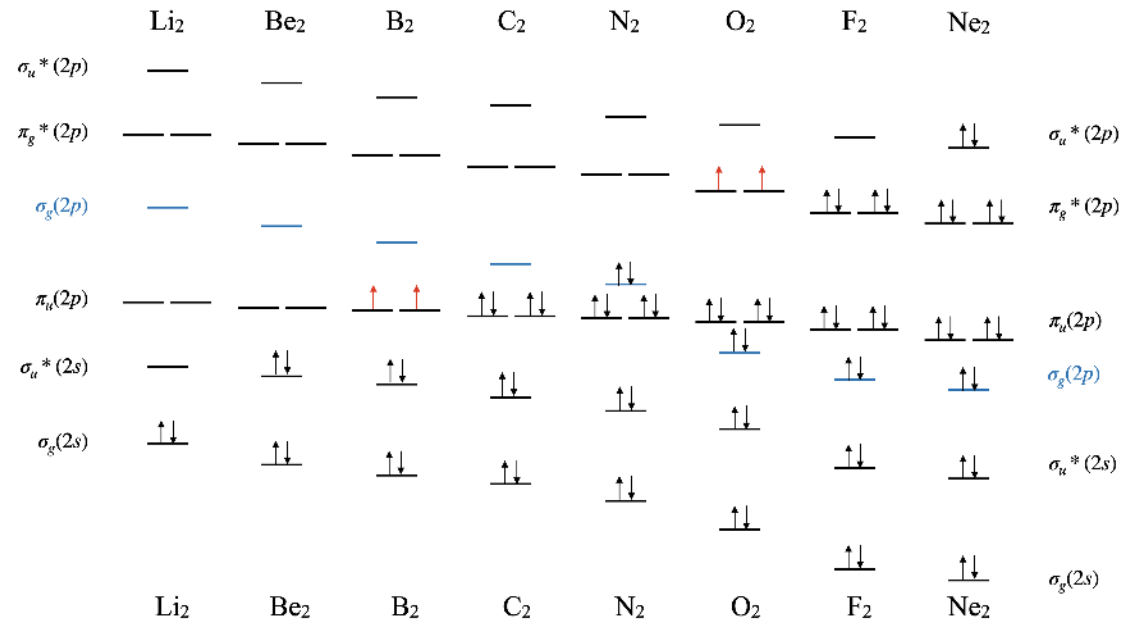


Figure for Exercise **3.7*B*.2**. Molecular orbital diagram of B_2. (CC-BY-NC-SA, Catherine McCusker)

Overview of Second Period Homonuclear Diatomic Molecules

Orbital mixing has significant consequences for the magnetic and spectroscopic properties of second period homonuclear diatomic molecules because it affects the order of filling of the $\sigma(2p)$ and $\pi(2p)$ orbitals. Early in period 2 (up to and including nitrogen), the $\pi(2p)$ orbitals are lower in energy than the $\sigma(2p)$ (see Figure **3.7*B*.1**). However, later in period 2, the $\sigma(2p)$ orbitals are pulled to a lower energy. This lowering in energy of $\sigma(2p)$ is not unique; all of the σ orbitals in the molecule are pulled to lower energy due to the increasing positive charge of the nucleus. The π orbitals in the molecule are also effected, but to a much lesser extent than σ orbitals. The reason has to do with the high penetration of s atomic orbitals compared to p atomic orbitals (recall our previous discussion on penetration and shielding, and its effect on periodic trends). The σ molecular orbitals have more s character and are thus their energy is more influence by increasing nuclear charge.

https://chem.libretexts.org/@go/page/332304



	Li_2	Be_2	B_2	C_2	N_2	O_2	F_2	Ne_2
Unpaired e⁻	0	0	2	0	0	2	0	0
Bond Order	1	0	1	2	3	2	1	0
Experimental* Bond Length (pm)	267.3	246.0	159.0	124.3	109.8	120.8	141.2	310.0

*Experimental bond lengths from "List of Experimental Diatomic Bond Lengths", NIST, https://cccbdb.nist.gov/diatomicexpbondx.asp

Figure **3.7*B*.8**: Molecular Orbital Energy-Level Diagrams for the Diatomic Molecules of the Period 2 Elements. In these diagrams, *only the valence molecular orbital energy levels for the **molecules** are shown here (atomic orbitals not shown for simplicity).* For Li_2 through N_2, the $\sigma(2p)$ orbital is higher in energy than the $\pi(2p)$ orbitals. In contrast, from O_2 onward, the $\sigma(2p)$ orbital is *lower* in energy than the $\pi(2p)$ orbitals due to the increase in the nuclear charge increases across the row. The experimental bond lengths correlate with calculated bond order. (CC-BY-NC-SA, Kathryn Haas)

Dilithium, Li_2 [$\sigma(2s)^2$]: This molecule has a bond order of one and is observed experimentally in the gas phase to have one Li-Li bond.

Diberylium, Be_2 [$\sigma(2s)^2\sigma(2s)^{*2}$]: This molecule has a bond order of zero due to equal number of electrons in bonding and antibonding orbitals. Although Be does not exist under ordinary conditions, it can be produced in a laboratory and its bond length measured (Figure **3.7*B*.9**). Although the bond is very weak, its bond length is surprisingly ordinary for a covalent bond of the second period elements.

Diboron, B_2 [$\sigma(2s)^2\sigma(2s)^{*2}\pi(2p)^2$]: The case of diboron is one that is much better described by molecular orbital theory than by Lewis structures or valence bond theory. This molecule has a bond order of one. The molecular orbital description of diboron also predicts, accurately, that dibornon is paramagnetic. The paramagnetism is a consequence of sp mixing, resulting in the $\sigma(2p)$ orbital at a higher energy than two degenerate $\pi(2p)$ orbitals.

Dicarbon, C_2 [$\sigma(2s)^2\sigma(2s)^{*2}\pi(2p)^4$]: This molecule has a bond order of two. Molecular orbital theory predicts two bonds with π symmetry, and no σ bonding. C_2 is rare in nature because its allotrope, diamond, is much more stable.

Dinitrogen, N_2 [$\sigma(2s)^2\sigma(2s)^{*2}\pi(2p)^4\sigma(2p)^2$]: This molecule is predicted to have a triple bond. This prediction is consistent with its short bond length and bond dissociation energy. The energies of the $\sigma(2p)$ and $\pi(2p)$ orbitals is very close, and their relative energy levels has been a subject of some debate.

Dioxygen, O_2 [$\sigma(2s)^2\sigma(2s)^{*2}\sigma(2p)^2\pi(2p)^4\pi(2p)^{*2}$]: This is another case where valence bond theory fails to predict actual properties. Molecular orbital theory correctly predicts that dioxygen is paramagnetic, with a bond order of two. Here, the molecular orbital diagram returns to its "normal" order of orbitals where orbital mixing could be somewhat ignored, and where $\sigma_g(2p)$ is lower in energy than $\pi_u(2p)$.

Difluorine, F_2 $[\sigma(2s)^2\sigma(2s)^{*2}\sigma(2p)^2\pi(2p)^4\pi(2p)^{*4}]$: This molecule has a bond order of one and like oxygen, the $\sigma(2p)$ is lower in energy than $\pi(2p)$.

Dineon, Ne_2 $[\sigma(2s)^2\sigma(2s)^{*2}\sigma(2p)^2\pi(2p)^4\pi(2p)^{*4}\sigma(2p)^{*2}]$: Like other noble gases, Ne exists in the atomic form and does not form bonds at ordinary temperatures and pressures. Like Be_2, Ne_2 is an unstable species that has been created in extreme laboratory conditions and its bond length has been measured (Figure **3.7*B*.9**)

Bond Lengths

The trends in experimental bond lengths are predicted by molecular orbital theory, specifically by the calculated bond order. The values of bond order and experimental bond lengths for the second period diatomic molecules are given in Figure **3.7*B*.8**, and shown in graphical format on the plot in Figure **3.7*B*.9**. From the plot, we can see that bond length correlates well with bond order, with a minimum bond length occurring where bond order is greatest (N_2). The shortest bond distance is at N_2 due to its high bond order of 3. From N_2 to F_2 the bond distance increases despite the fact that atomic radius decreases.

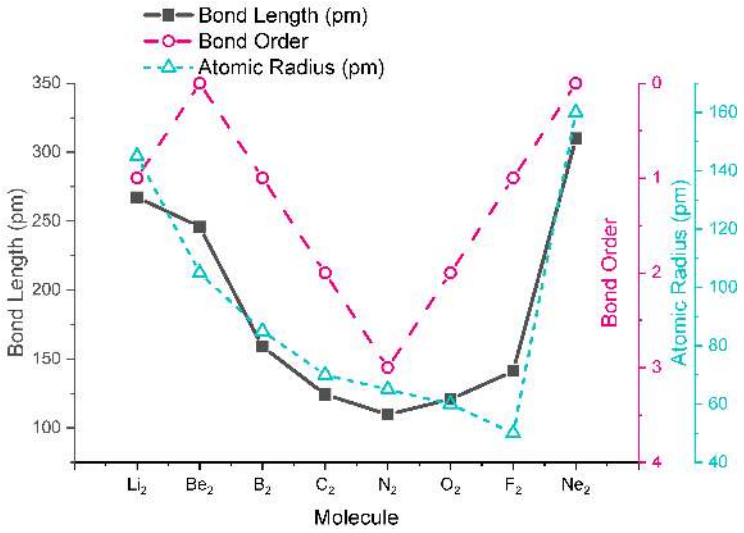


Figure **3.7*B*.9**: Overlayed plots of bond length (black squares), bond order (pink circles), and atomic radius (teal triangels) versus atomic number for second period homonuclear diatomic molecules. (CC-BY-NC-SA; Kathryn Haas)

References

1. Schöllkopf, W.; Toennies, J. P. Nondestructive Mass Selection of Small van der Waals Clusters. *Science* **1994**, *266* (5189), 1345–1348.
2. NIST, Calculated Geometries available for H_2^+ (Hydrogen cation) 2Σg+ D∞h, available at https://cccbdb.nist.gov/diatomicexpbondx.asp
3. Merritt, J. M.; Bondybey, V. E.; Heaven, M. C., Beryllium Dimer-Caught in the Act of Bonding. *Science* **2009,** *324* (5934), 1548-1551.
4. Meissler, G. L.; Fischer, P. J.; Tarr, D. A. *Inorganic Chemistry*, 5th Ed; Pearson, 2014.

Contributors and Attributions

- Stephen Lower, Professor Emeritus (Simon Fraser U.) Chem1 Virtual Textbook
- Curated or created by Kathryn Haas
- Modified by Catherine McCusker, ETSU

3.7B: Homonuclear Diatomic Molecules is shared under a CC BY-NC-SA 4.0 license and was authored, remixed, and/or curated by LibreTexts.

- **Current page** is licensed CC BY-NC-SA 4.0.
- **5.2.3: Diatomic Molecules of the First and Second Periods** by Kathryn Haas is licensed CC BY-SA 4.0.

3.7C: Heteronuclear Diatomic Molecules

Atomic Orbital Energies

Diatomic molecules with two non-identical atoms are called heteronuclear diatomic molecules. When atoms are not identical, the molecule forms by combining atomic orbitals of unequal energies. The result is a polar bond in which atomic orbitals contribute unevenly to each molecular orbital.

The application of molecular orbital theory to heteronuclear diatomic molecules is similar to the case of homonuclear diatomics, except that the atomic orbitals from each atom have different energies and contribute unequally to molecular orbitals. Recall that atomic orbitals must have compatible symmetry and similar energy to combine into molecular orbitals. In the case where atomic orbitals of like symmetry have different energies, they combine less favorably than orbitals that are closer to one another in energy. As a general rule, orbitals that have energy differences of greater than 10-14 eV do not combine favorably. In the molecular orbital diagram, the closer a molecular orbital is to an atomic orbital, the more that atomic orbital contributes to the molecular orbital. This last point is helpful for back-of-the napkin estimations of what the molecular orbitals "look" like.

In this section, you should learn how to generate molecular orbital diagrams of heteronuclear diatomic molecules. To approach such a problem, we must start with a knowledge of the relative energies of electrons in different atomic orbitals. In other words, we need knowledge of the orbital potential energies (or orbital ionization energies).

Orbital Ionization Energies

There are two approaches you can use to "know" or estimate the atomic orbital energy levels.

1. Use a table of atomic orbital ionization energies, like those found in Table **3.7C.1**.
2. When you do not have access to a table of values like the one below, use periodic trends in electronegativity and/or ionization energies as your guide to approximate relative values for different atoms.

Table **3.7C.1**: These are one-electron ionization energies of the valence orbitals calculated by average energies of both the ground-state and ionized-state configurations in eV. (From Harry Gray, “Electrons and Chemical Bonding,” Benjamin, 1964, Appendix)

Atom	1s	2s	2p	3s	3p
H	-13.64				
He	-24.55				
Li		-5.46			
Be		-9.30			
B		-14.01	-8.31		
C		-19.47	-10.66		
N		-25.54	-13.14		
O		-32.36	-15.87		
F		-46.37	-18.72		
Ne		-48.48	-21.57		
Na				-5.21	
Mg				-7.69	
Al				-11.28	-5.95
Si				-15.00	-7.81
P				-18.72	-10.17
S				-20.71	-11.65
Cl				-25.29	-13.76
Ar				-29.26	-15.87

MO Diagrams for Heteronuclear Diatomic Molecules

The molecular orbital diagram of a heteronuclear diatomic molecule is approached in a similar way to that of homonuclear diatomic molecule. The orbital diagrams may also look similar. A major difference is that the more electronegative atom will have orbitals at a lower energy level. Two examples of heteronuclear diatomic molecules will be explored below as illustrative examples.

Carbon monoxide MO diagram

Carbon monoxide is an example of a heteronuclear diatomic molecule where both atoms are second-row elements. The valence molecular orbitals in both atoms are the $2s$ and $2p$ orbitals. The molecular orbital diagram for carbon monoxide (Figure $3.7C.1$) is constructed similarly to how you would construct dicarbon or dioxygen, except that the oxygen orbitals have a lower potential energy than analogous carbon orbitals. The labeling of molecular orbitals in this diagram follows a convention by which orbitals are given serial labels according to type of orbital (σ, π, etc). The lowest energy orbitals of any type are assigned a value of 1 and higher energy orbitals of the same type are assigned by increasing intervals (..2, 3, 4...).

A consequence of unequal atomic orbital energy levels is that orbital mixing is significant. Notice the order of the molecular orbitals labeled 1π and 3σ in Figure $3.7C.1$. This is a similar order of π and σ orbitals as we saw in the case of N_2 and lighter diatomics of the second period. Because the oxygen $2p_z$ orbital is close in energy to both the carbon $2p_z$ and carbon $2s$, these three orbitals will have significant interaction (overlap). The result is an increase in the energy of the 3σ orbital and a decrease in energy of the $2\sigma^*$ orbital, resulting in the diagram shown in Figure $3.7C.1$.

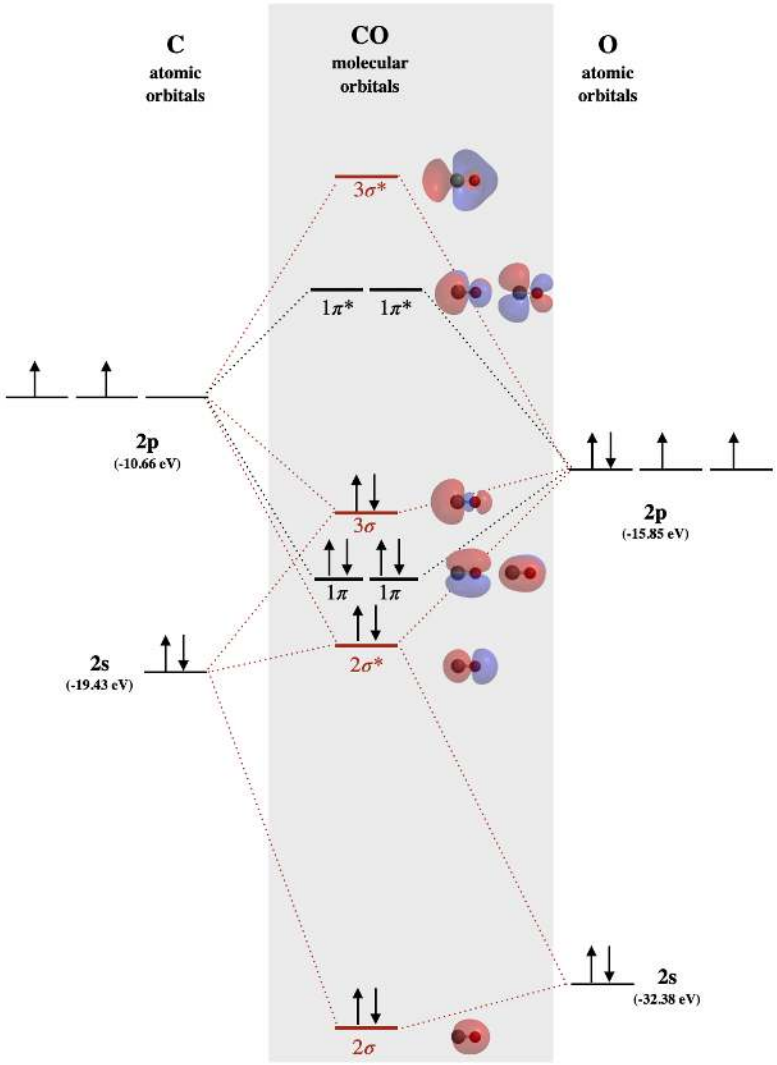


Figure 3.7C.1: Molecular orbital diagram of carbon monoxide. The labeling of molecular orbitals in this diagram follows a convention by which orbitals are given serial names according to type of orbital (σ, π, etc). The lowest energy orbitals of any type are assigned a value of 1 and higher energy orbitals of the same type are assigned by increasing intervals (..2, 3, 4...). Molecular orbital surfaces were calculated using Spartan software. (Kathryn Haas, CC-BY-NC-SA)

In the case of carbon monoxide (Figure 3.7C.1), atomic orbitals contribute unequally to each molecular orbital. For example, because the $2s$ orbital of oxygen is very close in energy to the 2σ molecular orbital, it contributes to that molecular orbital more than the $2s$ orbital from carbon. Notice the shape of this 2σ orbital and how it is unevenly distributed over the two atoms; it is more heavily distributed on the oxygen because it is most like the oxygen $2s$. This is in-line with the assumption that electron density is distributed more on oxygen because it is a more electronegative than carbon. Likewise, the 1π orbitals are unevenly distributed, with more distribution close to the oxygen.

Exercise 3.7C.1

Examine the shape of the 3σ orbital of carbon monoxide in Figure (3.7C.1). Describe what ways this shape is different from the shape of the σ_g orbitals from second period homonuclear diatomic molecules. Rationalize these differences. Both orbitals are re-created below for convenience.



Answer

The 3σ orbital is like the σ_g in that it has three lobes and two nodes distributed along the internuclear bond. They are different in their distribution. The two external lobes of σ_g are evenly distributed because the are an equal combination of two p_z orbitals (one from each atom). The 3σ orbital is more heavily distributed toward the carbon atom, the less electronegative atom, than toward the oxygen. The unequal distribution of 3σ is apparent in the unequal sizes of its exterior lobes, and the uneven shape of the interior lobe. The heavier distribution within the exterior lobe on carbon caused by the mixing of the carbon $2s$ orbital with carbon and oxygen $2p_z$ orbitals. The uneven shape of the interior lobe, where it leans toward oxygen, is best explained by the fact that the 3σ orbital is closer in energy to the oxygen $2p_z$ than the carbon $2p_z$.

Hydrogen fluoride MO diagram

Hydrogen fluoride is an example of a heteronuclear diatomic molecule in which the two atoms are from different periods. In this case, the valence orbital of H is $1s$ while those of F are $2s$ and $2p$. The molecular orbital diagram for HF is shown in Figure 3.7*C*.2.

Three of these orbitals have compatible symmetry for mixing; these are the hydrogen $1s$, fluorine $2s$, and fluorine $2p$. However, the extent to which they will interact depends on their relative energies. Fluorine is more electronegative than H, and the fluorine atom has a higher first ionization energy than does hydrogen. From these trends, we can expect that the fluorine valence orbitals are lower in energy than that of hydrogen. From Table 3.7*C*.1, we find that the 1s orbital of H (-13.6 eV) is higher in energy than both fluorine orbitals (-18.7 and -40.2 eV, respectively for $2p$ and $2s$). The energies of hydrogen $1s$ and fluorine $2p$ are a good match for combination, however, the $2s$ orbital is much too different to create a productive interaction. Therefore, we expect that the fluorine $2s$ will create a non-bonding molecular orbital, while the $1s$ and $2p_z$ orbital combine to make σ bonding and σ^* antibonding molecular orbitals. The remaining $2p_x$ and $2p_y$ orbitals do not have compatible symmetry for bonding with hydrogen, and they will form non-bonding π molecular orbitals. The non-bonding orbitals will have the same energy and character as their component atomic orbitals.

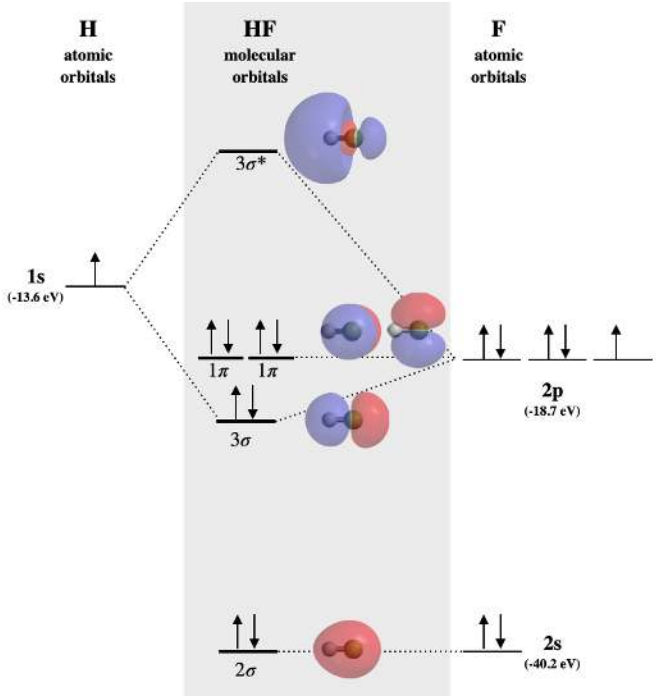


Figure 3.7*C*.2: Molecular Orbital diagram of hydrogen fluoride. Molecular orbitals calculated using Spartan software. (Kathryn Haas, CC-BY-NC-SA)

Chemical Reactivity

Knowledge of molecular orbital diagrams, and the shapes of molecular orbitals, can be used to accurately explain and predict chemical reactivity. Chemical reactions take place using the highest occupied molecular orbitals (HOMO) of a nucleophile or Lewis base, and the lowest unoccupied molecular orbital (LUMO) of an electrophile or Lewis acid.

> *Lewis bases react using electrons in the HOMO, while Lewis acids react using the empty LUMO.*

Example: Reactivity of CO with metal ions

CO is an excellent ligand for many metal ions. In fact, the strong affinity between CO and the heme iron (Fe) ions in hemoglobin can explain the mechanism of carbon monoxide poisoning. When CO binds in place of O_2 to hemoglobin, that hemoglobin can no longer carry O_2 to tissue cells. CO binding to hemoglobin is strong and practically irreversible. When CO binds to metal ions, it does so through the carbon atom. This is contrary to expectations based on the Lewis structure and the known bond polarity, where electron density is polarized toward oxygen. The distribution of the electron density of the HOMO of CO can explain this observation!

Exercise 3.7C.2

Refer to the MO diagram for CO. Identify the HOMO and explain why CO bonds to metal ions through the carbon atom rather than through the oxygen atom.

Answer

The HOMO of CO is the 3σ MO. That MO is closer in energy to both the C 2s and 2p than the contributing O atomic orbitals. This means the MO has more C character and is localized more on the C than the O. When CO acts as a Lewis base and bonds to a metal (a Lewis acid) it donates electrons from the HOMO orbital

---

Sources:

- Gray, Harry. *Electrons and Chemical Bonding*, Benjamin, 1964.
- Miessler, Gary L, and Donald A. Tarr. *Inorganic Chemistry*. Upper Saddle River, N.J: Pearson Education, 2014. Print.

Curated or created by Kathryn Haas

3.7C: Heteronuclear Diatomic Molecules is shared under a not declared license and was authored, remixed, and/or curated by LibreTexts.

- **Current page** has no license indicated.
- **5.3: Heteronuclear Diatomic Molecules** by Kathryn Haas is licensed CC BY-SA 4.0.
- **5.3.2: Polar bonds** by Kathryn Haas is licensed CC BY-SA 4.0.

CHAPTER OVERVIEW

4: Molecular Symmetry and Point Groups

Symmetry in Chemistry

Symmetry is actually a concept of mathematics and not of chemistry. However, symmetry, and the underlying mathematical theory for symmetry, group theory, are of tremendous importance in chemistry because they can be applied to many chemistry problems. For example it helps us to classify the structures of molecules and crystals, understand chemical bonding, predict vibrational spectra, and determine the optical activity of compounds. We will therefore first discuss the general foundations of symmetry and group theory, and then how they can be applied to chemical problems.

Let us first find a definition for symmetry. The human brain innately recognizes symmetry and patterns and we associate symmetry with beauty, but very familiar things are not necessarily easy to define scientifically. One common definition is that symmetry is the self-similarity of an object. The more similar parts it has the more symmetric it appears. For example, we would argue that the two wings of the butterfly depicted look similar. If the left wing was very different from the right wing the butterfly would look less symmetric.



Figure **4.1**: Symmetry depicted through an image of a butterfly (Photo by Alfred Schrock on Unsplash)

In other classes you have learned different ways to describe symmetry, radial and bilateral symmetry in biology; R and S enantiomers or cis and trans isomers in organic chemistry. Group theory gives us a universal language and tools to define and describe the symmetry of any object or molecule.

This TED talk explains symmetry from a mathematical and artistic perspective.

Learning Objectives

- Identify symmetry elements and operations in molecules and objects
- Use flowchart to assign a molecule to a point group
- Recognize the components of a character table
- Determine whether a vibrational mode is infrared allowed

Thumbnail image shows all the reflection planes in ferrocene. Image from Otterbein University symmetry gallery

4.1: Symmetry Operations and Elements

4.2: Point Groups
4.3: Introduction to Character Tables
4.4: Applications of Symmetry in Chemistry

4: Molecular Symmetry and Point Groups is shared under a not declared license and was authored, remixed, and/or curated by LibreTexts.

4.1: Symmetry Operations and Elements

Introduction

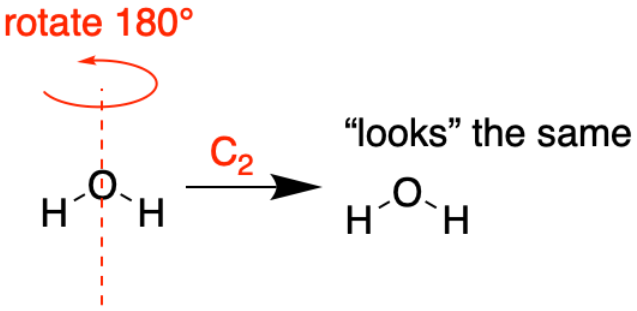


Figure **4.1.1**: An example of a symmetry operation is a 180° rotation where the resulting position is indistinguishable from the original. A 180° rotation is called a C_2 operation; the axis of rotation is the symmetry element. (CC-BY-NC-SA; Kathryn Haas)

The symmetry of a molecule consists of symmetry operations and symmetry elements. A symmetry operation is an operation that is performed to a molecule which leaves it indistinguishable and superimposable on the original position. Symmetry operations are performed with respect to symmetry elements (points, lines, or planes).

Definition: Symmetry Operation

Manipulation of an object around a symmetry element. The object must be indistinguishable before and after the operation.

Definition: Symmetry Element

A geometric entity (point, axis, or plane) around which a symmetry operation is performed

An example of a symmetry operation is a 180° rotation of a water molecule in which the resulting position of the molecule is indistinguishable from the original position (see Figure **4.1.1**). In this example, the symmetry operation is the rotation and the symmetry element is the axis of rotation.

There are five types of symmetry operations including **identity**, **reflection**, **inversion**, **proper rotation**, and **improper rotation**. The improper rotation is the sum of a rotation followed by a reflection. The symmetry elements that correspond to the five types of symmetry operations are listed in Table **4.1.1**.

Table **4.1.1**: Table of elements and operations

Element	Operation	Symbol
Identity	identity	E
Proper axis	rotation by (360/n)º	C_n
Symmetry plane	reflection in the plane	σ
Inversion center	inversion of a point at (x,y,z) to (-x,-y,-z)	*i*
Improper axis	rotation by (360/n)º, followed by reflection in the plane perpendicular to the rotation axis	S_n

Symmetry Operations and Elements

Identity (E)

All molecules have the identity element. The identity operation is a 360° rotation, essentially doing nothing to the molecule. It is included to fulfill the mathematical requirements of a group.

Proper Rotation and Proper Axis (C_n)

A "proper" rotation is just a simple rotation operation about an axis. The symbol for any proper rotation or proper axis is $C_{(360/n)}$, where n is the degree of rotation. Thus, a 180° rotation is a C_2 rotation around a C_2 axis, and a 120° rotation is a C_3 rotation about a C_3 axis. Figure \(\PageIndex{2}\) shows both the C_3 principal rotation axis and one of the C_2 rotation axes in BF_3.

Definition: Principal Rotation Axis

The principal axis of a molecule is the highest order proper rotation axis. For example, if a molecule had C_2 and C_4 axes, the C_4 is the principal axis.

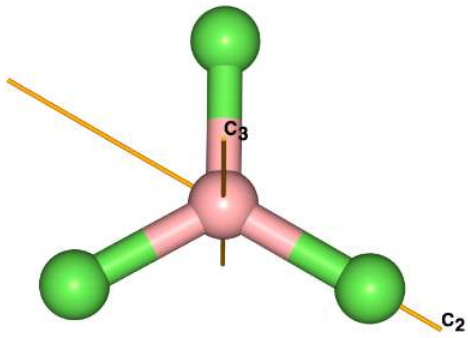


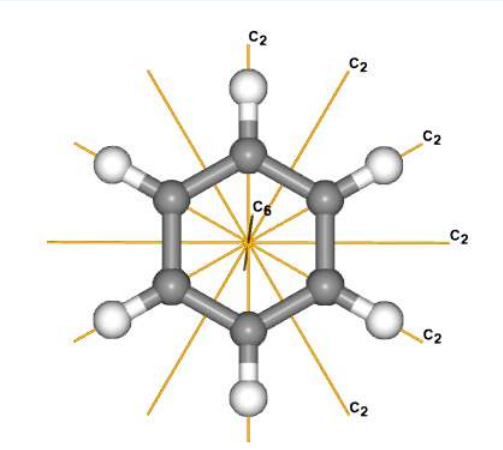
Figure 4.1.2:The C_3 and one of the C_2 rotation axes in BF_3. C_3 is the principal rotation axis. (Image source: https://symotter.org/gallery)

Exercise 4.1.1

What is the principal rotation axis in benzene (C_6H_6)?

Answer

Benzene is a planar molecule. It has one C_6 axis and 6 C_2 axes. The principal rotation axis is the C_6 as it has the highest order.



Reflection and Mirror Planes (σ)

A reflection operation occurs with respect to a mirror plane. Mirror planes can be classified based on their relationship to the principal rotation axis:

1. σ_h (horizontal): horizontal reflection planes are perpendicular to principal rotation axis
2. σ_v (vertical): vertical reflection planes contain the principal rotation axis
    - σ_d (dihedral): dihedral reflection planes are vertical reflection planes that bisect two C_2 rotation axes

Figure **4.1.3** shows the three types of mirror planes in the square planar $PtCl_4$. The horizontal reflection plane, shown in red, is in the plane of the molecule, and bisects the C_4 principal rotation axis. The vertical reflection planes, shown in orange, are along the Pt-Cl bonds and contain the C_4 principal rotation axis. The dihedral reflection planes, shown in yellow, bisect the Pt-Cl bonds (and the C_2 rotation axes along those bonds) and also contain the C_4 principal rotation axis.

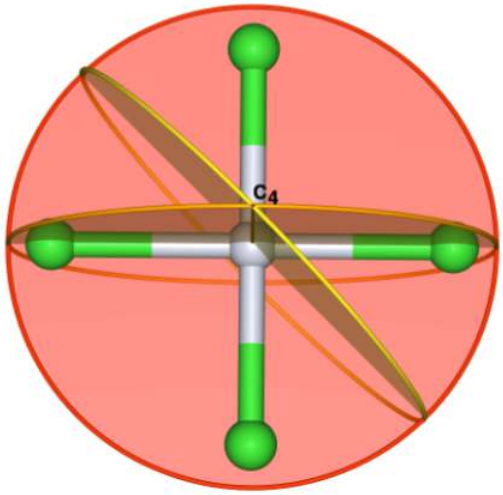


Figure **4.1.3**: The horizontal reflection plane (red), one of the vertical reflection planes (orange) and one of the dihedral reflection planes (yellow) in $PtCl_4$. (Image source: https://symotter.org/gallery)

Inversion and Inversion Center (i)

The inversion operation takes any point through the inversion center to an equidistant point on the opposite side of the inversion center. In other words, a point at the center of the molecule that can transform (x,y,z) into (-x,-y,-z) coordinates. The inversion center may be on the central atom or it may be at a point in space in the center of a molecule (Figure **4.1.4**).

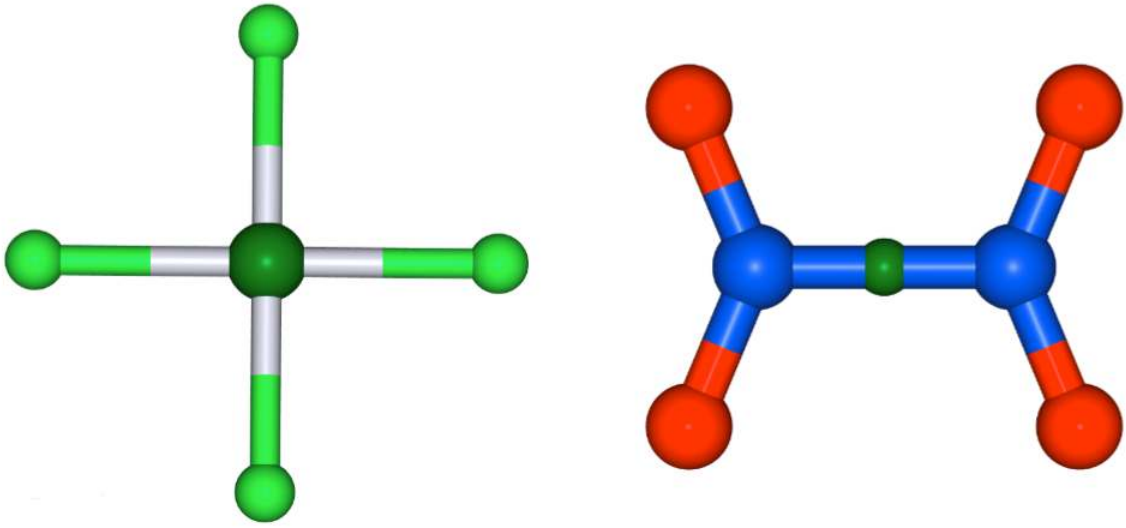


Figure **4.1.4**: The inversion center (dark green) in $PtCl_4$ and in N_2O_4. (Image source: https://symotter.org/gallery)

Improper Rotation and Improper Rotation Axis (S_n)

Improper rotation is by far the most difficult symmetry operation to visualize. It is a combination of a rotation with respect to an axis of rotation (C_n), followed by a reflection through a plane perpendicular to that C_n axis. The rotation and reflection may or may

not be valid symmetry operations on their own. In short, an S_n operation is equivalent to C_n followed by σ_h. In methane (Figure 4.1.5), the S_4 improper rotation axis will rotate 90° and rotate the in plane H's out of plane and vice versa. The perpendicular reflection then exchanges the in and out of plane H's, returning them to the original confirmation. In this example, neither the C_4 rotation or the perpendicular reflection are symmetry operations on their own.

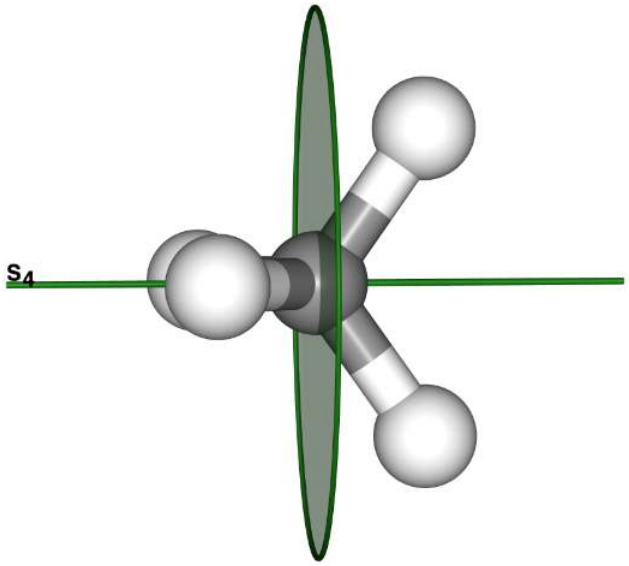


Figure 4.1.5: The improper rotation axis and reflection plane in methane. (Image source: https://symotter.org/gallery)

Successive Operations

Sometimes, new symmetry operations form by carrying out two or more simpler operations successively to result in an indistinguishable configuration. For example, the improper rotation axis above results from rotation about an axis of rotation (C_n) followed by reflection about a plane perpendicular to that axis (σ_h).

$$S_n = C_n \times \sigma_h \tag{4.1.1}$$

Note also that C_n in this case need not be a symmetry element for the molecule. For example, staggered ethane has an S_6 symmetry element although it does not have a C_6. Another example of a symmetry element that results from a combination of two different elements is the inversion center (i), which results from a C_2 rotation followed by a reflection about a plane perpendicular to that axis (σ_h).

$$i = C_2 \times \sigma_h \tag{4.1.2}$$

Note that an inversion center is a special case of an improper rotation axis because it results when, in the first equation, $n = 2$. That is,

$$i = S_2 \tag{4.1.3}$$

In fact, any symmetry operation can be carried out multiple time in a row. For example, when BH_3 is rotated twice by 120°, the two-step operation can be symboled by C_3^2. When the C_3 operation is performed a third time, the molecule returns to its original configuration; i.e,

$$C_3^3 = E \tag{4.1.4}$$

In general,

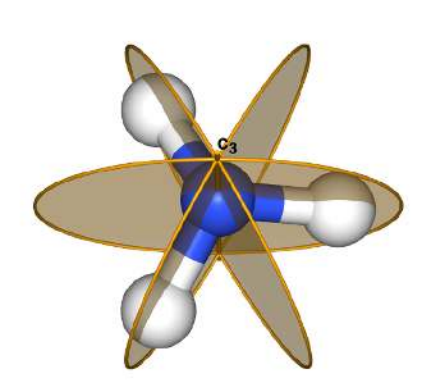
$$C_n^n = E \tag{4.1.5}$$

Exercise 4.1.1

List all of the symmetry elements in ammonia (NH_3).

Answer

Ammonia has a trigonal pyramidal geometry. It has one C_3 rotation axis (the principal rotation axis) which will exchange the three H atoms. It also has three vertical reflection planes, one along each N-H bond.



Sources:

1. Introduction to Molecular Symmetry by J. S Ogden
2. Inorganic Chemistry by Catherine Housecroft And Alan G. Sharpe.
3. Symmetry@Otterbien: https://symotter.org/

4.1: Symmetry Operations and Elements is shared under a CC BY-NC-SA 4.0 license and was authored, remixed, and/or curated by LibreTexts.

- **3.2: Symmetry Operations and Elements** is licensed CC BY-NC-SA 4.0.
- **Current page** is licensed CC BY-NC-SA 4.0.
- **3.3: Successive Operations** is licensed CC BY-NC-SA 4.0.

4.2: Point Groups

Introduction

In group theory, molecules or other objects can be organized into point groups based on the type and number of symmetry operations they possess. Every molecule in a point group will have all of the same symmetry operations as any other molecule in that same point group. The most common, and chemically relevant point groups are described below.

The Low Symmetry Point Groups

C_1 Point Group

Overall, we divide point groups into three major categories: High symmetry point groups, low symmetry point groups, dihedral point groups, and rotational point groups. Let us begin with the low symmetry point groups. As the name says, these point groups only have few symmetry elements and operations. The point group C_1 is the point group with the lowest symmetry. Molecules that belong to this point group only have the identity as symmetry element.

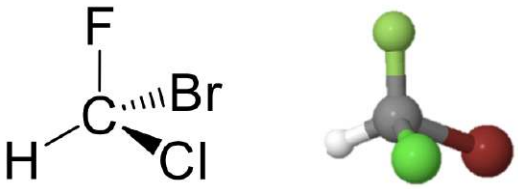


Figure **4.2.1** C_1 point group of bromochlorofluromethane (Attribution: symotter.org/gallery)

An example is the bromochlorofluromethane molecule (Figure **4.2.1**). It has no symmetry element except the identity (E). The name C_1 comes from the symmetry element C_1. A C_1 operation is the same as the identity.

C_s Point Group

The point group C_s has a mirror plane in a addition to the identity. An example is the 1,2-bromochloroethene molecule (Figure **4.2.2**).

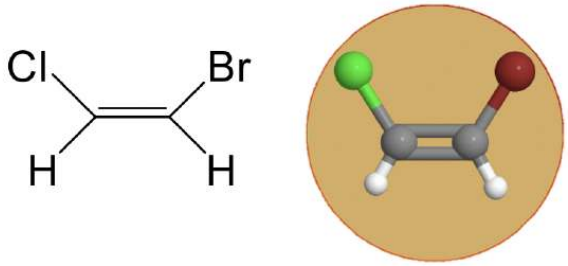


Figure **4.2.2** C_s point group of 1, 2-bromochloroethene (Attribution: symotter.org/gallery)

This is a planar molecule and the mirror plane is within the plane of the molecule. This mirror plane does not move any atoms when the reflection operation is carried out, nonetheless it exists because any point of the molecule above the mirror plane will be found below the mirror plane after the execution of the operation. Vice versa, any point below the mirror plane will be above the mirror plane. This mirror plane does not have a vertical or horizontal mirror plane designation because no proper rotational axes exist.

C_i Point Group

The point group C_i has the inversion as the only symmetry element besides the identity. The point group C_i is sometimes also called S_2 because an S_2 improper rotation-reflection is the same as an inversion. An example is the 1,2-dibromo 1,2-dichloro ethane (Figure **4.2.3**).

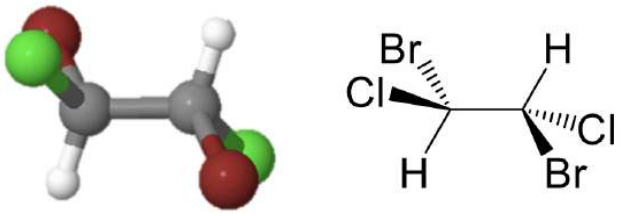


Figure **4.2.3** The C_i point group: 1,2-dibromo-1,2-dichloroethane (Attribution: symotter.org/gallery)

This molecule looks quite symmetric, but it has inversion center in the middle of the carbon-carbon bond as the only symmetry element. Upon execution of the inversion operation, the two carbons swap up their positions, and so do the two bromine, the two chorine, and the two hydrogen atoms.

The High Symmetry Point Groups

The symmetry elements of the high symmetry point groups can be more easily understood when the properties of platonic solids are understood first. Platonic solids are polyhedra made of regular polygons. In a platonic solid all faces, edges, and vertices (corners) are symmetry-equivalent. We will see that this is a property that can be used to understand the symmetry elements in high symmetry point groups. There are only five possibilities to make platonic solids from regular polygons (Figure **4.2.4**).

File:Platonic Solids Transparent.svgFigure **4.2.4** The platonic solids (Attribution: Drummyfish [CC0] https://commons.wikimedia.org/wiki/F...ransparent.svg)

The first possibility is to construct a tetrahedron from four regular triangles. The second platonic solid is the octahedron made of eight regular triangles. The third possibility is the icosahedron made of twenty triangles. In addition, six squares can be connected to form a cube, and twelve pentagons can be connected to form a dodecahedron. There are no possibilities to connect other regular polygons like hexagons to make a platonic solid.

The T_d Point Group

The tetrahedron, as well as tetrahedral molecules and anions such as CH_4 and BF_4- belong to the high symmetry point group T_d (Note that only tetrahedral molecules where all four outer atoms/groups are the same will be in the T_d point group). Let us find the symmetry elements and symmetry operations that belong to the point group T_d. First, we should not forget the identity operation, E. Next, it is useful to look for the principal axes.

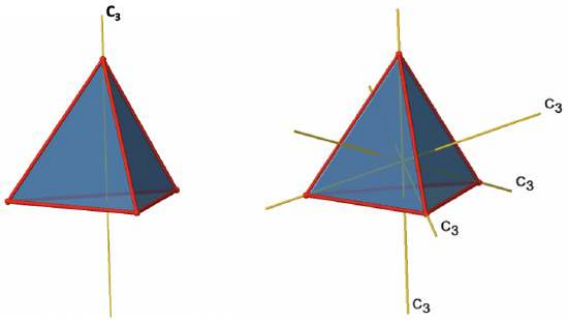


Figure **4.2.5** The C_3 axes in a tetrahedron (Attribution: symotter.org/gallery)

The tetrahedron has four principal C_3 axes (Figure **4.2.5**). It is a property of the high-symmetry point groups that they have more than one principal axis. The C_3 axes go through the vertices of the tetrahedron. Because each C_3 axis goes through one vertex, there are four vertices, and we know that in a platonic solid all vertices are symmetry-equivalent, we can understand that there are four C_3 axes. How many unique C_3 operations are associated with these axes? After three rotations around 120° we reach the identity. Therefore C_3^3=E, and we only need to consider the C_3^1 and the C_3^2 rotation about 120 and 240° respectively. Because there are

four C_3 axes, there are four C_3^1 and four C_3^2 operations and eight C_3 operations overall. In addition to the C_3 axes there are C_2 axes (Figure **4.2.6**).

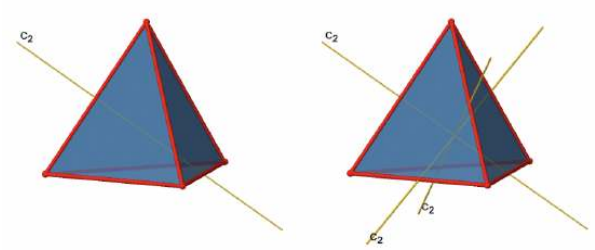


Figure **4.2.6** The C_2 axes in a tetrahedron belonging to the point group T_d (Attribution: symotter.org/gallery)

You can see that a C_2 axis goes through two opposite edges in the tetrahedron. Because a tetrahedron has six edges, and each C_2 axis go through two edges there are 6/2=3 C_2 axes. There is only one C_2 symmetry operation per C_2 axis because we produce the identity already after two rotations. Therefore there are three C_2^1 operations overall.

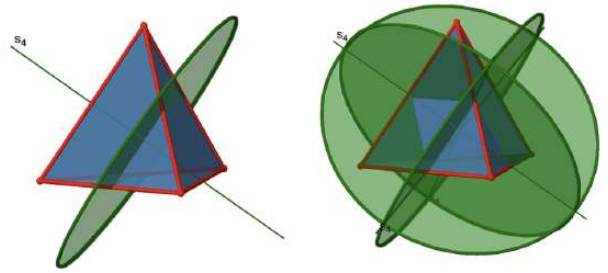


Figure **4.2.7** The S_4 axes in a tetrahedron (Attribution: symotter.org/gallery)

In addition, the T_d point group has S_4 improper rotation reflections. Like the C_2 axes, they pass through the middle of two opposite edges. This also means that they are superimposing the C_2 axes. Because there are six edges, and two S_4 axes per edge there are 6/2=3 S_4 axes (Figure **4.2.7**). How many operations are associated with these S_4 axes? The order of the axes are even, and therefore we need four S_4 operations to produce the identity. The S_4^2 operation is the same as a C_2^1 operation because reflecting two times is equivalent to not reflecting at all, and rotating two times by 90° is the same as rotating about 180°. Therefore overall, only S_4^1 and S_4^3 operations are unique operations. S_4^2 and S_4^4 can be expressed by the simpler operations C_2^1 and E respectively. Because there are 3 S_4 axes, there are three S_4^1 and three S_4^3 operations. Overall there are six S_4 operations.

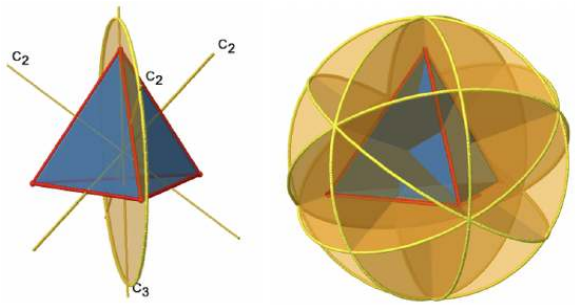


Figure **4.2.8** The mirror planes and C_2 axes in a tetrahedron belonging to the point group T_d (Attribution: symotter.org/gallery)

There are also mirror planes (Figure **4.2.8**). The planes contain a single edge of the tetrahedron, thereby bisecting the tetrahedron. There a six edges in a tetrahedron, and therefore there are 6/1=6 mirror planes.These planes are dihedral planes because each plane contains a C_3 principal axis and is bisects the angle between two C_2 axes. Overall, there are three C_2 axes and three C_2 operations. There is one reflection operation per mirror plane because reflecting two times produces the identity. Therefore, there are six σ_d reflection operations.

Symmetry Operations in the T_d Point Group

Every molecule or object in the T_d point group has the following symmetry operations:

- E, 8 C_3, 3 C_2, 6 S_4, and 6 σ_d

The Octahedral Point Group O_h

Another high symmetry point group is the point group O_h. Both the octahedron as well as the cube belong to this point group despite their very different shape Figure **4.2.9**. Because they belong to the same point group they must have the same symmetry elements and operations. There are many octahedrally shaped molecules, such as the SF_6.

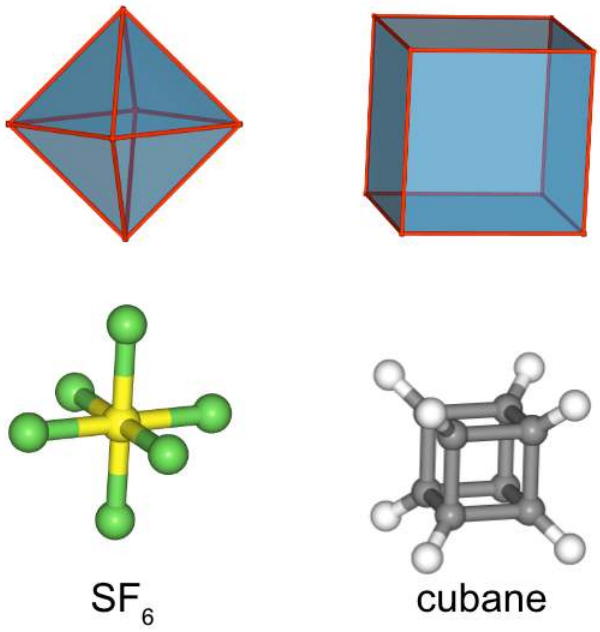


Figure **4.2.9**: SF_6 and cubane with cubic and octahedral shape, respectively, belong to the point group O_h (Attribution: symotter.org/gallery)

Molecules with cubic shapes are far less common, because a cubic shape often leads to significant strain in the molecule. An example is cubane C_8H_8. Let us determine the symmetry elements and operations for the point group O_h using the example of the octahedron. If we used the cube, we would get exactly the same results.

There are three C_4 principal axes in the octahedron. They go through two opposite vertices of the octahedron (Figure **4.2.10**). There are three C_4 axes because an octahedron has six vertices which are all symmetry-equivalent because the octahedron is a platonic solid.

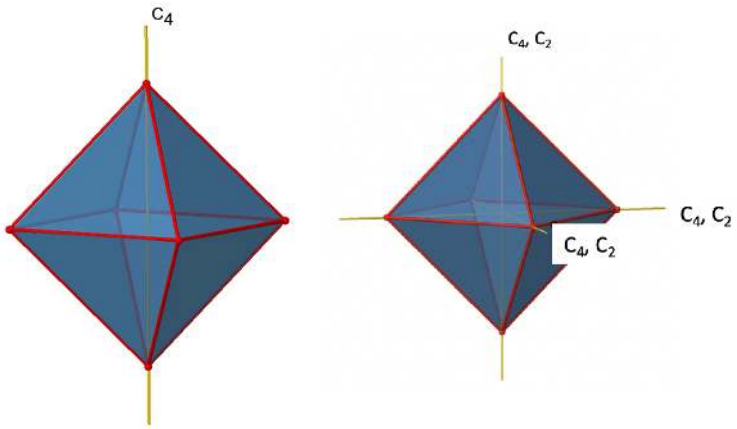


Figure **4.2.10**: The C_4 and C_2 axes in the octahedral point group O_h (Attribution: symotter.org/gallery)

We can see that there are also C_2 axes where the C_4 axes run. This is because rotating two times around 90° is the same as rotating around 180°. What are the symmetry operations associated with these symmetry elements? Rotating four times around 90° using the C_4 axes produces the identity. So we have to consider the operations C_4^1, C_4^2, C_4^3 and C_4^4. How many of these are unique? C_4^4 is the same as the identity, so it is not unique, In addition a C_4^2 is identical to a C_2^1, and thus C_4^2 is also not unique, and can be expressed by the simpler operation C_2^1. That leaves the C_4^1 and the C_4^3 as the only unique symmetry operations. Because we have three C_4 axes, there are 2x3=6 C_4 operations, in detail there are $3C_4^1$ and three C_4^3 operations. In addition, there are the three C_2^1 operations belonging the the three C_2 axes.

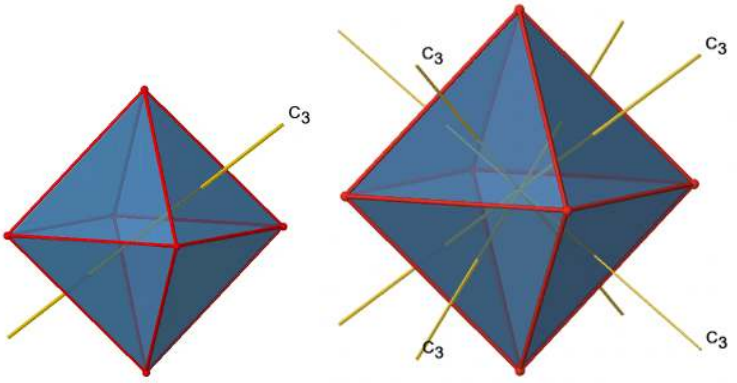


Figure **4.2.11**: The C_3 axes in the octahedral point group O_h (Attribution: symotter.org/gallery)

In addition, there are four C_3 axes (Figure **4.2.11**:). They are going through the center of two opposite triangular faces of the octahedron.You see above a single C_3 axis, and on the right hand side all four of these axes. How can we understand that there are four axes? An octahedron has overall eight triangular faces, and each C_3 axis goes through two opposite faces, so there are 8/2=4 C_3 axes. Each C_3 axis has the C_3^1 and the C_3^2 as unique symmetry operations. The C_3^3 is the same as the identity. So overall we have 4x2=8 operations, four of them are C_3^1, and four of them are C_3^2.

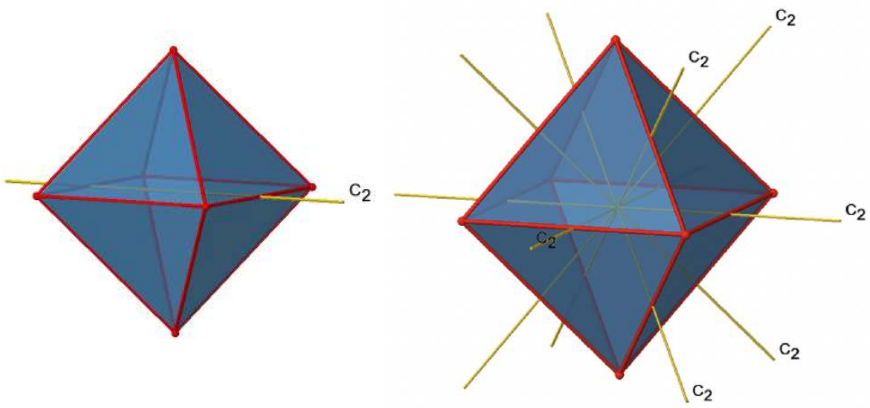


Figure **4.2.12**: The C_2' axes in the octahedral point group O_h (Attribution: symotter.org/gallery)

In addition to the C_2 axes that superimpose the C_4 axes, there are C_2' axes which go though two opposite edges of the octahedron (Figure **4.2.12**:). How many of them are there? An octahedron has twelve edges, and because each C_2' passes through two edges, there must be 12/2=6 C_2' axes. These axes have primes because they are not conjugate to the C_2 axes that superimpose the C_4 axes. For each C_2' axis there is only the C_2' ^{1} as the unique symmetry operation, and therefore there are overall 6 C_2'^{1} symmetry operations.

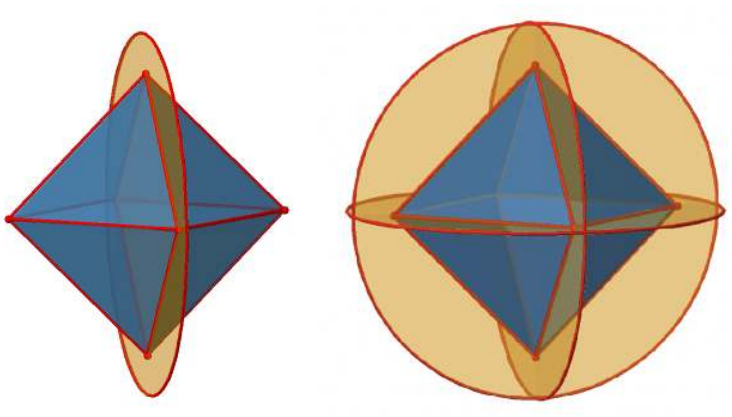


Figure **4.2.13**: The horizontal mirror planes in the octahedral point group O_h (Attribution: symotter.org/gallery)

Let us look at the horzontal mirror planes next (Figure **4.2.13**). There are horizontal mirror planes that stand perpendicular to the C_4 principal axes. Note that this mirror plane also contains two axes, in addition to the one to which it stands perpendicular. Because it contains two principal C_4 axes, it has also properties of a vertical mirror plane. Nonetheless, we call it a horizontal mirror plane because it stands perpendicular to the third C_4. The horizontal properties trump the vertical ones, so to say. You can see that a single mirror plane contains four edges of the octahedron. Because there are twelve edges, there are 12/4=3 horizontal mirror planes. There is one mirror plane per principal C_4 axis. There are three horizontal reflection operations because there is always only one reflection operation per mirror plane

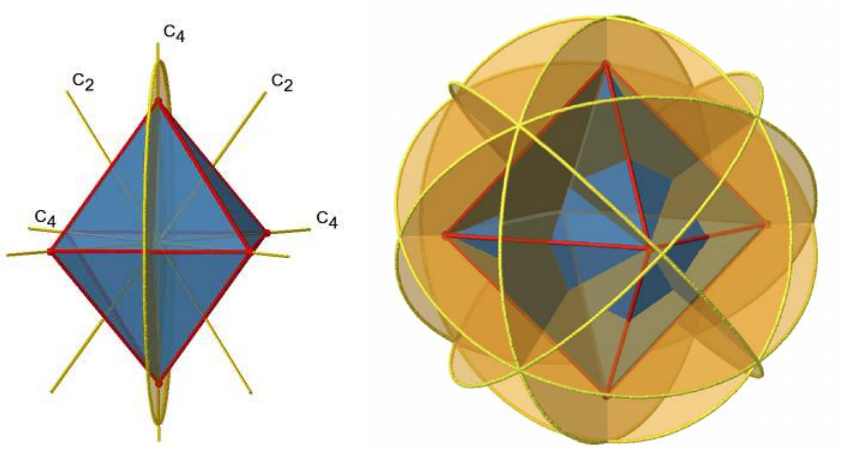


Figure 4.2.14: The vertical mirror planes in the octahedral point group O_h (Attribution: symotter.org/gallery)

Next let us look for vertical mirror planes (Figure **4.2.14**). You can see that - contrast to the horizontal mirror planes - it does not contain any edges. Rather, it cuts through two opposite edges. You can see that this plane contains a C_4 axis, but it does not stand perpendicular to the other two C_4 axes. Therefore it has only the properties of a vertical mirror plane. You can see however, that the mirror plane bisects the angle between two C_2' axes which also depicted. This makes the vertical mirror planes dihedral mirror planes, σ_d. How may of them do we have? As previously mentioned, each mirror plane cuts through two opposite edges. There are twelve edges in an octahedron, and thus there are 12/2=6 dihedral mirror planes. You can see all of them on the right side of Figure **4.2.14**. Each mirror plane is associated with one reflection operation, therefore there are six dihedral reflection operations.

Next we can ask if the point group O_h has an inversion center? Yes, there is one in the center of the octahedron (Figure **4.2.15**)!

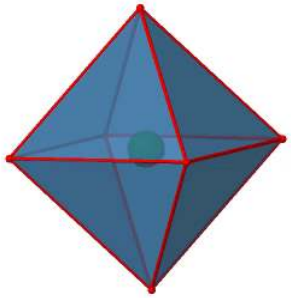


Figure 4.2.15: The inversion center of the octahedral point group O_h (Attribution: symotter.org/gallery)

Each point in the octahedron can be moved through the inversion center to the other side, and the produced octahedron will superimpose the original one. There is always one inversion operation associated with an inversion center.

Next, let us look for improper rotations. You can see an S_6 improper rotation operation below (Figure **4.2.16**, left).

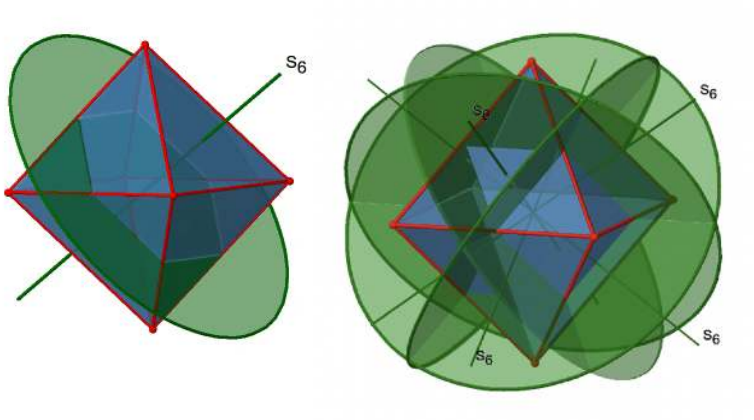


Figure **4.2.16**: The S_6 improper rotation element of the octahedral point group O_h (Attribution: symotter.org/gallery)

The improper S_6 axis passes though the centers of two opposite triangular faces. One can see that rotation about 60° alone does not make the octahedron superimpose. The reflection at a plane perpendicular to the improper axis is required to achieve superposition. Overall, the rotation-reflection swaps up the position of the two opposite triangular faces. How many S_6 improper axes are there? Since each S_6 passes through two faces, and an octahedron has 8 faces there must be 8/2=4 S_4 axes. You can see all of them above (Fig. 2.2.31, right). Note that they are in the same position as the $4C_3$ axes we previously discussed. How many unique operations are associated with them? For an S_6 axis we need to consider operations from S_6^1 to S_6^6. S_6^6 is the same as the identity so it is not unique. The S_6^2 is the same as a C_3^1 because rotating two times round 60° is the same as rotating around 120°, and reflecting twice is the same as not reflecting at all. Similarly, an S_6^4 is the same as an C_3^2. Rotating four time by 60° is the same as rotating two times by 120° and reflecting four times is the same as not reflecting at all. Further, an S_6^3 is the same as an inversion. After three 60° rotations we have rotated by 180°. If we reflect after that, then this is the same as an S_2^1 operation which is the same as an inversion. Therefore, only the S_6^1 and the S_6^5 operations are unique, all other operations can be expressed by simpler operations.

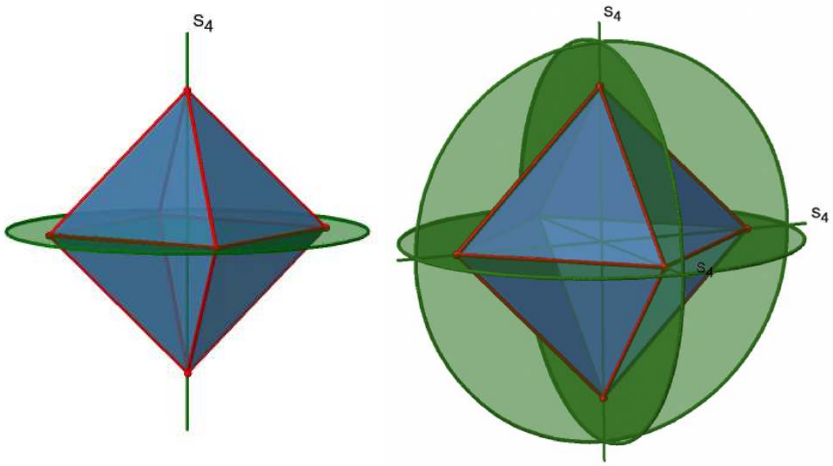


Figure **4.2.17**: The S_4 improper axis of the octahedral point group O_h (Attribution: symotter.org/gallery)

The octahedron also has S_4 improper axes, and you can see one of them in Figure **4.2.17**, right). It goes through two opposite corners of the octahedron. The S_4 improper axis seemingly does the same as the C_4 axis that goes through the same two opposite vertices, but actually does not. While rotating around 90° already makes the octahedron superimpose with its original form, executing the reflection operation after the rotation swaps up the position of the two vertices, and generally all points of the octahedron above and below the plane, respectively. Overall the S_4 moves the points within the object differently compared to the C_4 which makes it an additional, unique symmetry element. There are overall three S_4 improper axes because the octahedron has six vertices and one S_4 passes through two vertices.

Symmetry Operations in the O_h Point Group

Every molecule or object in the O_h point group has the following 48 symmetry operations:

- E, 8 C_3, 6 C_2, 6 C_4, 3 C_2 (C_4^2), i, 6 S_4, 8 S_6, 3 σ_h, and 6 σ_d

The I_h Point Group

The two remaining platonic solids, the icosahedron and the dodecahedron, belong both to the icosahedral point group I_h. This is despite they are made of different polygons. Because they belong to the same point group, they have exactly the same symmetry operations. An example for a molecule with icosahedral shape is the molecular anion $B_{12}H_{12}^{2-}$. Examples of molecules with dodecahedral shape include dodecahedrane ($C_{20}H_{20}$) and buckminsterfullerene (C_{60}). Let us determine the symmetry elements and symmetry operations for the example of the icosahedron. We could also use the dodecahedron, and the results would be the same. The principal axes of the icosahedron are the C_5 axes. You can see one of them, going through the center of the pentagon comprised of five triangular faces below (Figure **4.2.18**).

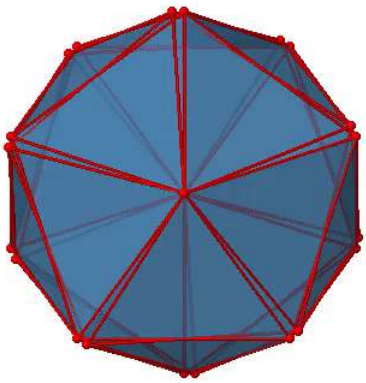


Figure **4.2.18**: One of the C_5 axes of the icosahedron stands perpendicular to the paper plane going through the center of a pentagon of the icosahedron (Attribution: symotter.org/gallery)

You can understand that there is a C_5 when considering that there are five triangular faces making a pentagon. The C_5 axis sits in the center of the pentagon. We can see that when we rotate around this C_5 axis, then the produced icosahedron superimposes the original one. The C_5 axis goes through two opposite vertices of the icosahedron. Because an icosahedron has 12 vertices, there must be six C_5 axes overall. You can see all of them below (Figure **4.2.19**). There are four unique symmetry operations associated with a single C_5 axis, namely the C_5^1, the C_5^2, the C_5^3, and the C_5^4. The C_5^5 is the same as the identity. Because there are six C_5 axes, there are overall 6x4=24 C_5 symmetry operations.

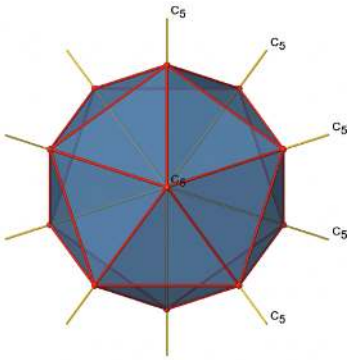


Figure **4.2.19**: The C_5 axes of the icosahedron (Attribution: symotter.org/gallery)



Figure **4.2.20**: One of the C_3 axes of the icosahedral point group (Attribution: symotter.org/gallery)

In addition, there are C_3 axes. One of them is shown below, and you can see that it passes through the centers of two opposite triangular faces (Figure **4.2.20**). As one rotates by 120° the atoms on the triangular faces change their position, and the resulting icosahedron superimposes the original one. As the name icosahedron says, there are twenty faces overall.

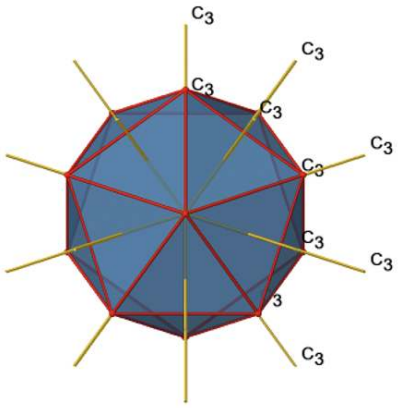


Figure **4.2.21**: The C_3 axes of the icosahedral point group (Attribution: symotter.org/gallery)

Because one C_3 passes through two opposite axes, there are 20/2=10 C_3 axes overall (Figure **4.2.21**:). Each C_3 axis is associated with two symmetry operations, namely C_3^1, and C_3^2. Thus, there are overall 10x2=20 C_3 symmetry operations.

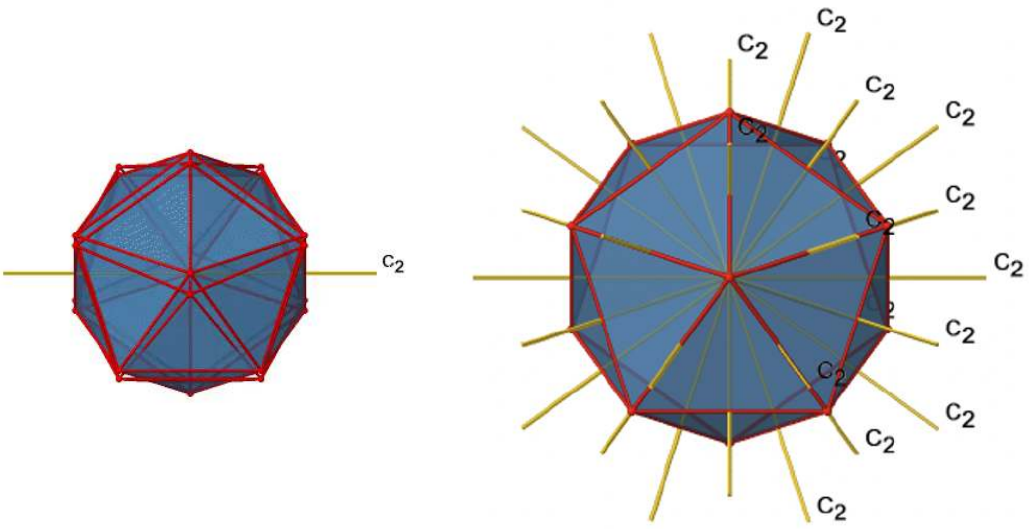


Figure 4.2.22: The C_2 axes of the icosahedral point group (Attribution: symotter.org/gallery)

There are also C_2 axes (Figure 4.2.21). They pass through the centers of two opposite edges of the icosahedron. Rotating around the C_2 axis shown makes the icosahedron superimpose. An icosoahedron has overall 30 edges. Because one C_2 axis passes through the centers of two opposite edges, we can understand that there are 30/2=15 C_2 axes. There is one unique C_2 operation per axis, and therefore there are 15 C_2 operations.

We have now found all proper rotations. Let us look for mirror planes, next. You can see a mirror plane below (Figure 4.2.22).

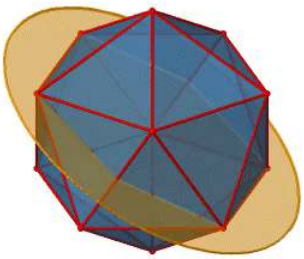


Figure 4.2.22: A mirror plane in the icosahedral point group (Attribution: symotter.org/gallery)

It contains two opposite edges. It also bisects two other edges. An icosahedron has overall 30 edges, therefore there are 30/2=15 mirror planes. You can see all of them below (Figure 4.2.23)).

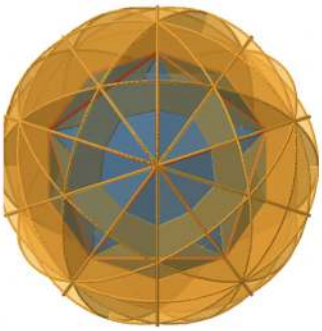


Figure **4.2.23**: All the mirror planes in the icosahedral point group (Attribution: symotter.org/gallery)

The icosahedron also has an inversion center in the center of the icosahedron (Figure **4.2.24**). As we carry out the associated symmetry operation, all points in the icosahedron move through the inversion center to the other side.



Figure **4.2.24**: The inversion center in the icosahedron (Attribution: symotter.org/gallery)

Let us now look for improper rotations. The improper rotational axes with the highest order are S_{10} axes. They are located in the same position as the C_5 axes, and go through two opposite corners (Figure **4.2.25**).

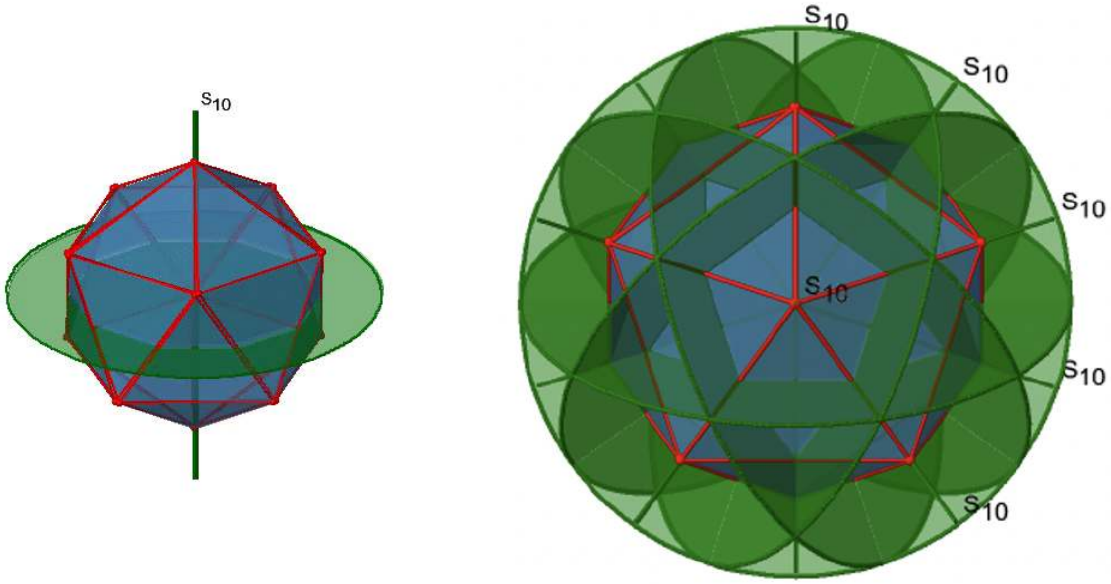


Figure 4.2.25: The S_{10} improper rotational axes in the icosahedral point group (Attribution: symotter.org/gallery)

The S_{10} exists because in an icosahedron there are pairs of co-planar pentagons that are oriented staggered relative to each other. The rotation around 36° brings one pentagon in eclipsed position relative to the other, but superposition is only achieved after the reflection at the mirror plane perpendicular to the rotational axis. Because one S_{10} passes through two opposite vertices, and there are 12 vertices there are 6 S_{10} improper axes. For each axis there are four unique symmetry operations, the S_{10}^1, the S_{10}^3, the S_{10}^7, and the S_{10}^9. Therefore, there are overall 4x6=24 operations possible.

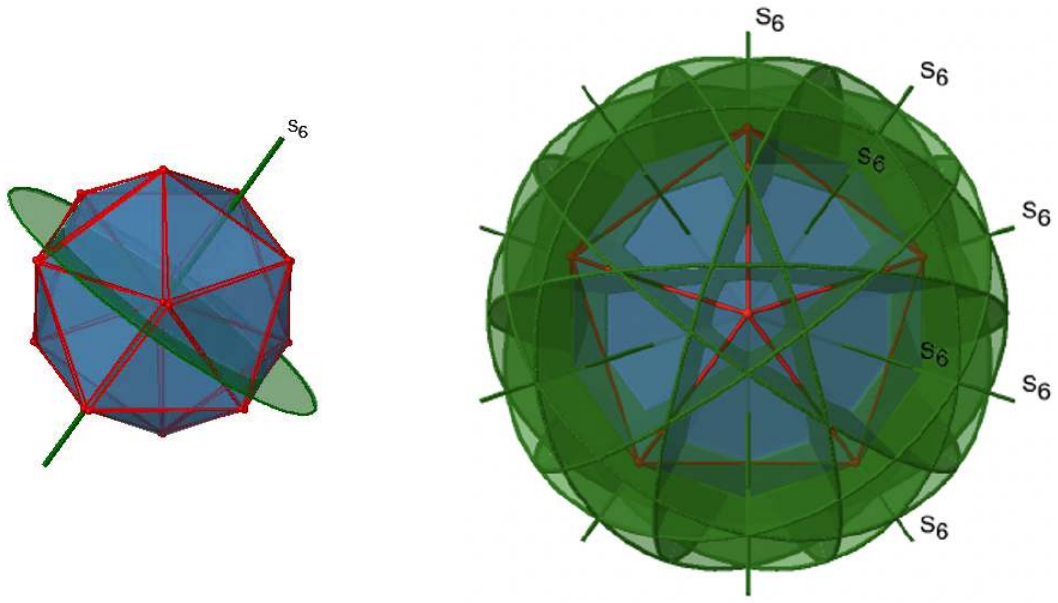


Figure 4.2.26: The S_6 rotation-reflections in the icosahedral point group (Attribution: symotter.org/gallery)

Are the lower order improper rotational axes? Yes, there are S_6 axes that pass through the centers of two opposite triangular faces (Figure 4.2.26). This symmetry element exists because the two triangular faces are in staggered orientation to each other. Rotation alone brings one face in eclipsed orientation relative to the other, but reflection at a mirror plane perpendicular to the axis is required to achieve superposition. The S_6 axes are in the same location as the C_3 axes. There are 10 S_6 axes because there are twenty faces and one axis passes through two opposite faces. Only the S_6^1 and the S_6^5 operations are unique S_6 operations, all others can be expressed by simpler operations. Therefore there are overall 10 S_6^1+10 S_6^5 = 20 S_6 operations.

We have now found all symmetry operations for the I_h symmetry. There are overall 120 operations making the point group I_h the point group with the highest symmetry.

Symmetry Operations in the I_h Point Group

Every molecule or object in the I_h point group has the following 120 symmetry operations:

- E, 24 C_5, 20 C_3, 15 C_2, i, 24 S_{10}, 20 S_6, and 15 σ

Rotational Point Groups

After having discussed high and low symmetry point groups, let us next look at rotational point groups. Unlike the high symmetry point groups, these only have a single proper rotational axis. The presence or absence of reflection planes further defines this class of point groups

C_n Point Groups

In the most simple case the point groups do not have any additional symmetry element such as mirror planes or improper rotations. These point groups are called pure rotation groups and denoted C_n whereby n is the order of the proper rotation axis. An example is the hydrogen peroxide molecule H_2O_2 (Figure **4.2.27**). It has a so-called roof-structure due to its non-planarity. One hydrogen atom points toward us, and the other points away from us. This structure is due to the two electron-lone pairs at each sp^3-hybridized oxygen atom. These electron-lone pairs consume somewhat more space than the H atoms, and there is electrostatic repulsion between the electron lone pairs. Therefore, the electron lone pairs at the different oxygen atoms try to achieve the greatest distance from each other. This forces the H-atoms out of the plane, leading to the roof-structure of the hydrogen peroxide. Because the H_2O_2 molecule is not planar, it only has a single C_2 axis, but no other symmetry element besides the identity. The C_2 axis passes through the center of the O-O bond. Execution of the C_2 operation swaps up both the O and the H atoms.

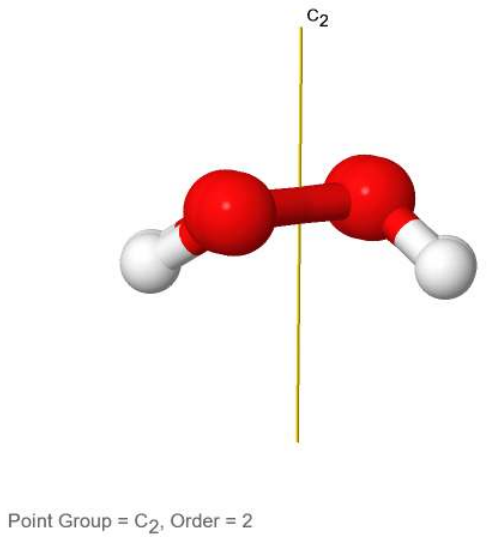


Figure **4.2.27**: The C_2 rotational axis of hydrogen peroxide (Attribution: symotter.org/gallery)

C_{nv} Point Groups

Another class of groups are the pyramidal groups, denoted C_{nv}. They have n vertical mirror planes containing the principal axis C_n in addition to the principal axis C_n. Generally molecules belonging to pyramidal groups are derived from an n-gonal pyramid. An n-gonal pyramid has an n-gonal polygon as the basis which is capped. For example a trigonal pyramid has a triangular basis which is capped, a tetragonal pyramid has a square which is capped, and so on. The proper axis associated with a specific pyramid has the order n and goes through the tip of the pyramid and the center of the polygon. An example of a molecule with a trigonal pyramidal shape is the NH_3 (Figure **4.2.28**).

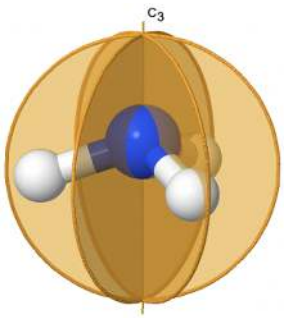


Figure 4.2.28: C_3 axis and vertical mirror planes in NH_3 (Attribution: symotter.org/gallery)

The three H atoms form the triangular basis of the pyramid, which is capped by the N atom. The NH_3 molecule belongs to the point group C_{3v}. The C_3 axis goes though the N atom which is the tip of the pyramid, and the center of the triangle defined by the H atoms. There are three vertical mirror planes that contain the C_3 axis. Each of them goes through an N-H bond.

C_{nh} Point Groups

If we add a horizontal mirror plane instead of n vertical mirror planes to a proper rotational axis C_n we arrive at the point group type C_{nh}. The presence of the horizontal mirror planes also generates an improper axis of the order n. This is because when one can rotate and reflect perpendicular to the rotational axes independently, then it must also be possible to do it in combination. An example of a molecule belong to a C_{nh} group is the trans-difluorodiazene N_2F_2 (Figure 4.2.29). It is a planar molecule with a C_2 axis going through the middle of the N-N double bond, and standing perpendicular to the plane of the molecule. The horizontal mirror plane stands perpendicular to the C_2 axis, and is within the plane of the molecule. There is an additional inversion center because an S_2 must exist which is the same as an inversion center. The inversion center is in the middle of the N-N bonds. Overall, the molecule has the symmetry C_{2h}.

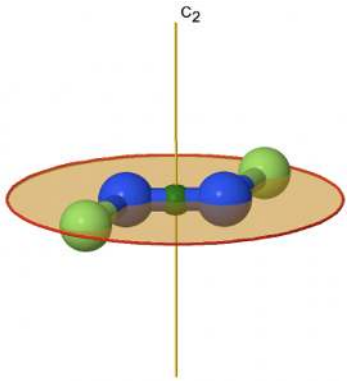


Figure 4.2.29: C_2 axis and horizontal mirror plane in trans-N_2F_2 (Attribution: symotter.org/gallery)

S_{2n} Point Groups

The category of rotational point groups to be discussed are the improper rotation point groups. The only have one proper rotational axis, and an improper rotational axis that has twice the order of the proper rotational axis (Figure 4.2.30). There may be an inversion center present depending on the order of the proper and improper axes. Molecules that fall into these point groups are rare. An example the tetramethylcycloocta-tetraene molecule (Figure 4.2.30).

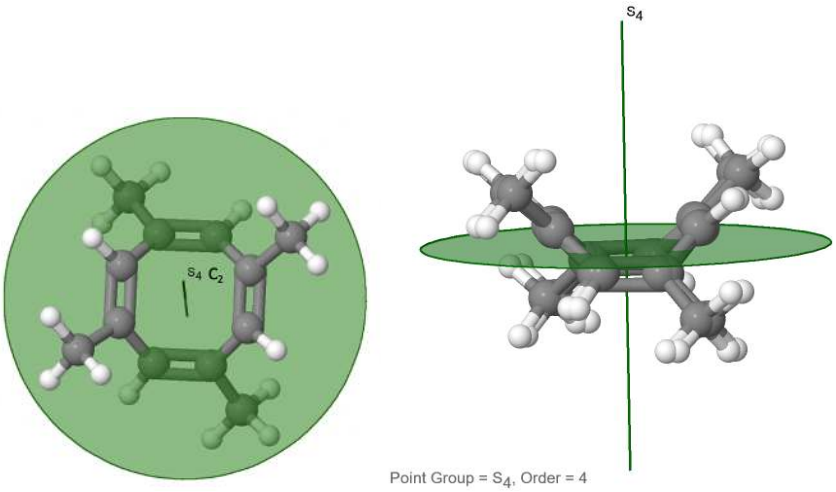


Figure **4.2.30**: The S_4 and an C_2 axes of tetramethyl cycloocta-tetraene

It has an S_4 and an C_2 axis as the only symmetry elements besides the identity. Rotating by 90° alone does not superimpose the molecule because two C-C double bonds lie above the plane and two below the plane. In addition, two opposite methyl groups lie above and below the plane respectively. Therefore it needs the additional reflection to achieve superposition. There is also a C_2 axis which is in the same locations as the S_4 axis.

Dihedral Groups

D_n Point Groups

Dihedral groups are point groups that have n additional C_2 axes that stand perpendicular to the principal axis of the order n. If there are no other symmetry elements, then the point group is of the type D_n. For example in the point group D_3 there is a C_3 principal axis, and three additional C_2 axes, but no other symmetry element (Fig. 2.2.75). The tris-oxolatoferrate(III) ion belongs to this point group (Figure **4.2.31**). You can see that the C_3 axis stands perpendicular to the paper plane, and there are three C_2 axes in the paper plane.

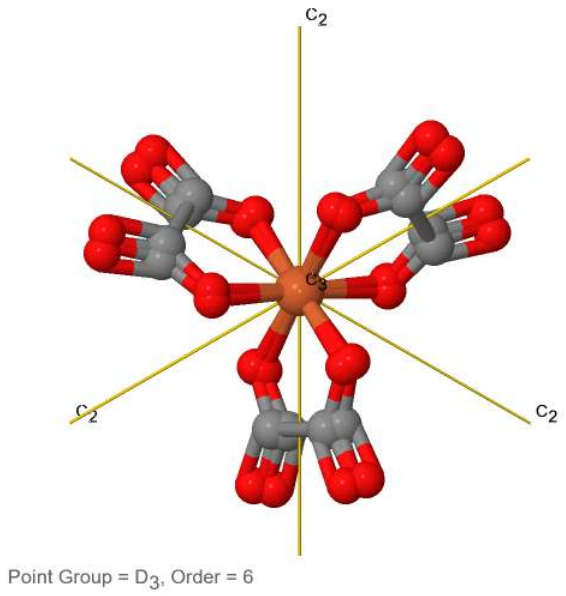


Figure **4.2.31**: The tris-oxolatoferrate(III) ion and its symmetry elements. (Attribution: symotter.org/gallery)

D_{nh} Point Groups

If a horizontal mirror plane is added to the C_n axis and the n C_2 axes we arrive at the D_{nh} point groups. The addition of the horizontal mirror plane generates further symmetry elements namely an S_n and n vertical mirror planes. An example for a molecule belonging to this class of point group is PF_5 (Figure **4.2.32**). It has a trigonal bipyramidal shape. The C_3 axis goes through the axial F atoms of the molecule, and the three C_2 axes go through the three equatorial F atom. The horizontal mirror plane stands perpendicular to the principal C_3 axis and is located within the equatorial plane of the molecule. In addition, there are the vertical mirror planes that contain the C_3 axis, and go through the three equatorial P-F bonds. There is also an S_3 axis which superimposes the C_3 axis.

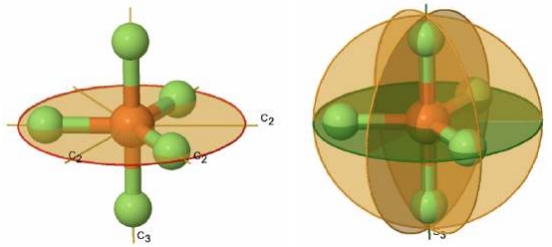


Figure **4.2.32**: The PF_5 molecule belonging to the point group D_{3h} and its symmetry elements. (Attribution: symotter.org/gallery)

D_{nd} Point Groups

If we add n vertical mirror planes to the principal axis and the n C_2 axes, we arrive at the point group D_{nd}. The vertical mirror planes are dihedral mirror planes because they bisect the angle between the C_2 axes. An example is the ethane molecule in staggered conformation which has the symmetry D_{3d} (Figure **4.2.33**:). The C_3 axis goes along the C-C bond, and the $3C_2$ axes pass through the middle of the carbon-carbon bond, and bisect the angle between two hydrogens and one carbon atom. The three dihedral mirror planes pass through the C-H bonds. In addition, the ethane molecule has an S_6 axis, and an inversion center.

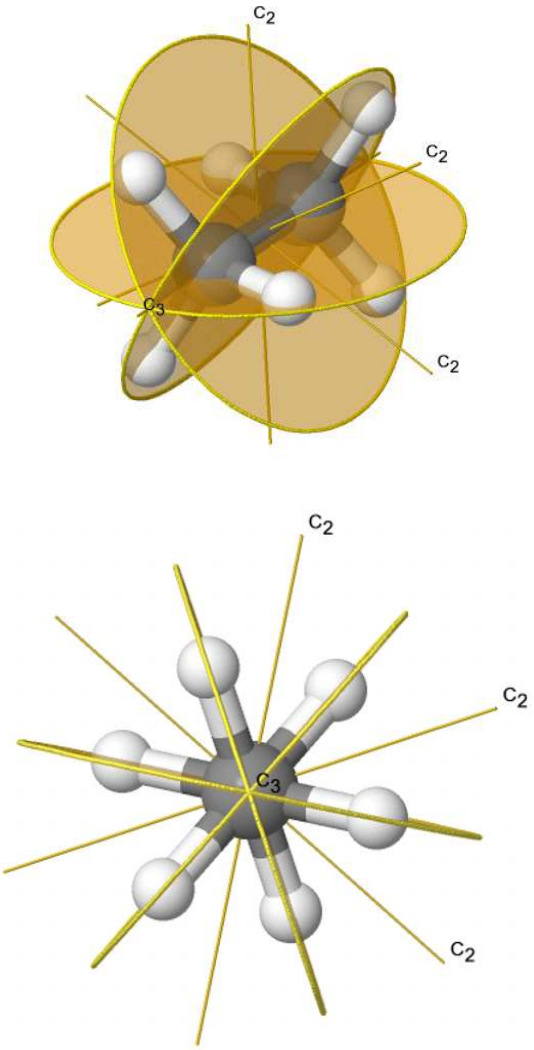


Figure **4.2.33**: The ethane molecule in the staggered conformation belongs to the point group type D_{nd} (Attribution: symotter.org/gallery)

Linear Point Groups

The principal rotation axis in a linear molecule is a C_∞ axis, meaning the molecule can be rotated along its bond axis an infinitely small amount and remain unchanged. Linear molecules can be subdivided based on the presence or absence of a horizontal reflection plane and inversion center.

$C_{\infty v}$ point groups

A special n-gonal polygon is the cone. A cone can be conceived as an n-gonal pyramid with an infinite number *n* of corners at the base (Figure **4.2.34**).

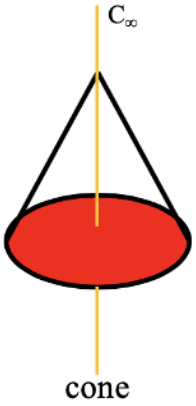


Figure **4.2.34**: Cone having a proper rotational axis with infinite order.

In this case the order of the rotational axis that passes through the tip of the cone and the center of the circular basis is infinite. This also means that there is an infinite number of vertical mirror planes that contain the C_∞ axis. The point group describing the symmetry of a cone is called the linear point group $C_{\infty v}$. Polar, linear molecules such as CO, HF, N_2O, and HCN belong to this point group. You can see the HCN molecule with its C_∞ axis and its infinite number of vertical mirror planes below (Figure **4.2.35**). The infinite number of mirror planes, shown in blue are forming a cylinder that surround the molecule.

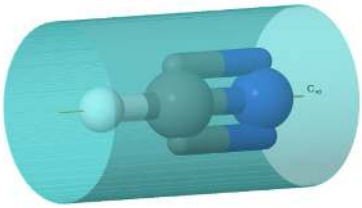


Figure **4.2.35**: C_∞ axis of the HCN molecule.

$D_{\infty h}$ point groups

A special case of a D_{nh} group is the linear group $D_{\infty h}$. An object that has this symmetry is a cylinder. A cylinder can be conceived as a prism with an infinite number of vertices. Thus, the principal axis that passes through a cylinder has infinite order. Because of the infinite order of the principal axis, there is an infinite number of C_2 axes that stand perpendicular to the principal axis. You can see one such C_2 going though the cylinder (Figure **4.2.36**:).

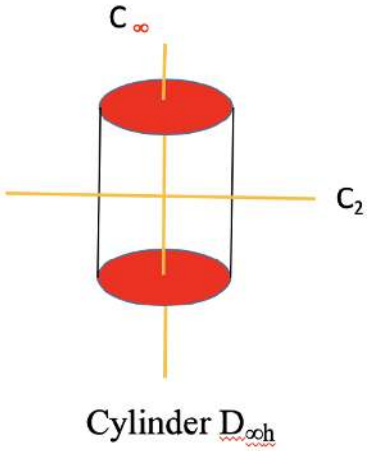
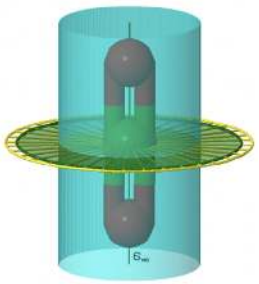


Figure **4.2.36**: Cylinder as an example of linear group $D_{\infty h}$.

There is now also an improper axis of infinite order, as well as an infinite number of vertical mirror planes. Non-polar linear molecules like H_2, CO_2, and acetylene C_2H_2 belong to the point group $D_{\infty h}$. You can see the C_∞ axis passing through a CO_2 molecule below (Figure **4.2.37**). You can see the infinite number of vertical mirror planes as a blue cylinder. The infinite number of C_2 axes is shown a yellow lines going around the molecule.



CO_2

Figure 4.2.37: C_∞ in a CO_2 molecule.

Guide for the Determination of Point Groups

The symmetry operations a molecule possesses will determine which point group the molecule is in. The key to success is that you are able to see the symmetry elements in the molecule which takes practice. Luckily, especially for high symmetry point groups, you don't need to identify every single symmetry operation to correctly assign a point group. You can use a flow chart to identify a point group more easily. These flow charts ask systematic questions about the presence or absence of key symmetry elements. Eventually, after having answered enough questions the guide will lead you to the respective point group. You can see an example flow chart below (Figure 4.2.38:).

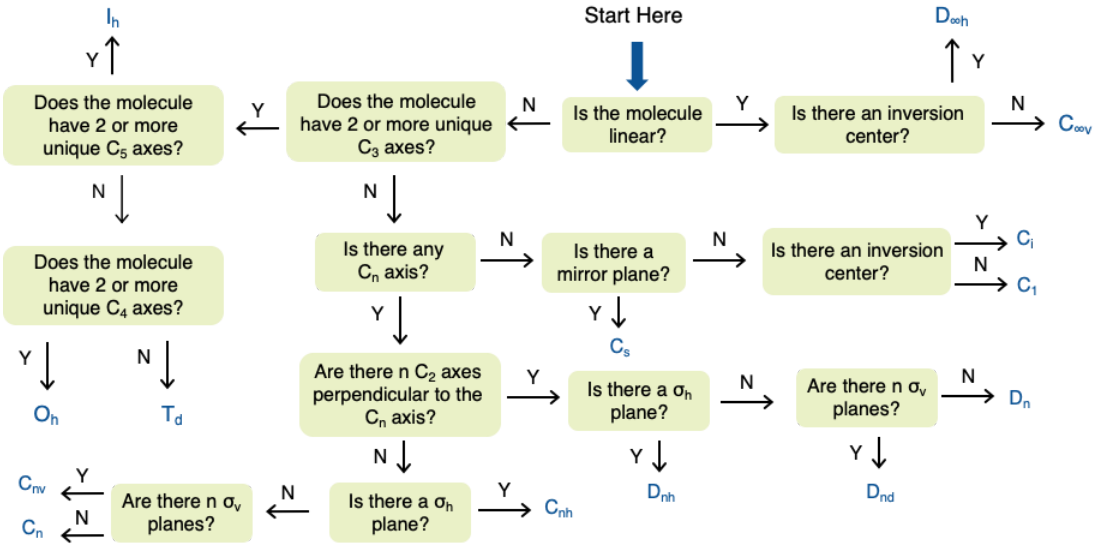


Figure 4.2.38: Flow chart for the determination of point groups. (CC BY-NC-SA; Catherine McCusker)

You can first ask if the molecule is linear (has a C_∞ rotation axis). Then we can ask next, if there is a high symmetry point group. This is the case when there are either $4C_3$, $3C_4$, or $6C_5$ rotational axes present, standing for tetrahedral, octahedral, and icosahedral symmetry, respectively. If there is are no C_n axes of any type present the molecule must be in a low symmetry point group. We ask if there are n $\perp C_2$ axes in addition to the C_n principal axis. If this is so, then we must have a dihedral group of the D type. If there are no $\perp$ C_2 axes in addition to the C_n, the group must be a rotational (C) group.

Example: Dibromonaphtalene

Let us practice the point group flow chart by example. Let us look at the dibromonaphtalene molecule (Figure 4.2.39).

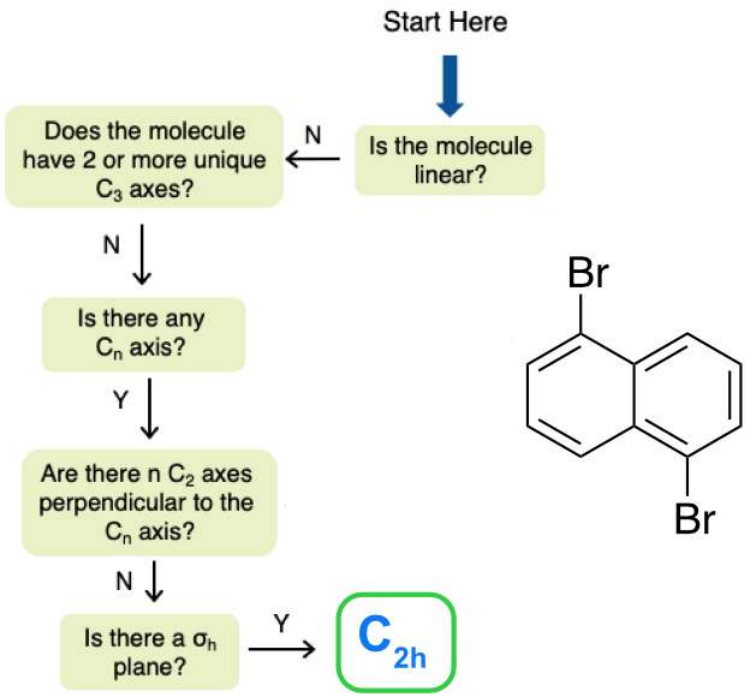


Figure 4.2.39: Guide for determining the point group of dibromonaphtalene

After determining that the molecule is not linear or in a high symmetry group (having 2 or more C_3 rotation axes), the first question we ask is: Can you see at least one proper rotational axis? The answer is yes. There is a C_2 proper rotational axis that stands perpendicular to the plane of the molecule and goes through the center of the C-C bond that is shared by the two aromatic rings. Next we can think about if the there are $2C_2$ axes in addition to the C_2 axes we already found. The answer is no, so the point group cannot be a dihedral (D) group. Next, we would ask: Is there a horizontal mirror plane. This is indeed the case. There is a horizontal mirror plane in the plane of the molecule. It does not move any atoms around, but as we discussed before, a mirror does not need to do this to exist. This identifies the point group as C_{2h}.

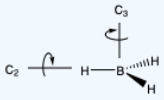
The Symmetry Challenge at Otterbein University is a great way to practice assigning molecules to point groups!

Exercise 4.2.1

Use the flow chart to assign the point group for (a) BH_3 and (b) H_2O.

Answer

(a) BH_3 has a trigonal planar geometry.



- It has a C_3 principal rotation axis
- It doesn't have C_5, C_4, or multiple C_3 axes
- It has 3 $\perp$ C_2 axes
- It has a σ_h (the plane of the molecule)
- The point group is **D_{3h}**

(b) H_2O has a bent geometry.



- It has a C_2 principal rotation axis
- It doesn't have any C_5, C_4, or C_3 axes
- It doesn't have $\perp$ C_2 axes
- It doesn't have a σ_h reflection plane
- It does have 2 σ_v reflection planes

- The point group is $\mathbf{C_{2v}}$

Dr. Kai Landskron (Lehigh University). If you like this textbook, please consider to make a donation to support the author's research at Lehigh University: Click Here to Donate.

This page titled 4.2: Point Groups is shared under a CC BY-NC-SA 4.0 license and was authored, remixed, and/or curated by Kai Landskron.

- **2.2: Point Groups** by Kai Landskron is licensed CC BY 4.0.
- **Current page** by Kai Landskron is licensed CC BY-NC-SA 4.0.

4.3: Introduction to Character Tables

Although the flow chart method of assigning a molecule to a point group requires some knowledge of the symmetry elements the molecule has, it does not require the consideration of all elements. For example, the molecule PF_5 can be assigned the point group D_{3h} using the flow chart by knowing that the molecule has a C_3 principal rotation axis, $\perp C_2$ axes, and a σ_h reflection plane. The point group assignment in this case did not require knowing that the molecule also has an improper rotation axis, for example. This type of knowledge is gained by examining character tables. A character table is a table that contains all the symmetry information of the point group. This information is essential for applying symmetry and group theory to chemical problems. In this course our goal is to become familiar with the information contained in character tables, in Advanced Inorganic we will use character tables for different chemical applications. As an example, the following table is the D_{4h} character table, a complete listing of character tables can be found under resources.

Table 1: *The character table of the point group D_{4h}.*

D_{4h}	E	$2C_4$	C_2	$2C_2'$	$2C_2''$	i	$2S_4$	σ_h	$2\sigma_v$	$2\sigma_d$		
A_{1g}	1	1	1	1	1	1	1	1	1	1		x^2+y^2, z^2
A_{2g}	1	1	1	-1	-1	1	1	1	-1	-1	R_z	
B_{1g}	1	-1	1	1	-1	1	-1	1	1	-1		x^2-y^2
B_{2g}	1	-1	1	-1	1	1	-1	1	-1	1		xy
E_g	2	0	-2	0	0	2	0	-2	0	0	(R_x, R_y)	(xz, yz)
A_{1u}	1	1	1	1	1	-1	-1	-1	-1	-1		
A_{2u}	1	1	1	-1	-1	-1	-1	-1	1	1	z	
B_{1u}	1	-1	1	1	-1	-1	1	-1	-1	1		
B_{2u}	1	-1	1	-1	1	-1	1	-1	1	-1		
E_u	2	0	-2	0	0	-2	0	2	0	0	(x, y)	

Components of Character Tables

Symmetry Operations

Across the top of each character table is a list of all the symmetry operations in the point group. Rather than being listed individually, they are grouped into classes. Symmetry operations in the same class will result in equivalent transformations.

Irreducible Representations

Down the left side of each character table is a list of irreducible representations. An irreducible representation describes how something (an atom, bond, orbital, etc.) changes when the different symmetry operations are performed. It could stay the same (1), become inverted (-1), or change completely (0). Representations with A and B labels are non-degenerate. Representations with E labels are two-fold degenerate, a set of two things that are the same energy like π bonding MOs formed from p_x and p_y atomic orbitals. Representations with T labels, found in high symmetry point groups, are three-fold degenerate. Representations with a subscript g are even (gerade) and stay the same after the inversion operation and representations with a subscript u are odd (ungerade) and are inverted after the the inversion operation.

Mathematical Functions

The last two columns contain mathematical functions, indicating which irreducible representation the functions belong to. When two or more of these functions are listed together in parentheses, (x, y) it means these functions are degenerate. In chemistry applications these mathematical functions can be used to assign orbitals to irreducible representations. For example, in the D_{4h}

point group the p_z orbital will have the same symmetry as the mathematical function z and will be in the A_{2u} irreducible representation and the d_{xy} orbital will have the same symmetry as the mathematical function xy and will be in the B_{2g} irreducible representation

---

4.3: Introduction to Character Tables is shared under a CC BY-NC-SA 4.0 license and was authored, remixed, and/or curated by LibreTexts.

- **3.5: Character Tables - An Introduction** is licensed CC BY-NC-SA 4.0.
- **Current page** is licensed CC BY-NC-SA 4.0.

4.4: Applications of Symmetry in Chemistry

In the previous sections of this chapter, the necessary tools to assign a point group to a molecule and to be able to read a character table were introduced. A good question at this point is: What is the importance of these tools in inorganic chemistry?

In fact, there are many applications in the study of inorganic chemistry where these symmetry tools become handy. In general, these applications belong to one of the following categories:

- Determining orbital overlap for molecular orbitals.
- Understanding the spectroscopic properties of molecules
- Identifying chiral molecular species

Orbital Overlap and Molecular Orbitals

As discussed previously, symmetry is one of the criteria for determining whether two or more atomic orbitals can overlap to form molecular orbitals. Once molecules get larger than two or three atoms drawing all the possible atomic orbital combinations to determine if they have the right symmetry to overlap is challenging and time consuming. Symmetry can be applied in this case to make the determination more quickly and easily, only orbitals that have the same irreducible representation have the correct symmetry to overlap and form a molecular orbital. As an example we will revisit the orbital overlap in water. Following the flow chart, the water molecule is in the C_{2v} point group because it has a C_2 principal rotation axis, no other rotation axes, no σ_h reflection plane and 2 σ_v reflection planes. Figure **4.4.1** shows the valence atomic orbitals of oxygen and hydrogen along with the irreducible representations they correspond to in the C_{2v} point group. Because only orbitals with the same irreducible representation can form molecular orbitals, both the $2p_z$ and 2s on O can overlap with the in-phase combination of 1s orbitals on the H atoms and the $2p_x$ on O can overlap with the out of phase combination of 1s orbitals on the H atoms. However, the $2p_y$ orbital on O has a different irreducible representation from both the H 1s combinations. This means the O $2p_y$ is non bonding in water.

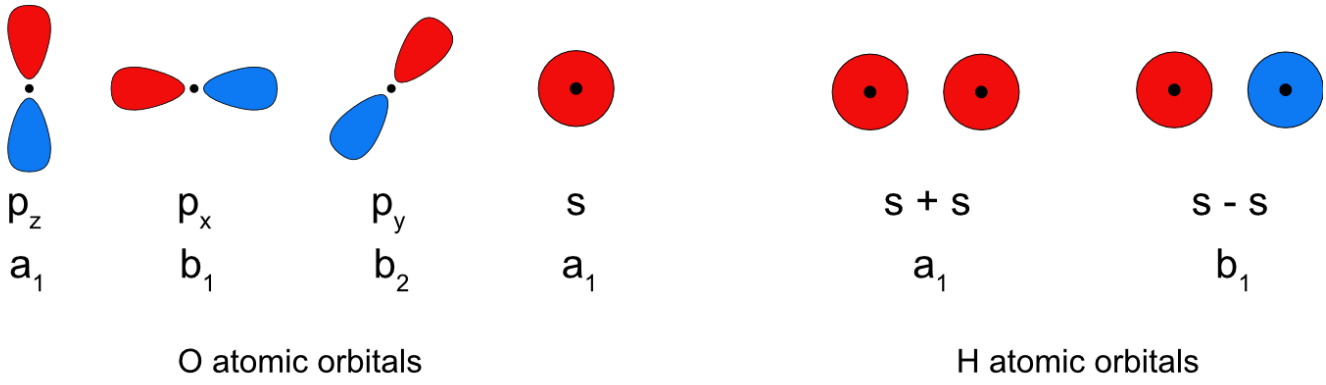


Figure **4.4.1**: Symmetries of the atomic orbitals in H_2O (C_{2v} point group). The valence atomic orbitals of O and their irreducible representations in the C_{2v} point group are on the left and the in phase and out of phase combinations of the two H 1s orbitals their irreducible representations in the C_{2v} point group are on the right (CC BY-NC-SA; Catherine McCusker)

Vibrational Spectroscopy

Every molecule has a total of $3n-6$ ($3n-5$ for linear) vibrational modes, but not all of those vibrations will necessarily appear in the infrared or Raman spectrum of the molecule. Symmetry can be used to develop selection rules, and easily determine which vibrational modes will be infrared active, which will be Raman active, and which will be both.

(a) (b)



Figure 4.4.2: Examples of different types of stretching vibrational modes (a) symmetric stretching and (b) antisymmetric stretching. (Image source: https://en.Wikipedia.org/wiki/Infrared_spectroscopy)

(a) (b) (c) (d)



Figure 4.4.3: Examples of different types of bending vibrational modes (a) scissoring, (b) rocking, (c) wagging, and (d) twisting. (Image source: https://en.Wikipedia.org/wiki/Infrared_spectroscopy)

Selection Rules

Infrared Spectroscopy

Infrared spectroscopy measures the frequency of absorption when a sample is irradiated with infrared electromagnetic radiation. The bonds between atoms can be thought of as a spring connecting two masses. In the spring-mass analogy the moving system can be approximated by a simple harmonic oscillator. The frequency oscillation is proportional to $\sqrt{\frac{k}{m}}$,where k is the spring constant and m is the mass of the object. In a similar approximation, the frequency of vibration between two atoms is unique and varies depending on the strength of the bond (k) and the size of the atoms (m). When the frequency of electromagnetic radiation matches the frequency of vibration between atoms, the energy can be possibly be absorbed. In order for a vibrational mode to be infrared active (absorb infrared light) the vibration must produce a change in the dipole moment of the molecule which can interact with the electric field. Any vibrational mode which has the same symmetry (corresponds to the same irreducible representation) as the mathematical functions x, y, and z will shift the charge distribution of the molecule in any of the x, y, or z directions resulting in a change in the dipole moment. Any vibrational mode which has the same symmetry as x, y, or z will be able to absorb infrared light and will appear in an infrared spectrum.

Raman Spectroscopy

Unlike IR spectroscopy which measures the energy absorbed, Raman spectroscopy is based on inelastic scattering of visible light. Upon a collision between a molecule and photon, a small amount of energy, equal to a vibrational frequency, can be transferred to or from the photon. The difference in the photon's energy before and after the collision is the Raman shift, and will have the same energies as the (Raman active) vibrational frequencies of the molecule. A vibrational mode will be Raman active if it causes a change in the molecular polarizability. Polarizability measures the ability for a molecule's electron cloud to become distorted. A dense electron cloud is more difficult to change than a more diffuse electron density. Any vibrational mode which has the same symmetry (corresponds to the same irreducible representation) as the product mathematical functions will cause a change in polarizability and will be Raman active. Product functions include any of the functions: \(xy, xz, yz, x^2, y^2, z^2\), or any combination, and are listed in the second column of math functions in a character table.

Rule of Mutual Exclusion

A molecule is centrosymmetric if it has a center of inversion and their corresponding point group contains the class for inversion. In such cases, the functions x, y, and z belong to ungerade (odd) irreducible representations, and the product functions belong to gerade (even) irreducible representations. As a result, vibrational modes in centrosymmetric molecules may be either infrared or Raman active, but they cannot be both.

Example 4.4.1

The bond stretching vibrations in $[PtCl_4]^{2-}$ are shown below, along with their corresponding irreducible representations. $[PtCl_4]^{2-}$ is a square planar molecule in the D_{4h} point group.

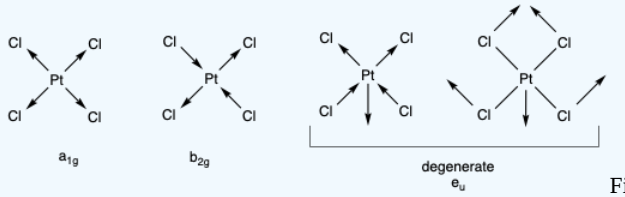


Figure 4.4.4: The four bond stretching vibrations in $[PtCl_4]^{2-}$ and their irreducible representations. (CC BY-NC-SA; Catherine McCusker)

By inspection we can see that the first two vibrations (a_{1g} and b_{2g}) won't change the dipole moment of the molecule, and are therefore not infrared active. This can be confirmed with the D_{4h} character table below. The mathematical functions x, y, and z (which represent a change in dipole moment) do not have a_{1g} or b_{2g} symmetry. The functions x and y are degenerate and have e_u symmetry. This means the last pair of vibrations will be infrared active, although because they are degenerate they will be at the same energy and appear as a single peak in the IR spectrum.

Raman active vibrations change the polarizability of the molecule, which is more difficult to determine by inspection. Any vibration that changes the polarizability of the molecule will have the same symmetry as the product math functions in the last column of the character table. By consulting the D_{4h} character table we cans see the math functions $x^2 + y^2$ and x^2 have a_{1g} symmetry, the math function xy has b_{2g} symmetry, and no product functions have eu symmetry. This means that only the first two vibrations (a_{1g} and b_{2g}) will be Raman active and will appear in the Raman spectrum.

You may also note that $[PtCl_4]^{2-}$ is a centrosymmetric molecule (has an inversion center) and the two infrared active vibrations belonged to an odd (u) symmetry irreducible representation and the two Raman active vibrations belonged to even (g) symmetry irreducible representations

D_{4h}	E	$2C_4$	C_2	$2C_2'$	$2C_2''$	i	$2S_4$	σ_h	$2\sigma_v$	$2\sigma_d$		
A_{1g}	1	1	1	1	1	1	1	1	1	1		x^2+y^2, z^2
A_{2g}	1	1	1	-1	-1	1	1	1	-1	-1	R_z	
B_{1g}	1	-1	1	1	-1	1	-1	1	1	-1		x^2-y^2
B_{2g}	1	-1	1	-1	1	1	-1	1	-1	1		xy
E_g	2	0	-2	0	0	2	0	-2	0	0	(R_x, R_y)	(xz, yz)
A_{1u}	1	1	1	1	1	-1	-1	-1	-1	-1		
A_{2u}	1	1	1	-1	-1	-1	-1	-1	1	1	z	
B_{1u}	1	-1	1	1	-1	-1	1	-1	-1	1		
B_{2u}	1	-1	1	-1	1	-1	1	-1	1	-1		
E_u	2	0	-2	0	0	-2	0	2	0	0	(x, y)	

Chirality

Around the year 1847, the French scientist Louis Pasteur provided an explanation for the optical activity of tartaric acid salts. when he carried out a particular reaction, Pasteur observed that two types of crystals precipitated. Patiently and carefully using tweezers, Pasteur was able to separate the two types of crystals. Pasteur noticed that the types rotated the plane polarized by the same amount but in different directions. These two compounds are called enantiomers.

What are Enantiomers?

Two compounds are enantiomers if they are non-superimposable mirror images of each other. As was mentioned, enantiomers are characterized by their ability to rotate plane-polarized light. They also have the same physical properties (e.g., melting point, etc.) relative to each other. As a result, they are also referred to as being optically active. When it comes to symmetry, there are some general rules of thumb that help determine whether a molecule is chiral or achiral. This can be very useful because sometimes molecules can have relatively complicated structures and geometries that knowing whether or not they are chiral becomes a daunting task. The goal, as a result, is to determine the point group of the molecule and the symmetry elements associated with it, then inferring the chirality of the molecule.

Using Symmetry to Determine Chirality

For a molecule to be chiral, it must lack:

1. Center of inversion i and a plane of symmetry σ.
2. An improper rotation axis (rotation-reflection axis) S_n.

However, since, by definition, an improper rotation axis is a rotation about an certain axis followed by reflection about a plane perpendicular to that axis, and an inversion center is simply S_2, the absence of an improper axis requires, in most cases, that absence of both a plane of symmetry and an inversion center. As a result, it suffices, in most cases, to check for improper rotation axes to determine whether a molecule is chiral or not.

As a result of the previous discussion, there are a few classes of point groups that lack an improper axis. Those classes are C_1, C_n, and D_n. *cis*-dichloridobis(ethylenediamine)cobalt(III) is in the C_2 point group and has two enantiomers that are chiral (Figure **4.4.5**). The *trans*-dichloridobis(ethylenediamine)cobalt(III) is achiral.

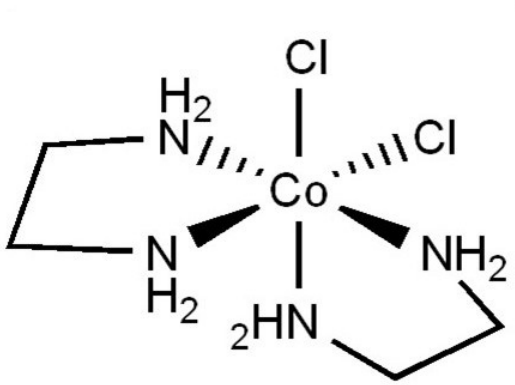


Figure **4.4.5**: One of the chiral enantiomers of *cis*-dichloridobis(ethylenediamine)cobalt(III).

4.4: Applications of Symmetry in Chemistry is shared under a CC BY-NC-SA 4.0 license and was authored, remixed, and/or curated by LibreTexts.

- **3.6: Significance of Recognizing Symmetry Elements** is licensed CC BY-NC-SA 4.0.
- **Current page** is licensed CC BY-NC-SA 4.0.
- **3.8: Chiral Molecules** is licensed CC BY-NC-SA 4.0.

CHAPTER OVERVIEW

5: Structure and Energetics of Solids

In the chemistry of molecular compounds, we are accustomed to the idea that properties depend strongly on structure. For example we can rationalize the polarity of the water molecule based on its shape. We also know that two molecules with the same composition (e.g., ethanol and dimethyl ether) have very different properties based on the bonding arrangements of atoms. It should come as no surprise that the properties of extended solids are also connected to their structures, and so to understand what they do we should begin with their crystal structures. Most of the metals in the periodic table have relatively simple structures and so this is a good place to begin.

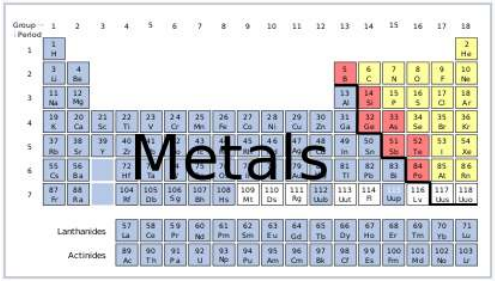


Figure **5.1**: Over $\frac{2}{3}$ of the elements in the periodic table are metals. All elemental metals (except the three - Cs, Ga, Hg - that are liquid at or near room temperature) are crystalline solids at room temperature, and most have one of three simple crystal structures.

With ionic solids we "graduate" from simple metal structures based on sphere packings to more complex structures where there are both anions and cations. In this chapter we will try to systematize the structures of inorganic solids - metal oxides, halides, sulfides, and related compounds - and develop some rules for which structures to expect based on electronegativity differences, hard-soft acid-base rules, and other periodic trends. We will see that many of these structures are based on the simple packing of spheres.



Figure **5.2**: The morphology of twinned crystals of iron pyrite (FeS_2) is related to the underlying cubic symmetry of the unit cell. Like NaCl, the pyrite crystal structure can be thought of as a face-centered cubic array of anions (S_2^{2-}) with cations (Fe^{2+}) occupying all the octahedral holes.

Inorganic solids often have simple crystal structures, and some of these structures are adopted by large families of ionic or covalent compounds. Examples of the most common structures include NaCl, CsCl, NiAs, zincblende, wurtzite, fluorite, perovskite, rutile, and spinel. We will develop these structures systematically from the close packed and non-close packed lattices.

Learning Objectives

- Determine the formula of an ionic solid based on the unit cell
- Predict relative lattice energies based on ion sizes and charges
- Understand how lattice energy plays a role in solubility
- Explain how particle size affects the material properties in nanomaterials

Thumbnail image shows the unit cell of the zincblende crystal structure

5.1: Crystal Structures and Unit Cells
5.2: Energetics of Ionic Solids- Lattice Energy
5.3: Lattice Enthalpies and Born Haber Cycles

5.4: Lattice Energy and Solubility
5.5: Bonding in Metals and Semicondoctors
5.6: Nanomaterials

5: Structure and Energetics of Solids is shared under a not declared license and was authored, remixed, and/or curated by LibreTexts.

5.1: Crystal Structures and Unit Cells

Introduction

The term "closest packed structures" refers to the most tightly packed or space-efficient composition of crystal structures (lattices). Imagine an atom in a crystal lattice as a sphere. While cubes may easily be stacked to fill up all empty space, unfilled space will always exist in the packing of spheres. To maximize the efficiency of packing and minimize the volume of unfilled space, the spheres must be arranged as close as possible to each other. These arrangements are called **closest packed structures**. The packing of spheres can describe the solid structures of crystals. In a crystal structure, the centers of atoms, ions, or molecules lie on the lattice points. Atoms are assumed to be spherical to explain the bonding and structures of metallic crystals. These spherical particles can be packed into different arrangements. In closest packed structures, the arrangement of the spheres are densely packed in order to take up the greatest amount of space possible.

Close-Packing of Identical Spheres

Crystals are of course three-dimensional objects, but we will begin by exploring the properties of arrays in two-dimensional space. This will make it easier to develop some of the basic ideas without the added complication of getting you to visualize in 3-D — something that often requires a bit of practice. Suppose you have a dozen or so marbles. How can you arrange them in a single compact layer on a table top? Obviously, they must be in contact with each other in order to minimize the area they cover. It turns out that there are two efficient ways of achieving this:



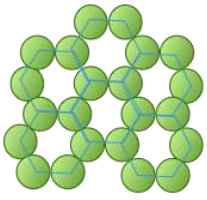
The essential difference here is that any marble within the interior of the square-packed array is in contact with four other marbles, while this number rises to six in the hexagonal-packed arrangement. It should also be apparent that the latter scheme covers a smaller area (contains less empty space) and is therefore a more efficient packing arrangement. If you are good at geometry, you can show that square packing covers 78 percent of the area, while hexagonal packing yields 91 percent coverage.

If we go from the world of marbles to that of atoms, which kind of packing would the atoms of a given element prefer?



If the atoms are identical and are bound together mainly by dispersion forces which are completely non-directional, they will favor a structure in which as many atoms can be in direct contact as possible. This will, of course, be the hexagonal arrangement.

Directed chemical bonds between atoms have a major effect on the packing. The version of hexagonal packing shown at the right occurs in the form of carbon known as *graphite* which forms 2-dimensional sheets. Each carbon atom within a sheet is bonded to three other carbon atoms. The result is just the basic hexagonal structure with some atoms missing.



The coordination number of 3 reflects the sp^2-hybridization of carbon in graphite, resulting in plane-trigonal bonding and thus the sheet structure. Adjacent sheets are bound by weak dispersion forces, allowing the sheets to slip over one another and giving rise to the lubricating and flaking properties of graphite.

Types of Holes From Close-Packing of Spheres

When a single layer of spheres is arranged into the shape of a hexagon, gaps are left uncovered. The hole formed between three spheres is called a **trigonal hole** because it resembles a triangle. In Figure **5.1.1**, two out of the the six trigonal holes have been highlighted green.

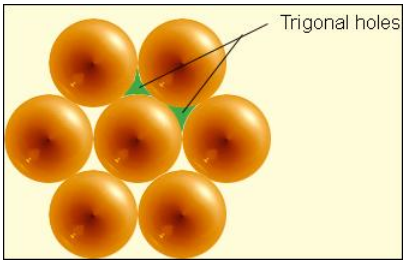


Figure **5.1.1**: Trigonal holes (green) between close packed spheres in a single layer

Once the first layer of spheres is laid down, a second layer may be placed on top of it. The second layer of spheres may be placed to cover the trigonal holes from the first layer. Holes now exist between the first layer (the orange spheres) and the second (the lime spheres), but this time the holes are different (Figure **5.1.2**). The triangular-shaped hole created over a orange sphere from the first layer is known as a **tetrahedral hole** because the surrounding spheres are in a tetrahedral arrangement. A hole from the second layer that also falls directly over a hole in the first layer is called an **octahedral hole** because the surrounding spheres are in an octahedral arrangement.

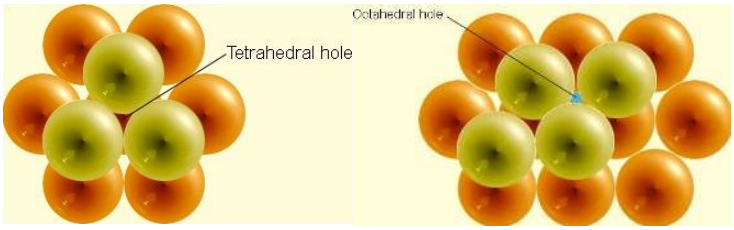


Figure **5.1.2**: Illustrations of tetrahedral (left) and octahedral (right) holes formed between two close packed layers

Close Packed Crystal Structures

Hexagonal Close-Packed (hcp)

In a hexagonal close-packed structure, the third layer has the same arrangement of spheres as the first layer and covers all the tetrahedral holes. Since the structure repeats itself after every two layers, the stacking for hcp may be described as "a-b-a-b-a-b." The atoms in a hexagonal close-packed structure efficiently occupy 74% of space while 26% is empty space.

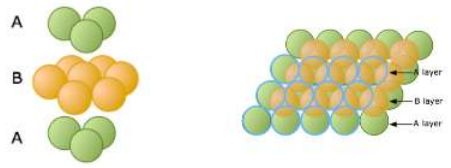


Figure **5.1.3**: Side and top views of the layers in the hexagonal close-packed (hpc) structure.

Cubic Close-Packed (ccp)

The arrangement in a cubic closest packing also efficiently fills up 74% of space. Similar to hexagonal closest packing, the second layer of spheres is placed on to of half of the depressions of the first layer. The third layer is completely different than that first two layers and is stacked in the depressions of the second layer, thus covering all of the octahedral holes. The spheres in the third layer are not in line with those in layer A, and the structure does not repeat until a fourth layer is added. The fourth layer is the same as the first layer, so the arrangement of layers is "a-b-c-a-b-c."

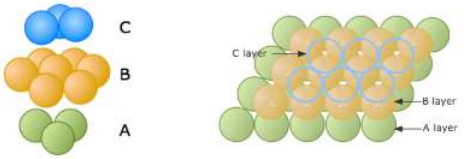


Figure 5.1.4: Side and top views of the layers in cubic close-packed (ccp) structure.

Coordination Number and Number of Atoms Per Unit Cell

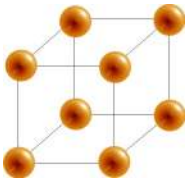
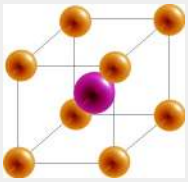
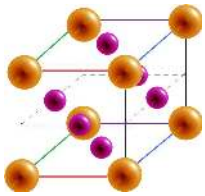
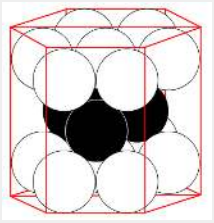
A unit cell is the smallest representation of an entire crystal. All crystal lattices are built of repeating unit cells. In a unit cell, an atom's coordination number is the number of atoms it is touching.

- The simple cubic has a sphere at each corner of a cube. Each sphere has a coordination number of 6 and there is 1 atom per unit cell.
- The body-centered cubic (bcc) has a sphere at each corner of a cube and one in the center. Each sphere has a coordination number 8 and there are 2 atoms per unit cell.
- The cubic closest packed, also called face-centered cubic (fcc) has has a sphere at each corner and each face of a cube. Each sphere has a coordination number of 12 and there are 4 atoms per unit cell.
- The hexagonal closest packed has spheres arranged in hexagons with one in the center. each sphere has a coordination number of 12 and there are 6 atoms per unit cell.

Atoms Per Unit Cell

The amount that an atom contributes to a unit cell depends on its position in the unit cell

- Each corner atom contributes $\frac{1}{8}$ to the unit cell in the cubic cells and $\frac{1}{6}$ to the unit cell in hcp
- Each edge atom contributes $\frac{1}{4}$ to the unit cell
- Each face atom contributes $\frac{1}{2}$ to the unit cell
- Each center atom contributes 1 to the unit cell

Unit Cell	Coordination Number	# of Atoms Per Unit Cell	% space
Simple Cubic 	**6**	**1**	**52%**
Body-Centered Cubic 	**8**	**2**	**68%**
Face-centered Cubic 	**12**	**4**	**74.04%**
Hexagonal Closest Packed 	**12**	**6**	**74.04%**

Inorganic Crystals

Many common inorganic crystals have structures that are related to cubic close packed (face-centered cubic) or hexagonal close packed sphere packings. One component of the material will pack in one of the arrangements above. The remaining component(s) will fill some or all of the holes between the layers. An interstitial atom filling a tetrahedral hole is coordinated to four packing atoms, and an atom filling an octahedral hole is coordinated to six packing atoms. In both the hexagonal close packed and cubic close packed lattices, there is one octahedral hole and two tetrahedral holes per packing atom.

Are Anions or Cations Better Packing Atoms?

We might expect that anions, which are often larger than cations, would be better suited to the positions of packing atoms. While this is often true, there are many examples of structures in which cations are the packing atoms, and others in which the distinction is arbitrary. The NaCl structure is a good example of the latter.

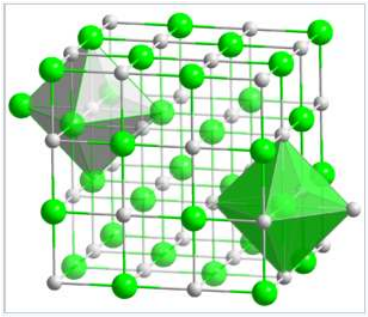


Figure **5.1.5**: Crystal structure of NaCl. Both the Na^+ (grey) and Cl^- (green) ions are octahedrally coordinated.

In the rock salt or NaCl structure, shown in Figure **5.1.5**, the green spheres are the Cl^- ions and the gray spheres are the Na^+ ions. The packing atoms (Na^+) are in a face centered cubic arrangement. The octahedral holes in a face-centered cubic lattice can be found at the edges and in the center of the unit cell, and they are filled by the chloride ions. Alternatively the structure can be described as the Cl^- ions in a fcc arrangement with the Na^+ ions occupying the octrahedral holes. Another way of stating this is that the structure consists of **two interpenetrating fcc lattices**, which are related to each other by a translation of half the unit cell along any of the three Cartesian axes. Thus the distinction between packing and interstitial atoms in this case is arbitrary.

NaCl is interesting in that it is a three-dimensional checkerboard, and thus there are no NaCl "molecules" that exist in the structure. When this structure was originally solved (in 1913 by using X-ray diffraction) by W. L. Bragg, his interpretation met resistance by chemists who thought that precise integer stoichiometries were a consequence of the valency of atoms in molecules. The German chemist Pfeiffer noted in 1915 that ‘the ordinary notion of valency didn’t seem to apply’, and fourteen years later, the influential chemist Armstrong still found Bragg’s proposed structure of sodium chloride ‘more than repugnant to the common sense, not chemical cricket’! Nevertheless, Bragg and his father, W. H. Bragg, persevered and used the then-new technique of X-ray diffraction to determine the structures of a number of other compounds, including diamond, zincblende, calcium fluoride, and other alkali halides. These experiments gave chemists their first real look at the atomic structure of solids, and laid the groundwork for X-ray diffraction experiments that later elucidated the structures of DNA, proteins, and many other compounds. For their work on X-ray diffraction the Braggs received the Nobel prize in Physics in 1915.

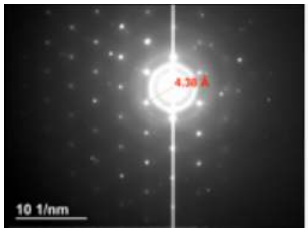


Figure **5.1.6**: X-ray difffraction pattern for a NaCl crystal. The lattice dimensions and positions of atoms in crystals such as NaCl are inferred from diffraction patterns.

Since each type of atom in the NaCl structure forms a face-centered cubic lattice, there are four Na and four Cl atoms per NaCl unit cell. It is because of this ratio that NaCl has a 1:1 stoichiometry. The shaded green and gray octahedra in the NaCl lattice (Figure **5.1.5**) show that the Na^+ ions are coordinated to six Cl^- ions, and vice versa.

Other materials with the NaCl structure

- Alkali Halides (except CsCl, CsBr, and CsI)
- Transition Metal Monoxides (TiO, VO,..., NiO)
- Alkali Earth Oxides and Sulfides (MgO, CaO, BaS... except BeO and MgTe)
- Carbides and Nitrides (TiC, TiN, ZrC, NbC) -these are very stable refractory, interstitial alloys (metallic)

Other Unit Cell Types

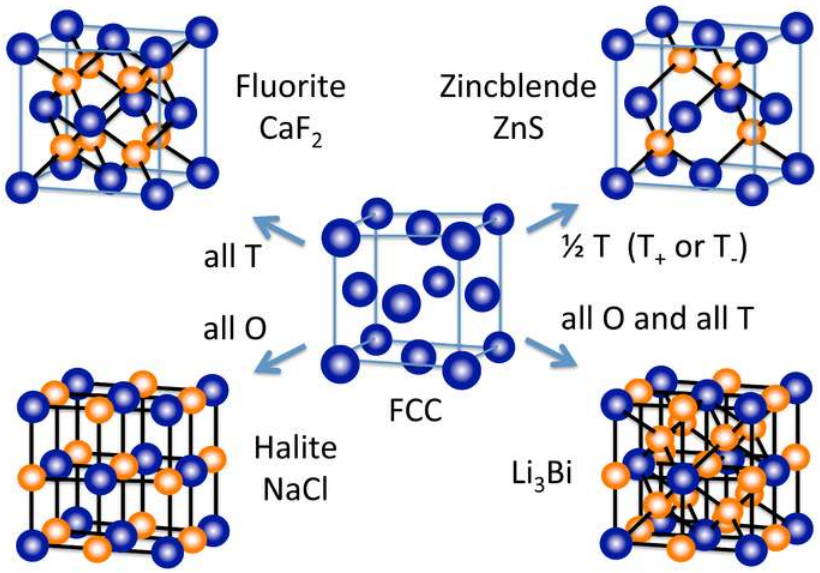


Figure **5.1.7**: Illustration of how different unit cell types are formed by filling holes in the fcc lattice

A number of other inorganic crystal structures are formed (at least conceptually) by filling octahedral and/or tetrahedral holes in close-packed lattices. Figure **5.1.7** shows some of the most common structures (fluorite, NaCl, and zincblende) as well as a rather rare one (Li_3Bi) that derive from the fcc lattice. From the hcp lattice, we can make the NiAs and wurzite structures, which are the hexagonal relatives of NaCl and zincblende, respectively.

An alternative and very convenient way to represent inorganic crystal structures (especially complex structures such as Li_3Bi) is to draw the unit cell in slices along one of the unit cell axes. This kind of representation is shown at the left for the fcc lattice and the NaCl structure. Since all atoms in these structures have z-coordinates of either 0 or 1/2, only those sections need to be drawn in order to describe the contents of the unit cell. It is a useful exercise to draw some of the fcc compound structures (above) in sections.

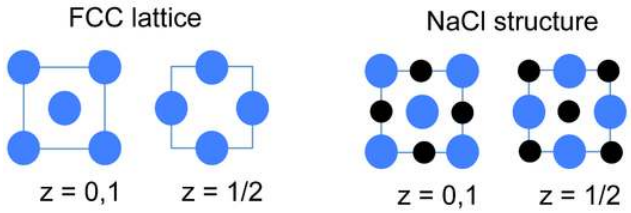


Figure **5.1.8**: Alternative representation of the fcc lattice (left) and the NaCl structure (right). The z = 0,1 represent the bottom and top faces of the unit cell. The z = $\frac{1}{2}$ represents a slice through the center of the unit cell

Fluorite

In ccp and hcp lattices, there are two tetrahedral holes per packing atom. A stoichiometry of either M_2X or MX_2 gives a structure that fills all tetrahedral sites, while an MX structure fills only half of the sites. An example of an MX_2 structure is fluorite, CaF_2, whose structure is shown in the figure at the left. The packing atom in fluorite is Ca^{2+} and the structure is composed of three interpenetrating fcc lattices. It should be noted that the Ca^{2+} ion (gray spheres) as a packing atom defies our "rule" that anions are larger than cations and therefore must be the packing atoms. The fluorite structure is common for ionic MX_2 (MgF_2, ZrO_2, etc.) and M_2X compounds (Li_2O). In contrast, the hcp relative of the fluorite structure is quite rare because of unfavorable close contacts between like-charged ions.

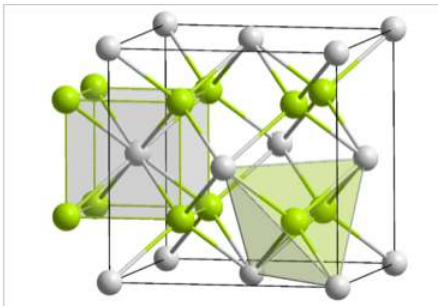


Figure 5.1.9: The fluorite (CaF_2) crystal structure showing the coordination environments of the Ca (grey) and F (green) atoms

In terms of geometry, Ca^{2+} is in cubic coordination with eight F^- neighbors, and the fluoride ions are tetrahedrally coordinated by four Ca^{2+} ions. The 8:4 coordination geometry is consistent with the 1:2 Ca:F stoichiometry; in all crystal structures the ratio of the coordination numbers is the inverse of the stoichiometric ratio. Looking more closely at the tetrahedral sites in fluorite, we see that they fall into two distinct groups: T_+ and T_-. If a tetrahedron is oriented with a vertex pointing upwards along the stacking axis, the site is T_+. Likewise, a tetrahedron with a vertex oriented downward is T_-. The alternation of T_+ and T_- sites allows for efficient packing of ions in the structure.

Zincblende and wurtzite

Tetrahedrally bonded compounds with a 1:1 stoichiometry (MX compounds) have only half of the tetrahedral sites (either the T_+ or T_- sites) filled. In this case, both the M and the X atoms are tetrahedrally coordinated. The zincblende and wurtzite structures of ZnS are 1:1 tetrahedral structures based on fcc and hcp lattices, respectively. Both structures are favored by p-block compounds that follow the octet rule, and these compounds are usually semiconductors or insulators. The zincblende structure, Figure 5.1.10, can be thought of as two interpenetrating fcc lattices, one of anions and one of cations, offset from each other by a translation of 1/4 along the body diagonal of the unit cell. Examples of compounds with the zincblende structure include CuCl, CuI, ZnSe, HgS, BeS, CdTe, AlP, GaP, SnSb, CSi, and diamond. Using ZnS as a representative of zincblende, the coordination of both Zn and S atoms is tetrahedral.

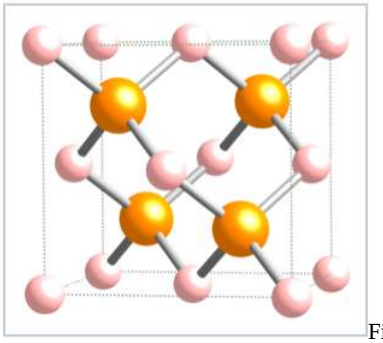


Figure 5.1.10: The zincblende structure of ZnS. The Zn^{2+} ions are in pink and the S^{2-} ions are in orange.

The wurtzite structure is a close relative of zincblende, based on filling half the tetrahedral holes in the hcp lattice. Like zincblende, wurtzite contains planes of fused six-membered rings in the chair conformation. Unlike zincblende, however, the rings joining these planes contain non-planar, six-membered rings. The structure aligns the anions so that they are directly above the cations in the structure, a less favorable situation sterically but a more favorable one in terms of electrostatics. As a result, the wurtzite structure tends to favor more polar or ionic compounds (e.g., ZnO, $NH_4^+F^-$) than the zincblende structure. As with zincblende, both ions are in tetrahedral (4:4) coordination and there are typically eight valence electrons in the MX compound. Examples of compounds with this structure include: BeO, ZnO, MnS, CdSe, MgTe, AlN, and NH_4F.

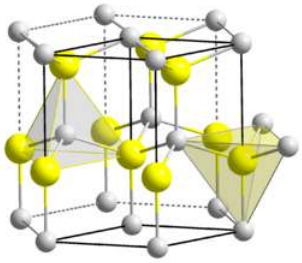


Figure 5.1.11: The wurtzite structure of ZnS with the tetrahedral coordination of anion and cation highlighted. The Zn^{2+} ions are in grey and the S^{2-} ions are in yellow. (Public domain; Solid State via Wikimedia Commons)

An interesting consequence of the layer stacking in the wurtzite structure is that the crystals are polar. When cleaved along the c-axis (the stacking axis), crystals of ZnO, ZnS, and GaN have one negatively charged face and an opposite positively charged face. An applied electric field interacts with the crystal dipole, resulting in compression or elongation of the lattice along this direction. For this reason crystals of compounds in the wurtzite structure are typically piezoelectric (increasing the pressure on the material generates a voltage in the material).

Some compounds are diamorphic and can have either the zincblende or wurtzite structure. Examples of these compounds that have intermediate polarities include CdS and ZnS. SiO_2 exists in polymorphs (crystobalite and tridymite) that resemble zincblende and wurtzite with O atoms midway between each of the Si atoms. The zincblende and wurtzite structures have efficient packing arrangements for tetrahedrally bonded networks and are commonly found in compounds that have tetrahedral bonding. Water, for example, has a tetrahedral hydrogen bonding network and is wurtzite-type. The undistorted wurtzite and zincblende structures are typically found for AX compounds with eight valence electrons, which follow the octet rule. AX compounds with nine or ten electrons such as GaSe and GaAs crystallize in distorted variants of the wurtzite structure. In GaSe, the extra electrons form lone pairs and this creates layers in the structure, as can be seen in the figure below. To the right of GaSe, the structures of As, Sb, and SbAs show an ever further breakdown of the structure into layers as more valence electrons are added.

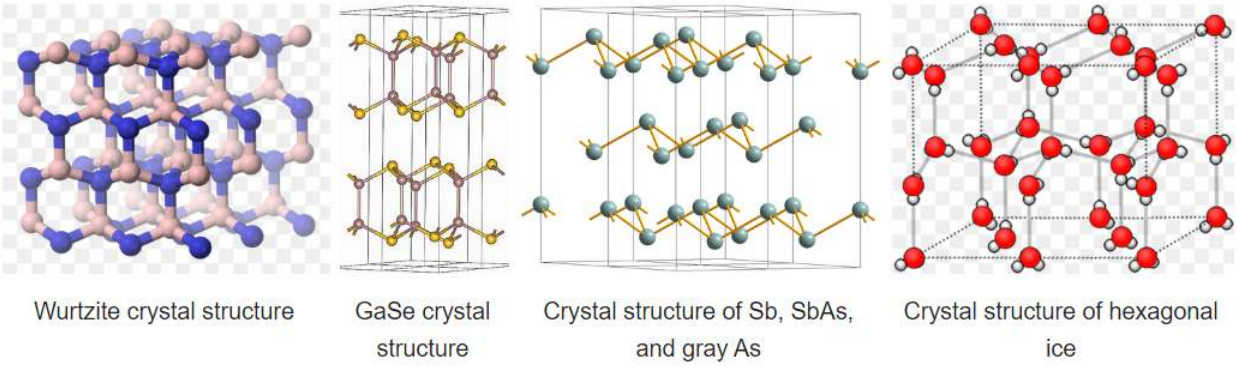


Figure 5.1.12: Different variations of the wurtzite crystal structure (Copyright; author via source)

Hexagonal ice is the most stable polymorph of ice, which is obtained upon freezing at 1 atmosphere pressure. This polymorph (ice-I) has a hcp wurtzite-type structure. Looking at the structure shown at the right, we see that there are irregular arrangements of the O-H---O bonds. In the structure, hydrogen bonding enforces the tetrahedral coordination of each water molecule, resulting in a relatively open structure that is less dense than liquid water. For this reason, ice floats in water.

References

1. Conway, J. H. and Sloane, N. J. A. *Sphere Packings, Lattices, and Groups, 2nd ed.* New York: Springer-Verlag, 1993.
2. Krishna, P. and Verma, A. R. Closed Packed Structures, Chester, UK: International Union of Crystallography, 1981.
3. Petrucci, Ralph H., William S. Harwood, F. Geoffrey Herring, and Jeffry D. Madura. "Crystal Structures" General Chemistry: Principles & Modern Applications, ninth Edition. New Jersey: Pearson Education, Inc., 2007. 501-508.

Contributors and Attributions

- Stephen Lower, Professor Emeritus (Simon Fraser U.) Chem1 Virtual Textbook
- Brittanie Harbick, Laura Suh, Jenny Fong

5.1: Crystal Structures and Unit Cells is shared under a CC BY-NC-SA 4.0 license and was authored, remixed, and/or curated by LibreTexts.

- **Current page** is licensed CC BY-NC-SA 4.0.
- **7.8: Cubic Lattices and Close Packing** by Stephen Lower is licensed CC BY 3.0. Original source: http://www.chem1.com/acad/webtext/virtualtextbook.html.
- **8.2: Close-packing and Interstitial Sites** by Chemistry 310 is licensed CC BY-SA 4.0. Original source: https://en.wikibooks.org/wiki/Introduction_to_Inorganic_Chemistry.
- **8.4: Tetrahedral Structures** by Chemistry 310 is licensed CC BY-SA 4.0. Original source: https://en.wikibooks.org/wiki/Introduction_to_Inorganic_Chemistry.

5.2: Energetics of Ionic Solids- Lattice Energy

Lattice Energy

Many ionic compounds have simple structures. Because the forces holding the atoms together are primarily electrostatic, we can calculate the cohesive energy of the crystal lattice with good accuracy. Interesting questions to ask about these lattice energy calculations are:

- How accurate are lattice energy calculations?
- What do they teach us about the chemical bonds in ionic crystals?
- Can we use lattice energies to predict properties such as solubility, stability, and reactivity?
- Can we use lattice energies to predict the crystal structures of ionic compounds?

Let's start by looking at the forces that hold ionic lattices together. There are mainly two kinds of force that determine the energy of an ionic bond.

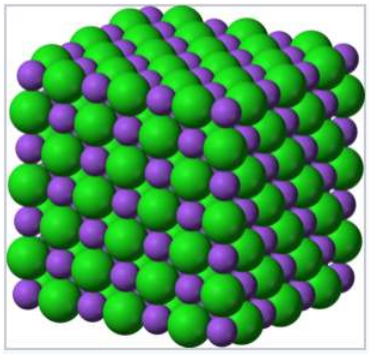


Figure **5.2.1**: The NaCl crystal structure is the archetype for calculating lattice energies and computing enthalpies of formation from Born-Haber cycles.

Electrostatic force

Electrostatic force is the attraction and repulsion between ions described by Coulomb's Law. Two ions with charges z_+ and z_-, separated by a distance r, experience a force F:

$$\mathbf{F} = -\frac{e^2}{4\pi\varepsilon_0}\frac{z_+z_-}{r^2} \tag{5.2.1}$$

where

e = 1.6022×10^{-19} C

4 π ε_0 = 1.112×10^{-10} C^2/(J m)

This force is attractive for ions of opposite charge and repulsive for ions of the same charge.

Closed-shell repulsion

When electrons in the core shells of one ion overlap with those of another ion, there is a repulsive force due to the Pauli exclusion principle. A third electron cannot enter an orbital that already contains two electrons. This force is short range, and is typically modeled as falling off exponentially or with a high power of the distance r between atoms. For example, in the Born approximation, B is a constant and ρ is a number with units of length, which is usually empirically determined from compressibility data. A typical value of ρ is 0.345 Å.

$$\mathbf{E}_{repulsion} = Bexp(\frac{-r}{\rho}) \tag{5.2.2}$$

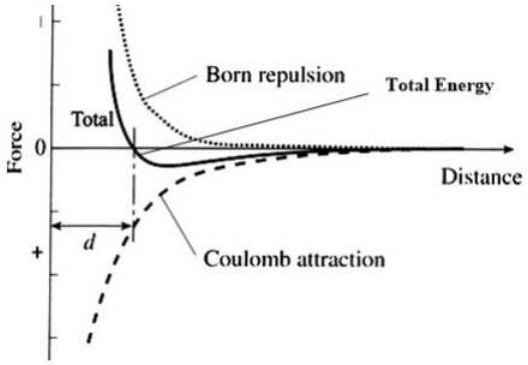


Figure **5.2.2**: Total energy of an ionic bond (solid) determined by the combination of Coulombic attraction (dashed) and Born (closed-shell) repulsion (dotted).

The energy of the ionic bond between two atoms is then calculated as the combination of net electrostatic and the closed-shell repulsion energies, as shown in Figure **5.2.2**. Note that for the moment we are ignoring the attractive van der Waals forces between ions. For a pair of ions, the equilibrium distance between ions is determined by the minimum in the total energy curve.

Madelung Constant

We can use the above equations to calculate the lattice energy of a crystal by summing up the interactions between all pairs of ions. Because the closed-shell repulsion force is short range, this term is typically calculated only for interactions between neighboring ions. However, the Coulomb force is long range, and must be calculated over the entire crystal. This problem was first solved in 1918 by Erwin Madelung, a German physicist.

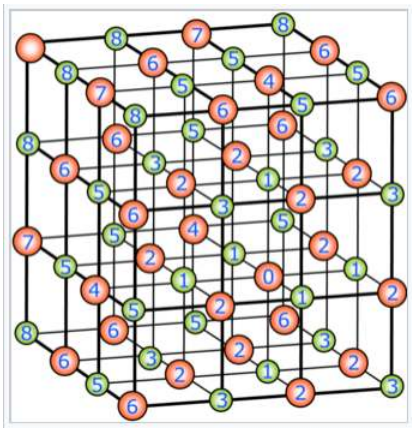


Figure **5.2.3**: The Madelung constant is calculated by summing up electrostatic interactions with ion labeled 0 in the expanding spheres method. Each number designates the order in which it is summed. For example, ions labeled 1 represent the six nearest neighbors (attractive interaction), ions labeled 2 are the 12 next nearest neighbors (repulsive interaction) and so on.

Consider an ion in the NaCl structure labeled "0" in Figure **5.2.3**. We can see that the nearest neighbor interactions (+ -) with ions labeled "1" are attractive, the next nearest neighbor interactions (- - and + +) are repulsive, and so on. In the NaCl structure, counting from the ion in the center of the unit cell, there are 6 nearest neighbors (on the faces of the cube), 12 next nearest neighbors (on the edges of the cube), 8 in the next shell (at the vertices of the cube), and so on. Their distances from ion "0" increase progressively: r_o, $\sqrt{2}\ r_o$, $\sqrt{3}\ r_o$, and so on, where r_o is the nearest neighbor distance.

We can now write the electrostatic energy at ion "0" as:

$$\mathbf{E}_{elec} = -6\frac{e^2}{4\pi\varepsilon_0}\frac{z_+z_-}{r_o} + 12\frac{e^2}{4\pi\varepsilon_0}\frac{z_+z_-}{\sqrt{2}r_o} - 8\frac{e^2}{4\pi\varepsilon_0}\frac{z_+z_-}{\sqrt{3}r_o} + \ldots \tag{5.2.3}$$

Factoring out constants and the nearest-neighbor bond distance r_o we obtain:

$$\mathbf{E}_{elec} = \frac{e^2}{4\pi\varepsilon_0}\frac{z_+z_-}{r_o}\left(6 - \frac{12}{\sqrt{2}} + \frac{8}{\sqrt{3}} - \frac{6}{\sqrt{4}} + \ldots\right) \tag{5.2.4}$$

Where the sum in parentheses, which is unitless, slowly converges to a value of A = 1.74756. Generalizing this formula for any three-dimensional ionic crystal we get a function:

$$\mathbf{E}_{elec} = \frac{e^2}{4\pi\varepsilon_0}\frac{z_+ z_-}{r_o}NA \tag{5.2.5}$$

where N is Avogadro's number (because we are calculating energy per mole of ions) and A is called the *Madelung constant*. The **Madelung constant** depends only on the geometrical arrangement of the ions and so it varies between different types of crystal structures, but within a given structure type it does not change. Thus MgO and NaCl have the same Madelung constant because they both have the NaCl structure.

Table **5.2.1**: Madelung Constants

Compound	*Crystal Lattice*	*M*	*A : C*	*Type*
NaCl	NaCl	1.74756	6 : 6	Rock salt
CsCl	CsCl	1.76267	6 : 6	CsCl type
CaF_2	Cubic	2.51939	8 : 4	Fluorite
$CdCl_2$	Hexagonal	2.244	6 : 3	
MgF_2	Tetragonal	2.381		
ZnS (wurtzite)	Hexagonal	1.64132	4 : 4	Wurtzite
TiO_2 (rutile)	Tetragonal	2.408	6 : 3	Rutile
$bSiO_2$	Hexagonal	2.2197		
Al_2O_3	Rhombohedral	4.1719	6 : 4	Corundum

A is the number of anions coordinated to cation and *C* is the numbers of cations coordinated to anion.

Born–Landé Equation

There are other factors to consider for the evaluation of lattice energy and the treatment by Max Born and Alfred Lande led to the formula for the evaluation of lattice energy for a mole of **crystalline solid**. The Born–Landé equation (Equation 5.2.6) is a means of calculating the lattice energy of a crystalline ionic compound and derived from the electrostatic potential of the ionic lattice and a repulsive potential energy term

$$U = \frac{N_A M Z^2 e^2}{4\pi\epsilon_o r}\left(1 - \frac{1}{n}\right) \tag{5.2.6}$$

where

- N_A is Avogadro constant;
- M is the Madelung constant for the lattice
- z^+ is the charge number of cation
- z^- is the charge number of anion
- e is elementary charge, 1.6022×10^{-19} C
- ε_0 is the permittivity of free space
- r_0 is the distance to closest ion
- n is the **Born exponent** that is typically between 5 and 12 and is determined experimentally. n is a number related to the electronic configurations of the ions involved (Table **5.2.3**).

Table **5.2.2**: n values for select solids

Atom/Molecule	*n*
He	5
Ne	7
Ar	9
Kr	10
Xe	12
LiF	5.9
LiCl	8.0
LiBr	8.7
NaCl	9.1
NaBr	9.5

Example 5.2.1: NaCl

Estimate the lattice energy for **NaCl**.

Solution

Using the values giving in the discussion above, the estimation is given by

$$U_{NaCl} = \frac{(6.022 \times 10^{23}/mol)(1.74756)(1.6022 \times 10^{-19})^2(1.747558)}{4\pi\,(8.854 \times 10^{-12} C^2/m)(282 \times 10^{-12}\ m)}\left(1 - \frac{1}{9.1}\right)$$
$$= -756\ kJ/mol$$

Much more should be considered in order to evaluate the lattice energy accurately, but the above calculation leads you to a good start. When methods to evaluate the energy of crystallization or lattice energy lead to reliable values, these values can be used in the Born-Hable cycle to evaluate other chemical properties, for example the electron affinity, which is really difficult to determine directly by experiment.



Figure 5.2.4: Lithium fluoride (shown here as a large single crystal in a beaker of water) is the only alkali halide that is not freely soluble in water. The lattice energy of LiF is the most negative of the alkali fluorides because Li^+ and F^- are both small ions and lattice energy is proportional to $1/r_0$.

5.2: Energetics of Ionic Solids- Lattice Energy is shared under a CC BY-NC-SA 4.0 license and was authored, remixed, and/or curated by LibreTexts.

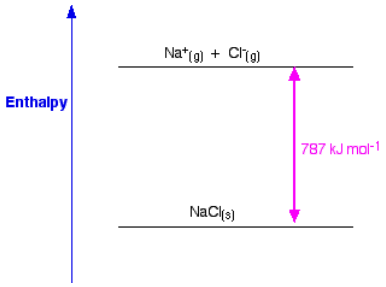
- **Current page** is licensed CC BY-NC-SA 4.0.
- **9.3: Energetics of Crystalline Solids- The Ionic Model** by Chemistry 310 is licensed CC BY-SA 4.0. Original source: https://en.wikibooks.org/wiki/Introduction_to_Inorganic_Chemistry.
- **6.13E: Madelung Constants** is licensed CC BY-NC-SA 4.0.

5.3: Lattice Enthalpies and Born Haber Cycles

Lattice enthalpy is a measure of the strength of the forces between the ions in an ionic solid. The greater the **lattice enthalpy**, the stronger the forces. This page introduces lattice enthalpies (lattice energies) and Born-Haber cycles.

Defining Lattice Enthalpy

There are two different ways of defining lattice enthalpy which directly contradict each other, and you will find both in common use. In fact, there is a simple way of sorting this out, but many sources do not use it. Lattice enthalpy is a measure of the strength of the forces between the ions in an ionic solid. The greater the lattice enthalpy, the stronger the forces. Those forces are only completely broken when the ions are present as gaseous ions, scattered so far apart that there is negligible attraction between them. You can show this on a simple enthalpy diagram.



For sodium chloride, the solid is more stable than the gaseous ions by 787 kJ mol^{-1}, and that is a measure of the strength of the attractions between the ions in the solid. Remember that energy (in this case heat energy) is released when bonds are made, and is required to break bonds.

So lattice enthalpy could be described in either of two ways.

- It could be described as the enthalpy change when 1 mole of sodium chloride (or whatever) was formed from its scattered gaseous ions. In other words, you are looking at a downward arrow on the diagram.
- Or, it could be described as the enthalpy change when 1 mole of sodium chloride (or whatever) is broken up to form its scattered gaseous ions. In other words, you are looking at an upward arrow on the diagram.

Both refer to the same enthalpy diagram, but one looks at it from the point of view of making the lattice, and the other from the point of view of breaking it up. Unfortunately, both of these are often described as "lattice enthalpy".

Definitions

- The *lattice dissociation enthalpy* is the enthalpy change needed to convert 1 mole of solid crystal into its scattered gaseous ions. Lattice dissociation enthalpies are **always positive**.
- The *lattice formation enthalpy* is the enthalpy change when 1 mole of solid crystal is formed from its separated gaseous ions. Lattice formation enthalpies are **always negative**.

This is an absurdly confusing situation which is easily resolved by never using the term "lattice enthalpy" without qualifying it.

- You should talk about "lattice dissociation enthalpy" if you want to talk about the amount of energy needed to split up a lattice into its scattered gaseous ions. For NaCl, the lattice dissociation enthalpy is +787 kJ mol^{-1}.
- You should talk about "lattice formation enthalpy" if you want to talk about the amount of energy released when a lattice is formed from its scattered gaseous ions. For NaCl, the lattice formation enthalpy is -787 kJ mol^{-1}.

That immediately removes any possibility of confusion.

Factors affecting Lattice Enthalpy

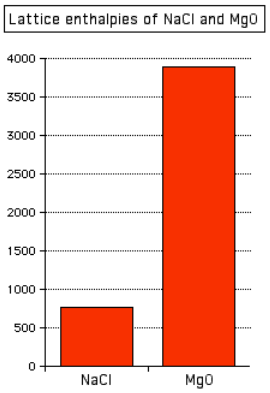
The two main factors affecting lattice enthalpy are

- The charges on the ions and

- The ionic radii (which affects the distance between the ions).

The charges on the ions

Sodium chloride and magnesium oxide have exactly the same arrangements of ions in the crystal lattice, but the lattice enthalpies are very different.

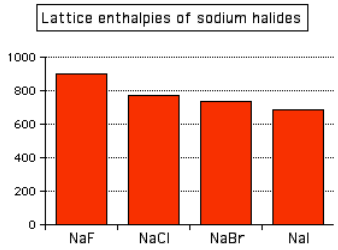


You can see that the lattice enthalpy of magnesium oxide is much greater than that of sodium chloride. That's because in magnesium oxide, 2+ ions are attracting 2- ions; in sodium chloride, the attraction is only between 1+ and 1- ions.

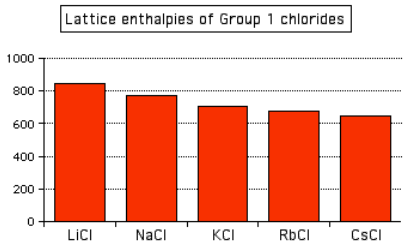
The Radius of the Ions

The lattice enthalpy of magnesium oxide is also increased relative to sodium chloride because magnesium ions are smaller than sodium ions, and oxide ions are smaller than chloride ions. That means that the ions are closer together in the lattice, and that increases the strength of the attractions.

This effect of ion size on lattice enthalpy is clearly observed as you go down a Group in the Periodic Table. For example, as you go down Group 7 of the Periodic Table from fluorine to iodine, you would expect the lattice enthalpies of their sodium salts to fall as the negative ions get bigger - and that is the case:



Attractions are governed by the distances between the centers of the oppositely charged ions, and that distance is obviously greater as the negative ion gets bigger. And you can see exactly the same effect if as you go down Group 1. The next bar chart shows the lattice enthalpies of the Group 1 chlorides.



Calculating Lattice Enthalpy

It is impossible to measure the enthalpy change starting from a solid crystal and converting it into its scattered gaseous ions. It is even more difficult to imagine how you could do the reverse - start with scattered gaseous ions and measure the enthalpy change when these convert to a solid crystal. Instead, lattice enthalpies always have to be calculated, and there are two entirely different ways in which this can be done.

1. You can can use a Hess's Law cycle (in this case called a Born-Haber cycle) involving enthalpy changes which can be measured. Lattice enthalpies calculated in this way are described as experimental values.
2. Or you can do physics-style calculations working out how much energy would be released, for example, when ions considered as point charges come together to make a lattice. These are described as theoretical values. In fact, in this case, what you are actually calculating are properly described as lattice energies.

Born-Haber Cycles

Standard Atomization Enthalpies

Before we start talking about Born-Haber cycles, we need to define the **atomization enthalpy**, ΔH_a^o. The standard atomization enthalpy is the enthalpy change when 1 mole of gaseous atoms is formed from the element in its standard state. Enthalpy change of atomization is always positive. You are always going to have to supply energy to break an element into its separate gaseous atoms. All of the following equations represent changes involving atomization enthalpy:

$$\frac{1}{2}Cl_2(g) \rightarrow Cl(g) \quad \Delta H_a^o = +122\,kJ\,mol^{-1}$$

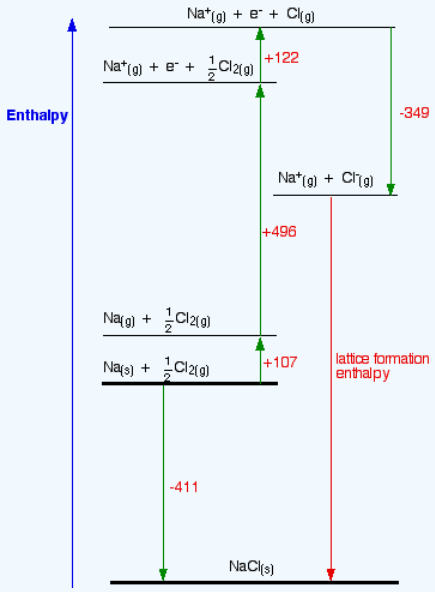
$$\frac{1}{2}Br_2(l) \rightarrow Br(g) \quad \Delta H_a^o = +122\,kJ\,mol^{-1}$$

$$Na(s) \rightarrow Na(g) \quad \Delta H_a^o = +107\,kJ\,mol^{-1}$$

Notice particularly that the "mol^{-1}" is per mole of atoms **formed** - NOT per mole of element that you start with. You will quite commonly have to write fractions into the left-hand side of the equation. Getting this wrong is a common mistake.

Example 5.3.1: Born-Haber Cycle for NaCl

Consider a Born-Haber cycle for sodium chloride, and then talk it through carefully afterwards. You will see that I have arbitrarily decided to draw this for lattice formation enthalpy. If you wanted to draw it for lattice dissociation enthalpy, the red arrow would be reversed - pointing upwards.



Focus to start with on the higher of the two thicker horizontal lines. We are starting here with the elements sodium and chlorine in their standard states. Notice that we only need half a mole of chlorine gas in order to end up with 1 mole of NaCl. The arrow pointing down from this to the lower thick line represents the enthalpy change of formation of sodium chloride.

The Born-Haber cycle now imagines this formation of sodium chloride as happening in a whole set of small changes, most of which we know the enthalpy changes for - except, of course, for the lattice enthalpy that we want to calculate.

- The +107 is the atomization enthalpy of sodium. We have to produce gaseous atoms so that we can use the next stage in the cycle.
- The +496 is the first ionization energy of sodium. Remember that first ionization energies go from gaseous atoms to gaseous singly charged positive ions.
- The +122 is the atomization enthalpy of chlorine. Again, we have to produce gaseous atoms so that we can use the next stage in the cycle.
- The -349 is the first electron affinity of chlorine. Remember that first electron affinities go from gaseous atoms to gaseous singly charged negative ions.
- And finally, we have the positive and negative gaseous ions that we can convert into the solid sodium chloride using the lattice formation enthalpy.

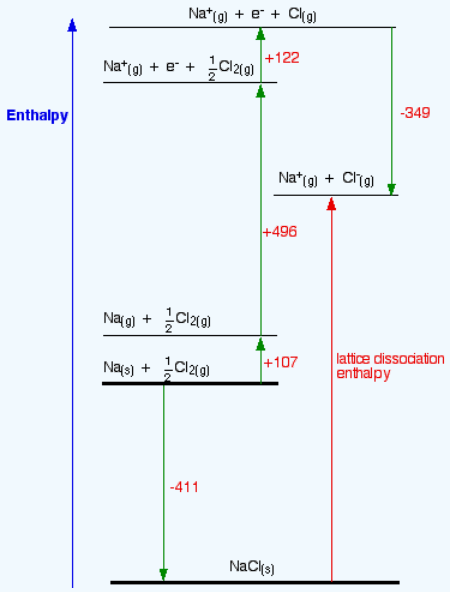
Now we can use Hess' Law and find two different routes around the diagram which we can equate. As drawn, the two routes are obvious. The diagram is set up to provide two different routes between the thick lines. So, from the cycle we get the calculations directly underneath it . . .

$$-411 = +107 + 496 + 122 - 349 + LE$$

$$LE = -411 - 107 - 496 - 122 + 349$$

$$LE = -787 \text{ kJ mol}^{-1}$$

How would this be different if you had drawn a lattice dissociation enthalpy in your diagram? Your diagram would now look like this:



The only difference in the diagram is the direction the lattice enthalpy arrow is pointing. It does, of course, mean that you have to find two new routes. You cannot use the original one, because that would go against the flow of the lattice enthalpy arrow. This time both routes would start from the elements in their standard states, and finish at the gaseous ions.

$$-411 + LE = +107 + 496 + 122 - 349$$

$$LE = +107 + 496 + 122 - 349 + 411$$

$$LE = +787 \text{ kJ mol}^{-1}$$

Once again, the cycle sorts out the sign of the lattice enthalpy.

Theoretical Estimates of Lattice Energies

Let's assume that a compound is fully ionic. Let's also assume that the ions are point charges - in other words that the charge is concentrated at the center of the ion. By doing physics-style calculations, it is possible to calculate a theoretical value for what you would expect the lattice energy to be. Calculations of this sort end up with values of *lattice energy*, and not *lattice enthalpy*. If you know how to do it, you can then fairly easily convert between the two.

There are several different equations, of various degrees of complication, for calculating lattice energy in this way. There are two possibilities:

- There is reasonable agreement between the experimental value (calculated from a Born-Haber cycle) and the theoretical value. Sodium chloride is a case like this - the theoretical and experimental values agree to within a few percent. That means that for sodium chloride, the assumptions about the solid being ionic are fairly good.
- The experimental and theoretical values do not agree. A commonly quoted example of this is silver chloride, AgCl. Depending on where you get your data from, the theoretical value for lattice enthalpy for AgCl is anywhere from about 50 to 150 kJ mol^{-1} less than the value that comes from a Born-Haber cycle. In other words, treating the AgCl as 100% ionic underestimates its lattice enthalpy by quite a lot.

The explanation is that silver chloride actually has a significant amount of covalent bonding between the silver and the chlorine, because there is not enough electronegativity difference between the two to allow for complete transfer of an electron from the silver to the chlorine. Comparing experimental (Born-Haber cycle) and theoretical values for lattice enthalpy is a good way of judging how purely ionic a crystal is.

Example 5.3.2: Born-Haber Cycle for $MgCl_2$

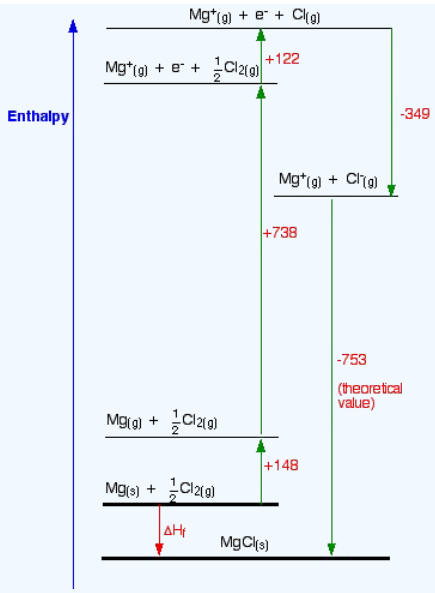
The question arises as to why, from an energetics point of view, magnesium chloride is $MgCl_2$ rather than MgCl or $MgCl_3$ (or any other formula you might like to choose). It turns out that $MgCl_2$ is the formula of the compound which has the most negative enthalpy change of formation - in other words, it is the most stable one relative to the elements magnesium and chlorine.

Let's look at this in terms of Born-Haber cycles of and contrast the enthalpy change of formation for the imaginary compounds MgCl and $MgCl_3$. That means that we will have to use theoretical values of their lattice enthalpies. We ca not use experimental ones, because these compounds obviously do not exist! I'm taking theoretical values for lattice enthalpies for these compounds that I found on the web. I can't confirm these, but all the other values used by that source were accurate. The exact values do not matter too much anyway, because the results are so dramatically clear-cut.

1. The Born-Haber cycle for MgCl

We will start with the compound MgCl, because that cycle is just like the NaCl one we have already looked at.

$$Mg(s) + \frac{1}{2} Cl_2(g) \rightarrow MgCl(s)$$



Find two routes around this without going against the flow of any arrows. That's easy:

$$\Delta H_f = +148 + 738 + 122 - 349 - 753$$

$$\Delta H_f = -94 \text{ kJ mol}^{-1}$$

So the compound MgCl is definitely energetically **more stable** than its elements. I have drawn this cycle very roughly to scale, but that is going to become more and more difficult as we look at the other two possible formulae. So I am going to rewrite it as a table. You can see from the diagram that the enthalpy change of formation can be found just by adding up all the other numbers in the cycle, and we can do this just as well in a table.

	kJ
atomization enthalpy of Mg	+148
1st IE of Mg	+738
atomization enthalpy of Cl	+122
electron affinity of Cl	-349
lattice enthalpy	-753
calculated ΔH_f	-94

2. The Born-Haber cycle for $MgCl_2$

The equation for the enthalpy change of formation this time is

$$\mathrm{Mg\,(s) + Cl_2\,(g) \rightarrow MgCl_2\,(s)}$$

So how does that change the numbers in the Born-Haber cycle?

- You need to add in the second ionization energy of magnesium, because you are making a 2+ ion.
- You need to multiply the atomization enthalpy of chlorine by 2, because you need 2 moles of gaseous chlorine atoms.
- You need to multiply the electron affinity of chlorine by 2, because you are making 2 moles of chloride ions.
- You obviously need a different value for lattice enthalpy.

	kJ
atomization enthalpy of Mg	+148
1st IE of Mg	+738
2nd IE of Mg	+1451
atomization enthalpy of Cl (x 2)	+244
electron affinity of Cl (x 2)	-698
lattice enthalpy	-2526
calculated ΔH_f	-643

You can see that much more energy is released when you make $MgCl_2$ than when you make MgCl. Why is that? You need to put in more energy to ionize the magnesium to give a 2+ ion, but a lot more energy is released as lattice enthalpy. That is because there are stronger ionic attractions between 1- ions and 2+ ions than between the 1- and 1+ ions in MgCl. So what about $MgCl_3$? The lattice energy here would be even greater.

3. The Born-Haber cycle for $MgCl_3$

The equation for the enthalpy change of formation this time is

$$\mathrm{Mg\,(s) + \tfrac{3}{2}\,Cl_2\,(g) \rightarrow MgCl_3\,(s)}$$

So how does that change the numbers in the Born-Haber cycle this time?

- You need to add in the third ionization energy of magnesium, because you are making a 3+ ion.
- You need to multiply the atomization enthalpy of chlorine by 3, because you need 3 moles of gaseous chlorine atoms.
- You need to multiply the electron affinity of chlorine by 3, because you are making 3 moles of chloride ions.
- You again need a different value for lattice enthalpy.

	kJ
atomization enthalpy of Mg	+148
1st IE of Mg	+738
2nd IE of Mg	+1451
3rd IE of Mg	+7733
atomization enthalpy of Cl (x 3)	+366
electron affinity of Cl (x 3)	-1047
lattice enthalpy	-5440
calculated ΔH_f	+3949

This time, the compound is hugely energetically unstable, both with respect to its elements, and also to other compounds that could be formed. You would need to supply nearly 4000 kJ to get 1 mole of $MgCl_3$ to form!

Look carefully at the reason for this. The lattice enthalpy is the **highest** for all these possible compounds, but it is not high enough to make up for the very large third ionization energy of magnesium.

Why is the third ionization energy so big? The first two electrons to be removed from magnesium come from the 3s level. The third one comes from the 2p. That is closer to the nucleus, and lacks a layer of screening as well - and so

much more energy is needed to remove it. The 3s electrons are screened from the nucleus by the 1 level and 2 level electrons. The 2p electrons are only screened by the 1 level (plus a bit of help from the 2s electrons).

Conclusion

Magnesium chloride is $MgCl_2$ because this is the combination of magnesium and chlorine which produces the most energetically stable compound - the one with the most negative enthalpy change of formation.

Contributors and Attributions

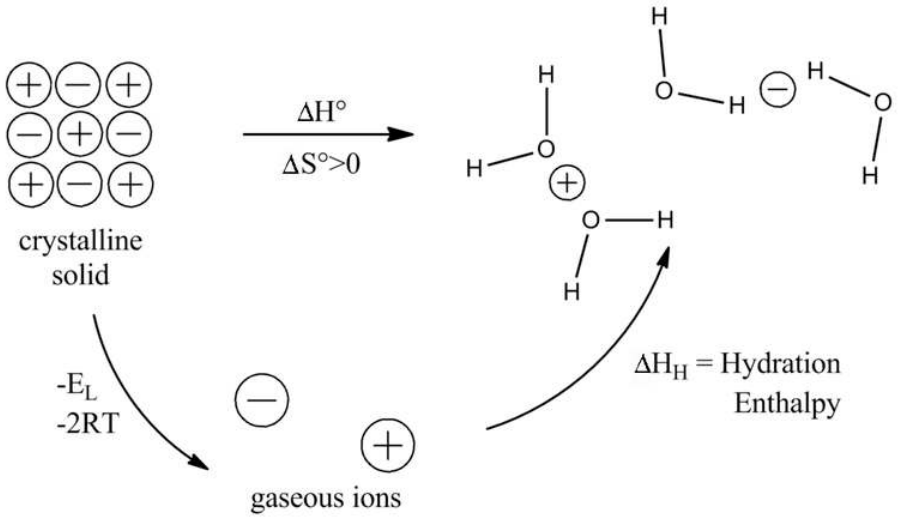
- Jim Clark (Chemguide.co.uk)

This page titled 5.3: Lattice Enthalpies and Born Haber Cycles is shared under a CC BY-NC 4.0 license and was authored, remixed, and/or curated by Jim Clark.

- **Lattice Enthalpies and Born Haber Cycles** by Jim Clark is licensed CC BY-NC 4.0.

5.4: Lattice Energy and Solubility

Lattice energies can also help predict compound solubilities. Let's consider a Born-Haber cycle for dissolving a salt in water. We can imagine this as the sum of two processes: (1) the vaporization of the salt to produce gaseous ions, characterized by the lattice enthalpy, and (2) the hydration of those ions to produce the solution. The enthalpy change for the overall process is the sum of those two steps. We know that the entropy change for dissolution of a solid is positive, so the solubility depends on the enthalpy change for the overall process.



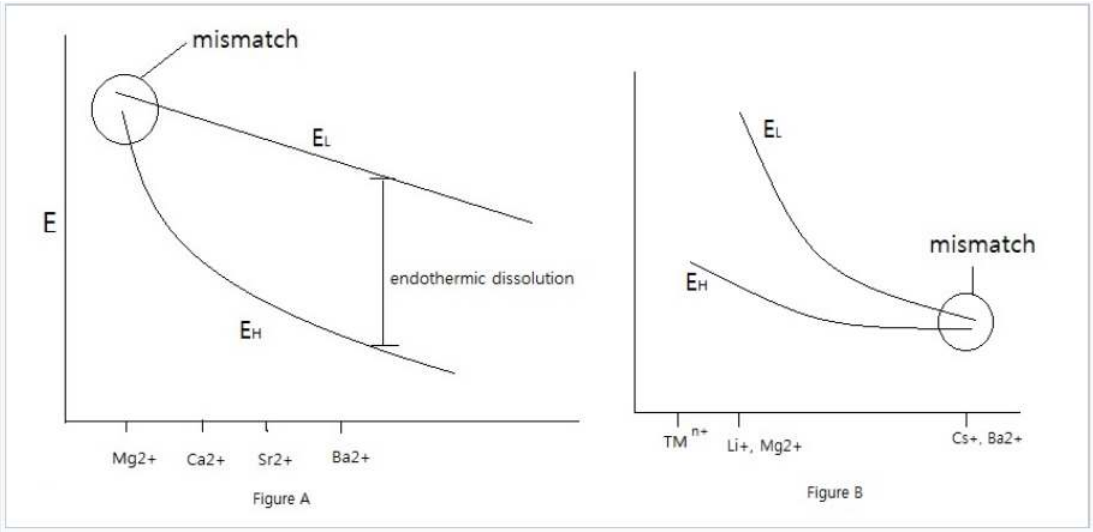
Here we need to consider the trends in both the lattice energy E_L and the hydration energy E_H. The lattice energy depends on the sum of the anion and cation radii ($r_+ + r_-$), whereas the hydration energy has separate anion and cation terms. Generally the solvation of small ions (typically cations) dominates the hydration energy because of the $1/r^2$ dependence.

$$E_L \alpha \frac{1}{r_+ + r_-} \tag{5.4.1}$$

$$E_H \alpha \frac{1}{r_+^2} + \frac{1}{r_-^2} \tag{5.4.2}$$

For salts that contain large anions, E_L doesn't change much as r_+ changes. That is because the anion dominates the $r_+ + r_-$ term in the denominator of the formula for E_L. On the other hand, E_H changes substantially with r_+, especially for small cations.

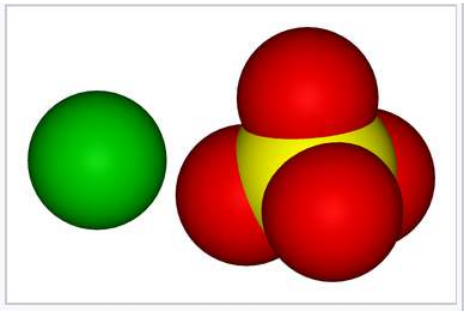
As a result, sulfate salts of small divalent cations, such as $MgSO_4$ (epsom salts), are soluble, whereas the lower hydration energy of Ba^{2+} in $BaSO_4$ makes that salt insoluble ($K_{sp} = 10^{-10}$).



Left: E_L diagram for sulfate salts. The large SO_4^{2-} ion is size-mismatched to small cations such as Mg^{2+}, which have large hydration energies, resulting soluble salts. With larger cations such as Ba^{2+}, which have lower E_H, the lattice energy exceeds the solvation enthalpy and the salts are insoluble.. Right: In the case of small anions such as F^- and OH^-, the lattice energy dominates with small cations such as transition metal ions (TM^{n+}), Mg^{2+}, and Li^+. Anion-cation size mismatch occurs with larger cations, such as Cs^+ and Ba^{2+}, which make soluble fluoride salts.

For small anions, E_L is more sensitive to r_+, whereas E_H does not depend on r_+ as strongly. For fluorides and hydroxides, LiF is slightly soluble whereas CsF is very soluble, and $Mg(OH)_2$ is insoluble whereas $Ba(OH)_2$ is very soluble.

Putting both trends together, we see that **low solubility** is most often encountered when the **anion and cation match well in their sizes**, especially when one or both are **multiply charged**.



Space-filling models showing the van der Waals surfaces of Ba^{2+} and SO_4^{2-}. The similarity in size of the two ions contributes to the low solubility of $BaSO_4$ in water.

Combining all our conclusions about solubility, we note the following trends:

1) Increasing **size mismatch** between the anion and cation leads to greater solubility, so CsF and LiI are the most soluble alkali halides.

2) Increasing **covalency** leads to lower solubility in the salts (due to larger E_L. For example, AgF, AgCl, AgBr, and AgI exhibit progressively lower solubility because of increasing covalency.

AgF > AgCl > AgBr > AgI

3) Increasing the **charge on the anion** lowers the solubility because the increase in E_L is large relative to the increase in E_H.

4) Small, polyvalent cations (having large E_H) make **soluble salts with large, univalent anions** such as I^-, NO_3^-, ClO_4^-, PF_6^-, and acetate.

Examples: Salts of transition metal and lanthanide ions

- Ln^{3+}: Nitrate salts are soluble, but oxides and hydroxides are insoluble.
- Fe^{3+}: Perchlorate is soluble, but sulfate is insoluble.

5) Multiple charged anions such as O^{2-}, S^{2-}, PO_4^{3-}, and SO_4^{2-} make insoluble salts with most M^{2+}, M^{3+}, and M^{4+} metals.

5.4: Lattice Energy and Solubility is shared under a CC BY-SA license and was authored, remixed, and/or curated by LibreTexts.

- **9.12: Lattice Energies and Solubility** by Chemistry 310 is licensed CC BY-SA 4.0. Original source: https://en.wikibooks.org/wiki/Introduction_to_Inorganic_Chemistry.
- **Current page** is licensed CC BY-SA 4.0.

5.5: Bonding in Metals and Semicondoctors

Band Theory

Band theory was developed with some help from the knowledge gained during the quantum revolution in science. In 1928, Felix Bloch had the idea to take the quantum theory and apply it to solids. In 1927, Walter Heitler and Fritz London discovered bands- very closely spaced orbitals with not much difference in energy. One way to conceptualize band theory is to view is as an extension of molecular orbital theory where the number of atomic orbitals mixed is increased to an infinite number and the energy difference between the molecular orbitals formed approaches 0 (Figure **5.5.1**).

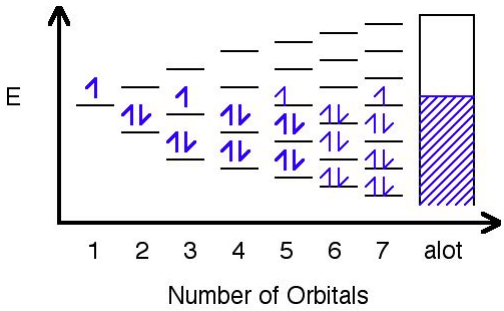


Figure **5.5.1**: In this image, orbitals are represented by the black horizontal lines, and they are being filled with an increasing number of electrons as their amount increases. Eventually, as more orbitals are added, the space in between them decreases to hardly anything, and as a result, a band is formed where the orbitals have been filled.

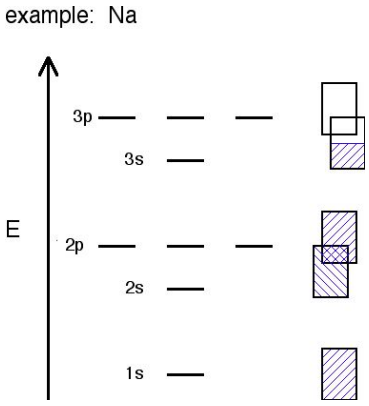


Figure **5.5.2**: Bands diagram of sodium metal. Filled bands are blue and empty bands are white. Because the 3s orbital is half filled in Na, the band formed form the 3s orbitals is also half filled.

Different metals will produce different combinations of filled and half filled bands depending on their valence electron configuration. Sodium's bands are shown in Figure **5.5.2**. As you can see, bands may overlap each other (the bands are shown askew to be able to tell the difference between different bands). The lowest unoccupied band is called the conduction band, and the highest occupied band is called the valence band.

Bands will follow a trend as you go across a period:

- In Na, the 3s band is 1/2 full.
- In Mg, the 3s band is full.
- In Al, the 3s band is full and the 3p band is 1/2 full... and so on.

In order for the material to conduct electricity, electrons should be in the conduction band where they are able to move freely through the material. The probability of finding an electron in the conduction band is shown by the equation:

$$P = \frac{1}{e^{\frac{\Delta E}{k_b T}} + 1} \tag{5.5.1}$$

The ΔE in the equation stands for the energy gap between the valence and conduction bands. k_b is the Boltzmann constant and T is temperature in K. That equation and the table below show that the larger the band gap between the valence band and the conduction band, the less likely electrons are to be found in the conduction band. This is because they don't have sufficient energy to make the jump up to the conduction band.

Table **5.5.1**: Band Gaps and Conduction Band Electron Densities for Group 4 Elements

ELEMENT	ΔE(kJ/mol) of energy gap	# of electrons/cm^3 in conduction band	material type
C (diamond)	524	10^{-27}	insulator
Si	117	10^{9}	semiconductor
Ge	66	10^{13}	semiconductor

Conductors, Insulators and Semiconductors

The conductivity of materials is directly related to the band gap and the probability of having electrons in the conduction band. Materials can be divided into three classes based on their band gaps (Figure **5.5.3**).

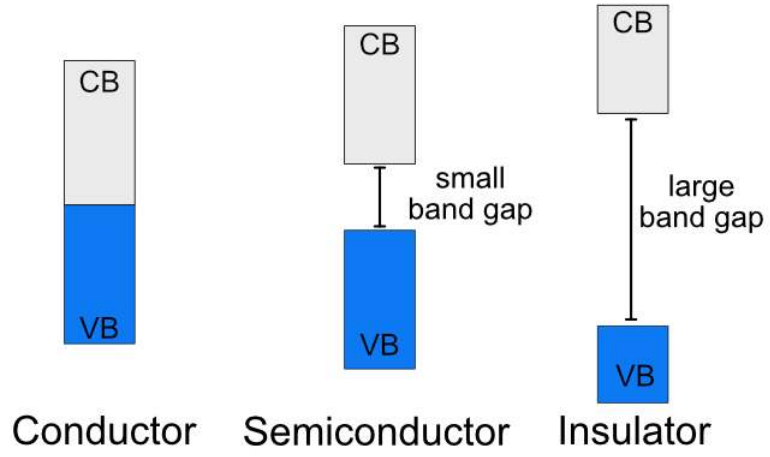


Figure **5.5.3**: Illustration of the energy difference between the valence band (VB) and conduction band (CB) in conductors, semiconductors and insulators. (CC BY-NC-SA; Catherine McCusker)

Conductors

Conductors have no band gap between their valence and conduction bands, since they overlap. There is no barrier for electrons to move from the valence to conduction band. Electrons can move freely through the material, which makes it able to conduct electricity. When the temperature of a conductor increases, the resistivity increases (and the conductivity decreases). Conductivity and resistivity are inversely proportional to each other. When conductivity is low, resistivity is high. When resistivity is low, conductivity is high. Since conductivity is the measure of how easily electricity flows, electrical resistivity measures how much a material resists the flow of electricity. As electrons move through a material, they come into contact with nuclei in the material. Collisions slow the electrons down. Each collision increases the resistivity of the material, and as temperature increases the electron are more likely to have collisions.

Insulators

Insulators have a large band gap between the valence and conduction bands. In insulators electrons do not have sufficient energy to jump from the valence band to the conduction band and the probability of finding an electron in the conduction band approaches 0. An insulator material won't conduct any electricity at any temperature.

Semiconductors

Semiconductors are an intermediate between conductors and insulators. They have a small energy gap between the valence band and the conduction band. Some electrons have sufficient energy that they can make the jump up to the conduction band. Semiconductors can conduct electricity, but not as easily as conductors. The probability of finding electrons in the conduction band of a semiconductor, and therefore it's ability to conduct electricity, will vary with the band gap and the temperature. Unlike conductors, semiconductors are more conductive at higher temperatures because more electrons have the energy to jump into the conduction band. There are two types of semiconductors: **intrinsic** and **extrinsic**.

Intrinsic Semiconductors

An intrinsic semiconductor is a pure material with a small band gap. For every electron that jumps into the conduction band, the missing electron will generate a hole that can move freely in the valence band. Both conduction band electrons and valence band holes can contribute to conducting electricity. The number of holes will equal the number of electrons that have jumped.

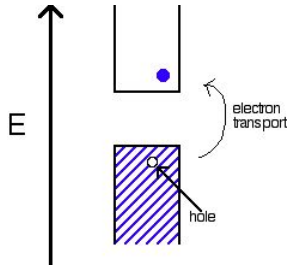


Figure **5.5.4**: Illustration of an intrinsic semiconductor. The electron in the conduction band (blue dot) leaves behind a vacancy (hole) in the valence band (white dot).

Extrinsic Semiconductors

Extrinsic semiconductors are not good conductors in their pure forms, they have larger band gaps than intrinsic semiconductors. In extrinsic semiconductors, the conductivity is controlled by purposefully adding small amounts of impurities to the material. This process is called doping. Doping, or adding impurities to the lattice can change the electrical conductivity of the lattice and therefore vary the efficiency of the semiconductor. In extrinsic semiconductors, the number of valence band holes will not equal the number of conduction band electrons. Silicon is one of the most common extrinsic semiconductors. If silicon is doped with an atom with fewer electron, such as boron, electron from the silicon valence band can hop to the boron atoms, leaving holes in the valence band to conduct electricity. If silicon is doped with an atom with more electrons, such as phosphorus, the extra electron from the phosphorus atoms can jump into the silicon conduction band.

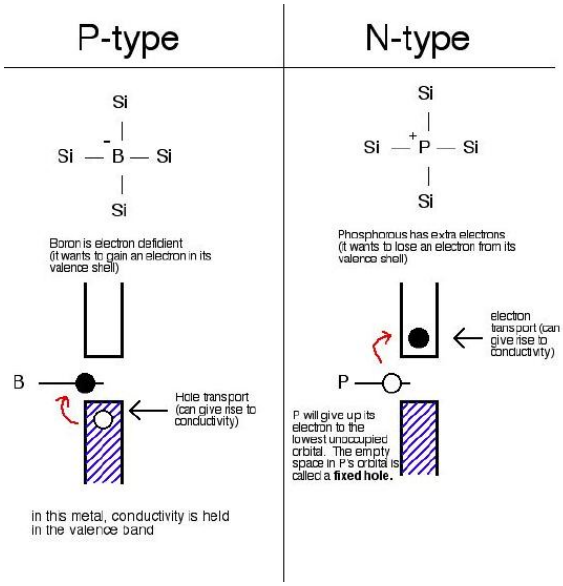


Figure 5.5.5: P-type (left) n-type (right) silicon semiconductors. In the p-type an electron from the valence band can jump to a vacancy on boron, leaving a hole in the valence band. In the n-type an electron from the phosphorus dopant can jump into the conduction band.

Exercise 5.5.1

Describe the difference between a valence band and a conduction band

Answer

The valence band is the highest band with electrons in it, the equivalent of the HOMO in MO theory. The conduction band is the highest band with no electrons in it, the equivalent of the LUMO in MO theory.

Exercise 5.5.2

A conductor material and a semiconductor material have the same conductivity at 100 K. Which will be more conductive when the temperature is increased to 200 K?

Answer

The conductivity of conductors will decrease as the temperature increases and the conductivity of semiconductors will increase as the temperature increases. Therefore at higher temperature the semiconductor material will have higher conductivity.

References

1. Electrical Conductivity and Resistivity, Heaney, Michael, Electrical Measurement, Signal Processing, and Displays. Jul 2003
2. Levy, Peter M., and Shufeng Zhang. "Electrical Conductivity of Magnetic Multilayered Structures." *Physical Review Letters* 65.13 (1990): 1643-646. Print.
3. Petrucci, Harwood, Herring, Madura. GENERAL CHEMISTRY Principles and Modern Applications 9th Edition. Macmillan Publishing Co: New Jersey. 1989.
4. Moore, John T. Chemistry Made Simple. Random House Inc: New York. 2004.

Contributors and Attributions

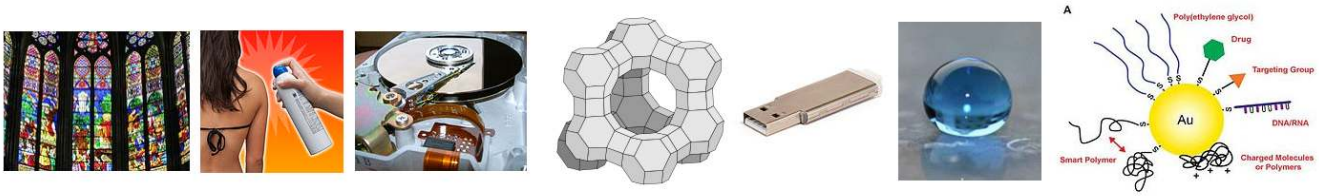
- Michael Ford (UCD) and Alexandra Christman (UCD)
- Sierra Blair (UCD)
- Jim Clark (Chemguide.co.uk)

5.5: Bonding in Metals and Semicondoctors is shared under a CC BY-NC-SA 4.0 license and was authored, remixed, and/or curated by LibreTexts.

- **Current page** is licensed CC BY-NC-SA 4.0.
- **6.8A: Electrical Conductivity and Resistivity** is licensed CC BY-NC-SA 4.0.

5.6: Nanomaterials

What do stained glass, sunscreen, magnetic hard drives, heterogeneous catalysts, consumer electronics, stain-resistant clothing, self-cleaning glass, and medical diagnostics all have in common? All of them derive some special property and utility from nanoscale materials: ordinary elements and inorganic compounds such as gold, silver, TiO_2, chromium, SiO_2, and silicon that acquire different properties when their characteristic dimensions are somewhere between 1 and 100 nm. In this section we will learn about the basic science of nanomaterials, i.e., what it is about their size that makes them different.



Surface Area

Nanoparticles have a substantial fraction of their atoms on the surface, as shown in Figure **5.6.1**. This high surface area to volume ratio is an important factor in many of the physical properties of nanoparticles, such as their melting point and vapor pressure, and also in their reactivity. In some cases, such as TiO_2, it can change which polymorph is most stable. The most stable form of bulk TiO_2 is rutile, but in TiO_2 nanoparticles, the most stable polymorph is anatase. Heterogeneous catalysts, for example, are often based on nanoparticles because the catalytically reactive atoms are those that are on the surface of the particle, and this allows for the most reactive surface sites with the smallest amount of material.

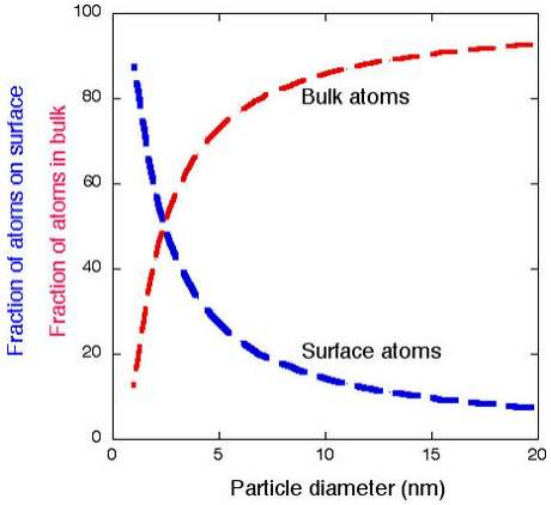


Figure **5.6.1**: Plot of how the ratio of surface to bulk atoms changes with particle size.

Surface Energy

The surface energy is always positive. A key quantity that is connected with the chemistry of all surfaces is the **surface energy**. This is the (thermodynamically unfavorable) energy of making "dangling bonds" at the surface. Atoms at the surface are under-coordinated, and because breaking bonds costs energy, surface atoms always have higher energy than atoms in the bulk. This happens regardless of whether the bonding is covalent (as in a metal), ionic (in a salt), or non-covalent (in a liquid such as water). We see this effect, for example, in water droplets that bead up on a waxy surface. The droplet contracts into a sphere (against the force of gravity that works to flatten it) in order to minimize the number of dangling hydrogen bonds at the surface.

In the case of metal or semiconductor particles, strong covalent bonds are broken at the surface. For example, a gold atom in bulk face-centered cubic Au has 12 nearest neighbors, but a gold atom on the surface of the crystal has six nearest neighbors in-plane and three underneath, for a total of 9. We might expect the surface energy of this crystal face to be a little less (because the remaining bonds will become slightly stronger) than 3/12 = 1/4 of the bonding energy of bulk Au, and this is in fact a fairly good

rule of thumb for many materials. When translated into energy per unit area, the surface energy of metals and inorganic salts is usually in the range of 1-2 J/m^2.

Example 5.6.1

The sublimation energy of bulk gold is 334 kJ/mol, and the surface energy is 1.5 J/m^2. What percentage of the bulk bonding energy is lost by atoms at the surface of a gold crystal?.

Solution

To solve this problem, we need to know the surface area per Au atom. Gold has the face-centered cubic structure, and the unit cell edge length is 4.08 Å. From this we can determine that the Au-Au distance is 4.08/1.414 = 2.88 Å. In a hexagonal array of gold atoms with this interatomic spacing, the surface area per atom is (2.88 Å)^2 x 0.866 = 7.2 Å^2. Multiplying by Avogadro's number, we find that the area per mole of Au surface atoms on the crystal face is 4.3 x 10^4 m^2.

Now we multiply this area by the surface energy:

$(4.3 \times 10^4 \frac{m^2}{mol}) \times (1.5 \frac{J}{mol}) \times (\frac{1kJ}{1000J}) = +65kJ$ per mole of Au surface atoms.

$\frac{65kJ}{334kJ} \times 100\% = 19\%$ of the bulk bonding energy is lost by atoms at the surface.

It is clear from the above example that the surface energy of nanoparticles can have a major effect on their physical properties, since a large fraction of the atoms in a nanoparticle are on the surface. A good example of this is the dramatic depression of the melting point. Solid nanocrystals are in general faceted, whereas liquid droplets made by melting nanocrystals adopt a spherical shape to minimize the surface area.

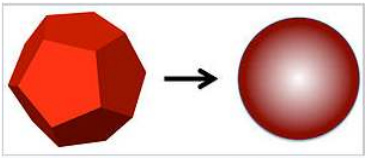


Figure 5.6.2: A faceted solid nanocrystal melts into a spherical droplet in order to minimize its surface energy.

Let's consider melting a silver nanocrystal that is 2 nm in diameter, meaning that about $\frac{1}{2}$ of the atoms are on the surface. The spherical liquid droplet has lower surface area than the faceted crystal. For example, a cube has 1.24 times the surface area of a sphere of the same volume. If the decrease in surface area is about 20% upon melting, and the surface energy is about 1/4 of the bulk bonding energy of the atoms, then for a 2 nm diameter nanocrystal we would estimate that:

$$\Delta H^o_{fusion} \approx \Delta H^o_{fusion,\ bulk} - (\frac{1}{2})(0.25)(\frac{1}{4})\Delta H^o_{vap} = \Delta H^o_{fusion,\ bulk} - 0.025\Delta H^o_{vap,\ bulk} \quad (5.6.1)$$

where $\Delta H^\circ_{vap,\ bulk}$, the heat of vaporization, is the total bonding energy of atoms in a bulk crystal. For silver, $\Delta H^\circ_{fusion,\ bulk}$ = 11.3 kJ/mol and $\Delta H^\circ_{vap,\ bulk}$ = 250 kJ/mol. From this we can calculate the heat of fusion of a 2 nm Ag nanocrystal:

$$\Delta H^o_{fusion} \approx 11.3 - (0.025)(25) = 5.1 \frac{kJ}{mol} \quad (5.6.2)$$

The melting point of bulk silver is 962 °C = 1235 K. Assuming that the entropy of fusion is the same in the bulk and in the nanocrystal, the melting point of the nanocrystal should be $1234K \times (\frac{5.1}{11.3}) = 557K = 284°C$, a drop of almost 700 degrees from the bulk value. Experimentally, the melting point of a 2 nm diameter silver nanocrystal drops about 800 degrees below that of the bulk, to 127 °C. This is a whopping big change in the melting point, which is in reasonable agreement with our rough estimate. The same effect - energetic destabilization of the surface atoms relative to bulk atoms - results in the lower boiling point, higher vapor pressure, higher solubility, and higher reactivity of nanocrystals relative to larger crystals of the same material.

Quantum Dots

One of the most fascinating and well-studied mesoscopic effects occurs with semiconductor particles of various shapes when one or more of their dimensions is in the range of a few nanometers. These so-called "quantum dots" (0D), "quantum rods" (1D) and "nanosheets" (2D) acquire striking new electronic and optical properties.

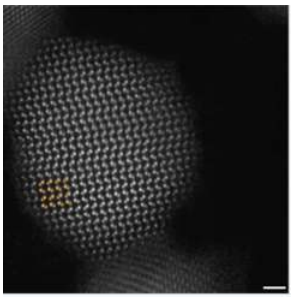


Figure 5.6.3: Atomic resolution image of a CdSe nanoparticle.

The synthesis of semiconductor quantum dots, which is discussed in more detail below, is sufficiently well controlled to give essentially perfect crystals of a few thousand atoms, something that is statistically impossible in a macroscopic crystal. An image of such a crystal is shown in Figure 5.6.3. The band gap in many of these quantum dots is in a range where absorption of visible light can promote an electron from the valence band to the conduction band as shown in Figure 5.6.4. Relaxation of that electron back into the valence band results in emission. The quantum yield for band gap emission of semiconductor quantum dots is typically high, giving rise to the bright emission colors shown in (Figure 5.6.5) for CdSe particles of different sizes. Because of their strong and narrow emission bands, quantum dots are of interest as luminescent tags for biological imaging applications, and also as light absorbers and emitters in solar cells and LEDs.

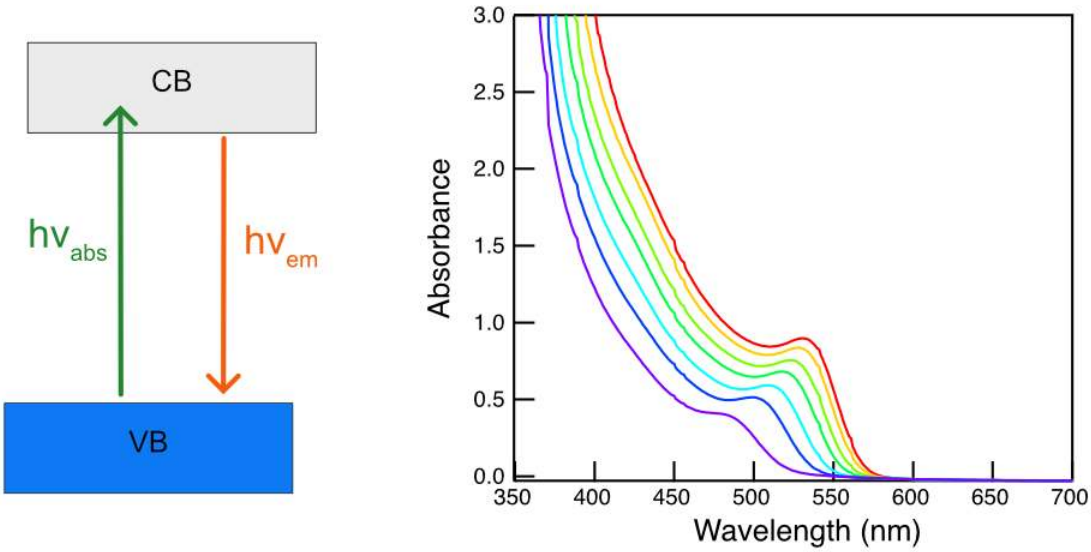


Figure 5.6.4: Diagram (left) showing the band gap absorption and emission of visible light in quantum dots. UV-visible spectrum (right) of a series of CdSe quantum dots. (CC BY-NC-SA, Catherine McCusker)

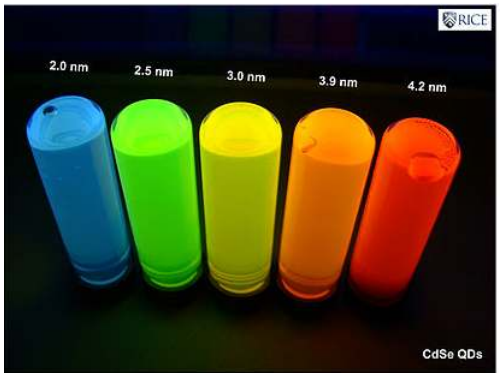


Figure 5.6.5: Emission colors of CdSe nanoparticles of different sizes. Smaller particles emit blue light because the exciton energy increases as the size decreases.

Size dependence

The size-dependence of the emission color comes primarily from a particle-in-a-box effect. The electron and hole that are created when the quantum dot absorbs light are bound together as an exciton by the confines of the "box". Louis Brus used first-order perturbation theory to determine that the band gap of a semiconductor quantum dot is given approximately by:

$$E_{gap} = E_{gap,bulk} + \frac{h^2}{8\mu R^2} - \frac{1.8e^2}{4R\pi\varepsilon\varepsilon_0} + ... \tag{5.6.3}$$

where R is the particle radius, μ is the electron-hole reduced mass ($1/\mu = 1/m_e^* + 1/m_h^*$), m_e^* and m_h^* are the electron and hole effective masses, and ε is the dielectric constant of the semiconductor. In this equation, the first term after the bulk bandgap is the kinetic energy due to confinement of the exciton, and the second term represents the electrostatic attractive energy between the confined electron and hole. Because the energy is a function of R^2, it can be widely tuned across the visible spectrum by changing the size of the quantum dot.

Definition: Exciton

A conduction band electron and its valence band hole together form an exciton. Excitons are formed when an electron is promoted from the valence band to the conduction band of a material.

Synthesis

Early work on the quantum size effect in semiconductor nanoparticles used simple metathesis reactions in the synthesis. For example, CdSe and PbS can be precipitated at ambient temperature by the reactions:

$$CdCl_{2\,(aq)} + H_2Se_{(g)} = CdSe_{(s)} + 2\,HCl_{(aq)}$$

$$Pb(NO_3)_2 + H_2S_{(g)} = PbS_{(s)} + 2\,HNO_{3\,(aq)}$$

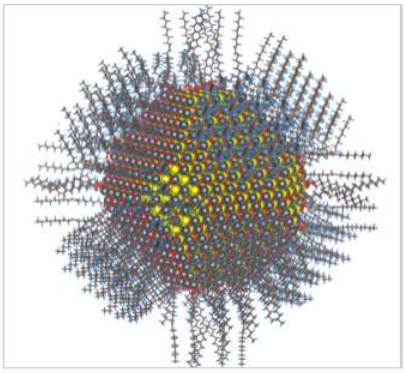


Figure 5.6.6: Complete atomistic model of a 5 nm diameter colloidal lead sulfide nanoparticle with surface passivation by oleic acid, oleyl and hydroxyl groups.

The growth of the particles was restricted by carrying out these reactions in different matrices, such as in polymer films or the silicate cages of zeolites, and capping ligands were also sometimes used to limit particle growth. While these reactions did produce nanoparticles, in general a broad distribution of particle sizes was obtained. The particles were also unstable to **Ostwald ripening** - in which large particles grow at the expense of smaller ones in order to minimize the total surface energy - because of the reversibility of the acid-forming synthetic reactions in aqueous media. The lack of good samples prevented detailed studies and the development of applications for semiconductor quantum dots.

A very important development in nanoparticle synthesis came in the early 1990's, when Murray, Norris, and Bawendi introduced the first non-aqueous, controlled growth process for II-VI semiconductor quantum dots. The keys to this synthesis were (1) to use non-aqueous solvents and capping ligands to stabilize the products against ripening, (2) to carry out the reaction at high temperature to ensure good crystallinity, and (3) to separate the steps of particle **nucleation** and **growth**, and thereby obtain particles of uniform size. This procedure is illustrated below in Figure 5.6.7.

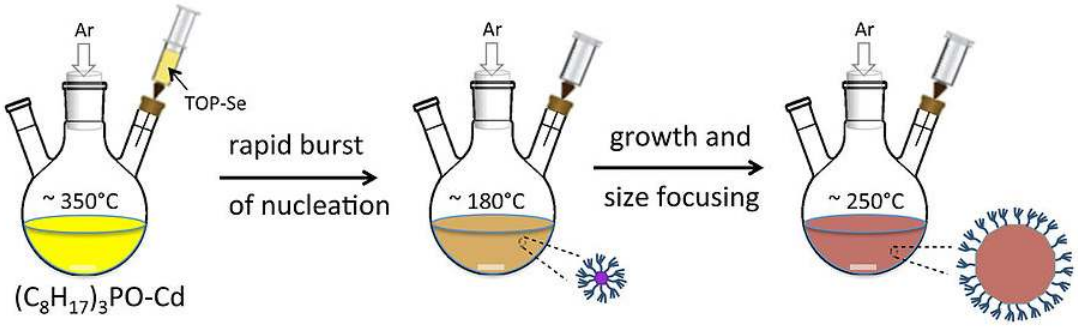


Figure **5.6.7**: Illustration of the steps of CdSe nanoparticle synthesis

The synthesis is carried out in a coordinating, high boiling solvent that is a mixture of trioctylphosphine (TOP) and trioctylphosphine oxide (TOPO). IAt the start of the reaction, a selenium source is rapidly injected into the hot (350 °C) reaction mixture containing Cd. The reaction causes a rapid burst of nanoparticle nucleation, but the temperature also drops as the cold solvent is injected and so the nucleation event ends quickly. The cooled solution now contains nanocrystal seeds. It is supersaturated in TOPO-Cd and TOP-Se, but particle growth proceeds slowly until the solution is heated again to the growth temperature, ca. 250°C. Particle growth and size-focusing occurs because small particles require less added material to grow by an amount ΔR than larger particles. This is because the volume of an added shell around a spherical seed is $4\pi R^2\Delta R$, so for larger R, ΔR is smaller. Very narrow particle size distributions can be obtained under conditions of high supersaturation, where the rate of nanoparticle growth is fast relative to particle dissolution and Ostwald ripening. Because the nanoparticles are capped with a ligand shell of TOP, they can be precipitated and re-suspended in organic solvents.

The high temperature synthesis of semiconductor quantum dots has been applied to a broad variety of materials. Monodisperse nanoparticles of controlled shapes can be made by variants of this method. For example, it is possible to adjust the conditions so that CdSe nucleates in the zincblende polymorph as tetrahedrally shaped seeds, and then grow polar wurtzite "arms" onto each triangular face, resulting in nanocrystal tetrapods. Numerous other nanocrystal shapes such as rods, arrowheads, rice (tapered rods), and polar structures such as Janus rods can be made by variants of this technique. These shape-control strategies often involve the use of ligands that adsorb specifically to certain crystal faces and inhibit their growth. For example, hexylphosphonic acid ligands adsorb selectively to Cd-rich crystal faces and thus lead to the growth of prismatic wurtzite-phase CdSe nanocrytals.

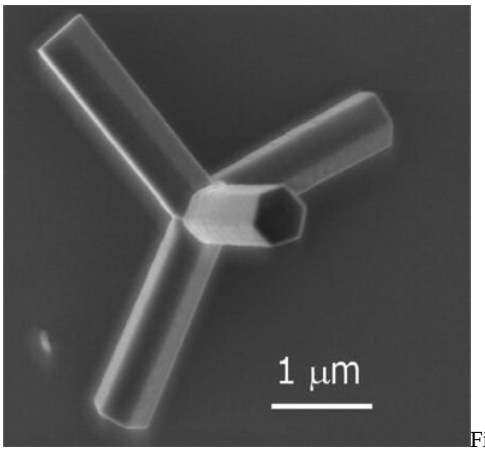
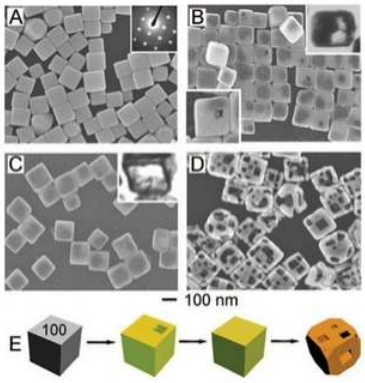
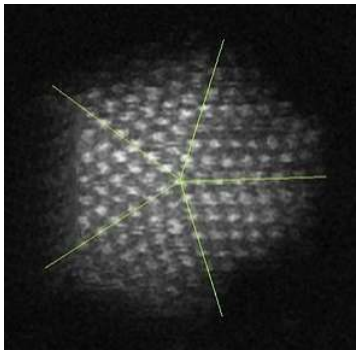


Figure **5.6.1**: Scanning electron microscope (SEM) image of a ZnO tetrapod nanocrystal. (CC BY-NC-ND 3.0; ScienceDirect via https://doi.org/10.1016/S1369-7021(07)70079-2)



Nanoscale metal particles have been the subject of intense research over the past 20 years, especially because of their unusual **optical**, **magnetic**, and **catalytic** properties. The synthesis of metal nanocrystals in various shapes has become increasingly sophisticated and rational, like the synthesis of semiconductor nanocrystals described above. By controlling the separate phases of nucleation and growth, and by using ligands that cap specific crystal faces during growth, it is possible to make metal nanocrystals of uniform size in a variety of interesting and useful shapes including cubes, truncated cubes, octahedra, triangular prisms, and high aspect ratio rods. By exploiting displacement reactions that replace one metal with another, complex hollow shapes such as nanocages (as shown at the left) can be made starting with other shapes. In this case, solid silver nanocubes are transformed to gold nanocages.



Five-fold twinning in a gold nanoparticle

The interesting optical properties of nanocrystalline Au, Ag, Cu, and a number of other metals, derive from the collective oscillation of their valence electrons, a phenomenon known as **plasmon resonance**. Remember that in these metals, the electron mean free path is long (about 100 times larger than the size of the atoms), so the valence electrons feel only the average positive charge of the atomic cores as they zoom around the crystal. Light impinging on the metal acts as an oscillating electric field, pushing and pulling on the valence electrons at the characteristic frequency of the light wave. The situation is very much like a pendulum or a weight on a spring. The electrons, pushed away from their equilibrium positions, feel a restoring force that is proportional to their displacement. Their motion can be described by **Hooke's Law**:

$$F = kx \tag{5.6.4}$$

where the spring constant k determines the "stiffness" of the spring. In the case of the plasmon resonance, k is proportional to the number density of valence electrons n, and the square of the electronic charge e:

$$k = \frac{ne^2}{\varepsilon_0} \tag{5.6.5}$$

The **resonant frequency** of the plasma oscillation is given by:

$$\omega_p = (\frac{k}{m})^{\frac{1}{2}} = (\frac{ne^2}{m_e \varepsilon_0}^{\frac{1}{2}} \tag{5.6.6}$$

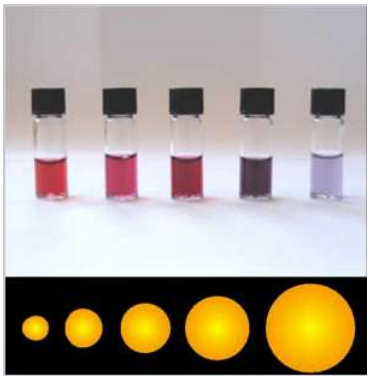
where m_e is the electron mass. For most metals, the plasmon resonance is in the ultraviolet part of the spectrum, but for a few metals like Au, Ag, and Cu it is in the visible.



The Lycurgus cup (4th century Roman glass) derives its unique coloration from noble metal nanoparticles. The cup is red in transmitted light and green in scattered (reflected) light.

For metal particles that are much smaller than the wavelength of light, this effect is called the **localized surface plasmon resonance**, or LSPR. There are three important consequences of the LSPR effect:

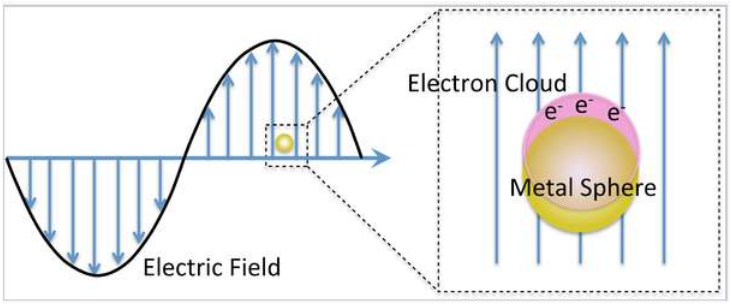
- The **local electric field** of the incoming light wave is greatly **enhanced** at the particle surface. This gives rise to huge enhancement factors in optical processes such as **Raman scattering** and **fluorescence**. Thus, certain analytical spectroscopic techniques are greatly enhanced by LSPR.
- Near the plasmon resonance frequency, metal nanocrystals **absorb** and **scatter light** very strongly. This makes them brightly reflective, and the strong light absorption can be exploited for light-induced local heating. These properties are being applied in medical diagnostics and therapy, e.g., for detection and photothermal destruction of cancer cells. By adjusting the size and shape of the gold nanoparticles, which are more stable than Ag and Cu in biological media, the plasmon frequency can be tuned to the tissue-transparent near-IR region of the spectrum between 700 and 900 nm. Small quantities of plasmonic Ag and Au particles also make brightly colored and strongly scattering pigments, e.g. in stained glass as shown above at the right.
- The plasmon frequency is sensitive to the refractive index of the particle's surroundings, i.e., its chemical environment. This makes metal nanoparticles of special interest for **sensing and biosensing** applications.



The colors of plasmonic gold nanoparticles depend on their size and shape.

Theory of light scattering and absorption by metal nanoparticles

The valence electrons in metal nanoparticles oscillate in the electric field of a light wave. While the nature of these oscillations is somewhat complex in metal particles that are non-spherical, the theory for spherical particles is relatively simple and in fact was worked out over 100 years ago by German physicist Gustav Mie.



Mie considered the interaction of a spherical particle with a **uniform electric field, E,** oscillating at angular frequency ω (= 2π f). This is a good approximation when the particle diameter is much smaller than the wavelength of light, as shown on the left. The particle is embedded in a uniform, insulating material (e.g. a solvent) that has a dielectric constant ε_{diel}. For insulators, ε_{diel} is a positive real number.

The dielectric constant ε of a metal is actually a complex number:

$$\varepsilon = \varepsilon' + i\varepsilon'' \tag{5.6.7}$$

Here the real part, ε', is related to the refraction of light, and the imaginary part, ε", is related to light absorption. Both ε' and ε" are dependent on the frequency of the light. For metals near the plasmon resonance frequency, ε' is typically a *negative number.*

The **cross-section for absorption** of the light wave by the particle is:

$$\sigma_{absorption} = \frac{9\omega}{c}\epsilon_{diel}^{\frac{3}{2}} V \frac{\epsilon''_{metal}}{(\epsilon'_{metal} + 2\epsilon_{diel})^2 + (\epsilon''_{metal})^2} \tag{5.6.8}$$

and the **cross-section for scattering** is:

$$\sigma_{scattering} = \frac{3}{2\pi}\left(\frac{\omega^4}{c}\right)\epsilon_{diel}^2 V^2 \frac{(\epsilon'_{metal} - \epsilon_{diel})^2 + (\epsilon''_{metal})^2}{(\epsilon'_{metal} + 2\epsilon_{diel})^2 + (\epsilon''_{metal})^2} \tag{5.6.9}$$

The sum of these two is the **cross-section for extinction**:

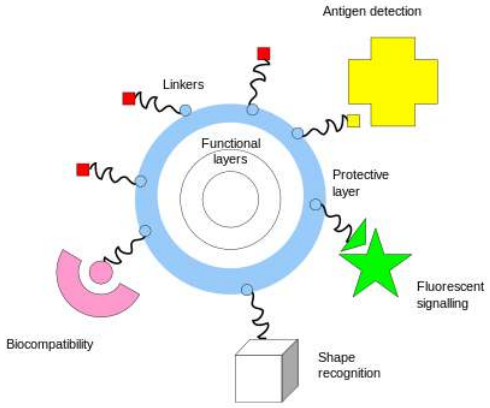
$$\sigma_{extinction} = \sigma_{absorption} + \sigma_{scattering} \tag{5.6.10}$$

These cross-sections become large when the ($\varepsilon'_{metal} + 2\varepsilon_{diel}$) term in the denominator becomes small. This occurs when

$$\epsilon'_{metal} \simeq -2\epsilon_{diel} \tag{5.6.11}$$

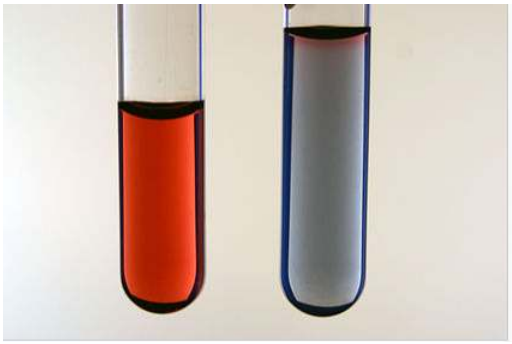
For 15 nm diameter gold nanoparticles in water, this happens at about 580 nm, resulting in the characteristic wine-red color of colloidal gold solutions. Changing the solution environment (e.g., by adsorbing a molecule onto the gold surface) changes ε_{diel} and thus alters the color slightly.

It is important to note that the cross-section for **scattering** is proportional to the **square of the volume** of the particle, V^2, whereas the absorption is proportional to V. This means that very small gold particles (< 5 nm) are strongly absorbing but not strongly scattering. Larger particles (>30 nm) scatter light very strongly. Depending on the application, therefore, we choose larger or smaller particles.



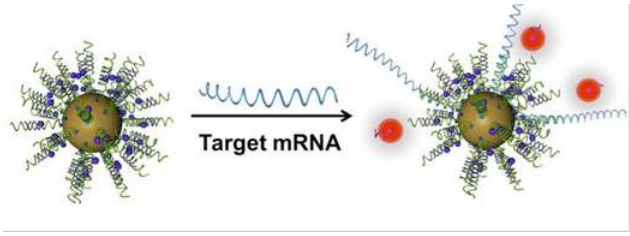
One of the key complementary properties of noble metal nanoparticles that is important to their use in biomedicine is the ease with which they can be **covalently conjugated** with polymers or small molecules, typically via thiol or amine bonds at their surface. This imparts biological recognition properties to the particles that enables them to bind to specific biomolecular targets. The figure at the left illustrates some of the functionality that can be imparted to nanoparticles through surface functionalization.

Functionalization of gold nanoparticles with thiol-terminated single-stranded DNA was the basis of one of the first nanoparticle sensors, developed by the Mirkin group at Northwestern University. **DNA-coated nanoparticles** have the characterstic wine-red plasmonic color of spherical nano-gold. However, when these particles are linked together by a complementary DNA strand, the resonance frequency shifs, resulting in a blue color. This color change, illustrated in the figure at the right, provides a "litmus test" for the presence of the target DNA sequence.[10] "Melting" of the DNA - heating it to the temperature at which double stranded DNA dissociates to make single strands - reverses the color change. The DNA hybridization/melting transition is highly **cooperative** because of the aggregation of many gold particles, so the transition temperature is very sharp. With proper temperature control, the color change can be sensitive to a **single base mismatch** in the target DNA that is detected by this method.



Aggregation of Au nanoparticles (in this case by adding salt to a colloidal solution) causes a color change from wine red (left) to blue (right). Photo credit: George Lisensky, Beloit College

Subsequent research has developed sophisticated diagnostic and therapeutic ("theranostic") applications for these **spherical nucleic acid**[11] particles. These particles easily penetrate cell membranes and can report on the chemistry happening inside living cells.



General schematic of nanoflare-based detection.

An important property of gold nanoparticles in these applications is their ability to **quench** the **fluorescence** of reporter molecules that are near their surface. Nucleic acid strands that contain a hairpin loop can position fluorescent molecules near the gold surface, where their fluorescence is turned off by nanoparticle quenching. Hybridization of these sequences to target RNA or DNA causes the fluorescence to turn on by moving the fluorescent molecule away from the nanoparticle surface. These so called "nanoflares" can thus signal the up- or down-regulation of specific genes inside cells. Nanoflares are the basis of the Verigene System, developed and commercialized by Nanosphere, Inc. to detect markers for infectious diseases and cancers.

References

1. K. J. Klabunde, J. Stark, O. Koper, C. Mohs, D. G. Park, S. Decker, Y. Jiang, I. Lagadic, and D. Zhang, "Nanocrystals as Stoichiometric Reagents with Unique Surface Chemistry," J. Phys. Chem. 1996, 100, 12142–12153. DOI: 10.1021/jp960224x.
2. Brus, Louis E. (1984). "Electron–electron and electron-hole interactions in small semiconductor crystallites: The size dependence of the lowest excited electronic state". J. Chem. Phys. 80, 4403. DOI: 10.1063/1.447218.
3. C. B. Murray, D. J. Norris, and M. G. Bawendi, "Synthesis and characterization of nearly monodisperse CdE (E = sulfur, selenium, tellurium) semiconductor nanocrystallites," J. Am. Chem. Soc. 1993, 115, 8706–8715. DOI: 10.1021/ja00072a025.
4. Y. Yin and A. P. Alivisatos, "Colloidal nanocrystal synthesis and the organic–inorganic interface," Nature 2005, 437, 664-670. DOI: 10.1038/nature04165
5. G. Zheng, F. Patolsky, Y. Cui, W. U. Wang and C. M. Lieber, "Multiplexed electrical detection of cancer markers with nanowire sensor arrays," Nature Biotechnol. 2005, 23, 1294 - 1301. DOi:10.1038/nbt1138.
6. Mirkin, C. A., et al., A DNA-based method for rationally assembling nanoparticles into macroscopic materials. *Nature* 1996, 382 (6592), 607-609.
7. Cutler, J. I., et al., Spherical Nucleic Acids. *J Am Chem Soc* 2012, 134 (3), 1376-1391.

5.6: Nanomaterials is shared under a CC BY-SA license and was authored, remixed, and/or curated by LibreTexts.

- **11.1: Prelude to Basic Science of Nanomaterials** by Chemistry 310 is licensed CC BY-SA 4.0. Original source: https://en.wikibooks.org/wiki/Introduction_to_Inorganic_Chemistry.
- **Current page** is licensed CC BY-SA 4.0.
- **11.5: Surface Energy** by Chemistry 310 is licensed CC BY-SA 4.0. Original source: https://en.wikibooks.org/wiki/Introduction_to_Inorganic_Chemistry.
- **11.3: Semiconductor Quantum Dots** by Chemistry 310 is licensed CC BY-SA 4.0. Original source: https://en.wikibooks.org/wiki/Introduction_to_Inorganic_Chemistry.
- **11.4: Synthesis of Semiconductor Nanocrystals** by Chemistry 310 is licensed CC BY-SA 4.0. Original source: https://en.wikibooks.org/wiki/Introduction_to_Inorganic_Chemistry.
- **11.6: Nanoscale Metal Particles** by Chemistry 310 is licensed CC BY-SA 4.0. Original source: https://en.wikibooks.org/wiki/Introduction_to_Inorganic_Chemistry.

CHAPTER OVERVIEW

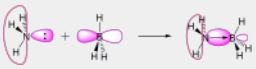
6: Acid-Base and Donor-Acceptor Chemistry

> *In a very real sense, we can make an acid anything we wish. The differences between the various acid-base concepts are not concerned with which is 'right', but which is most convenient to use in a particular situation.*
>
> *James E. Huheey, Ellen A. Keiter, and Richard L. Keiter*

The concept of acids and bases is often associated with the movement of hydrogen ions from one molecule or ion to another. However, a host of acid base concepts have been developed to help chemists organize and make sense of a wide range of reactions (Table 6.1).

Table 6.1. Summary of major acid-base models.

Definition	Theoretical paradigm and notable features.	Acid	Base	Illustrative sample reactions
Arrhenius (1894)	Interested in what the substance does to the state of an aqueous solution. In particular it assesses proton donation to & removal from water using [H_3O^+] as a proxy. Readily accommodates the pH concept as a measure of the state of a solution	Increases [H_3O^+]	Decreases [H_3O^+]	$\underset{acid}{HCl} + H_2O \rightarrow H_3O^+ + Cl^-$ $\underset{base}{NH_3} + H_2O \rightarrow NH_4^+ + OH^-$
Brønsted-Lowry (1923)	Envisions acid-base reactivity in terms of the transfer of a H^+ from one substance to another. Allows for conjugate acids and bases and solvent autoionization.	Donates H^+	Accepts H^+	$\underset{acid}{HCl} + \underset{base}{NH_3} \rightarrow \underset{conj.\ acid}{NH_4^+} + \underset{conj.\ base}{Cl^-}$ $\underset{acid}{HOAc} + \underset{base}{NH_3} \rightarrow \underset{conj.\ acid}{NH_4^+} + \underset{conj.\ base}{OAc^-}$ $\underset{amphoteric}{2\ H_2O} \rightarrow \underset{conj.\ acid}{H_3O^+} + \underset{conj.\ base}{OH^-}$
Lux-Flood (1939-~47)	Describes reactions involving oxides and oxyanions in terms of the transfer of oxide ion (O^{2-}). Mainly used in geochemistry, although it also can be used to describe some redox reactions.	Oxide acceptor	Oxide donor	$\underset{acid}{SiO_2} + \underset{base}{CaO} \rightarrow CaSiO_3$ $\underset{base}{H_2O} + \underset{acid}{CO} \rightarrow H_2 + CO_2$
Solvent System	Applies aspects of the Arrhenius, Brønsted-Lowry, and Lux-Flood acid base concepts to solvent cation & anion formation in a generalized reaction. Can be used to describe solution chemistry in nonaqueous solvent systems like BrF_3.	Is a solvent cation or increases the solvent cation concentration, often by receiving a lone pair bearing group	Is a solvent anion or increases the solvent anion concentration, often by donating a lone pair bearing group	$\underset{acid}{SbF_5} + \underset{base}{BrF_3} \rightarrow \underset{conj.\ base}{SbF_6^-} + \underset{conj.\ acid}{BrF_2^+}$ $\underset{amphoteric}{2\ BrF_3} \rightarrow \underset{conj.\ acid}{BrF_2^+} + \underset{conj.\ base}{BrF_4^-}$
Lewis (1923)	Envisions acid-base reactivity in terms of electron pair donation. Encompasses the Arrhenius, Brønsted-Lowry, Lux-Flood, and Solvent System definitions and readily	Accepts an electron pair	Donates an electron pair	$\underset{base}{:NH_3} + \underset{acid}{BF_3} \rightarrow H_3N \rightarrow BF_3$

Definition	Theoretical paradigm and notable features.	Acid	Base	Illustrative sample reactions
	integrates with molecular orbital descriptions of chemical reactivity in Frontier orbital theory.			
Nucleophile-Electrophile	Applies the Lewis concept to organic reactivity. Nucleophiles are Lewis bases which tend to react form a bond with Lewis acid sites called electrophilic centers.	(The electrophile) Tends to react by receiving an electron pair from a nucleophile, forming a bond in the process	(The nucleophile) Donates an electron pair to form a bond to an electrophile	$\underset{base}{Br^-} + \underset{acid}{CH_3-Cl} \rightarrow Br-CH_3 + Cl^-$
Usanovich (1939)	Extends Lewis theory to include the donation and acceptance of any number of electrons, whether through the formation of an adduct or electron transfer.	Accepts electrons	Donates electrons	$\underset{base}{:NH_3} + \underset{acid}{BH_3} \rightarrow \underset{adduct}{H_3N-BH_3}$ $\underset{acid}{Fe^{2+}} + \underset{base}{Zn^0} \rightarrow Fe^0 + Zn^{2+}$
Frontier Orbital (1960s)	Envisions Lewis Acid-base/Electrophile-nucleophile reactions in terms of the donation and acceptance of electrons between the reactant's frontier orbitals. Specifically, the reaction is envisioned in terms of donation of the base's HOMO electrons into the acid's HOMO level.	Possesses a LUMO capable of forming an occupied bonding MO on mixing with a base's HOMO.	Possesses an electron-bearing HOMO capable of forming a filled bonding MO on mixing with an acid's LUMO.	 base acid adduct

Some concepts involve defining acids and bases in particular ways that allow for the understanding of particular types of chemical systems. For example, the familiar Arhennius and Brønsted acids and base concepts used in general chemistry help chemists make sense of the behavior of compounds which can transfer H^+ ions among themselves, often in aqueous solution. However, the solvent system acid-base concept defines acids and bases in terms of the transfer of a lone-pair bearing group and is particularly useful for conceptualizing the reactivity of main group halides, oxides, and related compounds. Some acid-base definitions seek to encompass an extremely wide range of chemical reactions. For instance, the Lewis acid-base definition encompasses the Arrhenius, Brønsted, and solvent system definitions and has also found wide use in inorganic chemistry owing to the ease with which Lewis acid-base interactions may be described by the Frontier Orbital approach in terms of interacting molecular orbitals on the acid and base.

References

Huheey, J. E.; Keiter, E. A.; Keiter, R. L., *Inorganic Chemistry: Principles of Structure and Reactivity. 4th ed.*; HarperCollins: New York, NY, 1993, pg. 318.

Contributors and Attributions

- Stephen M. Contakes (Westmont College)

Learning Objectives

- Understand when to apply different acid and base theories
- Identify conjugate acids and bases, and rules for strong & weak acids/bases, in both Brønsted and Lewis acid-base systems
- Describe and rationalize acid/base chemistry of "non-traditional" Brønsted acids.
- Predict favorable and stable compounds using hard-soft acid-base (HSAB) theory.

Thumbnail image is the Lewis acid-base adduct formed between BF_3 and NH_3.

6.1: Arrhenius Model

6.2: Brønsted-Lowry Model

6.3: Lewis Concept and Frontier Orbitals

6.4: Hard and Soft Acids and Bases

6: Acid-Base and Donor-Acceptor Chemistry is shared under a CC BY-NC-SA 4.0 license and was authored, remixed, and/or curated by LibreTexts.

6.1: Arrhenius Model

The Arrhenius acid-base concept defines acids and bases in terms of how they affect the amount of hydronium ions, $\mathrm{H_3O^+}$, (and by extension hydroxide ions, $\mathrm{OH^-}$) in aqueous solutions. Simply, in the Arrhenius definition an acid is a substance that increases the concentration of hydronium ions when it is dissolved in water. This typically occurs when the acid dissociates by loss of a proton to water according to the general equation:

$$\mathrm{HA\,(aq) + H_2O\,(l) \rightleftharpoons H_3O^+\,(aq) + A^-\,(aq)} \tag{6.1.1}$$

where A is the deprotonated form of the acid. For example, what hydrochloric and acetic acid, $\mathrm{CH_3CO_2H}$, have in common is that both increase the amount of hydronium ion when they are dissociated in solution.

$$\mathrm{HCl\,(aq) + H_2O\,(l) \longrightarrow H_3O^+\,(aq) + Cl^-\,(aq)}$$

$$\mathrm{CH_3CO_2H\,(aq) + H_2O\,(l) \rightleftharpoons H_3O^+\,(aq) + CH_3CO_2{}^-\,(aq)}$$

In terms of the Arrhenius definition, the major difference between hydrochloric and acetic acid is that hydrochloric acid dissociates completely in solution to yield stoichiometric amounts of $\mathrm{H_3O^+}$, while acetic acid only partially dissociates. Acids like HCl that completely dissociate in water are classified as strong in the Arrhenius definition, while those like acetic acid that do not are classified as weak.

Although all weak acids incompletely dissociate, the extent of dissociation can vary widely. The relative strengths of weak Arrhenius acids is conveniently expressed in terms of the equilibrium constant for their acid dissociation reaction, K_a.

$$K_a = \frac{[\mathrm{H^+}][\mathrm{A^-}]}{[\mathrm{HA}]}$$

The $\mathrm{pK_a}$ values for selected weak acids are given in Table 6.1.1.

Table 6.1.1: Values of K_a, pK_a, K_b, and pK_b for selected monoprotic acids.

Acid	HA	K_a	pK_a	A^-	K_b	pK_b
sulfuric acid (2nd ionization)	HSO_4^-	1.0×10^{-2}	1.99	SO_4^{2-}	9.8×10^{-13}	12.01
hydrofluoric acid	HF	6.3×10^{-4}	3.20	F^-	1.6×10^{-11}	10.80
nitrous acid	HNO_2	5.6×10^{-4}	3.25	NO_2^-	1.8×10^{-11}	10.75
formic acid	HCO_2H	1.78×10^{-4}	3.750	HCO_2^-	5.6×10^{-11}	10.25
benzoic acid	$C_6H_5CO_2H$	6.3×10^{-5}	4.20	$C_6H_5CO_2^-$	1.6×10^{-10}	9.80
acetic acid	CH_3CO_2H	1.7×10^{-5}	4.76	$CH_3CO_2^-$	5.8×10^{-10}	9.24
pyridinium ion	$C_5H_5NH^+$	5.9×10^{-6}	5.23	C_5H_5N	1.7×10^{-9}	8.77
hypochlorous acid	$HOCl$	4.0×10^{-8}	7.40	OCl^-	2.5×10^{-7}	6.60
hydrocyanic acid	HCN	6.2×10^{-10}	9.21	CN^-	1.6×10^{-5}	4.79
ammonium ion	NH_4^+	5.6×10^{-10}	9.25	NH_3	1.8×10^{-5}	4.75
water	H_2O	1.0×10^{-14}	14.00	OH^-	1.00	0.00
acetylene	C_2H_2	1×10^{-26}	26.0	HC_2^-	1×10^{12}	−12.0
ammonia	NH_3	1×10^{-35}	35.0	NH_2^-	1×10^{21}	−21.0

*The number in parentheses indicates the ionization step referred to for a polyprotic acid.

As can be seen from the table the K_a values for weak acids are less than one (otherwise they would not be weak) and vary over many orders of magnitude. Consequently it is customary to tabulate acid ionization constants as pK_a values:

$$pK_a = -\log K_a$$

Because pK_a values essentially place the K_a values on a negative base ten logarithmic scale, the stronger the weak acid, the lower its pK_a. Weak acids with larger K_a values will have lower pK_a values than weaker acids with smaller K_a. Moreover, each unit increase or decrease in the pK_a corresponds to a tenfold increase or decrease in the corresponding K_a.

While Arrhenius acids increase the concentration of $\mathbf{H_3O^+}$ in aqueous solution, Arrhenius bases decrease $\mathbf{H_3O^+}$. Strong bases do this stoichiometrically. Most are hydroxide salts of alkali metals or quaternary ammonium salts that dissociate completely when dissolved in water:

$$\mathrm{MOH\,(aq) \longrightarrow M^+\,(aq) + OH^-\,(aq)}$$

This added hydroxide decreases the concentration of H_3O^+ by shifting the water autoionization equilibrium towards water.

$$\mathrm{2\,H_2O\,(l) \rightleftharpoons H_3O^+\,(aq) + OH^-\,(aq)}$$

In contrast, most weak bases react with water to produce an equilibrium concentration of hydroxide ion according to the base dissociation reaction

$$\mathrm{B\,(aq) + H_2O\,(l) \rightleftharpoons BH^+\,(aq) + OH^-\,(aq)}$$

in which **B** is the weak base. The ionization constant for this reaction, called the **base ionization constant** or K_b, is typically used as a measure of a weak base's strength.

Because both hydroxide and hydronium ion are products of water autoionization, the concentrations of hydronium ion and hydroxide ion in aqueous solution will vary reciprocally with one another. This means that Arrhenius acids can be recognized as substances that decrease the hydroxide concentration and Arrhenius bases as substances that increase it.

Since the Arrhenius acid-base concept is concerned about the state of the water autoionization reaction, Arrhenius acids and bases may also be recognized by their effect on the solution pH. Arrhenius acids decrease the pH and Arrhenius bases will increase it.

NOTE

To qualify as an Arrhenius acid, upon the introduction to water, the chemical must cause, either directly or otherwise:

- an increase in the aqueous hydronium concentration,
- a decrease in the aqueous hydroxide concentration, or
- a decrease in the solution pH.

Conversely, to qualify as an Arrhenius base, upon the introduction to water, the chemical must cause, either directly or otherwise:

- a decrease in the aqueous hydronium concentration,
- an increase in the aqueous hydroxide concentration, or
- an increase in the solution pH.

Because the Arrhenius acid-base model defines acids and bases in terms of their impact on the state of an aqueous solution the Arrhenius concept is unable to describe reactions in nonaqueous solvents, gases, molten liquids, and the solid state. Consequently other models should be used to describe reactions involving the transfer of H^+ and other fragments in nonaqueous media.

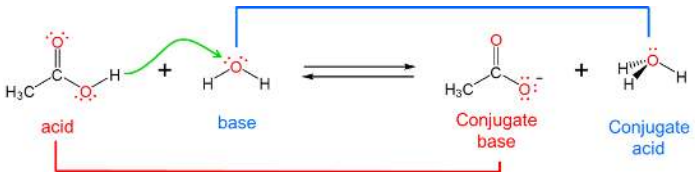
6.1: Arrhenius Model is shared under a CC BY-NC-SA 4.0 license and was authored, remixed, and/or curated by LibreTexts.

- **7.1A: Acid-Base Theories and Concepts** by Stephen M. Contakes is licensed CC BY-NC 4.0.
- **6.2: Arrhenius Concept** by Stephen M. Contakes is licensed CC BY 4.0.

6.2: Brønsted-Lowry Model

The Brønsted-Lowry Acid Base Concept

The Brønsted-Lowry acid base concept overcomes the Arrhenius system's inability to describe reactions that take place outside of aqueous solution by moving the focus away from the solution and onto the acid and base themselves. It does this by redefining acid-base reactivity as involving the transfer of a hydrogen ion, H^+, between an acid and a base. Specifically, a Brønsted acid is a substance that loses a H^+ ion by donating it to a base. This means that a Brønsted base is defined as a substance which accepts H^+ from an acid when it reacts.



Because the Brønsted-Lowry concept is concerned with H^+ ion transfer rather than the creation of a particular chemical species it is able to handle a diverse array of acid-base concepts. In fact, from the viewpoint of the Brønsted-Lowry concept, Arrhenius acids and bases are just a special case involving hydrogen ion donation and acceptance involving water. Arrhenius acids donate H^+ ion to water, which acts as a Brønsted base to give H_3O^+

$$\underset{\text{acid}}{HA(aq)} + \underset{\text{base}}{H_2O} \rightleftharpoons H_3O^+(aq) + A^-(aq) \tag{6.2.1}$$

Similarly, Arrhenius bases act as Brønsted bases in accepting a hydrogen ion from the Brønsted acid water:

$$\underset{\text{base}}{B(aq)} + \underset{\text{acid}}{H_2O(aq)} \rightleftharpoons BH^+(aq) + OH^-(aq) \tag{6.2.2}$$

In this way it can be seen that Arrhenius acids and bases are defined in terms of their causing hydrogen ions to be donated to and abstracted from water, respectively, while Brønsted acids and bases are defined in terms of their ability to donate and accept hydrogen ions to and from anything.

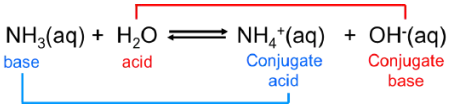
Because the Brønsted-Lowry concept can handle any sort of hydrogen ion transfer it readily accommodates many reactions that Arrhenius theory cannot, including those that take place outside of water, such as the reaction between gaseous hydrochloric acid and ammonia:

$$\underset{\text{base}}{NH_3(g)} + \underset{\text{acid}}{HCl(g)} \longrightarrow NH_4Cl(s) \tag{6.2.3}$$

The classification of acids as strong or weak usually refers to their ability to donate or abstract hydrogen ions to or from water to give H_3O^+ and OH^-, respectively, - *i.e.* their Arrhenius acidity and basicity. However, acids and bases may be classified as strong and weak under the Brønsted-Lowry definition based on whether they completely transfer or accept hydrogen ions; it is just that in this case it is important to specify the conditions under which a given acid or base acts strong or weak. For example, acetic acid acts as a weak base in water but is a strong base in triethylamine, since in the latter case it completely transfers a hydrogen ion to triethylamine to give triethylammonium acetate. Alternatively, the acidity or basicity of a compound may be specified using a thermodynamic scale like the Hammett acidity.

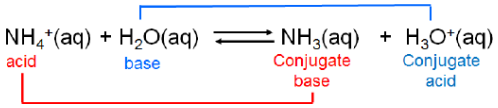
Conjugate Acids and Bases

By redefining acids and bases in terms of hydrogen ion donation and acceptance the Brønsted-Lowry system makes it easy to recognize that when an acid loses its hydrogen ion it becomes a substance that is capable of receiving it back again, namely a base. Consider, for example, the base dissociation of ammonia in water. When ammonia acts as a Brønsted base and receives a hydrogen ion from water ammonium ion and hydroxide are formed:



(6.2.4)

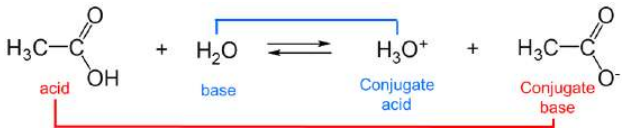
The ammonium ion is itself a weak acid that can undergo dissociation:



(6.2.5)

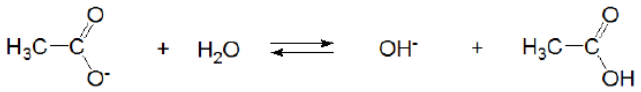
In this case ammonia and ammonium ion are acid-base conjugates. In general acids and bases that differ by a *single ionizable hydrogen ion* are said to be conjugates of one another.

The strengths of conjugates vary reciprocally with one another so that the stronger the acid the weaker the base and vice versa. For example, in water, acetic acid acts as a weak Brønsted acid:



(6.2.6)

and acetic acid's conjugate base, acetate, acts as a weak Brønsted base.



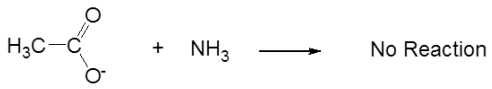
(6.2.7)

However, in liquid ammonia acetic acid acts as a strong Brønsted acid:



(6.2.8)

while its conjugate base, acetate, is neutral.



(6.2.9)

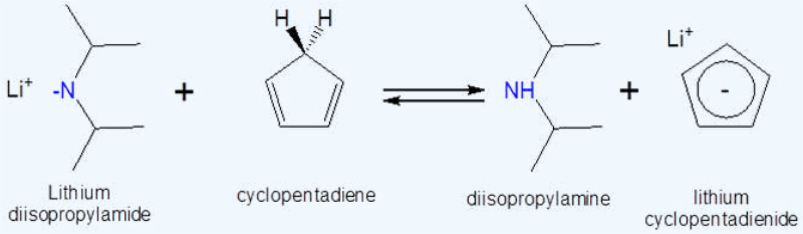
The reciprocal relationship between the strengths of acids and their conjugate bases has several consequences:

1. Under conditions when an acid or base acts as a weak acid or base its conjugate acts as weak as well. Conversely, when an acid or base acts as a strong acid or base its conjugate acts as a neutral species.

2. When a Brønsted acid and base react with one another the equilibrium favors formation of the weakest acid-base pair. That is why the acid-base reaction between acetic acid and ammonia in liquid ammonia proceeded to give the weak acid ammonium ion and neutral acetate. This consequence is particularly important for understanding the behavior of acids and bases in nonaqueous solvents, as illustrated by the following example.

Example 6.2.1

Can a solution of lithium diisopropylamide in heptane be used to form lithium cyclopentadienide? The pK_a of cyclopentadiene and diisopropylamine are ~15 and 40, respectively, and the proposed reaction is as follows:



Solution:

Since cyclopentadiene is a stronger acid than diisopropylamine (the stronger the acid the lower the pK_a) the equilibrium will favor protonation of the diisopropylamine by cyclopentadiene. Consequently addition of a heptane solution lithium diisopropylamide to monomeric cyclopentadiene should give lithium cyclopentadienide.

Molecular Structure and Brønsted Acidity and Basicity

Because the acidity of a given substance depends on the interplay between the relatively large values of its proton affinity and the energy associated with solvation of an acid's conjugate base it can be sometimes difficult to estimate the strength of an acid in a given solvent in the absence of detailed computations. Nevertheless a variety of simple ideas may be used to roughly estimate the relative strengths of acids. These should never be substituted for a detailed consideration of solvation but can serve as useful aids when thinking about trends and designing new Brønsted acids and bases.

Some simple factors that it can be helpful to consider when thinking about the strength of a given acid or base are:

Bond strength effects

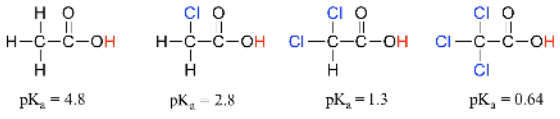
The weaker the bond to the ionizable hydrogen, the stronger the acid. Strongly bonded hydrogen ions are difficult to remove, weakly bonded ones much less so.

Inductive effects

Inductive effects involve the donation or withdrawal of electrons from an atom by a group connected to it through bonds. Electron donating groups increase the electron density while electron withdrawing groups decrease it. Atoms or groups that withdraw electron density away from a center increase its acidity while those which donate electrons to the center decrease its acidity. The reasons for this follow from the heterolytic bond cleavage of acid ionization:

$$E-H \rightarrow E:^- + H^+ \tag{6.2.10}$$

- When a bond to hydrogen is more polarized away from the H (more like $^{-\delta}E-H^{\delta+}$) it is easier to cleave off the hydrogen ion from that E-H bond. This may be seen from how the pK_a values of acetic acid and its mono-, di-, and tri-chlorinated derivatives decreases with the extent of chlorination of the methyl group.



- Polarized E-H bonds also make for stronger Brønsted acids because the resulting $E:^-$ conjugate base is more stable.

This leads to the third major factor that should be considered when thinking about acid strength.

Electronegativity effects

The more stable the acid's conjugate base, the stronger the Brønsted acid. All reactions are in theory reversible and so when considering the propensity of an acid to donate hydrogen ions it can be helpful to look at the reverse of hydrogen ion donation, namely protonation of the acid's conjugate base. If deprotonation of the acid gives a very stable conjugate base then deprotonation of the acid will be more favorable.

Two factors determine the stability of an acid's conjugate base.

- Conjugate bases in which a small amount of charge is on a large atom, spread over a large number atoms, and on electronegative atoms tend to be more stable. Conjugate bases in which a small amount of charge are spread over a large number of electronegative atoms are especially stable. That is why magic acid, a mixture of HF and SbF_5, is so acidic; the single negative charge on its conjugate base is spread over six F atoms and on Sb in SbF_6^-.
- Groups which tend to inductively polarize E-H bonds also tend to stabilize the conjugate base formed when that bond ionizes. In general, the more electronegative an atom, the better able it is to bear a negative charge. All other things being equal weaker bases have negative charges on more electronegative atoms; stronger bases have negative charges on less electronegative atoms. This is apparent from how inductive effects lead to an increase in the acidity of E-H bonds as the electronegativity of the element to which the acidic hydrogen is bound increases from left to right across a row of the periodic table. This horizontal periodic trend in acidity and basicity is apparent from the homologous series below in Figure 6.2.1.

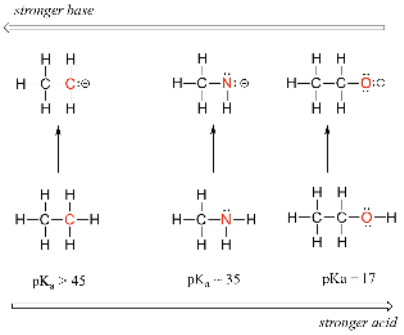


Figure 6.2.1: Horizontal periodic trend in acidity and basicity.

Notice how the inductive polarization of the E-H bond which results in greater acidity contributes to the greater stability of the conjugate base. For the case above look at where the negative charge ends up in each conjugate base. In the conjugate base of ethane, the negative charge is borne by a carbon atom, while on the conjugate base of methylamine and ethanol the negative charge is located on a nitrogen and an oxygen, respectively. Remember that electronegativity also increases as we move from left to right along a row of the periodic table, meaning that oxygen is the most electronegative of the three atoms, and carbon the least.

Thus, the methoxide anion is the most stable (lowest energy, least basic) of the three conjugate bases, and the ethyl carbanion anion is the least stable (highest energy, most basic). Conversely, ethanol is the strongest acid, and ethane the weakest acid.

Size effects

There are two classes of size effects to be considered:

a. The larger the atom to which a H is bound in an E-H bond, the weaker the bond and the stronger the acid.
b. Increased charge delocalization with increasing size. Electrostatic charges, whether positive or negative, are more stable when they are ‘spread out’ over a larger area. The greater the volume over which charge is spread in the acid's conjugate base, the more stable that base and the stronger the acid.

The impact of size effects are readily seen in the increase in acidity of the hydrogen halides, as illustrated by the vertical periodic trend in acidity and basicity below in Figure 6.2.2.

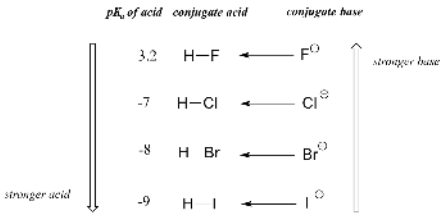
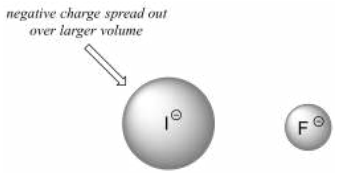


Figure **6.2.2**: Vertical periodic trend in acidity and basicity.

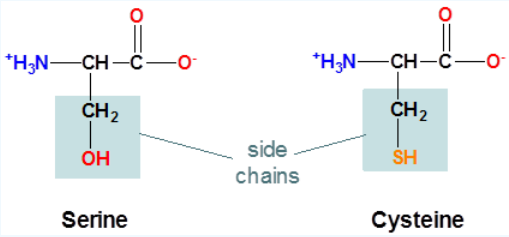
On going vertically down the halogen group from F to I the H-X bond strength decreases in the acid, making it easier to ionize, while the charge becomes more diffuse in the resultant X^- ion, making the conjugate base more stable.



The increase in the acidity of the hydrogen halides down a group suggests that size effects are more important than inductive effects. In the case of the hydrogen halides because fluorine is the most electronegative halogen element, we might expect fluoride to also be the least basic halogen ion. But in fact, it is the *least* stable, and the most basic! It turns out that when moving vertically in the periodic table, the *size* of the atom trumps its electronegativity with regard to basicity. The atomic radius of iodine is approximately twice that of fluorine, so in an iodide ion, the negative charge is spread out over a significantly larger volume.

Exercise 6.2.1

The structure of the amino acids serine and cysteine are shown below. Which do expect will have the more acidic side chain?



Answer

Cysteine, since the cysteine side chain possesses an ionizable S-H bond while serine's side chain possesses an ionizable O-H bond. Since S is larger than O cysteine's S-H bond will be weaker than serine's O-H bond the and cysteine side chain's thiolate conjugate base more stable than the serine side chian's alkoxide conjugate base. In fact, the side chain pK_a of cysteine is 8.3 while serine is considered to be nonionizable under physiological conditions.

Binary Hydrides

The compounds formed between the elements and hydrogen are called binary hydrides. All such compounds can in principle act as Brønsted acids in reactions with a suitably strong base. However, as the electronegativity decreases down a group and increases from left to right across the periodic table the acidity of binary hydrides increases. In fact, on the left side of the periodic table the hydrides of extremely electropositive alkali and alkaline earth metals are not acidic but basic. They are perhaps best considered to be ionic salts of the hydride ion (H^-). Consequently substances such as NaH and CaH_2 tend to act as Brønsted bases in their reactions.

$$NaH\,(s) + H_2O\,(l) \longrightarrow Na^+\,(aq) + OH^-\,(aq) + H_2\,(g) \tag{6.2.11}$$

$$CaH_2\,(s) + 2\,H_2O\,(l) \longrightarrow Ca^{2+}\,(aq) + 2\,OH^-\,(aq) + 2\,H_2\,(g) \tag{6.2.12}$$

https://chem.libretexts.org/@go/page/326202

On the right side of the periodic table the binary hydrides of the nonmetals exhibit appreciable acidity.

$$\mathrm{HBr\,(aq) + H_2O\,(l) \longrightarrow H^+\,(aq) + Br^-\,(aq)} \tag{6.2.13}$$

For this reason the binary nonmetal hydrides are termed acidic hydrides. Nevertheless not all are equally acidic. The dilute aqueous acid ionization constants for these hydrides are given in Figure **6.2.3**. As can be seen from the constants in Figure **6.2.2** the ability of the hydrides to transfer a hydrogen to water increases across a period and down a group.

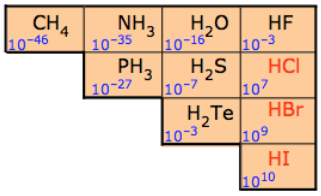


Figure **6.2.3**: The acid ionization constants of nonmetal hydrides increase across a period and down a group.

These trends are largely due to changes in the electronegativity and size of the nonmetal atom:

1. Going across a period the acid strength increases as there is an increase in electronegativity and the molecule gets more polar, with the hydrogen getting a larger partial positive charge. This makes it easier to heterolytically cleave the E-H bond to produce a stable anion.

$$\mathrm{E - H \rightarrow E:^- + H^+} \tag{6.2.14}$$

2. Going down a group the acid strength increases because the bond strength decreases as a function of increasing size of the nonmetal, and this has a larger effect than the electronegativity. In fact HF is a weak acid because it is so small that the hydrogen-fluorine bond is so strong that it is hard to break. Remember, the weaker the bond, the strong the acid strength. This is further illustrated in Table **6.2.1** where the weakest bond has produces the strongest acid.

Table **6.2.1** Acid strength as function of bond energy

Relative Acid Strength	HF	<<	HCl	<	HBr	<	HI
H–X Bond Energy (kJ/mol)	570		432		366		298
K_a	10^{-3}		10^{7}		10^{9}		10^{10}

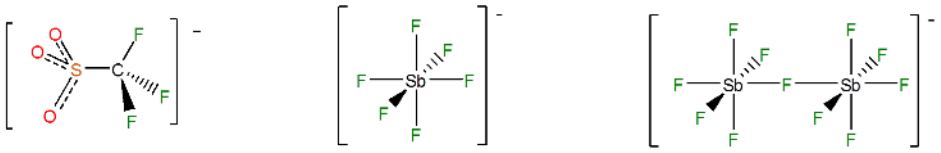
Superacids

Superacids are acids that are more acidic than pure sulfuric acid. They are able to dissociate completely because when they do so they give an extremely stable anion in which the residual negative charge is distributed among multiple electronegative atoms. For example, in mixtures of HF and antimony pentaflouride the dissociation of a hydrogen ion from the HF is promoted by the formation of a Lewis acid-base adduct between the HF fluoride and SbF_5.



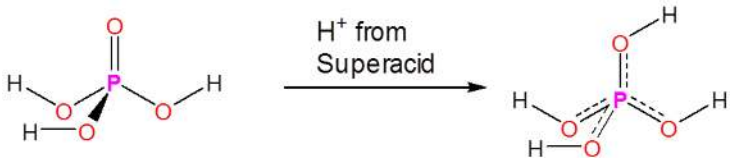
(6.2.15)

This gives extremely stable anions like SbF_6^- and $Sb_2F_{11}^-$, in which a single negative charge is delocalized among many electronegative groups and atoms; of these CF_3 and F are particularly common.

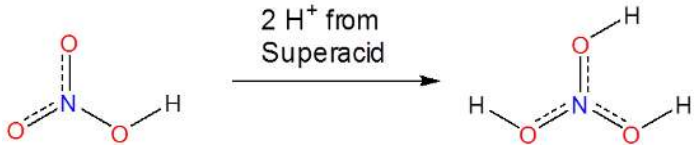


(6.2.16)

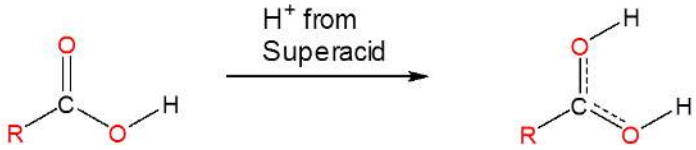
Superacids are able to protonate species that would otherwise act as neutral or even acidic species in water or aprotic media. Phosphoric, nitric, carboxylic, and other ordinary acids are all protonated when dissolved in superacids:



(6.2.17)



(6.2.18)



(6.2.19)

However, superacids also protonate many species that are not usually considered ot have acid base properties. Even alkanes can be protonated and, in fact, superacids are used to generate carbocations in a variety of synthetic applications. They do this by protonating alkanes to give unstable species which then decompose to carbocations in further reactions. For example, Mixtures of SbF_5 and FSO_3H called Magic Acid can even protonate methane, which subsequently decomposes to give a CH_5 cation:

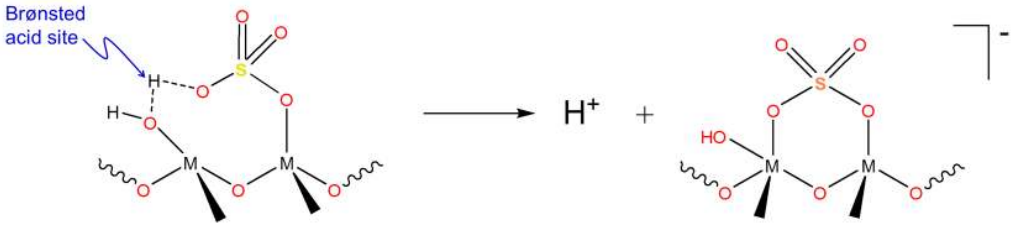
$$F_5Sb + FSO_3H + CH_4 \rightarrow F_5Sb - OSO_2F^- + CH_5^+ \tag{6.2.20}$$

which subsequently decomposes to give an ordinary carbocation

$$CH_5^+ \rightarrow CH_3^+ + H_2 \tag{6.2.21}$$

Solid superacids

Since liquid superacids are extremely corrosive and can be costly to separate from reaction mixtures solid superacids are used industrially instead. The main use these solid superacids to generate carbocations for use in hydrocarbon isomerization and alkylation chemistry. Many solids superacids consist of sulfuric acid/sulfates attached to a metal oxide surface to give structures similar to that shown below:

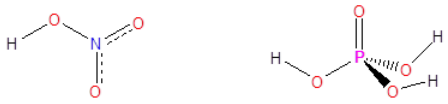


(6.2.22)

These structures exhibit Hammett acidity parameters in the superacid range. However, the mechanism by which these solid superacids generate carbocations isn't entirely clear since they contain both Brønsted acid sites (at OH) and Lewis acid sites (at M) that could be involved in the carbocation generation process.

Oxyacids

Oxyacids (also known as oxoacids) are compounds of the general formula $\mathbf{H_nEO_m}$, where **E** is a nonmetal or early transition metal and the acidic hydrogens are attached directly to oxygen (not **E**). This class of compounds includes such well-known acids as nitric acid, HNO_3, and phosphoric acid, H_3PO_4.



The acidity of oxyacids follows three trends:

Electronegativity of the central atom

In a homologous series the acidity increases with the electronegativity of the central atom. Elements in the same group frequently form oxyacids of the same general formula. For example, chlorine, bromine, and iodine all form oxyacids of formula HOE: hypochlorous, hypobromous and hypoiodous acids. In the case of these homologous oxyacids the acidity is largely determined by the electronegativity of the central element. Central atoms which are better able to inductively pull electron density towards themselves make the oxygen-hydrogen bond that is to be ionized more polar and stabilize the conjugate base, OE^-. Thus the acid strength in such homologous series increases with the electronegativity of the central atom. This may be seen from the data for the hypohalous acids in Table **6.2.2**, in which the acid strength increases with the electronegativity of the halogen so that the order of acidity is:

$$HClO > HBrO > HIO$$

Table **6.2.2**: Relationship of central atoms electronegativity to acid ionization constant in the hypohalous acids.

HOE	Electronegativity of E	K_a
HOCl	3.0	4.0×10^{-8}
HOBr	2.8	2.8×10^{-9}
HOI	2.5	3.2×10^{-11}

Note this the influence of central atom electronegativity on the strength of oxyacids is exactly the opposite to that observed for the binary hydrides in Table ***PageIndex5***, for which acidity increased down a group giving the order of acidity:

$$\mathbf{HI > HBr > HCl \gg HF} \tag{6.2.23}$$

The reason for this is that in the hydrogen halides the bond to be broken (H-E bond) decreased in strength down the group while in oxyacids the bond to be broken is always an O-H bond and so varies much less in strength with the electronegativity of central atom.

Central element's oxidation state

For oxoacids of a given central atom the acidity increases with the central element's oxidation state or, in other words, the number of oxygens bound to the central atom. Here we are looking at the trend for acids in which there are variable numbers of oxygen bound to a given central atom. An examples is the perchloric ($HClO_4$), chloric ($HClO_3$), chlorous ($HClO_2$), and hypochlorous (HClO) acid series. In such series the greater the number of oxygens the stronger the acid. This can be explained in several ways. From the viewpoint of the acid itself the key factor is again the inductive effect, in this case involving the ability of the oxygens attached to the central atom to pull on electron density across the OH bond. This is seen from the charge density diagram for the

chlorine oxoacids shown in Figure **6.2.4**, in which the partial positive charge on the acidic hydrogen increases with the number of oxygens present.

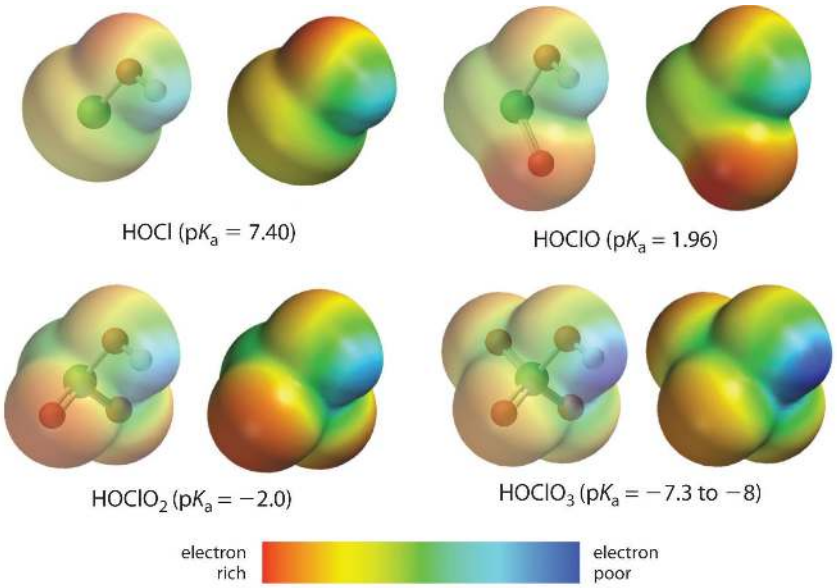


Figure **6.2.4**: Increasing number of oxygens increases K_a as evidenced by the decreased electron density on the acidic hydrogen (which is most blue in $HClO_4$). Note, $K_a = 10^{-pK_a}$, and so the larger pK_a, the smaller K_a. (CC BY-SA-NC; anonymous)

The increase in oxoacid acidity with the number of oxygens bound to the central atom may also be seen by considering the stability of the conjugate oxyanion. That the stability of the conjugate base increases with the number of oxygens may be seen from the charge distribution diagrams and Lewis bonding models for the chlorine oxyanions shown in figure **6.2.5**. As the negative charge is spread over more oxygen atoms it becomes increasingly diffuse.

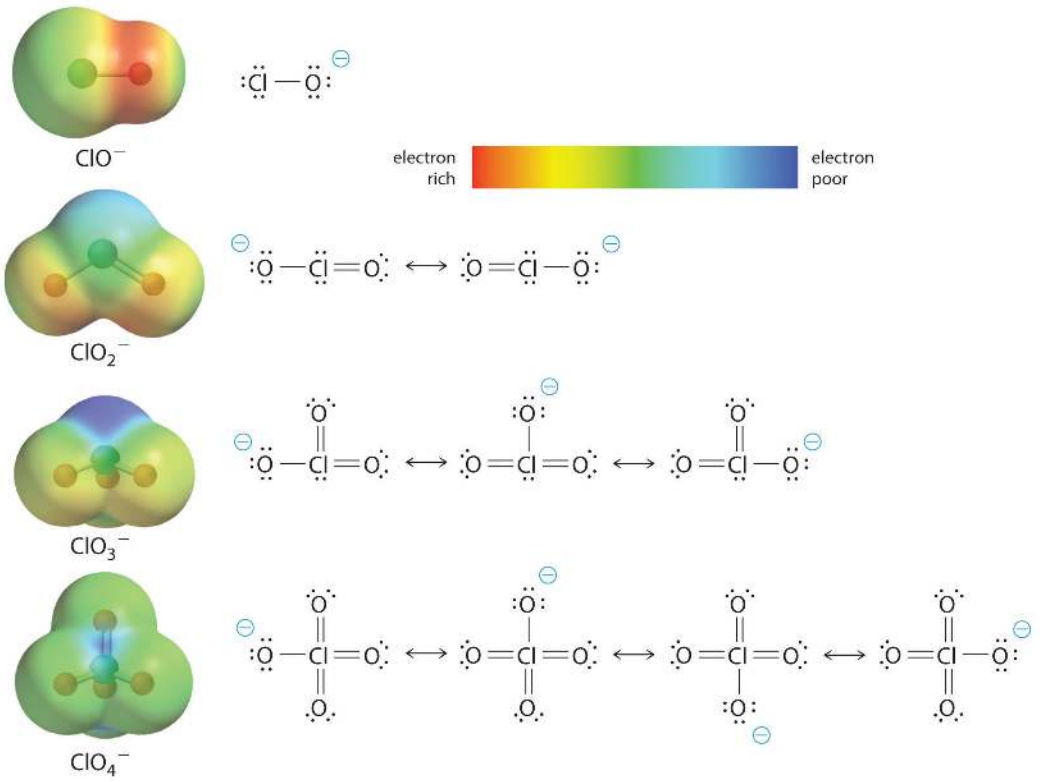


Figure **6.2.5**: Increased diffusion of charge in chlorine oxyanions with increasing number of oxygens. The larger the ion the more dispersed the charge and thus the less the charge density, making the perchlorate the most stable anion in the series. Even the simplistic treatment of bonding depicted in the resonance structures correctly show an increased dispersion of the charge density. (CC BY-SA-NC 3.0; anonymous)

Exercise 6.2.1

Sulfur and selenium both forms oxoacids of formula $\mathbf{H_2EO_4}$ where E is either S or Se. These are called sulfurous and selenous acid, respectively. Which oxoacid would you expect to be more acidic: selenous acid or sulfurous acid?

Answer

Sulfurous acid should be more acidic. Since sulfur is more electronegative than selenium sulfur will polarize OH bonds to a greater extent, making them more acidic. This prediction is borne out by a comparison of the pK_a values for the acids:

Acid	pK_{a1}	pK_{a2}
sulfurous acid, H_2SO_3	1.85	7.2
selenous acid, H_2SeO_3	2.62	8.32

Successive proton removal

For polyprotic oxoacids the acidity decreases as each successive proton is removed. Oxoacids with multiple O-H bonds are called **polyprotic** since they can donate more than one hydrogen ion. In this case hydrogen ions are removed in successive ionization reactions. Examples include phosphoric and carbonic acid:

$$H_3PO_4 \rightleftharpoons H^+ + H_2PO_4^- \qquad pK_{a1} = 2.2 \tag{6.2.24}$$

$$H_2PO_4^- \rightleftharpoons H^+ + HPO_4^{2-} \qquad pK_{a2} = 7.2 \tag{6.2.25}$$

$$HPO_4 \rightleftharpoons H^+ + PO_4^{3-} \qquad pK_{a3} = 12.4 \tag{6.2.26}$$

$$H_2CO_3 \rightleftharpoons H^+ + HCO_3^- \qquad pK_{a1} = 3.6 \tag{6.2.27}$$

$$HCO_3^- \rightleftharpoons H^+ + CO_3^{2-} \qquad pK_{a1} = 10.3 \tag{6.2.28}$$

The dissociation constants for successive ionization constants decrease by about five orders of magnitude between successive hydrogen ions. This is reflected in Linus Pauling's rule for oxoacids and their oxyanions.

Pauling's Rules

1. The pK_a or an oxyacid of general formula $\mathbf{E(OH)}_q\mathbf{(O)}_p$ is given by

$$pK_a = 8 - 5 \times p \tag{6.2.29}$$

2. As an oxoaxid undergoes successive ionizations the pK_a increases by five each time.

The central theme of Pauling's Rules is that the more oxygen there are on the central atom, the more resonance structure that can be constructed of the conjugate base, which increases it stability and increases the acidity of the acid. However, as the acids successively ionize, they have fewer resonance structure. Pauling's Rules are phenomenological (i.e., not based on a theoretical basis). As with many empirical rules, they often work quite well, but they are approximations which may not work in all situations.

Exercise 6.2.2: How well do Pauling's rules for oxoacids work?

Calculate the theoretical pK_a values for phosphoric and carbonic acid and their dissociation produces and compare the results with the experimental pK_a values.

Answer

For phosphoric acid, Pauling's rules (Equation 6.2.29) predict the pK_a values quite well:

- H_3PO_4: $p = 3$ and $q = 1$ and

$$pK_{a1,predicted} = 8 - 5 \times 1 = 3$$

  This slightly greater than the observed value of 2.2.
- $H_2PO_4^-$:

$$pK_{a2,predicted} = pK_{a1,experimental} + 5 = 7.2$$

  This Spot on with experiment.
- HPO_4^{2-}:

$$pK_{a3,predicted} = pK_{a2,experimental} + 5 = 12.2$$

  . This is slightly less than the experimental value of 12.4.

For carbonic acid Pauling's rules predict pK_{a1} reasonably well, but pK_{a2} less so:

- H_2CO_3: $p = 2$, $q = 1$ and

$$pK_{a1,predicted} = 8 - 5 \times 1 = 3$$

  This is slightly lower than the observed value of 3.6.
- HCO_3^-:

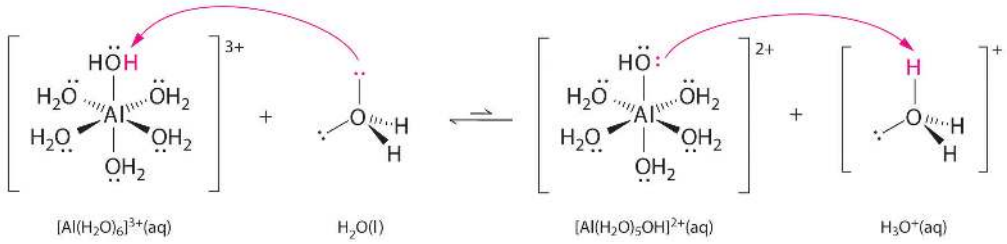
$$pK_{a2,predicted} = pK_{a1,experimental} + 5 = 8.6$$

  This is 1.7 units less than the experimental value of 10.3.

In some cases discrepancies between experimental pK_a values and those predicted by Pauling's rules suggest that structural rearrangements may be taking place upon ionization or else that the reported pK_a values do not really represent the ionization in question because they do not fully account for all the equilibria taking place in solution. In the case of carbonic acid, however, the reason for the discrepancy between the predicted and experimental pK_{a2} values is not entirely clear.

Metal Ions as Acids

Aqueous solutions of simple salts of metal ions can also be acidic, even though a metal ion cannot donate a proton directly to water to produce H_3O^+. Instead, a metal ion can act as a Lewis acid and interact with water, a Lewis base, by coordinating to a lone pair of electrons on the oxygen atom to form a hydrated metal ion.



A water molecule coordinated to a metal ion is more acidic than a free water molecule for two reasons. First, repulsive electrostatic interactions between the positively charged metal ion and the partially positively charged hydrogen atoms of the coordinated water molecule make it easier for the coordinated water to lose a proton.

Second, the positive charge on the Al^{3+} ion attracts electron density from the oxygen atoms of the water molecules, which decreases the electron density in the O–H bonds, as shown in Figure 6.2.6*b*. With less electron density between the O atoms and the H atoms, the O–H bonds are weaker than in a free H_2O molecule, making it easier to lose a H^+ ion. This is shown schematically in Figure 6.2.1.

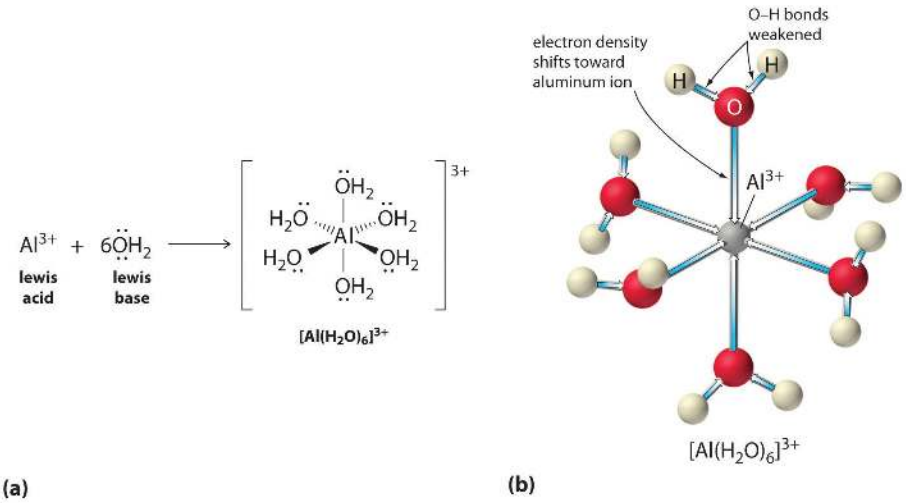


Figure 6.2.6: Effect of a Metal Ion on the Acidity of Water (a) Reaction of the metal ion Al^{3+} with water to form the hydrated metal ion is an example of a Lewis acid–base reaction. (b) The positive charge on the aluminum ion attracts electron density from the oxygen atoms, which shifts electron density away from the O–H bonds. The decrease in electron density weakens the O–H bonds in the water molecules and makes it easier for them to lose a proton. (CC BY-NC-SA 3.0; anonymous)

Trends in Acidity

The acidity of a given metal ion largely depends on its charge to size ratio and electronegativity, although in some cases hardness and ligand field effects also play a role. The magnitude of this effect depends on the following factors, of which the first two are generally considered the most important.

The charge on the metal ion

A divalent ion (M^{2+}) has approximately twice as strong an effect on the electron density in a coordinated water molecule as a monovalent ion (M^+) of the same radius.

The radius of the metal ion

For metal ions with the same charge, the smaller the ion, the shorter the internuclear distance to the oxygen atom of the water molecule and the greater the effect of the metal on the electron density distribution in the water molecule.

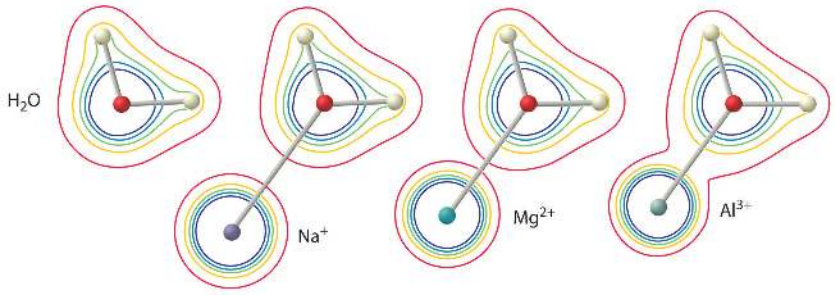


Figure **6.2.7**: The Effect of the Charge and Radius of a Metal Ion on the Acidity of a Coordinated Water Molecule. The contours show the electron density on the O atoms and the H atoms in both a free water molecule (left) and water molecules coordinated to Na^+, Mg^{2+}, and Al^{3+} ions. These contour maps demonstrate that the smallest, most highly charged metal ion (Al^{3+}) causes the greatest decrease in electron density of the O–H bonds of the water molecule. Due to this effect, the acidity of hydrated metal ions increases as the charge on the metal ion increases and its radius decreases. (CC BY-NC-SA 3.0; anonymous)

The first two of these factors explain why most alkali metal cations exhibit little acidity while aqueous solutions of small, highly charged metal ions, such as Al^{3+} and Fe^{3+}, are acidic:

$$[Al(H_2O)_6]^{3+}_{(aq)} \rightleftharpoons [Al(H_2O)_5(OH)]^{2+}_{(aq)} + H^+_{(aq)} \tag{6.2.30}$$

The $[Al(H_2O)_6]^{3+}$ ion has a pK_a of 5.0, making it almost as strong an acid as acetic acid. Because of the two factors described previously, the most important parameters for predicting the effect of a metal ion on the acidity of coordinated water molecules are the charge and ionic radius of the metal ion. Although the charge to size ratio is the simplest and most powerful predictor of metal ion acidity in water, three additional factors also can play a role:

Electronegativity

All other things being equal more electronegative elements are better able to withdraw electron density from a bound water ligand and consequently better at enhancing the ability of that water molecule to lose a hydrogen ion.

Hardness and Softness

Cation hardness or softness according to Pearson's Hard-Soft Acid Base Principle (HSAB). In general soft cations are more acidic than hard cations of the same charge and radius, as may be seen from the examples in Table **6.2.1**. The greater than expected acidity of softer cations is thought to reflect the importance of covalent contributions to the metal-water bond.

Table **6.2.1**: Comparison of the pK_a values at 25°C of hard and soft cations with approximately the same radius and charge. Based on Gutmann as reported by Burgess.

Cation	Classification	Radius (pm)	pK_a1
K^+	hard	1.33	14
Ag^+	soft	1.26	10
Mg^{2+}	hard	0.65	12.2
Cu^{2+}	soft	0.69	7.3
Ca^{2+}	hard	0.99	12.6
Cd^{2+}	soft	0.97	9.0
Sr^{2+}	hard	1.13	13.1
Hg^{2+}	soft	1.10	3.6

Ligand field effects

Ligand field effects involve bonding and antibonding interactions between the *d* orbitals on a transition metal and ligand orbitals. The importance of ligand field interactions on cation acidity is not well established but ligand field interactions might influence the acidity of a hydrated metal in two cases: (a) when the ligand field stabilization of the aqua complex (metal with H_2O or OH^-

bound) is greater or less than those in its conjugate base and (b) in complexes which undergo Jahn-Teller distortions that alter the metal's ability to polarize the OH bond.

Solvent Autoionization

The Brønsted-Lowry concept allows for an understanding of hydrogen ion transfer chemistry in amphoteric protic solvents. Amphoteric protic solvents are those which can both accept and receive hydrogen ions. From the viewpoint of the Brønsted-Lowry concept the acid-base chemistry in these solvents is governed by autoionization equilibria analogous to water autoionization.

$$2H_2O(l) \rightleftharpoons H_3O^+ + OH^- \qquad K_w = 1.0 \times 10^{-14} \tag{6.2.31}$$

For example, sulfuric acid ionizes according to the equation:

$$2H_2SO_4(l) \rightleftharpoons H_3SO_4^+ + HSO_4^- \qquad K = 4 \times 10^{-4} \tag{6.2.32}$$

The magnitude of the solvent autoionization constant in a given amphoteric solvent determines the amount of protonated and deprotonated* solvent present. Since sulfuric acid's autoionization constant is much larger than that of water $K_w = 10^{-14}$ the concentration of $H_3SO_4^+$ and HSO_4^- present in pure sulfuric acid is ~0.02 *M*, much greater than the 10^{-7} *M* H^+ amd OH^- present in pure water.

In contrast, ammonia's autoionization constant is much less than that of water and only ~10^{-14} \{*M* NH_4^+\} and \{NH_2^-\} are present in pure ammonia.

$$2NH_3(l) \rightleftharpoons NH_4^+ + NH_2^- \qquad K = 10^{-27} \tag{6.2.33}$$

Solvent Leveling Effect

The solvent leveling effect limits the strongest acid or base that can exist in acidic, basic, and amphoteric solvents. The conjugate acid and base of the solvent are the strongest Brønsted acid and bases that can exist in that solvent. To see why this is the case for acids consider the reaction between a Brønsted acid (HA) and solvent (*S*):

$$HA + S \rightleftharpoons HS^+ + A^- \tag{6.2.34}$$

This equilibrium will favor dissociation of whichever is a stronger acid - HA or HS^+. If the acid is stronger it will mostly dissociate to give HS^+, while if the solvent's conjugate acid is stronger the acid will be mostly un-ionized and remain as HA.

Any acid significantly stronger than HS^+ will act as a strong acid and effectively dissociate completely to give the solvent's conjugate acid HS^+. This also means that the relative acidity of acids stronger than HS^+ cannot be distinguished in solvent S. This is called the leveling effect since the solvent "levels" the behavior of acids much stronger acids than it to that of complete dissociation. For example, there is no way to distinguish the acidity of strong acids like $HClO_4$ and HCl in water since they both completely dissociate. However, it is possible to distinguish their relative acidities in solvents that are more weakly basic than the conjugate base of the strongest acid since then the acids will dissociate to different extents. Such solvents are called differentiating solvents. For example, acetonitrile (MeCN) acts as a differentiating solvent for $HClO_4$ and HCl. Both $HClO_4$ and HCl partially dissociate in MeCN, with the stronger acid $HClO_4$ dissociating to a greater extent than HCl.

The leveling effect can also occur in basic solutions. The strongest Brønsted base, B, that can exist in a solvent is determined by the relative acidity of the solvent and the base's conjugate acid, BH^+, determines whether the base will remain unprotonated and able to act as a base in that solvent. If the solvent is represented this time as HS then the relevant equilibrium is:

$$B + HS \rightleftharpoons BH^+ + S^- \tag{6.2.35}$$

The position of this equilibrium depends on whether B or S^- is the stronger base. If the solvent's conjugate base, S^- , is stronger then the base will remain unprotonated and available to act as a base. However, if B is a stronger base than S^- it will deprotonate the solvent to give BH^+ and S^-. In this way the strongest base that can exist in a given solvent is the solvent's conjugate base. The relative strength of Brønsted bases can only be determined in solvents that are more weakly acidic than BH^+; otherwise the bases will all be leveled to S^-.

It is important to consider the levelling effect of protic solvents when performing syntheses that require the use of basic reagents. For instance, hydride and carbanion reagents (Lithium aluminum hydride, Grignard reagents, alklyllithium reagents, etc.) cannot be

used as nucleophiles in protic solvents like water, alcohols, or enolizable aldehydes and ketones. Since carbanions are stronger bases than these solvent's conjugate bases they will instead act as Brønsted bases and deprotonate the solvent. For example if one adds n-butyllithium to water the result (along with much heat and possibly a fire) butane and a solution of lithium hydroxide will be obtained:

$$\underset{:}{CH_2CH_2CH_2CH_3} + H_2O(l) \rightarrow \overset{Li^+}{Li^+(aq)} + \overset{-}{OH^-}(aq) + CH_3CH_2CH_2CH_3(g) \tag{6.2.36}$$

Since hydride and carbanion reagents cannot be used as nucleophiles in protic solvents like water or methanol they are commonly sold as solutions in solvents such as hexanes (for alklyllithium reagents) or tetrahydrofuran (for Grignard reagents and $LiAlH_4$).

References

1. Wulfsberg, G. *Principles of Descriptive Inorganic Chemistry* University Science Books, 1991, pp. 28-30.
2. (a) Gutmann, V. *Allg. Prakt. Chem.* 1970, *21*, 116. (b) Gutmann, V. *Fortschr. Chem. Forsch.* 1972, *27*, 59.
3. Burgess, J. *Metal Ions in Solution* Ellis Horwood, 1978, pg. 268.

Contributors and Attributions

Stephen M. Contakes (Westmont College),

who expanded this section from a combination of

https://chem.libretexts.org/Courses/University_of_Arkansas_Little_Rock/Chem_1403%3A_General_Chemistry_2/Text/16%3A_Acids_and_Bases/16.6%3A_Molecular_Structure%2C_Bonding%2C_and_Acid-Base_Behavior

https://chem.libretexts.org/Bookshelves/Organic_Chemistry/Book%3A_Organic_Chemistry_with_a_Biological_Emphasis_(Soderberg)/Chapter_07%3A_Organic_compounds_as_acids_and_bases/7.3%3A_Structural_effects_on_acidity_and_basicity

https://chem.libretexts.org/Courses/University_of_Arkansas_Little_Rock/Chem_1403%3A_General_Chemistry_2/Text/16%3A_Acids_and_Bases/16.6%3A_Molecular_Structure%2C_Bonding%2C_and_Acid-Base_Behavior

https://chem.libretexts.org/Bookshelves/Organic_Chemistry/Book%3A_Organic_Chemistry_with_a_Biological_Emphasis_(Soderberg)/Chapter_07%3A_Organic_compounds_as_acids_and_bases/7.3%3A_Structural_effects_on_acidity_and_basicity

https://chem.libretexts.org/Courses/University_of_Arkansas_Little_Rock/Chem_1403%3A_General_Chemistry_2/Text/16%3A_Acids_and_Bases/16.6%3A_Molecular_Structure%2C_Bonding%2C_and_Acid-Base_Behavior

https://chem.libretexts.org/Bookshelves/General_Chemistry/Map%3A_General_Chemistry_(Petrucci_et_al.)/16%3A_Acids_and_Bases/16.7%3A_Ions_as_Acids_and_Bases

---

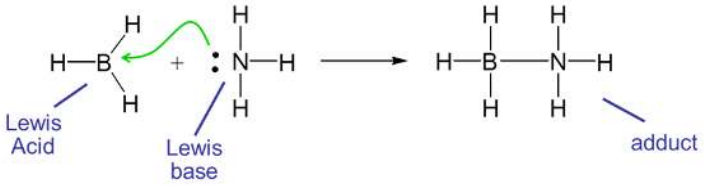
6.2: Brønsted-Lowry Model is shared under a CC BY-NC-SA 4.0 license and was authored, remixed, and/or curated by LibreTexts.

- **6.3.1: Brønsted-Lowry Concept** by Stephen M. Contakes is licensed CC BY 4.0.
- **Current page** is licensed CC BY-NC-SA 4.0.
- **6.3.2: Rules of Thumb for thinking about the relationship between Molecular Structure and Brønsted Acidity and Basicity*** by Stephen Contakes is licensed CC BY 4.0.
- **6.3.3: The acid-base behavior of binary element hydrides is determined primarily by the element's electronegativity and secondarily by the element-hydrogen bond strength** by Stephen M. Contakes is licensed CC BY 4.0.
- **6.3.4: Brønsted-Lowry Superacids and the Hammett Acidity Function** by Stephen M. Contakes is licensed CC BY 4.0.
- **6.3.7: The Acidity of an Oxoacid is Determined by the Electronegativity and Oxidation State of the Oxoacid's Central Atom*** by Stephen Contakes is licensed CC BY 3.0.
- **6.3.8: High Charge-to-Size Ratio Metal Ions Act as Brønsted Acids in Water** by Stephen M. Contakes is licensed CC BY 4.0.
- **6.3.10: Acid-Base Chemistry in Amphoteric Solvents and the Solvent Leveling Effect** by Stephen M. Contakes is licensed CC BY 4.0.
- **6.3.11: Non-nucleophilic Brønsted-Lowry Superbases** by Stephen M. Contakes is licensed CC BY 4.0.

6.3: Lewis Concept and Frontier Orbitals

Lewis Acids and Bases

The Lewis acid base concept generalizes the Brønsted and solvent system acid base concepts by describing acid-base reactions in terms of the donation and acceptance of an electron pair. Under the Lewis definition Lewis acids are electron pair acceptors and Lewis bases are electron pair donors. In Lewis acid-base reactions a Lewis base donates an electron pair to the Lewis acid, which accepts it. The reaction between borane, BH_3, and NH_3 is the classic example:



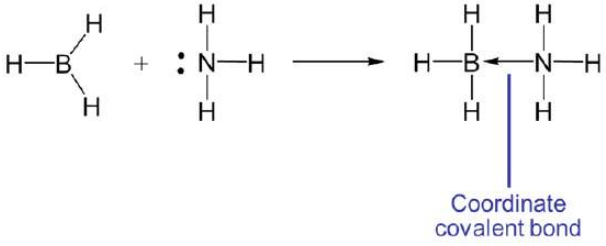
Definition: Lewis acid

A species that is an electron pair acceptor

Definition: Lewis base

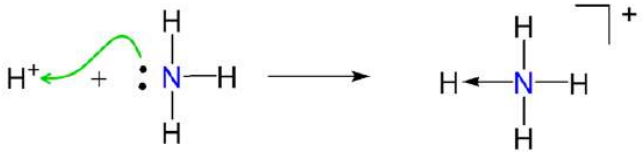
A species that is an electron pair donor

In this case the Lewis acid-base reaction results in the formation of a bond between BH_3, and NH_3 . When the acid and base combine to form a larger unit that unit is said to be an adduct and the resulting bond is said to be a coordinate covalent or dative bond. Such coordinate covalent bonds are sometimes represented by an arrow that indicates the direction of electron donation from the base to the acid. For instance the reaction between BH_3, and NH_3 could also have been written as



The arrow notation for the coordinate covalent bond is really just a convenient formalism - a bookkeeping tool to help keep track of where the electrons came from and where they might return if the reverse reaction occurs.

For example, in Brønsted acid base reactions the hydrogen ion is an acid because it accepts an electron pair from the Brønsted base. Consequently under the Lewis acid-base concept in Brønsted acid base reactions involve the formation of an adduct between H^+ and a base.

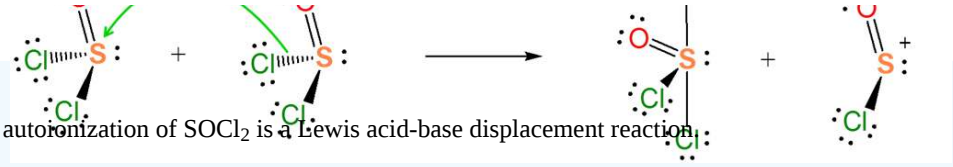


(6.3.1)

The Lewis acid base concept nicely explains ionization reactions involving nonaqueous solvents. For instance, the autoionization of $SOCl_2$ as an acid-base reaction between two $SOCl_2$ molecules.



https://chem.libretexts.org/@go/page/326213



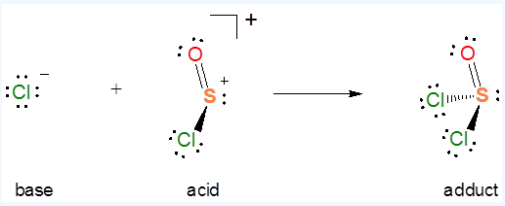
(6.3.2)

Example 6.3.1

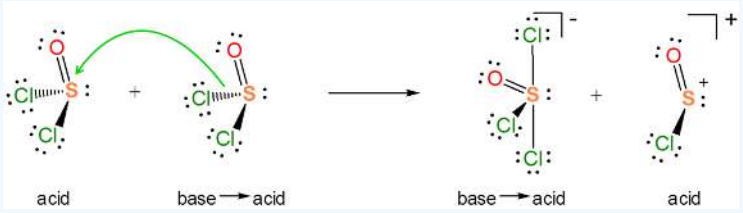
Explain how the autoionization of $SOCl_2$ is a Lewis acid-base displacement reaction.

Solution

In the autoionization of $SOCl_2$ the pair of electrons donated comes from the S-Cl bond and the S-Cl bond is broken to give a lone pair bearing Cl^- base and a $SOCl^+$ Lewis acid fragment. If you are having trouble seeing how this works it can be instructive to consider the reverse of this process. It is a Lewis acid-base reaction to give a Lewis acid-base adduct:



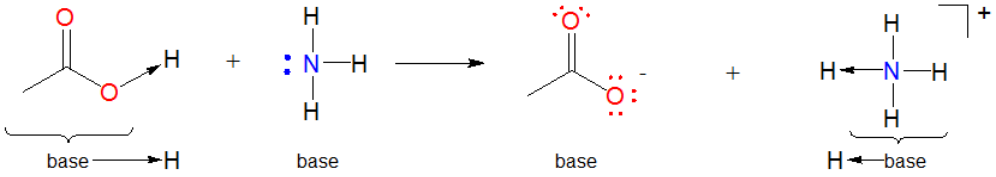
From the autoionization reaction it is also apparent that $SOCl_2$ itself acts as a Lewis acid towards the liberated Cl^-. So the autoionization reaction involves a transfer of the base Cl^- base between the two Lewis acids - a Lewis acid-base displacement reaction.



Lewis acid-base model and chemical reactions

It can be helpful to keep several distinctions in mind when using the Lewis acid-base concept to describe chemical reactions.

1. Many Lewis-Acid base reactions are displacement reactions. This is because the hydrogen ion is usually bound to something at the start of the reaction. In such cases the Lewis acid H^+ unit is transferred from one Lewis base and another. Such acid-base reactions are sometimes called displacement reactions since the base group in the initial Lewis acid-base complex is displaced by the incoming Lewis base to generate another complex.



(6.3.3)

2. Substances are sometimes considered amphoteric because they exhibit Lewis acidity and basicity at different types of atomic centers. The classic example is aluminum hydroxide, $Al(OH)_3$. In water $Al(OH)_3$ can act as a Lewis acid towards OH^- ion. The reaction occurs by formation of an adduct at $Al(OH)_3$'s Al^{3+} center:

$$Al(OH)_3 + OH^- \rightarrow Al(OH)_4^- \tag{6.3.4}$$

Notice that in addition to acting as a Lewis acid, in this reaction $Al(OH)_3$

- does not act as a Brønsted acid or base since no H^+ ion transfer occurs
- but does act as an Arhennius acid since OH^- ion is consumed from solution, decreasing $[OH^-]$ and increasing $[H^+]$

In water $Al(OH)_3$ also acts as a Lewis base towards H^+ through the lone pairs on its hydroxide ligands.

$$Al(OH)_3 + 3H^+ + 3H_2O \rightarrow Al(H_2O)_6^{3+} \quad (6.3.5)$$

Notice that in addition to acting as a Lewis base, in this reaction $Al(OH)_3$ also acts as a

- Brønsted base since a H^+ ion is transferred onto the OH^- ligand
- Arhennius base since H^+ ion is consumed from solution, decreasing $[H^+]$
- Lewis acid at its Al^{3+} center since Al-O metal-ligand bonds are formed

Frontier Orbitals

Another way the Lewis acid-base concept is widely employed for understanding chemical reactivity is through the frontier orbital approach to chemical reactions. The frontier orbital concept is a simplified version of molecular orbital theory where chemical bonding and reactivity are visualized in terms of the interactions between frontier molecular orbitals on the chemical species undergoing an interaction (*e.g.* molecules, atoms, ions, or groups as they interact to form a bond or undergo a reaction). Frontier orbitals are those at the frontier between occupied and unoccupied. They are often taken to be the highest energy occupied and lowest energy unoccupied molecular orbitals, called the HOMO and LUMO levels. However, it can sometimes be more convenient to think about them as atomic orbitals or Valence Bond approach-derived orbitals. When developing rough qualitative frontier orbital descriptions of the orbital interactions involved in a given system the choice of what types of orbitals to use is often a matter of what is the most informative and convenient.

In particular the frontier orbital concept envisions a Lewis acid-base interaction as involving an interaction between some of the frontier orbitals of the Lewis acid and base, specifically the donation of electrons from the bases' HOMO level into the acid's LUMO level. For example, in the frontier orbital approach adduct formation between NH_3 and BH_3 involves the donation of electrons from ammonia's HOMO into BH_3's LUMO level.

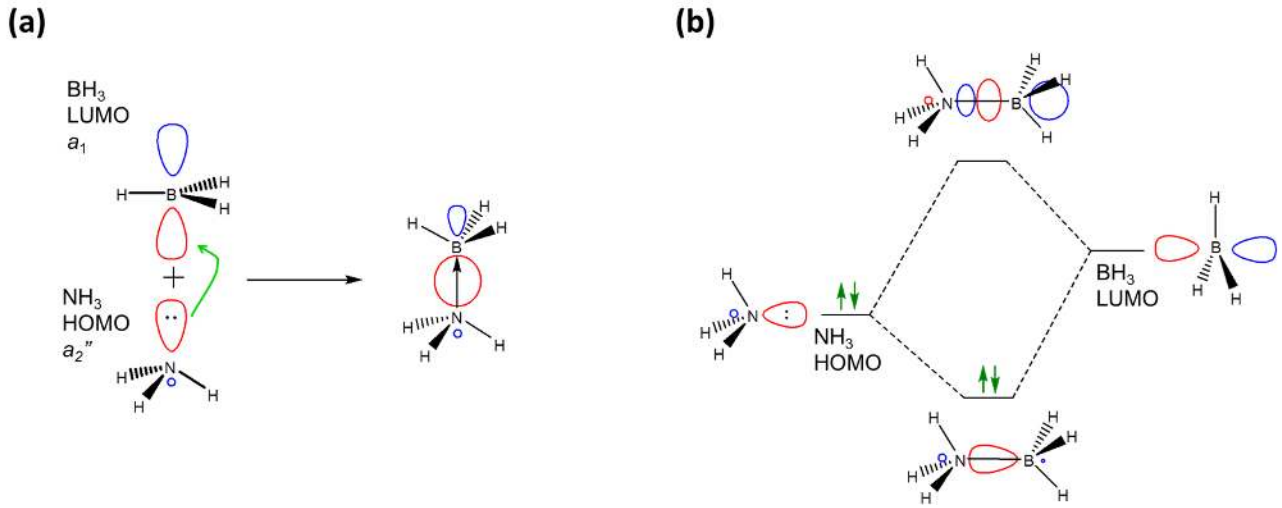


Figure **6.3.1**: Frontier orbital picture of adduct formation between ammonia and borane. (a) As NH_3 and BH_3 approach one another interaction between the NH_3 HOMO (lone pair on N) and BH_3 LUMO (unoccupied, non-bonding 2p orbital) gives a bonding MO. (b) Partial molecular orbital diagram for $NH_3 \rightarrow BH_3$ showing the stabilization of the base (NH_3) lone pair in a sigma bonding MO on adduct formation.

As expected when two orbitals of the appropriate symmetry combine, the result of the interaction is the formation of a lower energy bonding orbital between the acid and base (Figure **6.3.1**). Since it is occupied by an electron the net result of the interaction is the lowering of the base's lone pair as it interacts with the Lewis acid. In this case the interaction just follows the general pattern for Lewis-Acid base adduct formation, which is shown in Figure **6.3.2**.

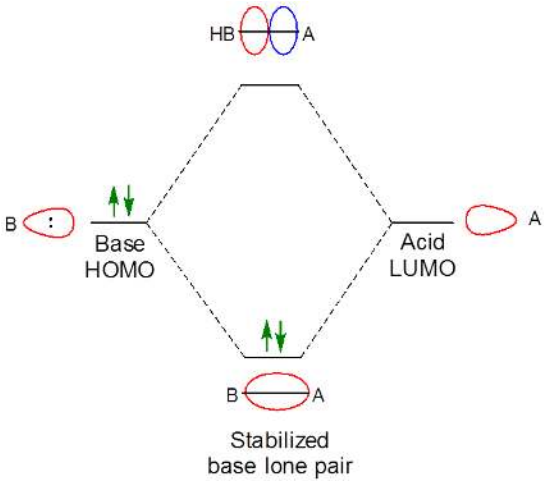
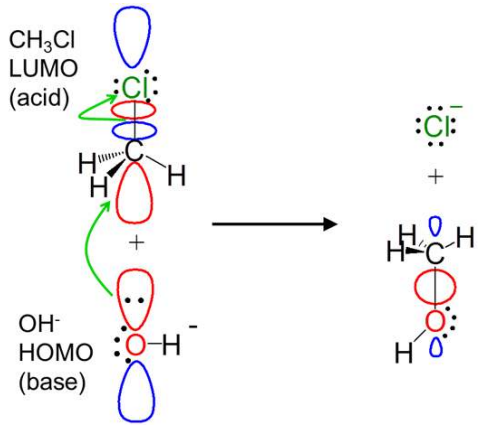


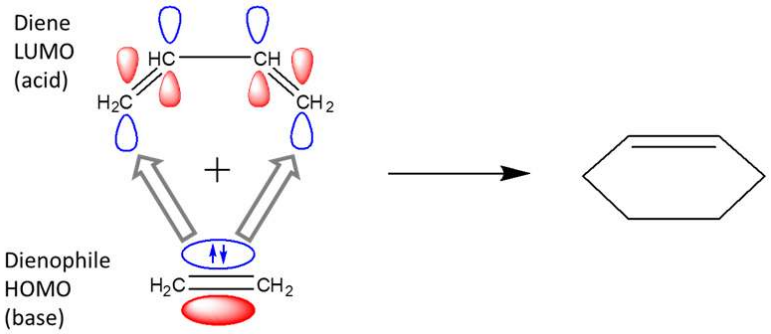
Figure **6.3.2**: Generalized frontier orbital picture for adduct formation between a Lewis base (B) and a Lewis acid (A) involving stabilization of the lone pair of the base HOMO by formation of a bonding orbital with the acid LUMO. The relative energies of the acid LUMO and base HOMO affect the character of the bonding and antibonding MOs but are otherwise unimportant in determining the general features of the interaction. In some cases the base HOMO is higher in energy; in others the acid LUMO is higher in energy; in still others they are equal in energy. In any case the net result is the stabilization of the base lone pair.

The frontier orbital concept illuminates the orbital interactions involved in reactions. For instance, from a frontier orbital perspective the alkyl halide substitution reaction between hydroxide and CH_3Cl via the S_N2 mechanism involves a Lewis acid-base interaction:

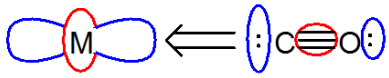


Notice how the frontier orbital approach even explains the displacement of the chloride leaving group. The donation of electrons from the hydroxide HOMO populates the antibonding CH_3Cl LUMO, breaking the C-Cl bond.

Using the frontier orbital approach it becomes apparent that pericyclic reactions are Lewis acid-base reactions. For example, in the Diels-Alder reaction the dienophile acts as a Lewis base and the diene as a Lewis acid.



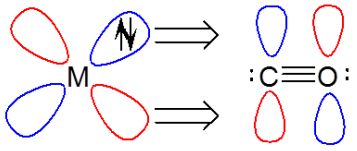
The orbital interactions involved in a given reaction can include both reactants acting as both an acid and base. In these cases the HOMO of each reactant interacts with the LUMO of the other. A good example of this involves **Π**-type interactions between a metal ion with occupied *d* orbitals and a pi-acceptor ligand. The ligand acts as a base and the metal as an acid to give a M-CO single bond.



Metal LUMO (d_{z^2}) acts as an acid

Carbon monoxide HOMO acts as a base

However, the metal can also act as a base towards the ligand LUMO (π^*) orbitals. Bonding between metals and ligands will be discussed further in chapter 9



Metal HOMO (d_{xz}, d_{xz}) acts as a base

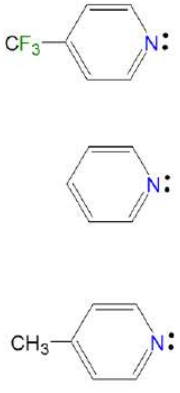
Carbon monoxide LUMO (π^*) acts as an acid

Substituent Effects

The electrons donated from a Lewis base to a Lewis acid in a Lewis acid-base reaction are donated and accepted at particular atomic centers. For instance, the formation of an adduct between ammonia and BF_3 involves the donation of the lone pair on the ammonia nitrogen atom to the Lewis acid site on BF_3.



Because Lewis acid-base reactions involve electron donation and acceptance at particular sites subsistent groups which alter the electron density at a site through inductively donating or withdrawing electron density will affect the Lewis acid-base properties of that site. For instance, the BF_3 affinities of 4-substituted pyridines increase slightly as the substituent on the aromatic ring is changed from electron donating Me to electron withdrawing CF_3.



BF_3 Affinity (kJ/mol)[a]
115.7 ± 0.4
128.1 ± 0.5
134.1 ± 0.6

a) Data from Laurence, C.; Gal, J.-F. o., *Lewis basicity and Affinity Scales: Data and Measurement. John Wiley: Chichester, West Sussex, U.K., 2010; pp. 91-101.*

Substituent inductive effects are much as one might predict. Since Lewis bases donate electron pairs and Lewis acids accept them:

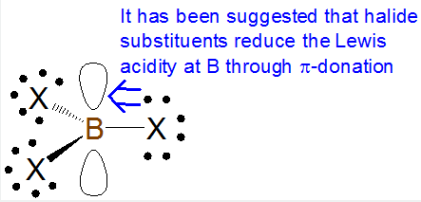
- electron withdrawing substituents tend to decrease the Lewis basicity of basic sites while electron donating substituents increase site Lewis basicity by making them more electron rich.
- electron withdrawing substituents increase the Lewis acidity of acidic sites by making those sites more electron deficient while electron donating substituents tend decrease Lewis acidity by making sites less electron deficient.

Nevertheless it can be difficult to predict substituent-based trends in Lewis acidity and basicity by inductive effects alone. This is because inductive effects are modest and often exists in competition with other substituent effects, such as

- Steric effects
- Hardness effects
- π-donation and acceptance effects, which can increase or decrease electron density at a given site as well as create an energy barrier for any structural distortions that might occur on adduct formation.

π Donation and Acceptance and Lewis Acid-Base Affinity

As with σ-based induction effectsπ-donation tends to increase Lewis basicity and decrease Lewis acditiy while π-withdrawal tends to decrease Lewis basicity and increase Lewis acidity. However, care needs to be taken in assessing the effect of π-donation effects on Lewis acidity and basicity. For example, some textbooks claim that the Lewis acidity of boron trihalides is dominated by the reduction of boron acidity throughπ-donation from the halide substituents:

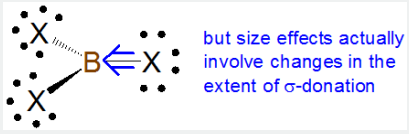


According to this explanation the extent of this π-donation decreases down the halogen group as the boron-halogen bond distance decreases. This is consistent with the observed trend in Lewis acidity of the boron trihalides towards most bases, which runs counter to that suggested by inductive effects alone:

$$BI_3 > BBr_3 > BCl_3 >> BF_3$$

However, computation work suggests that this explanation is incorrect since

- atomic size effects are important mainly for substituents in which the connected atom is row 3+ or higher
- atomic size effects mainly involve changes in the extent of σ-overlap. In other words the larger halogens are less able to reduce the electron deficiency at the boron center through σ interactions while π-interactions play little or no role.



References:

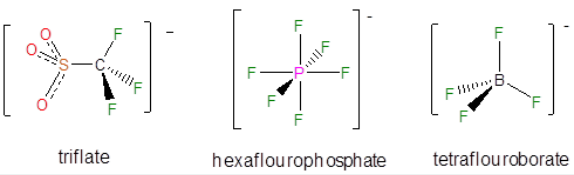
1. Plumley, J. A.; Evanseck, J. D., Periodic Trends and Index of Boron Lewis Acidity. *The Journal of Physical Chemistry A* 2009, 113 (20), 5985-5992.
2. Jupp, A. R.; Johnstone, T. C.; Stephan, D. W., Improving the Global Electrophilicity Index (GEI) as a Measure of Lewis Acidity. *Inorganic Chemistry* 2018, 57 (23), 14764-14771.

Conjugate Bases of Brønsted Superacids

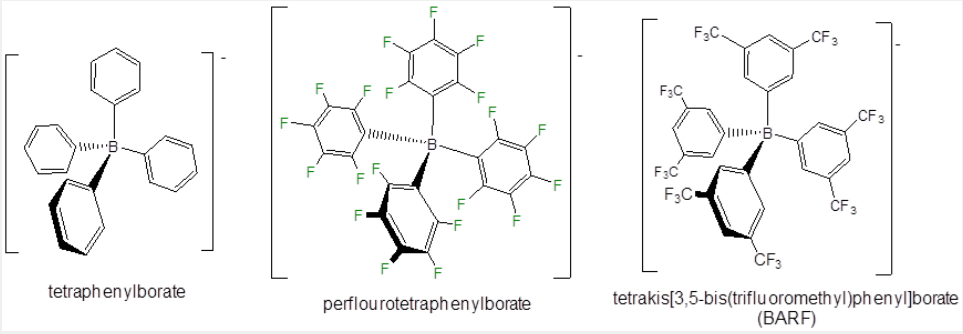
The nonreactivity of Brønsted superacids' conjugate bases towards hydrogen ions is often mirrored in nonreactivity towards other Lewis Acids/electrophiles, most notably metals. This makes these substances useful as inert or noncoordinating ions,

although since all are reactive towards a suitably electrophilic centers they are perhaps better understood as weakly coordinating.

A number of noncoordinating anions are commonly used in synthetic and other applications. The conjugate base of perchloric acid, perchlorate, was a common noncoordinating inert anion in classical coordination chemistry and continues to be used widely in electrochemistry. However metal perchlorate salts can be explosive, so synthesis of metal salts with perchlorate anions, especially on large scales is much less common in modern inorganic chemistry. In contrast, the conjugate bases of triflic acid, hexaflouroboric acid, and tetrafloroboric acid are now more commonly used as counterions for when isolating reactive cations.



Even less reactive noncoordinating anions include derivatives of tetraphenylborate, particularly those with electron withdrawing substituents.



Other classes of noncoordinating ions include floroantimonate clusters, derivatives of the carborane anion ($CB_{11}H_{11}^-$), and flourinated aluminum tetraalkoxides.

References:

1. Engesser, T. A.; Lichtenthaler, M. R.; Schleep, M.; Krossing, I., Reactive p-block cations stabilized by weakly coordinating anions. *Chemical Society Reviews* **2016**, *45 (4)*, 789-899.

Lewis Acid-Base Adducts

When a Lewis acid-base adduct is formed electron density and negative charge is transferred from the Lewis base to the acid.



(6.3.6)

For example, the formation of an adduct between borane and ammonia involves the transfer of a small amount of electron density, as shown by the movement of negative charge from NH_3 to BH_3 depicted in Figure **6.3.3**.

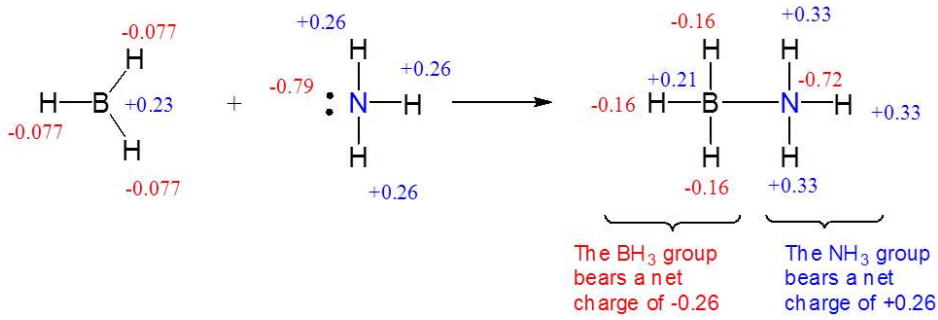


Figure **6.3.3**: Calculated change in atomic charge distribution on formation of an adduct between BH_3 and NH_3 in the gas phase. All partial charges were calculated for geometry optimized molecules at the 6-31G** level.

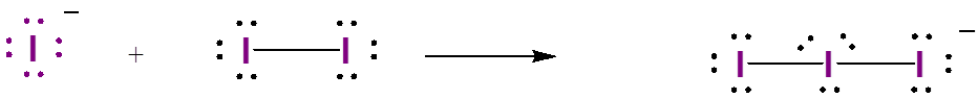
In many weakly bound Lewis acid-base complexes the transfer of electron density and consequently, charge, from the base group to the acid group is only partial:

$$A + B \rightleftharpoons A^{\delta-}B^{\delta+} \tag{6.3.7}$$

Such Lewis acid-base adducts are commonly called **charge transfer complexes (CT complexes)** or **donor-acceptor complexes (DA complexes)**. In these

- the base is called the **donor (D)** since it is a net donor of electrons and, consequently, their negative charge
- the acid is called the **acceptor (A)** since it is a net acceptor of electrons and, consequently, their negative charge

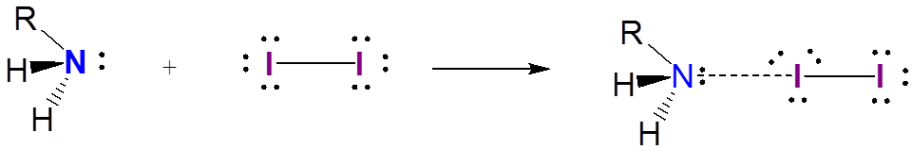
A particularly well-known class of charge transfer complexes are the iodine charge transfer complexes. In iodine charge transfer complexes the I_2 acts as a Lewis acid. This is possible since iodine is a Row 3+ element and so is capable of forming hypervalent complexes on reaction with a Lewis base. For example, I_2 reacts with I^- to give the triiodide ion.



(6.3.8)

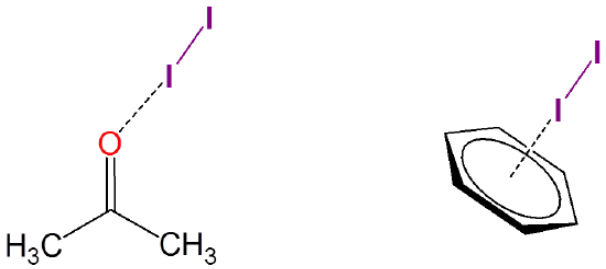
Triiodie is well-known from introductory chemistry from the bright blue color that appears when the triiodie is complexes with starch to give the dark blue starch-iodide complex.

In contrast to stable triiodide anion, iodine charge transfer complexes are only weakly associated. Complexes between iodine and amines are a well known example:



(6.3.9)

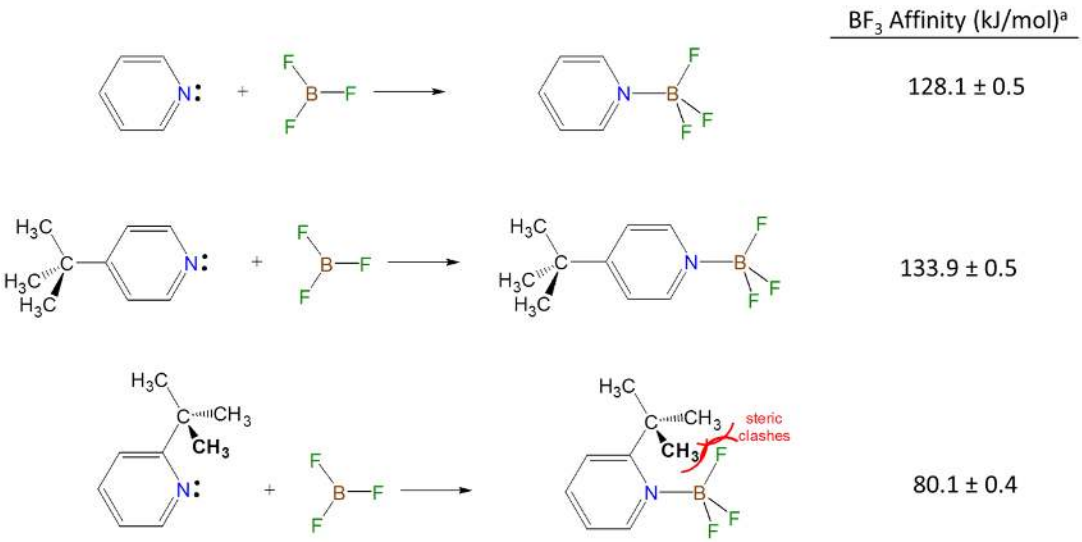
Iodine also forms weakly-associated charge transfer complexes with many solvents. For instance, iodine can weakly associate with both acetone and benzene:



Steric Effects

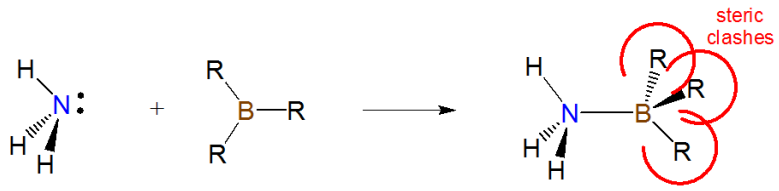
Steric effects can influence the ability of a Lewis acid or base to form adducts by introducing:

- **front strain (F-strain)** whereby bulky groups make it difficult for the Lewis acid and Lewis base centers to approach and interact.



a) Data from Laurence, C.; Gal, J.-F. o., *Lewis basicity and Affinity Scales: Data and Measurement. John Wiley: Chichester, West Sussex, U.K., 2010; pp. 91-101.*

- **back strain (B-strain)** associated with steric interactions that do not directly impede the Lewis acid and base centers from interacting but instead occur as the acid and base rearrange on adduct formation. For instance, when trivalent boron compounds form adducts with amines the boron center changes from a more open trigonal pyramidal geometry to a more hindered tetrahedral one:



- **internal strain (I-strain)** is also associated with the geometry changes incident on adduct formation. However, while B-strain involves direct steric clashes that occur on adduct formation I-strain is the strain involved in deforming bond and torsional angles away from more stable local geometries. Thus it is more important for Lewis base centers embedded in rings or clusters.

References

1. Alder, R. W., Strain effects on amine basicities. *Chemical Reviews* 1989, 89 (5), 1215-1223.

Contributors and Attributions

Stephen M. Contakes, Westmont College

Consistent with the policy for original artwork made as part of this project, all unlabeled drawings of chemical structures are by Stephen Contakes and licensed under a Creative Commons Attribution 4.0 International License.

6.3: Lewis Concept and Frontier Orbitals is shared under a CC BY-NC-SA 4.0 license and was authored, remixed, and/or curated by LibreTexts.

- **Current page** is licensed CC BY-NC-SA 4.0.
- **6.4: Lewis Concept and Frontier Orbitals** by Stephen M. Contakes is licensed CC BY 4.0.
- **6.4.1: The frontier orbital approach considers Lewis acid-base reactions in terms of the donation of electrons from the base's highest occupied orbital into the acid's lowest unoccupied orbital.** by Stephen M. Contakes is licensed CC BY 4.0.

- **6.4.2: All other things being equal, electron withdrawing groups tend to make Lewis acids stronger and bases weaker while electron donating groups tend to make Lewis bases stronger and acids weaker** by Stephen M. Contakes is licensed CC BY 4.0.
- **6.4.3: The electronic spectra of charge transfer complexes illustrate the impact of frontier orbital interactions on the electronic structure of Lewis acid-base adducts** by Stephen M. Contakes is licensed CC BY 4.0.
- **6.4.7: Bulky groups weaken the strength of Lewis acids and bases because they introduce steric strain into the resulting acid-base adduct.** by Stephen M. Contakes is licensed CC BY 4.0.
- **6.4.8: Frustrated Lewis pair chemistry uses Lewis acid and base sites within a molecule that are sterically restricted from forming an adduct with each other.** by Stephen M. Contakes is licensed CC BY 4.0.

6.4: Hard and Soft Acids and Bases

Origin of the Hard-Soft Acid-Base Principle

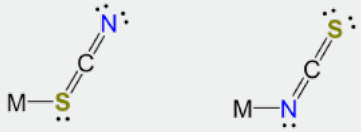
One of the strengths of the Lewis acid-base concept is the readiness with which it illuminates the role that covalent and electrostatic interactions in acid base behavior, specifically through its ability to explain chemical interactions in terms of frontier orbitals and the interactions between charged groups as electrons are donated from a base to an acid. However, simply acknowledging the presence of such interactions does little to illuminate the degree to which each mode of explanation best explains the bonding in a given system? To what extent is a given adduct better described as held together by covalent bonds as opposed to ionic ones - *e.g.* better described as a molecule rather than an ion pair? Moreover, does it even matter, given that the orbitals of quantum mechanics result from the combination of electrons' wavelike behavior with their electrostatic attraction to nuclei in either case? These questions and more are addressed by one of the most important conceptual tools in contemporary inorganic chemistry, the hard-soft acid-base principle.

The hard-soft acid-base (HSAB) principle stems from the recognition that some Lewis acids and bases seem to have a natural affinity for one another.* Consider the following:

- Some metals are commonly found in nature as salts of chloride or as oxide ores while others are found in combination with sulfur. Geochemists even use the Goldschmidtt classification scheme to classify the halide and oxide formers as lithophiles and the sulfide formers as chalcophiles.
- In living systems small highly charged metals ions like Fe^{3+} are usually found bound to N and O atoms while larger metals with lower charges such as Zn^{2+} are often found attached to at least one S atom. Similarly, metals prefer to bind to one coordination site over the other when forming complexes with ambidentate ligands. The most well-known instances involve complexes of cyanate and thiocyanate, which can coordinate metals through either the N or chalcogen atom. For instance, Cu^{2+} and Zn^{2+} form *N*-thiocyanato complexes in species like $[Cu(NCS)_2(py)_2]$ and $[Zn(NCS)_4]^{2-}$ while their larger cogeners Au^{3+} and Hg^{2+} preferentially forms *S*-thiocyanato complexes, giving speciles like $[Hg(SCN)_4]^{2-}$.

Ambidentate ligands

Ambidentate ligands possess multiple coordination sites through which a metal may bind. For instance, thiocyanate may coordinate metals (M) at either the S or N to give *S*-thiocyanato or *N*-thiocyanato complexes.



S-thiocyanato *N*-thiocyanato

- The solubility trends for the alklai metal halides and silver halides are opposite, even though both involve salts of formula M^+X^- (salts can be thought of as involving Lewis acid-base adduct formation between the anions and cations). Specifically, although the silver halides are all relatively insoluble in water, the very modest solubility they possess follows the order:

$$X = F >> Cl > Br > I \text{ (for the solubility of AgX)}$$

In contrast, the much more ample solubility of the alkali metal halides** follows the opposite order. For example, the order for the lithium halides is

$$X = F << Cl < Br << I \text{ (for the solubility of LiX)}$$

Notes

* Despite the fruitfulness of this observation, in general it is important to reduce the potential for observer bias by checking observations like these against compounds reported in the chemical literature and databases like the Inorganic Crystal Structure and Cambridge Crystallographic Databases.

** These are very soluble in water, to the point where some solutions are perhaps better described as solutions of water in the halide.

Qualitative HSAB Principle

The hard-soft acid-base principle is a conceptual tool for thinking about patterns of Lewis acid base reactivity. The explanation of the trends in metal distribution, halide salt solubility, and preferred metal coordination patterns is rooted in Arland, Chatt, and Davies' observation that *Lewis acids and bases could be classified into two groups based on their propensity to form stable compounds with one another* (*e.g.* acids in a class tend to form more stable adducts with bases in the same class than they did with bases in the other).[1] Arland, Chatt, and Davies somewhat boringly termed these groups class a and class b but today they are known by Ralph Pearson's name for them. Pearson called the class a acids and bases hard and class b acids and bases soft. These terms reflect how "soft" these substance's electron clouds are towards distortion or, in other words, their polarizability (Figure **6.4.1**). Pearson terms acids and bases which are relatively polarizable **soft** and those which are difficult to polarize **hard.**

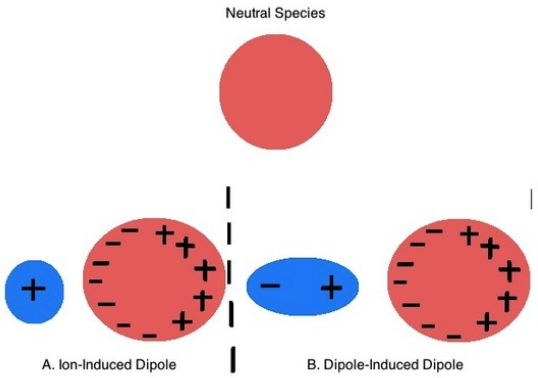


Figure **6.4.1**: Polarizability refers to the ease with which a substance's electron cloud may be distorted under the action of an electric field. An fragment's polarizability determines the degree to which its electron cloud is distorted by A.) an Ion and B.) a polar molecule to induce a dipole moment. The figure is taken from (and the caption expanded from) Cox, Kelly and Dana Reusser "Polarizability" in https://chem.libretexts.org/Bookshelves/Physical_and_Theoretical_Chemistry_Textbook_Maps/Supplemental_Modules_(Physical_and_Theoretical_Chemistry)/Physical_Properties_of_Matter/Atomic_and_Molecular_Properties/Intermolecular_Forces/Specific_Interactions/Polarizability

Recognizing Hard and Soft Acids and Bases

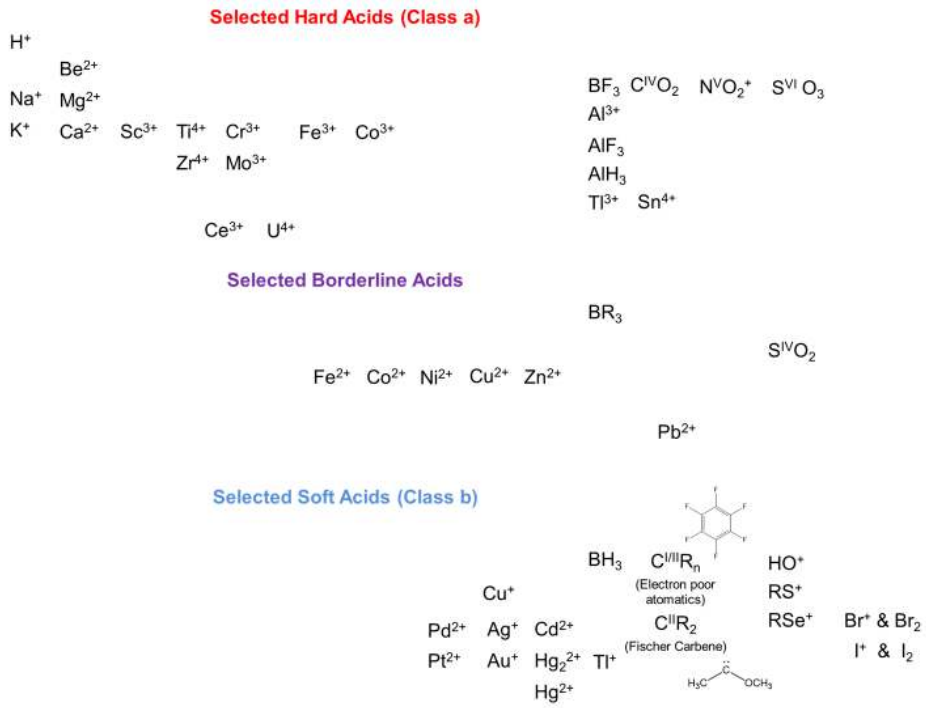
Hard acids and bases come in two varieties:

1. hard acid and base sites which possess few valence electrons and for which polarization therefore involves distorting core electrons, which are difficult to distort because they are close to the nucleus and experience a high nuclear charge. The most common examples of such substances are Lewis acids hard acids towards the left of the periodic table.
2. hard acids and base sites with a high charge density (highly charged relative to size) and/or which are electron deficient. In these cases polarization involves distorting electrons that already experience strong unshielded electrostatic interactions.

Soft acids and bases also come in two varieties

1. soft acids and bases which posses many valence electrons and so are more readily polarized. In consequence, all other tings being equal, soft acids and bases are more likely to be found towards the middle or right of the periodic table.
2. soft acids and bases with little charge density and/or which are relatively electron rich.

Note that the hard-soft classification should not be thought of as if all hard acids and bases are equally hard and all soft acids and bases equally soft. There is a graduation in hardness and softness and a number of intermediate acids and bases which do not fit neatly in either category. With this caveat in mind, representative **hard, soft, and borderline acids** are given below. Notice how they illustrate the trends just outlined.



As expected, hard acids tend to be found towards the left side of the periodic table and involve higher oxidation states and/or electron donating substituents while soft acids are more common to the right of the periodic table and involve lower oxidation states and/or electron donating substituents.

Illustrative hard, soft, and borderline bases are given below. Again, notice how these substances illustrate the general trends.

Selected Hard Bases (Class a)

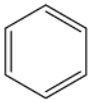
Nitrogen bases	Oxygen bases		small halides
NH_2^-	OH^-	CO_3^{2-}	F^-
NH_3	H_2O	RCO_2^-	Cl^-
RNH_2	ROH	NO_3^-	
NH_2NH_2	ROR	PO_4^{3-}	
		SO_4^{2-}	

Selected Borderline Bases

electron-poor Nitrogen bases		low oxidation state element oxyanions	intermediate halides
N_3^-		NO_2^-	
NO_2^-			Br^-
SCN^-		SO_3^{2-}	
N_2			

Selected Soft Bases (Class b)

Carbon bases	P and As bases	Sulfur bases	large halides & pseudohalides
R^-	PR_3	RS^-	H^-
CO	$P(OR)_3$	RSH	I^-
CN^-	AsR_3	RSR	
RNC		SCN^-	
$R_2C{=}CR_2$ (alkenes)			



(electron-rich aromatics)

Qualitative Estimation of the Relative Hardness and Softness of Lewis Acids and Bases

As can be seen from the examples above, **hard acids are relatively electron-poor and hard bases electron-rich** since they have comparatively

- small frontier orbitals, reflective of their relatively small atom/ion/fragment sizes
- high (for acids) or low (for bases) oxidation states on the base atom, reflected in a large positive formal charge (for acids) or negative formal charge (for bases)
- low polarizability, due to loss or gain of substantial numbers of electrons, or the localization of
  - positive charge on an electropositive element or an atom bearing electron-withdrawing substituents
  - negative charge on an electronegative element or an atom bearing electron-donating substituents

In contrast to hard acids and bases **soft acids are relatively electron-rich and soft bases larger and more electron poor** since they have comparatively

- large frontier orbitals, reflective of their relatively large atom/ion/fragment sizes
- low oxidation states, often resulting in small or nonexistent atomic charges
- high polarizability, as might be expected of species in which electron-electron repulsions are lower and electrons are spread over a large volume. Sometimes this is indicated by
  - positive charge on an electronegative element or an atom bearing electron-donating substituents
  - negative charge on an electropositive element or an atom bearing electron-withdrawing substituents

Exercise 6.4.1

Rank the acid or bases in each set in increasing order of expected hardness?

(a) Cr^{2+} and Cr^{3+}

(b) H^+, Cs^+, and Tl^+

(c) SCN^- (acting as a base at N) and SCN^- (acting as a base at S)

(d) AlF_3, AlH_3, $AlMe_3$

(e) The side chains of the following proteinogenic amino acids

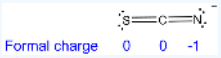


Answer

(a) $Cr^{2+} < Cr^{3+}$ All other things being equal, hardness increases with oxidation state.

(b) $Tl^+ < Cs^+ < H^+$ The order reflects Cs^+ and Tl^+'s larger size relative to H^+ (which doesn't possess any electrons that can be polarized anyway) and that Tl^+ still possesses two valence electrons while Cs^+ possesses none.

(c) SCN^- (acting as a base at S) < SCN^- (acting as a base at N) The order reflects that N is more elctronegative than S and possesses a more negative formal charge of -1.



(d) $AlH_3 < AlMe_3$, AlF_3 The hardness increases as the substituents on the Lewis acid Al center become less electron donating and more electron withdrawing (and, incidentally, harder bases) as their electronegativity increases in the order H^- < CH_3^- < F^-. Note that the order of electron donating ability for H^- and CH_3^- is the opposite observed for carbocations, for which hyperconjugation plays a larger role.

(e) Sec < Cys < Ser The hardness increases as the electronegativity of the Lewis base chalcogen increases on going from a selenol to a thiol to an alcohol.

Applications of HSAB Principle

The Hard-Soft acid-base principle (HSAB Principle) explains patterns in Lewis acid-base reactivity in terms of a *like reacts with like preference*. Both thermodynamically and kinetically hard acids prefer hard bases and soft acids soft bases. Specifically,

- Thermodynamically, hard acids form stronger acid-base complexes with hard bases while soft acids form stronger complexes with soft bases.
- Kinetically, hard acids/electrophiles react more quickly with hard bases/nucleophiles while soft acids/electrophiles react more quickly with soft bases/neucleophiles

Applications of the HSAB principle include

1. Predicting the equilibrium or speed of *Lewis acid-base metathesis and displacement reactions.* In a Lewis acid-base *metathesis reaction* the acids and bases swap partners

$$A_1{:}B_1 + A_2{:}B_2 \underset{}{\overset{k_1,\ K_{eq}}{\rightleftharpoons}} A_1B_2 + A_2{:}B_1 \tag{6.4.1}$$

For example, the equilibrium position of the metathesis reaction between TlF and K_2S favors the products:

$$2TlF + K_2S \rightleftharpoons Tl_2S + 2KF$$

(6.4.2)

consistent with the HSAB's hard-hard and soft-soft preference.

$$\underset{\text{soft hard}}{2\,Tl^{+}F^{-}} + \underset{\text{hard soft}}{(K^{+})_2S^{2-}} \rightleftharpoons \underset{\text{soft soft}}{(Tl^{+})_2\,S^{2-}} + \underset{\text{hard hard}}{2\,K^{+}F^{-}}$$

(6.4.3)

The HSAB principle also allows for prediction of the position of displacement reactions, in which a Lewis acid or base forms an adduct using a base or acid from an existing Lewis acid-base complex. In these reactions, the displacement of acid or base from the reactant complex to may be thought of as a sort of metathesis reaction, one in which in the unbound acid or base switches places with one in the complex. For example, the reaction between HI and methylmercury cation

$$HI + HgSCH_3^{+} \rightleftharpoons CH_3SHgI + H^{+}$$

(6.4.4)

involves displacement of an iodide from HI to give CH_3HgI. The position of the equilibrium favors CH_3HgI since both CH_3Hg^{+} and I^{-} are both soft, while H^{+} is a hard acid.

$$\underset{\text{hard-soft}}{H\text{-}I} + \underset{\text{soft}}{CH_3Hg^{+}} \rightleftharpoons \underset{\text{soft -soft}}{CH_3Hg\text{-}I} + \underset{\text{hard}}{H^{+}}$$

(6.4.5)

Exercise 6.4.2

Predict the position of equilibrium for the following reaction.

$$Fe_2O_3 + 3Ag_2S \rightleftharpoons Fe_2S_3 + 3Ag_2O$$

Answer

The equilibrium will favor the reactants (K<1) since the hard-hard and soft-soft interactions in the reactants are more stable than the hard-soft interactions in the products.

$$\underset{\text{hard hard}}{(Fe^{3+})_2\,(O^{2-})_3} + \underset{\text{soft soft}}{3\,(Ag^{+})_2S^{2-}} \rightleftharpoons \underset{\text{hard soft}}{(Fe^{3+})_2\,(S^{2-})_3} + \underset{\text{soft hard}}{3\,(Ag^{+})_2O^{2-}}$$

Exercise 6.4.3

Predict whether K for the following equilibria will be <<1, ~1, or >>1.

a. $2HF + (CH_3Hg)_2S \rightleftharpoons 2CH_3HgF + H_2S$

b. $Ag(NH_3)_2^{+} + 2PH_3 \rightleftharpoons Ag(PH_3)_2^{+} + 2NH_3$

c. $Ag(PH_3)_2^{+} + 2H_3B-SH_2 \rightleftharpoons 2H_3B-PH_3 + Ag(SH_2)_2^{+}$

d. $H_3B-NH_3 + F_3B-SH_2 \rightleftharpoons H_3B-SH_2 + F_3B-NH_3$

Answer

a. K< < 1 since the reactant adducts are hard-hard and soft-soft while the products involve hard-soft interactions

b. K>>1 since the reactant complex, diamine silver(I) is a complex of a hard base, NH_3, with the soft acid, Ag^+, while the product is a complex of the same soft acid with the soft base phosphine.

c. K~1 since all the adducts amongst the reactants and products involve soft acids and bases

d. K>>1 since BH_3 is a softer acid than BF_3 so it will form a stronger complex with the softer base H_2S while the harder BF_3 forms a stronger complex with the harder base NH_3.

2. Predicting the relative strengths of a given set of *Lewis acids or bases towards a particular substrate*. Consider, for example, the relative strengths of a BH_3, BMe_3, and BF_3 towards group 15 hydrides like NH_3, PH_3, and AsH_3. Of the boranes listed, the hardest acid BF_3 is the strongest acid towards the hard base NH_3 while BH_3 is the strongest towards AsH_3.[†]

Exercise 6.4.4

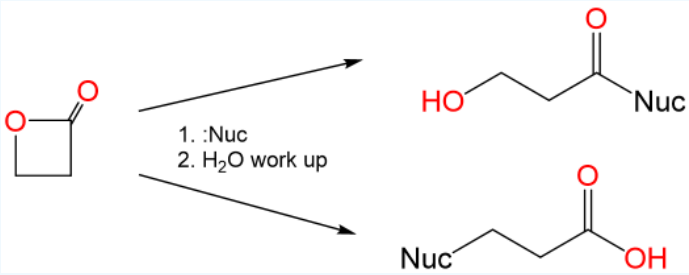
Which acid will form the most stable complex with CO - BH_3, BF_3, or BMe_3?

Answer

BH_3. Since CO forms complexes primarily through its carbon lone pair it is a soft base and so will form the strongest complex with the softest Lewis acid.

Exercise 6.4.5

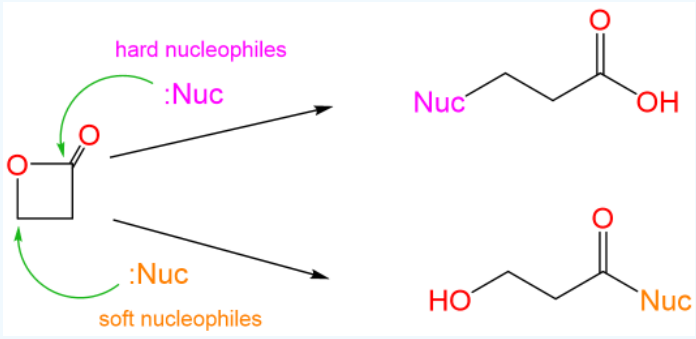
When lactones react with nucleophiles they can undergo ring opening reactions to give either an alcohol or carboxylic acid, as shown for propiolactone below:



In the reaction above, sterically unhindered alkoxides give one product and sterically unhindered thioalkoxides the other. Explain why this is the case and predict the products of the reaction between propiolactone and the sodium salts of ethoxide and thioethoxide.

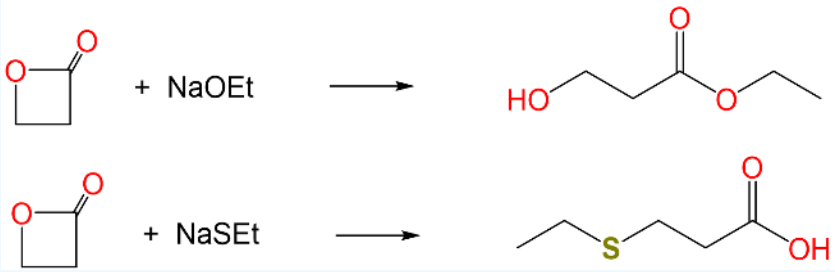
Answer

The two reaction products correspond to nucleophilic attack at the lactones two electrophilic carbon centers. Specifically, the acid is produced by attack at the softer C^I center of the CH_2 directly attached to the ester oxygen and the alcohol by nucleophilic attack at the harder C^{III} center of the ester carbonyl.



https://chem.libretexts.org/@go/page/326222

Consequently, it is reasonable to expect that the harder base ethoxide will nucleophilically attack the harder carbonyl carbon while the softer thioethoxide will attack the softer methylene carbon.



Theoretical Interpretation of the Hard Soft Acid-Base Principle

The Theoretical Interpretation of the Hard Soft Acid-Base Principle is that hard-hard preferences reflect superior electrostatic stabilization while soft-soft preferences reflect superior covalent stabilization. The hard-hard and soft-soft preferences in Lewis acid-base interactions reflect that

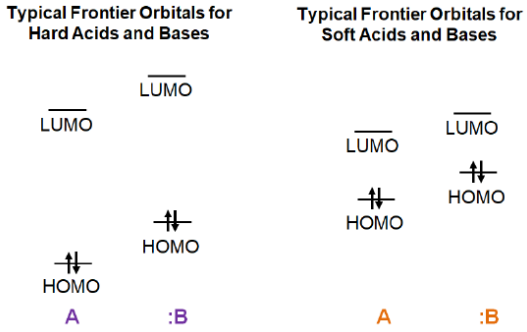
- The lone pair of a hard base is strongly stabilized electrostatically by a hard acid
- The lone pair of a soft base is strongly stabilized by forming a covalent bond with a soft acid
- The lone pair of a hard or soft base is comparatively weakly stabilized by an acid opposite to it in hardness or softness since the overall electrostatic and covalent stabilization of the adduct is comparatively weak.

To see why this is the case it is helpful to divide the contributions to the interaction energy between an acid and a base as follows:

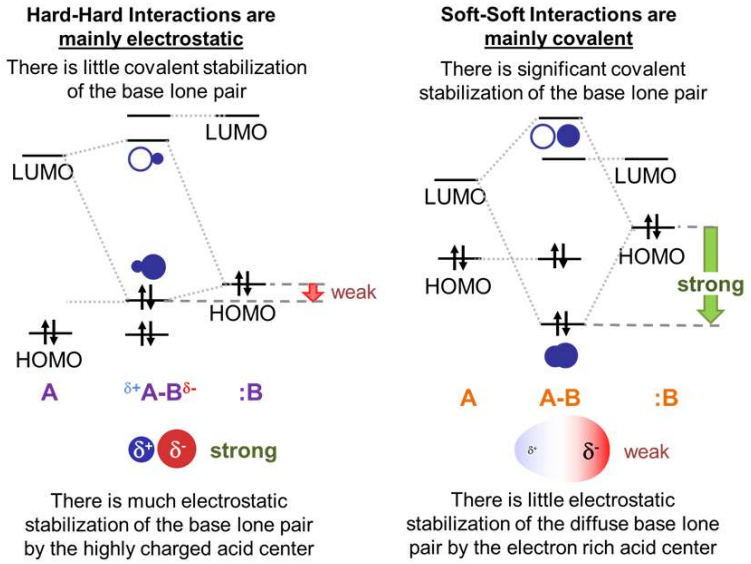
$$\text{Interaction Energy} = \underbrace{\text{Electrostatic attractions and repulsions of partial atomic charges}}_{\text{Ionic term}} + \underbrace{\text{Interactions between filled orbitals on one fragment and unfilled orbitals on the other}}_{\text{Covalent term}} + \underbrace{\text{Electrostatic repulsions between filled orbitals on the two fragments}}_{\text{Steric term}} \tag{6.4.6}$$

Of the three contributions to the interaction energy, only the ionic and covalent terms directly relate to the hardness of the interacting acid and base. One approach to thinking about how hardness influences the ionic and covalent contributions is to consider the frontier orbitals involved in the acid-base interaction. This is sometimes done through the use of the Salem-Klopman equation,[1,*] although in the treatment which follows a more qualitative approach will be employed.

Both hard acids and bases will have comparatively low energy HOMO levels and high energy LUMO levels, with a correspondingly high HOMO-LUMO gap. In contrast, soft acids and bases will have comparatively high-energy HOMO levels and low-energy LUMO levels, giving a comparatively smaller HOMO-LUMO gap.



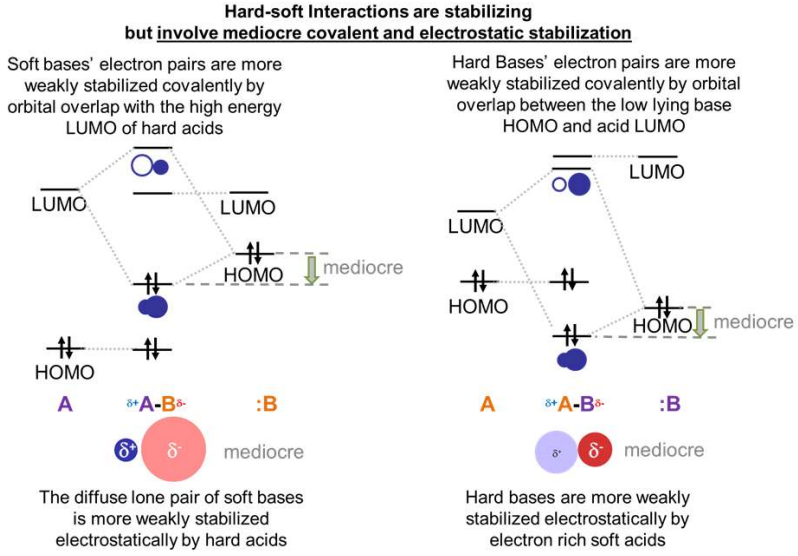
Given this, consider the frontier orbital interactions involved in the formation of an acid-base complex for the possible cases, as illustrated schematically below.



The large gap in energy between hard bases' highly stabilized HOMO lone pairs and the high energy LUMO of hard acids ensures that in **hard acid-hard base adducts the dominant stabilizing interaction will involve electrostatic attraction between the base lone pair and the electropositive Lewis acid center**. Fortunately, since the electron clouds in hard bases are relatively dense and electron rich while hard Lewis acids are highly charged and small these electrostatic interactions are strong.

In contrast, in **soft acid-soft base adducts the dominant stabilizing interaction will be covalent.** This is because the small gap in energy between a soft base HOMO and soft acid LUMO enables the formation of a well-stabilized bonding orbital with significant electron density between the acid and base.

The orbitals interactions between hard acids and soft bases and soft acids and hard bases are intermediate between the hard acid-hard base and soft acid-soft base cases.



This means that the adducts are stable relative to free acid and base – just not as well stabilized as in the hard acid and hard base case. In the case of hard acids and soft bases the hard acids are less able to stabilize the soft bases' relatively diffuse electron pair electrostatically and there isn't as much covalent stabilization as in adducts of soft acids and bases due to hard acid's high energy.

Notes

* Despite the fruitfulness of this observation, in general it is important to reduce the potential for observer bias by checking observations like these against compounds reported in the chemical literature and databases like the Inorganic Crystal Structure and Cambridge Crystallographic Databases.

** These are very soluble in water, to the point where some solutions are perhaps better described as solutions of water in the halide.

† This can be predicted based on the relative hardness of BF_3, BR_3, and BH_3 in the list of hard and soft acids. However, for those of you who may be confused as to why H is considered a better electron donor for the purposes of softening a Lewis acid center while alkyl groups are better electron donors for the purposes of stabilizing carbocations in organic chemistry, the dominant effect is the lower electronegativity of H relative to carbon (in CH_3). The effect of electron donation due to hyperconjugation isn't as great for thermodynamically stable bases like BX_3/BR_3.

†† For more on the Salem-Klopman equation see Fleming, I., Molecular orbitals and organic chemical reactions. Reference ed.; Wiley: Hoboken, N.J., 2010; pp. 138-143.

References

1. Ahrland, S.; Chatt, J.; Davies, N. R., The relative affinities of ligand atoms for acceptor molecules and ions. Quarterly Reviews, Chemical Society 1958, 12 (3), 265-276.

2. Pearson, R. G., Hard and Soft Acids and Bases. Journal of the American Chemical Society 1963, 85 (22), 3533-3539.

3. Fleming, I., Molecular orbitals and organic chemical reactions. Reference ed.; Wiley: Hoboken, N.J., 2010.

Contributors and Attributions

Stephen M. Contakes (Westmont College)

6.4: Hard and Soft Acids and Bases is shared under a CC BY-NC-SA 4.0 license and was authored, remixed, and/or curated by LibreTexts.

- **6.6: Hard and Soft Acids and Bases** by Stephen M. Contakes is licensed CC BY 4.0.
- **Current page** is licensed CC BY-NC-SA 4.0.
- **6.6.2: Hard-Hard and Soft-Soft preferences may be explained and quantified in terms of electrostatic and covalent and electronic stabilization on the stability of Lewis acid-base adducts** by Stephen M. Contakes is licensed CC BY 4.0.

CHAPTER OVERVIEW

7: Reduction and Oxidation Chemistry

Learning Objectives

- Balance a redox reaction in acidic or basic solution
- Calculate the cell potential and free energy of an electrochemical cell under standard and non-standard conditions
- Use Latimer diagrams to determine unknown reduction potential values and to quickly identify stable and unstable species
- Use Frost diagrams to determine which oxidation states of a species are stable and which are unstable
- Use Porbaix diagrams to determine which species will be present in solution under given conditions

Thumbnail image shows the Porbaix diagram of chromium (CC BY-SA 3.0, Denis Zhilin via Wikimedia Commons)

7.1: Balancing Redox Reactions

7.2: Electrochemical Potentials

7.3: Latimer Diagrams

7.4: Frost Diagrams

7.5: Pourbaix Diagrams

7: Reduction and Oxidation Chemistry is shared under a CC BY-NC-SA 4.0 license and was authored, remixed, and/or curated by LibreTexts.

7.1: Balancing Redox Reactions

Balancing Redox Reactions

In studying redox chemistry, it is important to remember balancing electrochemical reactions. Simple redox reactions (for example, $H_2 + I_2 \rightarrow 2\ HI$) can be balanced by inspection, but for more complex reactions it is helpful to have a systematic method. There are many different methods for doing this. The focus in this section will be on the **ion-electron method** allows one to balance redox reactions regardless of their complexity and allows for identification of the species changing valence states in the reaction. We illustrate this method with two examples. For a review of how to determine oxidation states see Oxidation States (Oxidation Numbers).

Steps to balance a redox reaction

1. Identify what is being oxidized and reduced and divide the reaction into two half reactions
2. For each half reaction, balance all the atoms EXCEPT oxygen and hydrogen.
3. For each half reaction, balance oxygen by adding H_2O
4. For each half reaction, balance hydrogen by adding H^+
5. For each half reaction, balance charge by adding electrons
6. Add the two half reaction together. If needed, multiply half reactions by coefficients so that there are an equal number of electrons in both half reactions
7. If the reaction is in BASIC solution, cancel any H^+ by adding OH^- to both sides or the reaction

Example 7.1.1

Determine the balanced redox reaction that occurs when I^- reacts with MnO_4^- to form IO_3^- and Mn^{2+} in basic solution.

Solution

Following the steps above:

Step 1. The I^- is oxidized and the MnO_4^- is reduced so the two half reactions are:

$$MnO_4^- \rightarrow Mn^{2+}$$

$$I^- \rightarrow IO_3^-$$

Step 2. The Mn and I are already balanced in the half reactions.

Step 3. Add H_2O to balance the O in each half reaction:

$$MnO_4^- \rightarrow Mn^{2+} + 4\ H_2O$$

$$3\ H_2O + I^- \rightarrow IO_3^-$$

Step 4. Add H^+ to balance H in each half reaction:

$$8\ H^+ + MnO_4^- \rightarrow Mn^{2+} + 4\ H_2O$$

$$3\ H_2O + I^- \rightarrow IO_3^- + 6\ H^+$$

Step 5. Add e^- to balance the charge in each half reaction:

$$8\ H^+ + MnO_4^- + 5\ e^- \rightarrow Mn^{2+} + 4\ H_2O$$

$$3\ H_2O + I^- \rightarrow IO_3^- + 6\ H^+ + 6\ e^-$$

Notice the electrons are on opposite sides in the two half reactions

Step 6. Multiply the half reactions by coefficients and add together. All the electrons should cancel in the final reaction:

Multiplying the top by 6 and bottom by 5 will give 30 electrons in each reaction

$$6(8\ H^+ + MnO_4^- + 5\ e^- \rightarrow Mn^{2+} + 4\ H_2O)$$

$$5(3\ H_2O + I^- \rightarrow IO_3^- + 6\ H^+ + 6\ e^-)$$

Add and cancel common species

$$\cancel{48}\ H^+ + 6\ MnO_4^- + \cancel{15\ H_2O} + 5\ I^- + \cancel{30\ e^-} \rightarrow 6\ Mn^{2+} + 5\ IO_3^- + \cancel{30\ H^+} + \cancel{30\ e^-} + \cancel{24}\ H_2O$$

$$18\ H^+ + 6\ MnO_4^- + 5\ I^- \rightarrow 6\ Mn^{2+} + 5\ IO_3^- + 9\ H_2O$$

Step 7. The reaction is in basic solution so add OH^- to each side:

$$18\ OH^- + 18\ H^+ + 6\ MnO_4^- + 5\ I^- \rightarrow 6\ Mn^{2+} + 5\ IO_3^- + 9\ H_2O + 18\ OH^-$$

$$OH^- + H^+ \rightarrow H_2O$$

$$\mathbf{9\ H_2O + 6\ MnO_4^- + 5\ I^- \rightarrow 6\ Mn^{2+} + 5\ IO_3^- + 18\ OH^-}$$

Example 7.1.2

Balance the redox reaction that occurs when $S_2O_3^{2-}$ reacts with H_2O_2 to form $S_4O_6^{2-}$ and water in acidic solution.

Solution

Following the steps above:

Step 1. The $S_2O_3^{2-}$ is oxidized and the H_2O_2 is reduced so the two half reactions are:

$$S_2O_3^{2-} \rightarrow S_4O_6^{2-}$$

$$H_2O_2 \rightarrow H_2O$$

Step 2. Balance the S.

$$2\ S_2O_3^{2-} \rightarrow S_4O_6^{2-}$$

$$H_2O_2 \rightarrow H_2O$$

Step 3. Add H_2O to balance the O in each half reaction:

$$2\ S_2O_3^{2-} \rightarrow S_4O_6^{2-}$$

$$H_2O_2 \rightarrow 2\ H_2O$$

Step 4. Add H^+ to balance H in each half reaction:

$$2\ S_2O_3^{2-} \rightarrow S_4O_6^{2-}$$

$$2H^+ + H_2O_2 \rightarrow 2\ H_2O$$

Step 5. Add e^- to balance the charge in each half reaction:

$$2\ S_2O_3^{2-} \rightarrow S_4O_6^{2-} + 2\ e^-$$

$$2H^+ + 2\ e^- + H_2O_2 \rightarrow 2\ H_2O$$

Notice the electrons are on opposite sides in the two half reactions

Step 6. The number of electrons is already the same on both sides. Add and cancel common species:

$$2\ S_2O_3^{2-} + 2H^+ + \cancel{2\ e^-} + H_2O_2 \rightarrow S_4O_6^{2-} + \cancel{2\ e^-} + 2\ H_2O$$

$$\mathbf{2\ S_2O_3^{2-} + 2H^+ + H_2O_2 \rightarrow S_4O_6^{2-} + 2\ H_2O}$$

Note that we did not need to know the oxidation states of S or O in the reactants and products in order to balance the reaction. In this case, assigning the valence states is a bit complex, because $S_4O_6^{2-}$ contains sulfur in more than one oxidation state.

7.1: Balancing Redox Reactions is shared under a CC BY-NC-SA 4.0 license and was authored, remixed, and/or curated by LibreTexts.

- **Current page** is licensed CC BY-NC-SA 4.0.
- **4.2: Balancing Redox Reactions** by Chemistry 310 is licensed CC BY-SA 4.0. Original source: https://en.wikibooks.org/wiki/Introduction_to_Inorganic_Chemistry.

7.2: Electrochemical Potentials

In electrochemical cells, or in redox reactions that happen in solution, the thermodynamic driving force can be measured as the **cell potential**. Chemical reactions are spontaneous in the direction of -ΔG, which is also the direction in which the cell potential (defined as $E_{cathode}$ - E_{anode}) is positive. A cell operating in the **spontaneous** direction (for example, a battery that is discharging) is called a **galvanic cell**. A cell that is being driven in the **non-spontaneous** direction is called an **electrolytic cell**. For example, let us consider the reaction of hydrogen and oxygen to make water:

$$2\,H_{2\,(g)} + O_{2\,(g)} = 2\,H_2O_{(l)} \tag{7.2.1}$$

Thermodynamically, this reaction is spontaneous in the direction shown and has an overall standard free energy change (ΔG°) of -237 kJ per mole of water produced.

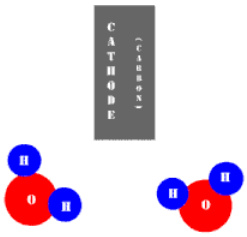
When this reaction occurs electrochemically in the spontaneous direction (e.g., in a hydrogen-air fuel cell), the two half cell reactions that occur are:

Anode: $H_{2\,(g)} \longrightarrow 2\,H^+_{(aq)} + 2\,e^-$

Cathode: $O_{2\,(g)} + 4\,H^+_{(aq)} + 4\,e^- \longrightarrow 2\,H_2O_{(l)}$

Here the anode is the negative electrode and the cathode is the positive electrode; under conditions of very low current density (where there are minimal resistive losses and kinetic overpotentials), the potential difference we would measure between the two electrodes would be 1.229 V.

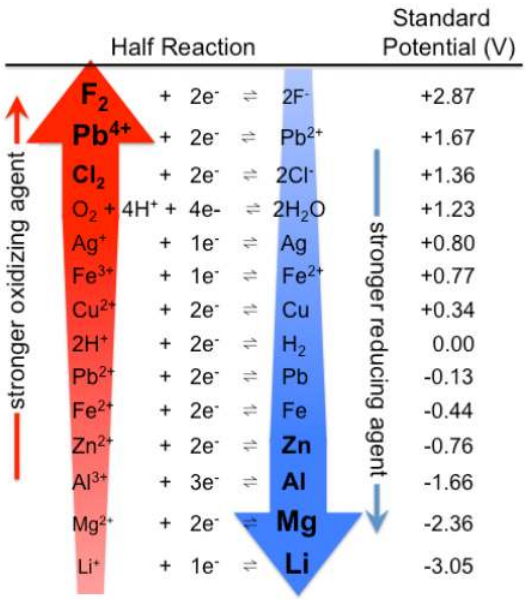
In an **electrolytic cell**, this reaction is run in reverse. That is, we put in electrical energy to split water into hydrogen and oxygen molecules. In this case, the half reactions (and their standard potentials) reverse. O_2(g) bubbles form at the anode and H_2(g) is formed at the cathode. Now the **anode** is the **positive** electrode and the **cathode** is **negative**. Electrons are extracted from the substance at the anode (water) and pumped into the solution at the cathode to make hydrogen. An animation of the cathode half reaction is shown below.



In both galvanic and electrolytic cells, **oxidation** occurs at the **anode** and **reduction** occurs at the **cathode**.

Half-cell potentials

As noted above, the equilibrium voltage of an electrochemical cell is proportional to the free energy change of the reaction. Because electrochemical reactions can be broken up into two half-reactions, it follows that the potentials of half reactions (like free energies) can be added and subtracted to give an overall value for the reaction. If we take the **standard hydrogen electrode** as our reference, i.e., if we assign it a value of zero volts, we can measure all the other half cells against it and thus obtain the voltage of each one. This allows us to rank redox couples according to their **standard reduction potentials** (or more simply their **standard potentials**), as shown in the table below.



Note that when we construct an electrochemical cell and calculate the voltage, we simply take the difference between the half cell potentials and do not worry about the number of electrons in the reaction. For example, for the displacement reaction in which silver ions are reduced by copper metal, the reaction is:

$$2\,Ag^{+}{}_{(aq)} + Cu_{(s)} = 2\,Ag_{(s)} + Cu^{2+}{}_{(aq)}$$

The two half-cell reactions are:

$$Ag^{+}_{(aq)} + e^{-} = Ag_{(s)} \quad +0.80V$$

$$Cu^{2+}_{(aq)} + 2e^{-} = Cu_{(s)} \quad +0.34V$$

and the standard potential $E^{o} = +0.80 - 0.34V = +0.46V$

The reason we don't need to multiply the Ag potential by 2 is that E^{o} is a measure of the free energy change **per electron**. Dividing the free energy change by the number of electrons (see below) makes E^{o} an **intensive property** (like pressure, temperature, etc.).

Relationship between E and ΔG. For systems that are in equilibrium, $\Delta G^{o} = -nFE^{o}_{cell}$, where n is number of moles of electrons per mole of products and F is the Faraday constant, ~96485 C/mol. Here the ^{o} symbol indicates that the substances involved in the reaction are in their standard states. For example, for the water electrolysis reaction, the standard states would be pure liquid water, H^{+} at 1M concentration (or more precisely, at unit activity), and O_2 and H_2(g) at 1 atmosphere pressure.

More generally (at any concentration or pressure), $\Delta G = -nFE$, where

$$E = E^{o} - \frac{RT}{nF} * lnQ \tag{7.2.2}$$

,

or at 298 K

$$E = E^{o} - \frac{0.0592}{n} * \log Q \tag{7.2.3}$$

where Q is the concentration ratio of products over reactants, raised to the powers of their coefficients in the reaction. This equation (in either form) is called the Nernst equation. The second term in the equation, when multiplied by -nF, is RT*lnQ. This is the free energy difference between ΔG and ΔG°. We can think of this as an entropic term that takes into account the positive entropy change of dilution, or the negative entropy change of concentrating a reactant or product, relative to its standard state.

7.2: Electrochemical Potentials is shared under a CC BY-NC-SA 4.0 license and was authored, remixed, and/or curated by LibreTexts.

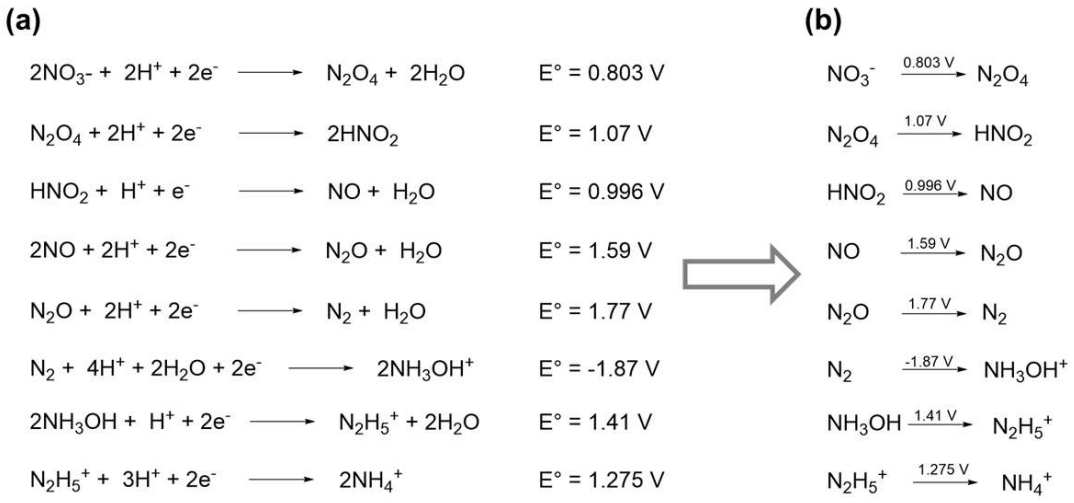
- **4.3: Electrochemical Potentials** by Chemistry 310 is licensed CC BY-SA 4.0. Original source: https://en.wikibooks.org/wiki/Introduction_to_Inorganic_Chemistry.

7.3: Latimer Diagrams

Latimer diagrams helpfully summarize elements' redox chemistry in a compact format.

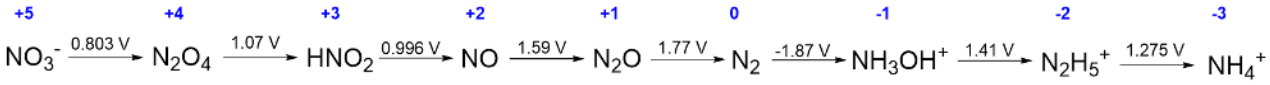
Latimer diagrams helpfully summarize elements' redox chemistry in a compact format.To see how Latimer diagrams work and why they are so useful it is helpful to start with an example. A selection of the redox reactions nitrogen is known to undergo in 1.0 *M* aqueous acid are given in Scheme **7.3.1*a***.

Scheme 7.3.1. (a) Full and (b) compact presentation of selected standard reduction half reactions for nitrogenous species in aqueous solution at pH 0.



The most important information in Scheme **7.3.1*a*** are the redox potentials and the identity of each nitrogen containing species. In fact, if the latter are known the number of electrons-, water molecules, and any H^+ (in acid) or OH^- (in base) involved in the reduction may be deduced by from the stoichiometry of the reaction. Consequently, the information in scheme **7.3.1*a*** may be presented more compactly by only giving the nitrogen-containing species and by writing the associated redox potential for each reaction above its reaction arrow, as is shown in Scheme **7.3.1*b***. Notice that in Scheme **7.3.1*b*** the product of each half reaction is the reactant in the succeeding one. Because of this it is possible to represent the entire sequence of redox reactions even more compactly by writing out the reactions on a single line, as shown in Scheme **7.3.2**.

Scheme 7.3.2. Simplified acidic Latimer diagram for nitrogen.



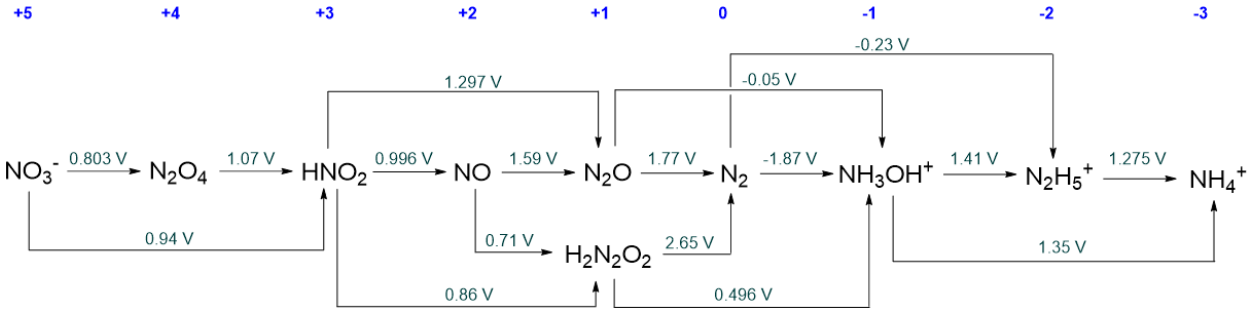
The type of diagram shown in Scheme **7.3.II** is called a **Latimer diagram**.

When interpreting Latimer diagrams it can be helpful to look for two pieces of information.

1. Whether the diagram corresponds to acidic (pH 0), basic (pH 14), or other solution conditions should be specified. In cases where it is not it is customary to assume the diagram refers to behavior in pH 0 aqueous solution. As redox chemistry can be pH dependent, a Latimer diagram is only valid at the specified pH.
2. The element's oxidation state, which makes it easier to keep track of the number of electrons involved in each reduction and to compare the redox behavior of related species. Oxidation states are commonly written above each chemical species, as is done in blue in Scheme **7.3.2**

When multiple pathways are available for interconverting two species in a Latimer diagram, these can be included by adding reaction arrows above and below the line. This is evident from the full pH 0 Latimer diagram for nitrogen given in Scheme **7.3.3**.

Scheme 7.3.3. Latimer diagram for nitrogen at pH 0. Redrawn from reference 1.



The diagram in Scheme **7.3.III** presents a large number of possible interconversions. However, every possible interconversion is not represented. For example, the reduction potential for the reduction of N_2O_4 to NO is not presented. This type of selectivity is common in Latimer diagrams but it does not necessarily mean that the missing conversions are not possible or that the potential has not been measured experimentally. Since $\Delta G^\circ = -nFE^\circ$ the potentials in Latimer diagrams are thermodynamic quantities and may always be calculated from solution thermodynamic parameters. In fact, some redox potentials reported in Latimer diagrams have been only determined that way. An example is the reduction potential of flourine,

$$F_2(g) + 2H^+ 2e^- \rightarrow 2HF \quad E^\circ = 3.053\ V \text{ in acid} \tag{7.3.1}$$

This potential has not been experimentally measured since F_2 is unstable in aqueous solution, reacting rapidly to give HF and O_2.

$$2\ F_2 + 2\ H_2O \xrightarrow{fast} 4\ HF + O_2 \tag{7.3.2}$$

When a potential is missing from a Latimer diagram it may always be calculated by constructing a thermodynamic cycle involving the known and unknown potentials, as explained in Note **7.3.1** at the bottom of this page.

Latimer Diagrams and Disproportionation.

Latimer diagrams permit are also useful for comparing elements' redox properties and determining whether a substance is stable to disproportionation. Latimer diagrams not only provide a compact summary of an element's redox chemistry, they also are useful for

1. Determining whether a species is thermodynamically unstable with respect to disproprotionation.

Disproprotionation occurs when a species reacts with itself to produce two or more stable products. For instance, in basic solution ReO_3 can undergo disproprotionation to ReO_4^- and $ReO_2{\cdot}2H_2O$.

$$2Re^{VI}O_3 + 2H_2O \rightarrow Re^{VII}O_4^- + Re^{V}O_2 \cdot 2H_2O \tag{7.3.3}$$

As with all redox reactions, disproprotionation reactions are thermodynamically favored when they possess a positive reaction potential. To see when this will be the case it is helpful to separate the disproprotionation reaction into its half reactions:

$$\text{Reduction}: Re^{VI}O_3 + H_2O + 2H^+e^- \rightarrow Re^{V}O_2 \cdot 2H_2O \quad E^\circ = -0.446V \tag{7.3.4}$$

$$\text{Oxidation}: Re^{VI}O_3 + H_2O \rightarrow Re^{VII}O_4^- + 2H^+ + e^- \quad E^\circ = +0.889V \tag{7.3.5}$$

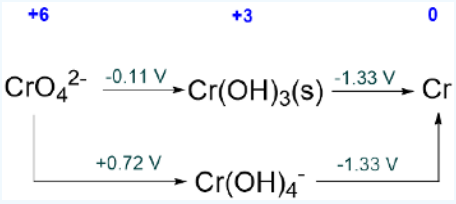
$$\text{Sum}: 2Re^{VI}O_3 + 2H_2O \rightarrow Re^{VII}O_4^- + Re^{V}O_2 \cdot 2H_2O \quad E^\circ = -0.446V + 0.889V = +0.443V \tag{7.3.6}$$

Notice that the disproprotionation of ReO_3 in basic solution is favored because the favorable reaction potential for ReO_3 oxidation is larger in magnitude than negative oxidation potential for ReO_3 reduction.

The ReO_3 disproportionation reaction is a specific instance of a general case. Any species possessing a standard reduction potential that is more positive than the standard reduction potential leading to their formation is thermodynamically unstable with respect to disproportionation. This situation is easy to recognize using a Latimer diagram; **species are unstable to disproportionation if the potential on their right is more positive than that on their left**.

Example 7.3.1

The Latimer diagram that has been reported for Cr in pH 14 aqueous solution is given below. Which, if any, species are unstable with respect to disproprotionation?

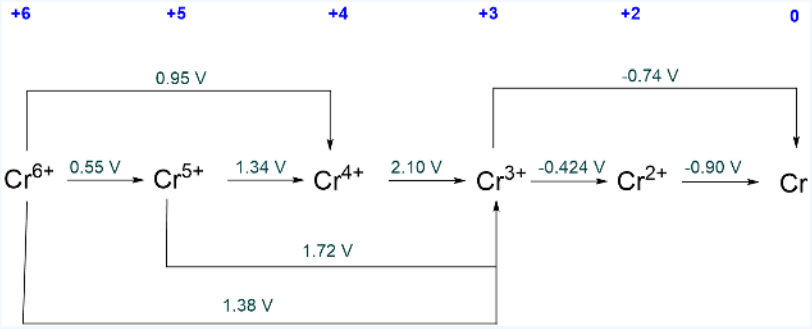


Solution

All of the species are stable with respect to disproprotionation since all the potentials on the right of all the Cr^{3+} intermediates are less than those on their left.

Example 7.3.2

The Latimer diagram for Cr in pH 0 aqueous solution is given below. Which, if any, species are unstable with respect to disproprotionation?

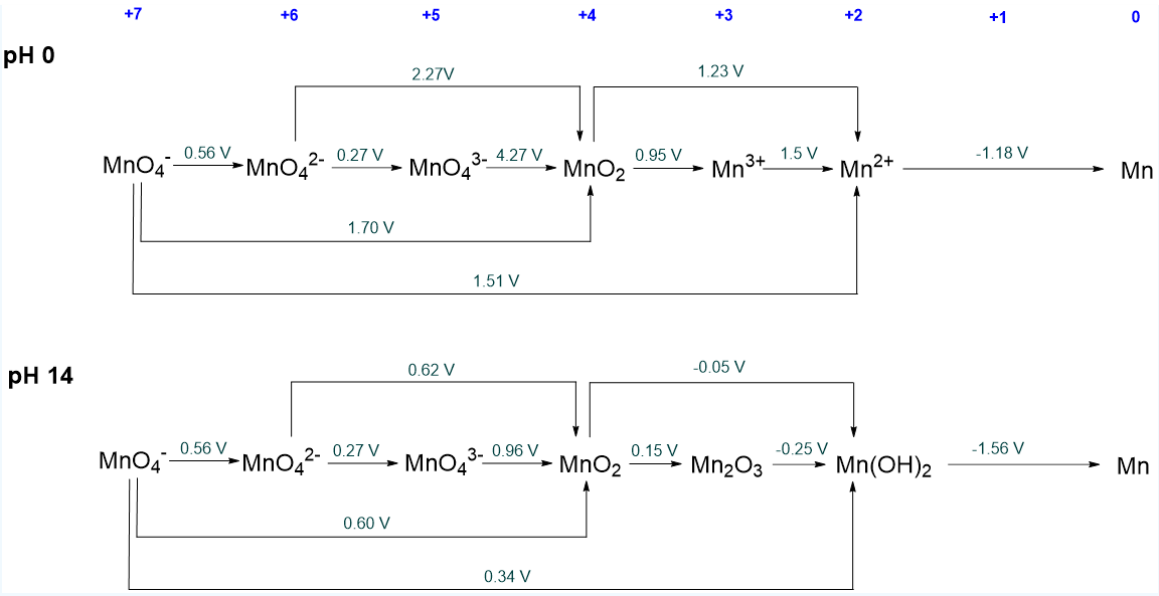


Solution

Both Cr^{5+} and Cr^{4+} are unstable towards disproprotionation since the potentials on their right (for their reduction) are greater than the potentials on their left (for their formation by reduction).

Example 7.3.3

Which manganese species are unstable with respect to disproportionation in aqueous solution under acidic and basic conditions? What will each of these metastable species give on sidproportionation? The Latimer diagrams for manganese are given below.



Solution

Under acidic conditions the following species are unstable with respect to disproprtionation:

- MnO_4^{2-} is unstable with respect to disproprtionation to MnO_4^- and MnO_2.
- MnO_4^{3-} is unstable with respect to MnO_4^{2-} and MnO_2. However, since MnO_4^{2-} is unstable with respect to disproprtionation the ultimate poducts of the disproprtionation will be MnO_4^- and MnO_2.
- Mn^{3+} is unstable towards disproprtionation to MnO_2 and Mn^{2+}.

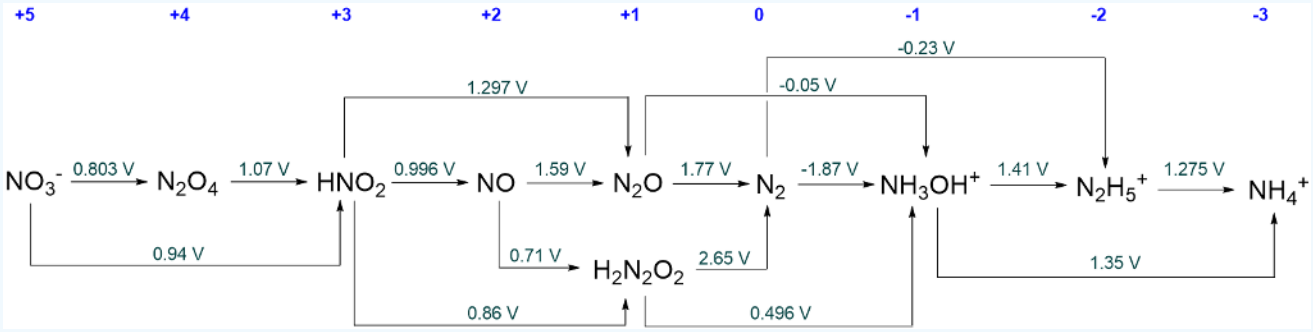
Under basic conditions the following species are unstable with respect to disproprtionation:

- MnO_4^{2-} is unstable with respect to disproprtionation to MnO_4^- and MnO_2.
- MnO_4^{3-} is unstable with respect to MnO_4^{2-} and MnO_2. However, since MnO_4^{2-} is unstable with respect to disproprtionation the ultimate poducts of the disproprtionation will be MnO_4^- and MnO_2.

Notice that the +3 oxidation state of Mn is stable under basic conditions but not acidic ones.

Exercise 7.3.1, part a

Which, if any of the species in nitrogen's Latimer diagram (Scheme **7.3.*III***, which for convenience is reproduced below) are unstable with respect to disproportionation?



Answer

They will be all the intermediate species for which the redox potential on their right is more positive than that on their left. These are N_2O_4, HNO_2, NO, N_2O, $H_2N_2O_2$, and NH_3OH^+.

Exercise 7.3.1, part b

As far as you are able, determine what each metastable nitrogen speices will disproprtionate to at pH 0.

Answer

Initially the metastable species will disproprtionate to give their immediate neighbors in the Latimer diagram.

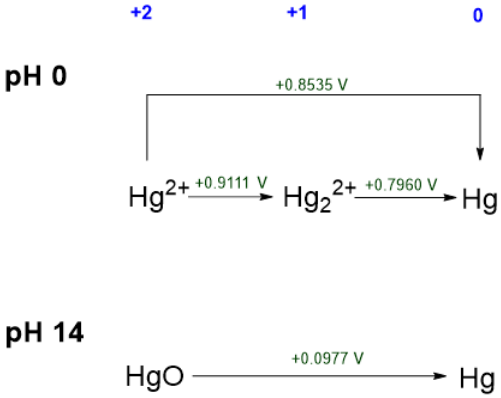
However, many of these neighbors are themselves metastable with respect to disproprtionation and so ultimately disproprtionation will only stop when species that are stable towards disproprtionation are reached.

In the case of N_2O_4, HNO_2, NO, N_2O, and $H_2N_2O_2$ disproprtionation will ultimately give NO_3^- and N_2.

For NH_3OH^+ disproprtionation will give N_2 and $N_2H_5^+$.

2. Comparing the redox chemistry of an element under different conditions (typically pH 0 and pH 14). This is well-illustrated by the Latimer diagrams of Chromium explored in Examples **7.3.1** and **7.3.2**. A simple instance involves the acidic and basic Latimer diagrams of mercury shown in Scheme **7.3.*IV***.

Scheme 7.3.*IV*. Latimer diagrams for mercury in aqueous solution.

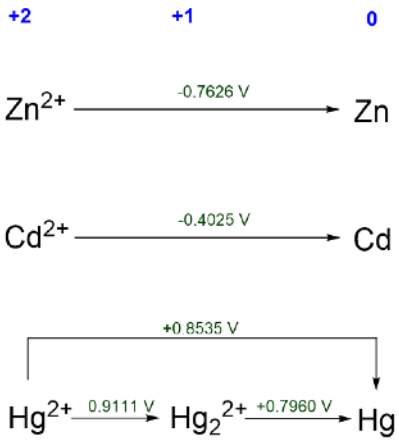


From Scheme **7.3.*IV*** several things are clear about mercury's redox chemistry under acidic and basic conditions:

- Mercury(I) ion, Hg_2^{2+}, is thermodynamically stable under acidic conditions, but it is not likely stable under basic conditions. This may be inferred from its absence in the pH 14 diagram, which suggests that it is not readily formed under basic conditions.
- Elemental mercury is the thermodynamically most stable form of the element under both acidic and basic conditions. This may be inferred that the standard reduction potential for all mercury +2 and +1 species is positive.
- In both its +1 and +2 oxidation states (Hg^{2+} and Hg_2^{2+} ions) mercury is a fairly powerful oxidant under acidic conditions (with \(\sf{E^{\circ}\) 0.796 - 0.9111 V). In contrast, under basic conditions the +2 form of mercury (HgO) is only a weak oxidant (E^{\circ}\) = 0.0977 V.
- All of the mercury species represented are thermodynamically stable towards disproprtionation.

3. Comparing the redox chemistry of different elements under similar conditions. For instance, the redox behavior of mercury and its cogeners in acid solution may be easily compared using the Latimer diagrams (Scheme **7.3.*V***.

Scheme 7.3.*V*. Latimer diagrams for the group 12 elements in pH 0 aqueous solution.



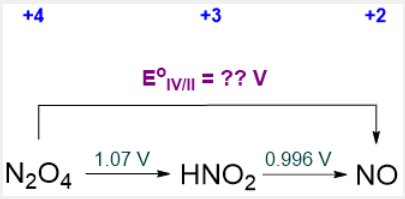
From Scheme **7.3.*V*** it is clear that Zn and Cd exhibit similar redox behavior. Both should dissolve at pH 0 to give dications. In contrast, elemental mercury should be stable towards acid. Mercury is also the only group 12 element for which the +1 oxidation state is stable.

As the examples above indicate Latimer diagrams are helpful summaries of elements' redox chemistry but it still requires a fair bit of careful reading to use them to make sense of trends in elements redox chemistry or to trace out the disproprtionation products of a given redox state. The published diagrams also tend to be limited to describing the redox chemistry of the elements under conditions of extreme pH. Fortunately, a variety of graphical representations of elements' redox chemistry have been developed that are particularly useful for estimating the dominant form of an element under a given set of conditions and for making sense of trends in elements' redox chemistry. These graphical methods will be described in the next two sections.

Note 7.3.1.

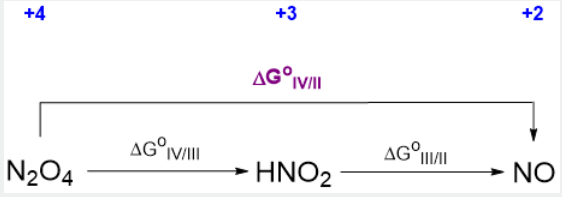
Potentials that are not shown in a Latimer diagram may always be calculated by constructing a **thermodynamic cycle**. Consider the interconversion of N_2O_4 to NO, $E^\circ_{IV/II}$, the value of which is not given in the standard Nitrogen Latimer diagram presented in Scheme **7.3.*sfII***. Part of that diagram is reproduced as Scheme **7.3.VI** below.

Scheme 7.3.VI. Partial Latimer diagram for nitrogen in acid.



The relevant thermodynamic cycle that may be used to calculate the unknown potential involves the free energies and is depicted in Scheme **7.3.VII**.

Scheme 7.3.VII. Thermodynamic cycle that may be used to determine $E^\circ_{N_2O_4 \rightarrow NO}$.



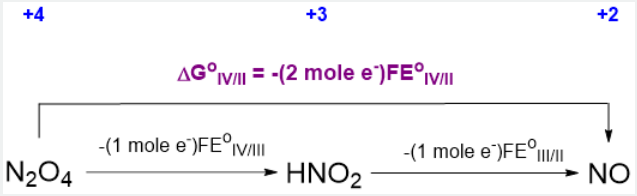
The free energies for each conversion step in the cycle is related to the corresponding potential by the relationship

$$\Delta G^\circ = nFE^\circ \qquad (7.3.7)$$

where n is the number of electrons involved in each step. Making this substitution the thermodynamic cycle above may be converted to the one shown in Scheme **7.3.VIII**.

https://chem.libretexts.org/@go/page/326228

Scheme 7.3.VIII. Thermodynamic cycle expressed in terms of standard potentials.



From Scheme **7.3.VIII** it may be seen that

$$\Delta G^{\circ}_{IV/II} = -(2\ mol\ e^{-})FE^{\circ}_{IV/II} = -(1\ mol\ e^{-})FE^{\circ}_{IV/III} - (1\ mol\ e^{-})FE^{\circ}_{III/II} \quad (7.3.8)$$

Cancelling the constant F and replacing the unknown potentials with the values in Scheme **7.3.VI** gives

$$-(2\ mol\ e^{-})E^{\circ}_{IV/II} = -(1\ mol\ e^{-})(1.07\ V) - (1\ mol\ e^{-})(0.996\ V) \quad (7.3.9)$$

from which $E^{\circ}_{IV/II}$ may be calculated, giving $E^{\circ}_{IV/II}$ = +1.033 V.

References

1. All standard reduction potentials are taken from Bard, A. J.; Parsons, R.; Jordan, J. Standard potentials in aqueous solution. M. Dekker: New York, 1985.

Contributors and Attributions

Stephen Contakes, Westmont College

Unless otherwise noted, all images and diagrams on this page are by Stephen Contakes and licensed under a Creative Commons Attribution 4.0 International License.

7.3: Latimer Diagrams is shared under a CC BY-NC-SA 4.0 license and was authored, remixed, and/or curated by LibreTexts.

- **8.1.4.1: Latimer Diagrams summarize elements' redox properties on a single line** by Stephen M. Contakes is licensed CC BY 4.0.
- **Current page** is licensed CC BY-NC-SA 4.0.

7.4: Frost Diagrams

Frost diagrams show how stable an element's redox states are relative to the free element

Frost diagrams represent how stable an element's redox states are relative to the free element. In a Frost diagram, a proxy for the free energy relative to that of the free element (oxidation state zero) is plotted as a function of oxidation state. To avoid ambiguity, sometimes the points are labeled with the identity of the chemical species involved.

The proxy used in place of the free energy is $\boldsymbol{NE°}$, sometimes expressed as $\boldsymbol{nE°}$. On this page $\boldsymbol{N}$ will be used in place of $\boldsymbol{n}$ to avoid confusion with the common use of $\boldsymbol{n}$ in redox chemistry to denote the number of electrons involved in individual oxidation or reduction reaction steps.

In Frost diagrams the quantity $\boldsymbol{NE°}$ is used since it is proportional to the standard free energy change for conversion of the free element to that oxidation state.

In $\boldsymbol{NE°}$

- $\boldsymbol{N}$ is the oxidation state.
- $\mathbf{E°}$ is the standard *reduction potential* associated with *interconversion between the free element and that oxidation state*.

For a proof that $\boldsymbol{NE°}$ is proportional to the free energy of an element's oxidation state and more information on how $\boldsymbol{NE°}$ may be calculated, see Note **7.4.1** at the end of this page.

Frost diagrams allow for rapid estimation of the relative stability of elements' redox states.

Because Frost diagrams directly show oxidation states' relative stabilities, they enable the rapid assessment of the following:

1. *The relative stability of an element's oxidation states under a given set of conditions.* Since $\boldsymbol{NE°}$ is a measure of thermodynamic stability, the lower its value the more stable the state. Moreover, since $\boldsymbol{NE°}$ measures stability relative to the free element, negative values of $\boldsymbol{NE°}$ indicate that a state is more stable than the element, while positive values indicate that the state is less stable.

Consider the Frost diagram for copper at pH 0 shown in Figure **7.4.1**.

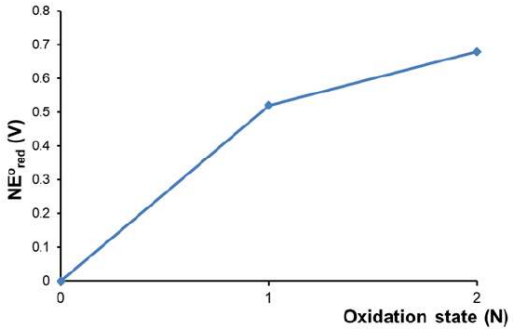


Figure **7.4.1**. Frost diagram for copper in aqueous acid. (CC BY-SA 4.0 International; Stephen Contakes)

As can be seen in Figure **7.4.1**, Cu^{+} and Cu^{2+} are both higher in free energy ($\propto \boldsymbol{NE°}$) than free Cu. This is consistent with copper's status as a noble metal that can only be dissolved in acid with the aid of oxidizing agents like O_2, H_2O_2, or NO_3^- (*e.g.*, as in HNO_3).

The acidic Frost diagram of Nickel shown in Figure **7.4.2** provides an example of a metal which dissolves in acid under otherwise nonoxidizing conditions (*i.e.*, without the aid of oxidants like O_2 or H_2O_2).

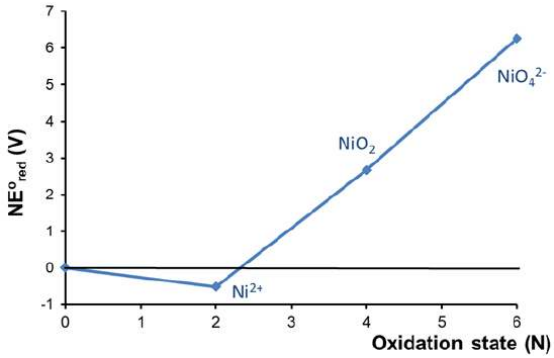


Figure **7.4.2**. Frost diagram for nickel in aqueous acid. (CC BY-SA 4.0 International; Stephen Contakes)

In this case the diagram shows that the Ni^{2+} oxidation state is lower in free energy than the free element, indicating that Ni spontaneously dissolves in acid to give Ni^{2+}. The diagram also reveals that higher nickel oxidation states (+4 and +6) are known but unstable with respect to both Ni^{2+} and free nickel.

Example 7.4.1. Interpreting a Frost Diagram

Consider the Frost diagram of Cr in acid shown in Figure **7.4.3**. What can be determined about the relative stability of chromium's oxidation states in acid?

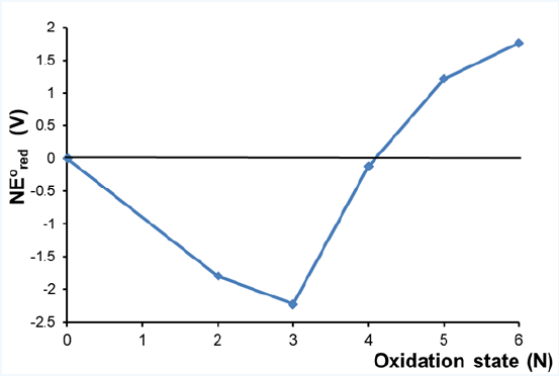


Figure **7.4.3**. Frost diagram for Cr in acidic solution. This work by Stephen Contakes is licensed under a Creative Commons Attribution 4.0 International License.

Solution

A cursory glance at the diagram reveals that

- The +3 oxidation state is the most stable since it has the lowest $\boldsymbol{NE°}$.
- The +2, +3, and +4 oxidation states are all more stable than the free element while the +5 and +6 oxidaton states are less stable.
- The diagram also reveals information about the susceptibility of the chromium species to undergo disproportionation and comproportionation reactions. For details see example 2.

2. *The redox behavior of an element under different conditions.* Consider the Frost diagrams of sulfur at pH 0 and 14 shown in Figure **7.4.4**.

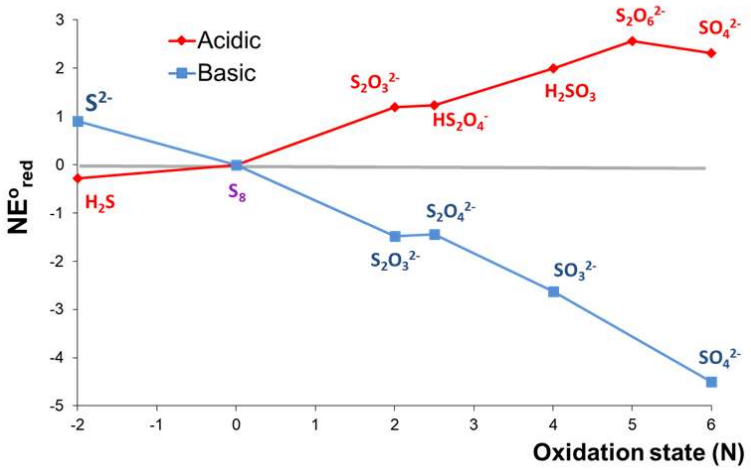


Figure **7.4.4**. Frost diagrams for sulfur at pH 0 and 14. This work by Stephen Contakes is licensed under a Creative Commons Attribution 4.0 International License.

As can be seen in Figure **7.4.4**, the relative stabilities of high and low sulfur oxidation states are roughly inverted between acidic and basic conditions. Under basic conditions, the oxidized forms of sulfur are all more stable than the free element, with sulfate most stable overall. In contrast, H_2S is the most stable form of sulfur under acidic conditions, while all the oxidized forms of sulfur are less stable than the free element.

3. *Comparison of the redox behavior of a series of elements.* Consider the pH 0 Frost diagrams of the group 6 elements shown in Figure **7.4.5**.

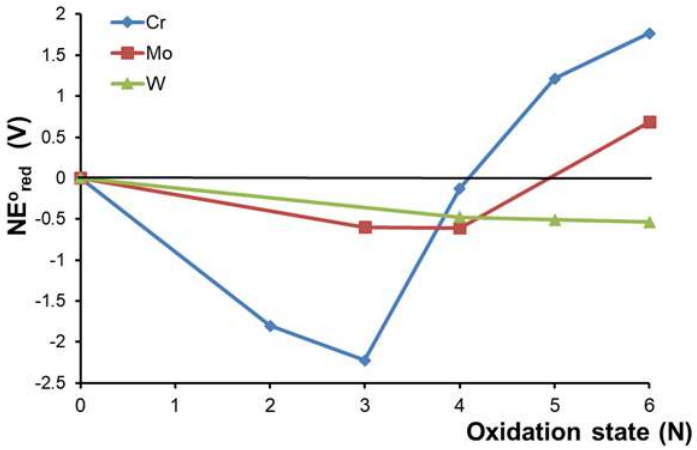


Figure **7.4.5**. Frost diagrams for the group 6 elements at pH 0. This work by Stephen Contakes is licensed under a Creative Commons Attribution 4.0 International License.

Several trends may be noted from the data in Figure **7.4.5**. First, on moving down the group from Cr to W, there is an increasing preference for higher oxidation states, with the most stable forms being Cr^{4+}, Mo^{4+}, and W^{6+}. Second, the coincidentally low stabilization of Cr^{4+} aside, the stabilization or destabilization of oxidation states relative to the free element decreases down a group - *i.e.*, Cr^{4+} is stabilized relative to Cr more so than Mo^{4+} is relative to Mo, and W^{6+} is stabilized relative to W even less so.

One of the most striking examples of the utility of Frost diagrams for comparing the empirical redox behavior of a series of elements involves the first row transition elements, the pH 0 Frost diagrams for which are shown in Figure **7.4.6**.[2,3] A number of trends may be noted. For example, as in the case of the group 6 elements, a shift in the most stable oxidation state may be observed, with Sc through Cr exhibiting a preference for the +3 oxidation state and Mn through Cu the +2 oxidation state. The diagram also shows that Sc through Mn lose all their valence electrons to form d^0 species, while similar species have not been observed for later members of the series (although an iron(VII) complex has been isolated[4] and iron's heavier cogeners, Ru and Os, do form d^0 species, RuO_4 and OsO_4).

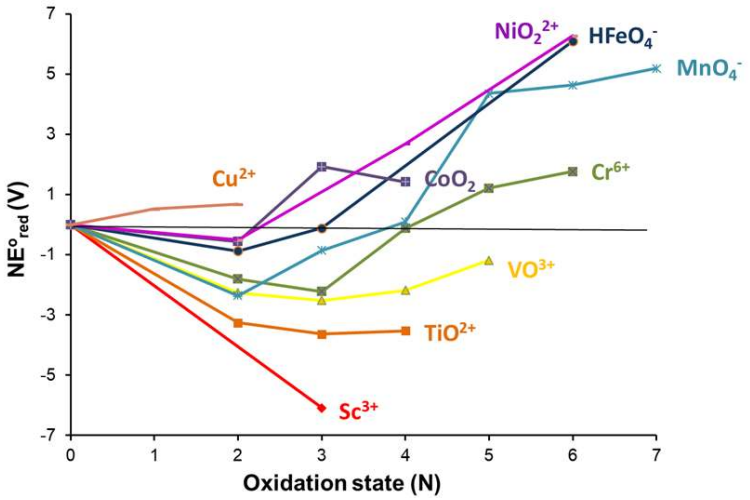


Figure **7.4.6**. Frost diagrams for the first transition series at pH 0. This work by Stephen Contakes is licensed under a Creative Commons Attribution 4.0 International License.

4. *Whether a redox state is unstable towards disproportionation* may be determined from the relative positions of that state and the states on either side of it on the diagram.[5] Remember that in **disproportionation** a species reacts with itself to produce two or more stable products. For example, NO can in principle undergo disproportionation in aqueous acid to give nitrate and N_2.

$$10\ NO\ +\ 2H_2O \rightarrow 3\ N_2 + 4\ NO_3^- + 4H^+$$

A Frost diagram can be used to determine when a redox state is unstable with respect to such disproportionation because the slope of a line between any two points is equal to the standard *reduction* potential interconverting the species involved. This means that *if a line is drawn between any two redox states then any states above the line will be unstable towards disproportionation to those states.* This is because in that case the potential for the reduction half reaction in the disproportionation will be more positive than the potential for the oxidation half reaction, rendering the overall reaction potential positive and so spontaneous. For proof of a specific example see Exercise 1.

To see how a disproportionation analysis may be performed using a Frost diagram, it can be helpful to examine the pH 0 Frost diagram for Cr more carefully. In this case the instability of Cr^{4+} and Cr^{5+} towards disproportionation may be revealed by placing a tie line drawn between the Cr^{3+} and Cr^{6+} states, as shown in Figure **7.4.7*a***.

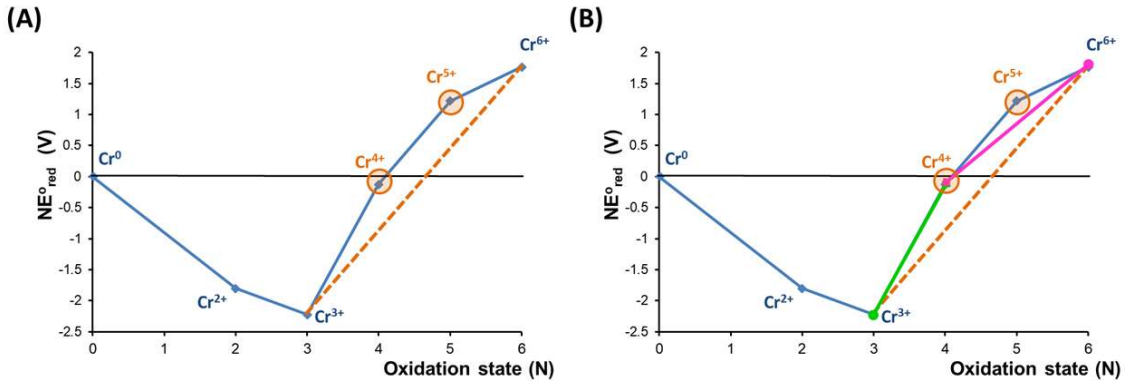


Figure **7.4.7**. (a) Frost diagram for Cr in acidic solution showing that the Cr^{4+} and Cr^{5+} states lie above a tie-line between the Cr^{3+} and Cr^{6+} states. (b) In the case of Cr^{4+}, disproportionation is favored because the $Cr^{4/3+}$ potential (slope of the green tie-line connecting the Cr^{4+} and Cr^{3+} states) is larger than the $Cr^{6/4+}$ potential (slope of the pink tie-line connecting Cr^{6+} and Cr^{4+}). This work by Stephen Contakes is licensed under a Creative Commons Attribution 4.0 International License.

As shown in Figure **7.4.7*a***, the Cr^{4+} and Cr^{5+} states are unstable towards disproportionation because they lie above a tie-line between the Cr^{3+} and Cr^{6+} states. This is because the potential for Cr^{4+} reduction to Cr^{3+}, represented by the tie-line connecting those species in Figure **7.4.7*b***, is larger than the potential for Cr^{6+} reduction to Cr^{4+}, as indicated by the lower slope of the tie-line connecting Cr^{6+} and Cr^{4+}.

Sometimes states which are unstable towards disproportionation correspond to concave down points on the Frost diagram. However, as this is not always the case, a systematic approach for finding metastable redox states is recommended. An example of such an approach is given in Example **7.4.2**.

✔ Example 7.4.2. Systematic identification of Mn redox states that are unstable towards disproportionation in acid.

Consider the Frost diagram of Mn in acid shown in Figure **7.4.8**. Which, if any, of manganese's oxidation states are unstable towards disproportionation at pH 0?

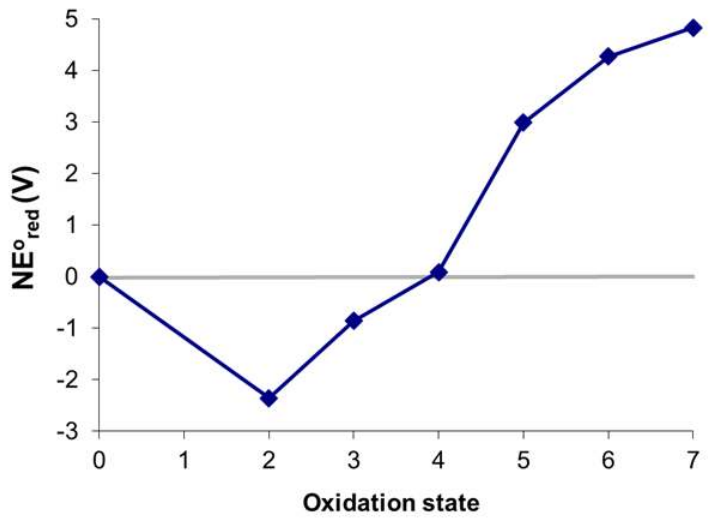
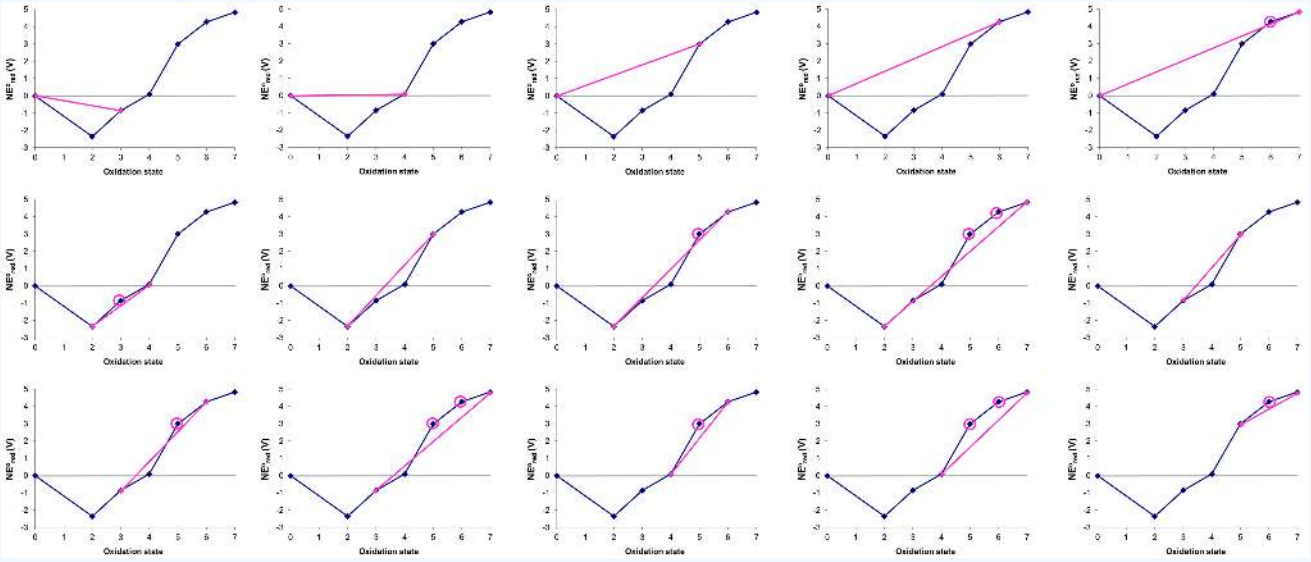


Figure **7.4.8**. Frost diagram for Mn at pH 0. This work by Stephen Contakes is licensed under a Creative Commons Attribution 4.0 International License.

Solution

States that are unstable towards disproportionation may be identified by drawing all the possible tie-lines between nonadjacent states spanning the lowest and highest oxidation states in the diagram, which in this case are Mn^0 and Mn^7. The possible permutations beginning with Mn^0 are given below



In the figure above the states that are thermodynamically unstable towards disproportionation (circled) are +3, +5, and +6.

The figure above by Stephen Contakes is licensed under a Creative Commons Attribution 4.0 International License.

4. Whether *two species are unstable towards comproportionation* may be assessed from the relative positions of the two species and all intervening species on the diagram. In **comproportionation,** two related species react to give a more stable product. For example, NO and hydrazinium ion can in principle undergo comproportionation in aqueous acid to give N_2.

$$2\ NO\ +\ N_2H_5^+ \rightarrow 2\ N_2\ +\ 2\ H_2O\ +\ H^+$$

A Frost diagram may be used to determine when two species are thermodynamically favored to undergo comproportionation. *Draw a line between the two species on the diagram. If there are states below the line then the two species are unstable towards forming those states by comproportionation.* Again, it can be helpful to examine the acidic condition Frost diagram for Cr to see how this works. In this case consider a tie line drawn between the Cr^{4+} and Cr^{2+} states, as shown in Figure **7.4.9*a***.

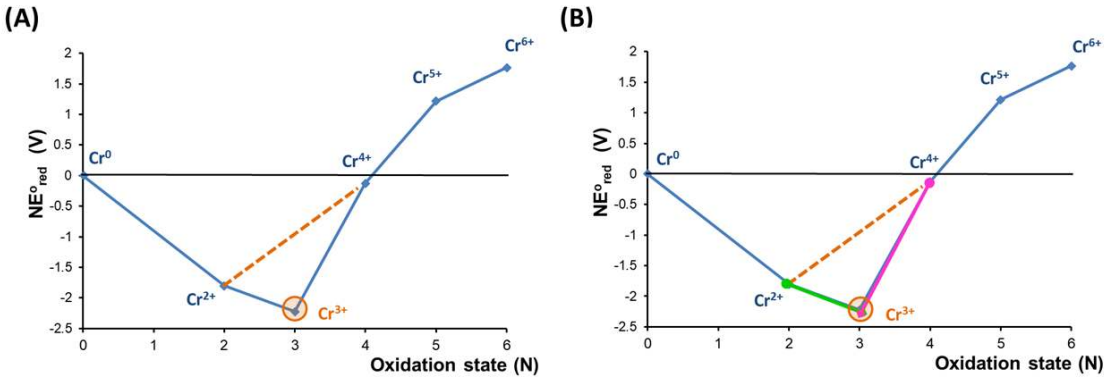


Figure **7.4.9**. (a) Frost diagram for Cr in acidic solution showing that the Cr^{3+} redox state lies below a tie-line between the Cr^{2+} and Cr^{4+} states. (b) The slope of the green line connecting the Cr^{2+} and Cr^{3+} states is less than that of the pink line connecting the Cr^{3+} and Cr^{4+} states. This work by Stephen Contakes is licensed under a Creative Commons Attribution 4.0 International License.

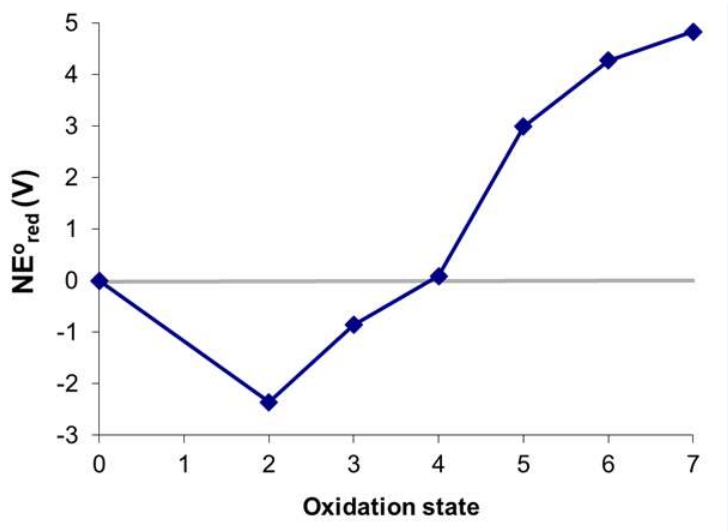
As shown in Figure **7.4.9*a***, a mixture of Cr^{2+} and Cr^{4+} is unstable towards comproportionation because on the Frost diagram Cr^{3+} lies below the tie-line between Cr^{2+} and Cr^{4+}. This shows that the standard potential for reduction of Cr^{3+} to Cr^{2+} (equal to the slope of the line connecting those states) is less than that for the reduction of Cr^{4+} to Cr^{3+} (again, equal to that of the line connecting the states), in consequence of which the potential for comproportionation will be positive.

The analysis of a Frost diagram for all favorable comproportionations is similar to the analysis used to detect species that are unstable towards disproportionation. The products of thermodynamically favored comproportionations are sometimes concave up points but since this is not always the case a systematic approach should be used. An example is given in Example **7.4.3**.

✔ Example **7.4.3**. Systematic identification of pairs of Mn redox states that are unstable towards comproportionation in acid.

Consider the Frost diagram of Mn at pH 0 in Figure **7.4.8** of Example **7.4.2**, which for convenience is reproduced below. Which, if any, pairs of manganese species are unstable towards comproportionation under these conditions and what products could they form?

https://chem.libretexts.org/@go/page/326229



Solution

The possible tie-lines were already identified in Exercise 7.4.2.

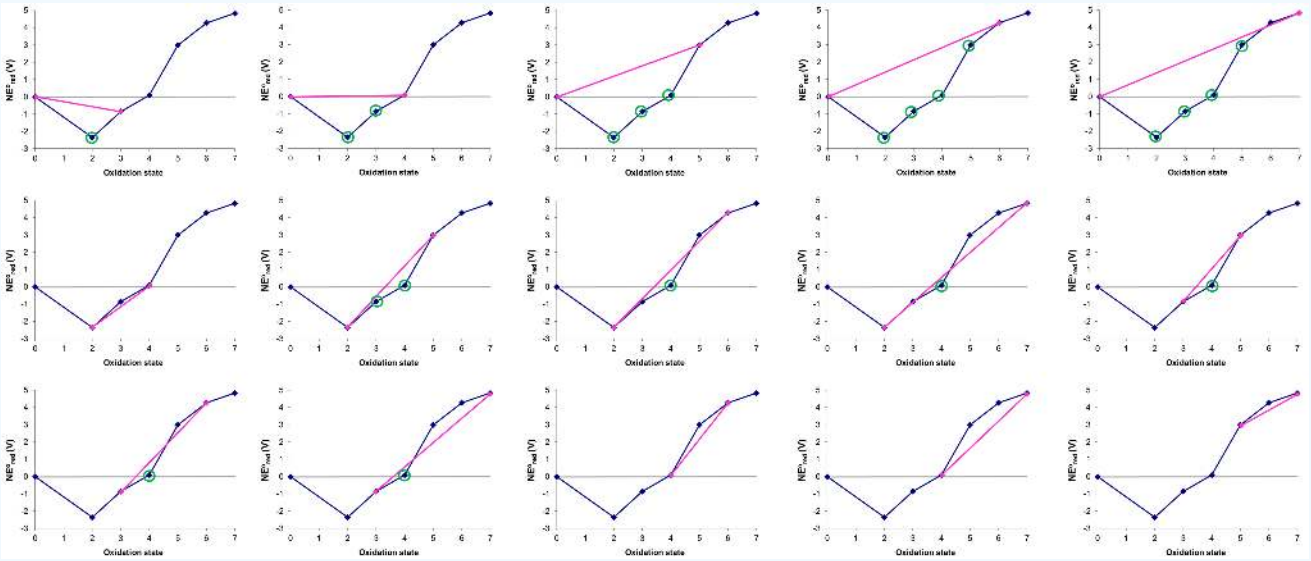


Figure above: the lower energy comproportionation products that species form are circled in green. The comproportionations identified involve the following pairs of oxidation states:

- 0 and +3 → +2
- 0 and +4 → +2 or +3
- 0 and +5 → +2 or +3 or +4
- 0 and +6 → +2 or +3 or +4 or +5
- 0 and +7 → +2 or +3 or +4 or +5
- +2 and +5 → +3 or +4
- +2 and +6 → +4
- +2 and +7 → +4
- +3 and +5 → +4
- +3 and +6 → +4
- +3 and +7 → +4

The figures in this problem are by Stephen Contakes and licensed under a Creative Commons Attribution 4.0 International License.

Additional analysis is needed to determined the thermodynamic product of many comproportionation reactions - but fortunately such an analysis is not necessary to understand the descriptive chemistry of the elements.

This list of possible comproportionation reactions identified in Example **7.4.3** raises several interesting questions:

1. When more than one comproportionation product is possible, which one(s) will be formed?

    In this case the answer is that all species can be formed in thermodynamically favored comproportionation reactions. However, the system still only possesses one state of lowest free energy. For example, depending on the stoichiometry of the reactants, the lowest energy products that can be formed from a mixture of Mn^0 and Mn^{VII} might be a mixture of Mn^{II} and Mn^{IV}. The identification of this state in a given case is complicated and involves minimizing the system energy subject to the constraints of a mass and charge balance. Fortunately, such an analysis is not needed to make sense of the chemistry of the elements.

    What should be noted is that if a comproportionation product can itself undergo a comproportionation reaction with one or more reactants, then that reaction can take place in solution. For instance, if the case of the comproportionation between Mn^0 and Mn^{IV} produces Mn^{III}, then that Mn^{III} can undergo an additional comproportionation reaction with Mn^0 to give Mn^{II}.

2. What happens if a species formed by comproportionation is susceptible to disproportionation?

    If the conditions allow, then that species will undergo disproportionation. Again, thermodynamic measures like those shown on Frost diagrams describe what can happen, not what will occur under a given set of conditions.

Exercises

? Exercise 7.4.1

Using the simplified Latimer diagram for Cr in aqueous acid, reproduced below, verify that the disproportionation of Cr^{4+} to Cr^{3+} and Cr^{6+} is thermodynamically spontaneous.



Answer

The disproportionation of Cr^{4+} to Cr^{3+} and Cr^{6+} is the sum of two processes:

$$Cr^{4+}\text{reduction}: \quad Cr^{4+} + e^- \rightarrow Cr^{3+} \qquad E^\circ_{Cr^{4/3+}} = 2.10\ V$$

$$Cr^{4+}\text{oxidation}: \quad Cr^{4+} \rightarrow Cr^{6+} + 2e^- \qquad E^\circ = -E^\circ_{Cr^{6/4+}}$$

$$\text{Sum}: \quad 3Cr^{4+} + \rightarrow Cr^{6+} + 2Cr^{3+} \qquad E^\circ_{disproportionation} = E^\circ_{Cr^{4/3+}} - E^\circ_{Cr^{6/4+}}$$

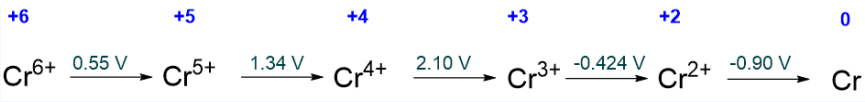
The value of $E^\circ_{Cr^{6/4+}}$ is just the sum of the $Cr^{6/5+}$ and $Cr^{5/4+}$ reduction potentials (+0.55 V + 1.34 V) or +1.89 V. Consequently,

$$E^\circ_{disproportionation} = E^\circ_{Cr^{4/3+}} \qquad E^\circ_{Cr^{6/4+}} = 2.10\ V - 1.89\ V = +0.21\ V$$

which is spontaneous.

? Exercise 7.4.2

Using the simplified Latimer diagram for Cr in aqueous acid, reproduced below, verify that the comproportionation of Cr^{2+} and Cr^{4+} to Cr^{3+} is thermodynamically spontaneous.



Answer

The comproportionation of Cr^{2+} and Cr^{4+} to Cr^{3+} is the sum of two processes:

$$Cr^{4+}\text{reduction}: \quad Cr^{4+} + e^- \rightarrow Cr^{3+} \qquad E^\circ_{Cr^{4+}/3+} = +2.10\ V$$

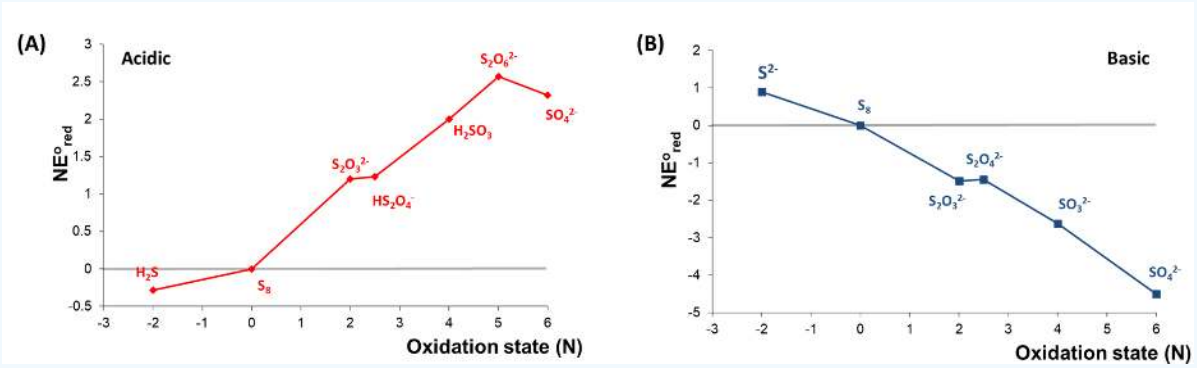
$$Cr^{2+}\text{oxidation}: \quad Cr^{2+} \rightarrow Cr^{3+} + e^- \qquad E^\circ = -E^\circ_{Cr^{3+}/2+} = -(-0.424\ V) = +0.424\ V$$

$$\text{Sum}: \quad Cr^{2+} + Cr^{4+} \rightarrow 2Cr^{3+} \qquad E^\circ_{\text{comproportionation}} = +2.10\ V + 0.424\ V = +2.524\ V$$

Since $E^\circ_{\text{comproportionation}}$ is positive, the comproportionation is spontaneous.

? Exercise 7.4.3. Identifying thermodynamically favored comproportionation and disproportionation reactions.

The Frost diagrams for acidic and basic solutions of sulfur are given below.



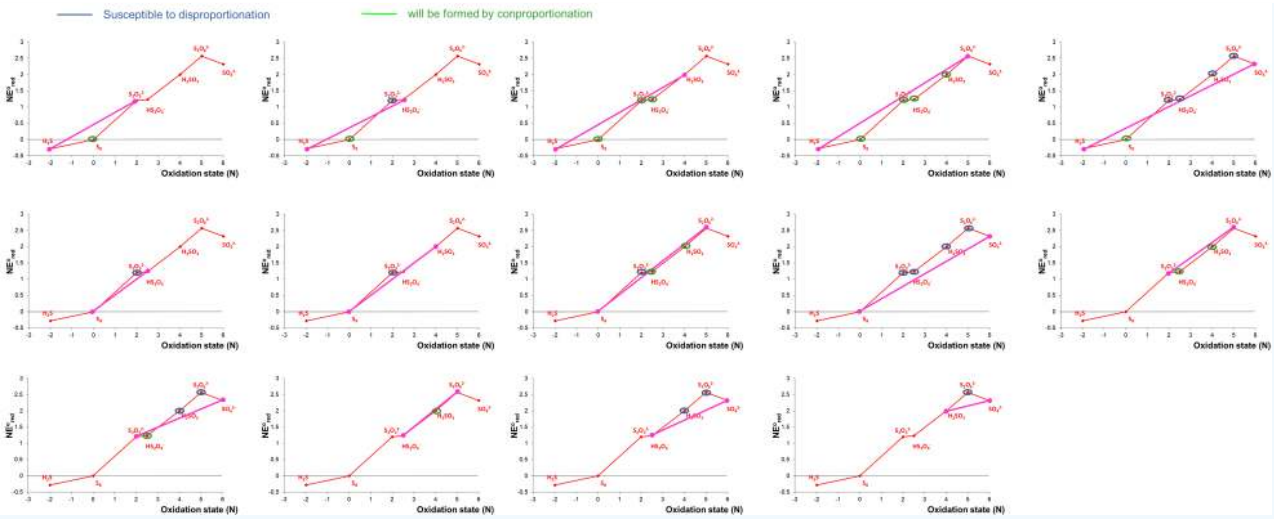
a. Identify any species that are unstable towards disproportionation under acidic or basic conditions.

b. Identify any species that can be formed by comproportionation under acidic or basic conditions.

Answer

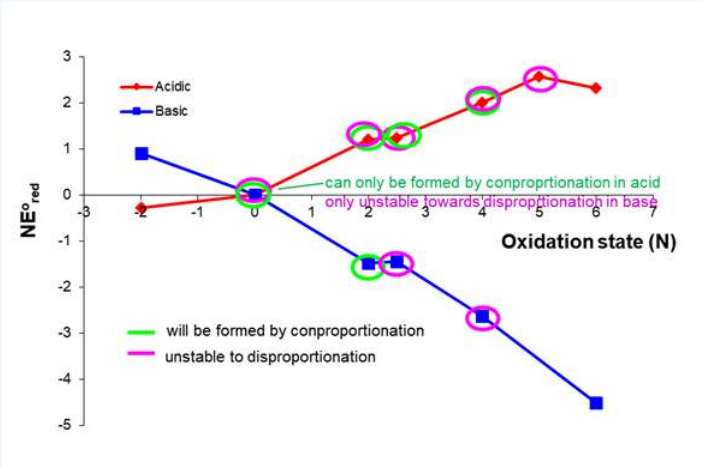
The species that are unstable towards *disproportionation* and *comproportionation* may be identified by constructing tie-lines between nonadjacent redox states and identifying any that fall above and below these lines. Species that are unstable to *disproportionation* will lie above a line; those that will be formed by *comproportionation* will lie below a line. Note that some species may be both capable of being formed by *comproportionation* and thermodynamically susceptible to *disproportionation.*

The possible tie-lines for acidic conditions are as follows:



Notice that in some cases it can be difficult to tell whether a point lies above or below a tie-line based on inspection alone. In these cases the relevant redox potential should be calculated to determine whether disproportionation or comproportionation is thermodynamically favored or even if the process is free energy neutral.

The possibilities for basic conditions are left as an exercise for the reader. To check your work the species that are susceptible to disproportionation and those which can be formed by comproportionation are summarized below.



The figures in this problem are by Stephen Contakes and licensed under a Creative Commons Attribution 4.0 International License.

Appendix

Note 7.4.1. Construction of a Frost Diagram.

Since Frost diagrams use $NE°$ as a proxy for oxidation free energy, the construction of a Frost diagram is a matter of calculating $NE°$ for each oxidation state, where $E°$ is the standard potential for the *formation of that oxidation state (O.S.)* from the free element. To see why this quantity is a useful proxy for oxidation state free energy, it is helpful to recognize that the oxidation state, N, is formally equal to the number of electrons that are *removed* from the free element when the oxidation state is formed. From this perspective the formation of negative oxidation states by adding electrons to the free element may be thought of as involving the removal of a negative number of electrons.

The free energy for formation of each oxidation state is determined as follows:

1. For free elements the free energy of formation, $E°$, and consequently $NE°$, are all by definition zero.

2. Negative oxidation states are formed by reduction of the free element

$$E + ne^- \rightarrow E^{O.S.} \qquad E^\circ = E^\circ_{red}$$

so that

$$\Delta G^\circ = -nFE^\circ_{red}$$

in which F is the Faraday constant.

In this case the oxidation state, N, is equal to $-n$ and the expression above becomes

$$\Delta G^\circ_{red} = F \times (NE^\circ)$$

from which it can also be seen why NE° is a useful proxy for free energy. It is proportional to ΔG°:

$$NE^\circ = \frac{1}{F}\Delta G^\circ_{red}$$

3. Positive oxidation states are formed by oxidation of the element:

$$E \rightarrow E^{O.S.} + ne^- \qquad E^\circ_{ox} = E^\circ = -E^\circ_{red}$$

in which the number of electrons, n, is equal to the oxidation state, N and

$$E^\circ_{ox} = E^\circ = -E^\circ_{red}$$

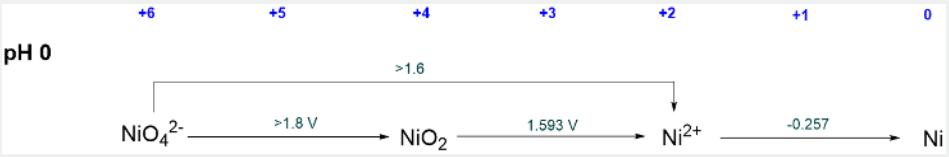
So that for positive oxidation states,

$$\Delta G^\circ_{ox} = -\Delta G^\circ_{red} = -(-nFE^\circ_{red}) = F(NE^\circ)$$

This is the same expression obtained for the negative oxidation states in which NE° is proportional to ΔG°.

From considering these cases, it is clear that as long as N is taken as the oxidation state and E° the associated standard reduction potential, the quantity NE° is proportional to the free energy.

In many cases the relevant standard reduction potentials are neither tabulated nor listed in the element's Latimer diagram. For example, in nickel's acidic Latimer diagram, the standard reduction potentials for formation of elemental Ni from NiO_4^{2-} or NiO_2 are not given.



In such cases the relevant reduction potential should be calculated by taking into account the fact that since free energy is a state function, the free energy for formation of that oxidation state is the sum of the free energies of the steps described in the Latimer diagram. For example, to calculate NE° for the formation of NiO_2, the following relationship may be used:

$$\Delta G^\circ_{NiO_2 \rightarrow Ni} = \Delta G^\circ_{NiO_2 \rightarrow Ni^{2+}} + \Delta G^\circ_{Ni^{2+} \rightarrow Ni}$$

But since $\Delta G = -nFE^\circ$, where n is the number of electrons involved in each reduction, then the above expression may be rewritten as

$$-n_{e^-,NiO_2 \rightarrow Ni} FE^\circ_{NiO_2 \rightarrow Ni} = -n_{e^-,NiO_2 \rightarrow Ni^{2+}} FE^\circ_{NiO_2 \rightarrow Ni^{2+}} + -n_{e^-,Ni^{2+} \rightarrow Ni} FE^\circ_{Ni^{2+} \rightarrow Ni}$$

which may be further simplified by cancelling the Faraday constant, F, from both sides, giving an expression for the desired value of NE°:

$$-n_{e^-,NiO_2 \rightarrow Ni} E^\circ_{NiO_2 \rightarrow Ni} = NE^\circ_{Ni \rightarrow NiO_2} = -n_{e^-,NiO_2 \rightarrow Ni^{2+}} E^\circ_{NiO_2 \rightarrow Ni^{2+}} + -n_{e^-,Ni^{2+} \rightarrow Ni} E^\circ_{Ni^{2+} \rightarrow Ni}$$

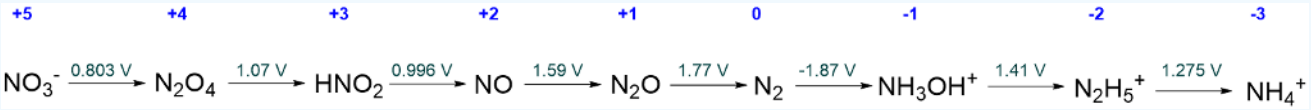
From this expression the value of $NE^\circ_{Ni \rightarrow NiO_2}$ may be calculated by inserting the relevant reduction potentials and number of electrons:

$$NE^{\circ}_{Ni \rightarrow NiO_2} = 2 \times (+1.593V) + 2 \times (-0.257V) = +2.672V$$

For complex cases it can be helpful to tabulate the calculations, as is done in the following example.

Example 7.4.1: Calculating the Frost Diagram for nitrogen in aqueous acid

Calculate the acidic Frost diagram of nitrogen from the information given in the simplified acidic Latimer diagram for nitrogen given below.



Solution

The value of NE° for each oxidation state is calculated as described in Table 7.4.1. The calculations follow the procedure:

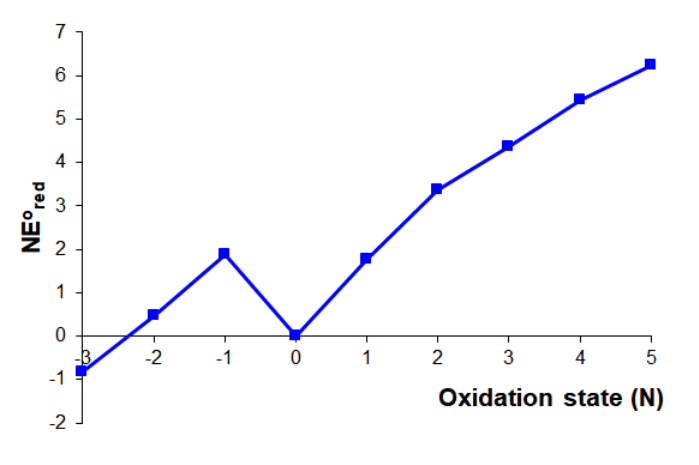
1. Set NE° = 0 for the free element.
2. Use NE° = O.S. × associated E° to calculate NE° for the lowest positive and negative oxidation states.
3. Iteratively use $NE^{\circ} = NE^{\circ}_{\text{last step}} + NE^{\circ}_{\text{one lower oxidation state}}$ to calculate NE° for all higher oxidation states.

Table 7.4.1: Calculation of NE° for each oxidation state of nitrogen.

Oxidation State	Step	$\mathbf{\Delta_r G^\circ}$ =	Calculated as the sum of the steps	Notes
5	$N_2 \rightarrow NO_3^-$	$5 \times (E^\circ_{NO_3^- \rightarrow N_2})$	$\mathbf{N_2 \rightarrow N_2O_4 \rightarrow NO_3^-}$ $NE^\circ = 1 \times E^\circ_{NO_3^- \rightarrow N_2O_4} + 4 \times E^\circ_{N_2O_4 \rightarrow N_2}$ $NE^\circ = 1 \times E^\circ_{NO_3^- \rightarrow N_2O_4} + NE^\circ_{+4\ O.S.}$ $NE^\circ = 1 \times 0.803V + 5.426V = 6.229V$	Calculate NE° for the +4 oxidation state, NO, first. Then use it in this calculation.
4	$N_2 \rightarrow N_2O_4$	$4 \times (E^\circ_{N_2O_4 \rightarrow N_2})$	$\mathbf{N_2 \rightarrow HNO_2 \rightarrow N_2O_4}$ $NE^\circ = 1 \times E^\circ_{HNO_2 \rightarrow NO} + 3 \times E^\circ_{HNO_2 \rightarrow N_2}$ $NE^\circ = 1 \times E^\circ_{N_2O_4 \rightarrow HNO_2} + NE^\circ_{+3\ O.S.}$ $NE^\circ = 1 \times 1.07V + 4.356V = 5.426V$	Calculate NE° for the +3 oxidation state, NO, first. Then use it in this calculation.
3	$N_2 \rightarrow HNO_2$	$3 \times (E^\circ_{HNO_2 \rightarrow N_2})$	$\mathbf{N_2 \rightarrow NO \rightarrow HNO_2}$ $NE^\circ = 1 \times E^\circ_{HNO_2 \rightarrow NO} + 2 \times E^\circ_{NO \rightarrow N_2}$ $NE^\circ = 1 \times E^\circ_{NO \rightarrow N_2O} + NE^\circ_{+2\ O.S.}$ $NE^\circ = 1 \times 0.996V + 3.36V = 4.356V$	Calculate NE° for the +2 oxidation state, NO, first. Then use it in this calculation.
2	$N_2 \rightarrow NO$	$2 \times (E^\circ_{NO \rightarrow N_2})$	$\mathbf{N_2 \rightarrow N_2O \rightarrow NO}$ $NE^\circ = 1 \times E^\circ_{NO \rightarrow N_2O} + 1 \times E^\circ_{N_2O \rightarrow N_2}$ $NE^\circ = 1 \times E^\circ_{NO \rightarrow N_2O} + NE^\circ_{+1\ O.S.}$ $NE^\circ = 1 \times 1.59V + 1.77V = 3.36V$	Calculate NE° for the +1 oxidation state, NO, first. Then use it in this calculation.
1	$N_2 \rightarrow N_2O$	$1 \times E^\circ_{N_2O \rightarrow N_2}$	$\mathbf{N_2 \rightarrow N_2O}$ $NE^\circ = 1 \times E^\circ_{N_2O \rightarrow N_2}$ $NE^\circ = 1 \times +1.77V = +1.77V$	
0	None	0 V	$NE^\circ = 0V$ by definition.	Defined as 0 V
-1	$N_2 \rightarrow NH_3OH^+$	$(-1) \times E^\circ_{N_2 \rightarrow NH_3OH^+}$	$\mathbf{N_2 \rightarrow NH_3OH^+}$ $NE^\circ = (-1)E^\circ_{N_2 \rightarrow NH_3OH^+}$ $NE^\circ = (-1) \times (-1.87V) = +1.87V$	
-2	$N_2 \rightarrow N_2H_5^+$	$(-2) \times E^\circ_{N_2 \rightarrow N_2H_5^+}$	$\mathbf{N_2 \rightarrow NH_3OH^+ \rightarrow N_2H_5^+}$ $NE^\circ = (-1) \times E^\circ_{N_2 \rightarrow NH_3OH^+} + (-1)E^\circ_{NH_3OH^+ \rightarrow N_2H_5^+}$ $NE^\circ = NE^\circ_{-1\ O.S.} + (-1)E^\circ_{NH_3OH^+ \rightarrow N_2H_5^+}$ $NE^\circ = +1.87V + (-1) \times 1.41V = 0.46V$	Calculate NE° for the -1 oxidation state, NO, first. Then use it in this calculation.

Oxidation State	Step	$NE°$ =	Calculated as the sum of the steps	Notes
-3	$N_2 \rightarrow NH_4^+$	$(-3) \times E°_{N_2 \rightarrow NH_4^+}$	$N_2 \rightarrow N_2H_5^+ \rightarrow NH_4^+$ $NE° = (-1)E°_{N_2 \rightarrow N_2H_5^+} + (-1)E°_{N_2H_5^+ \rightarrow NH_4^+}$ $NE° = NE°_{-2\ O.S.} + (-1)E°_{N_2H_5^+ \rightarrow NH_4^+}$ $NE° = +0.46V + (-1) \times 1.275V = -0.815V$	Calculate $NE°$ for the -2 oxidation state, NO, first. Then use it in this calculation.

The resulting Frost diagram for acidic aqueous nitrogen is given below.



The figure above by Stephen Contakes is licensed under a Creative Commons Attribution 4.0 International License.

References

1. Unless otherwise noted all potentials are for strongly acidic solutions and taken from Bard, A. J.; Parsons, R.; Jordan, J. Standard potentials in aqueous solution. M. Dekker: New York, 1985.
2. This diagram is inspired by the similar diagram given in M. Gerken Chemistry 2810 Lecture Notes. Posted on classes.uleth.ca/200501/chem2...lecture_20.pdf
3. The estimated $Fe^{6/3+}$ reduction potential of +2.07 V used to construct the Frost diagram for the first row transition metals is taken from Huheey, J. E.; Keiter, E. A.; Keiter, R. L., Inorganic chemistry : principles of structure and reactivity. 4th ed.; HarperCollins College Publishers: New York, NY, 1993; pg. 596.
4. Lu, J.-B.; Jian, J.; Huang, W.; Lin, H.; Li, J.; Zhou, M., Experimental and theoretical identification of the Fe(vii) oxidation state in FeO4−. Physical Chemistry Chemical Physics 2016, 18 (45), 31125-31131.
5. In some pedagogical applications only the adjoining states are considered.

Contributors and Attributions

- Stephen Contakes, Westmont College

7.4: Frost Diagrams is shared under a CC BY-NC-SA 4.0 license and was authored, remixed, and/or curated by LibreTexts.

- **8.1.4.2: Frost Diagrams show how stable element's redox states are relative to the free element** by Stephen Contakes is licensed CC BY 4.0.

7.5: Pourbaix Diagrams

Pourbaix Diagrams plot electrochemical stability for different redox states of an element as a function of pH.[3] As noted above, these diagrams are essentially phase diagrams that map the conditions of potential and pH (most typically in aqueous solutions) where different redox species are stable. We saw a simple example of such a diagram in section 4.2 for H_2O. Typically, the water redox reactions are plotted as dotted lines on these more complicated diagrams for other elements.

The lines in Pourbaix diagrams represent redox and acid-base reactions, and are the parts of the diagram where two species can exist in equilibrium. For example, in the Pourbaix diagram for Fe below, the horizontal line between the Fe^{3+} and Fe^{2+} regions represents the reaction $\mathbf{Fe^{3+}_{(aq)} + e^- = Fe^{2+}_{(aq)}}$, which has a standard potential of +0.77 V. While we could use standard potentials for all these lines, in practice Pourbaix diagrams are usually plotted for lower ion concentrations (often 1 mM) that are more relevant to corrosion and electrochemical experiments.

Example: Iron Pourbaix diagram

Areas in the Pourbaix diagram mark regions where a single species (Fe^{2+}(aq), Fe_3O_4(s), etc.) is stable. More stable species tend to occupy larger areas.

Lines mark places where two species exist in equilibrium.

- **Pure redox** reactions are **horizontal** lines - these reactions are not pH-dependent
- **Pure acid-base** reactions are **vertical** lines - these do not depend on potential
- Reactions that are **both** acid-base and redox have a slope of -0.0592 V/pH x # H^+/# e^-)

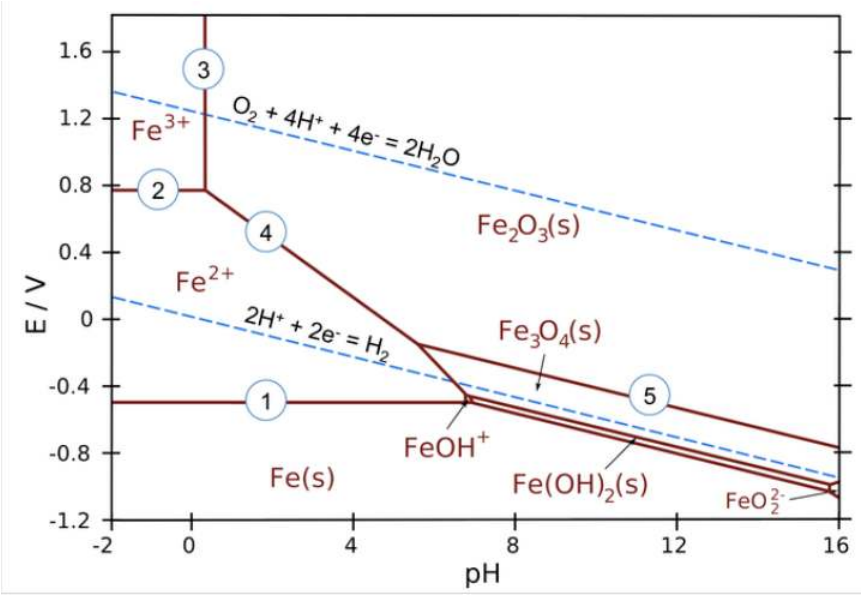


Figure **7.5.1**: Pourbaix diagram for iron at ionic concentrations of 1.0 mM. (CC BY-SA 3.0 Unported; Metallos via Wikipedia)

Examples of equilibria in the iron Pourbaix diagram (numbered on the plot):

1. $\mathbf{Fe^{2+} + 2e^- \longrightarrow Fe_{(s)}}$ (pure redox reaction - no pH dependence)
2. $\mathbf{Fe^{3+} + e^- \longrightarrow Fe^{2+}}$ (pure redox reaction - no pH dependence)
3. $\mathbf{2Fe^{3+} + 3H_2O \longrightarrow Fe_2O_{3\,(s)} + 6H^+}$ (pure acid-base, no redox)
4. $\mathbf{2Fe^{2+} + 3H_2O \longrightarrow Fe_2O_{3\,(s)} + 6H^+ + 2e^-}$ (slope = -59.2 x 6/2 = -178 mV/pH)
5. $\mathbf{2Fe_3O_{4\,(s)} + H_2O \longrightarrow 2H^+ + 2e^-}$ (slope = -59.2 x 2/2 = -59.2 mV/pH)

The water redox lines have special significance on a Pourbaix diagram for an element such as iron. Recall that liquid water is stable *only* in the region between the dotted lines. Below the H_2 line, water is unstable relative to hydrogen gas, and above the O_2 line, water is unstable with respect to oxygen. For active metals such as Fe, the region where the pure element is stable is typically below the H_2 line. This means that iron metal is unstable in contact with water, undergoing reactions:

$Fe_{(s)} + 2H^+ \longrightarrow Fe^{2+}{}_{(aq)} + H_2$ (in acid)

$fe_{(s)} + 2H_2O \longrightarrow Fe(OH)_{2\,(s)} + H_2$ (in base)

Iron (and most other metals) are also thermodynamically unstable in air-saturated water, where the potential of the solution is close to the O_2 line in the Pourbaix diagram. Here the spontaneous reactions are:

$4Fe_{(s)} + 3O_2 + 12H^+ \longrightarrow 4Fe^{3+} + 6H_2O$ (in acid)

\(\ce{4Fe_{(s)} + 3O2 -> 2Fe2O3_{(s)} (in base)

Corrosion and passivation. It certainly sounds bad for our friend Fe: unstable in water, no matter what the pH or potential. Given enough time, it will all turn into rust. But iron (and other active metals) can corrode, or can be stabilized against corrosion, depending on the conditions. Because our civilization is dependent on the use of active metals such as Fe, Al, Zn, Ti, Cr... for practically everything, it is important to understand this, and we can do so by referring to the Pourbaix diagram.

The **corrosion** of iron (and other active metals such as Al) is indeed rapid in parts of the Pourbaix diagram where the element is oxidized to a soluble, ionic product such as Fe^{3+}(aq) or Al^{3+}(aq). However, solids such as Fe_2O_3, and especially Al_2O_3, form a protective coating on the metal that greatly impedes the corrosion reaction. This phenomenon is called **passivation.**

Draw a vertical line through the iron Pourbaix diagram at the pH of tap water (about 6) and you will discover something interesting: at slightly acidic pH, iron is quite unstable with respect to corrosion by the reaction:

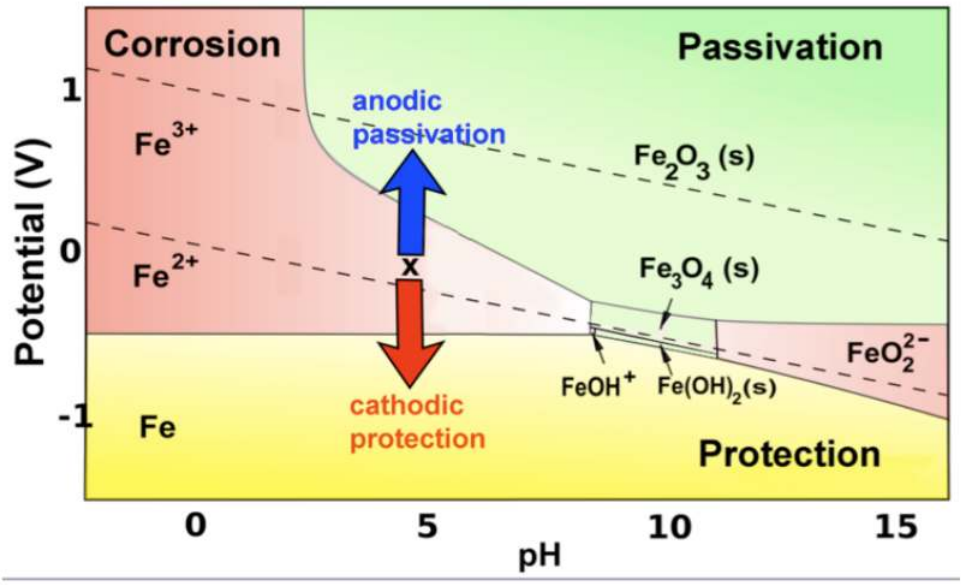
$$Fe_{(s)} + 2H^+ \longrightarrow Fe^{2+}{}_{(aq)} + H_2 \tag{7.5.1}$$

but *only in water that contains relatively little oxygen*, i.e., in solutions where the potential is near the H_2 line. Saturating the water with air or oxygen moves the system closer to the O_2 line, where the most stable species is Fe_2O_3 and the corrosion reaction is:

$$4Fe_{(s)} + 3O_2 \longrightarrow 2Fe_2O_{3\,(s)} \tag{7.5.2}$$

This oxidation reaction is orders of magnitude slower because the oxide that is formed *passivates* the surface. Therefore iron corrodes much more slowly in oxygenated solutions.

More generally, iron (and other active metals) are passivated whenever they oxidize to produce a solid product, and corrode whenever the product is ionic and soluble. This behavior can be summed up on the color-coded Pourbaix diagram below. The red and green regions represent conditions under which oxidation of iron produces soluble and insoluble products, respectively.



In the yellow part of the diagram, an active metal such as iron can be **protected** by a second mechanism, which is to bias it so that its potential is below the oxidation potential of the metal. This **cathodic protection** strategy is most frequently carried out by connecting a more active metal such as Mg or Zn to the iron or steel object (e.g., the hull of a ship, or an underground gas pipeline) that is being protected. The active metal (which must be higher than Fe in the activity series) is also in contact with the solution and slowly corrodes, so it must eventually be replaced. In some cases a battery or DC power supply - the anode of which oxidizes water to oxygen in the solution - is used instead to apply a negative bias.



The white patches visible on the ship's hull are zinc block sacrificial anodes.

Another common mode of corrosion of iron and carbon steel is **differential aeration.** In this case, part of the iron object - e.g., the base of a bridge, or the drill in an oil rig - is under water or in an anoxic environment such as mud or soil. The potential of the solution is close to the H_2 line in the Pourbaix diagram, where Fe can corrode to Fe^{2+} (aq). Another part of the iron object is in the air, or near the surface where water is well oxygenated. At that surface oxygen can be reduced to water, $O_2 + 4H^+ + 4e^- = 2\ H_2O$. The conductive iron object completes the circuit, carrying electrons from the anode (where Fe is oxidized) to the cathode (where O_2 is reduced). Corrosion by differential aeration can be rapid because soluble ions are produced, and the reaction has a driving force of over 1 V. Iron or carbon steel that is subjected to frequent weathering, such as the cast iron bridge and lamppost shown below, is corroded on the surface by differential aeration.



Rusty cast iron bridge and lamppost, North Ayrshire, Scotland

Differential aeration is involved in the formation of a rust ring around wet areas of cast iron, e.g., an iron frying pan left partially submerged in water for a day or more. (You may have seen this mechanism of corrosion in action when you did not get to the dirty dishes right away). Under the water, Fe is oxidized to soluble Fe^{2+}, and at the water line O_2 is reduced to H_2O. As Fe^{2+} ions diffuse towards the water surface, they encounter oxygen molecules and are oxidized to Fe^{3+}. However Fe^{3+} is insoluble at neutral pH and deposits as rust, typically just below the water line, forming the rust ring.

7.5: Pourbaix Diagrams is shared under a CC BY-NC-SA 4.0 license and was authored, remixed, and/or curated by LibreTexts.

- **4.6: Pourbaix Diagrams** by Chemistry 310 is licensed CC BY-SA 4.0. Original source: https://en.wikibooks.org/wiki/Introduction_to_Inorganic_Chemistry.

CHAPTER OVERVIEW

8: Coordination Chemistry- Structure and Isomers

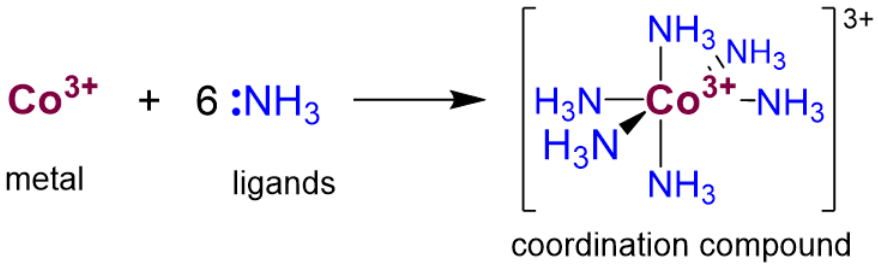
Introduction

Coordination compounds are important to all areas of chemistry, engineering, the life and environmental sciences, and beyond. In the synthetic laboratory catalytic amounts of coordination compounds enable organic chemists to synthesize new compounds selectively and in high yield under mild condition. Applied industrially, coordination compound catalysts serve as vital catalysts that facilitate the conversion of raw petrochemical or bio-derived feedstocks into useful industrial and consumer products. Without them life as we know it would be impossible as many biochemical systems are coordination complexes. Examples include the hemoglobin which transports oxygen around our bodies and the myoglobin which stores it, the photosystems which harvest light and use light energy in photosynthesis, the constituents of the respiratory chain, and many of the enzymes involved in the expression and transmission of genetic information. In studying coordination chemistry you are about to take your first steps into a vast and exciting world.

What is a Coordination Compound?

Coordination compounds consist of one or more metals bound to one or more Lewis base ligands. For example, hexaminechromium(III) ion is a coordination complex in which six ammonia ligands coordinate a Co^{3+} ion, as shown in Scheme 8.1.

Scheme 8.1: Formation of hexaminechromium(III) ion from Co^{3+} and NH_3.



(8.1)

Such complexes are called coordination compounds or complexes because the ligand-metal bond may be thought of as a coordinate covalent bond in which both of the bonding electrons come from the ligand, which is then said to coordinate the metal. This coordinate covalent model is a very useful formalism for understanding the basic features of coordination chemistry, although it does not always accurately reflect the actual details of the bonding in every coordination complex. Nevertheless, even in those cases where the simple coordinate covalent bond model breaks down the coordinate covalent bond concept supplies the language sophisticated models employ to describe the more complex bonding involved.

Additional Important Terms

Some of the common widely terms that follow from the coordinate covalent model of bonding in coordination complexes include

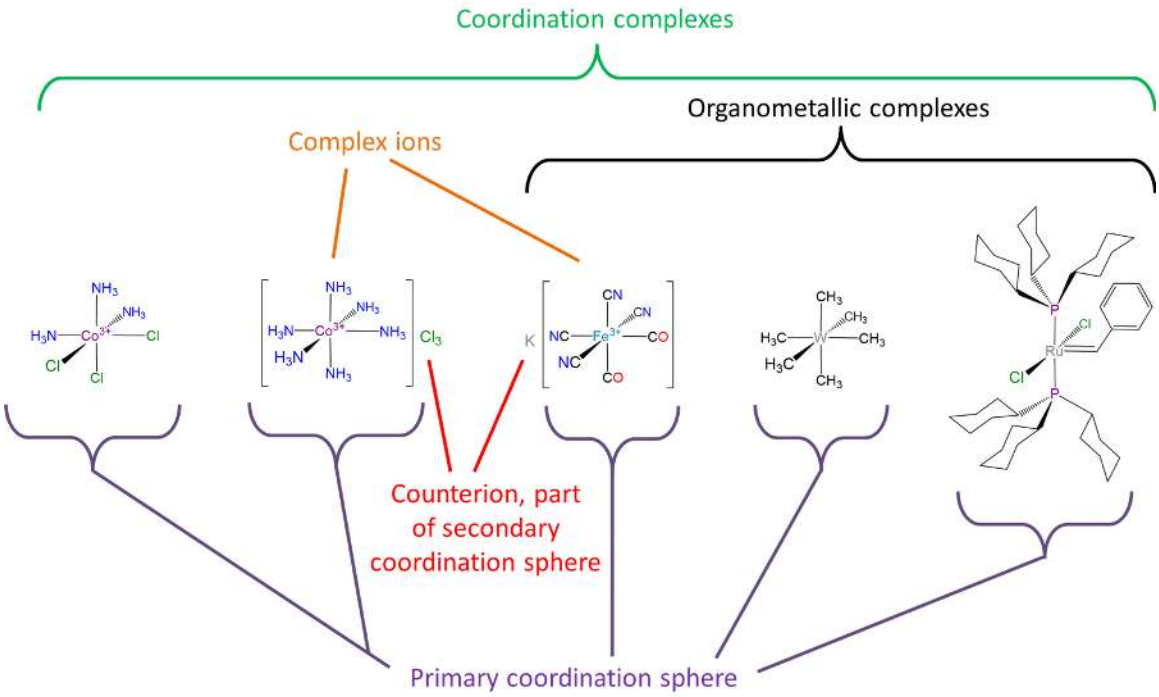
- Coordination compounds are also called **coordination complexes**, **metal complexes**, or just **complexes**. The term **complex** refers to coordination compounds' composite nature, in that they may be thought of as comprised of multiple ligand and metal ion parts that can be restored by breaking the coordinate covalent bonds holding the complex together. This is in contrast to inorganic or organic molecules which are more commonly thought about as whole molecules held together by the sharing of electrons contributed by all the atoms.
- Coordination complexes that are ions are called **complex ions.**
- Ligands bound to the coordination complex are said to reside in the **primary** or **inner coordination sphere**. These bound ligands are not readily exchangeable, in contrast to nearby counterions and solvent molecules, which are said to reside in the

secondary or **outer coordination sphere**.

- The portion of the complex contributing the electron pairs is said to be the **donor** and the portion which receives them the **acceptor**. In conventional coordination compounds the ligand is the donor and the metal the acceptor. In these cases it would be equally convenient to refer to the ligand donor as the Lewis base and the metal acceptor as the Lewis acid. However, in more complex bonding scenarios there may be multiple electron pair donation and acceptance interactions taking place between each pair of atoms and donor-acceptor language will be more convenient.
- The number of ligand sites donating lone pairs to the central atom is referred to as the **coordination number**. For most complexes this will just be equal to the number of ligand atoms bound to the metal. In simple complexes it is just equal to the number of ligands. For instance, the cobalt in Scheme **8.1** has a coordination number of six.
- Although technically compounds with metal-carbon bonds are coordination complexes term coordination complex is sometimes used to refer to complexes which do not possess metal-carbon bonds in their primary coordination sphere. Complexes which possess metal-carbon bonds are called organometallic compounds instead. The use of the terms organometallic and coordination to distinguish organometallic compounds from other types of coordination compounds is often convenient since many organometallic ligands engage in more than simple σ donor acceptor coordinate covalent bond formation with the metal center. However, this is true of some wholly inorganic ligands too so it should always be kept in mind that organometallic compounds are just a type of coordination compound and that inorganic ligands can in principle be tuned in interact with a metal center in much the same way an organic ligand does.

A summary of some of the concepts and terms used to describe coordination compounds is given in Scheme **8.2**.

Scheme **8.2**: Some terms used to describe coordination compounds. This work by Stephen Contakes is licensed under a Creative Commons Attribution 4.0 International License.



Contributors and Attributions

Stephen Contakes, Westmont College

Unless otherwise noted, all line drawings on this page are by Stephen Contakes and licensed under a Creative Commons Attribution 4.0 International License.

Learning Objectives

- Determine the correct name and chemical formula for a metal complex from its structure
- Identify the denticity of a ligand from its structure
- Recognize and name the different types of isomers in metal complexes

Thumbnail image is the structure of tris(oxalato)ferrate(III) from symmetry@otterbein

8.1: History

8.2: Nomenclature and Ligands

8.3: Coordination Numbers and Structures

8.4: Isomerism

8: Coordination Chemistry- Structure and Isomers is shared under a CC BY-NC-SA 4.0 license and was authored, remixed, and/or curated by LibreTexts.

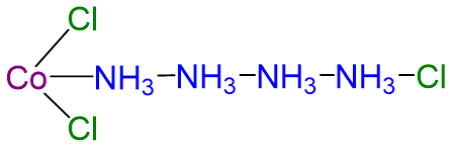
8.1: History

History of the Coordination Compounds

Coordination compounds have been known and used since antiquity; one of the oldest synthetic pigments is the blue pigment Egyptian blue, a copper complex of formula $CaCuSi_4O_{10}$ used by the Egyptians since the third Millenium B.C. (in ancient China the Ba analogue, Han blue, was discovered independently). The blue color of Egyptian blue is due to interlocked $Cu(Si_2O_7)_4$ units in which each copper is coordinated by four O atoms in a square planar arrangement. Later, in 1706, the Berlin painter Diesbach would discover another deep blue pigment, Prussian blue: $\mathbf{KFe_2(CN)_6}$.

Despite their long use, the chemical nature of coordination compounds was unclear for a number of reasons. For example, many compounds called "double salts" were known, such as $\mathbf{AlF_3 \cdot 3\,KF}$, $\mathbf{Fe(CN)_2 \cdot 4\,KCN}$, and $\mathbf{ZnCl_2 \cdot 2\,CsCl}$, which were combinations of simple salts in fixed and apparently arbitrary ratios. Why should $\mathbf{AlF_3 \cdot 3\,KF}$ exist but not $\mathbf{AlF_3 \cdot 4\,KF}$ or $\mathbf{AlF_3 \cdot 2\,KF}$? And why should a 3:1 KF:$\mathbf{AlF_3}$ mixture have different chemical and physical properties than either of its components? Similarly, adducts of metal salts with neutral molecules such as ammonia were also known—for example, $\mathbf{CoCl_3 \cdot 6\,NH_3}$, which was first prepared sometime before 1798. Like the double salts, the compositions of these adducts exhibited fixed and apparently arbitrary ratios of the components. For example, $\mathbf{CoCl_3 \cdot 6\,NH_3}$, $\mathbf{CoCl_3 \cdot 5\,NH_3}$, $\mathbf{CoCl_3 \cdot 4\,NH_3}$, and $\mathbf{CoCl_3 \cdot 3\,NH_3}$ were all known and had very different properties, but despite all attempts, chemists could not prepare $\mathbf{CoCl_3 \cdot 2\,NH_3}$ or $\mathbf{CoCl_3 \cdot NH_3}$.

Although the chemical composition of such compounds was readily established by existing analytical methods, their chemical nature was puzzling and highly controversial. The major problem was that what we now call valence (i.e., the oxidation state) and coordination number were thought to be identical. As a result, highly implausible (to modern eyes at least) structures were proposed for such compounds. Of these the most influential was the Blomstrand-Jørgensen chain theory of bonding in coordination compounds, which predicted the "Chattanooga choo-choo" model for $CoCl_3{\cdot}4NH_3$ shown in Scheme **8.1.I**.



Scheme **8.1.I**. Blomstrand-Jørgensen chain theory model of bonding in $CoCl_3{\cdot}4NH_3$.

Nevertheless, this theory was not wholly illogical and, in fact, explained much of the analytical data on coordination compounds available to chemists of the time. This data included the electrical conductivity of aqueous solutions of these compounds, which was roughly proportional to the number of ions formed per mole, and the number of free chloride ions present, which could be determined by precipitating them gravimetrically as AgCl. In the case of $CoCl_3{\cdot}4NH_3$, two ions and one chloride were produced when the compound was dissolved in water, which Jørgensen was able to explain using the chain structure shown above by postulating that chlorides attached to NH_3 could dissociate while those attached to Co could not. The modern theory of coordination chemistry, which overthrew the chain theory, is based largely on the work of Alfred Werner (1866–1919; Nobel Prize in Chemistry in 1913). In a series of careful experiments carried out in the late 1880s and early 1890s, he examined the properties of several series of metal halide complexes with ammonia. For example, five different "adducts" of ammonia with $PtCl_4$ were known at the time: $PtCl_4{\cdot}nNH_3$ (n = 2–6). Some of Werner's original data on these compounds are shown in Table **8.1.1**. Werner's data on $PtCl_4{\cdot}6NH_3$ in Table **8.1.1** showed that all the chloride ions were present as free chloride. In contrast, $PtCl_4{\cdot}2NH_3$, was a neutral molecule that did not give free chloride ions when dissolved in water.

Alfred Werner (1866–1919)

Werner, the son of a factory worker, was born in Alsace. He developed an interest in chemistry at an early age, and he did his first independent research experiments at age 18. While doing his military service in southern Germany, he attended a series of chemistry lectures, and he subsequently received his PhD at the University of Zurich in Switzerland, where he was appointed professor of chemistry at age 29. He won the Nobel Prize in Chemistry in 1913 for his work on coordination compounds, which he performed as a graduate student and first presented at age 26. Apparently, Werner was so obsessed with solving the riddle of the structure of coordination compounds that his brain continued to work on the problem even while he was asleep. In

1891, when he was only 25, he woke up in the middle of the night and, in only a few hours, had laid the foundation for modern coordination chemistry.

Table **8.1.1**: Werner's Data on Complexes of Ammonia with $PtCl_4$

Complex	Conductivity (ohm^{-1})	Number of Ions per Formula Unit	Number of Cl^- Ions Precipitated by Ag^+
$PtCl_4 \cdot 6NH_3$	523	5	4
$PtCl_4 \cdot 5NH_3$	404	4	3
$PtCl_4 \cdot 4NH_3$	299	3	2
$PtCl_4 \cdot 3NH_3$	97	2	1
$PtCl_4 \cdot 2NH_3$	0	0	0

These data led Werner to postulate that metal ions have two different kinds of valence: (1) a primary valence (oxidation state) that corresponds to the positive charge on the metal ion and (2) a secondary valence (coordination number) that is the total number of ligands bound to the metal ion. If Pt had a primary valence of 4 and a secondary valence of 6, Werner could explain the properties of the $PtCl_4 \cdot NH_3$ adducts by the following reactions, where the metal complex is enclosed in square brackets:

$$[Pt(NH_3)_6]Cl_4 \rightarrow [Pt(NH_3)_6]^{4+}(aq) + 4Cl^-(aq) \quad (8.1.1)$$

$$[Pt(NH_3)_5Cl]Cl_3 \rightarrow [Pt(NH_3)_5Cl]^{3+}(aq) + 3Cl^-(aq) \quad (8.1.2)$$

$$[Pt(NH_3)_4Cl_2]Cl_2 \rightarrow [Pt(NH_3)_4Cl_2]^{2+}(aq) + 2Cl^-(aq) \quad (8.1.3)$$

$$[Pt(NH_3)_3Cl_3]Cl \rightarrow [Pt(NH_3)_3Cl_3]^{+}(aq) + Cl^-(aq) \quad (8.1.4)$$

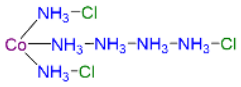
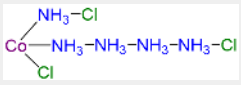
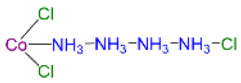
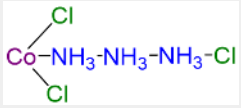
$$[Pt(NH_3)_2Cl_4] \rightarrow [Pt(NH_3)_2Cl_4]^{0}(aq) \quad (8.1.5)$$

Further work showed that the two missing members of the series—$[Pt(NH_3)Cl_5]^-$ and $[PtCl_6]^{2-}$—could be prepared as their mono- and dipotassium salts, respectively. Similar studies established coordination numbers of 6 for Co^{3+} and Cr^{3+} and 4 for Pt^{2+} and Pd^{2+}.

? Exercise 8.1.1. The $CoCl_3 x NH_3$ series.

The series $CoCl_3 \cdot xNH_3$ was particularly important in establishing the correctness of Werner's coordination theory over the rival chain theory. By ~1900 conductivity measurements suggested that the members of the series gave the number of ions shown in Table **8.1.1**.

Table **8.1.1**. The CoCl3·xNH3 series according to coordination theory, chain theory, and experiment.

Compound	Color	Werner formulation	Blomstrand-Jørgensen chain theory formulation	Number of ions in solution
$CoCl_3 \cdot 6NH_3$	yellow	$[Co(NH_3)_6]Cl_3$		4
$CoCl_3 \cdot 5NH_3$	violet	$[Co(NH_3)_5Cl]Cl_2$		3
$CoCl_3 \cdot 4NH_3$	green	$[Co(NH_3)_4Cl_2]Cl$		2
$CoCl_3 \cdot 3NH_3$	orange	$[Co(NH_3)_4Cl_3]$		0

What does this data suggest about the relative explanatory power of Werner's coordination theory and chain theory? Explain.

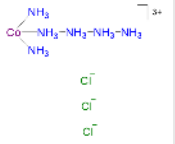
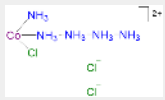
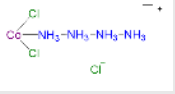
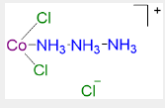
Answer

Remember that

- chain theory predicts that the number of ions is the number formed when the Cl atoms bound in a chain with NH_3 dissociate.
- coordination theory predicts the number of ions based on the number of complex ions and their counterions.

Based on this the predictions of coordination theory and chain theory can be compared with the experimental data, as is done in Table **8.1.2**.

Table **8.1.2**: Comparison of ions predicted for the $CoCl_3 \cdot xNH_3$ series by coordination theory and chain theory with the number observed experimentally.

Compound	Color	Ions predicted by Werner's coordination theory	Number of ions predicted by coordination theory	Ions predicted by Blomstrand-Jørgensen chain theory	Number of ions predicted by chain theory	Observed Number of ions in solution
$CoCl_3 \cdot 6NH_3$	yellow	$[Co(NH_3)_6]^{3+}$ Cl^- Cl^- Cl^-	4		4	4
$CoCl_3 \cdot 5NH_3$	violet	$[Co(NH_3)_5Cl]^{2+}$ Cl^- Cl^-	3		3	3
$CoCl_3 \cdot 4NH_3$	green	$[Co(NH_3)_4Cl_2]^+$ Cl^-	2		2	2
$CoCl_3 \cdot 3NH_3$	orange	None	0		2	0

As can be seen by comparing the number of ions predicted by coordination and chain theory in Table **8.1.2**, coordination theory successfully explains all the observed ion counts, while chain theory fails to explain the lack of ions observed for $CoCl_3 \cdot 3NH_3$.

Nevertheless, as is often the case when developing theoretical models using data from real experimental investigations, these observations did not convince Jørgensen, who could point to the experimental difficulty of determining the number of ions present from solution conductivity data.

What ultimately convinced Jørgensen of the correctness of Werner's coordination model over his own chain theory was how Werner's explanation of the structure of cobalt coordination complexes using an octahedral coordination geometry explained the existence of isomers in Co complexes containing Cl and NH_3 ligands. In the case of $[Co(NH_3)_4Cl_2]Cl$ two isomers were known: one red and the other green. Because both compounds had the same chemical composition and the same number of groups of the same kind attached to the same metal, there had to be something different about the arrangement of the ligands around the metal ion. Werner's key insight was that the six ligands in $[Co(NH_3)_4Cl_2]Cl$ had to be arranged at the vertices of an octahedron because that was the only structure consistent with the existence of two, and only two, stereoisomers (Figure 8.1.1). His conclusion was also corroborated by the existence of two and only two stereoisomers of the next compound in the series: $Co(NH_3)_3Cl_3$.

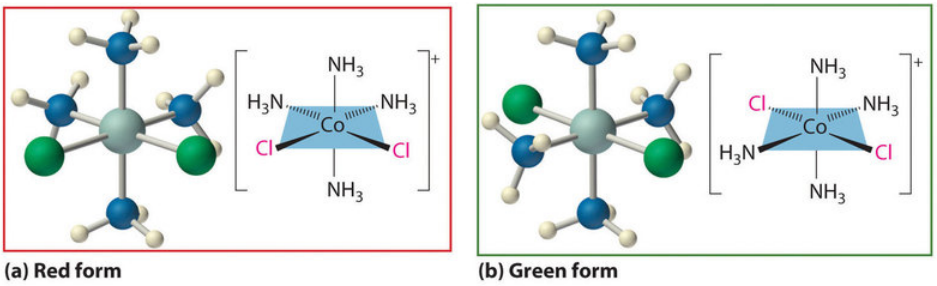


Figure **8.1.1**. The $[Co(NH_3)_4Cl_2]^+$ ion can have two different arrangements of the ligands, which results in different colors: if the two Cl^- ligands are next to each other (*cis*), the complex is red (a), but if they are opposite each other (*trans*), the complex is green (b).

Example 8.1.1: Why did Werner propose an octahedral geometry for 6-coordinate complexes?

In Werner's time, many complexes of the general formula MA_4B_2 were known, but no more than two different compounds with the same composition had been prepared for any metal. To confirm Werner's reasoning that this suggests these complexes possess an octahedral geometry, calculate the maximum number of different structures possible for six-coordinate MA_4B_2 complexes with each of the three most symmetrical possible structures the ligands will form about the central metal - a hexagon, a trigonal prism, and an octahedron.

Assuming that the absence of evidence for additional compounds in this case serves as reasonable circumstantial evidence for their absence, what does the fact that no more than two forms of any MA_4B_2 complex were known suggest about the three-dimensional structures of these complexes?

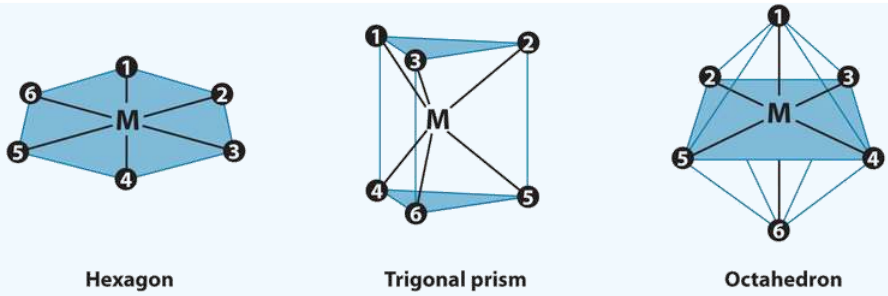
Solution

In this problem you are given

- the stochiometry of the complexes, MA_4B_2
- three possible coordination geometries - hexagonal, trigonal prismatic, and octahedral.

In order to calculate the number of isomers that could be present for each geometry it is best to follow a systematic approach. Since there are fewer B type ligands than A type ligands, the easiest way to do this for each geometry is to start by placing a B ligand at one vertex and then to determine how many different positions are available for the second B ligand.

The three regular six-coordinate structures are shown here, with each coordination position numbered so that we can keep track of the different arrangements of ligands. For each structure, all vertices are equivalent. We begin with a symmetrical MA_6 complex and simply replace two of the A ligands in each structure to give an MA_4B_2 complex:



For the hexagon, we place the first B ligand at position 1. There are now **three** possible places for the second B ligand:

- position 2 (or 6)
- position 3 (or 5)
- position 4

The (1, 2) and (1, 6) arrangements are chemically identical because the two B ligands are adjacent to each other. The (1, 3) and (1, 5) arrangements are also identical because in both cases the two B ligands are separated by an A ligand. Those of you who remember your ogranic chemistry might recognize that this situation is formally analogous to the *ortho-*, *meta-*, and *para-* isomerism in disubstituted benzenes.

Turning to the trigonal prism, we place the first B ligand at position 1. Again, there are three possible choices for the second B ligand:

- at position 2 or 3 on the same triangular face
- position 4 (on the other triangular face but adjacent to 1)
- position 5 or 6 (on the other triangular face but not adjacent to 1).

The (1, 2) and (1, 3) arrangements are chemically identical, as are the (1, 5) and (1, 6) arrangements.

In the octahedron, however, if we place the first B ligand at position 1, then we have only two choices for the second B ligand:

- position 2 (or 3 or 4 or 5)
- position 6.

In the latter, the two B ligands are at opposite vertices of the octahedron, with the metal lying directly between them. Although there are four possible arrangements for the former, they are chemically identical because in all cases the two B ligands are adjacent to each other.

The number of possible MA_4B_2 arrangements for the three geometries is thus: hexagon, 3; trigonal prism, 3; and octahedron, 2. The fact that only two different forms were known for all MA_4B_2 complexes that had been prepared suggested that the correct structure was the octahedron but did not prove it. For some reason one of the three arrangements possible for the other two structures could have been less stable or harder to prepare and had simply not yet been synthesized. When combined with analogous results for other types of complexes (e.g., MA_3B_3), however, the data were best explained by an octahedral structure for six-coordinate metal complexes.

? Exercise 8.1.1

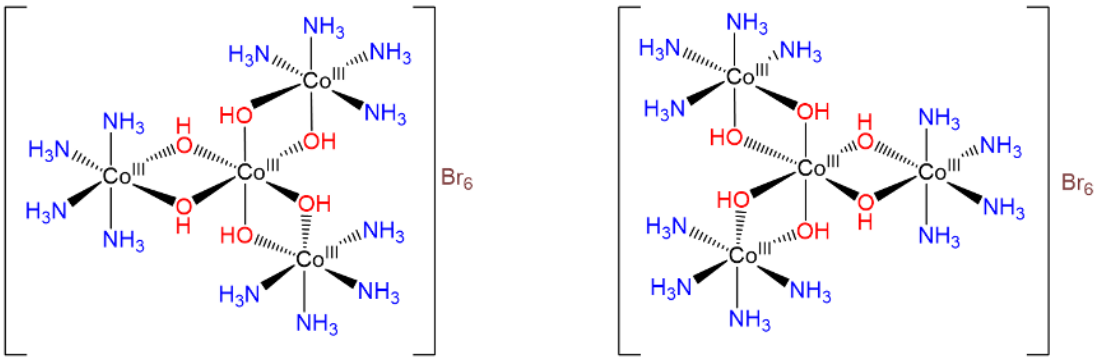
Determine the maximum number of structures that are possible for a four-coordinate MA_2B_2 complex with either a square planar or a tetrahedral symmetrical structure.

Answer

square planar, 2; tetrahedral, 1

Even Werner's explanation of isomerism in coordination complexes in terms of octahedral and other recognized coordination geometries did not convince all chemists until he was able to resolve a racemic mixture of *d*- and *l*-$[Co\{Co(NH3)_4(OH)_2\}_3]$ into its

enantiomers, which are shown in Scheme **8.1.II**. By doing so Werner demonstrated to chemists of his time (virtually none of whom knew group theory) that tetrahedral carbon atoms were not required for chirality; D_3 octahedral complexes were also chiral.



Scheme **8.1.II**: d- and l-enantiomers of $[Co\{Co(NH3)_4(OH)_2\}_3]$, colloquially referred to as hexol. This work by Stephen Contakes is licensed under a Creative Commons Attribution 4.0 International License.

8.1: History is shared under a CC BY-NC-SA 4.0 license and was authored, remixed, and/or curated by LibreTexts.

- **24.1: Werner's Theory of Coordination Compounds** by Anonymous is licensed CC BY-NC-SA 4.0.

8.2: Nomenclature and Ligands

Introduction

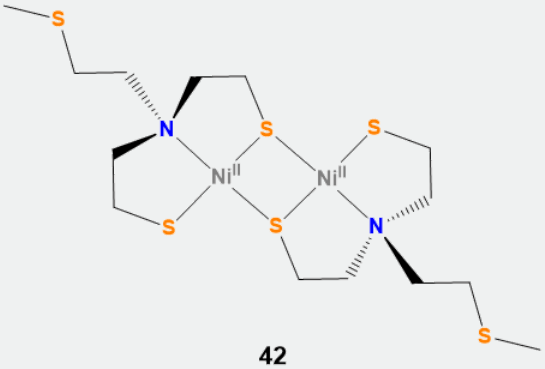
There are well-established rules for both naming and writing the formulae of coordination compounds. The purpose of these rules is to facilitate clear and precise communication among chemists. As with all such rules some are more burdensome than others to employ and some serve more crucial roles in the communication process while others are more peripheral - and all are poorly used in the service of pedantic tyranny, especially when against those who are otherwise doing good work. For this reason, you are urged to approach the rules in a spirit of generosity towards others in

- naming and writing formulas as reasonably accurately as you can so that ligands and metals are where readers expect them and thus can understand what you mean more easily.
- being gracious towards the many professional inorganic chemists who adhere loosely to some of the rules you are about to learn.
- recognizing that in cases when a structure is particularly complex and a picture may make be particularly useful you should supply one (See the note below).

Note 8.2.1: Sometimes the most helpful name to give a compound is 42.

Even though the IUPAC nomenclature rules permit specification of even the most complex structures, it is often much easier and more effective to supply a numbered structure that can be referred to instead of the IUPAC name. Consider bis{[(μ-2-mercaptoethyl)(2-mercaptoethyl)-methylthioethylaminato (2-)]Nickel(II)}. Which is easier, to expect readers and hearers to work out the structure from that name or to just refer them to compound **42** in Scheme **8.2.I**?

Scheme 8.2.I. Structure of bis{[(μ-2-mercaptoethyl)(2-mercaptoethyl)-methylthioethylaminato (2-)]Nickel(II)}. The authors of the synthesis of this compound in *Inorganic syntheses*[1] may have had to figure out an IUPAC name for this compound but if you have this scheme in your paper and your instructor is OK with it you can just call it **42**.



42

Coordination Complex Nomenclature

A variety of systems have been used for naming coordination compounds since the development of the discipline in the time of Alfred Werner. In this section the most common approaches as they are currently used by practicing chemists will be described. Those who need a more thorough and accurate acquaintance with the full IUPAC nomenclature rules are encouraged to consult the IUPAC brief guide to inorganic nomenclature followed by complete guidelines, commonly known as the IUPAC red book. If those are still not enough a careful read of note **8.2.1** is suggested.

The systems for naming coordination compounds used at present are additive, meaning that they consider coordination compounds as comprised of a central metal to which are added ligands. To specify the structure and bonding in this metal-ligand complex then involves

1. When there are several different ways of attaching the metal and ligands, specifying the structural or stereoisomer

2. systematically listing the ligands in a way that, as necessary, conveys information about how they are linked to the metal and their stereochemistry

3. providing the identity of the metal and its oxidation state, or if the oxidation state is unclear, at least the overall charge on the complex

4. specifying any counterions present

Since the stereochemistry of coordination compounds forms the subject of the next section, in this section it will be addressed in this section by simply giving the prefixes that designate stereochemistry as if they were self-evident. Do not worry about these for now. They will make sense after you have learned more about stereochemistry in the next section. At that time, you can go back over the examples in that section to solidify your understanding of how to name coordination compounds.

However, in order to name coordination compounds accurately you will need to learn about how to think about and name ligands first.

Ligands

Ligands are classified based on whether they bind to the metal center through a single site on the ligand or whether they bind at multiple sites. Ligands which bind through only a single site are called **monodentate** at the Latin word for tooth; in contrast those those which bind through multiple sites are called **chelating** after the Greek $\chi\alpha\lambda\epsilon$ for "claw". These relationships are summarized in Figure 8.2.1.

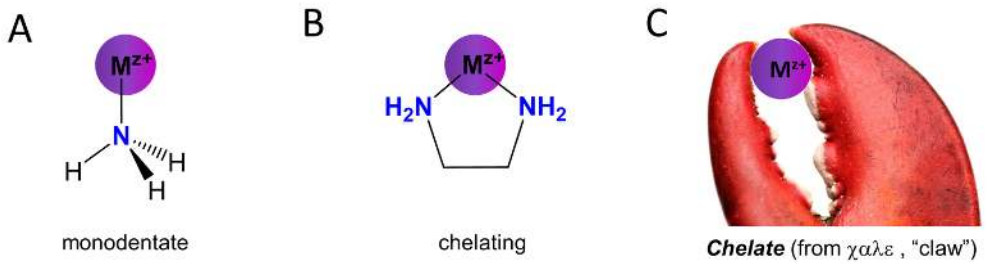
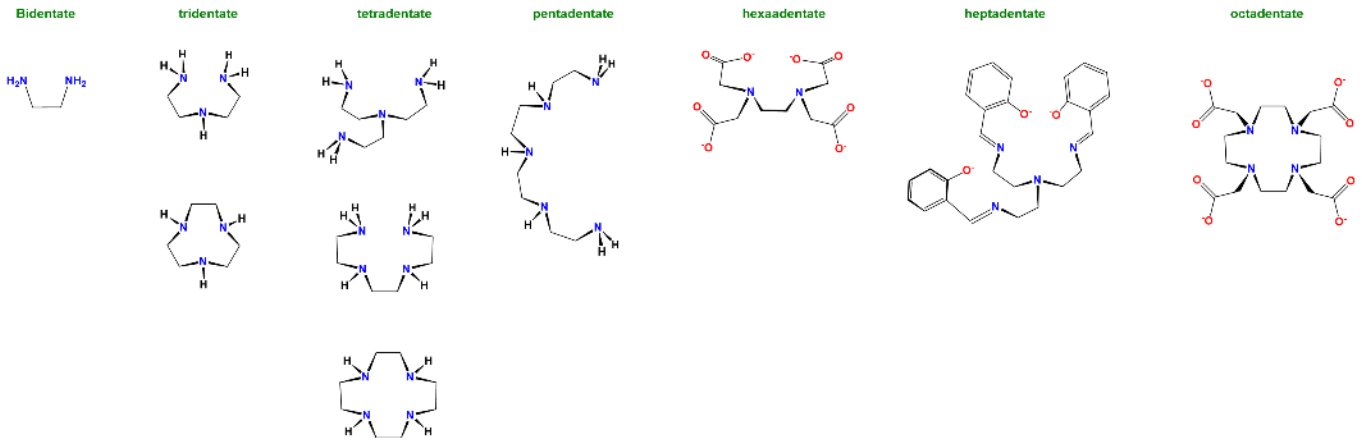


Figure 8.2.1. (A) Ammonia is monodentate ligand while (B) ethylene diamine is a chelating ligand owing to its capacity to bind metals via its two amine functional groups. (C) Chelating ligands act like a Lobster claw in attaching to the metal via multiple sites. The lobster claw image is adapted from https://www.clipart.email/download/1127636.html. Otherwise this work by Stephen Contakes is licensed under a Creative Commons Attribution 4.0 International License.

Following naturally from the classification of non-chelating ligands as monodentate, chelating ligands are further classified according to the number of sites which they can use to bind a metal center. This number of binding sites is called the denticity and ligands are referred to as monodentate (non chelating), bidentate, tridentate, etc. based on the number of sites available. Ligands with two binding sites have a denticity of two and are said to be bidentate; those with three are tridentate, four tetradentate, and so on. To illustrate this classification system examples of chelating ligands classified according to denticity are given in Scheme 8.2.I.

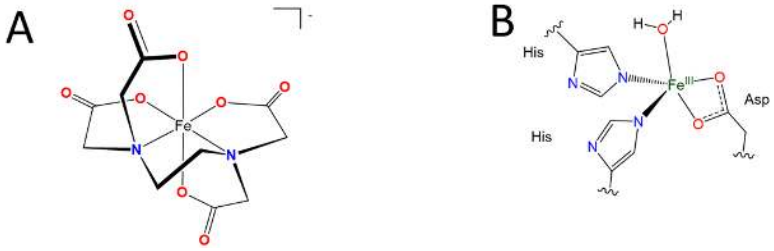
Scheme 8.2.I. A selection of chelating ligands classified according to denticity. this work by Stephen Contakes is licensed under a Creative Commons Attribution 4.0 International License.



The classification of several of the ligands in Scheme **8.2.I** requires a bit of explanation, specifically as to why the dentificity of the carboxylate-containing ligands is less than the total number of lone-pair bearing oxygen and nitrogens present. This is because only one of the carboxylate oxygens is counted. Only one is counted because in most cases only one oxygen binds to a metal at any given time. When that oxygen is bound the other oxygen faces away from the metal, as depicted for the iron complex shown in Scheme **8.2.IIA**. Because only one oxygen per carboxylate *typically* binds only one is counted when assigning a ligand's denticity.

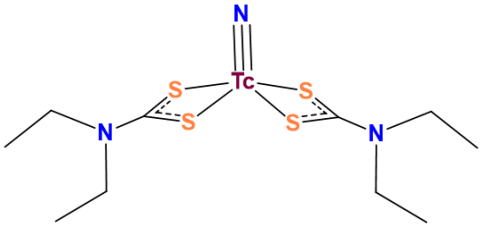
Although only one carboxylate oxygen usually binds to a metal it is still possible to bind a metal using both oxygens. As shown in Scheme **8.2.IIB** complexes in which both carboxylates bind to a metal are known, and in fact are common in the active sites of some enzymes. It is just that the binding of both oxygens gives a strained four-membered ring that is usually unstable.

Scheme 8.2.II. (A) Only one oxygen per carboxylate counts towards the denticity of EDTA since on binding the other oxygen generally points away from the metal center, as in the structure of $Fe(EDTA)^-$. This does not mean that both oxygens of a carboxylate can *never* both bind to metal centers in a complex. (B) Structures in which both oxygens of a carboxylate side chain bind to a metal are sometimes found in the active sites of some of the nonheme iron enzymes your body uses to break down amino acids. this work by Stephen Contakes is licensed under a Creative Commons Attribution 4.0 International License.



As was the case for carboxylate groups above, sometimes the classification of a group's denticity is based on experimental knowledge of their common binding modes. Carboxylates might commonly act as monodentate ligands but dithiocarbamates more commonly bind metals through both sulfur atoms (Scheme **8.2.III**) and are classified as bidentate.

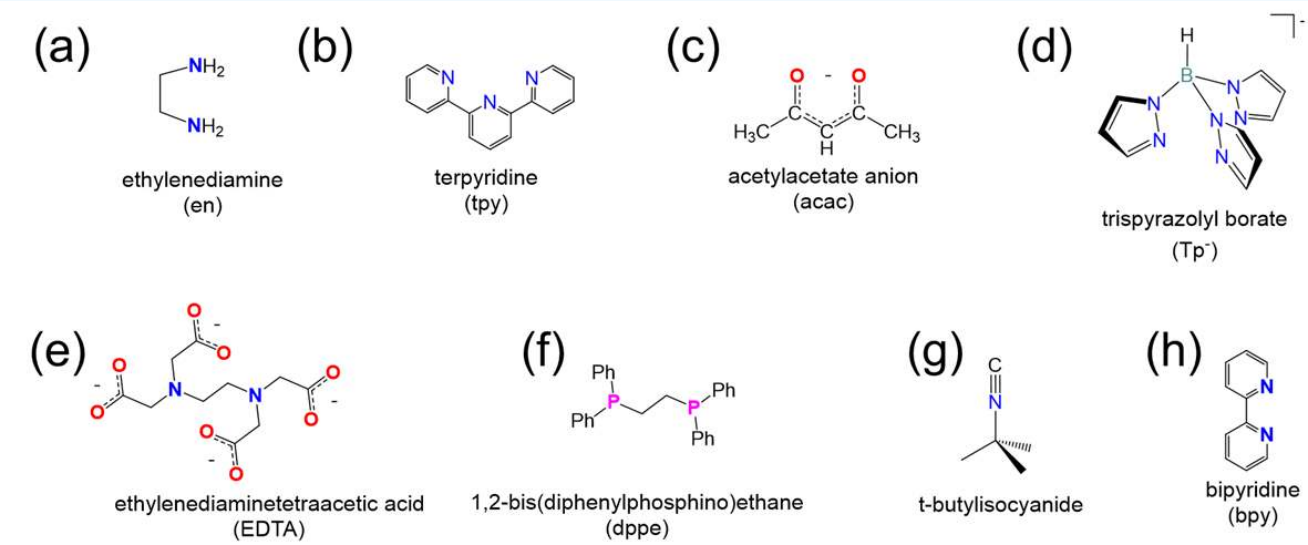
Scheme 8.2.III. As in this complex, dithiocarbamates commonly bind metals through both sulfur atoms. Consequently, dithiocarbamates are classified as bidentate. this work by Stephen Contakes is licensed under a Creative Commons Attribution 4.0 International License.



Because of these factors it is technically more correct to say that carboxylates *usually act as* monodentate ligands and dithiocarbamates bidentate ones than it is to say that carboxylates *are* monodentate ligands and dithiocarbamates bidentate ones. So in other words the ligand classifications presented here are just represent common binding modes.

Exercise 8.2.1

Determine the denticity of each ligand in the list below and classify them as monodentate, tridentate, etc.



Answer

(a) bidentate

(b) tridentate

(c) bidentate

(d) tridentate (only the lower N on each ring has a lone pair that can be used to bind the metal)

(e) hexadentate (remember that each carboxylate only counts as one point of attachment)

(f) bidentate

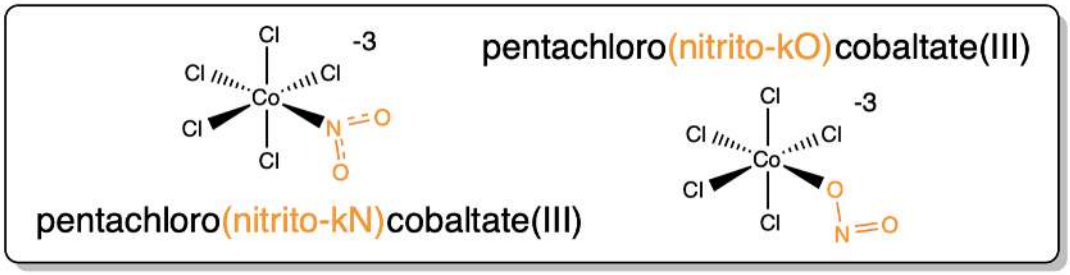
(g) monodentate (through the lone pair on the isocyanide C)

(h) bidentate

This experimentally-based classification of dithiocarbamates as bidentate and carboxylates as monodentate can be confusing to a beginner. Fortunately, such experimentally based classifications are embedded in the lists of common monodentate ligands are given in Table **8.2.1** and common chelating ligands in Table **8.2.2**.

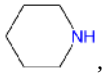
A perusal of the ligands in Table **8.2.1** reveals that several can bind to a metal in multiple ways. For example, thiocyanate, SCN^- can bind metal's through its S or N atoms. Such ligands are called **ambidentate ligands**. When naming an ambidentate ligand the atom through which it attaches to the metal is commonly specified after the ligand name using the italicized element symbol or, more formally a κ followed by the italicized element symbol. An example is given in Scheme **8.2.1**.[2]

Scheme 8.2.1. Two possible binding modes of nitrite acting as a ligand.[3]



https://chem.libretexts.org/@go/page/326233

Table 8.2.1. Common monodentate ligands. Most chemists still prefer common names over the IUPAC ones.

Ligand	Common name	IUPAC name
H^- (H ligands are always considered anions for naming purposes)	hydrido	hydrido
F^-	fluoro	fluorido
Cl^-	chloro	chlorido
Br^-	bromo	bromido
I^-	iodo	iodido
CN^-, M-CN	cyano	cyanido or cyanido-κC or cyanido-*C*
CN^-, as M-NC	isocyano	isocyanido or cyanido-κN or cyanido-*N*
CH_3NC	methylisocanide	methylisocyanide
N_3^-	azido	azido
SCN^-, *e.g.* thiocyanate as M-SCN	thiocyanato	thiocyanato-κS or thiocyanato-*S*
NCS^-, *e.g.* thiocyanate as M-NCS	isothiocyanato	thiocyanato-κN or thiocyanato-*N*
$CH_3CO_2^-$	acetato	ethanoato
N^{3-}	nitrido	nitrido
NH^{2-}	imido	azanediido
NH_2^-	amido	azanido
NH_3	ammine	ammine
RNH_2, R_2NH, R_3N	alkylamine, dialkylamine, trialkalyamine (*e.g.* methylamine for CH_3NH_2)	alkylamine, dialkylamine, trialkalyamine (*e.g.* methylamine for CH_3NH_2)
 , piperidine, abbreviated pip	piperidine	piperidine
 , pyridine, abbreviated py	pyridine	pyridine
CH_3CN, acetonitrile, abbreviated MeCN	acetonitrile	acetonitrile
P^{3-}	phosphido	phosphido
PH_3	phosphine	phosphane
PR_3	trialkylphosphine (*e.g.* trimethylphosphine for Me_3P)	trialkylphosphane (*e.g.* trimethylphosphane for Me_3P)
PAr_3	triarylphosphine (*e.g.* triphenylphosphine for Ph_3P)	triarylphosphane (*e.g.* triphenylphosphane for Ph_3P)
 , dimethylsulfoxide or DMSO or dmso	dimethylsulfoxide (sometimes called dimethylsulfoxo but this usage is rare and violates the nomenclature rules for neutral ligands)	(methanesulfinyl)methane or dimethyl(oxido)sulfur

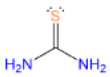
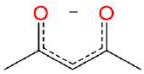
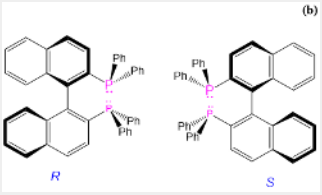
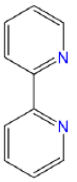
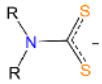
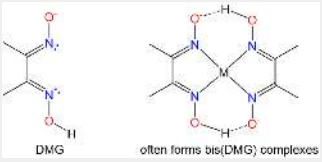
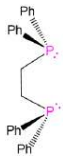
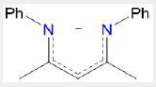
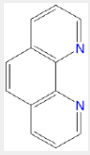
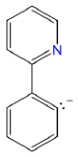
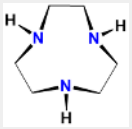
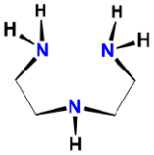
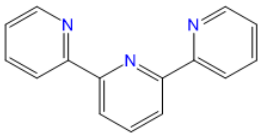
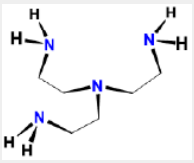
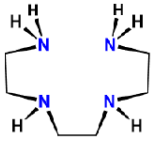
, thiourea or tu	thiourea	thiourea
O^{2-}	oxo	oxido
OH^-	hydroxo	hydroxido
H_2O	aqua	aqua
S^{2-}	sulfo	sulfo
HS^-	hydrosulfido	hydrosulfido
RS^-	alkanethiolate (*e.g.* ethanthiolate for EtS^-)	thioalkanoate
H_2S	hydrogen sulfide	hydrogen sulfide
R_2S	alkylsulfanylalkane (*e.g.* ethylsulfanylethane for Et_2S)	dialkyl sulfide
O_2	dioxygen	dioxygen
O_2^-, superoxide	superoxido	dioxido(1-) or superoxido
O_2^{2-}, peroxide	peroxido	dioxido(2-) or peroxido
N_2	dinitrogen	dinitrogen
NO (are always considered neutral for naming purposes)	nitrosyl	nitrosyl
CO	carbonyl	carbonyl
CS	thiocarbonyl	thiocarbonyl
SO, as M-SO	sulfino	sulfur monoxide-κ*S* or sulfur monoxide-*S*
NO_2, as M-NO_2	nitryl	nitrogen dioxide-κN or nitrogen dioxide-*N*
CO_3^{2-}	carbonato	carbonato
NO_2^-, as M-NO_2	nitro or nitrito-*N*	nitrito-κ*N* or nitrito-*N*
NO_2^-, as M-ONO	nitrito or nitrito-*O*	nitrito-κ*O* or nitrito-*O*
NO_3^-	nitrato	nitrato
SO_3^{2-}	sulfito	sulfito
SO_4^{2-}	sulfato	sulfato
$S_2O_3^{2-}$, as M-S-SO_2-O^-	thiosulfato-*S*	thiosulfato-κ*S* or thiosulfato-*S*
$S_2O_3^{2-}$, as M-O-SO_2-S^-	thiosulfato-*O*	thiosulfato-κ*O* or thiosulfato-*O*

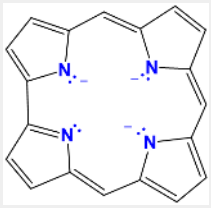
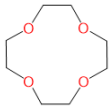
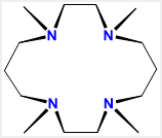
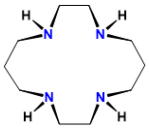
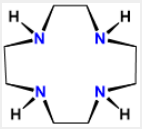
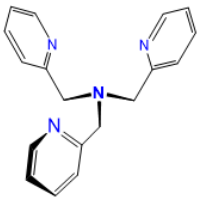
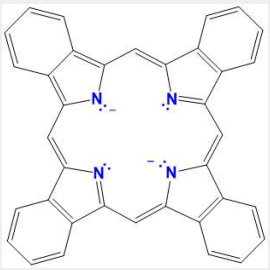
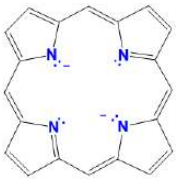
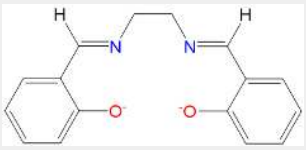
Table 8.2.2. Common chelating ligands organized by denticity. Most chemists use the common names and abbreviations to describe

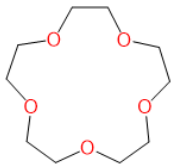
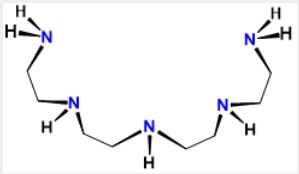
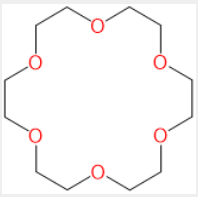
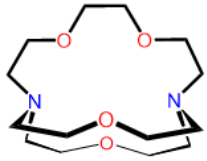
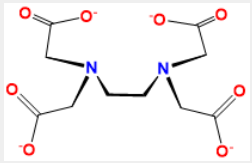
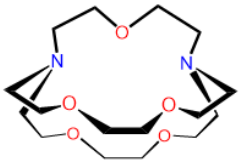
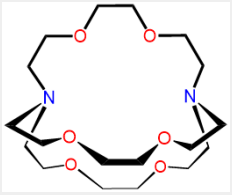
https://chem.libretexts.org/@go/page/326233

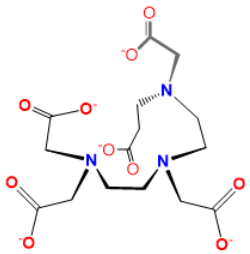
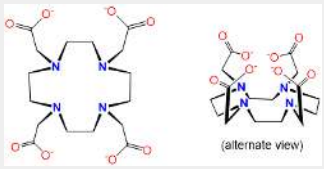
these ligands.

Common Ligand name	IUPAC ligand name	abbreviation (if applicable)	structure or representative/parent structure (shown in the ionization state in which they bind to a metal)
bidentate ligands			
acetylacetonato	2,4-pentanediono	acac	
R-BINAP and *S*-BINAP	*R*- or *S*-2,2'-bis(diphenylphosphino)-1,1'-binapthyl	BINAP	
2,2'-bipyridine	2,2'-bipyridine	bpy or bipy	
cyclooctadiene	1,5-cyclooctadiene	COD	 (binding to the metal occurs through the alkene π cloud)
dialkyldithiocarbamato	dialkylcarbamodithiolato	$R_2NCS_2^-$ or dtc	
dimethylgloximato	butanedienedioxime	Hdmg or DMG	
diphenylphosphinoethane or 1,2-(diphenylphosphino)ethane	Ethane-1,2-diylbis(diphenylphosphane)	dppe	
ethylenediamine	Ethane-1,2-diamine	en	
ethylenedithiolato	Ethane-1,2-dithiolato	$C_2H_2S_2^{2-}$	
nacnac	*N*,*N*'-diphenyl-2,4-pentanediiminato	nacnac	

oxalato	oxalato	ox	
1,10-phenanthroline or *o*-phenanthroline	1,10-phenanthroline	phen or *o*-phen	
phenylpyridinato	2-phenylpyridinato-C^2,*N* or 2-phenylpyridinato-κC^2,*N*	ppy	
tridentate ligands			
triazacyclononane	1,3,7-triazacyclononane	tacn	
diethylenetriamine	1,4,7-triazaheptane	dien	
pyrazoylborato (scorpionate)	hydrotris(pyrazo-1-yl)borato	Tp	
terpyridine or 2,2';6',2''-terpyridine	1^2,2^2:2^6,3^2-terpyridine or 2,6-bis(2-pyridyl)pyridine, tripyridyl, 2,2′:6′,2″-terpyridine	tpy or terpy	
tetradentate ligands			
β, *β*', *β*''-triaminotriethylamine	*β*, *β*', *β*''-tris(2-aminoethyl)amine	tren	
triethylenetetramine	1,4,7,10-tetraazadecane	trien	

corroles	variable and generally not used	cor or Cor	
12-crown-4	1,4,7,10-tetraoxacyclododecane	12-crown-4	
tetramethylcyclam	1,4,8,11-tetramethyl-1,4,8,11-tetraazacyclotetradecane	TMC or cyclam	
cyclam	1,4,8,11-tetraazacyclotetradecane	cyclam	
cyclen	1,4,7,10-tetraazacyclododecane	cyclen	
tris(2-pyridylmethyl)amine	1-pyridin-2-yl-*N*,*N*-bis(pyridin-2-ylmethyl)methanamine	tpa or TPA	
phthalocyanines	variable and generally not used	variable, usually a modified Pc	
porphyrins	variable and generally not used	variable, usually a modified por, Por, or P (e.g. TPP = tetraphenylporphyrin)	
salen	2,2'-ethylenebis(nitrilomethylidene) diphenoxido	salen	
pentadentate ligands			

15-crown-5	1,4,7,10,13-Pentaoxacyclopentadecane	15-crown-5	
tetraethylenepentamine	1,4,7,10,13-pentaazatridecane	tepa or TEPA	
hexadentate ligands			
18-crown-6	1,4,7,10,13,16-hexaoxacyclooctadecane	18-crown-6	
2,1,1-cryptand	4,7,13,18-Tetraoxa-1,10-diazabicyclo[8.5.5]icosane	2,1,1-crypt or [2.1.1]-cryptand kryptofix 211 and variations thereof	
ethylenediaminetetraaceto	2,2′,2″,2‴-(Ethane-1,2-diyldinitrilo)tetraaceto	EDTA, edta, Y^{4-}	
heptadentate ligands			
2,2,1-cryptand	4,7,13,16,21-pentaoxa-1,10-diazabicyclo[8.8.5]icosane	2,2,1-crypt or [2.2.1]-cryptand kryptofix 221 and variations thereof	
octadentate ligands			
2,2,2-cryptand	4,7,13,16,21,24-Hexaoxa-1,10-diazabicyclo[8.8.8]hexacosan	2,2,2-crypt or [2.2.2]-cryptand kryptofix 222 and variations thereof	

pentetato acid or diethylenetriaminepentaacetato or DTPA	2-[bis[2-[bis(carboxylatomethyl)amino]ethyl]amino]acetato	DTPA	
DOTA or tetraxetan	1,4,7,10-Tetraazacyclododecane-1,4,7,10-tetraacetic acid	Dota, DOTA	

Rules for Naming Coordination Compounds

As explained above, the name of a coordination compound communicates

- As appropriate, information about isomerism
- systematically listing the ligands in a way that as necessary conveys information about their oxidation state and how they are linked to the metal
- the identity of the metal and its oxidation state
- any counterions present

Before going into these rules it is worth pointing out a few things.

1. It is easiest to learn these rules by starting with one or two of the rules, learning how to apply them, and then adding additional rules one at a time. To that end, instructors who wish to use a more programmed approach may find it convenient to first direct their students to this page which focuses on getting the names of the ligands and metal right, without working about isomerism or stereochemistry.

2. The rules also assume some familiarity with common coordination geometries and patterns of isomerism in metal complexes. Thus it might be easiest to learn about common coordination geometries first, followed by common patterns of isomerism in metal complexes before beginning this section. If you decide to dive right in to this section you might find it helpful to know that when applying nomenclature and formula rules most textbooks *assume*

- complexes in which the metal has a coordination number of six are octahedral
- complexes in which the metal has a coordination number of five are trigonal bipyramidal
- complexes in which Pt^{II} , Pd^{II} , or Rh^{I}, or Ir^{I} have a coordination number of four are square planar
- other complexes in which the metal has a coordination number of four are tetrahedral

Like all assumptions these don't always work in real life but they should be good enough to get you through your first inorganic chemistry course.

For the pedants among you, note that the complexes given as examples and in exercises on this page have been selected for pedagogical utility. Although many are well-known compounds, others are hypothetical.

Now on to the rules.

Name the cation first, followed by the anion.

Examples:

$K_2[Pt^{II}Cl_4]$ potassium tetrachloroplatinate(2-)

$[Co^{III}(NH_3)_6](NO_3)_3$ hexaamminecobalt(3+) nitrate

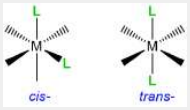
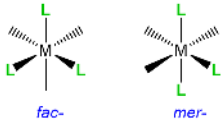
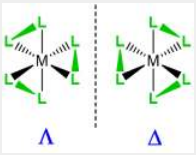
$[Co^{III}(NH_3)_6][Cr^{III}(C_2O_4)_3]$ hexaamminecobalt(3+) tris(oxalato)chromium(3-)

Designate the isomer in italics in front of the name

If you have not yet learned about isomerism in coordination compounds skip this rule for now and return to it after you have.

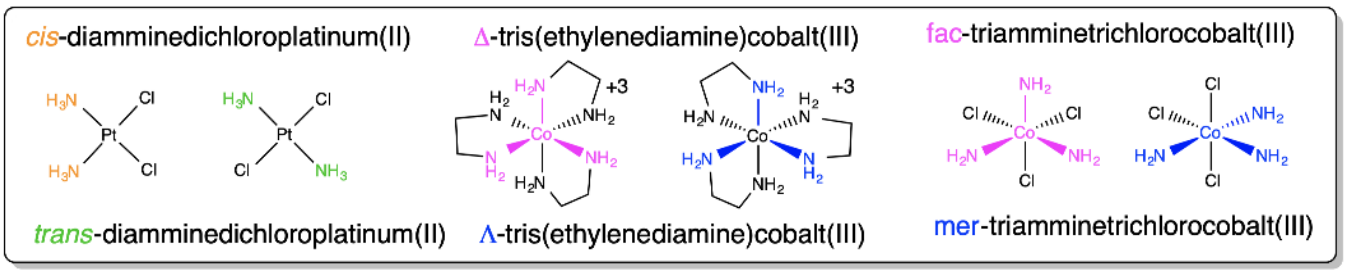
When a complex might exist as one of two stereosisomers prefixes are commonly used to designate which isomer is present. The most common cases are listed in Table **8.2.3**.

Table8.2.3. Prefixes used to specify isomerism about a metal center when naming and writing coordination compounds' formulae.

Type of isomerism	Graphical reminder	Prefixes
Geometric, *cis-* , *trans-*		*cis-* or *trans-*
Geometric, *fac- /mer-*		*fac-* or *mer-*
Enantiomers, **Λ-**, **Δ-**		**Λ-** or **Δ-**

Examples of how isomerism about a metal center is designated are given in Scheme **8.2.II**.

Scheme 8.2.II. Application of nomenclature rules for stereosimerism about a metal.[3]



There are a number of other cases where it might be advisable to specify the stereochemistry of a complex. These cases involve specifying

- the coordination geometry about a metal center (octahedral, trigonal prismatic, tetrahedral, square planar, etc.)
- the geometry cannot be unambigouously described by a single *cis/trans* or *fac/mer* relaionship of ligands

These cases may also be handled by using a designator to specify the coordination geometry and, as necessary, giving the position of ligated atoms in terms of designated numbered positions for that geometry. See the IUPAC red book for details as such cases fall outside the scope of what is normally advisable for an undergraduate course.

Specify the identity and number of the ligands in alphabetical order by ligand name.

Before specifying the metal, the ligands are written as prefixes of the metal.

In specifying the ligands several rules are followed.

1. The ligands are written in alphabetical order by the ligand name only; symbols are not considered and prefixes do not count in determining alphabetical order.

   Example: In the name of the complex ion $[Co(NH)_3Cl]^{2+}$, pentamminechlorocobalt(II), the ammine ligand is named before the chloro ligand because the order is alphabetical by the ligand name by virtue of which ammine comes before chloro.

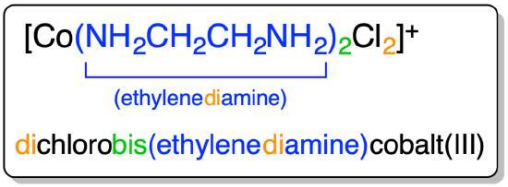
2. Prefixes are used to indicate the number of each ligand present. Specifically, *di-*, *tri-*, *tetra-* , *penta-*, *hexa-*, *etc.* prefixes are used to indicate multiple ligands of the same type EXCEPT when the ligand is polydentate or its name already has a *di-*, *tri-*, *tetra-* etc. In that case *bis-*,*tris-*, *tetrakis-*, etc. are used instead. These prefix rules are summarized in Table **8.2.3**.

Table 8.2.3. Prefixes used to specify the number of a given ligand present.

Number of identical ligands	prefix used when the ligand name is simple	prefix used when the ligand is polydentate or its name already has a *di-*, *tri-*, *tetra-* etc.
2	di-	bis-
3	tri-	tris-
4	tetra-	tetrakis-
5	penta-	pentakis-
6	hexa-	hexakis-
7	hepta-	heptakis-
8	octa-	octakis-
9	nona-	nonakis-
10	deca-	decakis-

An example of the application of the prefix rule is given in Scheme **8.2.III**.

Scheme 8.2.III. Example of the use of prefixes to specify the number of ligands of each type in a complex.[3]



3. Ligand names are based on their charge

- Neutral and cationic ligand names are the same as the names of their neutral compounds with two caveats

  i. names that involve spaces should either be put in parentheses or the spaces should be eliminated (preferred)

  Example: cis-dichlorobis(**dimethyl sulfoxide**)platinum(II) or *cis*-dichlorobis(**dimethylsulfoxide**)platinum(II)

  ii. A few ligands are given common names.

  - H_2O = aqua
  - NH_3 = ammine (notice that there are two m's)
  - CO = carbonyl
  - CS = thiocarbonyl
  - NO = nitrosyl

- For anionic ligands, the vowel at the end of their anion names is changed to an -"o"

  Examples: Cl^- = chlorido, NH_2^- = amido, N_3^- = azido

  Caveat: some anionic ligands have common names that may also be used

  Examples:

  I^- = iodo or iodino

  CN^- = cyano or cyanido

O^{2-} = oxo or oxido

The IUPAC and common names of many ligands are given in Tables 8.2.1. and 8.2.2.

4. When an ambidentate ligand is present the atom through which it is bound to the metal is indicated by giving either its element symbol or a κ and its element symbol in italics after the ligand name

   Example:

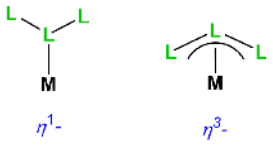
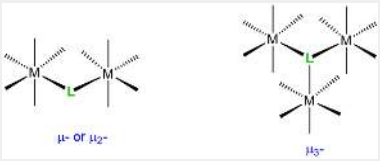
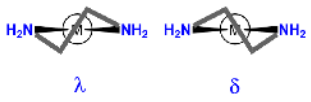
   M-SCN is thiocyanato-*S* or thiocyanato-κ*S*

   M-NCS = thiocyanato-*N or* thiocyanato-κ*N*

   The use of κ and an element symbol to indicate how a ligand and metal are linked is called a **k-term**. More complex k-terms might also involve specifying the atoms by number, though their use is outside the scope of this text.

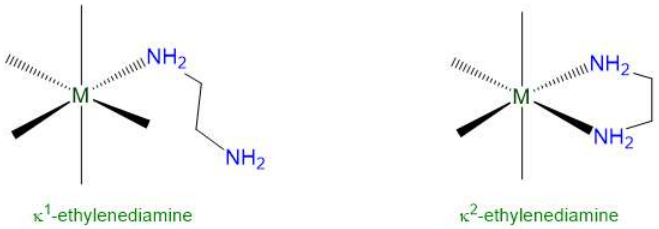
5. As appropriate, additional information about the way a ligand is bound to the metal center and/or its stereochemistry is specified using a prefix. The prefixes to provide linkage and stereochemistry for ligands are given in Table8.2.4.

Table8.2.4. Prefixes used to specify ligands' isomerism when naming and writing coordination compounds' formulae. Some of these types of isomerism will be discussed in later pages.

Type of isomerism	Graphical reminder	Prefixes
when a multidentate ligand binds through less than the full number of atoms		κ^n where n is the number of attached atoms; used when the attached atoms are not directly connected by a chemical bond. The metal-ligand bonding usually involves σ-type coordination.
hapticity		η^n where n is the number of attached atoms; used when the coordinated atoms are all connected by bonds. Usually the metal-ligand bonding involves for π-type coordination. In speech, η^1=monohapto; η^2=dihapto; η^3 =trihapto, etc.
bridging ligands		μ_n where n is the number of atoms bridged. The number n is usually omitted when n =2.
chelating ligand ring twist		λ- or δ-

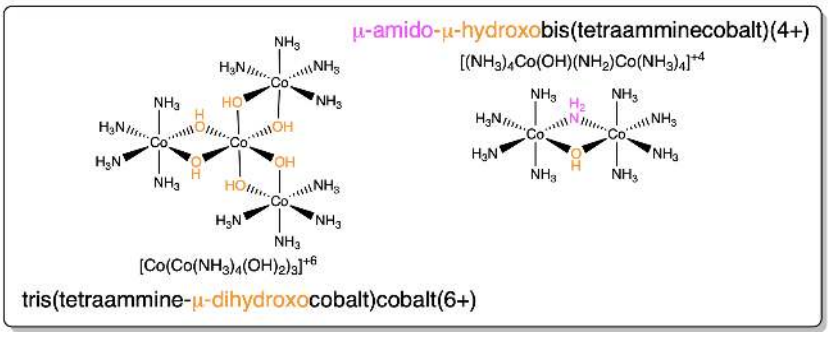
A example showing how the nomenclature rule is applied to a ligand that can have two coordination modes is given in Scheme 8.2.IV.

Scheme 8.2.IV. Use of the κ notation to specify the number of attached groups in a multidentate ligand.



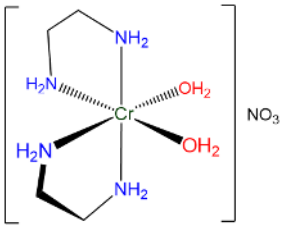
Two examples showing how the nomenclature rule is applied to bridging ligands are given in Scheme **8.2.V**. The names of the complexes follow the rules described in 9.2.6: multinuclear coordination complexes.

Scheme 8.2.V. Use of the μ notation to specify bridging ligands in metal complexes.[3]



6. If desired, parentheses *may* be used to delineate a ligand name to make it easier to identify in the name. This can be particularly helpful when the name contains a lot of information to keep track of. An example is given in Scheme **8.2.VI**.

   Scheme 8.2.VI. When naming the complex shown *cis*-diaquabis(ethylenediamine)chromium(III) nitrate is easier to read than *cis*-diaquabisethylenediaminechromium(III) nitrate.



Specify the metal

- In neutral and cationic complexes the metal's name is used directly

  - *e.g.* as in hexammineruthenium(III) for $[Ru(NH_3)_6]^{3+}$

- In anionic complexes, *-ate* replaces *-ium*, *-en*, or *–ese* or adds to the metal name.

  e.g. as in hexachloromanganate(IV) for $MnCl_6^{2-}$

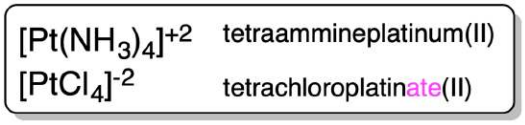
- In anionic complexes of some metals a Latin-derived name is used instead of the element's English name. These names are given in Table **8.2.5**.

  Table 8.2.5. Latin terms for Select Metal Ions. Redrawn from this page describing the nomenclature of coordination complexes.

Transition Metal	Latin
Copper	Cuprate
Gold	Aurate
Iron	Ferrate
Lead	Plumbate
Silver	Argentate
Tin	Stannate

An example of the application of the metal naming rules is given in Scheme \sf{\PageIndex{VII}}\).

Scheme 8.2.VII. Example of the application of the metal specification rules to a cationic and anionic platinum complexes.[3]



Specify the oxidation state of the metal.

Two different systems are used to specify the oxidation state of the metal.

1. In the **Stock system** the metal's oxidation state is indicated in Roman numerals after the metal name.

   Examples:

   $[CoCl(NH_3)_5]Cl_2$ = pentamminechlorocobalt(III) chloride

   $[PtBr_2(bpy)]$ = bipyridinedibromoplatinium(II)

   $K[Ag(SCN)_2]$ = potassium di-*S*-thiocyanatoargentate(I)

2. In the **Ewing-Bassett system** the charge on the complex is specified in Arabic numerals after the complex name. This provides a way of specifying a complex even when the oxidation state of the metal isn't known and, in cases where it is known, the value of the metal's oxidation state may be inferred from the complex ion's charge.

   $[CoCl(NH_3)_5]Cl_2$ = pentamminechlorocobalt(2+) chloride

   $[PtBr_2(bpy)]$ = bipyridinedibromoplatinium(0)

   $K[Ag(SCN)_2]$ = potassium di-*S*-thiocyanatoargentate(1-)

Summary

A graphical summary of the **rules for naming complexes** along with a few examples that you can use to review the nomenclature rules is given in Figure **8.2.1**. This work by Stephen Contakes is licensed under a Creative Commons Attribution 4.0 International License.

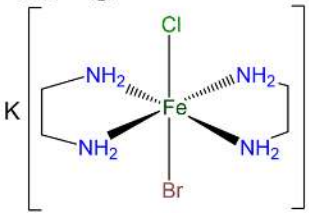
stereochemical prefix-	**Specify Ligands**	**Indicate Metal**	**Charge on the complex or metal oxidation state**
As appropriate use *cis-*, *trans-*, *fac-*, *mer-*, Λ-, Δ-, to indicate stereochemistry.	What ligands and how many? – List alphabetically by ligand name • Neutral – ligand name • Carionic – ligand name • Anionic – change last vowel to "o" – Indicate # by di-, tri-, tetra-, etc. (or bis-, tris-, tetrakis-, etc. if there is a di-, tri-, tetra, etc. in the ligand name) As appropriate, how are the ligands arranged? – Ambidentate – indicate linkage point by κ & italicized element symbol - other structure – use κ^n, η^n, μ_n, λ-, δ- For clarity, parentheses may be used to delineate ligands	Neutral, cationic: English name Anionic – change ending to "ate" - Latin names for Ag, Au, Cu, Fe, Pb, Sn; English for others	Stock system: Metal Oxidation state in capital Roman numerals Ewing-Bassett system: Complex's charge in Arabic numerals

Examples:

$[Ru(NH_3)_6](NO_3)_3$ hexammineruthenium(3+) nitrate or hexammineruthenium(III) nitrate

$K_2[PtCl_4]$ potassium tetrachloroplatinate(2-) or potassium tetrachloroplatinate(II)

$K[Ag(CN)_2]$ potassium dicyanoargentate(1-) or potassium dicyanoargentate(I)



potassium *trans*- bromochlorobis(ethylenediamine)iron(1+) (Ewing-Bassett)

-or-

potassium *trans*-bromochlorobis(ethylenediamine)iron(III) (Stock)

Figure 8.2.1. Summary of nomenclature rules for coordination complexes along with a few examples of their application.

When learning chemical nomenclature practice makes perfect. The following examples and exercises are provided to give you this practice. Additional examples and exercises on the https://chem.libretexts.org/ site include a set of simple examples with explained solutions, a set of simple exercises with solutions, and a set of more challenging exercises without solutions.

Exercise 8.2.2. Assigning metal oxidation states in a complex

In order to name a complex in the Stock system it is necessary to assign a formal oxidation state to the metal.

For this reason it is important to be able to assign the oxidation state of a metal in a complex. Fortunately, this is easy to do if you remember

1. The sum of all atom's oxidation states will equal the overall charge on the complex
2. When determining the metal's oxidation state the ligands can be treated as having an oxidation state equal to their charge - *i.e.* the charge they possess in the form they coordinate the metal so if they need to lose a proton to bind don't forget to account for that.

Given the above, assign the oxidation state of the metal in the following real and hypothetical complexes.

a. $K_3[Fe(CN)_6]$
b. $[CoCl(NH_3)_5](NO_3)_2$
c. $K_2[PtCl_4]$
d. [MnCl(por)]
e. $[Ru(bpy)_3]Cl_2$
f. $[PdCl_2(dppe)]$
g. $[Mn(en)_2(SCN)_2]$

Answer for $K_3[Fe(CN)_6]^{3-}$.

This contains $[Fe(CN)_6]^{3-}$; so O.S.$_{Fe}$ + 6 x (-1) (for CN^-) = -3 (the complexes' charge) so O.S.$_{Fe}$ = +3 or Fe^{3+}.

Answer for $[CoCl(NH_3)_5](NO_3)_2$.

This contains $[CoCl(NH_3)_5]^{2+}$; so O.S.$_{Co}$ + 1 x (-1) (for Cl^-) + 0 x 5 (for NH_3) = +2 (the complexes' charge) so O.S.$_{Co}$ = +3 or Co^{3+}.

Answer for $K_2[PtCl_4]$.

This contains $2K^+$ and $[PtCl_4]^{2-}$; so O.S.$_{Pt}$ + 4 x (-1) (for Cl^-) = -2 (the complexes' charge) so O.S.$_{Pt}$ = +2 or Pt^{2+}.

Answer for [MnCl(por)].

O.S.$_{Pt}$ + 1 x (-2) (for por; see table 9.2.2) + 1 x (-1) (for Cl^-) = +0 (the complexes' charge) so O.S.$_{Mn}$ = +3 or Mn^{3+}.

Answer $[Ru(bpy)_3]Cl_2$.

The complex is $[Ru(bpy)3]^{2+}$ so O.S.$_{Ru}$ + 0 x 3 (for bpy) = +2 (the complexes' charge) so O.S.$_{Ru}$ = +2 or Ru^{2+}.

Answer $[PdCl_2(dppe)]$.

O.S.$_{Pd}$ + 2 x (-1) (for Cl^-) + 0 x 3 (for dppe) = +0 (the complexes' charge) so O.S.$_{Pd}$ = +2 or Pd^{2+}.

Answer $[Mn(en)_2(SCN)_2]$.

O.S.$_{Mn}$ + (2 x 0) (for en) + 2 x (-1) (for SCN^-) = +0 (the complexes' charge) so O.S.$_{Mn}$ = +2 or Mn^{2+}.

Exercise 8.2.3: Simple Nomenclature Problems.

Name the following compounds in both the Stock and Ewing-Bassett systems:

a. $[Ru(NH_3)_6](NO_3)_3$
b. $K_2[PtCl_4]$
c. $K[Ag(CN)_2]$
d. $Cs[CuBrCl_2F]$
e. $[Cu(acac)_2]$

Answer

	Complex	Stock system name	Ewing-Bassett System name
a	$[Ru(NH_3)_6](NO_3)_3$	hexammineruthenium(III) nitrate	hexammineruthenium(3+) nitrate
b	$K_2[PtCl_4]$	potassium tetrachloroplatinate(II)	potassium tetrachloroplatinate(2-)
c	$K[Ag(CN)_2]$	potassium dicyanoargentate(I)	potassium dicyanoargentate(1-)
d	$Cs_2[CuBrCl_2F]$	cesium bromodichloroflourocuprate(II)	cesium bromodichloroflourocuprate(2-)
e	$[Cu(acac)_2]$	bis(acetylacetonato)copper(II)	bis(acetylacetonato)copper(0)

Exercise 8.2.4: More simple nomenclature problems.

Name the following compounds and ions in both the Stock and Ewing-Bassett systems.

a. $Cu(OH)_4^-$
b. $[AuXe_4]^{2+}$
c. $AuCl_4^-$
d. $Fe(CN)_6^{3-}$
e. $K_4[Fe(CN)_6]$
f. *trans*-$[Cu(en)_2(NO_2)_2]$ (the N is bound to Cu)
g. cis-$IrCl_2(CO)(PPh_3)$ (ignore stereochemistry)
h. $IrCl(PPh_3)$

Answer

	Compound	Stock System Name	Ewing-Bassett System Name
a	$Cu(OH)_4^-$	tetrahydroxocuprate(III) or tetrahydroxidocuprate(III)	tetrahydroxidocuprate(1-) or tetrahydroxidocuprate(1-)
b	$[AuXe_4]^{2+}$	tetraxenongold(II)	tetraxenongold(2+)
c	$AuCl_4^-$	tetrachloroaurate(III)	tetrachloroaurate(1-)
d	$Fe(CN)_6^{3-}$	hexacyanoferrate(III) or hexacyanidoferrrate(III)	hexacyanoferrate(3-) or hexacyanidoferrate(3-)
e	$K_4[Fe(CN)_6]$	potassium hexacyanoferrate(II) or potassium hexacyanidoferrrate(II)	potassium hexacyanoferrate(4-) or potassium hexacyanidoferrrate(4-)
f	*trans*-$[Cu(en)_2(NO_2)_2]$ (the N is bound to Cu)	bis(ethylenediamine)bisnitrocopper(II) or bis(ethylenediamine)bis(nitrito-κN)copper(II)	bis(ethylenediamine)bisnitrocopper(0) or bis(ethylenediamine)bis(nitrito-κN)copper(0)
g	*cis*-$IrCl_2(CO)(PPh_3)$	*cis*-dichlorocarbonyltriphenylphosphineiridium(I) or *cis*-dichloro(carbonyl)(triphenylphosphine)iridium(I)	*cis*-dichlorocarbonyltriphenylphosphineiridium(0) or *cis*-dichloro(carbonyl)(triphenylphosphine)iridium(0)
h	$IrCl(PPh_3)$	chlorotris(triphenylphosphine)iridium(I)	chlorotris(triphenylphosphine)iridium(0)

Exercise 8.2.5: Even more simple nomenclature problems.

Name the following compounds and ions in both the Stock and Ewing-Bassett systems. Ignore prefixes for designating isomers if you haven't learned about those.

a. $Fe(acac)_3$
b. $K_2[CuBr_4]$
c. ReH_9
d. $[Ag(NH_3)_2]BF_4$
e. $[Ag(NH_3)_2][Ag(CN)_2]$

f. $[Ni(CN)_4]^{2-}$
g. $[Co(N_3)(NH_3)_5]SO_4$
h. $[CoBrCl(H_2O)(NH_3)]I$ (ignore stereochemistry)

Sample Answers

	Complex	Stock system name	Ewing-Bassett System name
a	$Fe(acac)_3$	tris(acetoacetato)iron(III)	tris(acetoacetato)iron(0)
b	$Na_2[CuBr_4]$	sodium tetrabromocuprate(II)	sodium tetrabromocuprate(2-)
c	$[Co(NH_3)_6][Co(ox)_3]$	hexamminecobalt(III) tris(oxalato)cobalt(III)	hexamminecobalt(3+) tris(oxalato)cobalt(3-)
d	$[Ag(NH_3)_2]BF_4$	diamminesilver(I) tetrafluoroborate	diamminesilver(1+) tetrafluoroborate
e	$[Ag(NH_3)_2][Ag(CN)_2]$	diamminesilver(I) dicyanoargentate(I) or diamminesilver(I) dicyanidoargentate(I)	diamminesilver(1+) dicyanoargentate(1-) or diamminesilver(1+) dicyanidoargentate(1-)
f	$[Ni(CN)_4]^{2-}$	tetracyanonickelate(II) or tetracyanonickelate(II) ion	tetracyanonickelate(2-) or tetracyanonickelate(2-) ion
g	$[Co(N_3)(NH_3)_5]SO_4$	pentammineazidocobalt(III) sulfate	pentammineazidocobalt(2+) sulfate
h	$[CoBrCl(H_2O)(NH_3)]I$ (ignore stereochemistry)	ammineaquabromochlorocobalt(III) iodide	ammineaquabromochlorocobalt(1+) iodide

Exercise 8.2.6: Nomenclature problems, some of which involve consideration of isomerism.

Name the following compounds and ions in both the Stock and Ewing-Bassett systems. Ignore prefixes for designating isomers if you haven't learned about those.

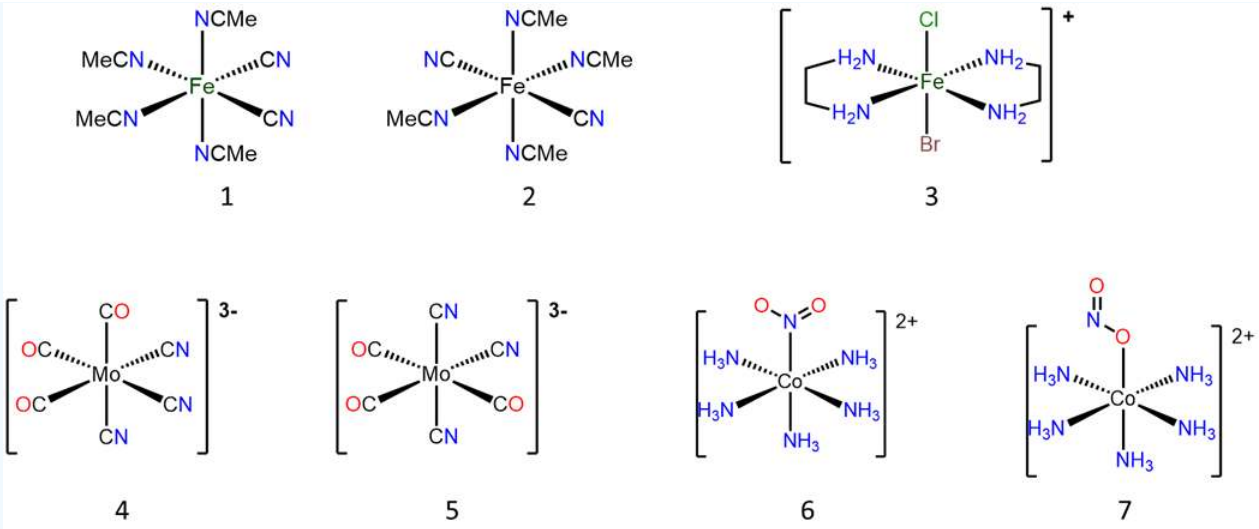
a. *trans*-$[Cu(dppe)_2(NO_2)_2]$ (the N is bound to Cu)
b. $[Pd(en)_2(SCN)_2]$, with the thiocyanates bound Pd-SCN
c. $[Mn(CO)_6]BPh_4$ (BPh_4 = tetraphenylborate)
d. $Rb[AgF_4]$
e. K_2ReH_9
f. K_3CrCl_6
g. $[Ru(H_2O)_6]Cl_2$
h. [*cis*-$Fe(CO)_4I_2$]
i. K_2[*trans*-$Fe(CN)_4(CO)_2$]
j. [*cis*-$MnCl(H_2O)_4(NH_3)$](NO_3)
k. K_3[*fac*-$RuCl_3(PMe_3)_3$]

Answer

	Complex	Stock system name	Ewing-Bassett System name
a	*trans*-$[Cu(dppe)_2(NO_2)_2]$	*trans*-bis(diphenylphosphinoethane)bisnitrocopper(II) or *trans*-bis(diphenylphosphinoethane)bis(nitrito-κN)copper(II)	*trans*-bis(diphenylphosphinoethane)bisnitrocopper(0) or *trans*-bis(diphenylphosphino)ethane bis(nitrito-κN)copper(0)
b	$[Pd(en)_2(SCN)_2]$, with the thiocyanates bound Pd-SCN	bis(ethylenediamine)bisthiocyanatopalladium(II) or bis(ethylenediamine)bis(thiocyanato-*S*)palladium(II) or bis(ethylenediamine)bis(thiocyanato-κS)palladium(II)	bis(ethylenediamine)bisthiocyanatopalladium(0) or bis(ethylenediamine)bis(thiocyanato-*S*)palladium(0) or bis(ethylenediamine)bis(thiocyanato-κS)palladium(0)
c	$[Mn(CO)_6]BPh_4$	hexacarbonylmanganese(I) tetraphenylborate	hexacarbonylmanganese(I) tetraphenylborate
d	$Rb[AgF_4]$	rubidium tetraflouroargentate(III)	rubidium tetraflouroargentate(1-)
e	K_2ReH_9	potassium nonahydridorhenium(VII)	potassium nonahydridorhenium(2-)
f	K_3CrCl_6 or $K_3[CrCl_6]$	potassium hexachlorochromium(III) or potassium hexachloridochromium(III)	potassium hexachlorochromium(3-) or potassium hexachloridochromium(3-)
g	$[Ru(H_2O)_6]Cl_2$	hexaaquaruthenium(II) chloride	hexaaquaruthenium(2+) chloride
h	[*cis*-$Fe(CO)_4I_2$]	*cis*-tetracarbonyldiiodoiron(II)	*cis*-tetracarbonyldiiodoiron(0)
i	K_2[*trans*-$Fe(CN)_4(CO)_2$]	potassium *trans*-dicarbonyltetracyanoferrate(II)	potassium *trans*-dicarbonyltetracyanoferrate(2-)
j	[*cis*-$MnCl(H_2O)_4(NH_3)$] (NO_3)	*cis*-amminetetraaquachloromanganese(0) nitrate	*cis*-amminetetraaquachloromanganese(1+) nitrate
k	K[*fac*-$RuCl_3(PMe_3)_3$]	potassium *fac*-trichlorotris(triphenylphosphine)ruthenium(II)	potassium *fac*-trichlorotris(triphenylphosphine)ruthenium(1-)

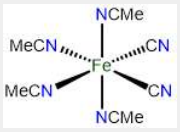
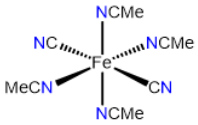
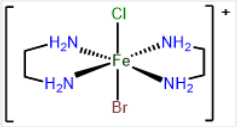
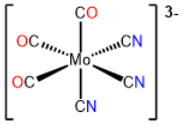
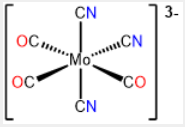
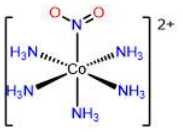
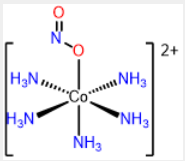
Exercise 8.2.7

Name the compounds and ions belowusing both the Stock and Ewing-Bassett systems. Ignore prefixes for designating isomers if you haven't learned about those.



https://chem.libretexts.org/@go/page/326233

Answer

#	Structure	Stock system name	Ewing-Bassett system name
1		*cis*-tetraacetonitriledicyanoiron(II) or *cis*-tetraacetonitriledicyanidoiron(II)	*cis*-tetraacetonitriledicyanoiron(0) or *cis*-tetraacetonitriledicyanoiron(0)
2		*trans*-tetraacetonitriledicyanoiron(II) or *trans*-tetraacetonitriledicyanidoiron(II)	*trans*-tetraacetonitriledicyanoiron(0) or *trans*-tetraacetonitriledicyanidoiron(0)
3		*trans*-bromochlorobis(ethylenediamine)iron(III) or *trans*-bromidochloridobis(ethylenediamine)iron(III)	*trans*-bromochlorobis(ethylenediamine)iron(1+) or *trans*-bromidochloridobis(ethylenediamine)iron(1+)
4		*fac*-tricarbonyltricyanomolybdate(0) or *fac*-tricarbonyltricyanidomolybdate(0)	*fac*-tricarbonyltricyanomolybdate(3-) or *fac*-tricarbonyltricyanidomolybdate(3-)
5		*mer*-tricarbonyltricyanomolybdate(0) or *mer*-tricarbonyltricyanidomolybdate(0)	*mer*-tricarbonyltricyanomolybdate(3-) or *mer*-tricarbonyltricyanidomolybdate(3-)
6		pentammineitrito-*N*-cobalt(III), pentammineitrito-**κ***N*-cobalt(III), or pentammineitrocobalt(III)	pentammineitrito-*N*-cobalt(2+), pentammineitrito-**κ***N*-cobalt(2+), or pentammineitrocobalt(2+)
7		pentammineitrito-*O*-cobalt(2+), pentammineitrito-**κ***O*-cobalt(2+), or pentammineitritocobalt(2+)	pentammineitrito-*O*-cobalt(2+), pentammineitrito-**κ***O*-cobalt(2+), or pentammineitritocobalt(2+)

Exercise 8.2.8

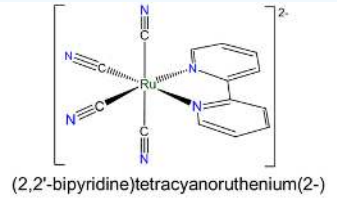
Draw structural formulae for the following compounds and ions. You may assume that

- complexes in which the metal has a coordination number of six are octahedral
- complexes in which the metal has a coordination number of five are trigonal bipyramidal
- complexes in which Pt^{II} , Pd^{II} , or Rh^{I}, or Ir^{I} have a coordination number of four are square planar
- other complexes in which the metal has a coordination number of four will be tetrahedral

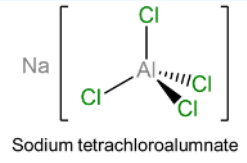
a. (2,2'-bipyridine)tetracyanoruthenium(2-)
b. sodium tetrachloroalumnate (note that since Al is a main group metal with a generally fixed oxidation state no oxidation state is given)
c. pentaamminechlorocobalt(2+) sulfate
d. carbonylhydridotris(triphenylphosphine)rhodium(I) (the ligands in this complex occupy sterically preferred positions)
e. bromotrichlorocobaltate(III)
f. hexaaquacopper(2+) sulfate
g. sodium tris(oxalato)cobalt(III)
h. *fac*-(1,10-phenanthroline)tricarbonylchlororhenium(I)
i. *mer*-triaquatrichlorochromium(III)
j. *trans*-dichlorobis(ethylenediamine)platinum(IV)

Answers

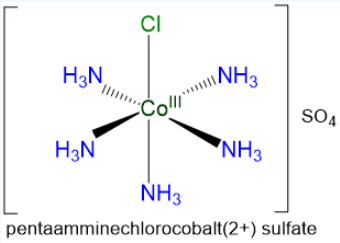
a



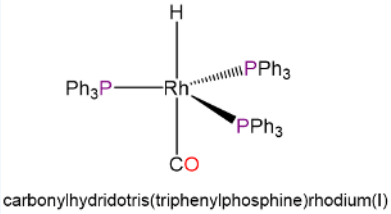
b



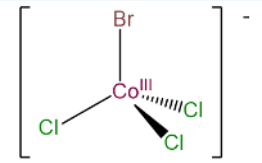
c



d

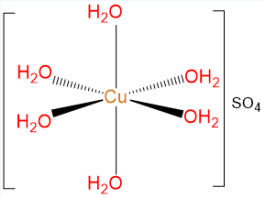


e



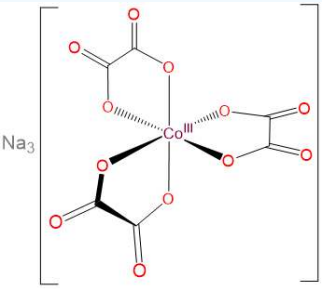
bromotrichlorocobaltate(III)

f



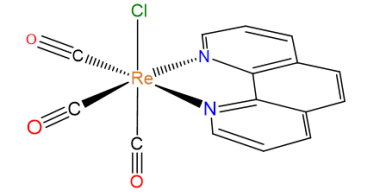
hexaaquacopper(2+) sulfate

g



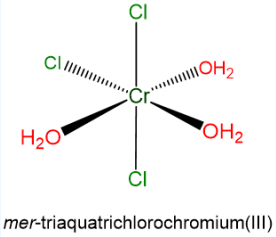
sodium tris(oxalato)cobalt(III)
Λ-enantiomer shown

h



fac-(1,10-phenanthroline)tricarbonylchlororhenium(I)

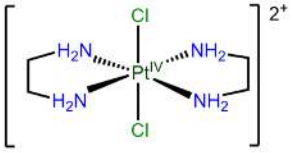
i



mer-triaquatrichlorochromium(III)

j

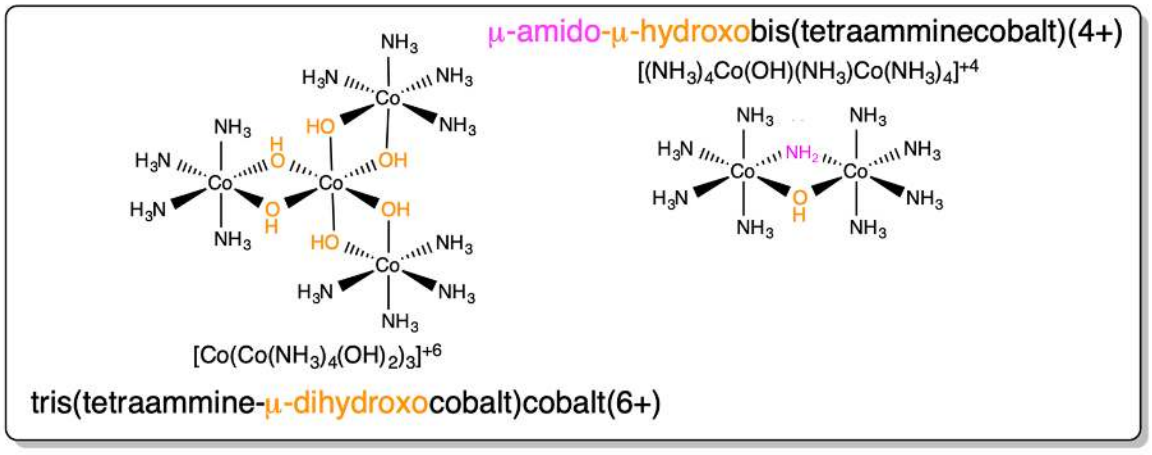
https://chem.libretexts.org/@go/page/326233



trans-dichlorobis(ethylenediamine)platinum(IV)

Exercise 8.2.9.

The name of the structure named tris(tetraammine-μ-dihydroxocobalt)cobalt(6+) in Scheme **8.2.III** (reproduced below) is incomplete. Give the complete name of the structure in both the Stock and Ewing-Basset systems.



Answer

Δ-tris(tetraammine-μ-dihydroxocobalt)cobalt(6+) or **Δ**-tris(tetraammine-μ-dihydroxocobalt(III)cobalt(III)

Rules for Writing Chemical Formulas

The rules for writing the formulas of coordination compounds follow the same general convention used to specify their names, but are not always adhered to in the chemical literature. Organized predictable formulae can be easier to read and understand than haphazardly written ones the rules for writing the formulae of coordination compounds have value. The rules as given here are adapted from a summary by Robert Lancashire.

1.If there are multiple ions present list the cations before anions.

2.Enclose all the constituents of each complex ion in square brackets.

3.For each complex ion,

- Give the **central metal** atom first.
- Then **ligands** next, listed in alphabetical order, ignoring prefixes according to the first letters in the ligand's symbol as written. This is true regardless of whether the symbol is an element symbol (like C, N, O, etc.) or a symbol for the ligand name (bpy, en, MeCN, etc.). Contrary to widely-circulated myths, the ligand's charge does not matter.[4]
- The formulae or abbreviations (*e.g.* en) for all polyatomic ligands should be enclosed in ordinary parentheses.
- As appropriate, use italicized atom symbols to indicate linkage isomerism and prefixes such as *cis*-, *trans*-, *fac*-, *mer*-, **Λ**-, **Δ**-, κ^n, η^n , μ_n, **λ**-, \or (\delta\)- to indicate stereochemistry.
- When a ligand is bound to a metal through a particular atom, preferably place that atom closest the metal - *e.g.* $[Fe(CN)_6]^{3-}$ not $[Fe(NC)_6]^{3-}$ (Note: this rule primarily is used for ambidentate ligands; although IUPAC reccomends that aqua ligands be written as OH_2 when the O would be closest to its coordinated metal they are still usually written as H_2O).

These rules are graphically summarized in Figure **8.2.2**.

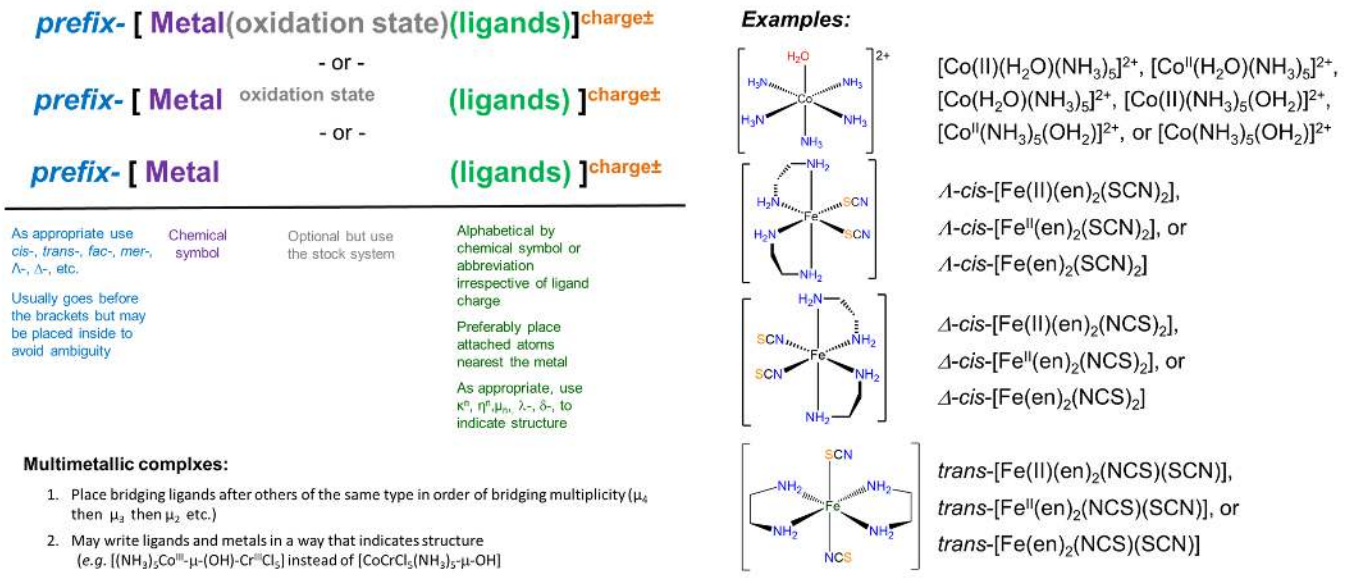
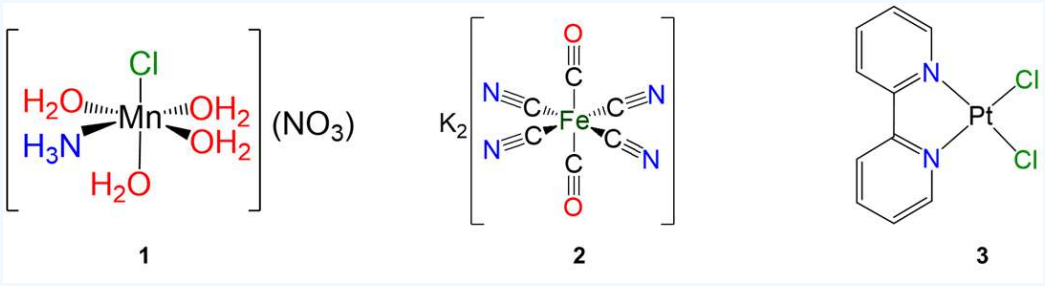


Figure **8.2.2.** Summary of the rules for writing the formula of a coordination complexes along with a few examples of their application. This work by Stephen Contakes is licensed under a Creative Commons Attribution 4.0 International License.

Exercise 8.2.10

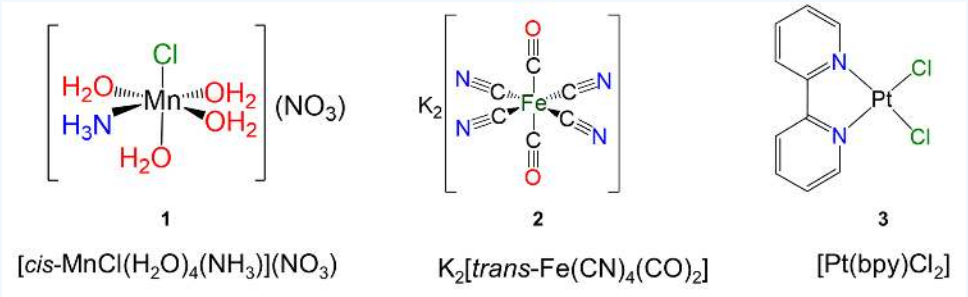
Give the formulae of the following complexes.



1 2 3

.

Answer



1 2 3

[*cis*-MnCl(H2O)4(NH3)](NO3) K2[*trans*-Fe(CN)4(CO)2] [Pt(bpy)Cl2]

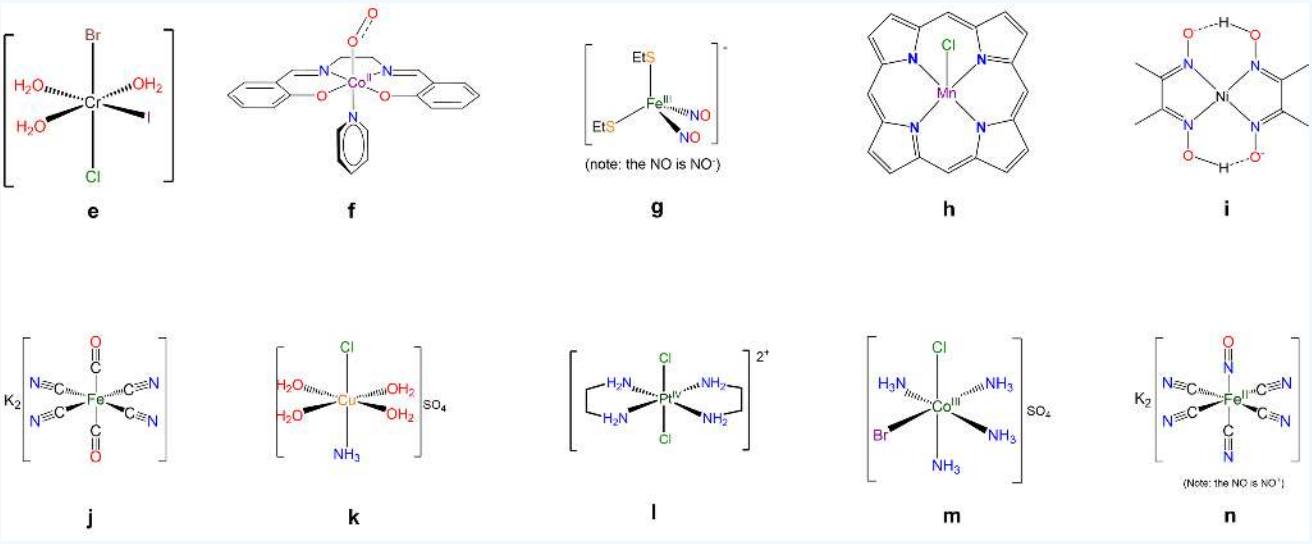
Exercise 8.2.11

Write formulae for each of the following compounds and ions. When multidentate ligands are present use suitable abbreviations.

a. pentaamminechlorocobalt(2+) sulfate
b. Δ-diamminebis(oxalato)manganate(III)

c. *trans*-tetraacetonitriledicyanoiron(II)

d. tricarbonyldichlorobis(triphenylphosphine)molybdenum



Answers

a.

$[CoCl(NH_3)_5](SO_4)$

b.

Δ-$[Mn(NH_3)_2(ox)_2]^-$

c.

trans-$[Fe(CN)_2(NCMe)_4]$

d.

$[MoCl_2(CO)_3(PPh_3)]$ or $MoCl_2(CO)_3(PPh_3)$

e.

mer-$[CrBrCl(H_2O)_3I]$

f.

$[Co(O_2)py(salen)]$

g.

$[Fe(NO)_2(SEt)_2]^-$

h.

[NiCl(por)] or $[MnCl(porphyrin)]^-$

i.

$[Ni(DMG)_2]$ or $[Ni(Hdmg)_2]$

j.

potassium *trans*-$[Fe(CN)_2(CO)_4]$

k.

trans-$[CuCl(H_2O)_4(NH_3)]SO_4$

l.

trans-$[PtCl_2(en)_2]^{2+}$

m.

cis-$[CoBrCl(NH_3)_4]SO_4$

n.

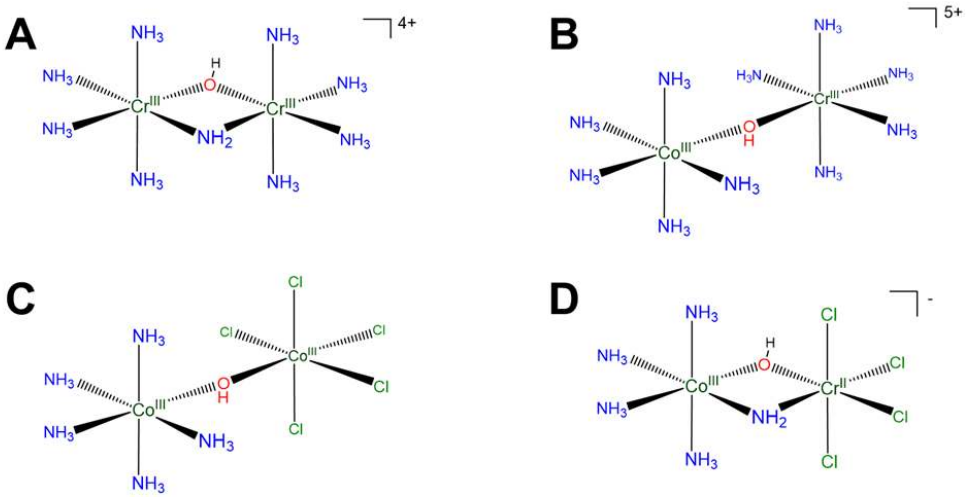
$K_2[Fe(CN)_5NO]$

Multinuclear Coordination Complexes

Multinuclear coordination complexes contain multiple metals connected by one or more bridging ligands. The structures of bridging complexes can usually be inferred from their μ-tagged ligands in their names and formulae. For the benefit of instructors who wish to have their students name multinuclear complexes.

Multinuclear complexes are named differently depending on whether the groups on either side of the bridging ligands are identical or different, as shown in Scheme **8.2.VIII**.

Scheme 8.2.VIII. Multinuclear coordination complexes may be named differently depending on whether the groups on either side of the bridging ligands are the same or different. The groups are the same if the metal, ligands, and ligand arrangement are identical. This is true in A but in B the metals differ, in C the ligands differ, and in D both the metal and ligands differ.



Naming multinuclear complexes

Let's look at the rules for naming symmetric and asymmetric multinuclear complexes.

Symmetric complexes

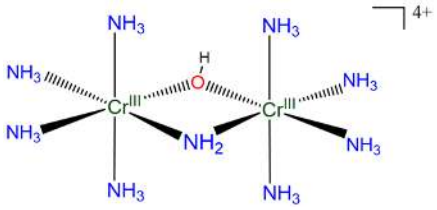
The IUPAC naming system helpfully avoids the sort of ambiguities and *ad hoc* choices involved in most textbook-level nomenclature systems for multimetallic complexes. Unfortunately, it is correspondingly difficult for beginners to employ. Thus it will only be applied in depth to the case of symmetric complexes. Symmetric complexes are particularly easy to name in the IUPAC system and several of its variants that find common use. In these

1. The ligands are given in alphabetical order. When there are bridging and non-bridging ligands of the same type the bridging ligands are given first. When there are multiple bridging ligands of the same type but which use different bridging modes (*e.g.* μ_4-, μ_3-, μ_2-) the bridging ligands are specified in decreasing order of bridging multiplicity, *e.g.* μ_3 -sulfido-di-μ-sulfido.
2. The groups bridged are given afterwards using names that follow the ordinary rules. Generally this either involves
   a. naming all the ligands followed by all the metals, in both cases using prefixes to indicate the number of each
   b. naming each group of atoms individually as in the less formal naming system, using prefixes to indicate the number of ligands (this is an unofficial variant of the IUPAC system that some textbook authors seem to prefer).

These two rules are sufficient to describe simple symmetric bridging complexes.

Example: The compound in Scheme **8.2.VIIIA**

https://chem.libretexts.org/@go/page/326233



may be named

[μ-amido-μ-hydroxo-octaamminedichromium(4+)] ion

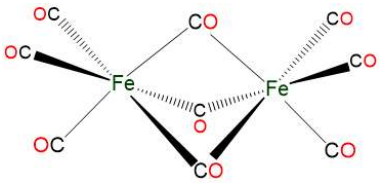
or

[μ-amido-μ-hydroxo-bis(tetraamminechromium(III))] ion

or

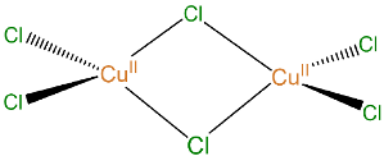
[μ-amido-μ-hydroxo-bis(tetraamminechromium)(4+)] ion

Example: The complex[5]



may be named [tri-μ-carbonyl-bis(tricarbonyliron)(0)], [tri-μ-carbonyl-bis(tricarbonyliron(0))], or [tri-μ-carbonyl-hexacarbonyldiiron)(0)]

Example: The complex



may be named di-μ-chlorido-tetrachloridodicopper(II), di-μ-chlorido-bis(dichlorocopper(II)), or di-μ-chlorido-bis(dichlorocopper)(0)

Asymmetric complexes

For a symmetrical complex like the $[Cu_2Cl_4(\mu\text{-}Cl)_2]$ considered above it is enough to specify the existence of the two bridging and four terminal chloro ligands; there is no need to number the chloro ligands or to specify exactly which ones are involved in bridging or to clarify that the bridging involves κ^2 coordination of the chloro ligands. In cases where the two metal centers or the chloro ligands differ it is necessary to specify the exact ligands and metals involved and how they are connected.

For example, a more extensive IUPAC name for $[Cu_2Cl_4(\mu\text{-}Cl)_2]$ in which the chloro ligands are individually and more completely specified would read di-μ_2-chlorido-tetrachlorido-1κ^2Cl,2κ^2Cl-dicopper(II).

Even more extensive systems would involve numbering the metals and specifying how they are connected together too. The details of how this is done are typically beyond the level of most undergraduate and graduate courses in inorganic chemistry. Those who want to know the details should consult the red book. In many cases it is sufficient to reserve the use of formal IUPAC names for use in publications and to employ a comvenient shorthand naming system for everyday use. An example of one type of system that is sometimes employed is given next.

Unofficial methods

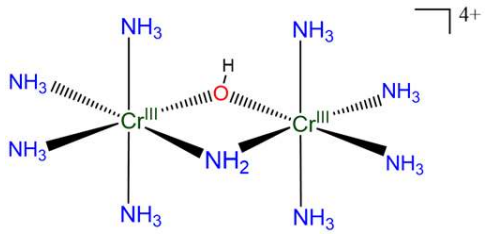
It can be quite complicated to use the IUPAC system to name asymmetric multinuclear coordination complexes. Fortunately it is rarely necessary and there are a variety of simpler somewhat *ad hoc* methods that work well for such cases. Since these methods

are commonly used by textbooks and inorganic instructors it is likely worth your while to learn about their general features. In these methods

1. A multinuclear complex is named as a derivative of one of the metal centers and the other metal centers and their ligands are treated as ligands to the prioritized metal center.
2. Unfortunately, most of the time the choice of which metals are part of the ligands and which one is central is made haphazardly. In other words, there is no agreed upon system for assigning which metal center is the central metal and which should be regarded as part of the ligands around it. One way to be more systematic about the selection of the central and ligand-embedded metals is to assign the central metal as the metal of highest priority in the IUPAC priority rules. In the IUPAC priority rules he central metal is the highest priority metal alphabetically by name; then if there is a tie the ligands on each tied metal center are ranked alphabetically and the tied metal center with the highest priority (or most highest priority) ligands wins.
3. The metal centers not chosen as the primary metal center and all ligands around them, including those bridging to the winning metal center, are then treated as a single ligand that coordinates the winning metal center.
4. When naming the ligands and the overall complex, again there is much that is haphazard. However, in the best systems each coordination sphere is named using the same rules as for mononuclear complexes - *i.e.* the ligands are given in alphabetical order, etc.
    - This is true of any metal center-containing ligands.
    - When there is a bridging and non-bridging ligand of the same type the bridging ligands are given first. When there are multiple bridging ligands of the same type but which use different bridging modes (*e.g.* μ_4-, μ_3-, μ_2-) the ligands are specified in decreasing order of bridging multiplicity, *e.g.* μ_3 -sulfido-di-μ-sulfido.

Let's apply these rules to the examples in Scheme **8.2.VIII**.

Compound A:



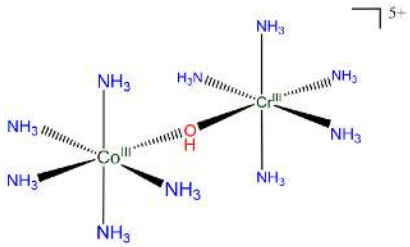
Using hydroxo for the OH^- it may be named

[(μ-amido-tetraammine-μ-hydroxochromium(III))tetraamminechromium(III)] ion

or

[(μ-amido-tetraammine-μ-hydroxochromium)chromium(4+)] ion

Compound B:



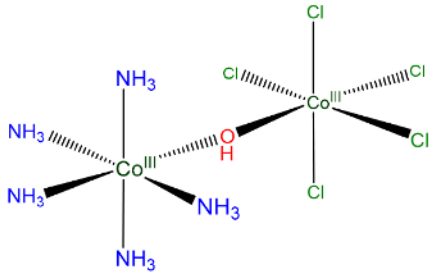
Using hydroxo for OH^- it may be named

[(pentaammine-μ-hydroxocobalt(III))tetraamminechromium(III)] ion

or

[(pentaammine-μ-hydroxocobalt)tetraamminechromium(5+)] ion

Compound C:



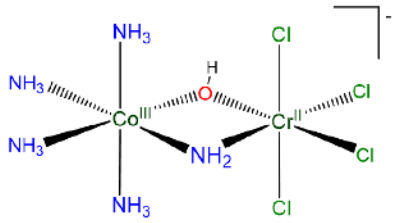
Using hydroxo for OH^- it may be named

[pentaammine(pentachloro-μ-hydroxocobalt(III))cobalt(III)]

or

[pentaammine(pentachloro-μ-hydroxocobalt)cobalt](0)]

Compound D:



Using hydroxo for OH^- and chloro for Cl^- it may be named

[pentaammine(pentachloro-μ-hydroxocobalt(III))chromate(III)] ion

or

[(tetrammine-μ-ammine-μ-hydroxocobalt)tetrachlorochromate](1-)] ion

As can be seen from the examples above this system gives serviceable names for multimetallic complexes but those names are not the IUPAC names and so should not be used to describe complexes outside of pedagogical and informal settings.

Writing and interpreting formulas for multinuclear complexes

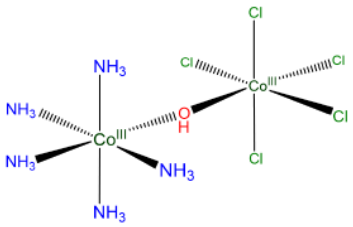
The rules for writing formulae for multinuclear complexes are the same as form mononuclear ones with two added details

1. Write bridging ligands after nonbridging ligands of the same type. For example, Cu_2Cl_6 should be written as $[Cu_2Cl_4$-μ-$Cl)_2]$
2. Although you may ignore that and other rules if you find it helpful to keep groups of metals and ligands together in a way that better convey how the atoms are connected. Just as the structure of ethane may be more clearly conveyed as H_3CCH_3 instead of CH_3CH_3 the complex $[Cu_2Cl_4\mu$-$Cl)_2]$ may be written as $[(Cl_2Cu)(\mu$-$Cl)_2(CuCl_2)]$

Other Examples:

For dichromate write, $[Cr_2O_6(\mu$-$O)]^{2-}$ or $[O_5Cr$-μ-O-$CrO_5]^{2-}$

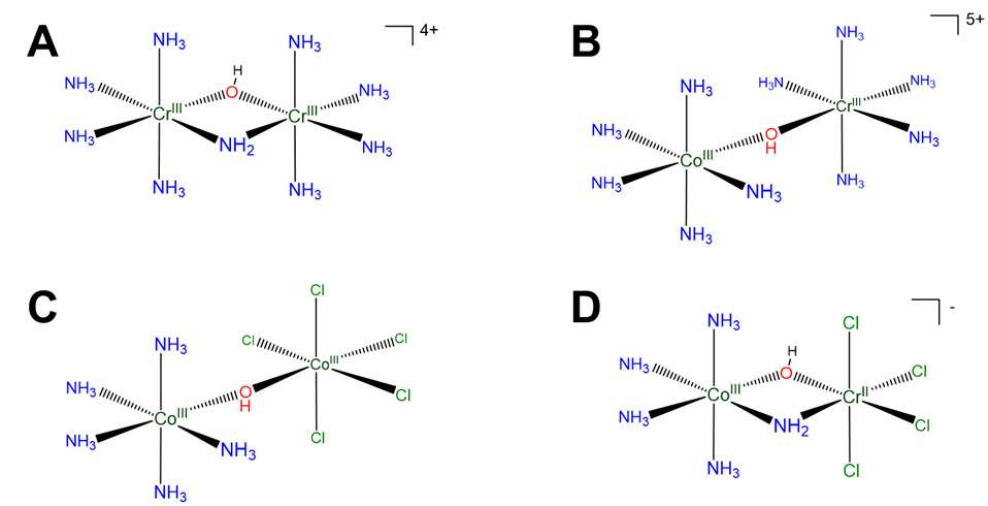
For compound C of Scheme **8.2.VIII**.



write $[Co_2Cl_5(NH_3)_5(\mu$-$OH)]$ or, even better, $[(H_3N)_5Co(\mu$-$OH)CoCl_5]$.

Exercise 8.2.10

Write reasonable formulae for complexes A, B, and D in Scheme **8.2.VIII**, which for convenience is reproduced below.



Sample answers for A

$[Cr_2(NH_3)_8\text{-}\mu(NH_2)\text{-}\mu(OH)]^{4+}$ or $[(H_3N)_4Cr^{III}\text{-}\mu(NH_2)\text{-}\mu(OH)\text{-}Cr^{II}(NH_3)_4]$ and variants thereof involving writing the H_3N as NH_3, μ as μ_2, etc.

Sample answers for B

$[CoCr(NH_3)_{10}\text{-}\mu(OH)]^{5+}$ or, better, $[(H_3N)_5Co^{III}\text{-}\mu(OH)\text{-}Cr^{III}(NH_3)_5]^{5+}$

Sample answers for C

This was already done as an example above, $[Co_2Cl_5(NH_3)_5\text{-}\mu(OH)]$ or, better, $[(NH_3)_5Co^{III}\text{-}\mu(OH)\text{-}Co^{III}Cl_5]$ and variants thereof

Sample answers for D

$[CoCrCl_4(NH_3)_4\text{-}\mu(NH_2)\text{-}\mu(OH)]$ or, better, $[(H_3N)_4Co^{III}\text{-}\mu(NH_2)\text{-}\mu(OH)\text{-}Cr^{II}Cl_4]$

References

1. International Union of Pure and Applied Chemistry *Nomenclature of Inorganic Chemistry* Cambridge, UK, 2005.

2. The structure and name is taken from Choudhury, S. B.; Allan, C. B.; Maroney, M.; Wodward, A. D.; Lucas, C. R. *Inorg. Synth.* **1998**, *32*, 98-107.

3. Haas, K. Naming Transition Metal Complexes. https://chem.libretexts.org/Courses/Saint_Mary's_College%2C_Notre_Dame%2C_IN/CHEM_342%3A_Bio-inorganic_Chemistry/Readings/Week_2%3A_Introduction_to_Metal-Ligand_Interactions_and_Biomolecules/2.1_Transition_metal_complexes/2.1.6%3A_Naming_Transition_Metal_Complexes

4. There is a widely-circulated myth that anionic ligands should be names before neutral ones. This myth is false. According to the IUPAC red book (bolding mine):

IR-2.15.3.4: Ordering ligands in formulae and names In formulae of coordination compounds,

The formulae or abbreviations representing the ligands **are cited in alphabetical order as the general rule**. Bridging ligands are cited immediately after terminal ligands of the same kind, if any, and in increasing order of bridging multiplicity. (See also Sections IR-9.2.3 and IR-9.2.5.)

IR-9.2.3.1 Sequence of symbols within the coordination formula

(i) The central atom symbol(s) is (are) listed first.

(ii) The **ligand symbols (line formulae, abbreviations or acronyms) are then listed in alphabetical order** (see Section IR-4.4.2.2).5 Thus, CH_3CN, MeCN and NCMe would be ordered under C, M and N respectively, and CO precedes Cl because single letter symbols precede two letter symbols. **The placement of the ligand in the list does not depend on the charge of the ligand.**

(iii) More information is conveyed by formulae that show ligands with the donor atom nearest the central atom; this procedure is recommended wherever possible, even for coordinated water.

5. Technically organometallic complexes are named according to slightly different rules but the coordination compound naming system works here. Note that this complex was once thought to possess an Fe-Fe bond, in accordance with the predictions of the 18 electron rule. Consequently, older sources often give an [*Fe-Fe*] after the name to reflect the presence of that bond. However, as the complex is no longer though to possess an Fe-Fe bond it is omitted here.

Contributors and Attributions

Stephen Contakes, Westmont College, to whom comments, corrections, and criticisms should be addressed.

with some examples taken from Naming Transition Metal Complexes by Kathryn Haas.

Consistent with the policy for original artwork made as part of this project, all unlabeled drawings of chemical structures are by Stephen Contakes and licensed under a Creative Commons Attribution 4.0 International License.

8.2: Nomenclature and Ligands is shared under a CC BY-NC-SA 4.0 license and was authored, remixed, and/or curated by LibreTexts.

- **9.3: Nomenclature and Ligands** by Stephen M. Contakes has no license indicated.
- **Current page** is licensed CC BY-NC-SA 4.0.

8.3: Coordination Numbers and Structures

Why Do Coordination Complexes Form the Structures They Do?

As with all chemical structure, coordination complexes form the structures they do so as to best stabilize the metal center and ligands through the formation of metal-ligand bonds. while avoiding destabilizing interactions like steric repulsions. The issue then is how many metal-ligand bonds should be formed and how those bonds should be arranged spatially to give the largest net stabilization possible. This question will eventually be considered in detail in connection with the nature of bonding in coordination compounds. For now, it will be helpful to think about it in terms of seven factors:

The stabilizing effect of metal-ligand bond formation

The driving force for complex formation is the stabilization of electrons in covalent chemical bonds. In the vast majority of cases this largely involves stabilization of the ligand lone pair is as it experiences the effective nuclear charge of the metal, although in a few involves stabilization of metal electrons by ligand nuclei (inverse ligand fields). Regardless, metal-ligand bond formation is stabilizing and classified in the way its effect is to preference the addition of ligands to the complex.

Steric effects

One reason coordination numbers do not increase indefinitely is that only so many ligands can fit around a metal. Exactly how many can fit depends on:

- **Size of metal center:** This is one of the more important factors and many metals tend to exhibit preferred coordination numbers, which depend on their oxidation state and size as shown in Figure **8.3.1**. Larger inner transition metals like the lanthanides and actinides can accommodate 9-12 sterically undemanding ligands while the smaller transition metals tend to accommodate up to six, although larger coordination numbers are more common for larger low valent metals. Thus molybdenum forms seven and eight coordinate $[Mo^{III}(CN)_7]^{4-}$ and $[Mo^{IV}(CN)_8]^{4-}$ with the sterically undemanding cyano ligand.
- **Size and shape of ligands:** As long as ligands are not excessively rigid and bulky their size is less important than the size of the metal in determining the number of ligands that coordinate. Ligands' ability to donate electrons to the metal center also tends to influence coordination number more than ligand size. However, all other things being equal for a given metal and ligand donor ability, small ligands allow higher coordination numbers while fewer bulky ligands will fit around the metal center. Ligands that are more sterically demanding in the vicinity of the metal center tend to limit the ability of other ligands to bind than those which bind through a small extended group. For example, a bulky isocyanide like tBuCN will sterically crowd the metal less than a bulky phosphine like $^{t}BuH_2P$ would. For this reason the effective size of a ligand is sometimes rated in terms of either a cone angle of space they are estimated to occupy around the metal (called the Tolman cone angle, it is commonly used to evaluate phosphines' steric bulk) or the in terms of the percentage of the metal's coordination sphere the ligand occupies (called the percent buried volume, it is used to estimate the steric impact of *N*-heterocyclic carbenes).

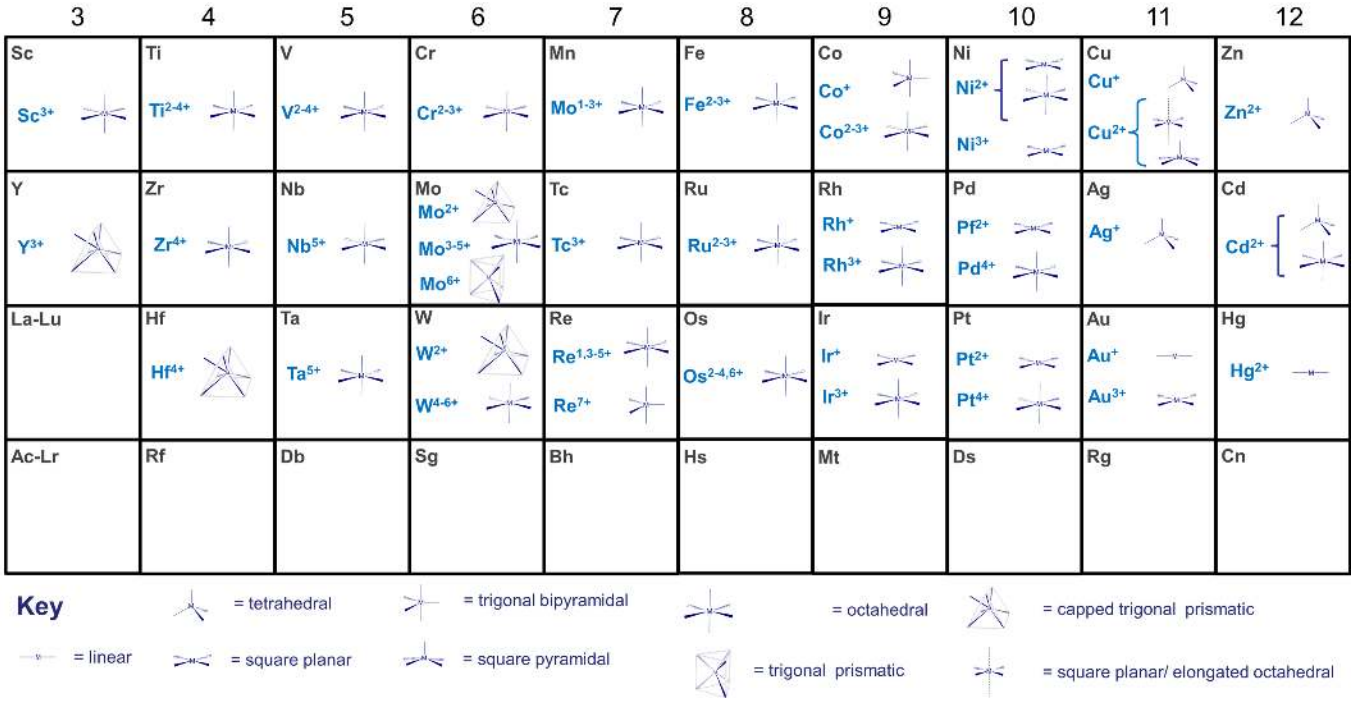


Figure **8.3.1**. Preferred coordination geometries of the transition elements. Assignments are as reported in reference 1 except for Cu^{2+}, which is assigned above as square planar/elongated octahedral instead of the square planar assignment given in that work. This work by Stephen Contakes is licensed under a Creative Commons Attribution 4.0 International License.

Repulsion between M-L bonding electrons

For many complexes steric effects are neither the only effects nor the most important. Among the additional factors that should be considered are the repulsions that occur between the electrons that different ligands donate to the metal-ligand bonding. These electron-electron repulsions affect the

- **Coordination number:** When a ligand donates its electrons to a metal center to form a new metal-ligand bond, the electron density around the metal increases, raising the overall energy of the other M-L bonding electrons. This increased repulsion often limits the number of coordinated ligands. As more ligands are added the electron-electron repulsions keep increasing until the lowering of energy of the ligand electrons in the new bond is insufficient to compensate for the raising of energy of the existing M-L bonding electrons. Based on this effect alone:
  - larger metals tend to achieve higher coordination numbers than smaller ones because the electron-electron repulsions are spread across a larger coordiantion sphere.
  - With a given metal, more electron donating ligands have a greater tendency to form complexes with lower coordination numbers than similar neutral ones do. This is why anionic ligands (which tend to be better electron donors) tend to give lower coordination numbers than comparable neutral ligands (which tend to be weaker donors). Thus Co^{2+} forms $CoCl_4^{2-}$ with chloro ligands but $[Co(H_2O)_6]^{2+}$ with aqua ligands.
- **Coordination geometry:** In the Kepert model for the shapes of coordination complexes, this intraligand repulsion determines the most stable coordination geometry by causing the ligands to move as far apart form one another on the metal's coordination sphere as possible.

Formally, according to the Kepert model:

- any of the metal's valence electrons not involved in metal-ligand bonds occupy (n-1)*d* orbitals and function as core electrons. As core electrons they do not influence the molecular shape
- electrons involved in bonding to a given ligand constitute an electron group that repels all other electron groups around the metal.
- all other things being equal the complex will form the geometry that minimizes the repulsions between electron groups.

Notice the similarities of these postulates to those of VSEPR theory. In predicting coordination geometries in terms of electron-electron repulsions, the Kepert model is just an extension of VSEPR theory to coordination compounds. The difference between VSEPR theory and the Kepert model is that in the Kepert model only electrons involved in metal-ligand bonds count.

Coordination geometries predicted by the Kepert model for coordination numbers two through nine are given in Figure **8.3.2**. As may be seen from the geoemtries listed in Figure **8.3.2**, these are just equivalent to VSEPR geometries for cases in which the number of electron groups is equal to the coordination number.

The difference between optimal and suboptimal coordination geometries is greater with few ligands and becomes smaller and ligands become increasingly dispersed across the metal's coordination sphere. In complexes containing five, seven, eight, or higher coordinate metals a number of geometries that are similar in energy to the preferred geometry. These geometries, which should be regarded as accessible, are also listed in Figure **8.3.2**.

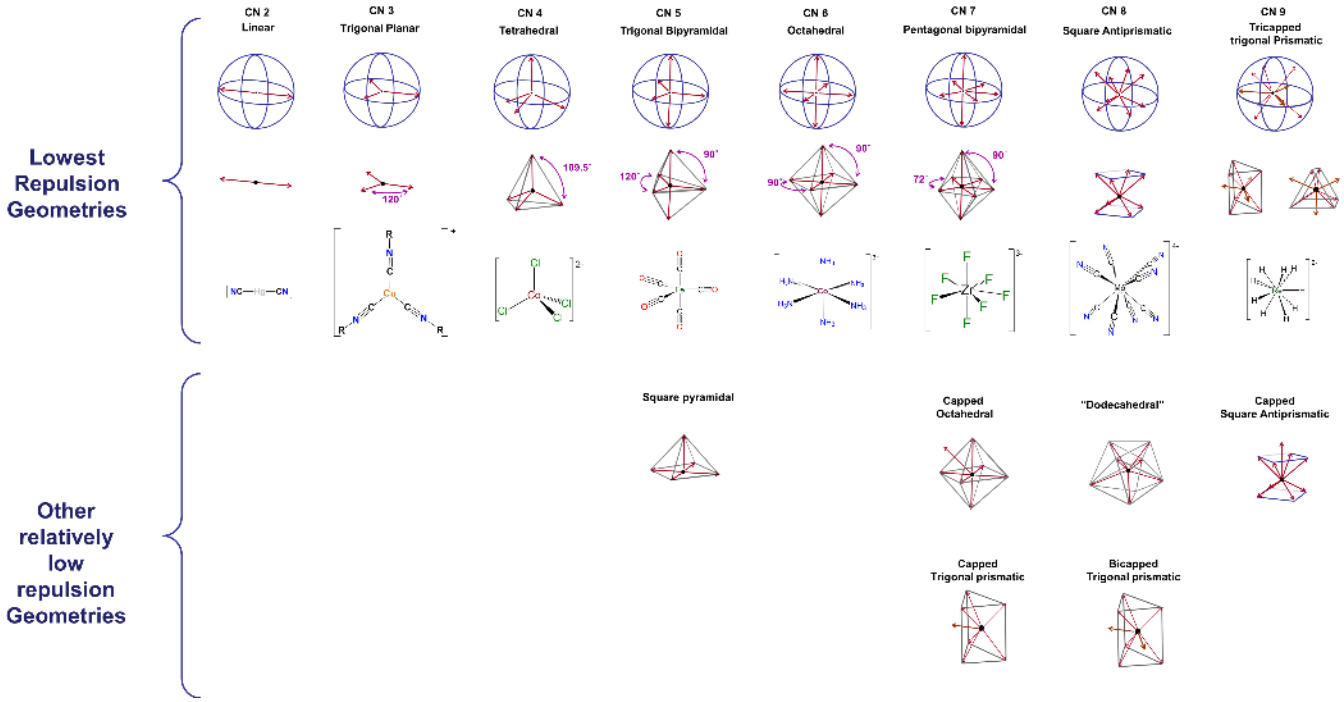


Figure **8.3.2**. Coordination geometries predicted by the Kepert model for coordination numbers two through nine along with other coordination geometries similar in energy to the lowest repulsion geometry. This work by Stephen Contakes is licensed under a Creative Commons Attribution 4.0 International License.

Ligand field effects

A few coordination geometries are noticeably absent from the Kepert-preferred and Kepert-accessible geometries in Figure **8.3.2**. These include the trigonal prismatic geometries formed by compounds like $W(CH_3)_6$ and the very common square planar geometry illustrated by complexes like $[PtCl_4]^{2-}$ and $[IrClH(PPh_3)_2]$. One of the reasons the Kepert model fails to predict the existence of such structures is its neglect of directional interactions involving *d* electrons on the metal center. Metal *d* electrons exert on profound influence on almost all properties of transition metal complexes, including their structures. The way in which this occurs will be explored at length in the next chapter. For now, it is enough to note that both the ligand-donated electrons surrounding a metal center and the electrons occupying particular *d* orbitals on that metal are oriented in specific directions relative to one another. Because of this the strength of the interactions between the ligand and metal *d* electrons depend on both the number of *d* electrons present, how strongly metal-ligand binding affects their energy, and how the ligands are arranged about the metal center. The impact of these effects, here termed ligand field effects, differ from case to case and can include

- distortions of the complex's geometry. For instance, an ideal octahedral coordination geometry might be tetragonally distorted by flattening or elongating it.
- imparting a strong preference for a non-Kepert coordination geometries. This is why, for example, 2nd and 3rd row complexes in which the metal has a d^8 electron configuration are almost always square planar.

- stabilizing non-Kepert geometries enough to permit complexes to adopt them in the presence of a rigid or semirigid ligand that prefers to coordinate the metal in that geometry.[3]

Because of these effects square planar and trigonal prismatic geometries are also observed and the list of coordination geometries given in Figure **8.3.2** may be extended to that shown in Figure **8.3.3**.

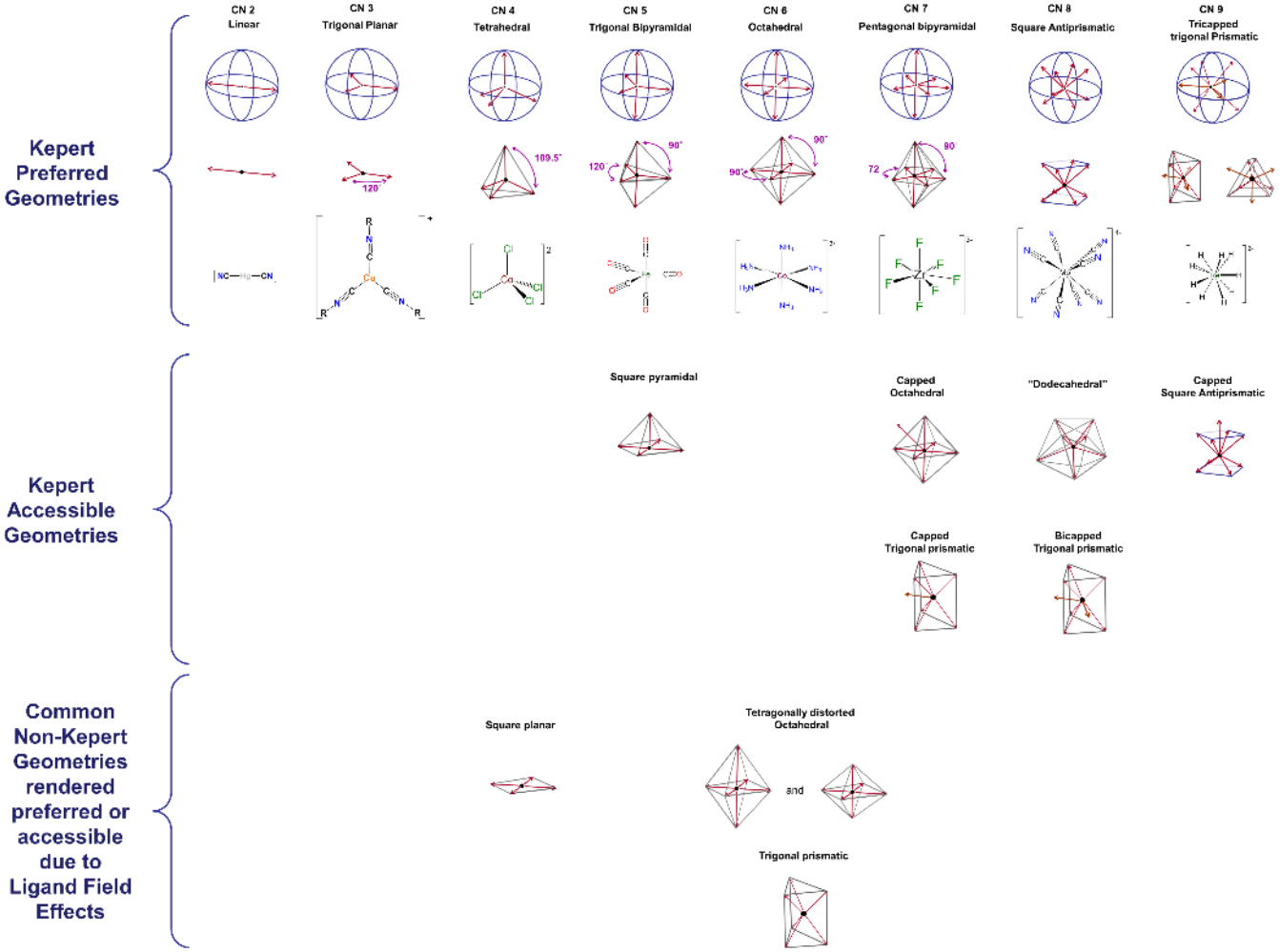


Figure **8.3.3**. Coordination geometries accessible in for 2-9 coordinate complexes even without constraint by rigid or semirigid ligands. This work by Stephen Contakes is licensed under a Creative Commons Attribution 4.0 International License.

Ligand geometry constraints

Rigid or semirigid ligands influence the coordination geometry of metal complexes in two main ways:

- Bulky rigid ligands that crowd the metal center prevent other ligands from binding. Such ligands are useful for preparing low-coordinate complexes.
- Rigid and semirigid ligands can impose their preferred coordination geometry on a metal center. This is because these ligands energetically prefer to adopt a particular conformation when they bind a metal center. In doing so they shift the coordination geometry energy landscape toward that preferred geometry. If the shift is large enough relative to the native preference due to ligand repulsion and ligand field effects the complex will either adopt the ligand-preferred geometry or be distorted in the direction of the ligand-preferred geometry. Examples are given in Figure **8.3.4**.

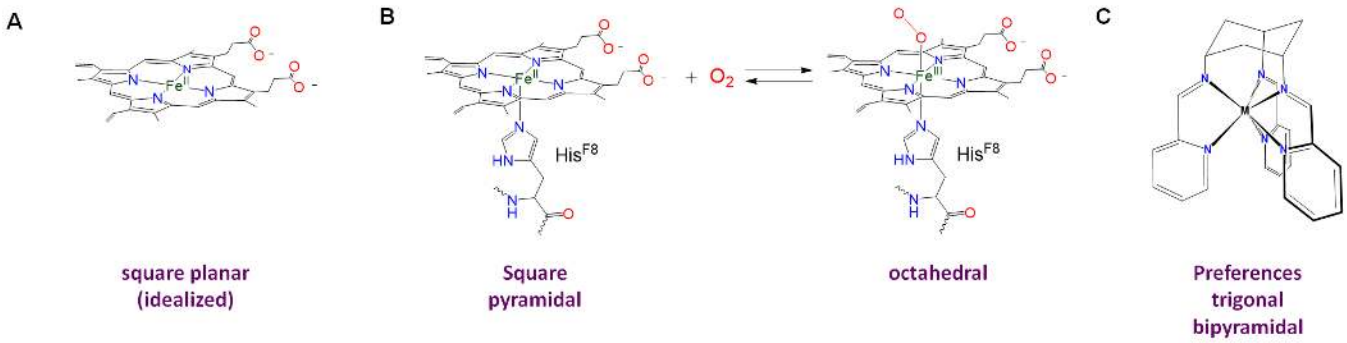


Figure 8.3.4. Examples of rigid or semirigid ligands that can impose their preferred coordination geometry on a metal center. Porphyrins, phyhalocyanines and related macrocycles tend to impose a slightly bent square planar coordination geometry, although (B) many such complexes, including the iron of myoglobin's heme cofactor coordinate additional ligands to give square pyramidal or octahedral complexes. (C) Synthetic multidentate ligands have been developed to preference trigonal prismatic coordination geometries, including the one shown here. It forms roughly trigonal prismatic complexes with Co^{II} and $Zn^{II,}$ albeit imperfect ones.[3] This work by Stephen Contakes is licensed under a Creative Commons Attribution 4.0 International License.

The influence of ligands on coordination geometry is important in living systems in which proteins and nucleic acids can act as rigid or semirigid ligands. The ability of these ligands to distort the coordination geometries of metal atoms in ways that enable them to perform specific functions is so common that the resulting distorted geometries are termed entactic states. A particulary spectacular case of an entactic state involves the blue copper proteins azurin and plastocyanin, the structure of which is given in Figure 8.3.5.

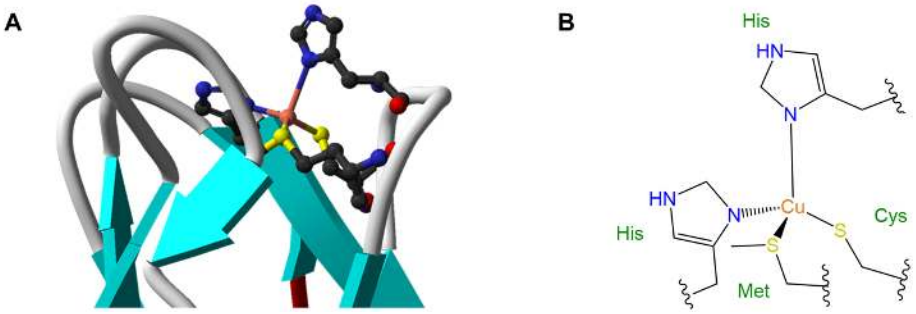


Figure 8.3.5. (A) Structure and (B) schematic of the plastocyanin active site showing the distorted tetrahedral coordination environment that the protein imposes on the copper center (tan), which is most evident from the long vertically oriented Cu-Histidine bond. The image in part A is cropped from an original image by Ben Mills - Own work, Public Domain, https://commons.wikimedia.org/w/inde...?curid=6202620. The image in part B is by Stephen Contakes and licensed under a Creative Commons Attribution 4.0 International License.

As may be seen from the structure in Figure 8.3.5, the copper in plastocyanin exibits a distorted tetrahedral coordination geometry. The protein is said to act like a medieval torture device called a rack in stretching the metal into its distorted geometry. This distortion makes its easier for the copper center to undergo facile redox reactions, enabling it to better function as an electron carrier.

Crystal packing effects

This effect is similar to that of ligand constraints except that in this case arise not from the structure internal to a ligand but out of the forces involves in maximizing the stabilization energy of a crystal. With lower coordination number complexes packing effects can shift the conformations of flexible ligands but only give rise to very small distortions of the overall coordination geometry. Packing effects can drive a shift in the overall coordination geometry of higher coordination number complexes, for which packing effects are significant relative to the small difference in energy between geometries. Thus while $[Mo(CN)_8]^{4-}$ has a square antiprismatic coordination geometry in solution it exhibits a docecahedral coordination geometry in the crystals of many of its salts.

Relativistic effects on orbital energies

The proximity of fast moving electrons to massive nuclei in the heavier transition elements results in relativistic expansion and contraction of orbitals. The net results are that

- heavier elements tend to be smaller than expected. This effect preferences lower coordination numbers.
- the relative energies of orbitals shift. Orbitals which become contracted are lowered in energy while those which are expanded increase in energy, as shown for the case of gold in Figure **8.3.6*A***.

The combination of smaller sizes and altered orbital energies affect coordination preferences. Relatavistic effects contribute to the greater tendency of Au(I) relative to other group 11 metals to form linear two coordinate complexes. As shown in Figure **8.3.6*B***, the relative closeness in energy of the 6*s* and 5*d* orbitals of gold makes mixing of these orbitals more favorable, facilitating the ability of gold to form two coordinate complexes with strong sigma bonds oriented 180° from one another.

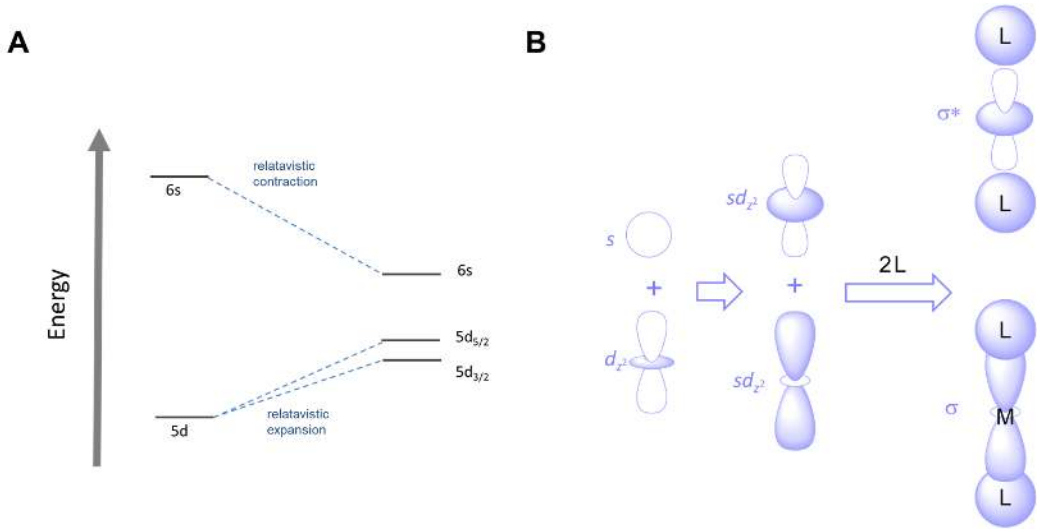


Figure **8.3.6**. (A) Gold experiences relatavistic expansion and contraction of its 5*d* and 6*s* orbitals, resulting in shifts to their relative energies. (B) This makes mixing of these orbitals more favorable, facilitating the ability of gold to form two coordinate complexes with strong sigma bonds that involve considerable sd_{z^2} character. This work by Stephen Contakes is licensed under a Creative Commons Attribution 4.0 International License.

What Structures do Coordination Complexes Form?

Metal complexes with coordination numbers ranging from one to 16 are known, although values greater than seven are rare for the transition metals. In this section examples of common coordination geometries will be presented in order of coordination number.

Coordination Number 1

Condensed phase monocoordinate complexes are unknown for the transition metals, although the post transition metals Tl and In form monocoordinate complexes with the bulky ligands triazapentadienyl and 2,6-tris(2,4,6-triisoprophylphenyl)benzene as shown in Figure **8.3.7**.

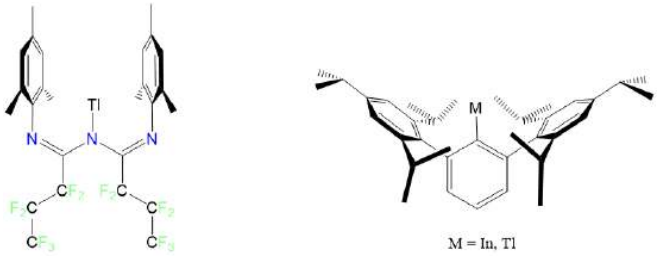
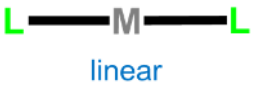


Figure **8.3.7**. No monocoordiante transition metal complexes are known but Tl^+ and In^+ form monocoordinate complexes with extremely bulky ligands. This work by Stephen Contakes is licensed under a Creative Commons Attribution 4.0 International License.

Coordination Number 2

This coordination number is rare outside of d^{10} complexes of the group 11 metals and mercury, specifically, Cu^+, Ag^+, Au^+, and Hg^{2+}. In accordance with the predictions of the Kepert model these give linear complexes.



linear

Among these:

- Cu^+ more commonly gives tetrahedral complexes but can be coaxed to give linear ones. The most prominent example is $[CuCl_2]^-$, which forms when CuCl is treated with concentrated HCl under anerobic conditions.
- Ag^+ also commonly forms tetrahedral or trigonal planar complexes but can give linear ones. The most prominent example is $[Ag(NH_3)_2]^+$, which can be formed by treating silver salts with concentrated aqueous or liquid ammonia.
- Au^+ almost always forms linear complexes but many of these formally two coordinate complexes associate as depicted in Figure 8.3.8. The ability of Au^+ to form linear complexes with cyanide is even used to selectively extract metallic gold from low grade ores. The stability of $[Au(CN)_2]^-$ means that the dissolution of metallic gold in aqueous cyanide is thermodynamically favorable under aerobic conditions.

$$4\ Au + 8\ CN^- + O_2 + 2\ H_2O \longrightarrow 4\ [Au(CN)_2]^- + 4\ OH^- \quad (8.3.1)$$

- Hg^{2+}, like Au^+, benefits from relativistic effects and more commonly forms two-coordinate complexes with a linear geometry. Among these is $[Hg(CN)_2]$. However, its preference for linearity is not as rigid as for Au^+ and so complexes with a variety of coordination geometries are known.

An by means of honorary mention the mercury(I),Hg_2^{2+}, forms linear complexes of the type L-Hg-Hg-L, although since Hg_2^{2+} is often considered as a single unit these aren't always considered to be two coordinate complexes.

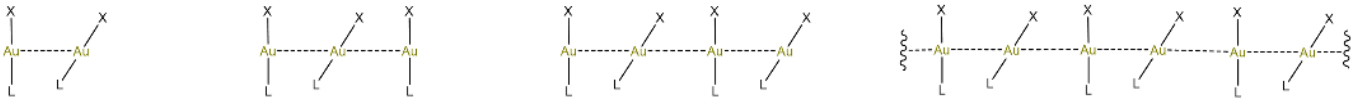
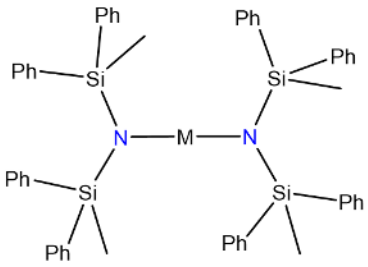


Figure 8.3.8. Many "linear" gold complexes associate side-on to form dimers, trimers, tetramers, and chains. Although in this chapter L is usually taken to represent a generic ligand, in this scheme L represents a neutral ligand that donates two electrons to the metal (py, PR_3, CO etc.) and X an anionic one (*e.g.* Cl^-, CN^-, etc.). Exactly which structure forms depends on the identity of L and X. Redrawn from reference 5. This work by Stephen Contakes is licensed under a Creative Commons Attribution 4.0 International License.

Two coordinate complexes may also be formed through the use of bulky ligands that only allow for the binding of two to the metal center. Classic examples are given in Figure 8.3.9.

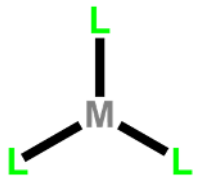


M = Mn, Fe, Co

Figure 8.3.9. Two coordinate complexes form between Mn^{2+}, Fe^{2+}, and Co^{2+} and $N(SiMePh_2)_2$.[6] This work by Stephen Contakes is licensed under a Creative Commons Attribution 4.0 International License.

Coordination Number 3

Three coordinate complexes are similar to two coordinate ones in that they are rare and, aside from the constraining influence of ligands, usually limited to d^{10} metal ions such as Cu^+, Ag^+, Au^+, Hg^{2+}, and Pt^0. As expected from the Kepert model, in the absence of constraining ligands three coordinate complexes are trigonal planar.



Trigonal planar

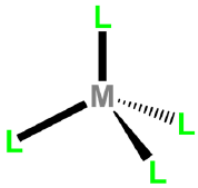
Many of the examples involve soft ligands. They include $[Cu(SPMe_3)_3]^+$, $[Ag(PPh_3)_3]^+$, $[Au(PPhCy_2)_3]^+$, HgI_3^-, and $[Pt(PPh_3)_3]$. Non-d^{10} metal centers have successfully been constrained to adopt a three coordinate trigonal planar geometry using bulky and semirigid ligands. Examples of such three-coordinate complexes are given in Figure **8.3.10**.



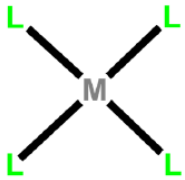
Figure **8.3.10**: Three coordinate complexes prepared using bulky and semirigid ligands. This work by Stephen Contakes is licensed under a Creative Commons Attribution 4.0 International License.

Coordination Number 4

Four is one of the most common coordination numbers found in transition metal complexes. The two common four coordinate geometries are tetrahedral and square planar.



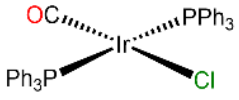
tetrahedral



Square planar

Tetrahedral complexes are commonly formed by metals possessing either a d^0 or d^{10} electron configuration. Monometallic examples of the former include $TiCl_4$, VO_4^{3-}, WS_4^{2-}, MnO_4^-, CrO_4^{2-}, and OsO_4 while d^{10} examples are $[Ni(CO)_4]$, $[HgBr_4]^{2-}$, $[ZnCl_4]^{2-}$, $[CdI_4]^{2-}$. Otherwise tetrahedral complexes are known but much less common. Examples usually involve good donor ligands and include $[FeCl_4]^-$ (d^5), $[CoCl_4^{2-}]$ (d^6), and $[NiCl_4]^{2-}$ (d^7).

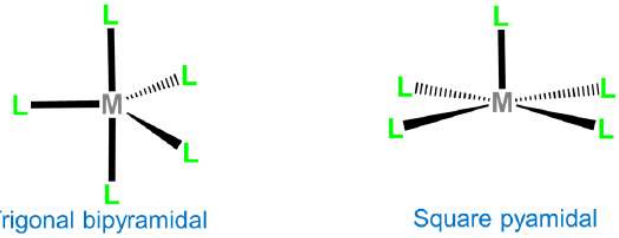
Second and third row transition metal centers with d^8 electron configurations like Rh^+, Ir^+, Pd^{2+}, and Pt^{2+}, Au^{3+} almost exclusively exhibit square planar geometries. Beyond this, square planar geometries are often formed by Ni^{2+} (d^8), Ni^{3+} (d^7), and Cu^{2+} (d^9). Examples of square planar complexes include $[Cu(acac)_2]$; $[PtCl_4]^{2-}$;Wilkinson's catalyst, $[RhCl(PPh_3)_3]$; and Vaska's complex, *trans*-$[Ir(CO)Cl(PPh_3)_2]$. Porphyrins, phthalocyanines, and other rigid macrocycles can also impose a square planar geometry on coordinated metals.



Vaska's Complex

Coordination Number 5

The two common coordination geometries for five coordinate complexes are trigonal bipyramidal and square pyramidal.



Five coordinate complexes are rare. Complexes that exhibit trigonal bipyramidal geometry include $[Fe(CO)_5]$ and $[CuCl_5]^{3-}$ and complexes containing tripodal ligands that preference formation of a trigonal pyramidal structure with an open coordination site, as shown in Figure **8.3.11**.

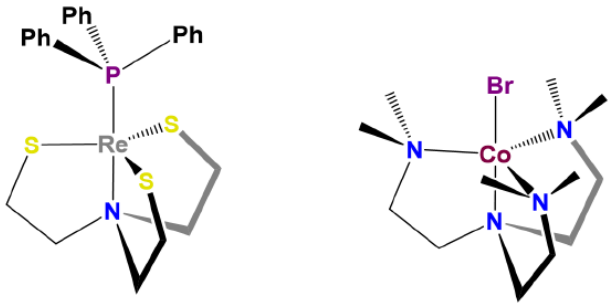


Figure **8.3.11**: Some tripodal ligands preference the formation of trigonal bipyramidal complexes. This work by Stephen Contakes is licensed under a Creative Commons Attribution 4.0 International License.

Homoleptic $[Ni(CN)_5]^{3-}$ possesses a square pyramidal structure, although the geometry is more common for macrocyclic complexes like the iron protoporphyrin of deoxymyoglobin shown in Figure **8.3.4** and for complexes containing oxo and nitrido ligands, examples of which are shown in Figure **8.3.12**.

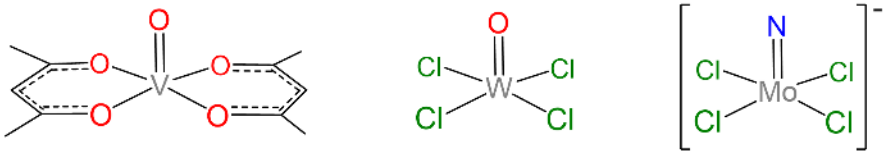


Figure **8.3.12**: Some square pyramidal oxo and nitrido complexes. This work by Stephen Contakes is licensed under a Creative Commons Attribution 4.0 International License.

In the absence of rigid constraining ligands the relatively low energy difference between the trigonal bipyramidal and square pyramidal coordination geometries provides a mechanism for interconversion of the axial and equatorial ligands in a trigonal planar complex. For example, pentacarbonyliron(0) exhibits fluxionality involving a square pyramidal intermediate via a Berry pseudorotation mechanism, as shown in Figure **8.3.13**

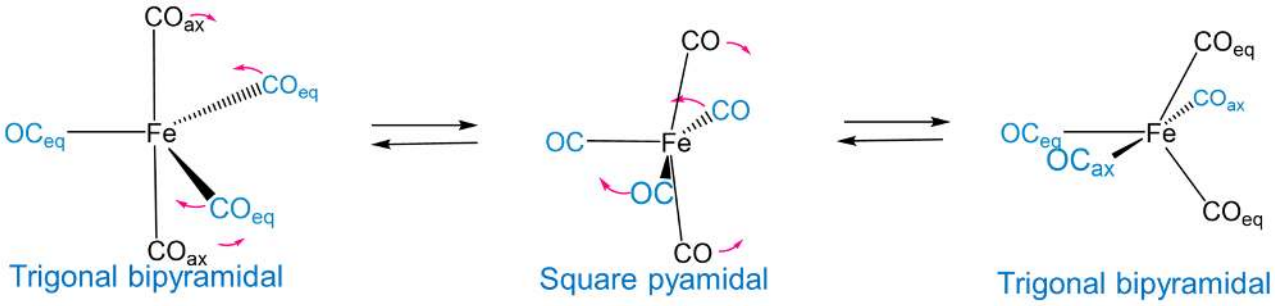
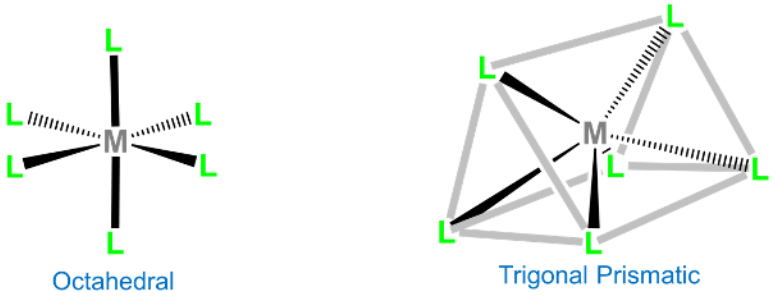


Figure **8.3.13**: Fluxionality in pentacarbonyliron(0) involves exchange of axial and equatorial carbonyl ligands via Berry pseudorotation. Interconversion of the axial and equatorial carbonyl groups occurs faster than the NMR timescale at room temperature. As a result the ^{13}C NMR spectrum of $Fe(CO)_5$ exhibits a single signal rather than two separate signals for the axial and equatorial carbonyl carbons. This work by Stephen Contakes is licensed under a Creative Commons Attribution 4.0 International License.

Coordination Number 6

The two common octahedral coordination geometries are octahedral and trigonal prismatic.



Octahedral

Of these octahedral is by far the most common mode of coordination exhibited by transition metals. Most metals can be induced to form octahedral complexes and examples exist for every d electron configuration ranging from d^0 to d^{10}. Among these are the 28 metal oxidation states listed in Figure **8.3.1** for which octahedral is the most common coordination geometry. Because of this it is worth pointing out that octahedral complexes possessing d^4, d^7 , or d^9 electron configurations commonly exhibit tetragonal distortions depicted in Figure **8.3.14**.

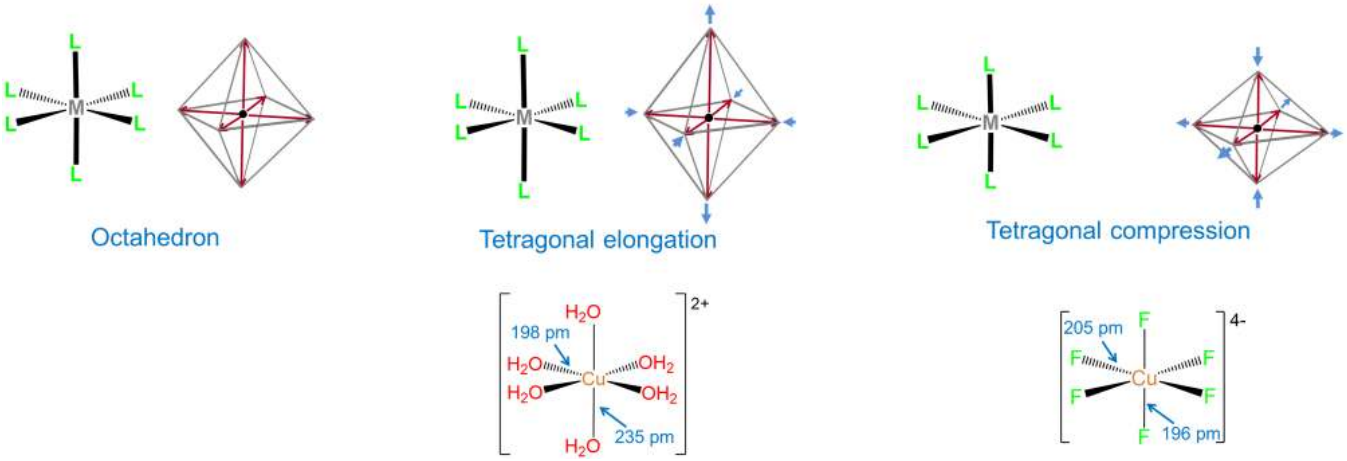


Figure **8.3.14**: Tetragonal distortions commonly occur for d^4, d^7 , and d^9 octahedral complexes. The most common type involves axial elongation in which the octahedron is stretched along a single *trans*-L-M-L axis but axial compressions in which the octahedron is compressed along such an axis instead are sometimes observed. An example of an axial elongated complex is $[Cu(H_2O)_6]^{2+}$ in solution while $[CuF_6]^{4-}$ is axially compressed when doped into a Ba_2ZrF_6 lattice (it is elongated when doped into a Bond distances are taken from references 7 and 8. This work by Stephen Contakes is licensed under a Creative Commons Attribution 4.0 International License.

Trigonal prismatic

Trigonal prismatic coordination is related to octahedral coordination as shown in Figure **8.3.15**. As may be seen in Figure **8.3.15**, an octahedral coordination sphere is just a trigonal antiprism in which all edge lengths are identical. Rotation of one triangular face relative to its opposite until the two are eclipsed gives a triganal prismatic geometry. In fact, since continuation of this rotation gives another octahedral complex the trigonal prismatic geometry is an intermediate in isomerization reactions involving octahedral complexes.

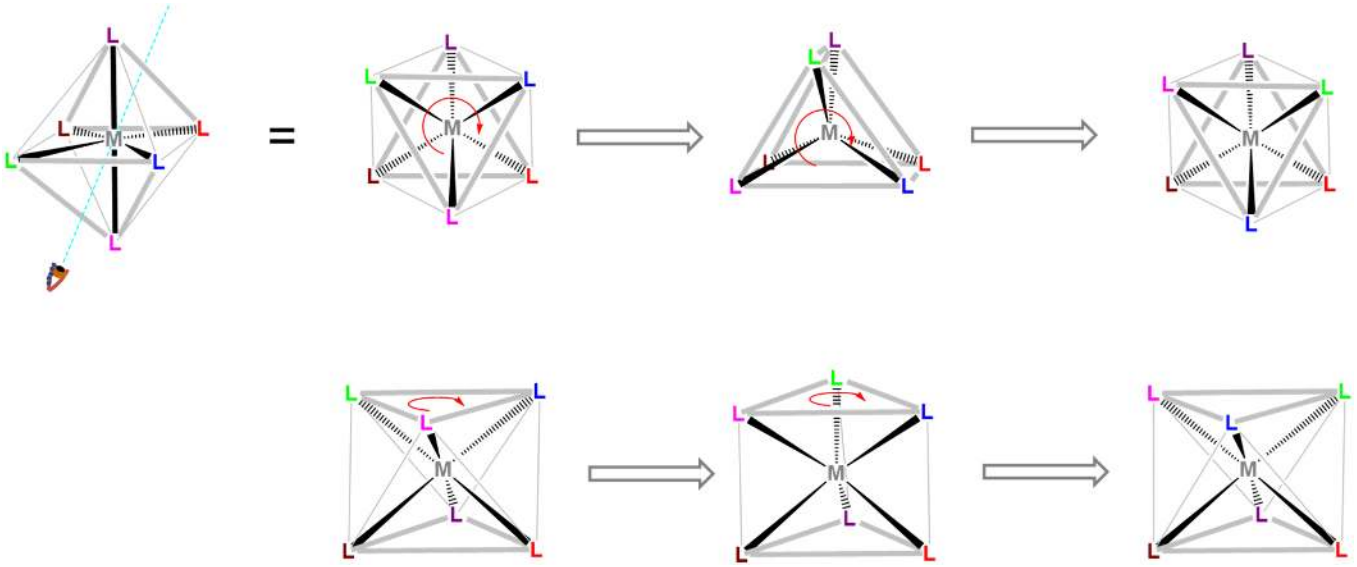


Figure 8.3.15: Since an octahedron is a trigonal antiprism a trigonal prism may be produced by rotating or "twisting" one face of the octahedron relative to its opposite. Since continuation of the rotation gives an isomer of the original octahedron, when the energy landscape for twists like these is thermally or photochemically accessible twists like these provide one pathway for isomerisation reactions involving octahedral complexes. In tris- and bis-chelates such isomerizations are said to occur by Bailar and Ray-Dutt twists, which differ only in the relationship between the chelate rings and the faces twisted. Top: View down looking down an axis bisecting a pair of opposing faces. Bottom: View perpendicular to that shown at top. This work by Stephen Contakes is licensed under a Creative Commons Attribution 4.0 International License.

In contrast to octahedral coordination geometries, trigonal prismatic coordination (and distorted versions thereof) are rare and occur mostly for d^0, d^1, and d^2 configurations. Examples of trigonal prismatic metal centers include the d^2 Mo^{4+} centers in MoS_2, d^1 $[Re(S_2C_2Ph_2)_3]^-$, and d^0 $[Ta(CH_3)_6]^-$, of which the latter two structures are given in Figure 8.3.16. Semirigid ligands like that shown in Figure 8.3.4*C* may be used to encourage the adoption of a trigonal prismatic geometry, although once the number of *d* electrons present the preference for octahedral coordination is too great for a trigonal prismatic geometry to occur.

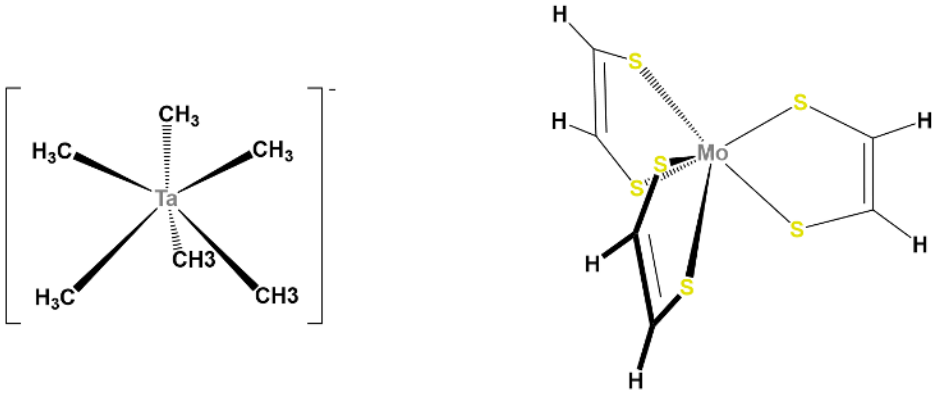
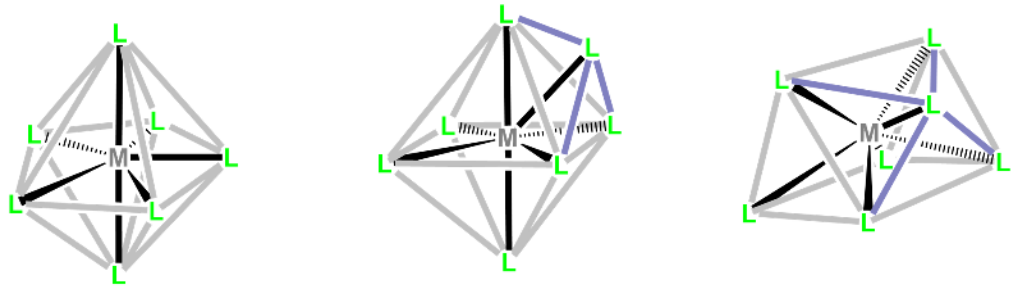


Figure 8.3.16: The complexes $[Ta(CH_3)_6]^-$ and $[Mo(S_2C_2H_2)_3]$ adopt a trignal prismatic geometry. Trigonal primatic coordination is common for d^0 and d^1 complexes with alkyl and dithiolene ligands. It is also typical for the dithiolene ligands to coordinate along the rectangular edges of the trigonal prism instead of the triangular ones. This work by Stephen Contakes is licensed under a Creative Commons Attribution 4.0 International License.

Coordination Number 7

Seven coordinate complexes are rare outside of the relatively large early transition metals, lanthanides, and actinides. The three common seven coordinate geometries are pentagonal bipyramidal, monocapped octahedral, and monocapped trigonal prismatic. The latter two are often called capped octahedral, and capped trigonal prismatic, with the mono- prefix being understood.



Although intraligand repulsions are smaller in the pentagonal bipyramidal coordination geometry than the capped octahedral and capped trigonal prismatic geometries the difference is small and the three structures are often close in energy. As a result the structure observed is often dependent on ligand-based constraints, crystal packing, and solvent effects that preference one geometry over the others.

Heptacyano complexes are often pentagonal bipyramidal. Examples include $[Mo(CN)_7]^{3-}$, $[W(CN)_7]^{3-}$, and $[Os(CN)_7]^{3-}$. Seven coordinate complexes containing oxo ligands commonly are pentagonal bipyramidal with the oxo ligand(s) in the less sterically hindered axial position. Examples include $[NbOF_6]^{3-}$ and, for the inner transition metals, $[UO_2F_5]^{3-}$. Ligands that have been used to promote formation of seven-coordinate species include 15-crown-5 and 2,2':6',2":6",2"'-quaterpyridine and 15-crown-5. Representative complexes are given in (Figure **8.3.17**.

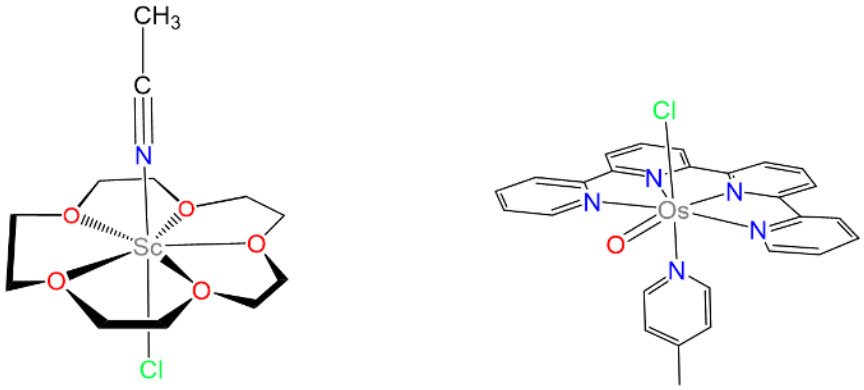


Figure **8.3.17**: Seven coordinate complexes containing ligands that encourage the formation of seven-coordinate geometries. Note that while in $[NbOF_6]^{3-}$ and $[UO_2F_5]^{3-}$ the oxo ligands occupy axial positions the Osmium complex shown possesses an oxo ligand in an equatorial position. This is likely because the parent octahedral complex, in which the oxo ligand is not present, possesses an expanded outer N-Os-N angle of 121.655° that opens to 154.161° to accommodate the oxo group. Drawn based on the structures reported in references 9 and 10. This work by Stephen Contakes is licensed under a Creative Commons Attribution 4.0 International License.

Capped trigonal prismatic geometries are common for complexes of the early transition metals. Examples include $[NbF_7]^{2-}$, $[TaF_7]^{2-}$, and $[ZrF_7]^{3-}$ in $(NH_4)_3[ZrF_7]$.

Capped octahedral geometries are found in $[MoMe_7]^-$, $[WMe_7]^-$, and $[WBr_3(CO)_4]$, which contains three pairs of *trans*-Br and CO with the final CO capping the octahedron's $(CO)_3$ face, as shown in Figure **8.3.18**.

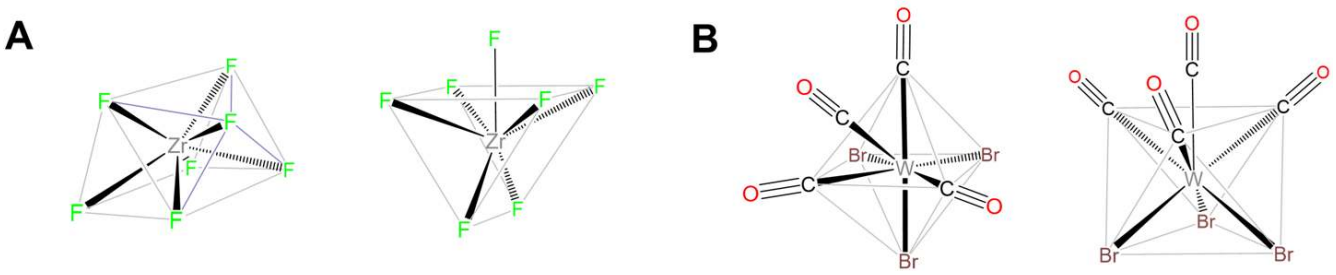


Figure **8.3.18**: Examples of complexes that adopt monocapped triconal prismatic and monocapped octahedral geometries.(A) Two views of the structure of (A) capped trigonalprismatic $[ZrF_7]^{3-}$ and (B) capped octahedral $[WBr_3(CO)_4]$. This work by Stephen Contakes is licensed under a Creative Commons Attribution 4.0 International License.

In seven and higher coordinate complexes ligand and crystal packing effects frequently give distorted coordination geometries. These geometries are intermediate between two or more of the idealized seven coordinate geometries, making it difficult to tell exactly which structure they are a distortion of (Figure **8.3.19**.

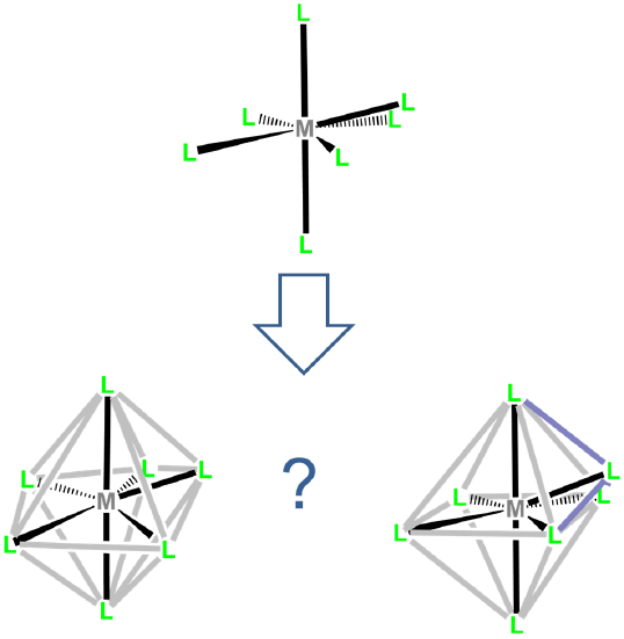
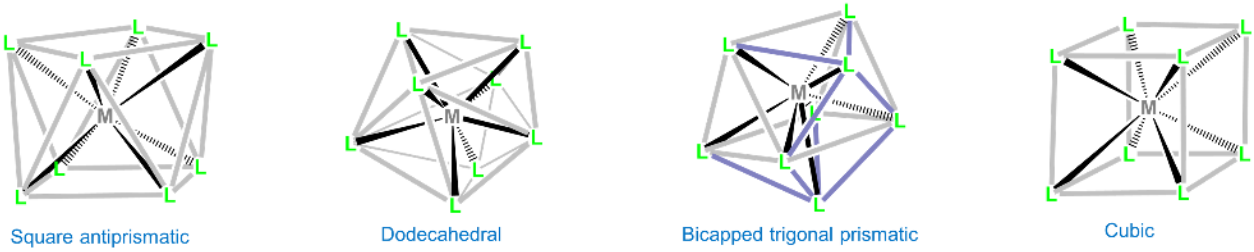


Figure **8.3.19**: Many seven-coordinate structures are distorted and can be difficult to classify. For example, how should the geometry of this complex be described - as distorted trigonal bipyramidal or distorted monocapped octahedral? This work by Stephen Contakes is licensed under a Creative Commons Attribution 4.0 International License.

Coordination Number 8

Eight coordinate complexes are rare and occurs in discrete molecules and ions only for the relatively large early transition metals, lanthanides, actinides. The three common eight coordinate geometries are square antiprismatic, dodecahedral, and bicapped trigonal prismatic. In contrast, the cubic coordination geometry is only found in ionic lattices like that of CsCl and in complexes of the inner transition metals such as $Na_3[UF_8]$.



The simplest structure is the cube, which is rare because it does not minimize interligand repulsive interactions. Square antiprismatic, dodecahedral, and bicapped trogonal prismatic coordination are more common. Of these the square antirpismatic and dodecahedral geometries can both be considered as distorted cubic structures. As shown in Figure **8.3.20**, the square antiprism may be made by twisting one face of a cube relative to one another and the dodecahedron by folding opposing faces towards one another.

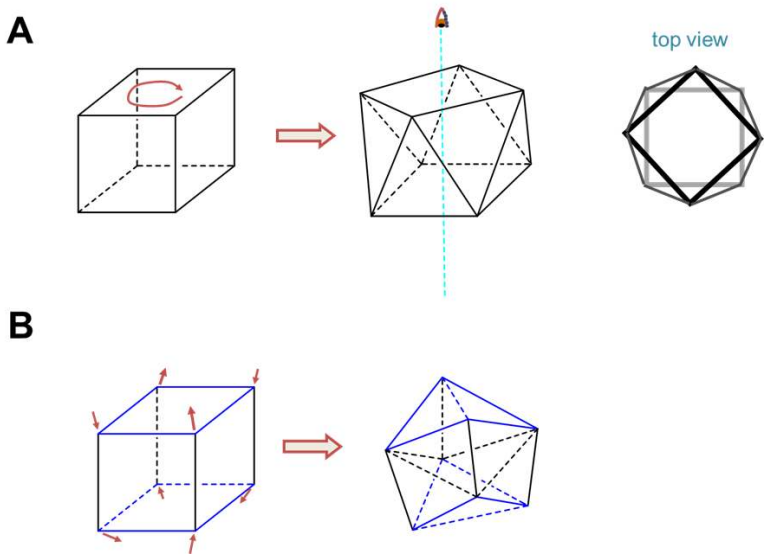


Figure **8.3.20**: The (A) square antiprismatic and (B) dodecahedral coordination geometries are distorted cubic geometries. (A) The square antiprismaric coordination geometry is just a cubic coordination geometry in which one face has been rotated 45° relative to its opposite (and for which the distance between those faces need not be equal to the distance between adjacent atoms within a face) (B) The dodecahedral geometry may be thought of as a cube in which opposing faces are folded up and down relative to one another as shown. This work by Stephen Contakes is licensed under a Creative Commons Attribution 4.0 International License.

As with other high-coordinate structures the energy difference between these eightfold coordination geometries is small enough that packing effects can significantly influnece the observed structure. For example, octacyanomolybdates commonly adopt a square antiprismatic coordination geometry but depending on the counterions present can give dodecahedral or bicapped trigonal prismatic complexes. Examples are given in Figure **8.3.21**.

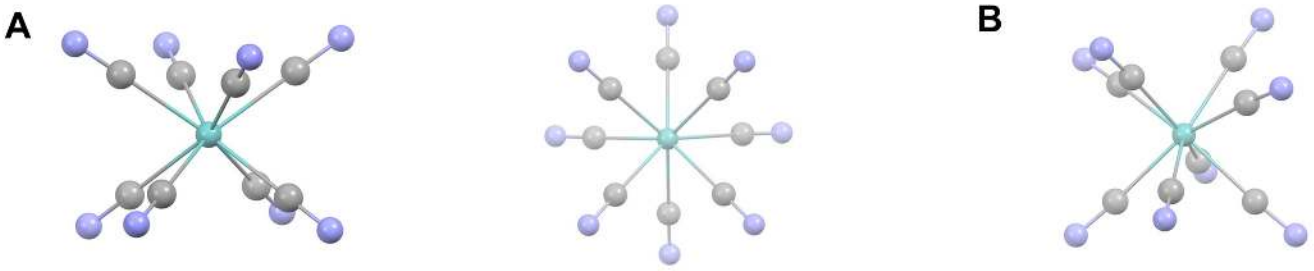
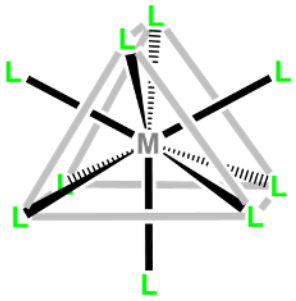


Figure **8.3.21**: Structures reported for (A) square antiprismatic $[Mo(CN)_8]^{3-}$ as a solid 4,4'-Diazenediyldipyridinium salt and (B) dodecahedral $[Mo(CN)_8]^{4-}$ as a solid tetra-n-butylammonium salt.

Coordination Number 9

Again, nine coordinate complexes typically require larger transition metals, lanthanides, and actinides. Coordination geometries are typically either tricapped trigonal prismatic or idosynchraitcally determined by the ligands. Simpleexamples include the aqua complexes $[Sc(H_2O)_9]^{3+}$, $[Y(H_2O)_9]^{3+}$, and $[La(H_2O)_9]^{3+}$ as well as $[TcH_9]^{2-}$ and $[ReH_9]^{2-}$.



Tricapped trigonal Antiprism

The classic example of a nine-coordinate complex, $[ReH_9]^{2-}$, is shown in Figure **8.3.22**.

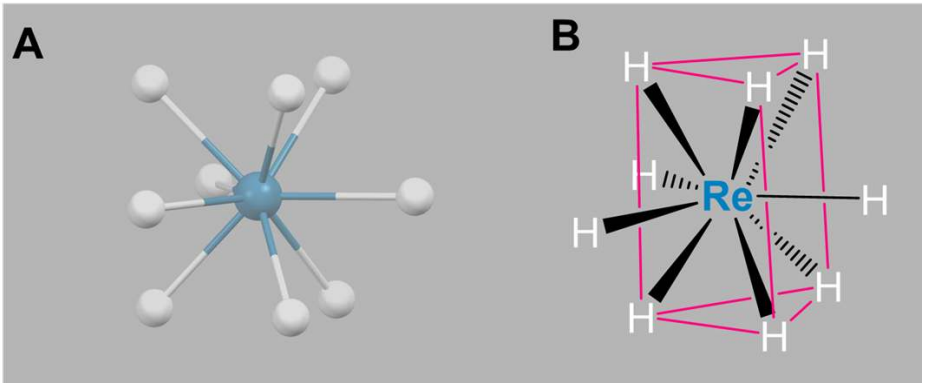


Figure **8.3.22**: (A) Structure of $[ReH_9]^{2-}$ in $K_2[ReH_9]$ and (B) schematic showing how the structure maps onto a tricapped trigonal pyramidal coordination geometry. This work by Stephen Contakes is licensed under a Creative Commons Attribution 4.0 International License.

Coordination Numbers 10-16

Coordination numbers higher than nine are extremely rare for compounds that bind in κ fashion (form conventional metal-ligand bonds)[14] and usually involve some combination of large metals, sterically undemanding ligands, and special ligand structures that promote higher coordination. Noteworthy examples include

1. Twelve-coordinate $[Hf(BH_4)_4]$, which illustrates how small multidentate ligands promote higher coordination numbers. As shown in Figure **8.3.23**, $[Hf(BH_4)_4]$ has a cubooctahedral structure in which BH_4^- acts as a tridentate ligand, with BH_3 units occupying triangular faces of the cubooctahedron to give a tetrahedron of BH_4^- ligands around the Hf.

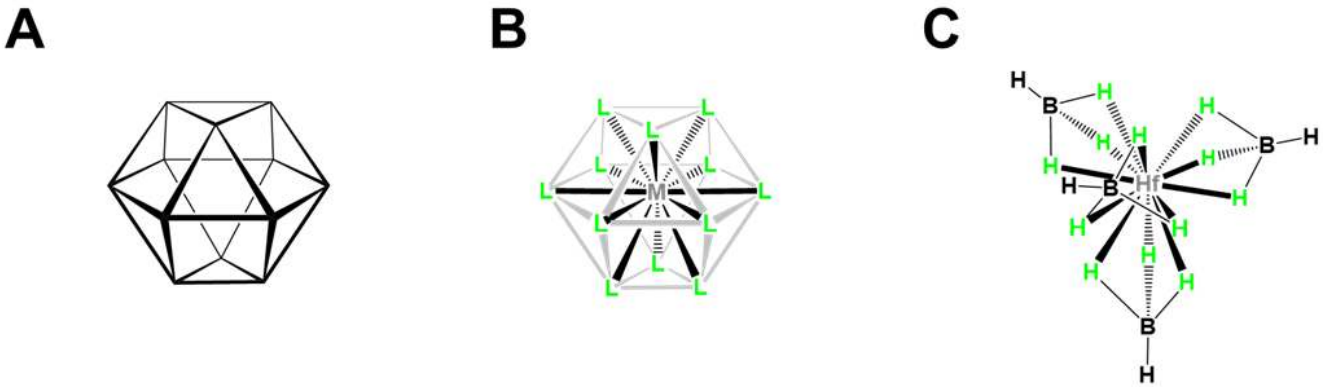


Figure **8.3.23**: The anticubooctahedral coordination geometry is observed for $[Hf(BH_4)_4]$. (A) An anticubooctahedron consists of a hexagonal ring capped with antiparallel triangles above and below the ring. (B) Idealized anticubooctahedral complex. (C) Structure of $[Hf(BH_4)_4]$. This work by Stephen Contakes is licensed under a Creative Commons Attribution 4.0 International License.

2. Twelve coordinate $[Ce(NO_3)_6]^{2-}$, in which the nitrate oxygens define an icosahedral coordination geometry as shown in Figure **8.3.24**. The nitrates in the structure bind the Ce center in bidentate fashion in an octahedral array.

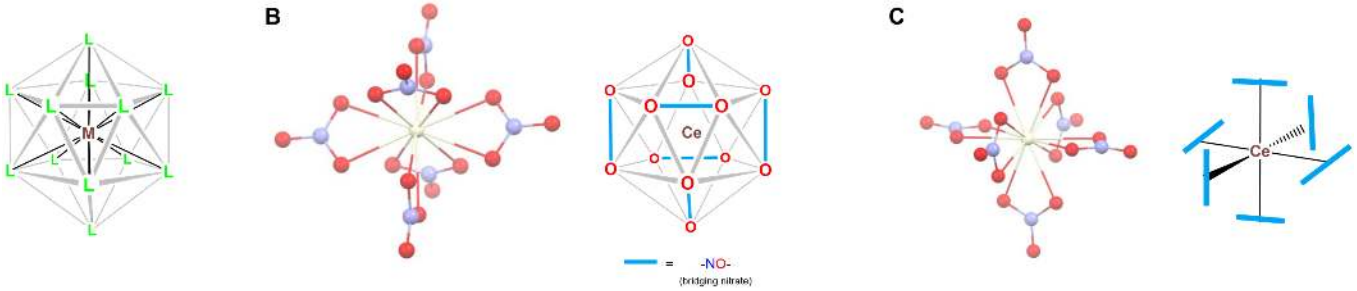


Figure **8.3.24**: Coordination geometry of $[Ce(NO_3)_6]^{2-}$ in $[Mg(H_2O)_6][Ce(NO_3)_6]\cdot H_2O$. (A) Idealized icosahedral coordination. (B) View of the structure of $[Ce(NO_3)_6]^{2-}$ showing how it maps onto the icosahedral coordination geometry. (C) The structure may also be thought of as comprising an octahedral geometry in which each vertex of the octahedron is occupied by a κ^2-NO_3^-. The structure of $[Ce(NO_3)_6]^{2-}$ is rendered in Mercury from the cif data in reference 15. This work by Stephen Contakes is licensed under a Creative Commons Attribution 4.0 International License.

3. Fifteen-coordinate, $[Th(H_3BNMe_2BH_3)_4]$, which also uses bridging H-B-H units that occupy little of the coordination sphere. In $[Th(H_3BNMe_2BH_3)_4]$ three of the four $H_3BNMe_2BH_3$ bind in κ^4 fashion and one binds κ^3, giving the fifteen fold coordination.[16]

4. Sixteen-coordinate $[CoB_{16}]^-$, which possesses the highest coordination number yet observed. Its structure is given in Figure **8.3.25** The coordination geometry is an octahedral antiprism and the complex should be considered as involving a Co center in the midst of a B_{16}^- "molecular drum" held together by cluster bonds.

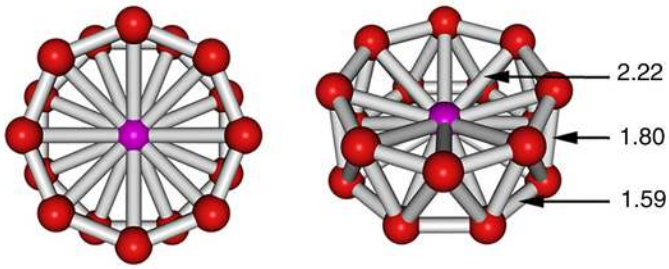


Figure **8.3.25**: Structure of the D_{8d} isomer of the 16 coordinate complex $[CoB_{16}]^-$, with distances shown in Ångstroms. The image is Figure 2A from from Popov, I., Jian, T., Lopez, G. *et al*. Cobalt-centred boron molecular drums with the highest coordination number in the CoB_{16}^- cluster. *Nat Commun* **6,** 8654 (2015). https://doi.org/10.1038/ncomms9654, which is is licensed in that publication under a Creative Commons Attribution 4.0 International License.

References

1. Dudev, M.; Wang, J.; Dudev, T.; Lim, C., Factors Governing the Metal Coordination Number in Metal Complexes from Cambridge Structural Database Analyses. *The Journal of Physical Chemistry B* **2006**, *110(4)*, 1889-1895.

2. Kuppuraj, G.; Dudev, M.; Lim, C., Factors Governing Metal−Ligand Distances and Coordination Geometries of Metal Complexes. *The Journal of Physical Chemistry B* 2009, 113 (9), 2952-2960.

3. Cremades, E.; Echeverría, J.; Alvarez, S., The Trigonal Prism in Coordination Chemistry. *Chemistry – A European Journal* 2010, 16 (34), 10380-10396.

4. Xiong, X.-G.; Wang, Y.-L.; Xu, C.-Q.; Qiu, Y.-H.; Wang, L.-S.; Li, J., On the gold–ligand covalency in linear $[AuX_2]^-$ complexes. *Dalton Transactions* 2015, 44 (12), 5535-5546.

5. Concepción Gimeno, M. The Chemistry of Gold in Laguna, Antonio (ed.) *Modern Supramolecular Gold Chemistry: Gold-Metal Interactions and Applications*. Wiley, 2008.

6. Andersen, R. A.; Faegri, K.; Green, J. C.; Haaland, A.; Lappert, M. F.; Leung, W. P.; Rypdal, K., Synthesis of bis[bis(trimethylsilyl)amido]iron(II). Structure and bonding in M[N(SiMe3)2]2 (M = manganese, iron, cobalt): two-coordinate transition-metal amides. *Inorganic Chemistry* 1988, 27 (10), 1782-1786.

7. Persson, I., Hydrated metal ions in aqueous solution: How regular are their structures? Pure and Applied Chemistry 2010, 8*2(10)*, 1901.

8. Aramburu, J. A.; García-Fernández, P.; García-Lastra, J. M.; Moreno, M., Jahn–Teller and Non-Jahn–Teller Systems Involving CuF_6^{4-} Units: Role of the Internal Electric Field in Ba2ZnF6:Cu2+ and Other Insulating Systems. *The Journal of Physical Chemistry C* 2017, *121(9)*, 5215-5224.

9. Brown, M. D.; Levason, W.; Murray, D. C.; Popham, M. C.; Reid, G.; Webster, M., Primary and secondary coordination of crown ethers to scandium(iii). Synthesis, properties and structures of the reaction products of ScCl3(thf)3, ScCl3·6H2O and Sc(NO3)3·5H2O with crown ethers. Dalton Transactions 2003, (5), 857-865.

10. Liu, Y.; Ng, S.-M.; Lam, W. W. Y.; Yiu, S.-M.; Lau, T.-C., A Highly Reactive Seven-Coordinate Osmium(V) Oxo Complex: [OsV(O)(qpy)(pic)Cl]2+. Angewandte Chemie International Edition 2016, 55 (1), 288-291.

11. Popov, I., Jian, T., Lopez, G. *et al.* Cobalt-centred boron molecular drums with the highest coordination number in the CoB_{16}^- cluster. *Nat Commun* **6,** 8654 (2015). https://doi.org/10.1038/ncomms9654

12. The structures are rendered from cif data reported in the following publications (A) square antiprismatic $[Mo(CN)_8]^{3-}$: Wen-Yan Liu, Hu Zhou, Ai-Hua Yuan, *Acta Crystallographica Section E: Structure Reports Online*, 2008, 64, m1151, (B) dodecahedral $[Mo(CN)_8]^{4-}$: B.J.Corden, J.A.Cunningham, R.Eisenberg, *Inorganic Chemistry*, 1970, 9, 356.

13. The structure of ReH_9^{2-} is rendered from the structure reported in Abrahams, S.C.; Ginsberg, A.P.; Knox, K. Transition metal-hydrogen compounds. II. The crystal and molecular structure of potassium rhenium hydride, K_2ReH_9 *Inorganic Chemistry*, **1964**, *3*, 558-567.

14. There are other complexes in which a metal may be said to interact with more than sixteen "ligand atoms" but these are not usually considered to possess a higher coordination number. For example in some π complexes like η^5-Cp_4U technically there are 20 C atoms fastened to the U but these complexes are better considered as 12 coordinate than twenty (since each cyclopentadienl ring is isolobal with a *fac* coordinated set of 3 L ligands) while the metal centers in endohedral fullerene species like $La@C_{60}$ do not interact with all sixty carbon atoms at once are so are better thought of as a metal trapped in a spacious sixty-carbon cage.

15. Zalkin, A.; Forrester, J.D.; Templeton, D.H. Crystal structure of cerium magnesium nitrate hydrate *Journal of Chemical Physics*, **1963**, *39*, 2881-2891.

16. Daly, S. R.; Piccoli, P. M. B.; Schultz, A. J.; Todorova, T. K.; Gagliardi, L.; Girolami, G. S., Synthesis and Properties of a Fifteen-Coordinate Complex: The Thorium Aminodiboranate [Th(H3BNMe2BH3)4]. Angewandte Chemie International Edition 2010, 49 (19), 3379-3381.

17. Popov, I., Jian, T., Lopez, G., Boldyrev, A. I.; Wang, L-S. Cobalt-centred boron molecular drums with the highest coordination number in the CoB_{16}^- cluster. *Nat Commun* **6,** 8654 (2015).

Contributors

Stephen Contakes, Westmont College, to whom comments, corrections, and criticisms should be addressed.

Consistent with the policy for original artwork made as part of this project, all unlabeled drawings of chemical structures are by Stephen Contakes and licensed under a Creative Commons Attribution 4.0 International License.

8.3: Coordination Numbers and Structures is shared under a CC BY-NC-SA 4.0 license and was authored, remixed, and/or curated by LibreTexts.

- **9.5: Coordination Numbers and Structures** by Stephen M. Contakes is licensed CC BY 4.0.
- **Current page** is licensed CC BY-NC-SA 4.0.

8.4: Isomerism

Metal complexes present a rich, interesting, and diverse structural chemistry. Major points of variation in the structural chemistry of metal complexes include

1. **coordination number** and **coordination geometry**, which involve differences in how many ligands surround a central metal and their overall geometric arrangement. Examples of the latter include the tetrahedral and square planar geometries commonly observed for four-coordinate metal centers. Tetrahedral, square planar, and octahedral coordination serve as a backdrop to the discussion of isomerism on this page. Readers who are unfamiliar with these structures might consider reading the section on coordination geometries before this one.
2. **structural iosmerism** involves differences in how potential ligand atoms are bound to metals in a complex. Possibilities for structural isomerism include
   - linkage or ambidentate isomerism
   - hydrate/solvate isomerism
   - ionization isomerism
   - coordination isomerism.

   Of these, linkage isomerism should always be considered when working with ambidentate ligands. As classifications, the last three forms of structural isomerism are mainly of academic interest since they represent permutations of ordinary structure patterns for solvates, salts, and coordination complexes, respectively.
3. **stereochemistry**, which includes
   - which coordination geometry is adopted for a metal with a given set of ligands in a particular oxidation state. For instance, $[Ni^{II}Cl_4]^{2-}$ is tetrahedral while $[Pt^{II}Cl_4]^{2-}$ is square planar. Since this geometry is usually fixed by the metal and ligands it is typically not a source of stereoisomeric varierty.
   - metal-centric stereoisomerism involving possible variations in where ligands are located relative to one another around the metal. The possibilities depend on the coordination number, geometry, and number of different types of ligands. For instance, square planar complexes can exhibit *cis-/trans-* isomerism while tetrahedral ones cannot. Tetrahedral complexes with four different ligands exhibit *R* and *S* chirality but complexes of that type are relatively rare. The more common cases include *cis* and *trans* isomerism in square planar complexes and *cis* & *trans-*, *mer* & *fac-*, and Λ & Δ isomerism in octahedral ones, although some multidentate ligands present additional possibilities for stereochemical variation
   - Stereoisomerism centered on the ligands bound to a metal center. Possibilities include
     - stereoisomerism inherent to a ligand. This would include cases where the ligand itself is chiral or, as in the case of amines, exists as a rapidly interconverting mixture of isomers. Thus this sort of stereoisomerism is an extension of the isomerism encountered in ordinary organic and other main group compounds. The main new issues introduced by binding of such ligands to a metal center involve the creation of new possibilities for diastereoisomerism based on the stereochemistry of the metal center and the freezing out of stereocenter inversion on binding to a metal. The latter is particularly important for amines, which as free amines racemize rapidly by nitrogen inversion.
     - or conformational isomerism involving five-membered **chelate rings** created when a multidentate ligand binds to a metal. This isomerism is often called chelate ring twist since individual rings can exhibit one of two conformations depending on how they twist on binding.

A summary of these forms of isomerism is given in Figure **8.4.1**.

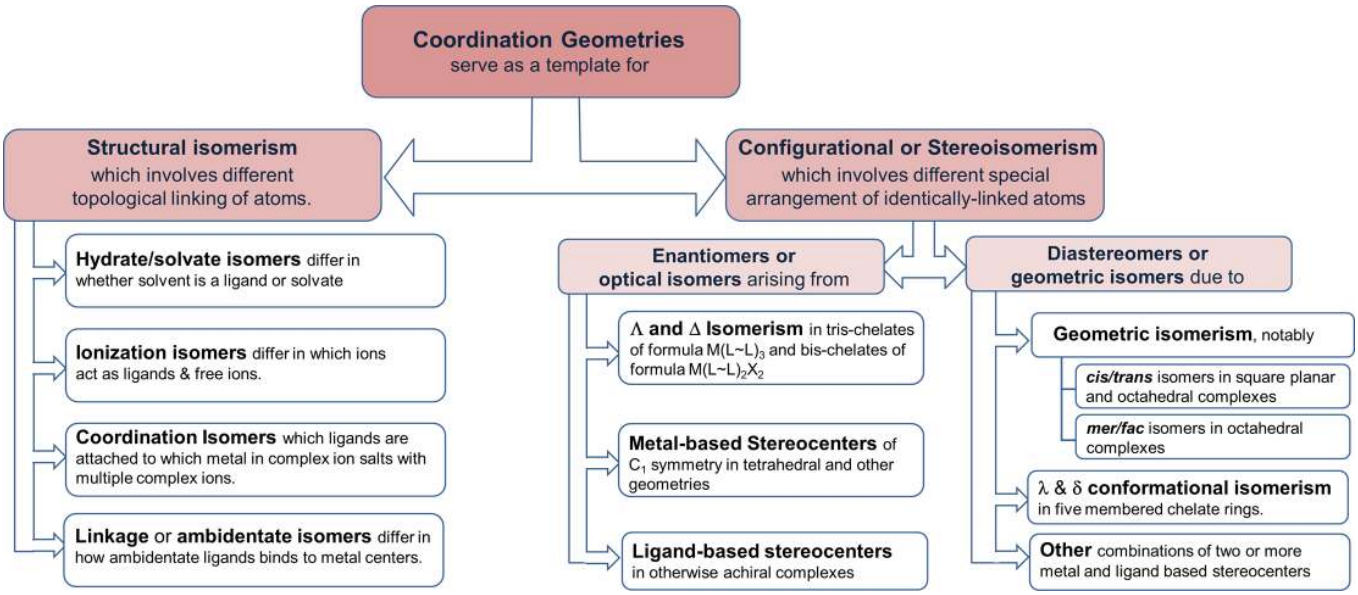


Figure **8.4.1**. Relationship among the common types of isomerism in metal complexes. This work by Stephen Contakes is licensed under a Creative Commons Attribution 4.0 International License.

Structural isomers

Structural isomerism involves different topological linkages of atoms. Differences in atomic linkages distinctive to coordination chemistry involve the linkages between metals and ligands. The main variations are:

1. Hydrate/solvate isomerism

Solvate isomers differ in terms of whether a molecule acts as a ligand or whether it acts as a solvate by occupying a lattice site in the crystal. Among solvate isomers, the case in which water is the ligand or solvate is the best known. The resulting isomers are called **hydrate isomers** after the term for water acting as a solvate, hydrate. A well-known example that illustrates how solvate isomerism works is the series $[CrCl_x(H_2O)_{6-x}]Cl_{3-x}{\cdot}xH_2O$, for which x = 0-2. The structures of the complex ions involved in this series are shown in Figure **8.4.2**.[1]

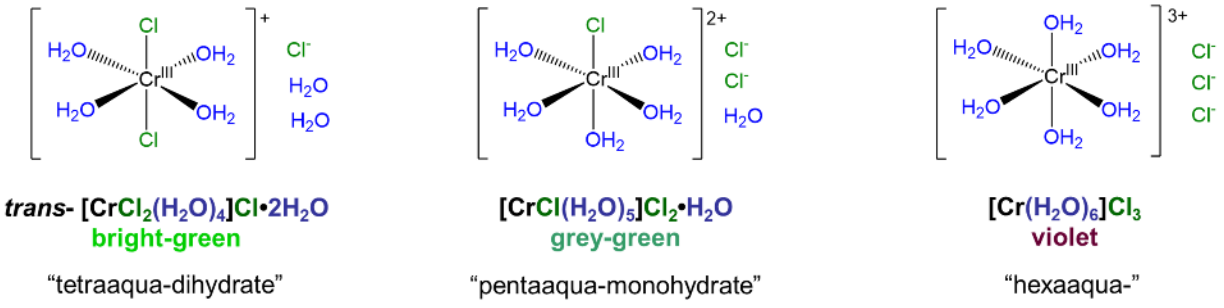


Figure **8.4.2**. Complexes of the hydrate isomer series $[CrCl_x(H_2O)_{6-x}]Cl_{3-x}{\cdot}xH_2O$ (x = 0-2). This work by Stephen Contakes is licensed under a Creative Commons Attribution 4.0 International License.

As can be seen from the compounds in Figure **8.4.2**, hydrate isomers differ both in terms of whether water acts as a ligand or hydrate *and* in terms of whether a potential counterion acts as a counterion or ligand. Thus, in *trans*-$[CrCl_2(H_2O)_4]Cl{\cdot}2H_2O$ two chlorides act as chloro ligands and four waters as aqua ligands while in $[CrCl(H_2O)_5]Cl_2{\cdot}H_2O$ five water molecules act as aqua ligands while only one chloride acts as a chloro ligand. In this way, solvate isomers simply represent cases in which two or more of the possible permutations for metal ligand binding among a set of solvent and counterion molecules are stable.

2. Ionization isomerism

In **ionization isomerism** there are two or more potential ions that can act as ligands. The ionization isomers differ in terms of which of these ions act as counterions and which act as ligands. Consider, for instance, the complexes shown in Figure **8.4.3**. These complexes differ in terms of whether the chloride or sulfate acts as a ligand, with the other acting as a counterion.

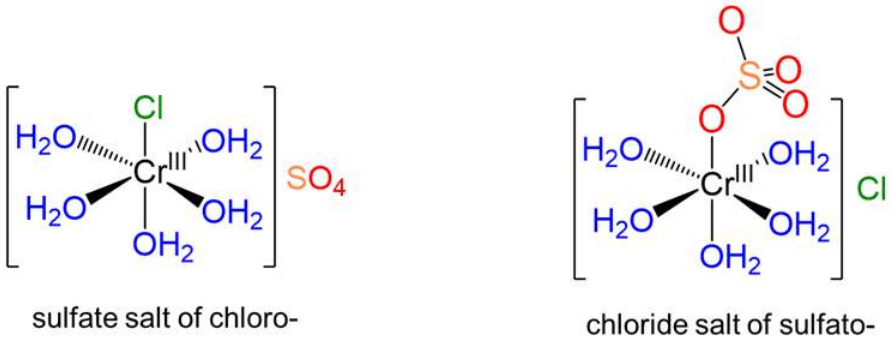


Figure **8.4.3**. Ionization isomers comprising a pentaaquachromium(III) fragment and the anions chloride and sulfate. As with all ionization isomers, the isomers differ in terms of which anion acts as a ligand and which a counterion. This work by Stephen Contakes is licensed under a Creative Commons Attribution 4.0 International License.

3. Coordination isomerism

Coordination isomers exist in compounds containing two or more complexes, each of which possesses a different set of ligands that can in principle be swapped with a ligand of the other complex. An example involves $[Co^{III}(NH_3)_6][Cr^{III}(ox)_3]$, depicted in Figure **8.4.4A**.[1] Coordination isomers of this complex involve swapping the ammine ligands around the Co^{3+} center for oxalato ligands surrounding the Cr^{3+} center. For instance, swapping all the ammine and oxalato ligands between the metal centers gives the coordination isomer $[Cr^{III}(NH_3)_6][Co^{III}(ox)_3]$ shown in Figure **8.4.4B**.

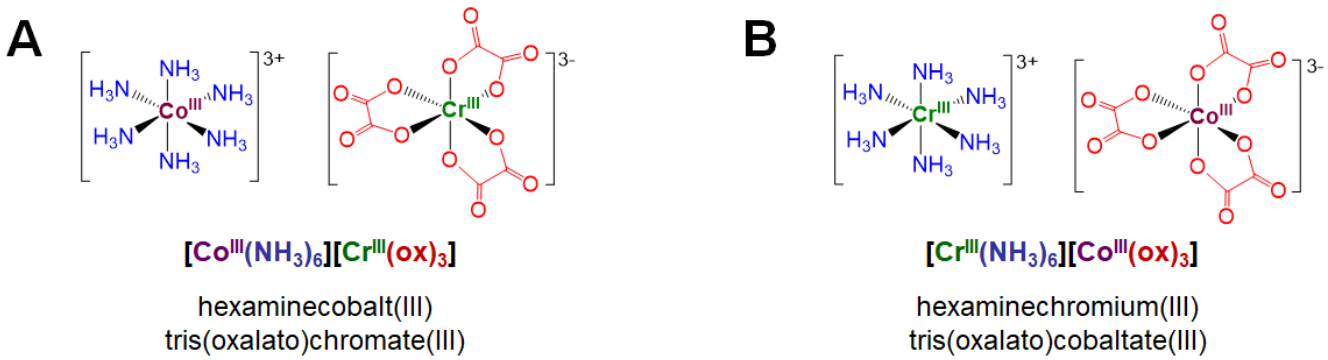
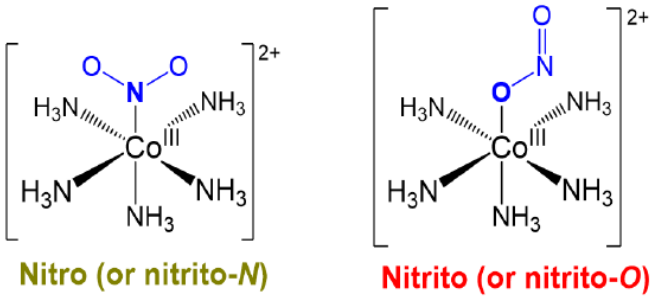


Figure **8.4.4**. Two coordination isomers comprising a Co^{3+} ,Cr^{3+}, six NH_3. and three oxalato ligands. The isomers differ in terms of which ligand type is bound to which metal. This work by Stephen Contakes is licensed under a Creative Commons Attribution 4.0 International License.

As classifications, hydrate/solvate, ionization, and coordination isomerism represent permutations of ordinary structure patterns for solvates, salts, and coordination complexes, respectively. As a result these forms of isomerism are rarely used as independent conceptual frameworks when thinking and talking about the structure of coordination compounds. Not so the final type of structural isomerism, linkage isomerism. That is because linkage isomerism has to do with the special *capacity* of ambidentate ligands to bind metals in multiple ways.

4. Linkage or ambidentate isomerism

Linkage or ambidentate isomers differ in how one or more ambidentate ligands bind to metal centers in a complex. The classic example dating from the work of Jørgensen and Werner is given in Scheme **8.4.I**.



Scheme **8.4.I**. Linkage isomers of penaamminenitritocobalt(III) ion. This work by Stephen Contakes is licensed under a Creative Commons Attribution 4.0 International License.

Just as alkenes exist as *E* and *Z* isomers, compounds possessing ambidentate ligands exist as one among the possible linkage isomers. As such, when working with ambidentate ligands the particular linkage isomer formed should be determined experimentally and considered when interpreting the complex's chemical and physical behavior.

The main ambidentate ligands which give rise to linkage isomerism are

- cyanide, CN^-
- thiocyanate, SCN^-, and the O and Se analogues, OCN^- and $SeCN^-$
- nitrite, NO_2^-
- sulfite, SO_3^-
- nitrosyl, NO

Although ambidentate ligands can bind metals in multiple ways, most exhibit a preferred binding mode (*i.e.*, prefer to bind metal centers in one of the possible ways). For instance, cyanide almost always binds through its carbon atom and thiocyanate almost always binds through its nitrogen (*μ-N*). However, the other binding mode can sometimes be formed kinetically or by using conditions that particularly favor its formation. Thus thiocyanate forms M-SCN^- linkages in the presence of exceptionally soft metal centers or in hard polar solvents (in which Lewis acid groups can stablize the terminal nitrogen of a bound thiocyanate ligand).

Ambidentate ligands are of significant research interest because many don't just bind to metal centers in two ways; the linkage isomers sometimes have significantly different physical properties. In addition, the possibility of two binding modes introduces the possibility of exploiting linkage isomerism to take advantage of some of these ligands:

a. different structural chemistry in different coordination modes. In mononuclear complexes the coordination mode influences which side of the ligand faces away from the complex and might be susceptible to stabilization by interaction with solvent. Additionally, the orientation of the ligand relative to the metal center might differ between one coordination mode and another. For instance, as predicted from the minor contributor to its resonance structure, thiocyanate binds nonlinearly via its S atom and linearly via its N (Figure **8.4.5**). Because of this the apparent steric bulk of the ligand around the metal center might differ between forms.

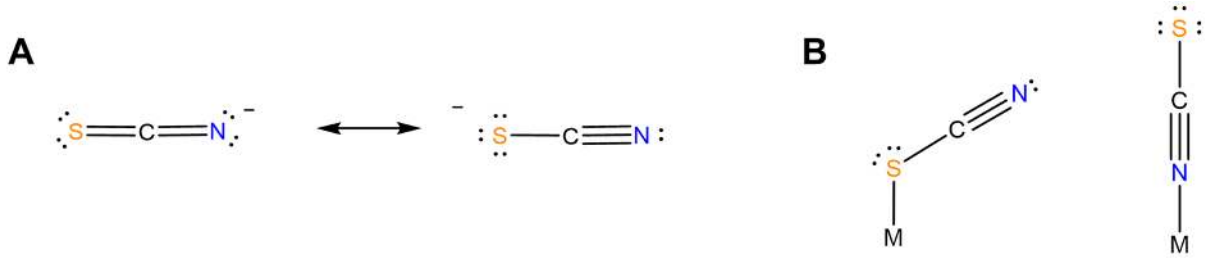


Figure **8.4.5**. Thiocyanate generally prefers to bind metals nonlinearly but in some cases forms linear M-SCN bonds. This work by Stephen Contakes is licensed under a Creative Commons Attribution 4.0 International License.

b. bind two different metal centers at the same time, linking them together. Perhaps the best-known examples involve thiocyanate and cyanide. The latter forms linkages of the type M-C≡N-M'. In the dye Prussian blue these take the form Fe^{II}-C≡N-Fe^{III}. An example from the author's graduate research involved tetrahedral clusters containing four metal atoms linked by six cyano ligands, as shown in Figure **8.4.6**.

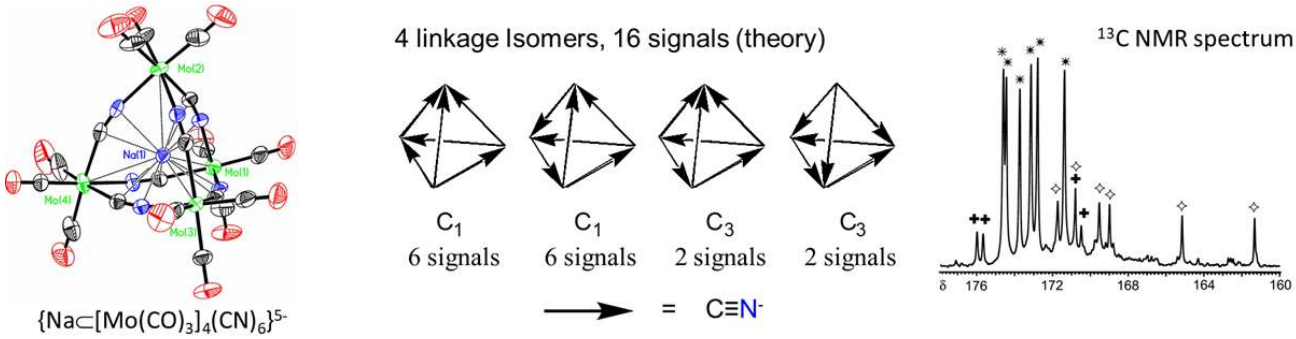


Figure **8.4.6**. (A) Structure of $\{Na@[Mo(CO)_3]_4(CN)_6\}$ showing the linking of four Mo centers by six CN ligands. Thermal ellipsoids for the C atoms are shown in black; those of the N atoms in blue. (B) The complex exists as a mixture of four linkage isomers in which the bridging CN^- ligands are oriented in different ways, as may be seen from the presence of the expected sixteen signals in its ^{13}C NMR spectrum. Based on work reported in reference 2.

c. can be induced to change from one binding mode to another in response to a stimulus. The classic example involves the light-driven transformation of the thermodynamically more stable yellow nitro complex of pentamminecobalt(III), $[Co(NH_3)_5NO_2]^{2+}$ to the less stable red *O*-nitrito complex, $[Co(NH_3)_5ONO]^{2+}$. Less stable cyanometallate coordination networks like those in the red $K\{Fe^{II}[Cr^{III}(CN)_6]\}$ transform into the more stable green $K\{Fe^{II}[Cr^{III}(NC)_6]\}$ form on heating, as shown in Figure **8.4.7**.[3]

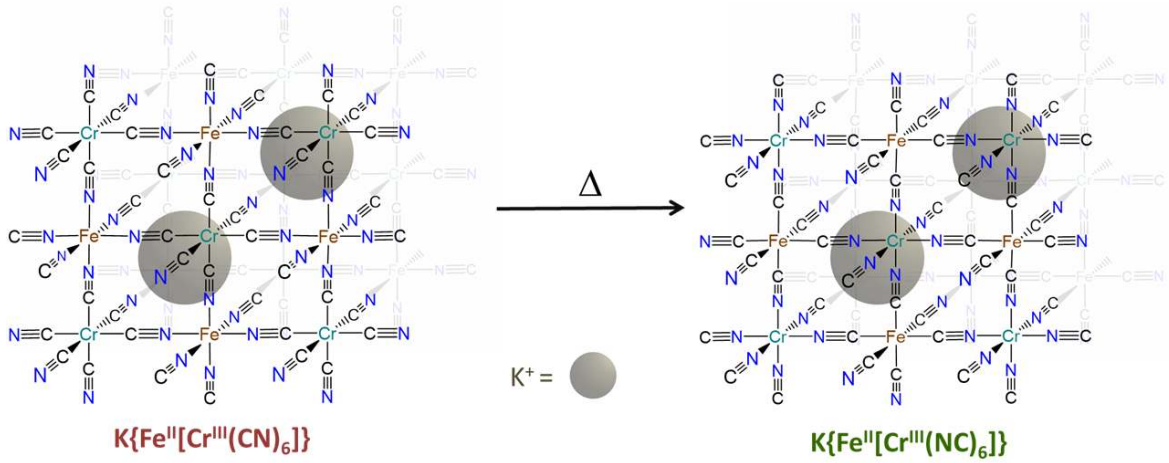


Figure **8.4.7**. Thermally-induced transformation of one $K\{Fe^{II}[Cr^{III}(CN)_6]\}$ into its more stable green linkage isomer $K\{Fe^{II}[Cr^{III}(NC)_6]\}$ involves "flipping" the cyano ligands. This work by Stephen Contakes is licensed under a Creative Commons Attribution 4.0 International License.

? Exercise 8.4.1: Bridging ambidentate ligands and the Hard-Soft Acid- Base Principle.

The hard-soft acid-base principle helps explain the preference of bridging ambidentate ligands for particular binding modes. How might the greater stability of the green $K\{Fe^{II}[Cr^{III}(NC)_6]\}$ over red $K\{Fe^{II}[Cr^{III}(CN)_6]\}$ be explained in terms of the hard and soft acid-base concept?

Answer

The greater stability of $K\{Fe^{II}[Cr^{III}(NC)_6]\}$ over $K\{Fe^{II}[Cr^{III}(CN)_6]\}$ reflects the greater stability of the Fe^{II}-CN-Cr^{III} linkages in the former over the Fe^{II}-NC-Cr^{III} linkages in the latter. This is consistent with the preference for hard-hard and soft-soft Lewis acid-base interactions of the Hard-Soft Acid-Base Principle.

The Fe^{II}-CN-Cr^{III} linkages are more stable because they possess bonds between

- the softer Lewis acid (Fe^{II}) and Lewis base (the C end of CN^-)
- the harder Lewis acid (Cr^{III}) and Lewis base (the N end of CN^-)

In contrast, the Fe^{II}-NC-Cr^{III} linkages in the less stable linkage isomer involve bonds between

- the softer base (the C end of CN^-) and harder acid (Cr^{III})
- the harder base (the N end of CN^-) and softer acid (Fe^{II})

Stereoisomerism

Optical Isomerism/Chirality

Molecules of D_n, C_n, or C_1 symmetry with only proper rotation axes (including $E = C_1$) are chiral and exhibit optical isomerism. As described in Figure **8.4.1**, the main sources of such optical isomerism in coordination chemistry are:

1. Chirality inherent to an organic or main group ligand.

   This type of isomerism is just an extension of the sort described in undergraduate organic texts and consequently does not merit separate discussion here, other than to note that some forms of optical isomerism which are of little importance in organic chemistry lead to optical activity in coordination compounds. In particular, the nitrogen inversion process which serves to rapidly racemize chiral amines is frozen out on formation of a metal-ligand bond. Because of this chiral amine, ligands bound to a metal form non-interconvertible *R* and *S* enantiomers, as shown in Figure **8.4.8**.

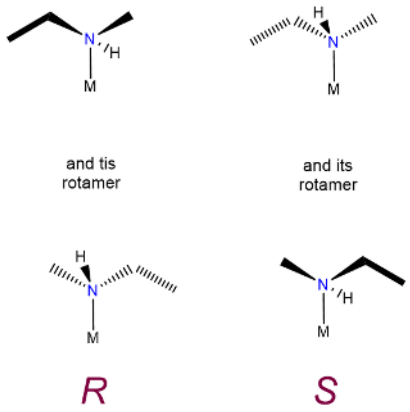


Figure **8.4.8**. Two views of *R* and *S* enantiomers formed when the chiral amine ethylmethylamine binds a metal that are commonly used to represent chiral amines in complexes. This work by Stephen Contakes is licensed under a Creative Commons Attribution 4.0 International License.

2. Chirality arising from the symmetry of ligands about a metal center.

   The two common situations through which such chirality arises involve:

   i. Chirality at a tetrahedral metal center surrounded by four different ligand attachment points.

      Such cases are often referred to as MABCD or Mabcd where M stands for the metal and a, b, c, and d the four different ligand attachment points. An example of such a complex is given in Figure **8.4.9A**. The chirality of such complexes is analogous to the chirality arising from a tetrahedral carbon stereocenter. There are two caveats, though. First, it is not enough to have a four-coordinate complex; the metal must possess tetrahedral symmetry since, as shown in Figure **8.4.9B**, square planar M complexes with four different ligands are identical to their mirror images. Second, such chirality is most easily realized using macrocyclic ligands like proteins. Metal ligand bonds involving sterically unhindered monodentate complexes like that in the example of Figure **8.4.9A** are in general weaker and more flexible than analogous carbon-carbon bonds. Consequently, in such cases it is likely that the enantiomers would interconvert through a fluxional process, making their resolution difficult if not impossible.

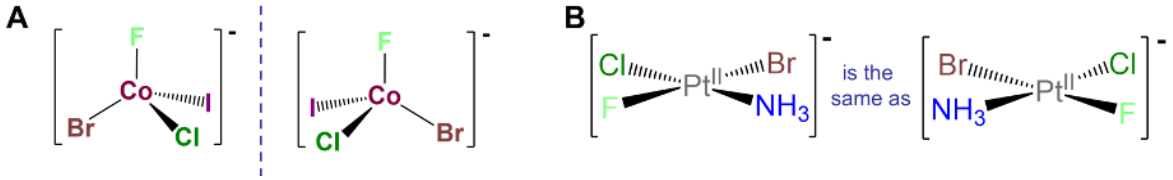


Figure **8.4.9**. (A) In principle tetrahedral metal centers surrounded by four different ligands (Mabcd) exhibit chirality analogous to the chirality of tetrahedral carbon stereocenters; (B) in contrast, square planar Macbd complexes like $[PtBrClF(NH_3)]^-$ are not chiral since they are the same as their mirror images. (It is easiest to see this by either working out its point group (C_s) or by rotating the left $[PtBrClF(NH_3)]^-$ structure clockwise 180 degrees to give its mirror image. This work by Stephen Contakes is licensed under a Creative Commons Attribution 4.0 International License.

ii. **Λ** and **Δ** isomerism at octahedral metal centers surrounded by two or three chelating ligands.

Specifically,

a. Octahedral tris-chelates of formula $M(L\sim L)_3$ exhibit D_3 symmetry.
b. cis-octahedral bis-chelates of formula $M(L\sim L)_2XY$ exhibit C_2 or C_1 symmetry: C_2 if X = Y and C_1 if $X \neq Y$.

As shown in Figure **8.4.10A**, octahedral tris-chelates like $[V(ox)_3]^{3-}$ are chiral and can exist as nonsuperimposable **Λ** and **Δ** enantiomers. The chirality of these tris-chelates is analogous to that of pinwheels. As shown in Figure **8.4.10B**, when looking directly at the head of any individual pinwheel from above, the blades will be angled from back to front going around the pinwheel in either the clockwise or counterclockwise direction. As shown in Figure **8.4.10C**, the case for which the blades are angled in the clockwise direction is analogous to the **Λ** enantiomer and the case when they are angled in the counterclockwise direction the **Δ**.

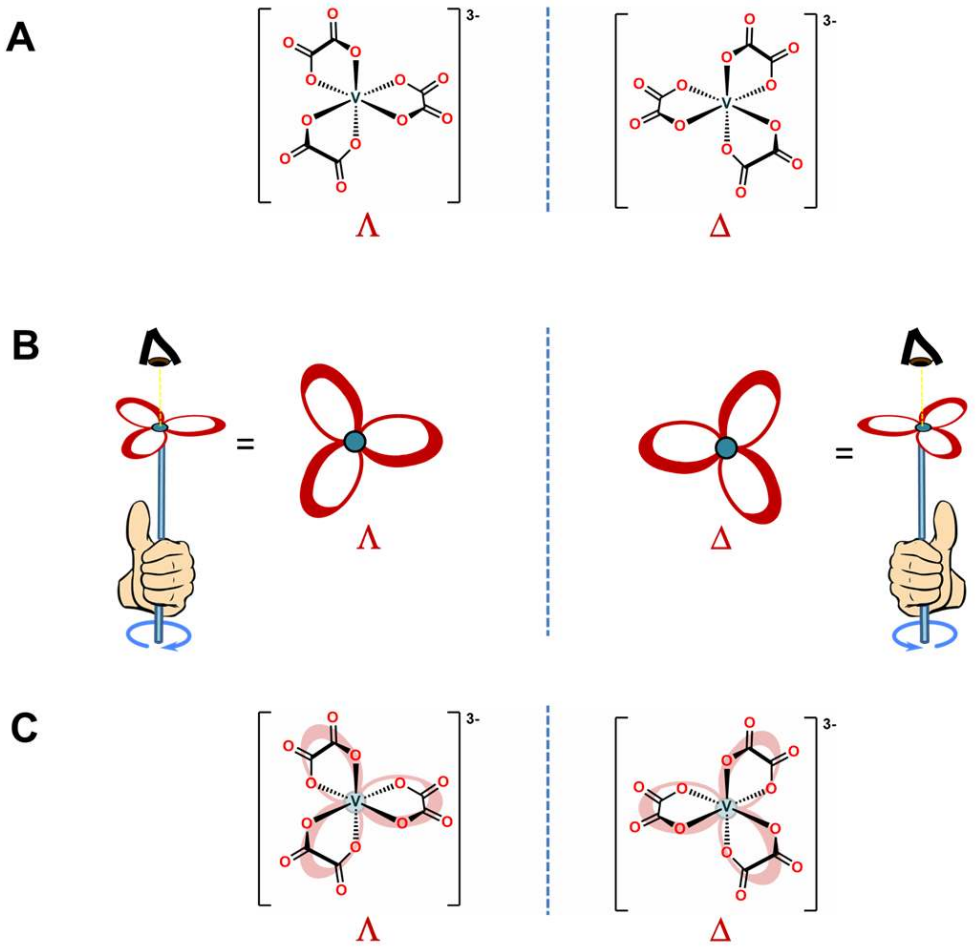


Figure **8.4.10**. (A) Octahedral tris-chelates like $[V(ox)_3]^{3-}$ are chiral and can exist as **Λ** and **Δ** enantiomers. (B) The chirality in these systems is analogous to that of a pinwheel, with the **Λ** enantiomer exhibiting the symmetry of a left-handed pinwheel and the **Δ** enantiomer that of a right handed one. (C) The pinwheel-like nature of **Λ** and **Δ** enantiomers is easiest to see by overlaying the structures of $[V(ox)_3]^{3-}$ from A with the pinwheel structures of B. One way to recognize **Λ** and **Δ** enantiomers is to draw them in these projections. If a left hand is curled around the **Λ** enantiomer with the thumb facing up the curl of the fingers will flow from the back of each ligand towards the front. The same will be true if the right hand is curled around the **Δ** enantiomer. Credits: Although the image is largely an original drawing, the hand images used in part B are adapted from an image by SVGguru / CC BY-SA (https://creativecommons.org/licenses/by-sa/4.0). Otherwise this work by Stephen Contakes is licensed under a Creative Commons Attribution 4.0 International License.

The **Λ** and **Δ** chirality in octahedral bis-chelates is analogous to that in the tris-chelates except this time the third chelating ligand is replaced by an arbitrary pair of ligands. This lowers the symmetry of the complex to either C_2 or C_1, as shown for the C_2 complex $[CoCl_2(en)_2]^+$ in Figure **8.4.11A**. In either case the result is that such complexes exist as **Λ** and **Δ** enantiomers analogous to those in the metal tris-chelates, as shown in Figure **8.4.11B**.

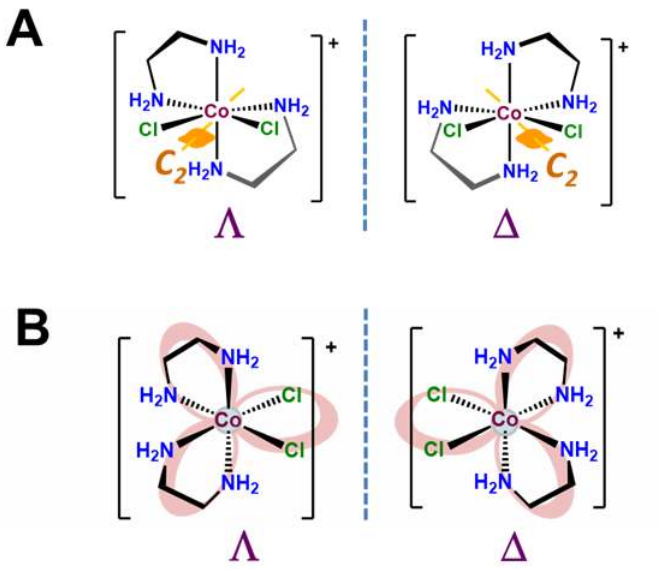


Figure **8.4.9C**. This work by Stephen Contakes is licensed under a Creative Commons Attribution 4.0 International License.

Octahedral complexes containing ligands with denticities of four or more also exhibit **Λ** and **Δ** chirality; it is just that in such cases the bound ligand defines multiple rings within the complex that can be defined as existing in either **Λ** or **Δ** orientations relative to each other. The procedure for making these assignments is beyond the scope of most introductory inorganic courses but the result is that such complexes are designated as **ΛΛ**, **ΔΔ**, **ΔΛ**, **ΔΔΔ**, etc., depending on the number of relationships involving the rings defined by the bound ligand. Interested readers should consult reference 4 for more details.

Circular dichroism may be used to characterize optically active metal complexes.

At the present the most definitive way to determine the absolute configuration of an optically active coordination compound is to determine its 3D molecular structure using single crystal X-ray crystallography.[5] However, as that is not always possible or convenient, the optical activity of coordination complexes is also commonly studied using circular dichroism (CD) spectroscopy. CD spectroscopy is used because, unlike most chiral organics, optically active coordination complexes possess low-energy electronic transitions that occur in the far UV and visible range. This means that it is often convenient to use the ability of a complex to refract and absorb different circular polarizations of light to derive information about both the configuration of an optically active complex and its electronic structure. The focus of this section will be to explain how the determination of absolute configuration by circular dichroism and optical rotatory dispersion work, as well as the relationship of these techniques to the more ordinary sort of polarimetry used to measure optical rotation in organic systems. Only brief notes will be made about the instrumental and electronic structure applications of these techniques since the electronic spectra of metal complexes will be discussed in Chapter 11: Coordination Chemistry III - Electronic Spectra and the instrumental aspects of CD are well-treated elsewhere.

Both polarimetry and circular dichroism spectroscopy are grounded in the recognition that plane polarized light is equivalent to a superposition of left and right circularly polarized light, as shown in Figure **8.4.12**.

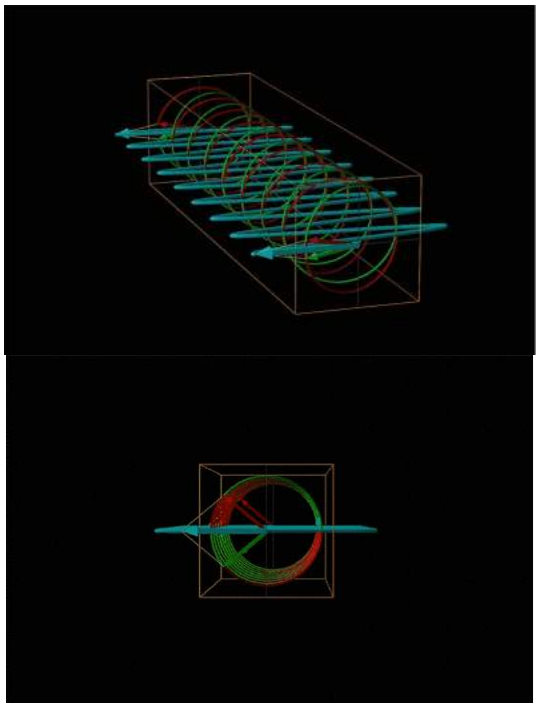


Figure **8.4.12**. Angled and front view of plane polarized light (light blue) as the vector sum of left circularly polarized light (red) and right circularly polarized light (green). Created using EMANIM Version 1.2 (2011 July) by Andras Szilagyi (www.enzim.hu/~szia/emanim). This work by Stephen Contakes is licensed under a Creative Commons Attribution 4.0 International License.

When plane polarized light passes through a chiral medium, its left and right circularly polarized components move at different rates (*i.e.*, have different indices of refraction). This causes the plane of polarization to rotate in the direction of the faster component according to the relationship

$$\alpha = \frac{n_l - n_r}{\lambda}$$

where α is the angle of rotation, λ the light's wavelength, and n_l and n_r the refractive indices experienced by left and right circularly polarized light.

An example of such a rotation is shown in Figure **8.4.13**.

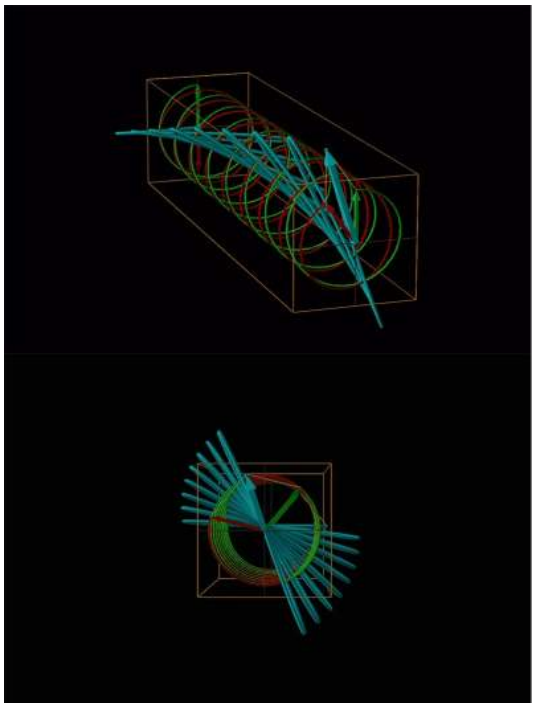


Figure **8.4.13**. Angled and front view of plane polarized light (light blue) as it passes through a medium (represented by the orange box) in which left circularly polarized light (red) experiences a higher refractive index (and so moves slower) than right circularly polarized light (green). Created using EMANIM Version 1.2 (2011 July) by Andras Szilagyi (www.enzim.hu/~szia/emanim) with a refractive index of 1.05 for left circularly polarized light and 1.00 for right circularly polarized light. This work by Stephen Contakes is licensed under a Creative Commons Attribution 4.0 International License.

Chemists typically call this rotation of light by a chiral medium optical rotation. In organic chemistry it is common to measure the optical rotation at the sodium D wavelength of 589.29 nm, a much longer wavelength than most organics are able to absorb. Because of this the optical rotations commonly measured by organic chemists are largely independent of absorption and mainly serve as a characteristic physical property similar to melting points or are used to establish the purity of a mixture of enantiomers. The sort of spectroscopic data used to characterize chiral coordination compounds more commonly makes use of the relationship between absorption and optical rotation.

In coordination chemistry the wavelength-dependence of optical rotation is used to discern information about compounds' electronic spectra. This measurement of the wavelength dependence of optical rotation is called **optical rotatory dispersion (ORD)** and the resulting plots are called optical rotatory dispersion or ORD spectra or curves. Such ORD curves are useful for characterizing the chiral environment in a coordination complex because the ORD curves exhibit a characteristic shape. This characteristic shape is because according to the **Cotton Effect,** the optical rotation changes sign at the absorption maximum of a chromophore in the compound. For one configuration the rotation will go from negative to positive with increasing wavelength and is called a **positive cotton effect**; for the other configuration the rotation will go from positive to negative or exhibit a **negative cotton effect**. This behavior is summarized in the top two curves of Figure **8.4.14**.

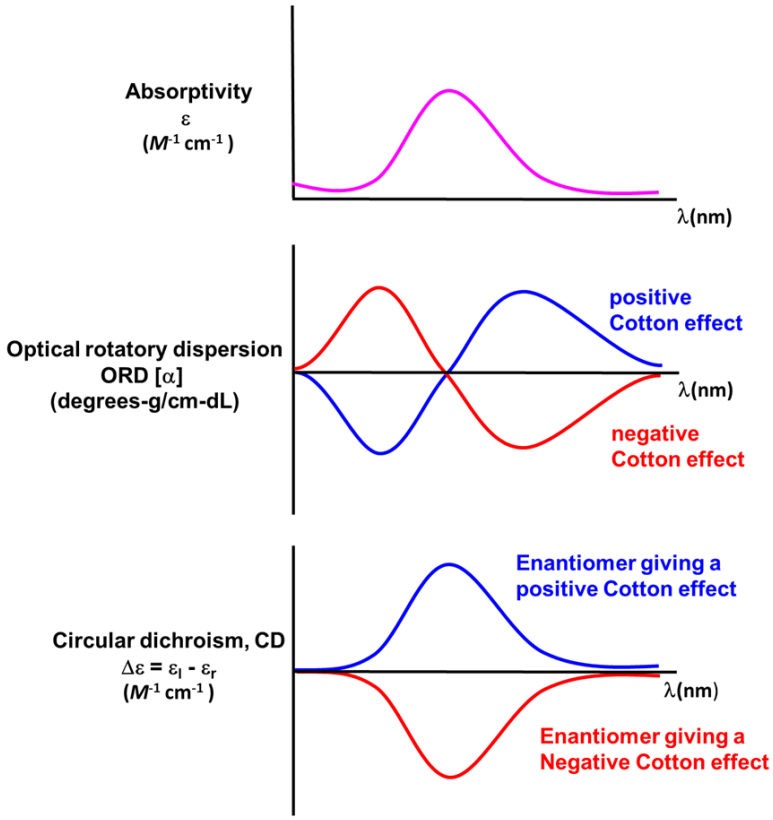


Figure 8.4.14. Idealized relationship between absorbance, ORD, and CD spectra for enantiomers exhibiting a positive and negative Cotton effect. This work by Stephen Contakes is licensed under a Creative Commons Attribution 4.0 International License.

A technique used even more often than ORD is **circular dichroism (CD)**, represented by the lowest spectrum in Figure 8.4.14. Circular dichroism arises from the differential absorption of left and right circularly polarized light by a chiral compound. This gives elliptically polarized light as shown in Figure 8.4.15.

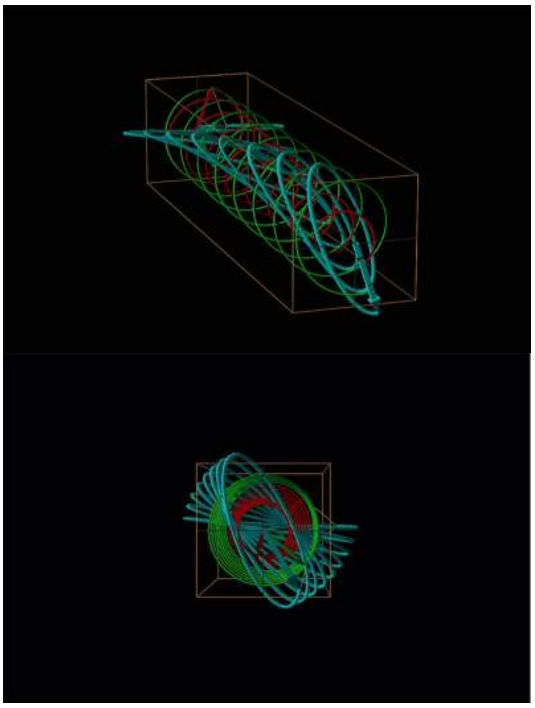


Figure **8.4.15**. Angled and front view of plane polarized light (light blue) as it passes through a medium (represented by the orange box) in which left circularly polarized light (red) both experiences a higher refractive index and greater absorption than right circularly polarized light (green). Created using EMANIM Version 1.2 (2011 July) by Andras Szilagyi (www.enzim.hu/~szia/emanim) with a refractive index of 1.05 and an extinction coefficient of 0.05 for left circularly polarized light and a refractive index of 1.00 and extinction coefficient of 0 for right circularly polarized light. This work by Stephen Contakes is licensed under a Creative Commons Attribution 4.0 International License.

In circular dichroism (CD) spectroscopy a sample is irradiated with polarized light resulting in the transmission of elliptically polarized light due to differential refraction and absorption of the polarized light's left and right circularly polarized components. For achiral molecules the handedness doesn't affect absorbance, but for chiral molecules, which chiral ground and excited states the handedness of an EM wave affects can determine how readily that wave can distort the chiral ground state into the chiral excited one. For this reason chiral molecules absorb left and right circularly polarized light differently.

In CD spectroscopy the magnitudes of the left and right circularly polarized components of light that is transmitted by the sample are measured and used to determine how much light of each was absorbed (just as in regular absorbance spectroscopy). The difference in absorption between left and right circularly polarized light constitutes the primary signal in CD spectroscopy. More specifically, circular dichroism spectra (CD spectra) show the difference in extinction coefficients for left and right circularly polarized light, $\Delta\epsilon$, as a function of wavelength, where

$$\Delta\epsilon = \epsilon_l - \epsilon_r$$

where Missing open brace for subscript and Missing open brace for subscript are the extinction coefficients observed with left and right circularly polarized light, respectively.

As with ORD spectra, the signs of the features in CD spectra like that of Δ–$[Co(en)_3]Cl_3$ given in Figure **8.4.16** are enantiomer-dependent. As illustrated in the lower spectrum in Figure **8.4.14** , the CD spectra of enantiomers mirror one another. Because of this difference in behavior it is possible in principle to determine the absolute configuration of a complex from its CD spectrum.

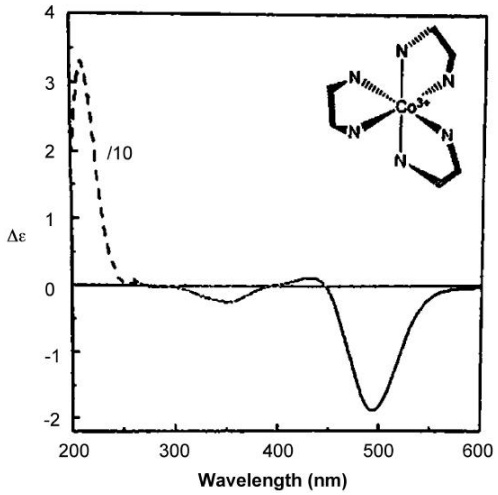


Figure **8.4.16**. CD spectrum of Δ–$[Co(en)_3]Cl_3$. Taken from reference 6.

There are several ways that ORD and CD spectra can be useful for determining the absolute configuration of a chiral complex.

1. First, the sign of the Cotton effect and peaks in CD spectra exhibited by a given absolute configuration is often consistent across a series of compounds. Thus if a new member of the series is isolated, its configuration can be determined based on which enantiomer has the same Cotton effect. For instance, if both the **Λ** isomer of a metal diimine complex like $[Ru(bpy)_3]^{2+}$ exhibit a positive Cotton effect and a newly resolved metal diimine exhibits a negative Cotton effect it might reasonably be inferred that the newly-resolved complex is in the opposite or **Δ** configuration.
2. Second, for some systems the expected sign of the Cotton effect and CD peaks for each enantiomer may be predicted semi-empirically based on the spatial locations of substituents relative to the chromophore (the part of the molecule that changes electronic structure during the transition), although the details are beyond the scope of the present discussion.
3. Consideration of interactions between multiple chromophores in a compound can be used to infer absolute configuration. Again, the details are beyond the scope of the present discussion. Interested readers are referred to reference 7 for details.

Common patterns of Diastereomerism

Geometric isomerism

Geometric isomerism involves differences in the geometric placement of atoms in a compound. In coordination chemistry, geometric isomerism involves differences in the relative placement of a set of ligands about a metal center. There are two main types:

cis and *trans* isomerism

This type of isomerism has to do with how two ligands are oriented relative to one another in a square planar or octahedral complex. As shown in Figure **8.4.17**, ligands that are next to one another with a L-M-L bond angle of 90° are said to be *cis*; those on opposite sides of the metal with a L-M-L bond angle of 180° are in the *trans* arrangement.



Figure **8.4.17**. *cis* and *trans* arrangement of ligands around (A) square planar and (B) octahedral metal centers. Since both types of complexes feature 90° L-M-L bond angles, the arrangements are fundamentally the same in both cases. This work by Stephen Contakes is licensed under a Creative Commons Attribution 4.0 International License.

Simple *cis* and *trans* geometric isomers can be identified when there are two identical ligands (A) or chelating ligands with distinguishable attachment points (A~B) oriented about either a square planar or octahedral center. Examples are given in Figure

8.4.18. Notice from the example given in Figure 8.4.18C that multidentate ligands have the potential to constrain complexes to adopt a particular geometry.

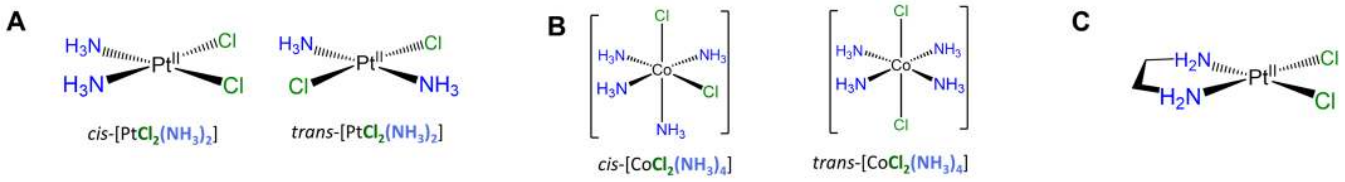


Figure 8.4.18. Examples of square planar and octahedral *cis* and *trans* isomers. (A) *cis* and *trans* isomers of $[PtCl_2(NH_3)_2]$; the former is medicinally important. Sold under the name cisplatin, the *cis* isomer is used as a chemotheraphy against various forms of cancer. (B) *cis* and *trans* isomers of $[CoCl_2(NH_3)_4]$, a compound of more academic interest. (C) $PtCl_2$(en) only exists as the *cis* isomer because the chelating en ligand can only bind in a *cis* arrangement. This work by Stephen Contakes is licensed under a Creative Commons Attribution 4.0 International License.

Slightly more involved examples involve perturbations of the simple cases above in which there are multiple distinguishable *cis* and/or *trans* relationships. Two square planar examples are given in Figure 8.4.19.

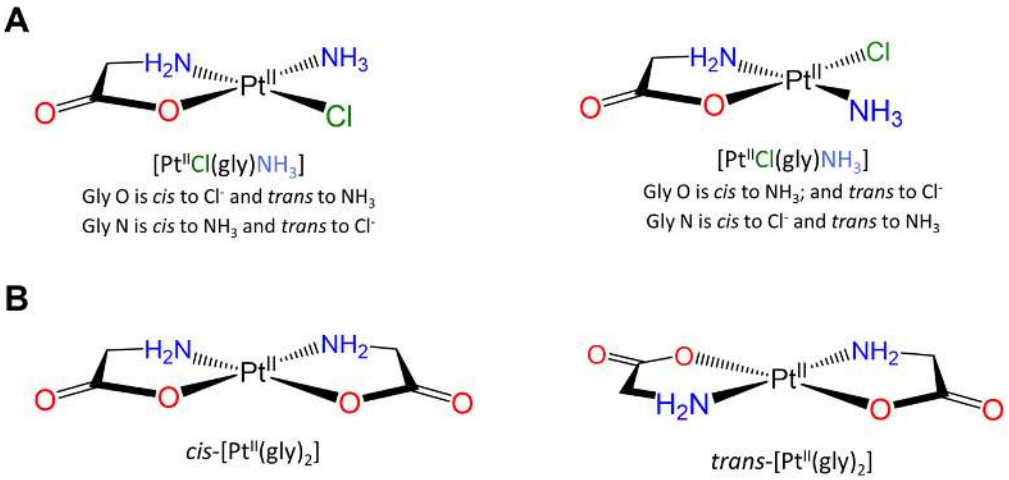


Figure 8.4.19. Examples of more complex square planar systems. (A) Geometric isomers of $[PtCl(gly)NH_3]$, a MA_2BC system for which A = gly^-, B = Cl^-, and C = NH_3. Swapping of the ammine and chloro ligands changes both the *cis* and *trans* relationships involving the Gly ligand. (B) Geometric isomers of $[Pt(gly)_2]$, an $M(A\sim B)_2$ system for which A = the *κO* glycine carboxy group and B its *κN* amine. The only possible geometric isomerism involves swapping the orientation of one glycine relative to the other. For this reason the two complexes shown can be designated as *cis* and *trans* isomers based on whether the *κO* and *κ*N ends of the glycine are *cis* or *trans* to one another. This work by Stephen Contakes is licensed under a Creative Commons Attribution 4.0 International License.

More complex examples of *cis* and *trans* relationships between ligands in octahedral complexes are given in the exercises that conclude this page, which also demonstrates how a systematic approach may be used to identify isomers.

mer and *fac* isomerism

This type of isomerism has to do with how three ligands are oriented relative to one another in an octahedral complex. The arrangements are represented in Figure 8.4.20.

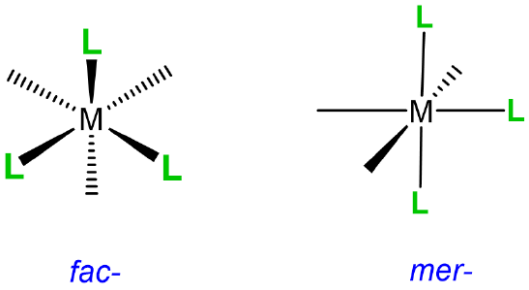


Figure 8.4.20. Simple representation of the *fac* and *mer* arrangements of ligands around an octahedral metal center. This work by Stephen Contakes is licensed under a Creative Commons Attribution 4.0 International License.

Since it can help to visualize the *mer* and *fac* geometry from multiple points of view, several representations are given in Figure 8.4.21. As shown in Figure 8.4.21, in ***fac*** or **facial arrangements**, the ligands occupy the same "face" of the octahedral coordination sphere, while in the ***mer*** or **meridional geometry** the ligands form a T shape in the same plane or its "meridian."[8]

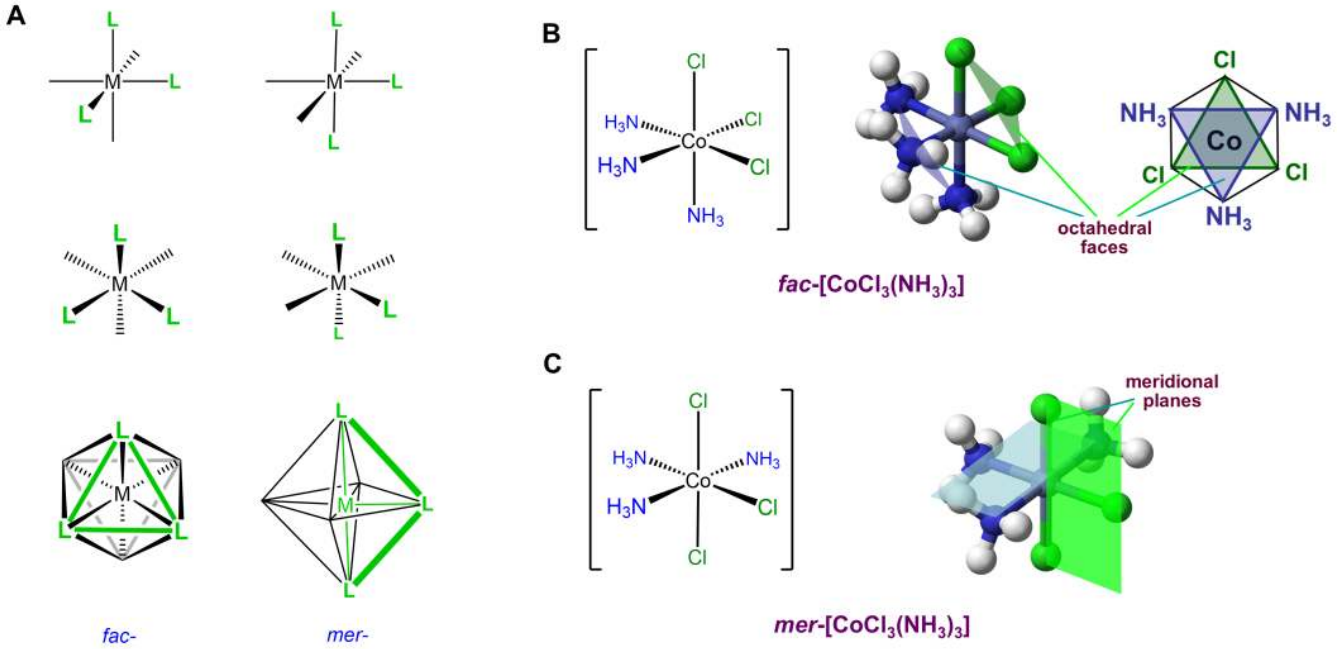
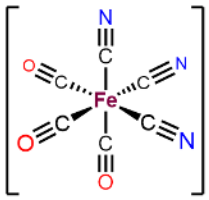
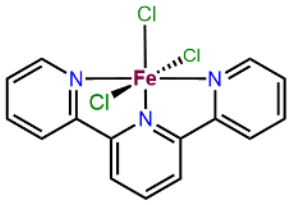
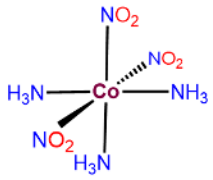


Figure 8.4.21. (A) Three projections of *fac* and *mer* arrangements of ligands around an octahedral metal center emphasizing that in the *fac* arrangement the ligands are oriented along a face of the octahedron while in the *mer* arrangement they are oriented in a plane. (B) Structure of *fac*-$[CoCl_3(NH_3)_3]$ showing the octahedral faces occupied by the chloro and amine ligands. (C) Structure of *mer*-$[CoCl_3(NH_3)_3]$ showing the planar arrangement of the chloro and ammine ligands. The ball and stick models are modified from images by Benjah-bmm27 - Own work, Public Domain, https://commons.wikimedia.org/w/inde...?curid=1874872 and curid=1874873. Otherwise this work by Stephen Contakes is licensed under a Creative Commons Attribution 4.0 International License.

Octahedral complexes with three identical ligands oriented about an octahedral center can only exist in *mer* and *fac* arrangements. Consequently, such complexes can be designated as *mer* and *fac* isomers. Examples are given in Figure 8.4.22.







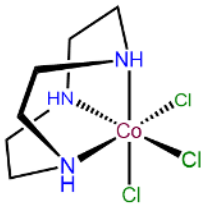


Figure 8.4.22. Examples of *fac* and *mer* octahedral complexes. Note how some chelating ligands preferentially bind to the metal in a *fac* or *mer* arrangement and, in so doing, force the other ligands to also form a *mer* or *fac* arrangement. This work by Stephen Contakes is licensed under a Creative Commons Attribution 4.0 International License.

Diastereomerism arising from multiple ligand-associated chiral centers

Diastereomerism can also arise when two or more chiral ligands bind to a metal center. Such cases typically give rise to a complex mixture of isomers, as shown by the example in Figure 8.4.23. As may be seen from Figure 8.4.23, the differences between these isomers can arise from both changes in the stereochemical configuration of the ligand and the relationship of particular ligand centers relative to one another. For instance, the leftmost two structures in Figure 8.4.23 possess one *R* and *S* nitrogen center each but differ in whether the centers are oriented so that the *R* and *S* centers on the two ligands are *trans* or *cis* to one another.

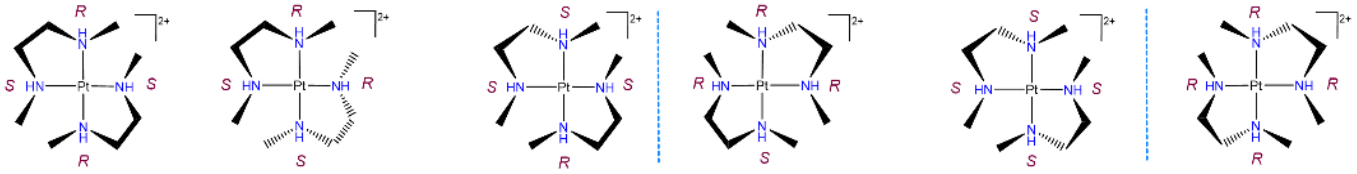


Figure 8.4.23. Diastereomers that can in principle be formed when two *N*,*N*′-dimethylethylenediamine ligands coordinate a Pt^{2+} center. This work by Stephen Contakes is licensed under a Creative Commons Attribution 4.0 International License.

Diastereomerism arising from λ and δ ring conformation isomerism.

Chelate rings are formed when a chelating ligand binds a metal

As may also be seen from the structures in Figure 8.4.23, when a multidentate ligand coordinates a metal, the ligand and metal center comprise one or more **chelate rings**. Examples of such chelate rings are shown in Figure 8.4.24.

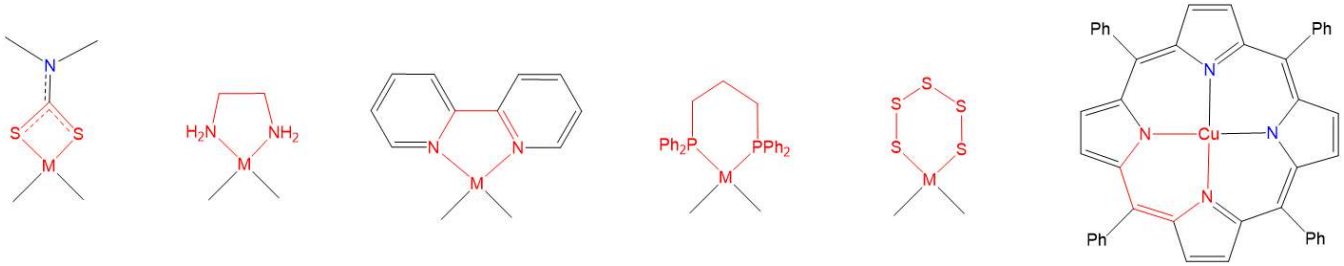


Figure 8.4.24. Four, five, and six-membered chelate rings (shown in red) formed by coordination of selected bidentate ligands to a metal center. This work by Stephen Contakes is licensed under a Creative Commons Attribution 4.0 International License.

As may be inferred from the examples in Figure 8.4.24, chelate rings may be of different sizes, although four, six, and especially five-membered rings are particularly common. Exactly which ring sizes will be more stable for a given system depends on the

coordination geometry and, due to differences in M-L bond lengths, to a lesser degree on the metal. As a result, for octahedral and square planar complexes with 90° L-M-L bond angles between *cis* ligands, *five-membered rings tend to be especially stable* (Figure **8.4.25**).

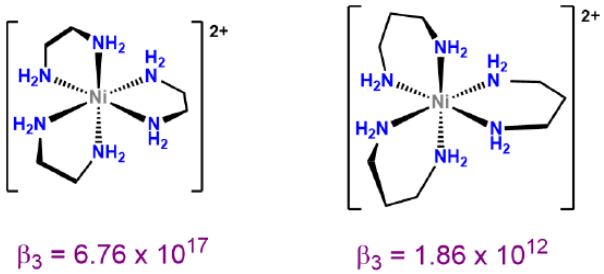


Figure **8.4.25**. The greater stability of five-membered chelate rings involving Ni^{2+} and organic ligands is reflected in the higher overall formation constant (β_3) for the five-membered chelate rings contained in $[Ni(en)_3]^{2+}$ compared to that of $[Ni(et)_3]^{2+}$, which has six-membered rings. The data in this figure is taken from Stability of Metal Complexes and Chelation by Robert Lancashire. This work by Stephen Contakes is licensed under a Creative Commons Attribution 4.0 International License.

Not all metal chelates prefer to form five-membered rings. The steric requirements of chelate rings depend on both the preferred coordination geometry of the metal center and the stereochemistry of the ligand. Both of these effects are typically considered in terms of preferred L-M-L bond angles. From the perspective of the metal center, the preferred bond angle is determined by the coordination geometry. Octahedral and square planar metals prefer 90° L-M-L bond amgles, trigonal bipyramidal systems 90 and 120° L-M-L bond angles, and tetrahedral complexes 109.5° L-M-L angles. The larger preferred bond angles in tetrahedral and trigonal bipyramidal systems often require the formation of larger six or seven-membered chelate rings for maximum stability. The size of the chelate ring actually formed between a metal and ligand is determined by the ligand's structure. As the contributor of all the atoms in the chelate ring but one, the ligand directly determines the chelate ring size. More subtly, ligands naturally prefer to coordinate metals at a particular L-M-L angle, called the **bite angle**, as shown in Figure **8.4.26A**. Ligands with bite angles corresponding to the ideal L-M-L angle for a metal's preferred geometry tend to form more stable complexes, although in turn ligand bite angles can cause metals with a weak coordination geometry preference to adopt the ligand's preferred geometry instead.[10] As may be seen from the values in Figure **8.4.26B**, bite angles roughly increase with the size of the chelate ring formed but are also influenced by the types of structures used to connect the ligand's Lewis base sites. This facilitates the use of diphosphine ligands to tailor the structure and reactivity of phosphine-containing organometallic catalysts.



Figure **8.4.26**. (A) Definition of the bite angle as the angle at which the ligand's preferred L-M-L angle when coordinating a metal center. (B) Bite angles of selected diphosphines.[9] The bite angles of many such diphosphines have been determined to facilitate the design of phosphine-containing organometallic catalysts. This work by Stephen Contakes is licensed under a Creative Commons Attribution 4.0 International License.

λ and δ isomerism involves differences in the conformation of nonplanar five-membered chelate rings

As shown in Figure **8.4.27**, some chelate ring systems are planar while others are not.

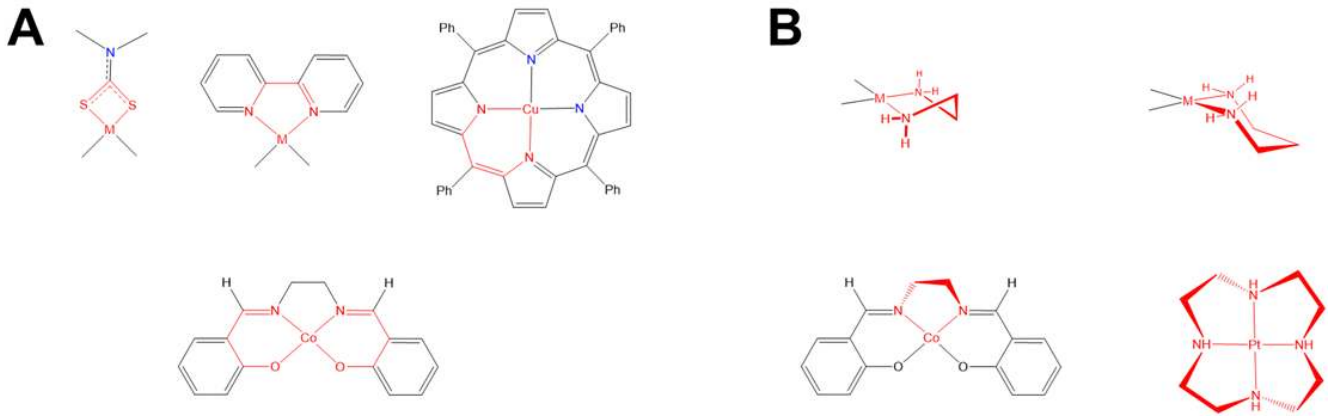


Figure 8.4.27. (A) Planar and (B) Nonplanar chelate rings shown highlighted in red. Notice how [Co(salen)] possesses a nonplanar chelate ring and two planar ones. This work by Stephen Contakes is licensed under a Creative Commons Attribution 4.0 International License.

Among the nonplanar chelate ring systems are ligands like en and dppe, which contain tetrahedral C, N, O, P, and S atoms. Because these atoms create kinks in the chelate ring they introduce additional opportunities for diastereomerism due to differences in the chelate ring conformation, called **ring twist**. Ring twist in nonplanar systems has been most extensively explored for five-membered chelates like those formed by dppe and by en and other chelating amines. Unlike the more rigid four-membered chelate rings, five-membered chelates tend to be conformationally flexible, but not so conformationally flexible that their conformers are rapidly interconverting at room temperature (at least not when the rings are substituted to introduce additional steric strain). This balance between flexibility and rigidity enables some five-membered chelate rings to exist as mixtures of distinguishable conformational isomers at room temperature.

To understand the two most stable conformers that five-membered chelates rings tend to form, it is helpful to think of five-membered chelate rings as involving two components (Figure 8.4.28):

- a planar L-M-L group, where L are the atoms directly attached to the metal, M, and
- the remaining two ring atoms, E, which form a rigid E-E bar across the back of the chelate ring.

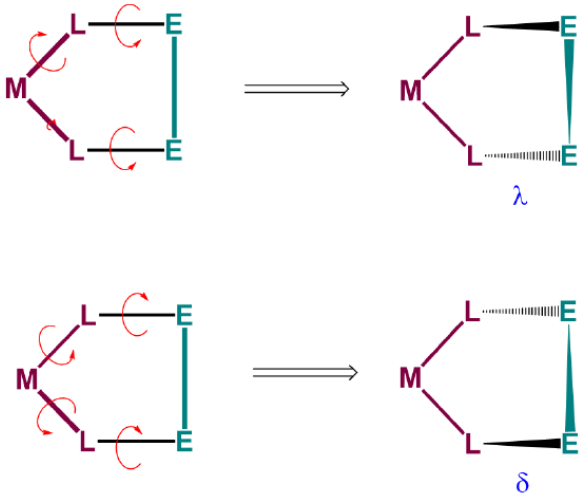


Figure 8.4.28. Five-membered chelate rings consist of a planar L-M-L group connected to a rigid E-E bar. Conformers arise as rotation about the M-L and L-E bonds causes twisting of the E-E bar relative to the L-M-L plane. This work by Stephen Contakes is licensed under a Creative Commons Attribution 4.0 International License.

As can be seen from Figure 8.4.28 , rotation about the M-L and L-E bonds causes twisting of the E-E bar relative to the L-M-L plane. The two most stable conformers produced by these motions are the λ or δ conformations as shown in Figures 8.4.29 and 8.4.29.

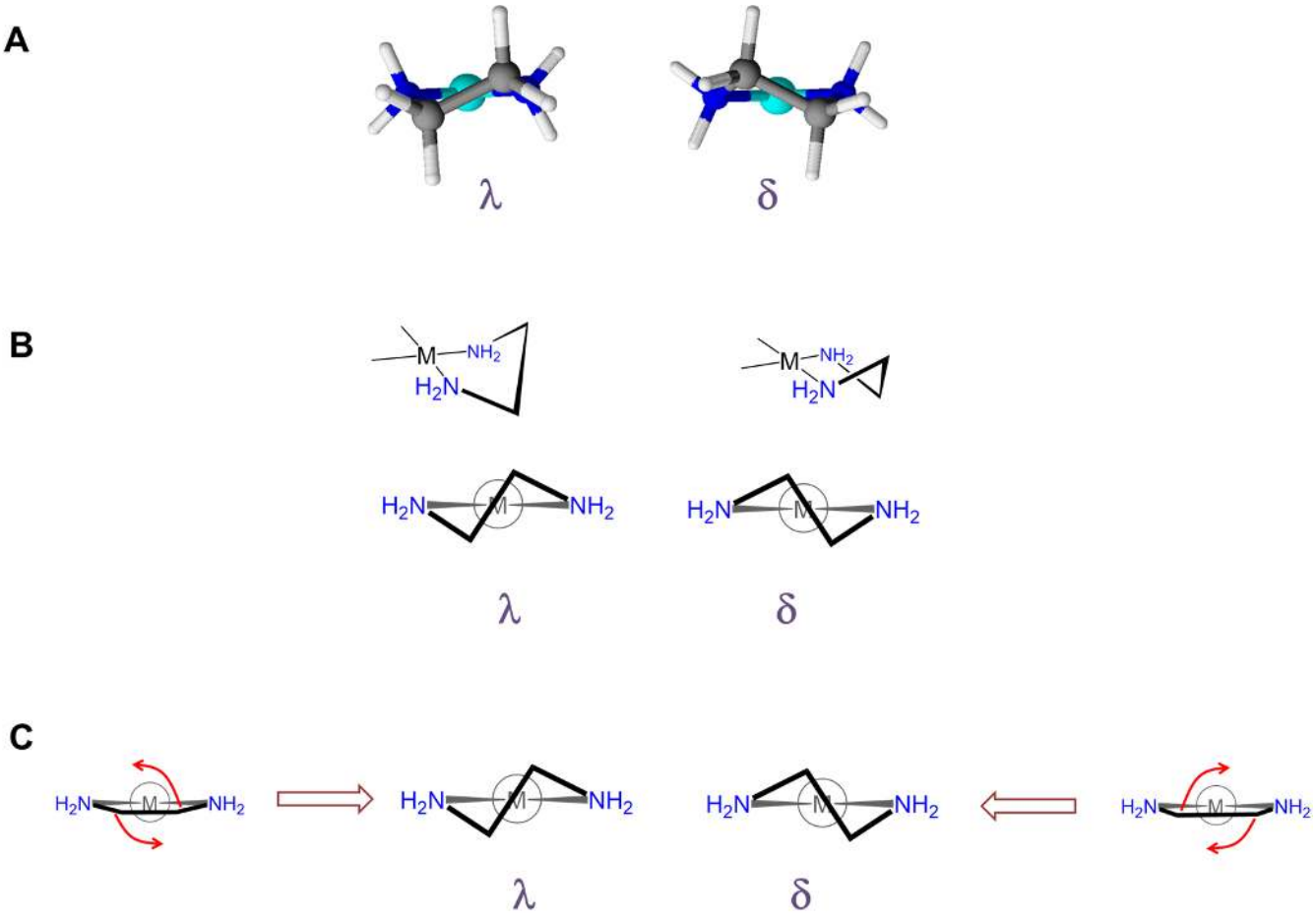


Figure **8.4.29**. (A) **λ** and ***δ*** ring twist in a square planar metal ethylenediamine complex (B) along with several ways to represent it in line drawing form. (C) Of these, the projection looking down an axis bisecting the chelate ring makes it easiest to see that, starting with a planar chelate ring the **λ** conformer corresponds to a counterclockwise twist of the CH_2CH_2 bond relative to the N-M-N plane and the ***δ*** conformer a clockwise twist relative to the N-M-N plane. This work by Stephen Contakes is licensed under a Creative Commons Attribution 4.0 International License.

The relative stability of the **λ** and ***δ*** conformers will depend on the configuration of any stereocenters present and steric factors. As with organic ring systems, steric effects tend to favor conformers in which bulky groups are placed in the less sterically strained equatorial positions while the configuration of the stereocenters present can serve to restrict the allowable ring twist conformations, as illustrated in Figure **8.4.30**. A detailed treatment of such systems is beyond the scope of this page. Interested readers are referred to reference 12 for more details.

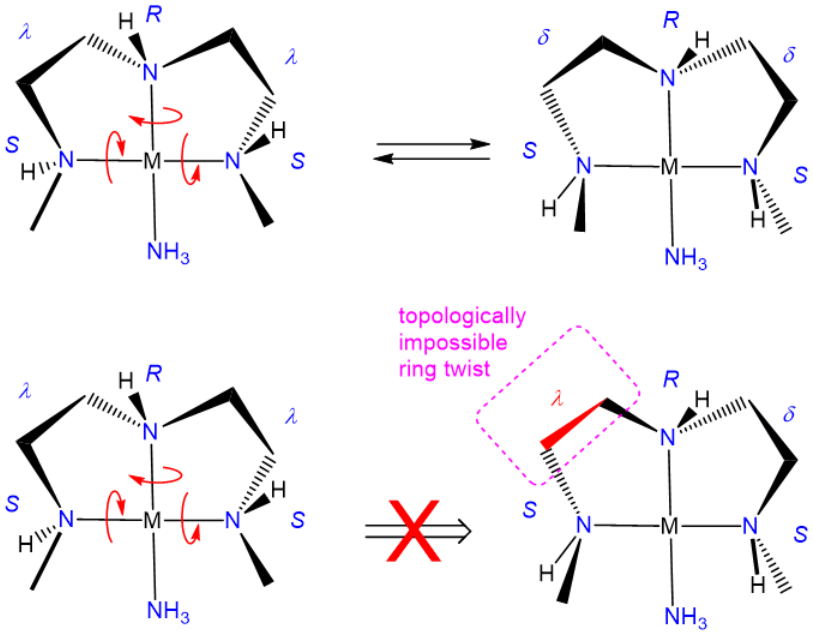


Figure 8.4.30. The configurations at nitrogen in the complex shown restrict the chelate ring conformations to either a λλ or δδ conformation because the rotations needed to enable a λδ configuration are topologically impossible. This work by Stephen Contakes is licensed under a Creative Commons Attribution 4.0 International License.

In closing, it should be noted that it might seem to be making much of small effects in pointing out that one source of diastereomerism in metal complexes involves the freezing out of chelate ring conformations. However, that would be to mistake the impacts that ring conformations can have on the steric accessibility of a coordination site and shaping the course of processes that might occur there. As illustrated in Figure 8.4.31, a simple shift in the conformation of one ring in a square planar, pyramidal, or octahedral complex containing coplanar ethylene diamine ligands can exert a significant effect on the steric profile of the complex perpendicular to the MN_4 square plane. Because of effects like these, ring conformation isomerism plays a role in the design of stereoselective transition metal catalysts.

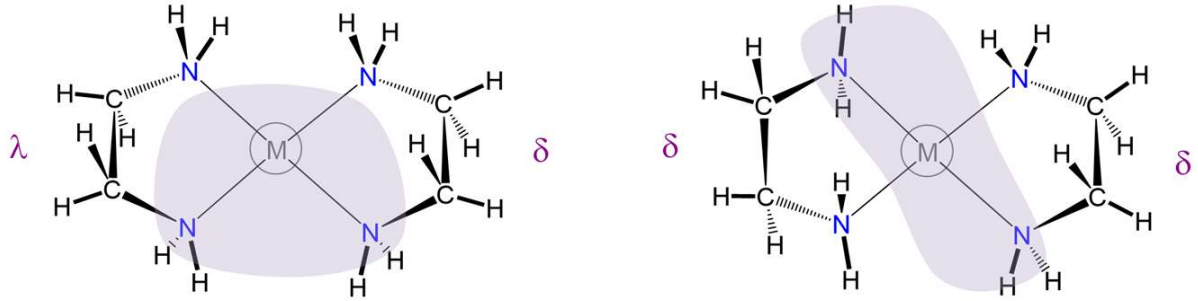


Figure 8.4.31. Schematic illustrating how the conformation of ethlyenediamine ligands bound to a metal center affects the steric accessibility of the metal (shown shaded in violet) to potential ligands attempting to bind from above the MN_4 plane. This work by Stephen Contakes is licensed under a Creative Commons Attribution 4.0 International License.

Exercises

? Exercise 8.4.1. Identify the type of isomerism

What type of isomers are

a. $[CoCl(NH_3)_5](NO_3)$ and $[Co(NH_3)_5(N\text{-}NO_2)]Cl$?
b. $[Co(NH_3)_5\text{-}CN\text{-}Ru(NH_3)_5]^{4+}$ and $[Co(NH_3)_5\text{-}NC\text{-}Ru(NH_3)_5]^{4+}$
c. $[Cr(CN)_5\text{-}CN\text{-}Co(NH_3)_5]$ and $[Co(CN)_5\text{-}CN\text{-}Cr(NH_3)_5]$
d. *cis*-$[Mn(en)_2(CN)_2]$ and *trans*-$[Mn(en)_2(CN)_2]$

Answer a.

Ionization isomers.

Answer b.

Linkage isomers.

Answer c.

Coordination isomers.

Answer d.

Geometric isomers, specifically *cis*/*trans* isomers.

? Exercise 8.4.2. Assigning metal oxidation states in a complex

Many properties of transition metal complexes depend on the metal's oxidation state. For instance,

- octahedral complexes of Co^{II} lose and gain ligands rapidly
- octahedral complexes of Co^{III} lose and gain ligands very slowly
- four-coordinate complexes are generally tetrahedral
- EXCEPT four-coordinate complexes of metals like Pt^{II} , Pd^{II} , Rh^{I}, and Ir^{I}, among others, are square planar

For this reason it is important to be able to estimate the formal oxidation state of a metal in a complex. Fortunately, this is easy to do if you remember

1. The sum of all atoms' oxidation states will equal the overall charge on the complex
2. When determining the metal's oxidation state, the ligands can be treated as having an oxidation state equal to their charge - *i.e.*, the charge they possess in the form in which they coordinate the metal - so if they need to lose a proton to bind, don't forget to account for that.

Given the above, estimate the oxidation state of the metal in the following real and hypothetical complexes.

a. $Na_4[Fe(CN)_6]$
b. $[Cu(phen)_2]BF_4$
c. $[PtF_4(NH_3)_2]$
d. $[Ni(en)_2]SO_4$
e. $Co(acac)_3$
f. [MnCl(O)(salen)]

Answer for $Na_4[Fe(CN)_6]$.

This contains $[Fe(CN)_6]^{4-}$; so $O.S._{Fe}$ + 6 x (-1) (for CN^-) = -4 (the complex's charge) so $O.S._{Fe}$ = +2 or Fe^{2+}.

Answer for $[Cu(phen)_2]BF_4$.

Since tetrafluoroborate is a monoanion, the complex is $[Cu(phen)_2]^+$ so $O.S._{Cu}$ + 0 x 2 (for phen) = +1 (the complex's charge) so $O.S._{Cu}$ = +1 or Cu^+.

Answer for $[PtF_4(NH_3)_2]$.

$O.S._{Pt}$ + 4 x (-1) (for F^-) + 0 x 2 (for NH_3) = +0 (the complex's charge) so $O.S._{Pt}$ = +4 or Pt^{4+}.

Answer $[Ni(en)_2]SO_4$.

The complex is $[Ni(en)_2]^+$ so $O.S._{Ni}$ + 0 x 2 (for en) = +2 (the complex's charge) so $O.S._{Ni}$ = +2 or Ni^{2+}.

Answer $Co(acac)_3$.

$O.S._{Co}$ + 3 x (-1) (for acac; see table 9.2.2) = +0 (the complex's charge) so $O.S._{Co}$ = +3 or Co^{3+}.

Answer [MnCl(O)(salen)].

$O.S._{Mn}$ + 1 x (-1) (for Cl^-) + 1 x (-2)(for oxo) + 1 x (-2) (for salen; see table 9.2.2) = +0 (the complex's charge) so $O.S._{Mn}$ = +5 or Mn^{5+}.

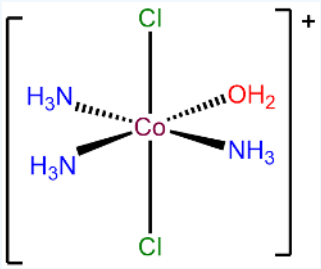
Exercise 8.4.3. Drawing isomers from descriptions

Draw structures that match the descriptions given, assuming that

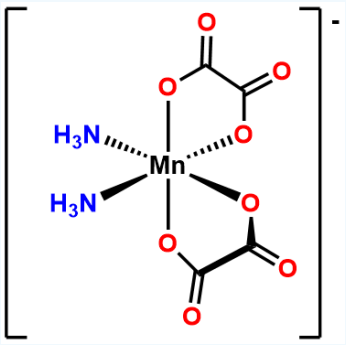
- complexes in which the metal has a coordination number of six are octahedral
- complexes in which the metal has a coordination number of five are trigonal bipyramidal
- complexes in which Pt^{II} , Pd^{II} , or Rh^{I}, or Ir^{I} have a coordination number of four are square planar
- other complexes in which the metal has a coordination number of four will be tetrahedral

a. *mer*-triammineaqua-*trans*-dichlorocobalt(III) ion
b. **Δ**-diaminebis(oxalato)manganate(III)
c. $[CoCl_4]^{2-}$
d. *trans*-diamminebis(ethylenediamine)Nickel(2+) tetracyanopalladate(2-)
e. **Λ**-bis(ethylenediamine)cobalt(III)- μ-amido μ-hydroxo-**Δ**-bis(ethylenediamine)cobalt(III)

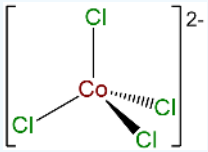
Answer a. *mer*-triammineaqua-*trans*-dichlorocobalt(III) ion.



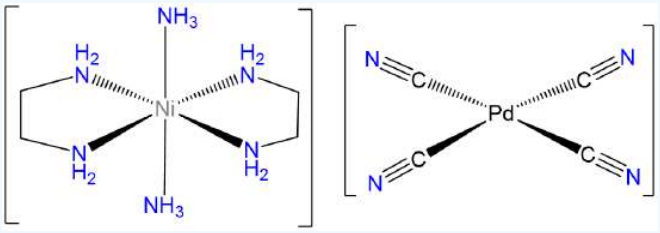
Answer b. Δ-diaminebis(oxalato)manganate(III).



Answer c. $[CoCl_4]^{2-}$.



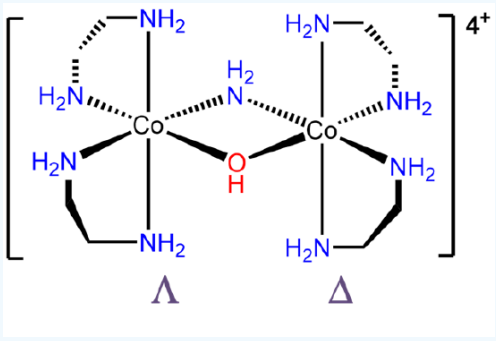
Answer d. *trans*-diamminebis(ethylenediamine)Nickel(2+) tetracyanopalladate(2-).



Note that since the Pd in $[Pd(CN)_4]^{2-}$ is Pd^{2+} it will be square planar.

https://chem.libretexts.org/@go/page/326235

Answer e. Λ-bis(ethylenediamine)cobalt(III)- μ-amido μ-hydroxo-Δ-bis(ethylenediamine)cobalt(III).



Exercise 8.4.4. Stereoisomers of complexes containing only monodentate ligands.

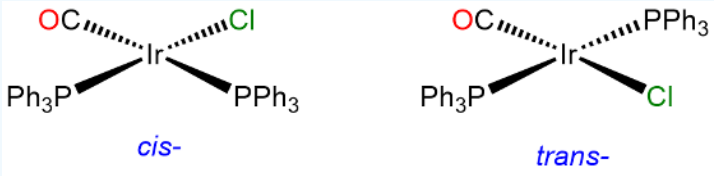
Draw all the stereoisomers of the following real and hypothetical complexes. You may assume that

- complexes in which the metal has a coordination number of six are octahedral
- complexes in which the metal has a coordination number of five are trigonal bipyramidal
- complexes in which Pt^{II} , Pd^{II} , or Rh^{I}, or Ir^{I} have a coordination number of four are square planar
- other complexes in which the metal has a coordination number of four will be tetrahedral

a. $[IrCl(CO)(PPh_3)_2]$
b. $[CoCl_3(NH_3)_3]$
c. $[CoCl_2(H_2O)_2(NH_3)_2]^+$
d. $[CoBrCl(H_2O)_2(NH_3)_2]^+$
e. $[CoBrClI(NH_3)_3]$

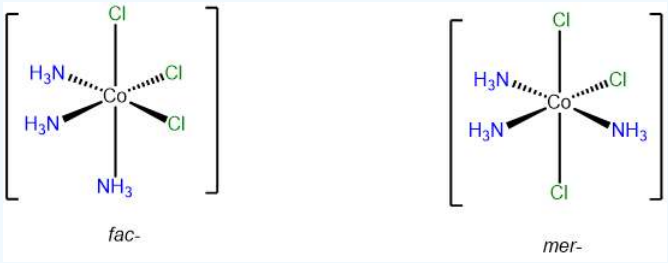
Answer a. $[IrCl(CO)(PPh_3)_2]$

This is a 4-coordinate Ir^{I} complex and, as such will be square planar. Since two of the ligands are identical, it will have *cis* and *trans* isomers. The *trans* isomer is famous for its ability to form adducts and is called Vaska's complex.



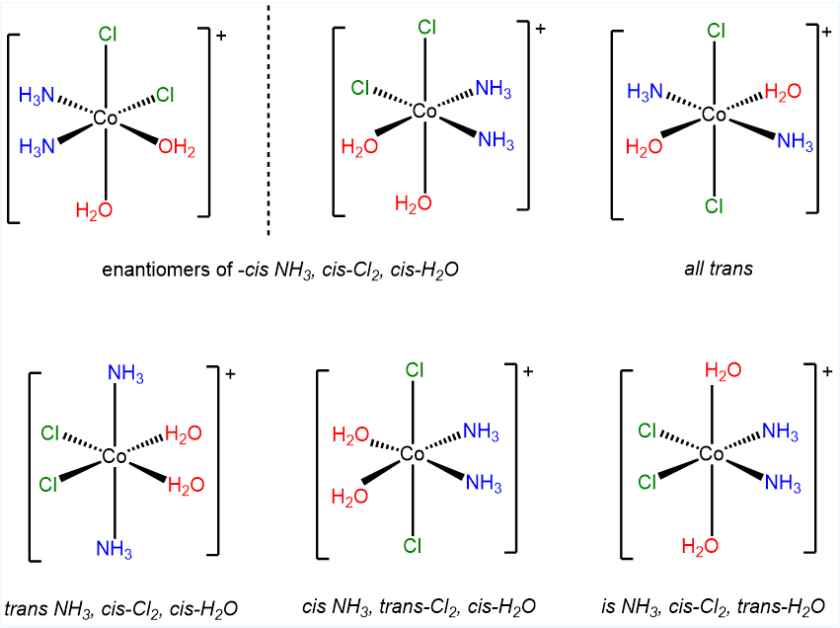
Answer b. $[CoCl_3(NH_3)_3]$

This complex contains three ammine and three chloro ligands and so will have *fac* and *mer* isomers.



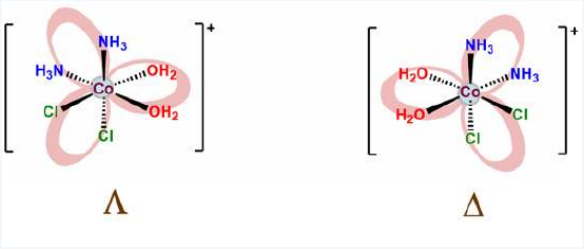
Answer c. $[CoCl_2(H_2O)_2(NH_3)_2]^+$

This is a case of an $MA_2B_2C_2$ system (A = Cl^-, B = H_2O, C = NH_3) involving multiple *cis* and *trans* relationships. The six stereoisomers are shown below.



Since it may not be obvious how to arrive at a set of isomers like the ones above, it is worth considering how one might work through the possibilities for a system of ligands like this one. Several systems may be used to systematically identify isomers. Once approach is the Macbdef system described in Note **8.4.1** at the end of these exercises. The solutions presented here and in subsequent problems employ a variant of that approach.

- Start by fixing one set of ligands. In this case the chloro ligands were first fixed as *cis* to one another. Then the remaining ligands might be *cis* or *trans* to one another, although since the *chloro* ligands are already *cis*, the ammine and aqua ligands cannot both be *trans* at the same time. Thus for *cis* chloro ligands the possibilities for the others are:
  - *cis*-H_2O ,*cis*-NH_3,
  - *cis*--H_2O, *trans*-NH_3
  - *trans*-H_2O, *cis*-NH_3
- Swap the configuration of the ligand set you started with. In this case it means placing the chloro ligands *trans* to one another. From that configuration, the possibilities for the ammine and aqua ligands are
  - *cis*-H_2O ,*cis*-NH_3,
  - *trans*-H_2O, *trans*-NH_3
- Check for enantiomers and create mirror images of any chiral complexes you drew. The easiest way to do this is to assign point groups. However, it turns out that the octahedral all-*cis* case is D_3 and formally equivalent to the symmetry of a tris chelate, as shown below.

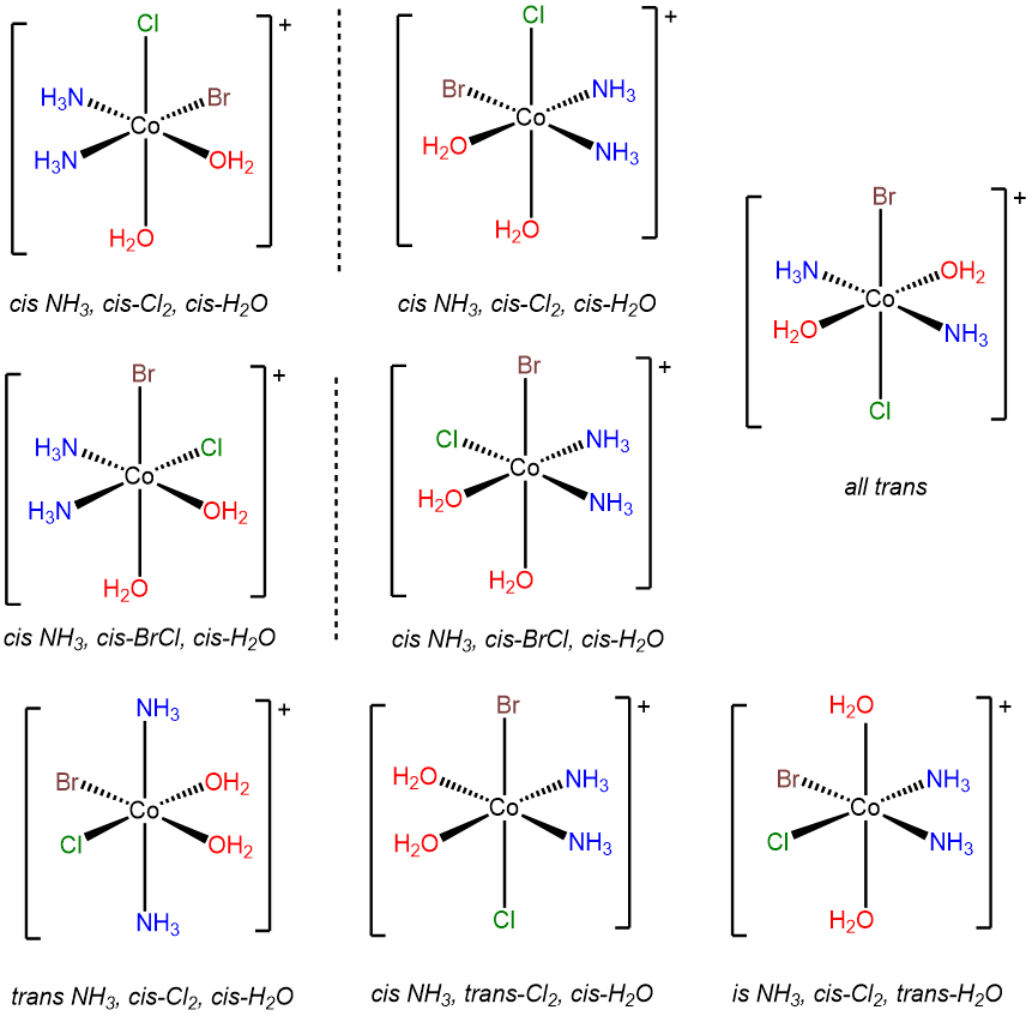


- finally, check to make sure you didn't include the same complex twice. Humans do make mistakes after all.

Answer d. $[CoBrCl(H_2O)_2(NH_3)_2]^+$

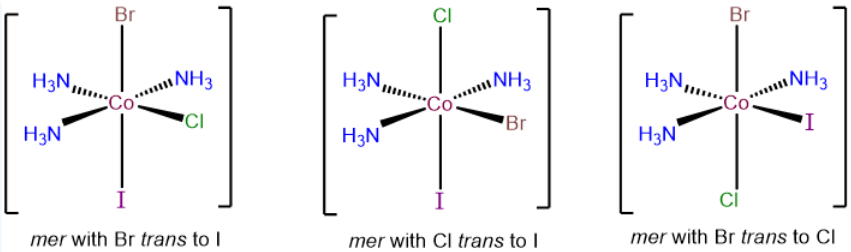
This problem is analogous to the one above except that this complex contains a bromo and chloro ligand in place of the two chloro ligands in $[CoCl_2(H_2O)_2(NH_3)_2]^+$. Consequently, when the bromo and chloro ligands are *cis* to one

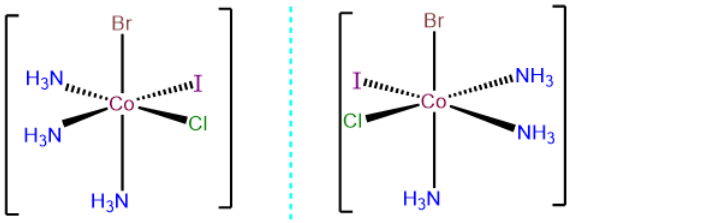
another, additional possibilities for isomers arise based on whether ammine or aqua ligands are *trans* to the chloro and bromo. The result is eight isomers.



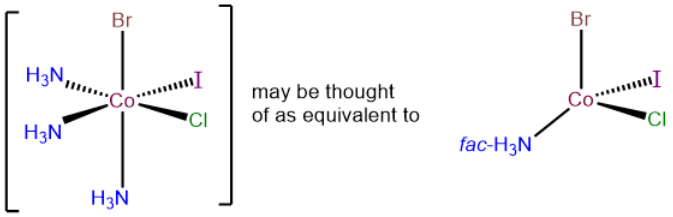
Answer e. [$CoBrClI(NH_3)_3$]

There are two possibilities for this complex - a *fac*-$(NH_3)_3$ and a *mer*-$(NH_3)_3$ arrangement. These may be taken as starting points for examining the possible permutations for the Cl^-, Br^-, and I^- ligands. The top row presents the three possibilities within the *mer*-$(NH_3)_3$ arrangement; each corresponds to a different ligand *trans* to an ammine ligand. The bottom row presents the two possible isomers with a *fac*-$(NH_3)_3$ arrangement. In each, the Cl^-, Br^-, and I^- ligands are *trans* to ammine ligands. However, the complexes possess C_1 symmetry and so are chiral and exist as enantiomers.





(C_1 symmetry or it you think of the *fac*-$(H_3N)_3$ as being "one uniform group" then the symmetry is equivalent to that of a chiral carbon)



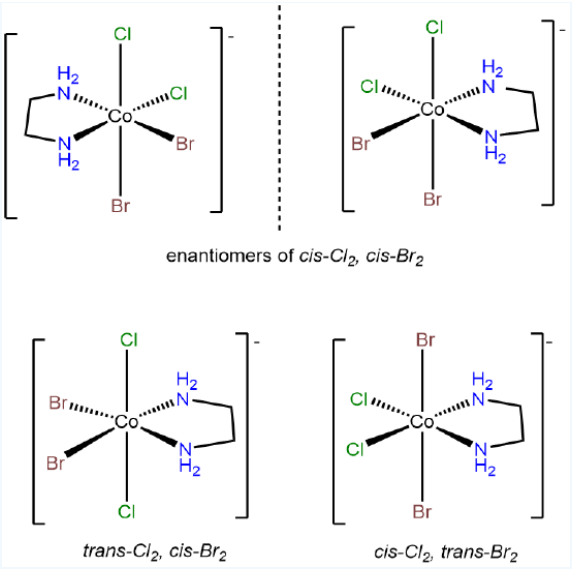
Exercise 8.4.5. Stereoisomers of complexes with bidentate ligands (ignoring ring twist).

Ignoring ring twist, draw all the stereoisomers of the following real and hypothetical octahedral complexes.

a. $[CoBr_2Cl_2(en)]^-$
b. $[CoBrCl(en)_2]^+$
c. $[CoBrCl(gly)_2]^-$
d. $[Co(en)_3]^{3+}$
e. $[Co(gly)_3]$

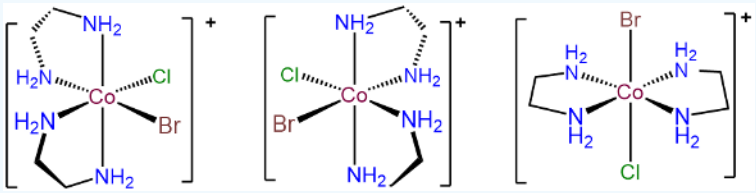
Answer a. $[CoBr_2Cl_2(en)]^-$

This complex is analogous to $[CoCl_2(H_2O)_2(NH_3)_2]^+$ in possessing pairs of identical ligating groups. The main difference is that in $[CoBr_2Cl_2(en)]^-$ the two amine ligating group of the en ligand are restricted to a *cis* arrangement. Under the MABCDEF system explained in Note **8.4.1**, $[CoCl_2(H_2O)_2(NH_3)_2]^+$ may be $MA_2B_2C_2$, but this complex, $[CoBr_2Cl_2(en)]^-$, is $M(AA)B_2C_2$. The isomers are:



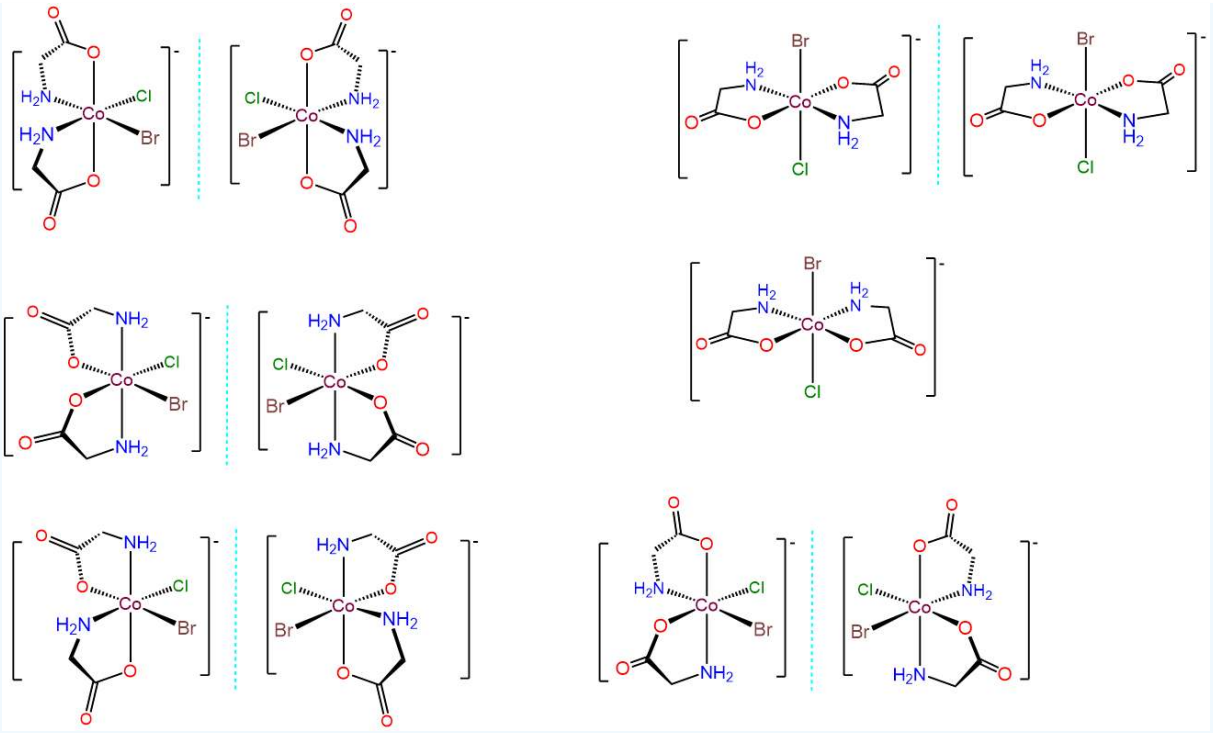
Answer b. $[CoBrCl(en)_2]^+$

The key to problems like this is to focus on the unique ligands, in this case Br^- and Cl^-. These can exist in either a *cis* or *trans* arrangement. The *trans* form is achiral, but in the case where Br^- and Cl^- are *cis*, **Λ** and **Δ** enantiomers are possible. The result is three isomers.



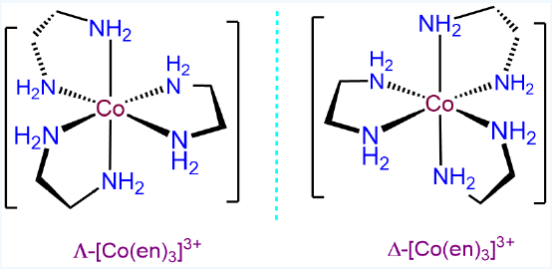
Answer c. $[CoBrCl(gly)_2]^-$

This case is analogous to the one above, but this time the bidentate ligand, gly, possesses distinguishable binding sites. Thus there are additional permutations involving how the gly ligands are bound relative to one another and/or whether the O or N end of the gly is bound *trans* to Br or Cl. The result is 11 different isomers, which are given below.



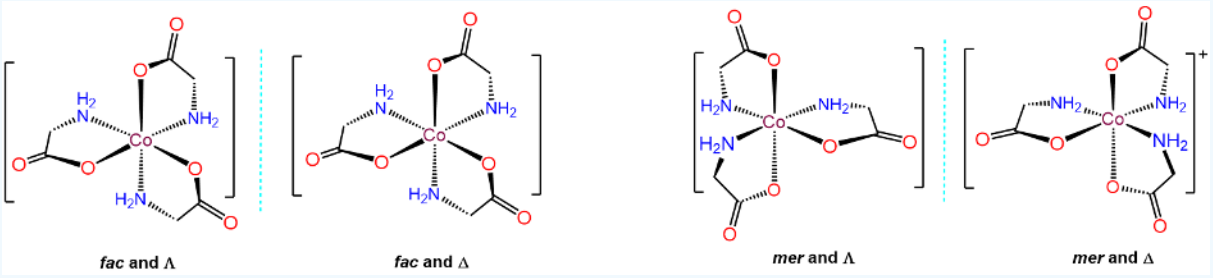
Answer d. $[Co(en)_3]^{3+}$

As a tris-chelate of symmetric bidentate ligands, ignoring ring twist, $[Co(en)_3]^{3+}$ will only exhibit **Λ** and **Δ** isomerism.



Answer e. $[Co(gly)_3]$

Since there are three gly ligands, each of which have carboxy and amine ends, the allowable arrangements involve whether the resulting three carboxy and three amine ends are oriented in a *mer* or *fac* arrangement. This gives two possibilities, each of which can exist as either the **Λ** or **Δ** enantiomer, for a total of four isomers, which are given below.



https://chem.libretexts.org/@go/page/326235

Exercise 8.4.6. More stereoisomers: Now featuring linkage isomerism

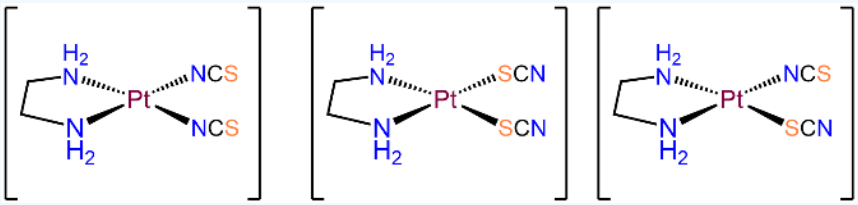
Ignoring ring twist, draw all chemically reasonable stereoisomers for the following real and hypothetical complexes. You may assume that

- complexes in which the metal has a coordination number of six are octahedral
- complexes in which the metal has a coordination number of five are trigonal bipyramidal
- complexes in which Pt^{II} , Pd^{II} , or Rh^{I}, or Ir^{I} have a coordination number of four are square planar
- other complexes in which the metal has a coordination number of four will be tetrahedral

a. $[Pt(en)(SCN)_2]$
b. $[Pt(NH_3)_2(SCN)_2]$
c. $[Co(en)_2(SCN)_2]^+$

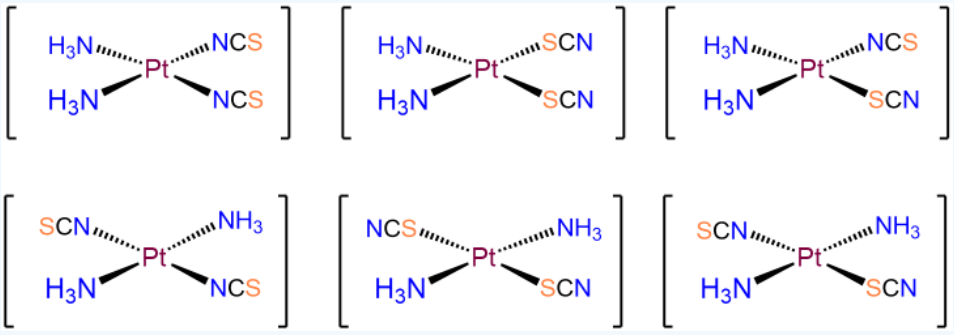
Answer a. $[Pt(en)(SCN)_2]$

The Pt in this neutral complex must be Pt^{2+} to balance the negative charges of the two SCN^- ligands. Complexes of Pt^{2+} are square planar and four coordinate, consistent with the bidentate en and two thiocyanato ligands. Of the ligands, the en ligand must bind in a *cis* arrangement. Consequently, the two SCN^- ligands will be in a *cis* arrangement as well. The isomers will therefore only differ in whether the two SCN^- bind κN or κS. The possibilities are:



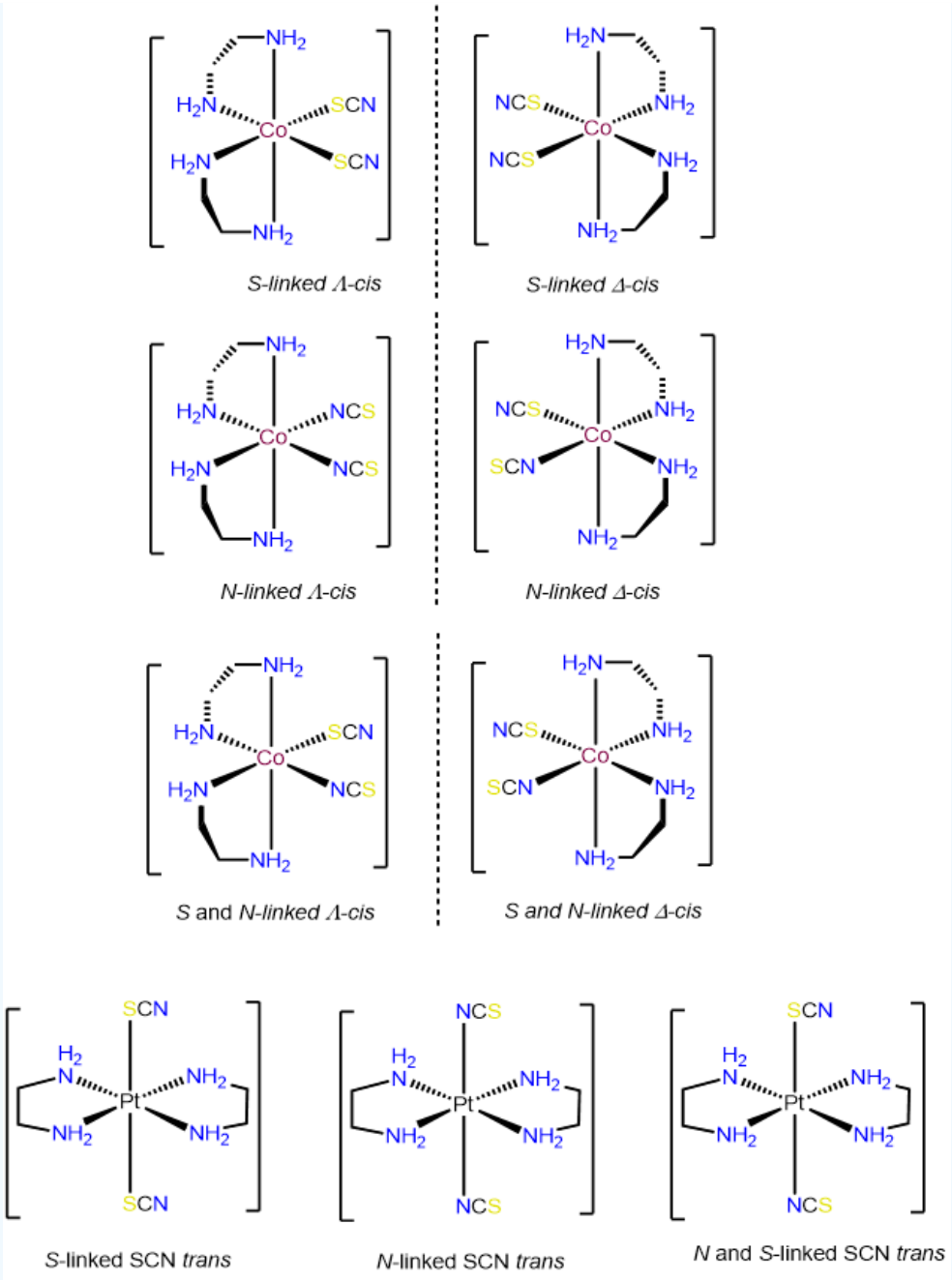
Answer b. $[Pt(NH_3)_2(SCN)_2]$

As with the preceding example, this will be a square planar Pt^{2+} complex. The main difference is that this time the coordinated nitrogens are not constrained to adopt a *cis* arrangement so there will be both *cis* and *trans* isomers.



Answer c. $[Co(en)_2(SCN)_2]^+$

https://chem.libretexts.org/@go/page/326235



? Exercise 8.4.7. Stereoisomer free for all.

Ignoring ring twist, draw all chemically reasonable stereoisomers for the following real and hypothetical complexes. You may assume that

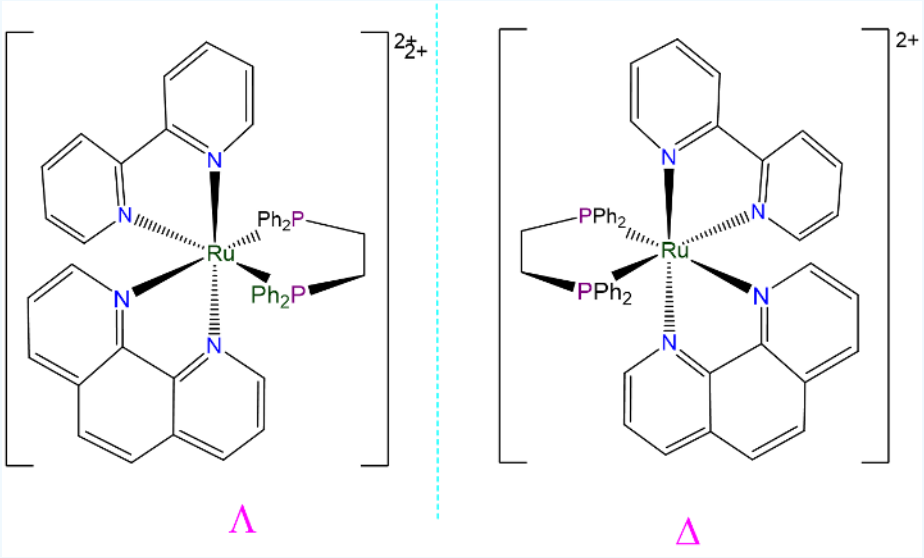
- complexes in which the metal has a coordination number of six are octahedral
- complexes in which the metal has a coordination number of five are trigonal bipyramidal
- complexes in which Pt^{II} , Pd^{II} , or Rh^{I}, or Ir^{I} have a coordination number of four are square planar
- other complexes in which the metal has a coordination number of four will be tetrahedral

a. $[Ru(bpy)(phen)(dppe)]^{2+}$
b. $[CoClF(PPh_3)(py)]^{-}$
c. $[Ni(en)_2(NO_2)_2]$

d. $[Fe(H_2O)_3(SCN)_3]$
e. $[PtClF(PPh_3)(py)]$
f. $[CoBr_2Cl(NH_3)_3]$

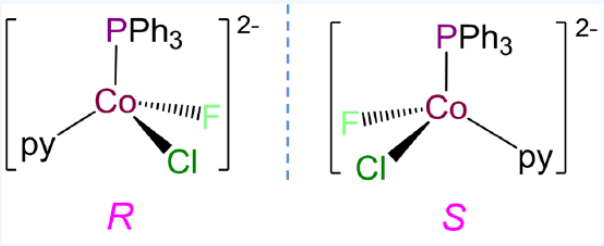
Answer a. $[Ru(bpy)(phen)(dppe)]^{2+}$

This complex is an octahedral tris-chelate containing symmetric ligands. As such it will exhibit **Λ** and **Δ** isomers:



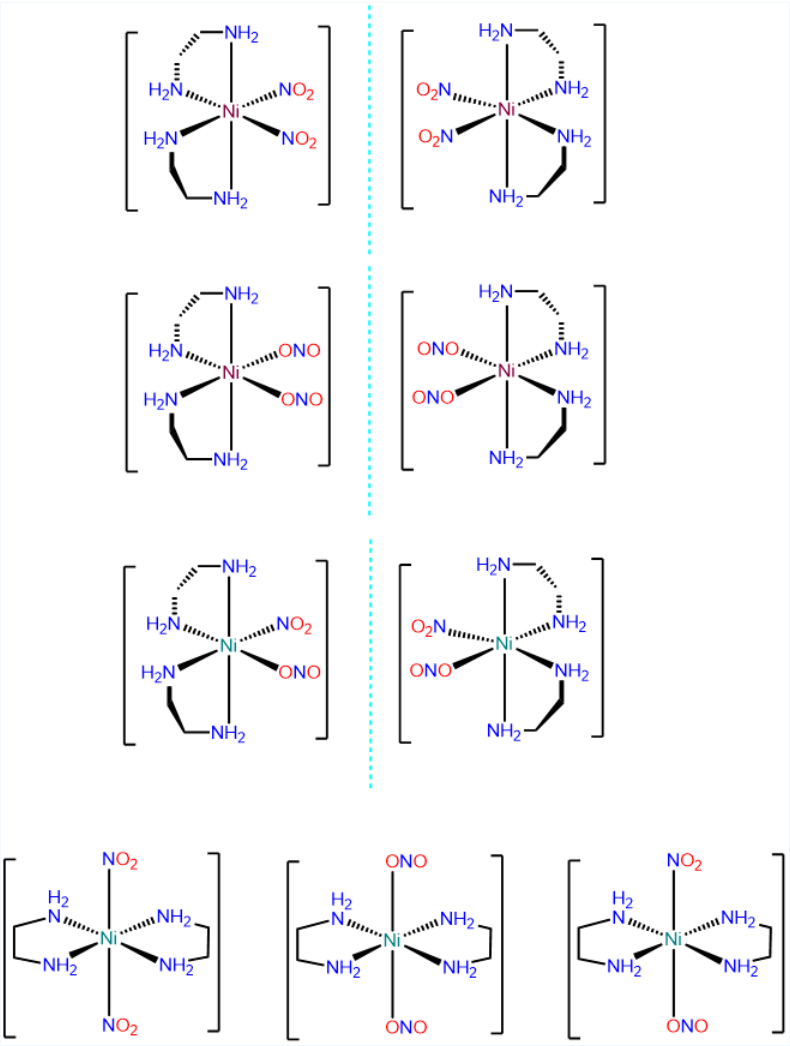
Answer b. $[CoClF(PPh_3)(py)]^-$

This complex has a coordination number of 4 and contains a Co^{2+} ion with a d^7 electron configuration, so a tetrahedral geometry is expected. Tetrahedral complexes like this one with four different ligands are chiral and can form *R* and *S* enantiomers.



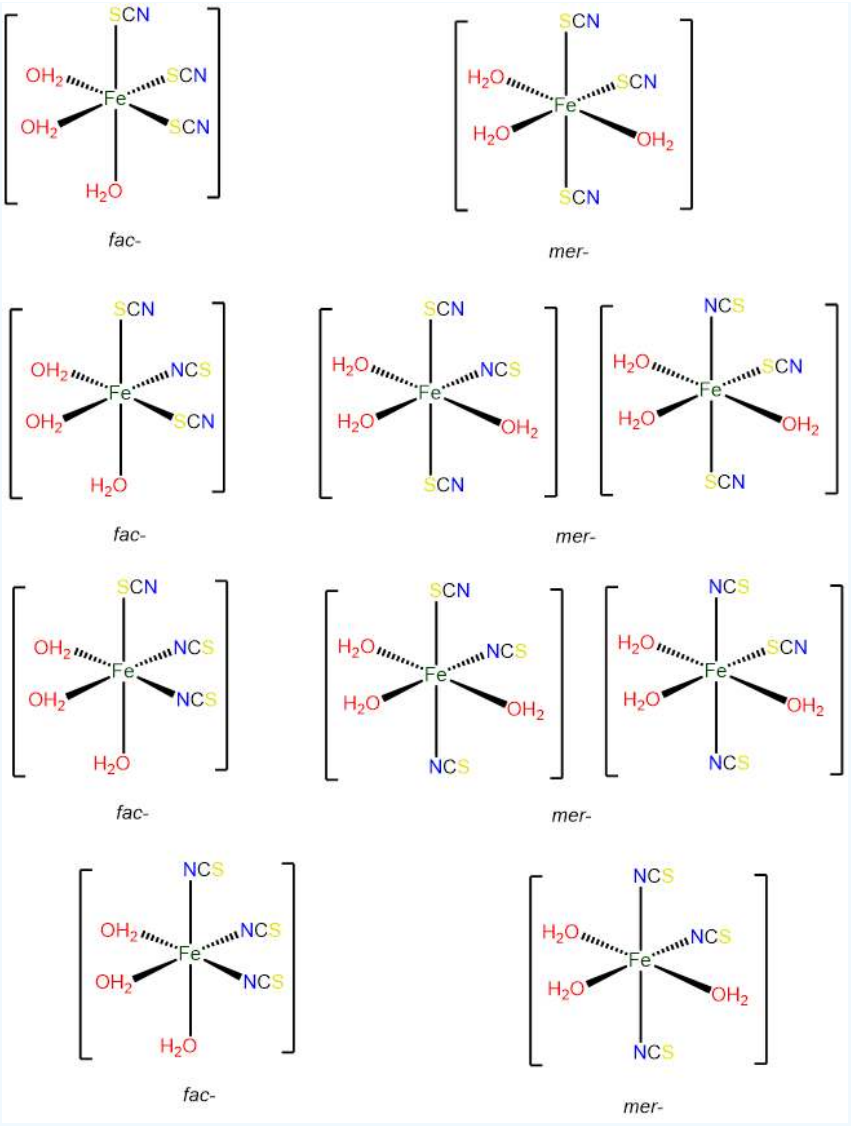
Answer c. $[Ni(en)_2(NO_2)_2]$

This is an octahedral bis-chelate and will exist in **Λ** and **Δ** configurations. Within each configuration the NO_2^- ligands can exist as *κN* and *κO*, leading to the following possibilities:



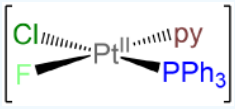
Answer d. $[Fe(H_2O)_3(SCN)_3]$

As an octahedral complex with three identical ligands it can exist in *mer* and *fac* configurations, with the ambidentate SCN ligand providing additional possibilities for isomerism.



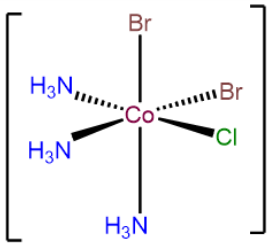
Answer e. [PtClF(PPh$_3$)(py)]

As a square planar complex with four nonidentical ligands, this complex exists as a single isomer.

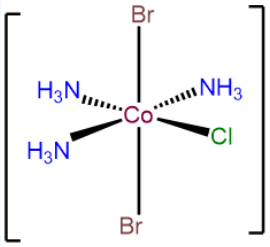


Answer f. [CoBr$_2$Cl(NH$_3$)$_3$]

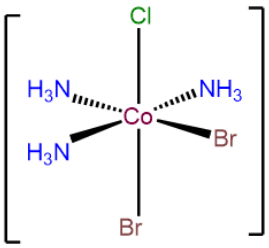
As an octahedral complex with three identical ligands it will exhibit *mer* and *fac* isomerism. In addition, it will have two *mer* configurations that differ in terms of the cis and trans relationships between the bromo and chloro ligands.



fac



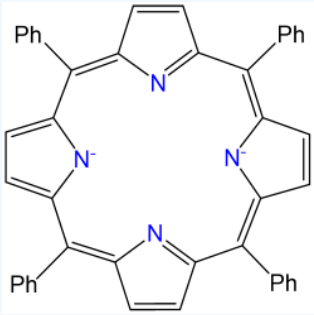
mer with Br *trans* to Br



mer with Cl *trans* to Br

Exercise 8.4.8

Complexes of formula $Ru(TPP)py_2$ have been prepared, in which TPP is tetraphenylporphyrin, which binds metals in the form given below. Draw all isomers of $Ru(TPP)py_2$.

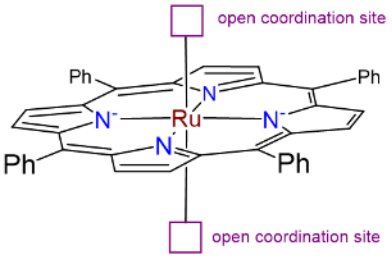


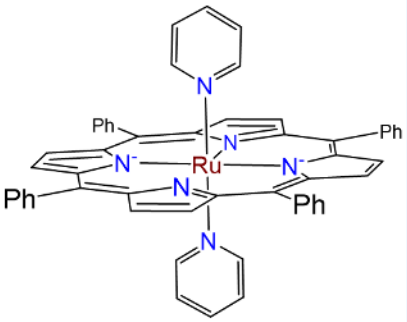
Answer

There is only one isomer. While normally complexes containing two identical ligands (in this case py) can exhibit *cis* and *trans* isomerism, in this case the planar tetraphenylporphyrin ring ligates the Ru^{2+} ion in a square planar arrangement, as shown at left in the image below. This leaves only a pair of *trans* coordination sites for the chloro ligands to occupy, giving the isomer shown at right below.

https://chem.libretexts.org/@go/page/326235

When TPP ligates Ru^{2+} it leaves only *trans* open coordination sites so only the *trans* isomer can form.

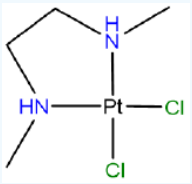




trans-[Ru(py)$_2$(TPP)]

Exercise 8.4.9

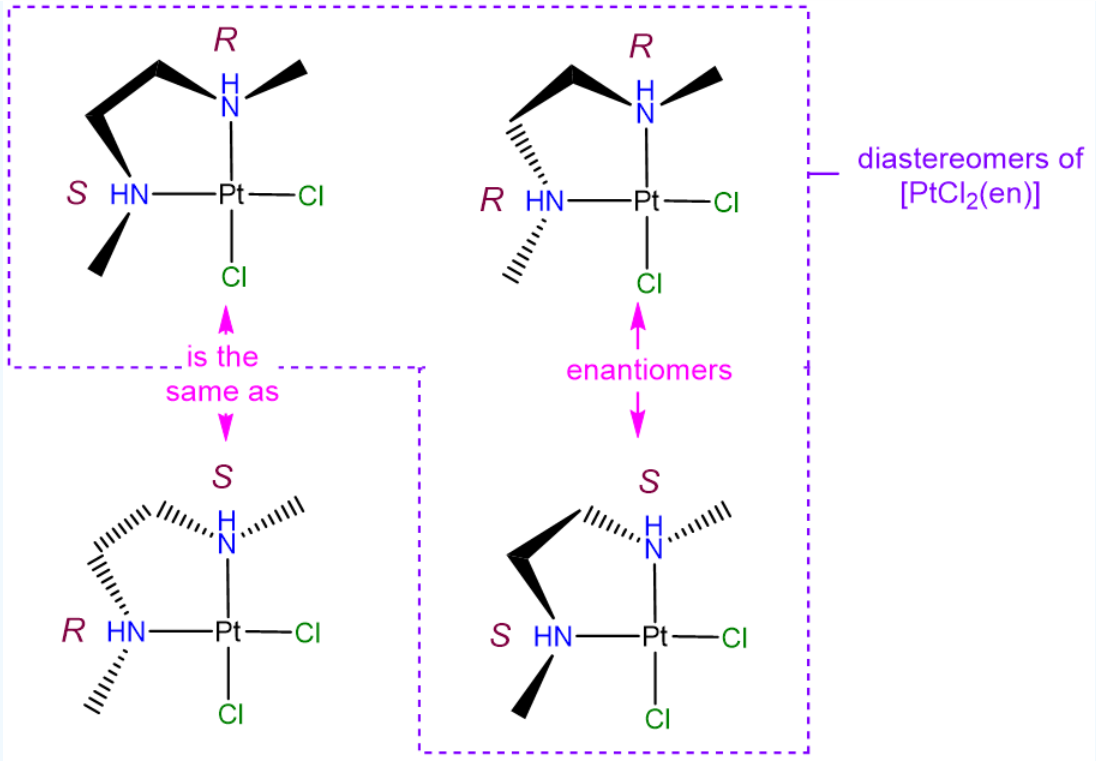
Draw the diastereomers formed due to the chirality of the amine nitrogen atoms in [$PtCl_2$(*N*,*N*'-dimethylethane-1,2-diamine)] which has the atomic connectivity represented below



Answer

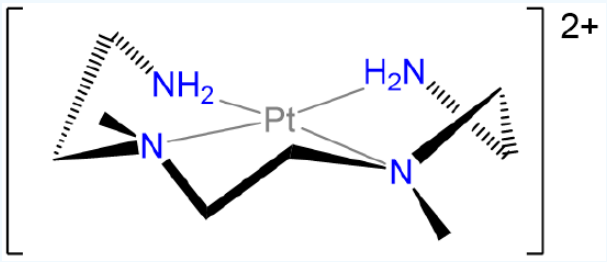
The diastereomers will differ in whether the N atoms adopt an *R* or *S* configuration at the nitrogen atoms. The possible permutations are (*R*,*R*), (S,*S*), (*R*,*S*), and (S,*R*). However, as may be seen from the image below, the (*R*,*S*) and (S,*R*) configurations are identical (the two projections shown can be interconverted through a C_2 rotation along an axis bisecting the Cl-Pt-Cl unit). As a result there are only three unique isomers. Of these, the (*R*,*R*) and (S,*S*) configurations are enantiomers (they are mirror images by reflection in the $PtCl_2N_2$ plane). Note that in solving problems like this one it can be helpful to keep track of possible isomers by assigning the stereochemistry at each chiral center as *R* or *S* using the Cahn-Ingold-Prelog-convention, though it is not strictly necessary to do so.

https://chem.libretexts.org/@go/page/326235

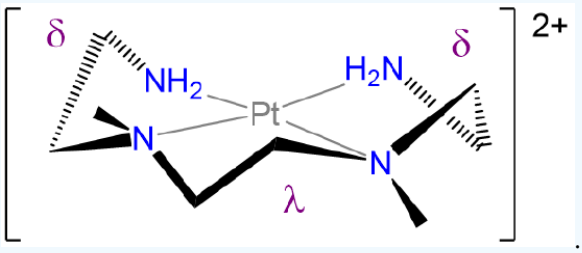


? Exercise 8.4.10

Label the conformations of all chelate rings in the structure below.



Answer



Appendix: The MABCDEF bookkeeping system for identifying isomers

The Mabcdef or MABCDEF system is one method for identifying the number of isomers in an octahedral complex, although since it is really just a bookkeeping and organizational system it can easily be extended to other geometries as well. The M in Mabcdef stands for metal and the other letters are used to stand in for ligands. The basic approach involves

- classifying the ligands as A, B, C, D, E, or F in order of multiplicity. Thus for

$[Cr(NH_3)_6]^{3+}$ A = NH_3; there are no B, C, D,E, or F ligands; and the complex is classified as MA_6

$[CoCl(NH_3)_5]^{2+}$ A = NH_3, B = Cl^-, and the complex is MA_5B

$[CrCl_2(H_2O)_2(NH_3)_2]^+$ A = Cl^-, B = H_2O, C = NH_3, and the complex is $MA_2B_2C_2$

- in the classification above, multidentate ligands are typically classified before monodentate ones and are designated AA, AB, ABC, ABA, etc. based on the symmetry of the attachment points. Thus

  en has identical attachment amine points and is AA

  gly has a carboxy and amine attachment points and is AB

  trien is ABA

  $CoCl_2(en)_2^+$ is $M(AA)_2B_2$

  $CoCl_2(gly)_2^-$ is $M(AB)_2C_2$

  $CoCl_2(en)(gly)$ is $M(AA)(AB)C_2$

- Systematically list out the possible *trans* arrangements of ligands by
  1. assigning one pair of ligands to be *trans* to one another.
  2. Then systematically list out the other possible *trans* pairs by permuting the remaining trans arrangements. It can help to organize the permutations in a table, such as that shown below for an MABCDEF complex where A and B are assigned *trans*. In looking at the table notice how the second set of trans permutations is systematically varied. This helps ensure that no possibility is skipped.
  3. Go through the list of isomers and remove any duplicates you generated so far. For instance, notice in the table below that the last three stereoisomers are identical with the first three (*e.g.*, stereoisomer 4 is identical to stereoisomer 3, 5 with 2, and 6 with 1).

Stereoisomer 1	Stereoisomer 2	Stereoisomer 3	Stereoisomer 4 (same as isomer 3)	Stereoisomer 5 (same as isomer 2)	Stereoisomer 6 (same as isomer 1)
trans AB (fixed)	*trans* AB (fixed)	*trans* AB (fixed)	*trans* AB (fixed)	*trans* AB (fixed)	*trans* AB (fixed)
trans CD	*trans* CE	*trans* CF	*trans* DE	*trans* DF	*trans* EF
trans EF	*trans* DF	*trans* DE	*trans* CF	*trans* CE	*trans* CD

  4. If the complex possesses multidentate ligands that demand that certain groups exist and *cis* pairs, then also remove any configurations which do not agree with the known binding capability of the ligand (*e.g.*, the two amine groups of ethylenediamine cannot be *trans* to one another, so if you have an en ligand, remove configurations like that from the list).

5. Next, swap or permute the original *trans* pair and repeat the process you just followed. In the case of Mabcdef this gives the following results:

Isomer	"fixed" trans pair	Additional trans pairs	
1	AB	CD	EF
2	AB	CE	DF
3	AB	CF	DE
4	AC	BD	EF
5	AC	BE	BF
6	AC	BF	DE
7	AD	BC	EF
8	AD	BE	CF
9	AD	BF	CE
10	AE	BC	DF
11	AE	BD	CF
12	AE	BF	CD
13	AF	BC	DE
14	AF	BD	CE
15	AF	BE	CD

- Since the procedure explained above only identifies isomers based on unique *trans* pairings, **it does not identify when a configuration is chiral and corresponds to a pair of enantiomers.** Any enantiomers can be identified by drawing out the complexes and either classifying their point groups or by drawing their mirror images and checking if they are superimposable. In the MABCDEF case - *i.e.*, where all the ligands are different - all of the isomers identified have C_1 symmetry so are chiral. This means there will be a pair of enantiomers for each, giving 15 x 2 = 30 different stereoisomers.

References

1. These examples are taken from http://wwwchem.uwimona.edu.jm/courses/inorgnom.html

2. Contakes S. M.; Rauchfuss, T.B. *Chem. Commun.* 2001, 553-554.

3. Shriver, D. F.; Shriver, S. A.; Anderson, S. E., *Inorg. Chem.* 1965, *4(5)*, 725-730.

4. Zelewsky, A. v., *Stereochemistry of Coordination Compounds* Wiley, 1996.

5. In the past it was difficult to determine absolute configurations from X-ray data alone, but recent advances have made it easier to do so.

6. Pavan M. V. Raja & Andrew R. Barron "Circular Dichroism Spectroscopy and its Application for Determination of Secondary Structure of Optically Active Species" in *Physical Methods in Chemistry and Nano Science* https://chem.libretexts.org/Bookshelves/Analytical_Chemistry/Book%3A_Physical_Methods_in_Chemistry_and_Nano_Science_(Barron)/07%3A_Molecular_and_Solid_State_Structure/7.07%3A_Circular_Dichroism_Spectroscopy_and_its_Application_for_Determination_of_Secondary_Structure_of_Optically_Active_Species

7. Berova, N.; Bari, L. D.; Pescitelli, G., *Chemical Society Reviews* 2007, 36 (6), 914-931.

8. Of course, if one set of ligands occupies a meridional plane, then the other three ligands will be oriented in an equatorial one. The reason they may both be considered meridional is because if the complex were rotated, the equatorial plane would be meridional and vice versa. From that point of view both might be considered meridional planes - albeit not at the same time.

9. Bite angles are taken from Mansell, S. M., Catalytic applications of small bite-angle diphosphorus ligands with single-atom linkers. Dalton Transactions 2017, 46 (44), 15157-15174.

10. Hancock, R. D., The pyridyl group in ligand design for selective metal ion complexation and sensing. Chemical Society Reviews 2013, 42 (4), 1500-1524.

11. Sasi, D.; Ramkumar, V.; Murthy, N. N., Bite-Angle-Regulated Coordination Geometries: Tetrahedral and Trigonal Bipyramidal in Ni(II) with Biphenyl-Appended (2-Pyridyl)alkylamine N,N'-Bidentate Ligands. ACS Omega 2017, 2 (6), 2474-2481.

12. Ehnbom, A.; Ghosh, S. K.; Lewis, K. G.; Gladysz, J. A., Octahedral Werner complexes with substituted ethylenediamine ligands: a stereochemical primer for a historic series of compounds now emerging as a modern family of catalysts. Chemical Society Reviews 2016, 45 (24), 6799-6811.

8.4: Isomerism is shared under a CC BY-NC-SA 4.0 license and was authored, remixed, and/or curated by LibreTexts.

- **9.4: Isomerism** by Stephen M. Contakes is licensed CC BY 4.0.

CHAPTER OVERVIEW

9: Coordination Chemistry- Bonding

With the exception of molecular orbital theory, the bonding models discussed previously for main group complexes are not easily applied to transition metal complexes. This chapter describes bonding models that are used to explain the bonding and electronic structures of coordination complexes. As with many theories, the crystal field and ligand field theories discussed in this chapter were developed because existing bonding theories couldn't explain the observed properties of some transition metal complexes.

As an example let us consider the following two transition metal complexes, $[Fe(NH_3)_6]^{2+}$ and $[Co(NH_3)_6]^{3+}$. The Fe^{2+} and the Co^{3+} centers both have a valence electron configuration of $3d^6$ and have the same ligands coordinated. Lewis, VSEPR, and valence bond theories predict that two isoelectronic molecules should have very similar properties, but in the case of $[Fe(NH_3)_6]^{2+}$ and $[Co(NH_3)_6]^{3+}$ that is not true. The light absorption properties (and colors) of the two are quite different. The iron complex absorbs very little visible light and therefore appears a very pale yellow color and the cobalt complex strongly absorbs visible light and has a dark red-orange color. Also, the iron complex is paramagnetic (having unpaired electrons) and the cobalt complex is diamagnetic (having no unpaired electrons). Crystal field theory, and later ligand field theory were developed in part to explain the spectroscopic and magnetic properties of transition metal complexes.

Complex	**$[Fe(NH_3)_6]^{2+}$**	**$[Co(NH_3)_6]^{3+}$**
Valence electron configuration	[Ar] $3d^6$	[Ar] $3d^6$
Color	pale yellow	Red-orange
Magnetic properties	paramagnetic	diamagnetic

Learning Objectives

- Draw a crystal field diagram for a given metal complex and use to identify the number of unpaired electrons
- Identify whether a given metal complex will be high or low spin
- Calculate the crystal field stabilization energy for a given metal complex
- Use ligand field theory to explain the spectrochemical series

Thumbnail image shows pi donation from a ligand to a metal

9.1: Crystal Field Theory
9.2: Crystal Field Stabilization Energy
9.3: Jahn-Teller Distortions
9.4: Factors That Affect Crystal Field Splitting
9.5: Ligand Field Theory

9: Coordination Chemistry- Bonding is shared under a CC BY-NC-SA 4.0 license and was authored, remixed, and/or curated by LibreTexts.

9.1: Crystal Field Theory

Crystal Field Theory

Crystal field theory (CFT) describes the breaking of orbital degeneracy in transition metal complexes due to the presence of ligands. CFT qualitatively describes the strength of the metal-ligand bonds. Based on the strength of the metal-ligand bonds, the energy of the system is altered. This may lead to a change in magnetic properties as well as color. This theory was developed by Hans Bethe and John Hasbrouck van Vleck in the late 1920's. Crystal field theory is a purely electrostatic theory and uses classical potential energy equations that take into account the attractive and repulsive interactions between charged particles (that is, Coulomb's Law interactions).

$$E \propto \frac{q_1 q_2}{r} \tag{9.1.1}$$

with

- E the bond energy between the charges and
- q_1 and q_2 are the charges of the interacting ions and
- r is the distance separating them.

For this simple approach to work, CFT makes some assumptions and simplifications. All ligands are modeled as negative point charges with no orbitals and the metal orbitals are modeled as clouds of negative charge. This approach leads to the correct prediction that large cations of low charge, such as K^+ and Na^+, should form few coordination compounds. For transition metal cations that contain varying numbers of d electrons in orbitals that are NOT spherically symmetric, however, the situation is quite different. The shape and occupation of these d-orbitals then becomes important in an accurate description of the bond energy and properties of the transition metal compound.

Orientation of *d*-Orbitals

To understand CFT, one must first understand the shape and orientation of the d orbitals:

- d_{xy}: lobes lie in-between the x and the y axes.
- d_{xz}: lobes lie in-between the x and the z axes.
- d_{yz}: lobes lie in-between the y and the z axes.
- $d_{x^2-y^2}$: lobes lie on the x and y axes.
- d_{z^2}: there are two lobes on the z axes and there is a donut shape ring that lies on the xy plane around the other two lobes.

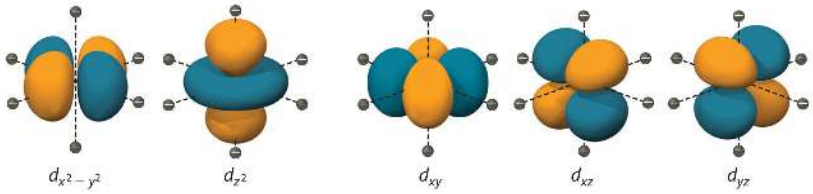


Figure **9.1.1**: Spatial arrangement of ligands in the an octahedral ligand field with respect to the five d-orbitals.

Octahedral Crystal Field

When examining a single transition metal ion in free space, the five d-orbitals have the same energy (Figure **9.1.2**). When ligands approach the metal ion, the ligand negative point charges destabilize the metal d-orbital based on the geometric structure of the molecule. Since ligands approach from different directions, not all d-orbitals interact equally. These interactions, however, create a splitting due to the electrostatic environment, orbitals with more interaction are higher in energy and orbitals with less interaction are lower in energy.

Definition: Barycenter

In crystal field theory the barycenter is the energy of the d orbitals in a spherical crystal field, where the negative lignad charges are evenly distributed around the metal ion in a sphere. The splitting of the d orbitals in other crystal fields will be symmetric around the barycenter (i.e. the total amount of stabalization will always be equal to the total amount of destabalization)

For example, consider a molecule with octahedral geometry. Ligands approach the metal ion along the x, y, and z axes. Therefore, the electrons in the d_{z^2} and $d_{x^2-y^2}$ orbitals (which lie along these axes) experience greater repulsion and are therefore at higher energy. Compared to a spherical field, where ligands are evenly distributed around the metal center, the d orbitals that lie between the axes (d_{xy}, d_{xz}, and d_{yz} experience less repulsion when the ligands are in an octahedral arrangement and are stabilized. This causes a splitting in the energy levels of the d-orbitals, known as crystal field splitting. For octahedral complexes, crystal field splitting is denoted by Δ_o (or Δ_{oct}) (in older texts and papers it may also be labeled as 10Dq). Any orbital that has a lobe on the axes moves to a higher energy level. The energies of the e_g symmetry orbitals (d_{z^2} and $d_{x^2-y^2}$) increase due to greater interactions with the ligands. The t_{2g} symmetry orbitals (d_{xy}, d_{xz}, and d_{yz}) decrease in energy with respect to the spherical energy level and become

more stable. This splitting is symmetric around the barycenter (the theoretical energy of the d orbitals with spherical charge distribution) which means that the energy levels of e_g are higher (by $0.6\Delta_o$) while t_{2g} are lower (by $0.4\Delta_o$). It should be noted that the labels t_{2g} and e_g come from group theory and the octahedral point group. The energy difference between the t_{2g} and e_g orbitals dictates the energy that the complex will absorb causing electrons to move from one level to the next. For transition metal complexes, the absorbed energy is typically in the visible part of the spectrum and thus this will determine the color of the complex. Whether the complex is paramagnetic or diamagnetic will be determined by the spin state. If there are unpaired electrons, the complex is paramagnetic; if all electrons are paired, the complex is diamagnetic.

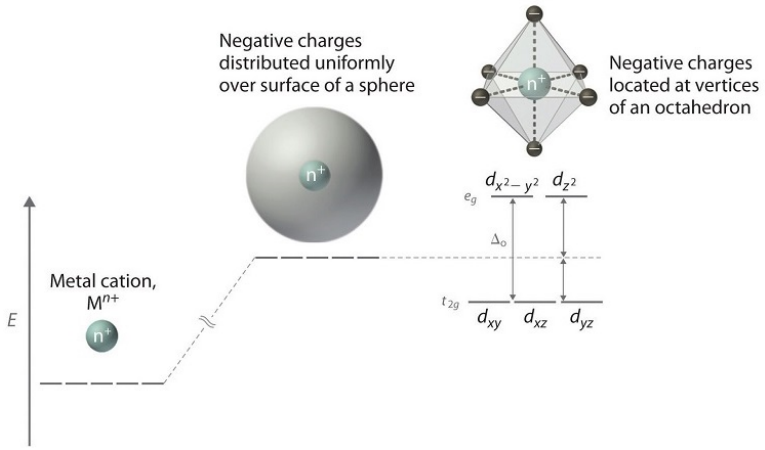


Figure **9.1.2**: (a) Distributing a charge of −6 uniformly over a spherical surface surrounding a metal ion causes the energy of all five d orbitals to increase due to electrostatic repulsions, but the five d orbitals remain degenerate. Placing a charge of −1 at each vertex of an octahedron causes the d orbitals to split into two groups with different energies: the $d_{x^2-y^2}$ and d_{z^2} orbitals increase in energy, while the, d_{xy}, d_{xz}, and d_{yz} orbitals decrease in energy. The average energy of the five d orbitals is the same as for a spherical distribution of a −6 charge, however. Attractive electrostatic interactions between the negatively charged ligands and the positively charged metal ion (far right) cause all five d orbitals to decrease in energy but does not affect the splittings of the orbitals. (b) The two e_g orbitals (left) point directly at the six negatively charged ligands, which increases their energy compared with a spherical distribution of negative charge. In contrast, the three t_{2g} orbitals (right) point between the negatively charged ligands, which decreases their energy compared with a spherical distribution of charge.

Filling Electrons in Orbitals

d^1 - d^3

For one, two, or three d electrons the filling is straightforward. According to the Aufbau principle, electrons are filled from lower to higher energy orbitals. In an octahedral crystal field, this corresponds to the d_{xy}, d_{xz}, and d_{yz}) orbitals. Following Hund's rule, electrons are filled in order to have the highest number of unpaired electrons. Therefore, each electron occupies one of the t_{2g} symmetry orbitals d_{xy}, d_{xz}, or d_{yz}) and all the electrons are orientated in the same direction to maximize spin multiplicity as shown in Figure **9.1.3**.

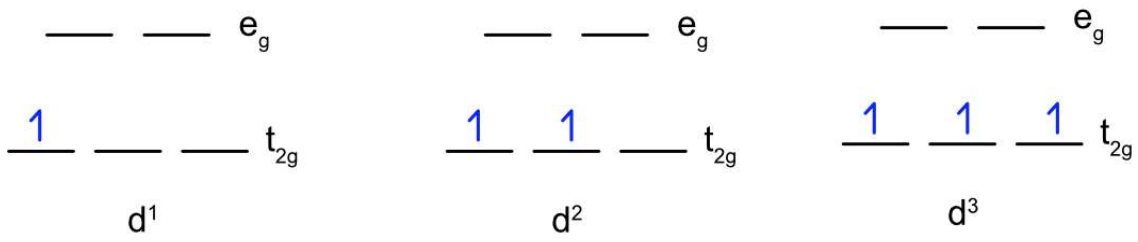


Figure **9.1.3**: Arrangement of the d electrons in a octahedral crystal field for 1, 2, and 3 d electrons. (CC-BY-NC-SA; Catherine McCusker)

d^4 - d^7

When a complex has between 4 and 7 d electrons there are two ways the electrons can be arranged into the d orbitals. As an example, in d^4 the first three electrons are placed one in each of the t_{2g} symmetry orbitals. The fourth electron can either be placed in one of the empty e_g symmetry orbitals or it can be paired in one or the t_{2g} symmetry orbitals, as shown in Figure **9.1.4**. The first configuration is called high spin because it maximizes the number of unpaired electrons and the second is called low spin. Whether a complex will have the high spin or low configuration depends on the relative magnitude of the spin pairing energy (the energy required to place two negatively charged electrons in the same orbital) and the crystal field splitting (Δ_o). In cases where the spin pairing energy is larger than Δ_o the complex will adopt the high spin configuration because it requires less energy to place an electron in a higher energy e_g orbital than is does to pair two electrons in the same t_{2g} orbital. In cases where Δ_o is larger than the spin pairing energy the complex will adopt a low spin configuration because it requires less energy to place a second electron in a t_{2g} orbital than it does to place one in the higher energy e_g orbitals.

Definition: Spin Pairing Energy

The spin pairing energy is the energy required to pair two electrons in an orbital. It is based on the Coulombic repulsion between the two negative charges. Larger, more diffuse orbitals will have lower spin pairing energy because the two electrons can be further apart

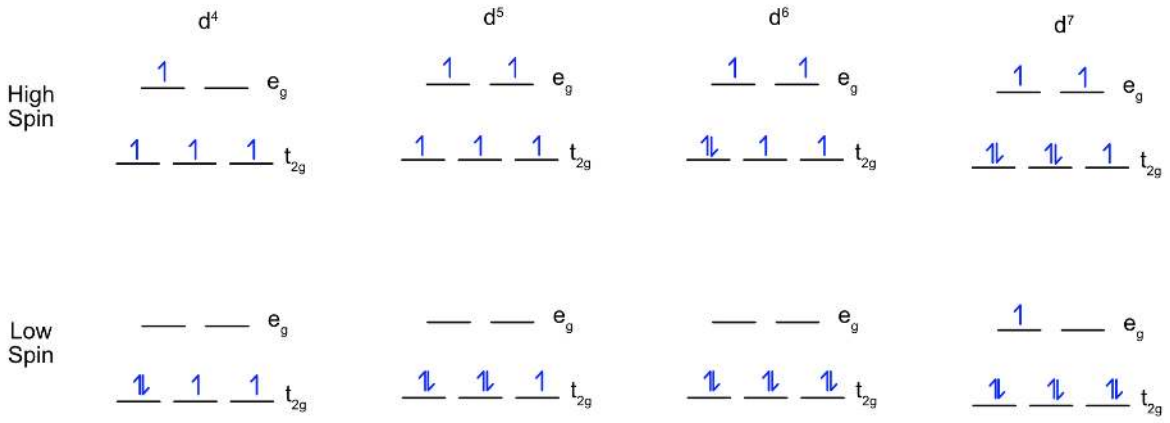


Figure **9.1.4**: High spin and low spin arrangements of electrons for d^4 - d^7. (CC-BY-NC-SA; Catherine McCusker)

d^8 - d^{10}

For complexes with 8 - 10 d electrons there is again only one way to arrange the electrons. Whether or not the e_g orbitals are filled before electrons are paired in the t_{2g} orbitals the final electron configurations are as shown in Figure **9.1.5**.

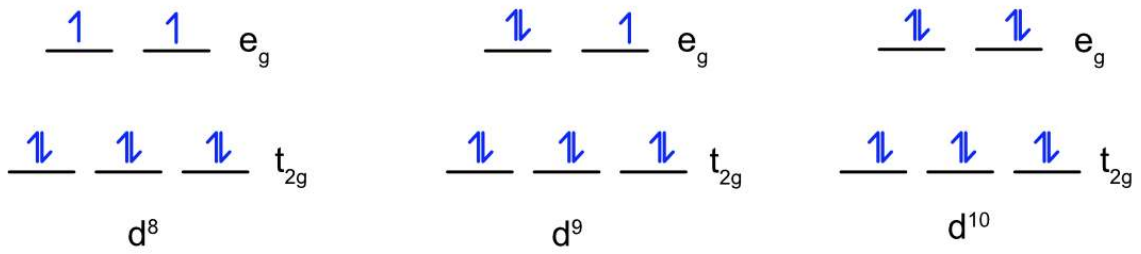


Figure **9.1.5**: Arrangement of the d electrons in a octahedral crystal field for 8, 9, and 10 d electrons. (CC-BY-NC-SA; Catherine McCusker)

Tetrahedral Crystal Field

In a tetrahedral complex, the four ligands are orientated at opposite corners of a cube as shown in Figure **9.1.6*a*** rather than along the axes. With the ligands between the axes, the three d orbitals which lie between the axes, d_{xy}, d_{xz}, and d_{yz} (t_2 symmetry in tetrahedral), now interact more with the ligands and are destabilized relative to the spherical crystal field. Conversely, the two d orbitals that lie along the axes, $d_{x^2-y^2}$ and d_{z^2} (e symmetry in tetrahedral), now interact less with the d orbitals and are stabilized relative to the spherical crystal field. As shown in Figure **9.1.6*b*** the splitting of the d orbitals in a tetrahedral crystal field is essentially the inverse of the octahedral crystal field. The crystal field splitting energy in a tetrahedral crystal field is Δ_t. Because a tetrahedral complex has fewer ligands than an octahedral complex, and those ligands are not ideally orientated to overlap with the d orbitals Δ_t is less than Δ_o for the same metal and ligands:

$$\Delta_t \approx \frac{4}{9}\Delta_o \tag{9.1.2}$$

Consequentially, Δ_t is typically smaller than the spin pairing energy, so tetrahedral complexes are usually high spin. As seen with octahedral compounds, the labels for the groups of orbitals, t_2 and e in this case, come from group theory and the tetrahedral point group.

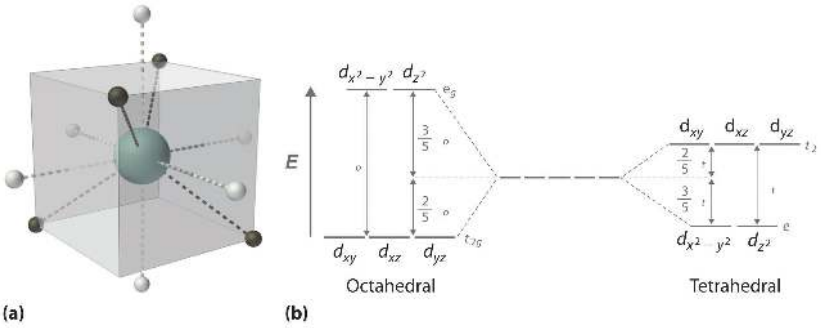


Figure **9.1.6**: (a) Tetrahedral ligand field surrounding a central transition metal (teal sphere). (b) Splitting of the degenerate d-orbitals (without a ligand field) due to an octahedral ligand field (left diagram) and the tetrahedral field (right diagram).

Square Planar Crystal Field

In a complex with four ligands, the other possible arrangement of ligands is square planar. The easiest way to visualize the square planar geometry is to start with an octahedral complex and remove the two ligands that are along the z axis. The four remaining ligands are in the xy plane, along the x and y axes. From a crystal field splitting perspective, when the z ligands are removed the d orbitals split further. In an octahedral crystal field both $d_{x^2-y^2}$ and d_{z^2} are destabilized. When the z ligands are removed the d_{z^2} orbital is stabilized because it no longer interacts with ligands on the z axis. Conversely the $d_{x^2-y^2}$ orbital is further destabilized because all of the ligand negative charges are concentrated in the xy plane. Removing the z ligand has a similar effect on the d_{xy}, d_{xz}, and d_{yz} orbitals, although the magnitude of the stabilization and destabilization is less because those orbitals do not directly interact with the ligands. The d_{xy} orbital is destabilized because it also lies in the xy plane and the d_{xz} and d_{yz} orbitals are stabilized because they have lost the (indirect) interaction with the ligands on the z axis. Overall the $d_{x^2-y^2}$ orbital is significantly more destabilized than the other d orbitals, meaning the square planar geometry is most favored in complexes with 8 electrons where the $d_{x^2-y^2}$ is empty and the other more stabilized d orbitals are filled.

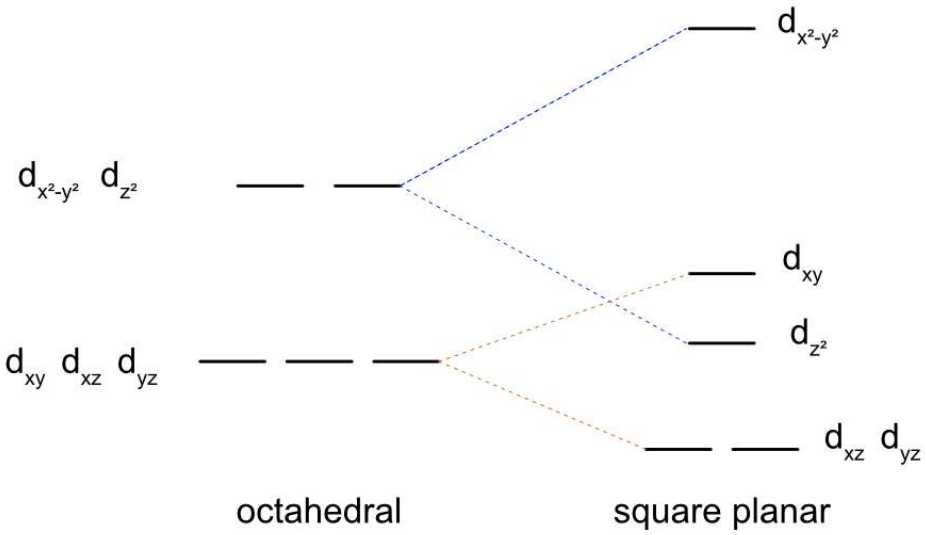
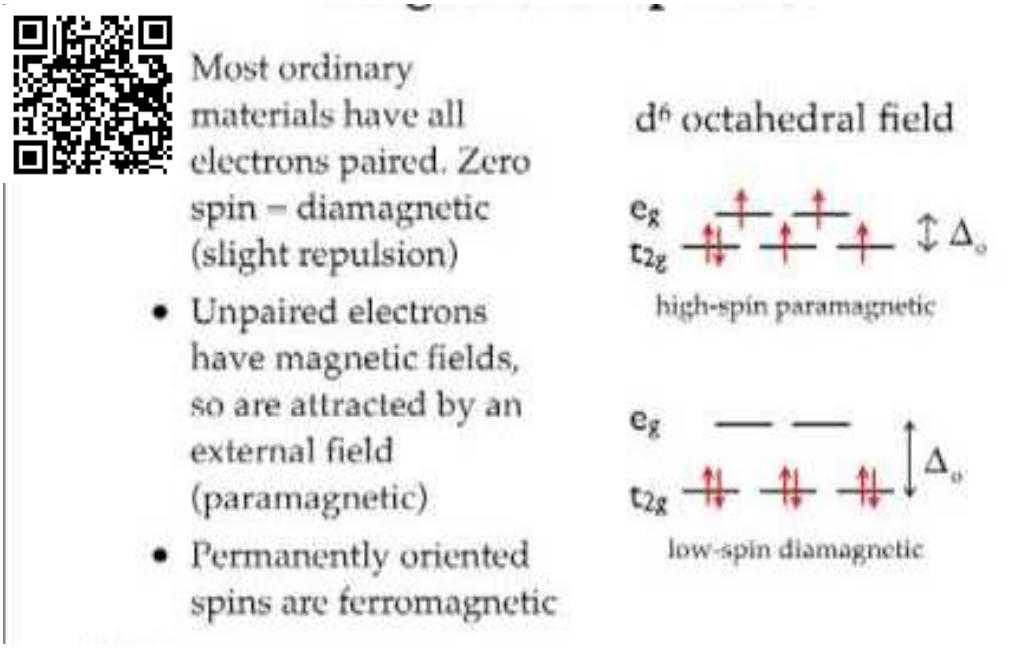


Figure **9.1.7**: Comparison between octahedral and square planar crystal field splittings, showing how the energies of the d orbitals change when the two z ligands are removed from an octahedral complex to form a square planar complex. (CC-BY-NC-SA; Catherine McCusker)

Video:



Tetrahedral vs Square Planar

From VSEPR theory we know that sterically the most favorable way to arrange four ligands around a metal ion is in the tetrahedral arrangement. That puts the most possible space between the four ligands. Because of this, a four coordinate metal complex will prefer a tetrahedral geometry UNLESS there is a larger crystal field stabilization energy (CFSE) for the square planar arrangement. As discussed above, this means square planar is the preferred geometry for most metal complexes with 8 d electrons, especially when the crystal field splitting (Δ) is large. While not every d^8 complex is square planar, almost all square planar complexes are d^8 (there are examples of d^7 and d^9 square planar complexes but they are less common)

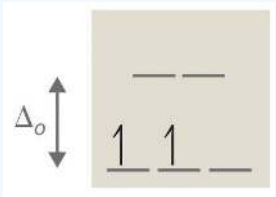
Exercise 9.1.3

For each of the following, sketch the d-orbital splitting diagram, fill the diagram with the correct number of d-electrons, list the number of unpaired electrons, and label whether they are paramagnetic or diamagnetic:

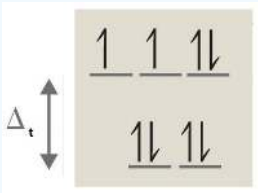
1. $[Ti(H_2O)_6]^{2+}$
2. $[NiCl_4]^{2-}$ (tetrahedral)
3. $[CoF_6]^{3-}$ (high spin)
4. $[Co(NH_3)_6]^{3+}$ (low spin)

Answer

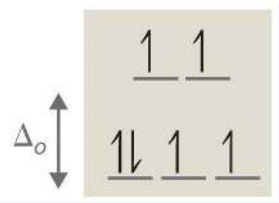
1. 2 unpaired electrons, paramagnetic



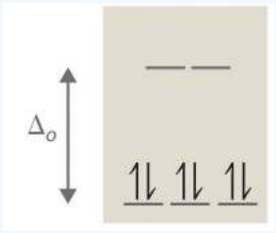
2. 2 unpaired electrons, paramagnetic



3. 4 unpaired electrons, paramagnetic



4. 0 unpaired electrons, diamagnetic



Contributors and Attributions

- Asadullah Awan (UCD), Hong Truong (UCD)
- Prof. Robert J. Lancashire (The Department of Chemistry, University of the West Indies)
- Modified by Catherine McCusker (East Tennessee State University)

9.1: Crystal Field Theory is shared under a CC BY-NC-SA 4.0 license and was authored, remixed, and/or curated by LibreTexts.

9.2: Crystal Field Stabilization Energy

Crystal Field Stabilization Energy

A consequence of crystal field theory is that the distribution of electrons in the d orbitals may lead to net stabilization (decrease in energy) of some complexes depending on the specific ligand geometry and metal d-electron configurations. It is a simple matter to calculate this stabilization since all that is needed is the electron configuration and knowledge of the splitting patterns.

Definition: Crystal Field Stabilization Energy (CFSE)

The crystal field stabilization energy is defined as the energy of the electron configuration in the crystal field minus the energy of the electronic configuration in the spherical field.

$$CFSE = \Delta E = E_{\text{crystal field}} - E_{\text{spherical field}} \tag{9.2.1}$$

The CSFE will depend on multiple factors including:

- Geometry (crystal field splitting pattern)
- Number of d-electrons
- Spin Pairing Energy (the contribution of spin pairing energy is often negligible in comparison to other contributions and is omitted at times)

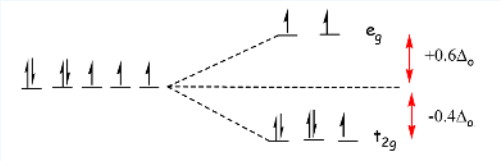
For an octahedral complex, each of the more stable t_{2g} orbitals are stabilized by $-0.4\Delta_o$ relative to spherical field whereas the higher energy e_g orbitals are destabilized by $+0.6\Delta_o$. For a complex the stabilization or destabilization of each electron is summed. Any electrons that are paired within a single orbital, also contribute spin pairing energy (+P). The overall CFSE for a complex is expressed as a multiple of the crystal field splitting parameter Δ_o.

Example 9.2.1: CFSE for a high Spin d^7 complex

What is the CFSE for a high spin d^7 octahedral complex?

Solution

The splitting pattern and electron configuration for both spherical and octahedral ligand fields are compared below.



The energy of the spherical field ($E_{\text{spherical field}}$) is

$$E_{\text{spherical field}} = 7 \times 0 + 2P = 2P$$

The energy of the octahedral crystal field $E_{\text{oct field}}$ is

$$E_{\text{oct field}} = (5 \times -0.4\Delta_o) + (2 \times 0.6\Delta_o) + 2P = -0.8\Delta_o + 2P$$

So via Equation 9.2.1, the CFSE is

$$\begin{aligned} CFSE &= E_{\text{oct field}} - E_{\text{spherical field}} \\ &= (-0.8\Delta_o + 2P) - 2P \\ &= -0.8\Delta_o \end{aligned}$$

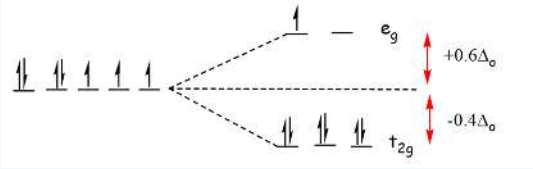
Notice that the spin pairing energy cancels out in this case (and will when calculating the CFSE of high spin complexes) since the number of paired electrons in the octahedral field is the same as that in spherical field of the free metal ion.

Exercise 9.2.1

What is the CFSE for a low spin d^7 octahedral complex?

Answer

The splitting pattern and electron configuration for both spherical and octahedral ligand fields are compared below.



The energy of the spherical field is the same as calculated for the high spin configuration in Example 1:

$$E_{\text{spherical}} = 7 \times 0 + 2P = 2P$$

The energy of the octahedral ligand\) field $E_{\text{oct field}}$ is

$$\begin{aligned} E_{\text{oct field}} &= (6 \times -0.4\Delta_o) + (1 \times 0.6\Delta_o) + 3P \\ &= -1.8\Delta_o + 3P \end{aligned}$$

So via Equation 9.2.1, the CFSE is

$$\begin{aligned} CFSE &= E_{\text{oct field}} - E_{\text{spherical field}} \\ &= (-9/5\Delta_o + 3P) - 2P \\ &= -9/5\Delta_o + P \end{aligned}$$

This appears more a more stable configuration than the high spin d^7 configuration in Example 9.2.1, but we have then to take into consideration the pairing energy P to know definitely, which varies between $200 - 400\ kJ\ mol^{-1}$ depending on the metal.

Table 9.2.1: Crystal field stabilization energies (CFSE) for high and low spin octahedral complexes

Total d-electrons	Spherical Field	Octahedral Field				Crystal Field Stabilization Energy	
		High Spin		Low Spin			
	$E_{\text{spherical field}}$	Configuration	$E_{\text{crystal field}}$	Configuration	$E_{\text{crystal field}}$	High Spin	Low Spin
d^0	0	$t_{2g}^0\ e_g^0$	0	$t_{2g}^0 e_g^0$	0	0	0
d^1	0	$t_{2g}^1\ e_g^0$	-2/5 Δ_o	$t_{2g}^1 e_g^0$	-2/5 Δ_o	-2/5 Δ_o	-2/5 Δ_o
d^2	0	$t_{2g}^2\ e_g^0$	-4/5 Δ_o	$t_{2g}^2 e_g^0$	-4/5 Δ_o	-4/5 Δ_o	-4/5 Δ_o
d^3	0	$t_{2g}^3\ e_g^0$	-6/5 Δ_o	$t_{2g}^3 e_g^0$	-6/5 Δ_o	-6/5 Δ_o	-6/5 Δ_o
d^4	0	$t_{2g}^3\ e_g^1$	-3/5 Δ_o	$t_{2g}^4 e_g^0$	-8/5 Δ_o + P	-3/5 Δ_o	-8/5 Δ_o + P
d^5	0	$t_{2g}^3\ e_g^2$	0 Δ_o	$t_{2g}^5 e_g^0$	-10/5 Δ_o + 2P	0 Δ_o	-10/5 Δ_o + 2P
d^6	P	$t_{2g}^4\ e_g^2$	-2/5 Δ_o + P	$t_{2g}^6 e_g^0$	-12/5 Δ_o + 3P	-2/5 Δ_o	-12/5 Δ_o + P
d^7	2P	$t_{2g}^5\ e_g^2$	-4/5 Δ_o + 2P	$t_{2g}^6 e_g^1$	-9/5 Δ_o + 3P	-4/5 Δ_o	-9/5 Δ_o + P
d^8	3P	$t_{2g}^6\ e_g^2$	-6/5 Δ_o + 3P	$t_{2g}^6 e_g^2$	-6/5 Δ_o + 3P	-6/5 Δ_o	-6/5 Δ_o
d^9	4P	$t_{2g}^6\ e_g^3$	-3/5 Δ_o + 4P	$t_{2g}^6 e_g^3$	-3/5 Δ_o + 4P	-3/5 Δ_o	-3/5 Δ_o
d^{10}	5P	$t_{2g}^6\ e_g^4$	0 Δ_o + 5P	$t_{2g}^6 e_g^4$	0 Δ_o + 5P	0	0

P is the spin pairing energy and represents the energy required to pair up electrons within the same orbital. For a given metal ion P (pairing energy) is constant, but it does not vary with ligand and oxidation state of the metal ion).

Octahedral Preference

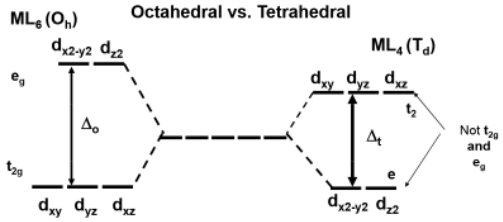
Similar CFSE values can be constructed for non-octahedral ligand field geometries once the knowledge of the d-orbital splitting is known and the electron configuration within those orbitals known, e.g., the tetrahedral complexes in Table **9.2.2**. These energies geoemtries can then be contrasted to the octahedral CFSE to calculate a thermodynamic preference for a metal-ligand combination to favor the octahedral geometry. This is quantified via an octahedral site preference energy defined below.

Definition: Octahedral Site Preference Energies (OSPE)

The octahedral site preference energy (OSPE) is defined as the difference of CFSE energies for a non-octahedral complex and the octahedral complex. For comparing the preference of forming an octahedral ligand field vs. a tetrahedral ligand field, the OSPE is thus:

$$OSPE = CFSE_{(oct)} - CFSE_{(tet)} \tag{9.2.2}$$

The OSPE quantifies the preference of a complex to exhibit an octahedral geometry vs. another geometry. The OSPE for octahedral vs tetrahedral geometries is illustrated below.



Note: the conversion between Δ_o and Δ_t used for these calculations is:

$$\Delta_t \approx \frac{4}{9}\Delta_o \tag{9.2.3}$$

which is applicable for comparing octahedral and tetrahedral complexes that involve same ligands only.

Table **9.2.2**: Octahedral Site Preference Energies (OSPE)

Total d-electrons	CFSE(Octahedral)	CFSE(Tetrahedral)	OSPE (for high spin complexes)**

Total d-electrons	CFSE(Octahedral)		CFSE(Tetrahedral)		OSPE (for high spin complexes)**
	High Spin	Low Spin	Configuration	**Always High Spin***	
d^0	0 Δ_o	0 Δ_o	e^0	0 Δ_t	0 Δ_o
d^1	-2/5 Δ_o	-2/5 Δ_o	e^1	-3/5 Δ_t	-6/45 Δ_o
d^2	-4/5 Δ_o	-4/5 Δ_o	e^2	-6/5 Δ_t	-12/45 Δ_o
d^3	-6/5 Δ_o	-6/5 Δ_o	$e^2t_2^1$	-4/5 Δ_t	-38/45 Δ_o
d^4	-3/5 Δ_o	-8/5 Δ_o + P	$e^2t_2^2$	-2/5 Δ_t	-19/45 Δ_o
d^5	0 Δ_o	-10/5 Δ_o + 2P	$e^2t_2^3$	0 Δ_t	0 Δ_o
d^6	-2/5 Δ_o	-12/5 Δ_o + P	$e^3t_2^3$	-3/5 Δ_t	-6/45 Δ_o
d^7	-4/5 Δ_o	-9/5 Δ_o + P	$e^4t_2^3$	-6/5 Δ_t	-12/45 Δ_o
d^8	-6/5 Δ_o	-6/5 Δ_o	$e^4t_2^4$	-4/5 Δ_t	-38/45 Δ_o
d^9	-3/5 Δ_o	-3/5 Δ_o	$e^4t_2^5$	-2/5 Δ_t	-19/45 Δ_o
d^{10}	0	0	$e^4t_2^6$	0 Δ_t	0 Δ_o

P is the spin pairing energy and represents the energy required to pair up electrons within the same orbital.

Note

Tetrahedral complexes are always high spin since the splitting is appreciably smaller than ***P*** (Equation 9.2.3).

After conversion with Equation 9.2.3. The data in Tables **9.2.1** and **9.2.2** are represented graphically by the curves in Figure **9.2.1** below for the high spin complexes only. The low spin complexes require knowledge of ***P*** to graph, which will vary depending on the identiy of the metal ion.

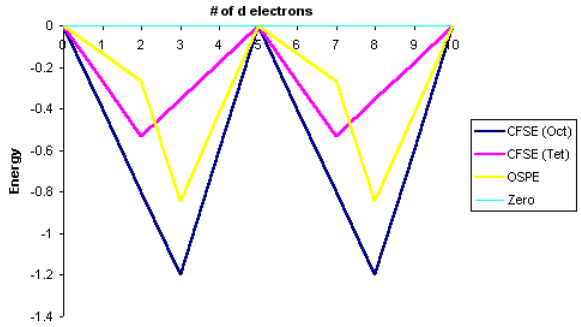


Figure **9.2.1**: Crystal Field Stabilization Energies for both high spin octahedral fields ($CFSE_{oct}$) and tetrahedral fields ($CFSE_{tet}$). Octahedral Site Preference Energies (OSPE) are in yellow. This is for high spin complexes only.

From a simple inspection of Figure **9.2.1**, the following observations can be made:

- The OSPE is *small* in d^1, d^2, d^5, d^6, d^7 high spin complexes and other factors influence the stability of the complexes including steric factors
- The OSPE is *large* in d^3 and d^8 high spin complexes which strongly favor octahedral geometries

Applications

The "double-humped" curve in Figure **9.2.1** is found for various properties of the first-row transition metals, including hydration and lattice energies of the M(II) ions, ionic radii as well as the stability of M(II) complexes. This suggests that these properties are somehow related to crystal field effects.

In the case of hydration energies describing the complexation of water ligands to a bare metal ion:

$$M^{2+}(g) + H_2O \rightarrow [M(OH_2)_6]^{2+}(aq) \tag{9.2.4}$$

Table **9.2.3** and Figure **9.2.2** shows this type of curve. Note that in any series of this type not all the data are available since a number of ions are not very stable in the M(II) state in water.

Table **9.2.3**: Hydration energies of M^{2+} ions

M	ΔH°/kJmol^{-1}	M	ΔH°/kJmol^{-1}
Ca	-2469	Fe	-2840
Sc	no stable 2+ ion	Co	-2910
Ti	-2729	Ni	-2993
V	-2777	Cu	-2996
Cr	-2792	Zn	-2928
Mn	-2733		

Graphically the data in Table 2 can be represented by:

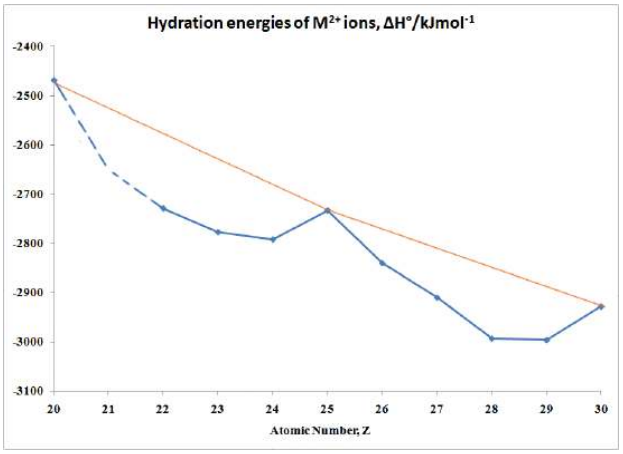


Figure **9.2.2**: Hydration energies of M^{2+} ions

Contributors and Attributions

- Prof. Robert J. Lancashire (The Department of Chemistry, University of the West Indies)

9.2: Crystal Field Stabilization Energy is shared under a CC BY-NC-SA 4.0 license and was authored, remixed, and/or curated by LibreTexts.

9.3: Jahn-Teller Distortions

The Jahn-Teller effect is a geometric distortion of a non-linear molecular system that reduces its symmetry and energy. This distortion is typically observed among octahedral complexes where the two axial bonds can be shorter or longer than those of the equatorial bonds. This effect can also be observed in tetrahedral compounds. This effect is dependent on the electronic state of the system.

Introduction

In 1937, Hermann Jahn and Edward Teller postulated a theorem stating that "stability and degeneracy are not possible simultaneously unless the molecule is a linear one," in regards to its electronic state.[1] This leads to a break in degeneracy which stabilizes the molecule and by consequence, reduces its symmetry. Since 1937, the theorem has been revised which Housecroft and Sharpe have eloquently phrased as "any non-linear molecular system in a degenerate electronic state will be unstable and will undergo distortion to form a system of lower symmetry and lower energy, thereby removing the degeneracy."[2] This is most commonly observed with transition metal octahedral complexes, however, it can be observed in tetrahedral compounds as well.

For a given octahedral complex, the five d atomic orbitals are split into two degenerate sets when constructing a molecular orbital diagram. These are represented by the sets' symmetry labels: t_{2g} (d_{xz}, d_{yz}, d_{xy}) and e_g (d_{z^2} and $d_{x^2-y^2}$). When a molecule possesses a degenerate electronic ground state, it will distort to remove the degeneracy and form a lower energy (and by consequence, lower symmetry) system. The octahedral complex will either elongate or compress the z ligand bonds as shown in Figure **9.3.1** below:

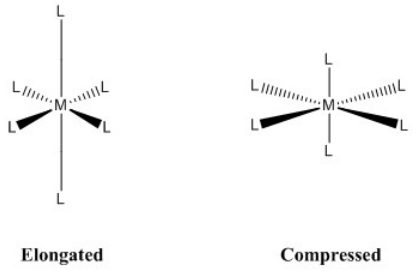


Figure **9.3.1**: Jahn-Teller distortions for an octahedral complex.

When an octahedral complex exhibits elongation, the axial bonds are longer than the equatorial bonds. For a compression, it is the reverse; the equatorial bonds are longer than the axial bonds. Elongation and compression effects are dictated by the amount of overlap between the metal and ligand orbitals. Thus, this distortion varies greatly depending on the type of metal and ligands. In general, the stronger the metal-ligand orbital interactions are, the greater the chance for a Jahn-Teller effect to be observed.

Elongation

Elongation Jahn-Teller distortions occur when the degeneracy is broken by the stabilization (lowering in energy) of the d orbitals with a z component, while the orbitals without a z component are destabilized (higher in energy) as shown in Figure **9.3.2** below:

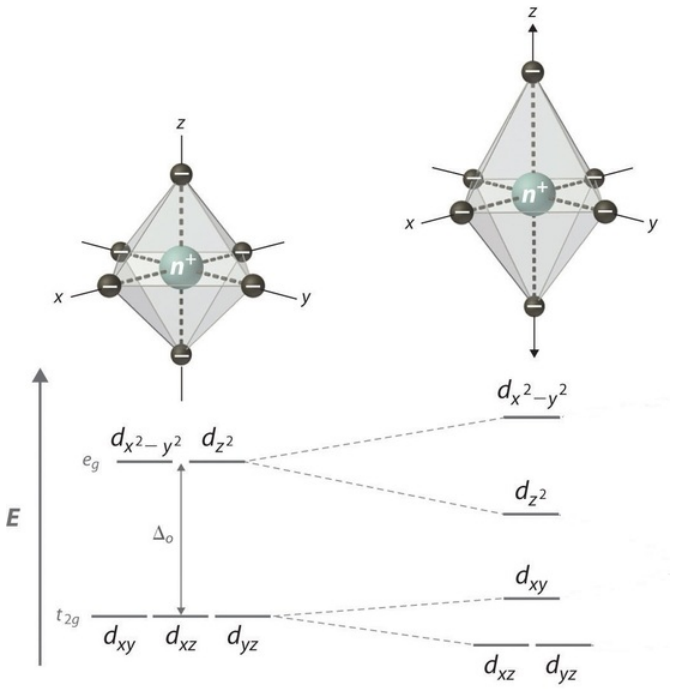


Figure **9.3.2**: Illustration of tetragonal distortion (elongation) for an octahedral complex.

This is due to the d_{xy} and $d_{x^2-y^2}$ orbitals having greater overlap with the ligand orbitals, resulting in the orbitals being higher in energy. Since the $d_{x^2-y^2}$ orbital is antibonding, it is expected to increase in energy due to elongation. The d_{xy} orbital is still nonbonding, but is destabilized due to the interactions. Jahn-Teller elongations are well-documented for copper(II) octahedral compounds. A classic example is that of copper(II) fluoride as shown in Figure **9.3.3**.

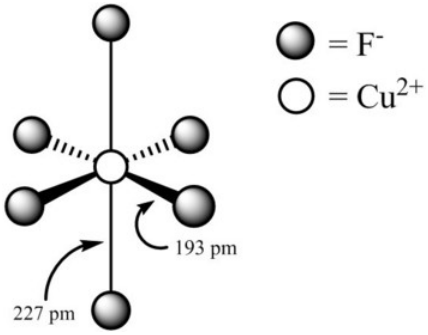


Figure **9.3.3**: Structure of octahedral copper(II) fluoride.[3]

Notice that the two axial bonds are both elongated and the four shorter equatorial bonds are the same length as each other. According the theorem, the orbital degeneracy is eliminated by distortion, making the molecule more stable based on the model presented in Figure **9.3.2**.

Compression

Compression Jahn-Teller distortions occur when the degeneracy is broken by the stabilization (lowering in energy) of the d orbitals *without* a *z* component, while the orbitals with a *z* component are destabilized (higher in energy) as shown in Figure **9.3.4** below:

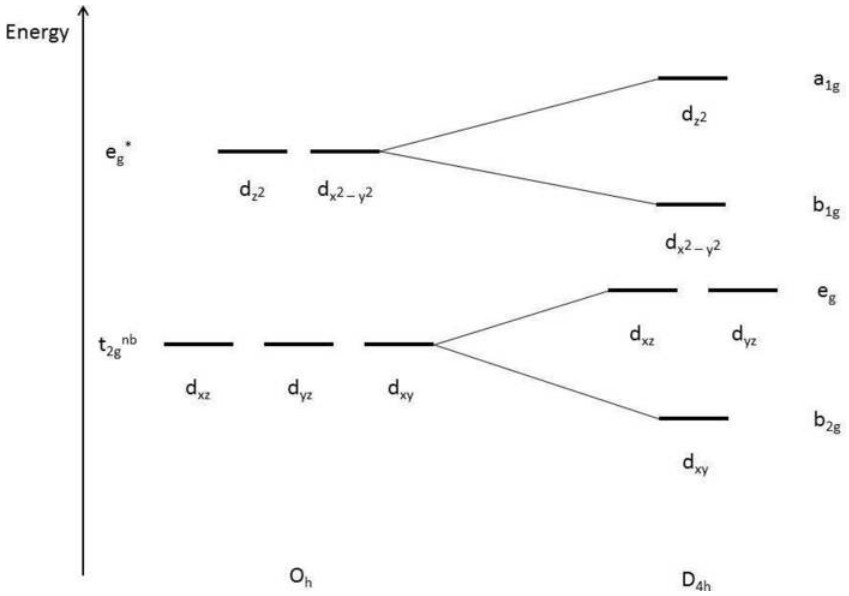


Figure **9.3.4**: Illustration of tetragonal distortion (compression) for an octahedral complex.

This is due to the *z*-component d orbitals having greater overlap with the ligand orbitals, resulting in the orbitals being higher in energy. Since the d_{z^2} orbital is antibonding, it is expected to increase in energy due to compression. The d_{xz} and d_{yz} orbitals are still nonbonding, but are destabilized due to the interactions.

Electronic Configurations

For Jahn-Teller effects to occur in transition metals there must be degeneracy in either the t_{2g} or e_g orbitals. The electronic states of octahedral complexes depend on the number of d-electrons and the splitting energy, **Δ**. When **Δ** is large and is greater than the energy required to pair electrons, electrons pair in t_{2g} before occupying e_g. On the other hand, when **Δ** small and is less than the pairing energy, electrons will occupy e_g before pairing in t_{2g}. The **Δ** of an octahedral complex is dictated by the chemical environment (ligand identity), and the identity and charge of the metal ion. If there electron configurations for any d-electron count is different depending on **Δ**, the configuration with more paired electrons is called low spin while the one with more unpaired electrons is called high spin.

The electron configurations diagrams for d1 through d10 with large and small **Δ** are illustrated in the figures below. Notice that the electron configurations for d^1, d^2, d^3, d^8, d^9, and d^{10} are the same no matter what the magnitude of **Δ**. Low spin and high spin configurations exist only for the electron counts d^4, d^5, d^6, and d^7.

Large Δ

Figure **9.3.5** (below) shows the various electronic configurations for octahedral complexes with large **Δ**, including the low-spin configurations of d^4, d^5, d^6, and d^7:

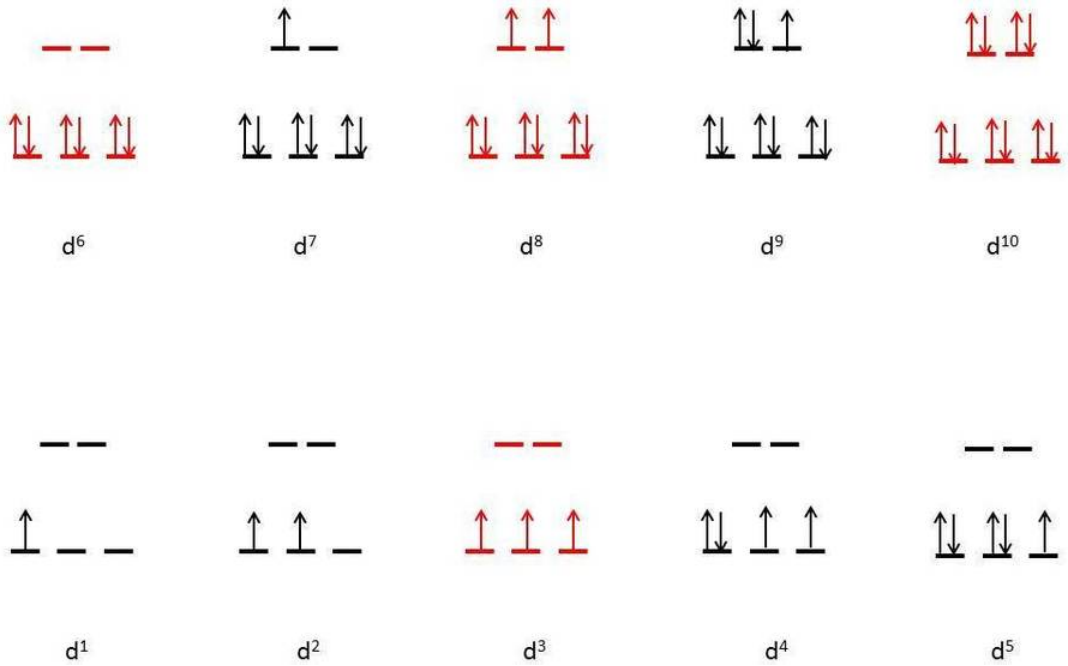


Figure 9.3.5: Electron configuration diagram of octahedral complexes (red indicates no degeneracies possible, thus no Jahn-Teller effects).

The figure illustrates the electron configurations in the case of large **Δ**. The electron configurations highlighted in red (d^3, low spin d^6, d^8, and d^{10}) **do not** exhibit Jahn-Teller distortions. On the other hand d^1, d^2, low spin d^4, low spin d^5, low spin d^7, and d^9, would be expected to exhibit Jhan-Teller distortion. These electronic configurations correspond to a variety of transition metals. Some common examples include Cr^{3+}, Co^{3+}, and Ni^{2+}.

Small Δ

Figure 9.3.6 (below) shows the various electronic configurations for octahedral complexes with small **Δ**, including the high-spin configurations of d^4, d^5, d^6, and d^7::

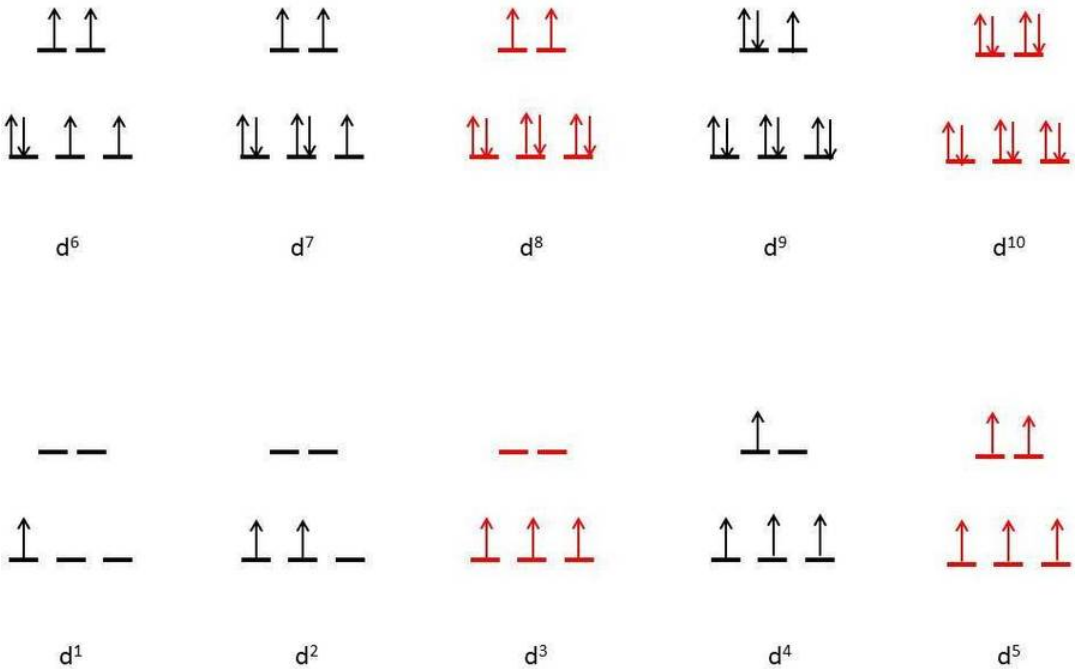


Figure 9.3.6: High spin octahedral coordination diagram (red indicates no degeneracies possible, thus no Jahn-Teller effects).

The figure illustrates the electron configurations in the case of small Δ. The electron configurations highlighted in red (d^3, high spin d^5, d^8, and d^{10}) **do not** exhibit Jahn-Teller distortions. In general, degenerate electronic states occupying the e_g orbital set tend to show stronger Jahn-Teller effects. This is primarily caused by the occupation of these high energy orbitals. Since the system is more stable with a lower energy configuration, the degeneracy of the e_g set is broken, the symmetry is reduced, and occupations at lower energy orbitals occur.

Spectroscopic Observation

Jahn-Teller distortions can be observed using a variety of spectroscopic techniques. In UV-VIS absorption spectroscopy, distortion causes splitting of bands in the spectrum due to a reduction in symmetry (O_h to D_{4h}). Consider a hypothetical molecule with octahedral symmetry showing a single absorption band. If the molecule were to undergo Jahn-Teller distortion, the number of bands would increase as shown in Figure **9.3.7** below:

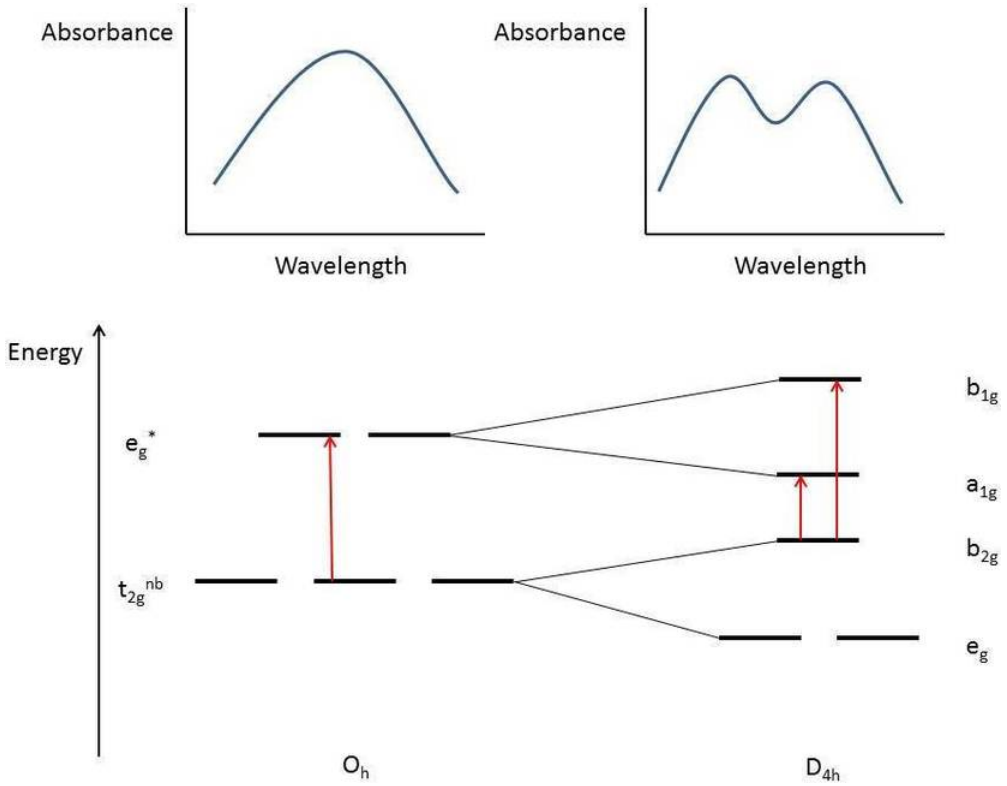


Figure **9.3.7**: Hypothetical absorption spectra of an octahedral molecule (left) and the same molecule with Jahn-Teller elongation (right). The red arrows indicate electronic transitions.

A similar phenomenon can be seen with IR and Raman vibrational spectroscopy. The number of vibrational modes for a molecule can be calculated using the 3n - 6 rule (or 3n - 5 for linear geometry) rule. If a molecule exhibits an O_h symmetry point group, it will have fewer bands than that of a Jahn-Teller distorted molecule with D_{4h} symmetry. Thus, one could observe Jahn-Teller effects through either IR or Raman techniques. This effect can also be observed in EPR experiments as long as there is at least one unpaired electron.

Table **9.3.1**: Examples of Jahn-Teller distorted complexes

$CuBr_2$	4 Br at 240 pm 2 Br at 318 pm
$CuCl_2$	4 Cl at 230 pm 2 Cl at 295 pm
$CuCl_2.2H_2O$	2 O at 193 pm 2 Cl at 228 pm 2 Cl at 295 pm
$CsCuCl_3$	4 Cl at 230 pm 2 Cl at 265 pm
CuF_2	4 F at 193 pm 2 F at 227 pm
$CuSO_4.4NH_3.H_2O$	4 N at 205 pm 1 O at 259 pm 1 O at 337 pm
K_2CuF_4	4 F at 191 pm 2 F at 237 pm
$KCuAlF_6$	2 F at 188 pm 4 F at 220 pm
CrF_2	4 F at 200 pm 2 F at 243 pm
$KCrF_3$	4 F at 214 pm 2 F at 200 pm
MnF_3	2 F at 209 pm 2 F at 191 pm 2 F at 179 pm

The Jahn-Teller Theorem predicts that distortions should occur for *any degenerate state*, including degeneracy of the t_{2g} level, however distortions in bond lengths are much more distinctive when the degenerate electrons are in the e_g level.

References

1. Jahn, H. A.; Teller, E. *Proc. R. Soc. London A*, **1937**, *161*, 220-235. DOI: 10.1098/rspa.1937.0142
2. Housecroft, C.; Sharpe, A. G. *Inorganic Chemistry*. Prentice Hall, 3rd Ed., 2008, p. 644. ISBN: 978-0-13-175553-6
3. Billy, C.; Haendler, H. A. *J. Am. Chem. Soc.*, **1957**, *79*, 1049–1051. DOI: 10.1021/ja01562a011

References

- Janes, R.; Moore, E. A. *Metal-ligand bonding*. The Open University, 2004, p. 23. ISBN 0-85404-979-7
- P.T.Miller, P.G.Lenhert and M.D.Joesten, *Inorg. Chem.*, 11, 2221, 1972.
- J.S.Wood, C.P.Keijzers and R.O.Day, *Acta Crystallogr., Sect.C (Cr. Str. Comm.)*, 40, 404, 1984.
- M.D.Joesten, M.S.Hussain and P.G.Lenhert, *Inorg. Chem.*, 9, 151, 1970.

Practice Questions

1. Why do d^3 complexes not show Jahn-Teller distortions?
2. Does the spin system (high spin v. low spin) of a molecule play a role in Jahn-Teller effects?
3. What spectroscopic method would one utilize in order to observe Jahn-Teller distortions in a diamagnetic molecule?
4. What spectroscopic method(s) would one utilize in order to observe Jahn-Teller distortions in a paramagnetic molecule?
5. Why are Jahn-Teller effects most prevalent in inorganic (transition metal) compounds?

Answers

1. Complexes with d^3 electron configurations do not show Jahn-Teller distortions because there is no ground state degeneracy.
2. Yes. Examining the d^5 electron configuration, one finds that the high spin scenario contains all singly occupied d orbitals (no degeneracy). However, the low spin d^5 electron configuration shows degeneracy, which then leads to possible Jahn-Teller effects.
3. UV-VIS absorption spectroscopy is one of the most common techniques for observing these effects. In general, it is independent of magnetism (diamagnetic v. paramagnetic). Thus, one would see the effect in the spectrum of UV-VIS absorption analysis. Note that EPR requires at least one unpaired electron, and therefore not EPR active.
4. Inorganic, specifically transition metal, complexes are most prevalent in showing Jahn-Teller distortions due to the availability of d orbitals. The most common geometry that the Jahn-Teller effect is observed is in octahedral complexes (see **Figures 2, 4, 5** and **6** above) due to the splitting of d orbitals into two degenerate sets. Due to stabilization, the degeneracies are removed, making a lower symmetry and lower energy molecule.

5. In addition to UV-VIS absorption, one can also employ EPR spectroscopy if a molecule possesses and unpaired electron.

9.3: Jahn-Teller Distortions is shared under a CC BY-NC-SA 4.0 license and was authored, remixed, and/or curated by Kamran Ghiassi & Robert Lancashire.

9.4: Factors That Affect Crystal Field Splitting

Magnitude of Crystal Field Splitting

The magnitude of the crystal field splitting (Δ) dictates whether a complex with four, five, six, or seven d electrons (in an octahedral complex) is high spin or low spin, which affects its magnetic properties, structure, and reactivity. Large values of Δ (i.e., Δ > P) yield a low-spin complex, whereas small values of Δ (i.e., Δ < P) produce a high-spin complex. The magnitude of Δ depends on four factors: the valence of the metal, the principal quantum number of the metal (and thus its location in the periodic table), the geometry, and the nature of the ligand(s). Values of Δ for some representative transition metal complexes are given in Table **9.4.1**.

Table **9.4.1**: Crystal Field Splitting Energies for Some Octahedral (Δ_o)* and Tetrahedral (Δ_t) Transition-Metal Complexes

Octahedral Complexes	Δ_o (cm^{-1})	Octahedral Complexes	Δ_o (cm^{-1})	Tetrahedral Complexes	Δ_t (cm^{-1})
$[Ti(H_2O)_6]^{3+}$	20,300	$[Fe(CN)_6]^{4-}$	32,800	VCl_4	9010
$[V(H_2O)_6]^{2+}$	12,600	$[Fe(CN)_6]^{3-}$	35,000	$[CoCl_4]^{2-}$	3300
$[V(H_2O)_6]^{3+}$	18,900	$[CoF_6]^{3-}$	13,000	$[CoBr_4]^{2-}$	2900
$[CrCl_6]^{3-}$	13,000	$[Co(H_2O)_6]^{2+}$	9300	$[CoI_4]^{2-}$	2700
$[Cr(H_2O)_6]^{2+}$	13,900	$[Co(H_2O)_6]^{3+}$	27,000		
$[Cr(H_2O)_6]^{3+}$	17,400	$[Co(NH_3)_6]^{3+}$	22,900		
$[Cr(NH_3)_6]^{3+}$	21,500	$[Co(CN)_6]^{3-}$	34,800		
$[Cr(CN)_6]^{3-}$	26,600	$[Ni(H_2O)_6]^{2+}$	8500		
$Cr(CO)_6$	34,150	$[Ni(NH_3)_6]^{2+}$	10,800		
$[MnCl_6]^{4-}$	7500	$[RhCl_6]^{3-}$	20,400		
$[Mn(H_2O)_6]^{2+}$	8500	$[Rh(H_2O)_6]^{3+}$	27,000		
$[MnCl_6]^{3-}$	20,000	$[Rh(NH_3)_6]^{3+}$	34,000		
$[Mn(H_2O)_6]^{3+}$	21,000	$[Rh(CN)_6]^{3-}$	45,500		
$[Fe(H_2O)_6]^{2+}$	10,400	$[IrCl_6]^{3-}$	25,000		
$[Fe(H_2O)_6]^{3+}$	14,300	$[Ir(NH_3)_6]^{3+}$	41,000		

*Energies obtained by spectroscopic measurements are often given in units of wave numbers (cm^{-1}); the wave number is the reciprocal of the wavelength of the corresponding electromagnetic radiation expressed in centimeters: 1 cm^{-1} = 11.96 J/mol.

Source of data: Duward F. Shriver, Peter W. Atkins, and Cooper H. Langford, Inorganic Chemistry, 2nd ed. (New York: W. H. Freeman and Company, 1994).

Valence of the metal

Increasing the valence of a metal ion has two effects: the radius of the metal decreases and ligands are more strongly attracted to it due to Coulombic attraction. Both factors decrease the metal–ligand distance, which in turn causes the ligands to interact more strongly with the d-orbitals. Consequently, the magnitude of Δ_o increases as the valence of the metal increases. Typically, Δ_o for a M(III) is about 50% greater than for the M(II) of the same metal; for example, for $[V(H_2O)_6]^{2+}$, Δ_o = 11,800 cm^{-1}; for $[V(H_2O)_6]^{3+}$, Δ_o = 17,850 cm^{-1}.

Principal quantum number of the metal

For a series of complexes of metals from the same group in the periodic table with the same charge and the same ligands, the magnitude of Δ_o increases with increasing principal quantum number: Δ (3d) < Δ (4d) < Δ (5d). The data for hexaammine complexes of the trivalent Group 9 metals illustrate this point:

$$[Co(NH_3)_6]^{3+}: \Delta_o = 22{,}900\ cm^{-1}$$

$$[Rh(NH_3)_6]^{3+}: \Delta_o = 34{,}100\ cm^{-1}$$

$$[Ir(NH_3)_6]^{3+}: \Delta_o = 40{,}000\ cm^{-1}$$

The increase in Δ with increasing principal quantum number is due to the larger radial extension of the d orbitals as n increases. In addition, repulsive ligand–ligand interactions are most important for smaller metal ions. Relatively speaking, this results in shorter M–L distances and stronger d orbital–ligand interactions. The increase in Δ going from 3d to 4d and 5d is so large that all 4d and 5d metals will form low spin complexes.

Geometry of the complex

The number of ligands in a complex as well as how well the ligand geometry overlaps with the d orbitals is also a factor in the magnitude of the crystal field splitting. For example, comparing octahedral and tetrahedral geometries the octahedral geometry has 6 ligands, and those 6 ligands overlap directly with the two d orbitals that lie along the axes, $d_{x^2-y^2}$ and d_{z^2}. The tetrahedral geometry has fewer ligands than octahedral, and those ligands overlap less ideally with the ligands that lie between the axes, d_{xy}, d_{xz}, and d_{yz}. Because of this the crystal field splitting of a tetrahedral complex is generally less than half ($\frac{4}{9}$ than an octahedral complex with the same metal and ligands. For example $[FeCl_4]^-$ has a $\Delta_t = 5{,}200\ cm^{-1}$ and $[FeCl_6]^{3-}$ has a $\Delta_o = 11{,}600\ cm^{-1}$.

Nature of the ligands

In crystal field theory ligands are all modeled as negative point charges, which means that all ligands should behave identically. Experimentally, it is found that the Δ_o observed for a series of complexes of the same metal ion depends strongly on the nature of the ligands. For a series of chemically similar ligands, the magnitude of Δ_o decreases as the size of the donor atom increases. For example, Δ_o values for halide complexes generally decrease in the order F > Cl > Br > I because smaller, more localized charges, such as we see for F, interact more strongly with the d-orbitals of the metal. In addition, a small neutral ligand with a highly localized lone pair, such as NH_3, results in significantly larger Δ_o values than might be expected. Because the lone pair points directly at the metal ion, the electron density along the M–L axis is greater than for a spherical anion such as F. The experimentally observed order of the crystal field splitting energies produced by different ligands is called the spectrochemical series.

Ligands are classified as strong field or weak field based on the spectrochemical series:

weak field $I^- < Br^- < Cl^- < \underline{S}CN^- < F^- < OH^- < ox^{-2} < \underline{O}NO < H_2O < SC\underline{N}^- < NH_3 <$ en $< \underline{N}O_2 < CN^-$, CO strong field

Note that SCN and NO_2 ligands are represented twice in the above spectrochemical series since there are two different Lewis base sites (e.g., free electron pairs to share) on each ligand (e.g., for the SCN ligand, the electron pair on the sulfur or the nitrogen can form the bond to a metal). The specific atom that binds in such ligands is underlined. Ligands on the weak field end of the series (halogens, OH, H_2O) will tend to form high spin complexes and ligands on the strong field end of the series (CN, CO, NO_2) will tend to form low spin complexes. Intermediate ligands in the midle of the series could form high or low spin complexes depending on other factors.

How to determine if a complex is high or low spin

1. How many d electrons does the complex have?
   - Only complexes with 4-7 d electrons have high spin and low spin configurations
2. What period is the metal?
   - 3d metals could either be high or low spin
   - 4d and 5d metals will ALWAYS be low spin
3. What is the geometry of the complex?
   - Tetrahedral complexes with 3d metals will almost always be high spin because Δt is generally less than spin pairing energy

- Square planar complexes will almost always be low spin because they are favored over tetrahedral when crystal field splitting is large
- Octahedral complexes could be either high or low spin

4. What are the ligands?
   - Strong field ligands will form low spin complexes
   - Weak field ligands will form high spin complexes
   - Intermediate field ligands could form high or low spin complexes. Additional information (like number of unpaired electrons) is needed

- Adapted by Catherine McCusker (East Tennessee State University)

9.4: Factors That Affect Crystal Field Splitting is shared under a CC BY-NC-SA 4.0 license and was authored, remixed, and/or curated by LibreTexts.

9.5: Ligand Field Theory

Extension of Crystal Field Theory

Experimentally it is known that the nature of the ligand plays an important role in the magnitude of the crystal field splitting in metal complexes and can determine whether a complex is high or low spin. Empirically ligands can be ordered in the spectrochemical series, but using crystal field theory we cannot rationalize where ligands fall in the series. For example, why is the neutral CO one of the strongest field ligands in the series while the anionic halogens are weak field ligands? To understand why ligands behave differently we have to consider how ligand orbitals interact with the metal d orbitals. Ligand field theory is essentially a combination between crystal field theory and molecular orbital theory where we focus only on the orbital overlap between the metal d orbitals and select ligand orbitals (rather than considering all of the valence orbitals on both the metal and ligand)

Metal-Ligand σ Bonding

The bond between a metal and a ligand is primarily a Lewis acid-base interaction where the ligand is a Lewis base and donates a pair of electron to the metal, the Lewis acid. This interaction forms a coordinate covalent bond. As with molecular orbital theory we have to decide how (or if) the ligand lone pairs will overlap with each of the d orbitals, and what type of bonding will be formed In an octahedral complex the ligands and their lone pairs lie along the x, y, and z axes. As shown in Figure **9.5.1**, the two on axis d orbitals ($d_{x^2-y^2}$ and d_{z^2}) have to correct orientation to form sigma bonds with the ligands. With the three off axis d orbitals (d_{xy}, d_{xz}, and d_{yz}) the ligand lone pair overlaps with a node in these orbitals (Figure **9.5.1***c*). This means there is no net overlap and no bonding (or antibonding) molecular orbital can be formed.

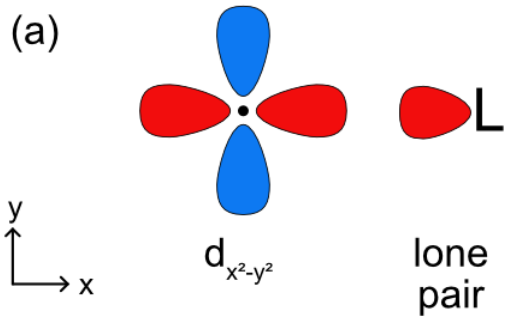


Figure **9.5.1*a***: Overlap between a ligand lone pair orbital and the metal $d_{x^2-y^2}$ orbital to form a sigma bond (CC BY-NC-SA, Catherine McCusker)

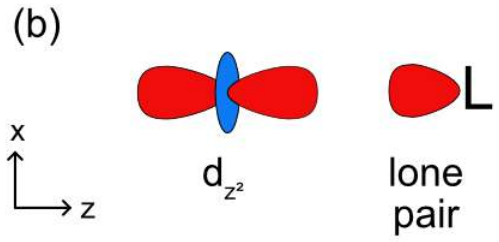


Figure **9.5.1*b***: Overlap between a ligand lone pair orbital and the metal d_{z^2} orbital to form a sigma bond (CC BY-NC-SA, Catherine McCusker)

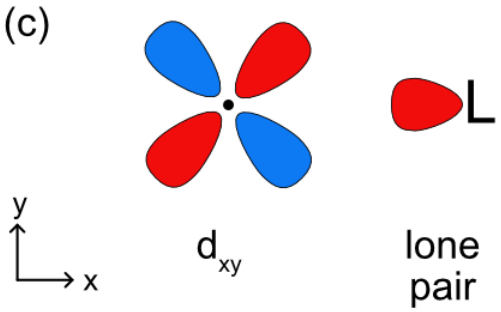


Figure **9.5.1*c***: There is no net overlap between the ligand lone pair orbital and the d_{xy} metal orbital, so this is a non bonding interaction (CC BY-NC-SA, Catherine McCusker)

Knowing this, we can construct a ligand field splitting diagram (a simplified molecular orbital diagram) (Figure **9.5.2**). In the free metal ion all 5 of the d orbitals are degenerate and before they interact with the metal all 6 of the ligand lone pair orbitals are at the same energy as well. Generally, based on electronegativity the ligand lone pair orbitals will be lower in energy than the metal d orbitals. When the ligand lone pairs interact with metal d orbitals the on axis set of d orbitals ($d_{x^2-y^2}$ and d_{z^2}) will form sigma bonding (e_g) and sigma antibonding (e_g*) molecular orbitals. The off axis set of d orbitals are nonbonding and are not stabilized or destabilized by the ligand lone pairs. Unlike a complete molecular orbital diagrams, a ligand field diagram won't necessarily have the same number of molecular orbitals as atomic orbitals becuse not every possible bonding interaction is included (for example, any overlap between the ligand orbitals and the metal s and p orbitals are not included). As in crystal field theory we can define an octahedral ligand field splitting energy (Δ_o), which will be the difference between the two molecular orbitals with the most metal d orbital character. In Figure **9.5.2** the t_{2g} set of d orbitals are nonbonding and therefore 100% metal character. The e_g bonding orbital is closer in energy to the ligand lone pairs and will have a higher % contribution from the ligands, and the e_g* antibonding orbital is closer in energy to the metal d orbitals and will have a higher % contribution from the metal. The relevant energy difference is between the t_{2g} and e_g* orbitals, as highlighted in green in Figure **9.5.2**. The splitting energy will increase as there is a stronger interaction between the metal and ligand orbitals (based on the criteria discussed previously) and the e_g* is more destabilized.

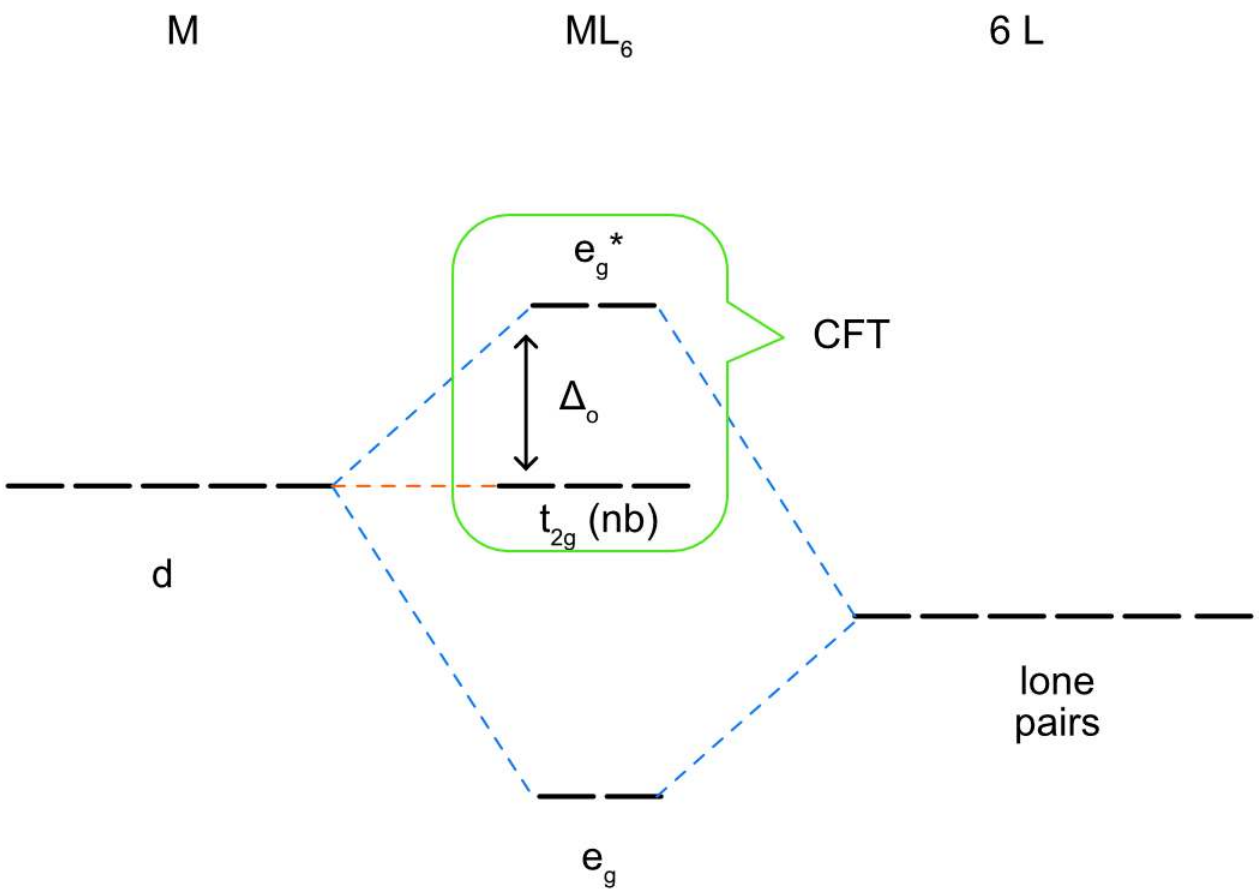


Figure **9.5.2**: Octahedral ligand field splitting diagram for only sigma bonding. The $d_{x^2-y^2}$ and d_{z^2} metal orbitals form sigma bonding (e_g) and antibonding molecular orbitals (e_g*). The d_{xy}, d_{xz}, and d_{yz} orbital are nonbonding (t_{2g} (nb)). The green outline highlights the portion of the diagram that is equivalent to the crystal field splitting diagram. (CC BY-NC-SA; Catherine McCusker)

Metal-Ligand π Bonding

In addition to sigma bonding, some ligands have orbitals available which can form π bonds with metals as well. These could include p orbitals on a single donor atom such as a halogen ion or π bonding or antibonding molecular orbitals on a molecular ligand. To determine how π bonding will change the ligand field splitting picture in Figure **9.5.2**, we will visualize how a ligand p orbital will interact with the metal d orbitals. The $d_{x^2-y^2}$ and d_{z^2} orbitals do not have the correct symmetry to form any type of bond with a ligand p orbital as shown in Figures **9.5.3***a* – *b* The d_{xy}, d_{xz}, and d_{yz} orbitals all have the correct symmetry to form π bonds with a ligand p orbital (Figure **9.5.3***c*).

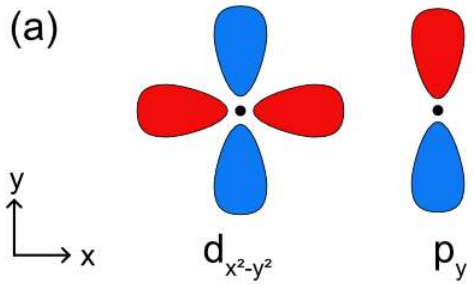


Figure 9.5.3*a*: There is no net overlap between the ligand p orbital and the $d_{x^2-y^2}$ metal orbital, so this is a non bonding interaction (CC BY-NC-SA, Catherine McCusker)

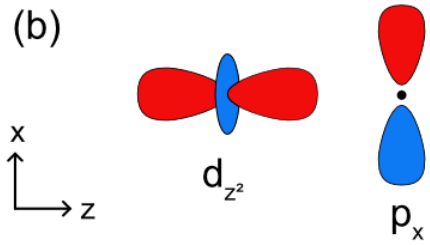


Figure 9.5.3*b*: There is no net overlap between the ligand p orbital and the d_{z^2} metal orbital, so this is a non bonding interaction (CC BY-NC-SA, Catherine McCusker)

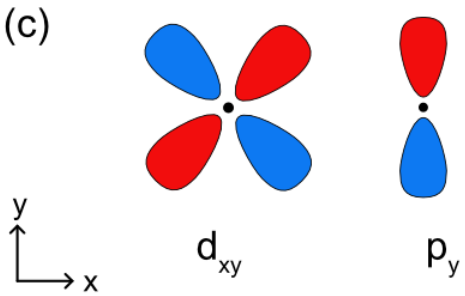


Figure 9.5.3*c*: Overlap between a ligand p orbital and the metal d_{xy} orbital to form a π bond (CC BY-NC-SA, Catherine McCusker)

Unlike metal-ligand σ bonding, where electrons are always donated from the ligand to the metal, electrons in metal-ligand π bonding can be donated from either the metal or the ligand depending on the nature of the orbitals involved. In cases where ligands have empty p or π symmetry orbitals that are close in energy to the metal d orbitals, they can accept electrons from a filled metal orbital. This is also known as π backbonding because the direction of electron donation is opposite of that found in sigma metal ligand bonding. These ligands are called π acceptor ligands. In cases where ligands have filled p or π symmetry orbitals that are close in energy to the metal d orbitals, they can donate electrons to an empty metal orbital. These ligands are called π donor ligands.

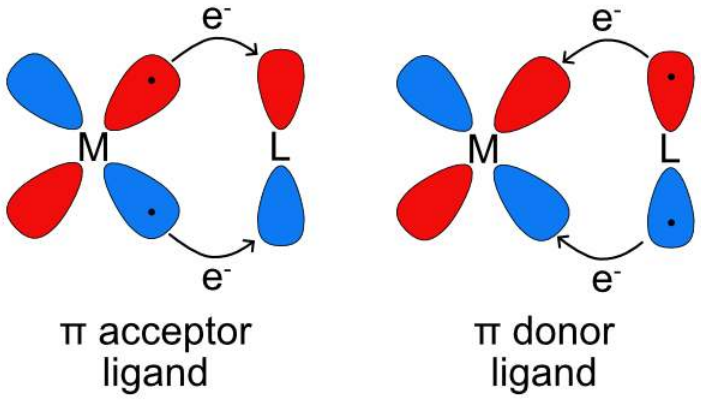


Figure **9.5.4**: Illustration of metal-ligand π bonding with π acceptor and donor ligands. Filled orbitals are represented with black dots. (CC BY-NC-SA, Catherine McCusker)

π Acceptors

Ligands that are π acceptors have empty, low energy π symmetry orbitals available to accept electrons from the metal center. Most often this is a π^* antibonding molecular orbital but it could also be an empty p orbital. Due to the aufbau principle, these empty orbitals will be higher in energy than any filled lone pairs on the ligands and will also generally be higher energy than the metal d orbitals. Similar to multiple bonding in main group compounds π bonding always occurs in combination with sigma bonding so in the ligand field splitting diagram of metal-ligand bonding with a π acceptor ligand the lone pairs for sigma bonding must be included as well as the empty orbitals for π bonding. As seen in Figure **9.5.3**, the $d_{x^2-y^2}$ and d_{z^2} orbitals do not overlap with the ligand p orbitals. The on axis d orbitals will form sigma bonding (e_g) and sigma antibonding (e_g^*) molecular orbitals. Unlike the sigma bonding only diagram, the off axis d orbitals (d_{xy}, d_{xz}, and d_{yz}) overlap with the ligand p orbitals to form π bonding (t_{2g}) and π antibonding (t_{2g}^*) molecular orbitals as seen in Figure **9.5.5**. Rather than being nonbonding, like in the sigma bonding only picture, the metal based t_{2g} molecular orbital is bonding. This increases the energy difference between the t_{2g} and e_g^* and therefore increases Δ_o.

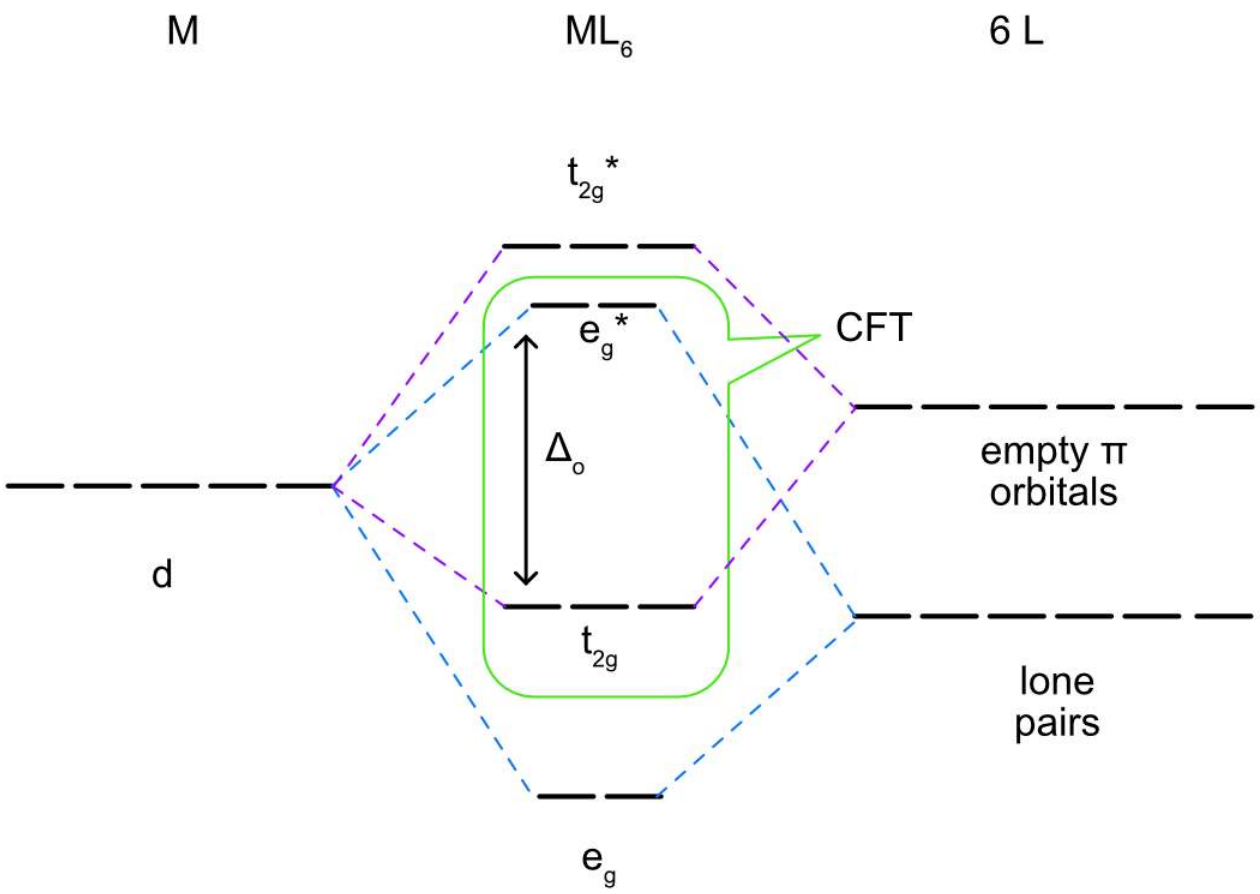


Figure 9.5.5: Octahedral ligand field splitting diagram with a π acceptor ligand. The $d_{x^2-y^2}$ and d_{z^2} metal orbitals form sigma bonding (e_g) and antibonding molecular orbitals (e_g*) with the ligand lone pairs. The d_{xy}, d_{xz}, and d_{yz} orbital form pi bonding (t_{2g}) and pi antibonding molecular orbitals (t_{2g}*) with the empty π symmetry orbitals. The green outline highlights the portion of the diagram that is equivalent to the crystal field splitting diagram. (CC BY-NC-SA; Catherine McCusker)

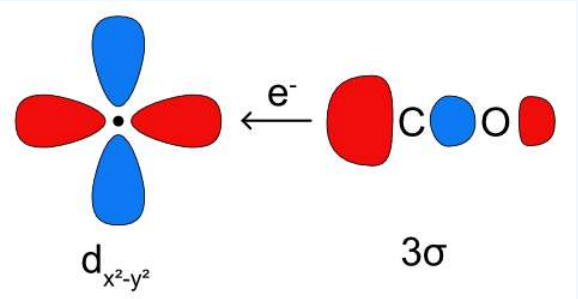
Exercise 9.5.1

Carbon monoxide is one of the most common, and strongest π acceptor ligands in inorganic chemistry. Refer to the molecular orbital diagram of CO and sketch likely metal-ligand orbital interactions for both sigma and pi bonding in a metal-CO complex. Indicate the direction of electron donation in both cases.

Answer

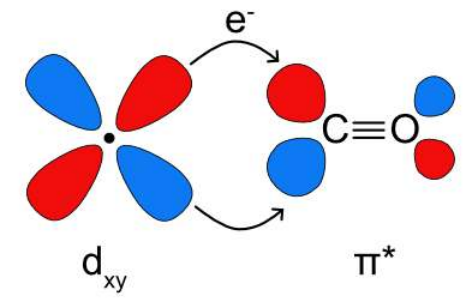
Sigma bonding:

Sigma bonding between a metal ion and a CO ligand involves overlap between the HOMO of CO (3σ) and the metal $d_{x^2-y^2}$ or d_{z^2} orbitals. Electrons are donated from the ligand to the metal.



Pi bonding:

Pi bonding between a metal ion and CO ligand involves overlap between the LUMO of CO (π^*) and the metal d_{xy}, d_{xz}, or d_{yz} orbitals. Electrons are donated from the metal to the ligand.



π Donor Ligands

Ligands that are π donors have filled π symmetry orbitals that are high enough in energy to donate electrons to the metal center. Most often this is a filled p orbital, but it could also be a π bonding molecular orbital. As lone pairs are generally the highest occupied orbitals is a molecule, the filled π orbitals will be lower in energy as seen in Figure **9.5.6**. The sigma interaction between the ligand lone pairs and the metal $d_{x^2-y^2}$ and d_{z^2} remain the same as previously described, forming the e_g bonding and e_g* antibonding molecular orbitals. The d_{xy}, d_{xz}, and d_{yz} overlap with the filled π orbitals to form π bonding (t_{2g}) and π antibonding (t_{2g}*) molecular orbitals. The difference between the *pi* acceptor and donor ligands is the energy and character of the t_{2g} and t_{2g}* molecular orbitals. In the π acceptor case above, the t_{2g} orbital is above the e_g and has a higher contribution from the metal and the t_{2g}* is above the e_g* and has a higher contribution from the ligand. In the π donor case the opposite is true. The t_{2g} orbital is below the e_g and has a higher contribution from the ligand and the t_{2g}* is below the e_g* and has a higher contribution from the metal. In this case Δ_o is smaller than in the sigma only picture because the t_{2g} symmetry molecular orbital has gone from nonbonding to antibonding and the energy difference between t_{2g}* and e_g* is smaller.

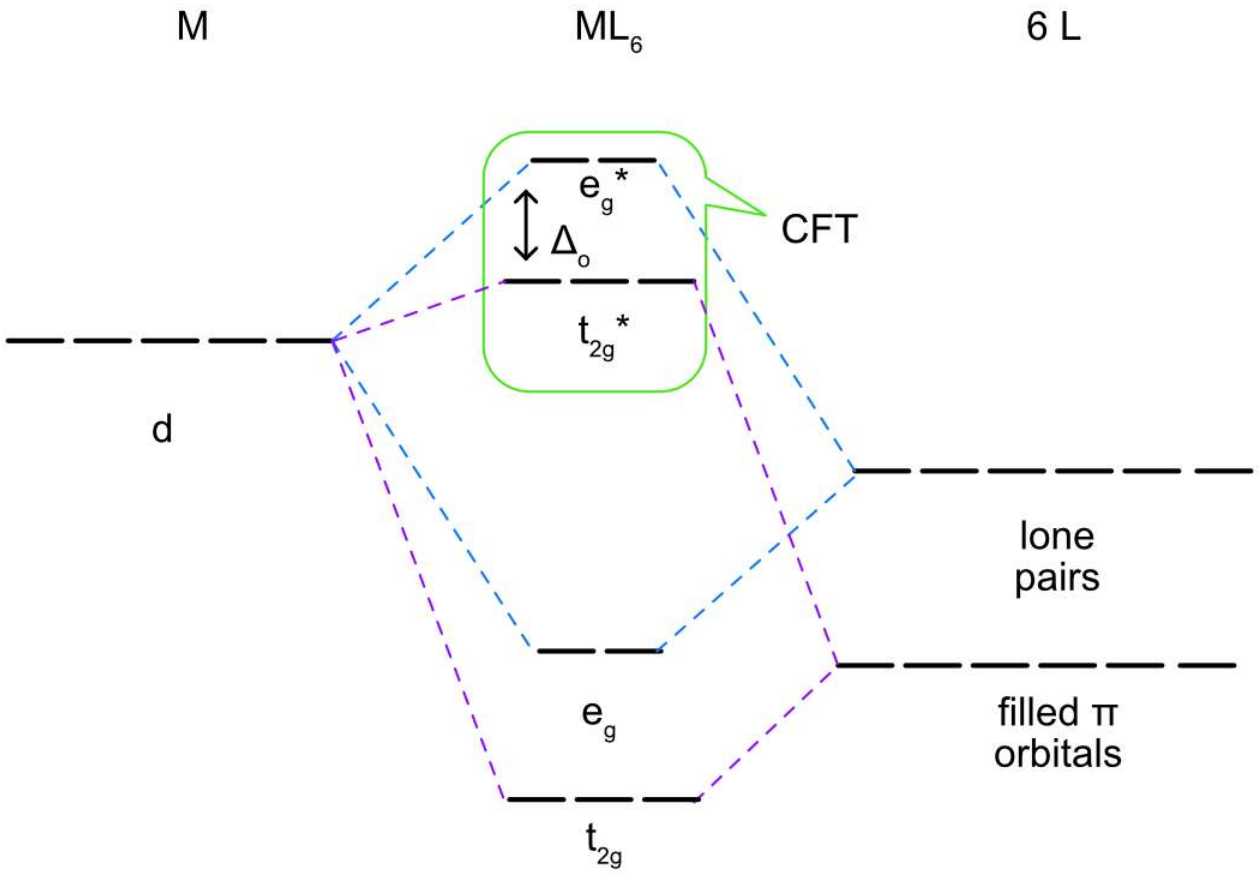


Figure **9.5.6**: Octahedral ligand field splitting diagram with a π donor ligand. The $d_{x^2-y^2}$ and d_{z^2} metal orbitals form sigma bonding (e_g) and antibonding molecular orbitals (e_g*) with the ligand lone pairs. The d_{xy}, d_{xz}, and d_{yz} orbital form pi bonding (t_{2g}) and pi antibonding molecular orbitals (t_{2g}*) with the filled π symmetry orbitals. The green outline highlights the portion of the diagram that is equivalent to the crystal field splitting diagram. (CC BY-NC-SA; Catherine McCusker)

The Spectrochemical Series

As discussed above, crystal field theory alone can't distinguish the behaviors of different ligands or explain why some ligands inherently produce larger splittings than others. Armed with ligand field theory we can now revisit the spectrochemical series and explain why ligands fall where they do within the series.

Strong field ligands

Strong field ligands are ones that produce large splittings between the d orbitals and form low spin complexes. Examples of strong field ligands include CO, CN^-, and NO_2. From a ligand field theory perspective all three of these ligands have strong π bonds (either double or triple bonds) and have empty π* molecular orbitals available for backbonding. Strong field ligands are both sigma donors (all ligands are sigma donors) and π acceptors. π backbonding between a metal and a ligand stabilizes the metal based t_{2g} molecular orbital and increases Δ_o.

Weak field ligands

Weak field ligands are ones that produce small splittings between the d orbitals and form high spin complexes. Examples of weak field ligands include the halogens, OH^- and H_2O. From a ligand field perspective these ions or molecules all have filled orbitals

which can π bond with the metal d orbitals. In the case of the halogens these are filled p orbitals and in the case of OH^- and H_2O these are lone pairs which are perpendicular to the metal-ligand bond. Weak field ligands are both sigma donors and π donors. The π donation from the ligand to the metal destabilizes the metal based t_{2g} molecular orbital and decreases Δ_o.

Intermediate field ligands

Intermediate field ligands produce intermediate splittings between the d orbitals and could form high or low spin complexes. Examples of intermediate field ligands include NH_3 or ethylenediamine (en). From a ligand field perspective these ligands only have a single lone pair available for sigma bonding. All of the other orbitals on nitrogen are used for sigma bonding to the H or C atoms within the molecule. Intermediate ligands are those which are only sigma donors, and are not π donors or π acceptors. In this case the t_{2g} symmetry d orbitals are nonbonding and the Δ_o is determined by the strength of the metal ligand sigma interaction (and amount of destabilization of the e_g* molecular orbital)

This page titled 9.5: Ligand Field Theory is shared under a CC BY-NC-SA 4.0 license and was authored, remixed, and/or curated by Catherine McCusker.

CHAPTER OVERVIEW

10: Coordination Chemistry- Reactions and Mechanisms

Learning Objectives

- Determine whether an metal ion will be labile or inert.
- Use kinetic data to determine if a ligand substitution occurs by an associative or dissociative mechanism
- Predict the product of a square planar ligand substitution reaction based on the trans effect and trans influence
- Explain the difference between and inner sphere and outer sphere electron transfer reaction

Thumbnail image shows the structure of the Creutz-Taube complex used to study inner sphere electron transfer reactions (CC0, Jynto via Wikimedia Commons)

10.1: Thermodynamic Stability of Metal Complexes

10.2: Trends in Kinetic Lability

10.3: Ligand Substitution Mechanisms

10.4: The Trans Effect

10.5: Electron Transfer Reactions

10: Coordination Chemistry- Reactions and Mechanisms is shared under a CC BY-NC-SA 4.0 license and was authored, remixed, and/or curated by LibreTexts.

10.1: Thermodynamic Stability of Metal Complexes

Chelate Complexes

As seen in Chapter 8, ligands like chloride, water, and ammonia are monodentate More complex ligands can, however, be bidentate, tridentate, or, in general, polydentate Ethylenediamine ($H_2NCH_2CH_2NH_2$, often abbreviated as en) and diethylenetriamine ($H_2NCH_2CH_2NHCH_2CH_2NH_2$, often abbreviated as dien) are examples of a bidentate and a tridentate ligand, respectively, because each nitrogen atom has a lone pair that can be shared with a metal ion. When a bidentate ligand such as ethylenediamine binds to a metal such as Ni^{2+}, a five-membered ring is formed. A metal-containing ring like that shown is called a chelate ring. Correspondingly, a polydentate ligand is a chelating agent, and complexes that contain polydentate ligands are called chelate complexes.



A chelate complex

Experimentally, it is observed that metal complexes of polydentate ligands are significantly more stable than the corresponding complexes of chemically similar monodentate ligands; this increase in stability is called the chelate effect. For example, the complex of Ni^{2+} with three ethylenediamine ligands, $[Ni(en)_3]^{2+}$, should be chemically similar to the Ni^{2+} complex with six ammonia ligands, $[Ni(NH_3)_6]^{2+}$. In fact, the equilibrium constant for the formation of $[Ni(en)_3]^{2+}$ is almost 10 orders of magnitude larger than the equilibrium constant for the formation of $[Ni(NH_3)_6]^{2+}$ (Table E4):

$$[Ni(H_2O)_6]^{2+} + 6NH_3 \rightleftharpoons [Ni(NH_3)_6]^{2+} + 6H_2O(l) \quad K_f = 4 \times 10^8 \tag{10.1.1}$$

$$[Ni(H_2O)_6]^{2+} + 3en \rightleftharpoons [Ni(en)_3]^{2+} + 6H_2O(l) \quad K_f = 2 \times 10^{18} \tag{10.1.2}$$

The formation constants are formulated as ligand exchange reactions with aqua ligands being displaced by new ligands (NH_3 or en) in the examples above.

> *Chelate complexes are more stable than the analogous complexes with monodentate ligands.*

The stability of a chelate complex depends on the size of the chelate rings. For ligands with a flexible organic backbone like ethylenediamine, complexes that contain five-membered chelate rings, which have almost no strain, are significantly more stable than complexes with six-membered chelate rings, which are in turn much more stable than complexes with four- or seven-membered rings. For example, the complex of nickel (II) with three ethylenediamine ligands is about 363,000 times more stable than the corresponding nickel (II) complex with trimethylenediamine ($H_2NCH_2CH_2CH_2NH_2$, abbreviated as tn):

$$[Ni(H_2O)_6]^{2+} + 3en \rightleftharpoons [Ni(en)_3]^{2+} + 6H_2O(l) \quad K_f = 6.76 \times 10^{17} \tag{10.1.3}$$

$$[Ni(H_2O)_6]^{2+} + 3tn \rightleftharpoons [Ni(tn)_3]^{2+} + 6H_2O(l) \quad K_f = 1.86 \times 10^{12} \tag{10.1.4}$$

*The above measurements were done in a solution of ionic strength 0.15 at 25° C.

Example 10.1.1

Arrange $[Cr(en)_3]^{3+}$, $[CrCl_6]^{3-}$, $[CrF_6]^{3-}$, and $[Cr(NH_3)_6]^{3+}$ in order of increasing stability.

Given: four Cr(III) complexes

Asked for: relative stabilities

Strategy:

A Determine the relative basicity of the ligands to identify the most stable complexes.

B Decide whether any complexes are further stabilized by a chelate effect and arrange the complexes in order of increasing stability.

Solution

A The metal ion is the same in each case: Cr^{3+}. Consequently, we must focus on the properties of the ligands to determine the stabilities of the complexes. Because the stability of a metal complex increases as the basicity of the ligands increases, we need to determine the relative basicity of the four ligands. Our earlier discussion of acid–base properties suggests that ammonia and ethylenediamine, with nitrogen donor atoms, are the most basic ligands. The fluoride ion is a stronger base (it has a higher charge-to-radius ratio) than chloride, so the order of stability expected due to ligand basicity is

$$[CrCl_6]^{3-} < [CrF_6]^{3-} < [Cr(NH_3)_6]^{3+} \approx [Cr(en)_3]^{3+}.$$

B Because of the chelate effect, we expect ethylenediamine to form a stronger complex with Cr^{3+} than ammonia. Consequently, the likely order of increasing stability is

$$[CrCl_6]^{3-} < [CrF_6]^{3-} < [Cr(NH_3)_6]^{3+} < [Cr(en)_3]^{3+}.$$

Exercise 10.1.1

Arrange $[Co(NH_3)_6]^{3+}$, $[CoF_6]^{3-}$, and $[Co(en)_3]^{3+}$ in order of decreasing stability.

Answer: $[Co(en)_3]^{3+} > [Co(NH_3)_6]^{3+} > [CoF_6]^{3-}$

The Chelate Effect

The chelate effect can be seen by comparing the reaction of a chelating ligand and a metal ion with the corresponding reaction involving comparable monodentate ligands. For example, comparison of the binding of 2,2'-bipyridine with pyridine or 1,2-diaminoethane (ethylenediamine=en) with ammonia. It has been known for many years that a comparison of this type always shows that the complex resulting from coordination with the chelating ligand is **much more thermodynamically stable**. This can be seen by looking at the values for adding two monodentates compared with adding one bidentate, or adding four monodentates compared to two bidentates, or adding six monodentates compared to three bidentates.

> *The Chelate Effect is that complexes resulting from coordination with the chelating ligand is much more thermodynamically stable than complexes with non-chelating ligands.*

A number of points should be highlighted from the formation constants in Table E4. In Table **10.1.1**, it can be seen that the ΔH° values for the formation steps are almost identical, that is, heat is evolved to about the same extent whether forming a complex involving monodentate ligands or bidentate ligands. What is seen to vary significantly is the ΔS° term which changes from negative (unfavorable) to positive (favorable). Note as well that there is a dramatic increase in the size of the ΔS° term for adding two compared to adding four monodentate ligands. (-5 to -35 $JK^{-1}mol^{-1}$). What does this imply, if we consider ΔS° to give a measure of disorder?

In the case of complex formation of Ni^{2+} with ammonia or 1,2-diaminoethane, by rewriting the equilibria, the following equations are produced.

$$\begin{array}{lcl} [Ni(H_2O)_6]^{2+} + 6\,NH_3 \overset{\beta_6}{\Leftrightarrow} [Ni(NH_3)_6]^{2+} + 6\,H_2O & & \textbf{1f} \\ [Ni(NH_3)_6]^{2+} \Leftrightarrow [Ni(H_2O)_6]^{2+} + 6\,NH_3 & & \textbf{1d} \\ [Ni(H_2O)_6]^{2+} + 3\,en \overset{\beta_3}{\Leftrightarrow} [Ni(en)_3]^{2+} + 6\,H_2O & & \textbf{2f} \\ \hline [Ni(NH_3)_6]^{2+} + 3\,en \Leftrightarrow [Ni(en)_3]^{2+} + 6NH_3 & & \textbf{3} \end{array}$$

Using the equilibrium constant for the reaction (3 above) where the *three* bidentate ligands replace the *six* monodentateligands, we find that at a temperature of 25° C:

$$\Delta G° = -2.303\,RT\,\log_{10} K \tag{10.1.5}$$

$$= -2.303\,RT\,(18.28 - 8.61) \tag{10.1.6}$$

$$= -54\ \text{kJ mol}^{-1} \tag{10.1.7}$$

Based on measurements made over a range of temperatures, it is possible to break down the $\Delta G°$ term into the enthalpy and entropy components.

$$\Delta G^\circ = \Delta H^\circ - T\Delta S^\circ \tag{10.1.8}$$

The result is that: $\Delta H^\circ = -29 kJ mol^{-1}$

$$- T\Delta S^\circ = -25 \text{ kJ mol}^{-1}$$
and at 25C (298K)
$$\Delta S^\circ = +88 \text{ J K}^{-1} \text{ mol}^{-1}$$

Caution

For many years, these numbers have been **incorrectly recorded** in textbooks. For example, the third edition of "Basic Inorganic Chemistry" by F.A. Cotton, G. Wilkinson and P.L. Gaus, John Wiley & Sons, Inc, 1995, on page 186 gives the values as:

$$\Delta G^\circ = -67 \text{ kJ mol}^{-1}$$
$$\Delta H^\circ = -12 \text{ kJ mol}^{-1}$$
$$-T\Delta S^\circ = -55 \text{ kJ mol}^{-1}$$

The conclusion they drew from these incorrect numbers was that the chelate effect was essentially an entropy effect, since the $T\Delta S^\circ$ contribution was nearly 5 times bigger than ΔH°.

In fact, the breakdown of the ΔG° into ΔH° and $T\Delta S^\circ$ shows that the two terms are nearly equal (-29 and -25 kJ mol^{-1}, respectively) with the ΔH° term a little bigger! The entropy term found is still much larger than for reactions involving a non-chelating ligand substitution at a metal ion. How can we explain this enhanced contribution from entropy? One explanation is to count the number of species on the left and right hand side of the equation above.

It will be seen that on the left-hand-side there are 4 species, whereas on the right-hand-side there are 7 species, that is a net gain of 3 species occurs as the reaction proceeds. This can account for the increase in entropy since it represents an increase in the disorder of the system. An alternative view comes from trying to understand how the reactions might proceed. To form a complex with 6 monodentates requires 6 separate favorable collisions between the metal ion and the ligand molecules. To form the tris-bidentate metal complex requires an initial collision for the first ligand to attach by one arm but remember that the other arm is always going to be nearby and only requires a rotation of the other end to enable the ligand to form the chelate ring.

If you consider dissociation steps, then when a monodentate group is displaced, it is lost into the bulk of the solution. On the other hand, if one end of a bidentate group is displaced the other arm is still attached and it is only a matter of the arm rotating around and it can be reattached again. **Both** conditions favor the formation of the complex with bidentate groups rather than monodentate groups.

This page titled 10.1: Thermodynamic Stability of Metal Complexes is shared under a CC BY-NC-SA 4.0 license and was authored, remixed, and/or curated by Robert J. Lancashire.

10.2: Trends in Kinetic Lability

Introduction

Kinetics is a branch of chemistry that is concerned with the rates of chemical reactions. In this section, we will discuss the rates of metal-ligand (M-L) substitution reactions.

Let's start with some examples. In the table below are three examples of ligand substitution reactions of hexaaquo metal complexes to form hexaammine complexes. These reactions are nearly identical with the exception of the metal ion. The products are thermodynamically favored in all cases.

Reaction	Rate constant (k)	Labile or Inert
$[Ni(OH_2)]^{2+} + 6NH_3 \rightleftharpoons [Ni(NH_3)_6]^{2+}$	$k = 10^4 s^{-1}$	Labile (happens in < 1 min)
$[Cr(OH_2)]^{3+} + 6NH_3 \rightleftharpoons [Cr(NH_3)_6]^{3+}$	$k = 10^{-3} s^{-1}$	Inert (slow, takes hours)
$[Cu(OH_2)]^{2+} + 6NH_3 \rightleftharpoons [Cu(NH_3)_6]^{2+}$	$k = 10^8 s^{-1}$	Very Labile (happens in seconds)

Definitions

- **Labile** - Metal complexes that undergo "kinetically fast" substitution reactions are **labile**. These reactions usually happen in less than one minute.
- **Inert** - Metal complexes that undergo "kinetically slow" substitution reactions are **inert** or **non-labile**. These reactions usually take hours.
- **Intermediate** - Metal complexes that undergo "kinetically intermediate" substitution reactions are **intermediate**.

A common pitfall is to confuse the meaning of kinetic terms, like *labile* and *inert*, with thermodynamic terms, like *stable* and *unstable*. It is important to distinguish between kinetics and thermodynamics. For example, the complex $[Fe(H_2O)Cl]^{2+}$ has a large formation constant and is thermodynamically stable; yet it is also labile. On the other hand, the complex $[Co(NH_3)_6]^{3+}$ is unstable in acidic aqueous solution and decomposes spontaneously to $[Co(H_2O)_6]^{3+}$; yet it decomposes slowly because it is inert. It is good practice to distinguish between meanings by using terms such as "kinetically labile" or "kinetically inert" and "thermodynamically stable" and "thermodynamically unstable".

Reaction Coordinate Diagrams

One way to visualize chemical reactions is through reaction coordinate diagrams (Figure **10.2.1**). These diagrams illustrate the relative free energy of the reactants and products, when the free energy of the products is lower than the reactants ΔG_{rxn} is negative and the reaction is spontaneous. This is what determines thermodynamic stability. These diagrams also illustrate the changes in free energy as the reaction progresses from reactants to products. In the case of a single step, concerted reaction the reactants go through a higher energy transition state before (potentially) forming products. The free energy difference between the reactants and the transition state is the free energy of activation ($\Delta G^{\ddagger}$), which determines the rate of the reaction. A larger $\Delta G^{\ddagger}$ yields a slower reaction rate because fewer reactants have sufficient energy to form products. In cases where the reaction occurs in 2 steps an intermediate is formed. The step with the largest $\Delta G^{\ddagger}$ will be the slowest, rate determining step. The magnitude of $\Delta G^{\ddagger}$ is what determines kinetic lability.

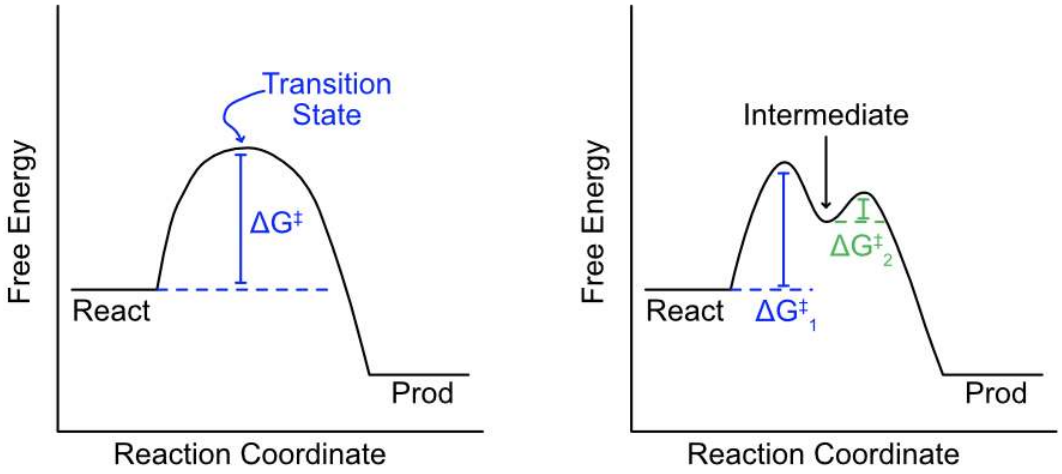


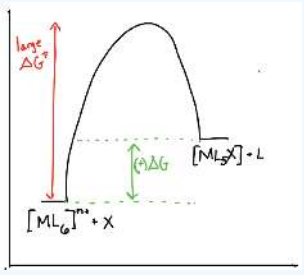
Figure **10.2.1**: Example reaction coordinate diagrams for a single step reaction (left) and a reaction with an intermediate (right). $\Delta G^{\ddagger}$ is the free energy of activation. (CC BY-NC-SA; Catherine McCusker)

Exercise 10.2.1

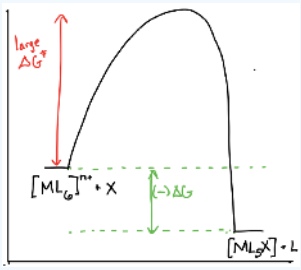
Draw the reaction coordinate diagrams for a reaction of the form $[ML_6]^{n+} + X \rightleftharpoons [ML_5X]^{n+} + L$ in the following scenarios:

a. $[ML_6]^{n+}$ is thermodynamically stable and kinetically inert.
b. $[ML_6]^{n+}$ is thermodynamically unstable and kinetically inert.
c. $[ML_6]^{n+}$ is thermodynamically stable and kinetically labile.
d. $[ML_6]^{n+}$ is thermodynamically unstable and kinetically labile.

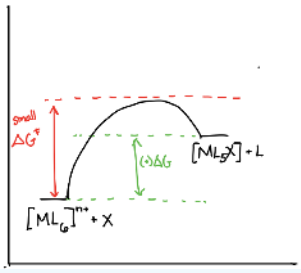
Answer a)



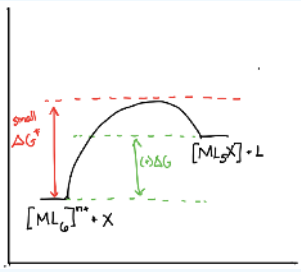
Answer b)



Answer c)



Answer d)



Self Exchange Reactions

$$[ML_5L]^{n+} + L \rightleftharpoons [ML_5L]^{n+} + L \tag{10.2.1}$$

The rate of a chemical reaction depends on both thermodynamic and kinetic factors. One way to isolate the kinetic factors is to study self exchange reactions. In a self exchange reaction the incoming and outgoing ligand are the same and the ΔG_{rxn} of the reaction is 0. In practice this is often done by dissolving hexaaqua metal complexes in isotopically labeled water and monitoring the ligand exchange reaction by NMR. These experiments have found reaction rates for different metals that span more than 12 orders of magnitude as shown in Figure 10.2.2.

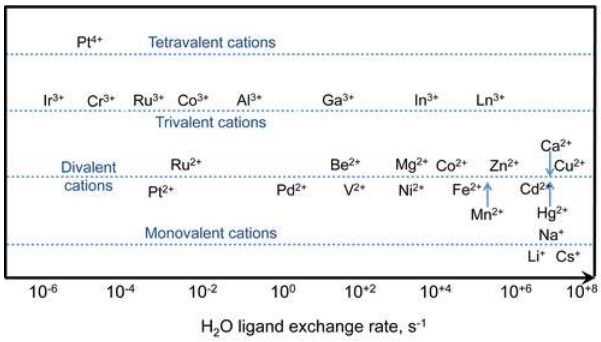


Figure 10.2.2: Water exchange rates measured by NMR for a series of metal ions. (CC BY-SA; Tem5psu via Wikimedia)

Factors that Affect Rates of Substitution Reactions

Some of the factors that affect rates of ligand substitution reactions are those that also affect thermodynamic stability. It is important to remember that kinetic and thermodynamic factors are related, yet separate. The same factors that make a complex stable can also make it more inert. However, it is incorrect to assume that stability is always correlated with reaction rates.

Why are kinetic factors related to thermodynamic stability? For a complex to react or exchange one ligand for another, it must change its geometry to form an intermediate or transition state. For example, inert octahedral complexes often have stable electron configurations. When the reactant electron configuration is particularly stable, it can result in a higher activation energy associated with moving away from the stable configuration.

Factors to consider

1. Electron configuration and LFSE: Electron configurations that place electrons in higher-energy orbitals (particularly antibonding orbitals) result in more labile complexes. As long as there are not electrons in higher-energy orbitals, the lability correlates roughly with LFSE. The more negative the LFSE, the more inert.
2. Size and charge of the metal ion: In general, higher charge density on the metal ion leads to stronger electrostatic attraction between metal and ligand; higher charge density generally correlates with slower rates of ligand substitution.

Taube's Observations of Substitution Rates

Henry Taube (Nobel Prize, 1983) tried to understand lability by comparing the factors that govern bond strengths in ionic complexes to observations about the rates of reaction of coordination complexes. He saw some things that were unsurprising. He also drew some new conclusions based on ligand field theory. Taube observed that many M^{+1} ions are more labile than many M^{+3} ions, in general. That isn't too surprising, since metal ions function as electrophiles or Lewis acids and ligands function as nucleophiles or Lewis bases in forming coordination complexes. In other words, metals with higher charges ought to be stronger Lewis acids, and so they should bind ligands more tightly. However, there were exceptions to that general rule. For example, Taube also observed that Mo^{+5} compounds are more labile than Mo^{+3} compounds. So, there must be more going on here than just the effects of electrostatic attraction.

Another factor that governs ionic bond strengths is the size of the ion. Typically, ions with smaller atomic radii form stronger bonds than ions with larger radii. Taube observed that Al^{3+}, V^{3+}, Fe^{3+} and Ga^{3+} ions are all about the same size. All these ions exchange ligands at about the same rate. That isn't surprising, because they have the same charge and the same radius. However, Cr^{3+} is also about the same size as those ions and it also has the same charge, but it is much less labile. Once again, there are exceptions to our regular expectations based on simple electrostatic considerations. Furthermore, 4d and 5d transition metals (Y→Cd, and Ac→Hg) are much more inert than 3d transition metals (Sc→Zn). This is unexpected when we consider size; the 4d and 5d metals are much larger than the 3d metals. This unexpected behavior tells us that electrostatics alone cannot predict lability.

Exercise 10.2.2

In which compound from each pair would you expect the strongest ionic bonds? Why?

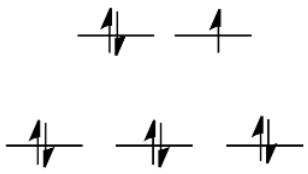
a) LiF vs KBr
b) $CaCl_2$ vs. KCl

Answer a

The ions in LiF are both smaller than in KBr, so the force of attraction between the ions in LiF is greater because of the smaller separation between the charges.

Answer b

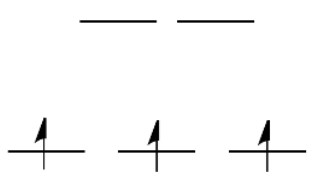
Calcium has a 2+ charge in $CaCl_2$, whereas potassium has only a + charge, so the chloride ions are more strongly attracted to the calcium than to the potassium.



Cu^{2+}

Taube came up with a hypothesis that could explain the seeming contradictory observations described above: *kinetic lability must be affected by d-electron configuration*. This idea forms the basis of Taube's rules about lability. For example, metals like Ni^{2+} and Cu^{2+} are very labile. The d orbital splitting diagrams for those compounds would have d electrons in the e_g set. Remember, the e_g

set arises from interaction with the ligand donor orbitals; this set corresponds to a σ antibonding level. By comparison, V^{2+} is rather inert. The d orbital splitting diagram in this case has electrons in the t_{2g} set, but none in the e_g set. So, having electrons in the higher energy, antibonding e_g level weakens the bond to the ligand, so the ligand can be replaced more easily. In the absence of those higher energy electrons, the bond to the ligand is stronger, and the ligand isn't replaced as easily.



V^{2+}

On the other hand, metals like Ca^{2+}, Sc^{3+} and Ti^{4+} are pretty labile. The d orbital splitting diagrams in those cases are pretty simple: there are no d-electrons at all in these ions. That means having no electrons in these mostly non-bonding levels leaves the complex susceptible to ligand replacement. But it's hard to see why population of an orbital that is mostly non-bonding would have an effect on ligand bond strength. Instead, this factor probably has something to do with the part of ligand substitution that we have ignored so far. Not only does one ligand need to leave, but a second one needs to bond in its place. So, having an empty orbital for the ligand to donate electrons into (or, put another way, not having electrons in the way that may complicate donation from the ligand) makes that part of the reaction easier.

Electron configurations can be generally classified as inert or labile based on crystal field stabilization energy. Configurations with high CFSE will be inert and configurations with low CFSE will be labile. Configurations that are most susceptible to Jahn-Teller distortions will be exceptionally labile, as the elongated bonds will be weaker and those ligands more easily exchanged.

Labile and inert electron configurations

Inert	Labile	Very labile
d^3, ls d^4, ls d^5, ls d^6,	d^1, d^2, hs d^5, hs d^6, hs d^7, d^{10}	hs d^4, d^9

Exercise 10.2.3

Put the metal ions in order of decreasing reaction rate (from labile to inert):

a) Al^{3+}, Na^{+}, Mg^{2+}

b) $Ca^{2+}, Mg^{2+}, Sr^{2+}$

Answer (a)

Most labile to most inert: $Na^{+} > Mg^{2+} > Al^{3+}$

These are metal ions with similar size and varying charge. They are in order of increasing charge and increasing density from left to right.

Answer (b)

Most labile to most inert: $Sr^{2+} > Ca^{2+} > Mg^{2+}$

These metal ions have the same charge, and vary in size. They are in order of decreasing charge and increasing charge density from left to right.

Exercise 10.2.4

Predict whether octahedral complexes of the following metals are labile or inert

a) Co^{3+} (high spin)

b) Co^{3+} (low spin)

c) Fe^{2+} (low spin)

d) Fe^{2+} (high spin)

e) Zn^{2+}

Answer a

hs d^6 labile (electrons in higher energy d orbital set)

Answer b

ls d^6 inert (all electrons in lower energy d orbitals)

Answer c

ls d^6 inert (all electrons in lower energy d orbitals)

Answer d

hs d^5 labile (electrons in higher energy d orbital set, CFSE = 0)

Answer e

d^{10} labile (electrons in higher energy d orbital set, CFSE = 0)

Overall Generalizations for Kinetics

1. s-block metals are very labile, except for those with very high charge density (eg. Mg^{2+} *is inert*)
2. d^{10} metals are labile (eg: Zn^{2+}, Cu^{+}, Hg^{2+})
3. Other ions with a full shell are labile (eg: La^{3+} of f-block)
4. 3d M^{2+}, *when high spin*, are generally labile (eg. Cu^{2+}*is very labile*)
5. 4d and 5d are usually inert due to higher CFSE (low spin, high CFSE)
6. M^{2+} is more labile than the same metal as M^{3+}
7. d^3 and low spin d^6 are inert (eg. Cr^{3+}, Co^{3+}, low spin Fe^{2+})

Attribution

Chris P Schaller, Ph.D., (College of Saint Benedict / Saint John's University)

Curated or created by Kathryn Haas

- Modified by Catherine McCusker (East Tennessee State University)

10.2: Trends in Kinetic Lability is shared under a not declared license and was authored, remixed, and/or curated by LibreTexts.

10.3: Ligand Substitution Mechanisms

Ligand Substitution Reactions

Ligand substitution is one of the simplest reactions a metal complex may undergo. In general, ligand substitution involves the exchange of one ligand for another, with no change in oxidation state at the metal center. The incoming and outgoing ligands may be neutral or ionic but the charge of the complex changes if the ligand charge changes. Keep charge conservation in mind when writing out ligand substitutions.

How do we know when a ligand substitution reaction is favorable? The thermodynamics of the reaction depend on the relative strength of the two metal-ligand bonds, and the stability of the departing and incoming ligands (or salts of the ligand, if they're ionic). It's often useful to think of X-for-X substitutions like acid-base reactions, with the metal and spectator ligands serving as a "glorified proton." Like acid-base equilibria in organic chemistry, we look to the relative stability of the two charged species (the free ligands) to draw conclusions. Of course, we don't necessarily need to rely just on thermodynamics to drive ligand substitution reactions. Photochemistry, neighboring-group participation, relative concentrations, and other tools can facilitate otherwise difficult substitutions.

Ligand substitution is characterized by a continuum of mechanisms bound by associative (A) and dissociative (D) extremes. At the associative extreme, the incoming ligand first forms a bond to the metal, then the departing ligand takes its lone pair and leaves. At the dissociative extreme, the order of events is opposite—the departing ligand leaves, then the incoming ligand comes in. Associative substitution is common for square planar (like d8 complexes of Ni, Pd, and Pt), while dissociative substitution is more common for octahedral complexes. Then again, reality is often more complicated than these extremes. In some cases, evidence is available for simultaneous dissociation and association, and this mechanism has been given the name interchange (IA or ID).

Associative Substitution

The associative substitution reaction is the inorganic analog of an S_{N2} reaction. In associative ligand substitution, the incoming ligand (Y) forms a new bond with the metal (M) before the bond to the leaving ligand (X) breaks. The first step, formation of the new M-Y bond is generally rate-determining. A typical mechanism for associative ligand substitution in both octahedral and square planar complexes is shown in Figure **10.3.1**.

$$ML_nX \xrightarrow{Y} ML_nXY \rightarrow ML_nY + X \tag{10.3.1}$$

In an octahedral complex the intermediate is 7 coordinate, so associative ligand exchange in octahedral complexes is rare and only favored with larger metal ions and ligands that are not sterically demanding. In contrast, ligand substitution in square planar complexes almost always occurs via an associative mechanism, involving approach of the incoming ligand to the open coordination sites above or below the plane. Let's begin with the kinetics of the reaction. How can we spot an associative mechanism in experimental data, and what are some of the consequences of this mechanism?

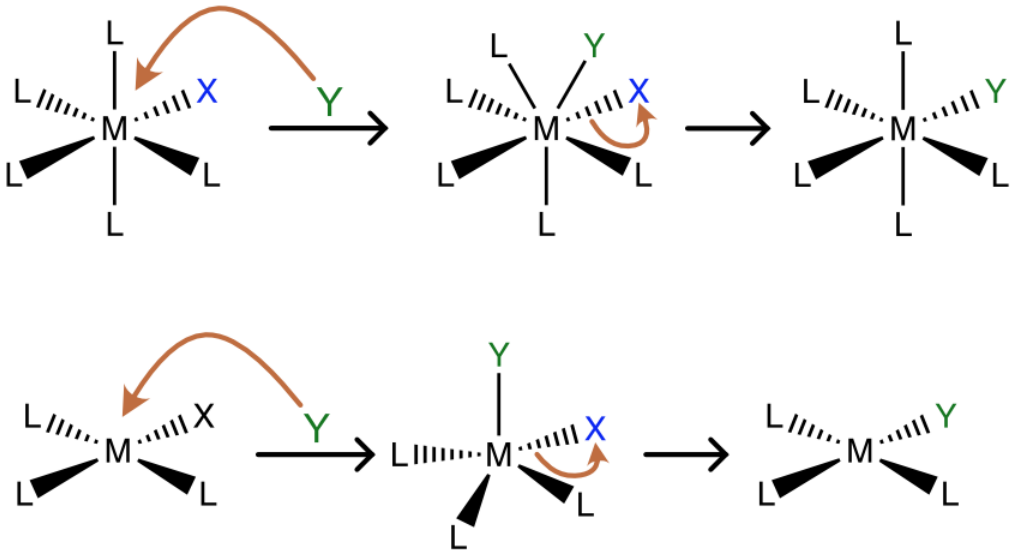


Figure 10.3.1: Scheme of associative ligand substitution in an octahedral (top) and square planar (bottom) metal complex. (CC BY-NC-SA; Catherine McCusker)

Reaction Kinetics

$$L_nM\text{–}X + Y \xrightarrow{k_1} L_nM\text{–}Y + X \tag{10.3.2}$$

$$\frac{d[L_nM\text{–}Y]}{dt} = rate = k_1[L_nM\text{–}X][Y] \tag{10.3.3}$$

Reaction kinetics are commonly used to elucidate reaction mechanisms, and ligand substitution is no exception. Different mechanisms of substitution may follow different rate laws, so plotting the dependence of reaction rate on concentration often allows us to distinguish mechanisms. In the associative mechanism, the rate law is second order overall, first order in both L_nMX and Y. (Figure 10.3.2). If a large excess of Y is used in the reaction is will become pseudo first order, where the reaction appears first order because the [Y] doesn't change significantly over the course of the reaction.

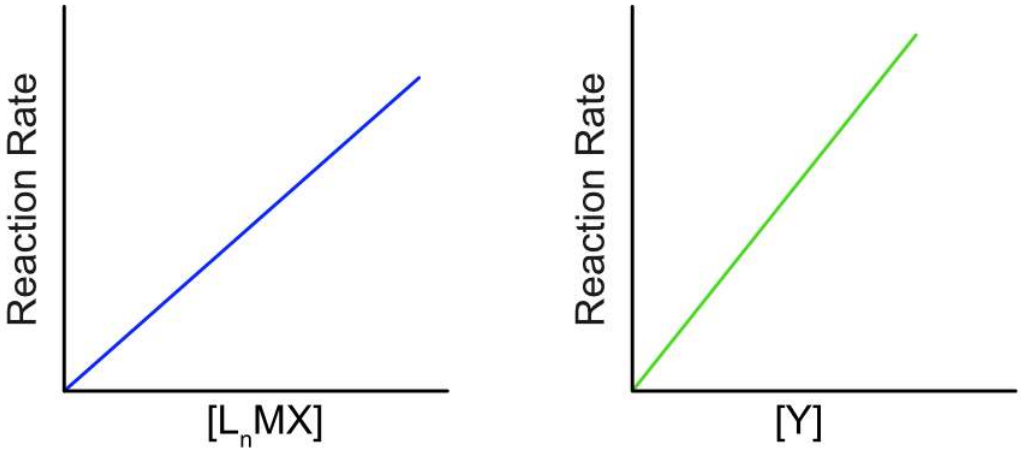


Figure 10.3.2: Dependence of associative reaction rate on concentration of the starting metal complex [ML_nX] and the incoming ligand [Y]. (CC BY-NC-SA; Catherine McCusker)

Dissociative Substitution

The associative substitution mechanism is unlikely for 6 coordinate complexes. For octahedral complexes dissociative substitution mechanisms involving 5 coordinate intermediates are more likely. In

a slow step, the departing ligand leaves, generating a coordinatively unsaturated 5 coordinate intermediate. The incoming ligand then enters the coordination sphere of the metal to generate the product. We'll focus on the kinetics of the reaction and the nature of the unsaturated intermediate (which influences the stereochemistry of the reaction). The reverse of the first step, re-coordination of the departing ligand (rate constant k_{-1}), is often competitive with dissociation.

$$ML_nX \rightarrow ML_n + X + Y \rightarrow ML_nY + X \tag{10.3.4}$$

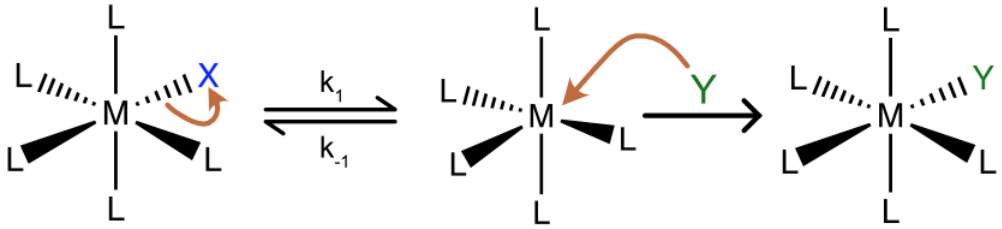


Figure 10.3.3: A general scheme for dissociative ligand substitution in an octahedral complex. (CC BY-NC-SA; Catherine McCusker)

Reaction Kinetics

Let's begin with the general situation in which k_1 and k_{-1} are similar in magnitude. Since k_1 is rate limiting, k_2, the rate of the second step is assumed to be much larger than k_1 and k_{-1}. Most importantly, we need to assume that variation in the concentration of the unsaturated intermediate is essentially zero. This is called the steady state approximation, and it allows us to set up an equation that relates reaction rate to observable concentrations.

$$\text{rate} = k_2[L_nM][Y] \tag{10.3.5}$$

Of course, the unsaturated complex is present in very small concentration and is unmeasurable, so this equation doesn't help us much. We need to remove the concentration of the unmeasurable intermediate from (1), and the steady state approximation helps us do this. We can express variation in the concentration of the unsaturated intermediate as (processes that make it) minus (processes that destroy it), multiplying by an arbitrary time length to make the units work out. All of that equals zero, according to the steady state approximation.

$$\Delta[L_nM] = 0 = (k_1[L_nM\text{–}X] – k_{-}1[L_nM][X] – k_2[L_nM][Y])\Delta t \tag{10.3.6}$$

$$0 = k_1[L_nM\text{–}X] – k_{-1}[L_nM][X] – k_2[L_nM][Y] \tag{10.3.7}$$

Rearranging to solve for [L_nM], we arrive at the following.

$$[L_nM] = k_1\frac{[L_nM\text{–}X]}{(k_{-1}[X] + k_2[Y]} \tag{10.3.8}$$

Finally, substituting into Equation 10.3.5 we reach a verifiable rate equation.

$$\text{rate} = k_2k_1\frac{[L_nM\text{–}X][Y]}{(k_{-1}[X] + k_2[Y])} \tag{10.3.9}$$

When k_{-1} is negligibly small, Equation 10.3.9 reduces to the familiar Equation 10.3.10, typical of dissociative reactions like S_N1.

$$\text{rate} = k_1[L_nM\text{–}X] \tag{10.3.10}$$

This rate does not depend on the concentration of incoming ligand. For reactions that are better described by Equation 10.3.9, we can use a large excess of Y to make $k_2[Y]$ far greater than $k_{-1}[X]$, essentially forcing the reaction to fit Equation 10.3.10.

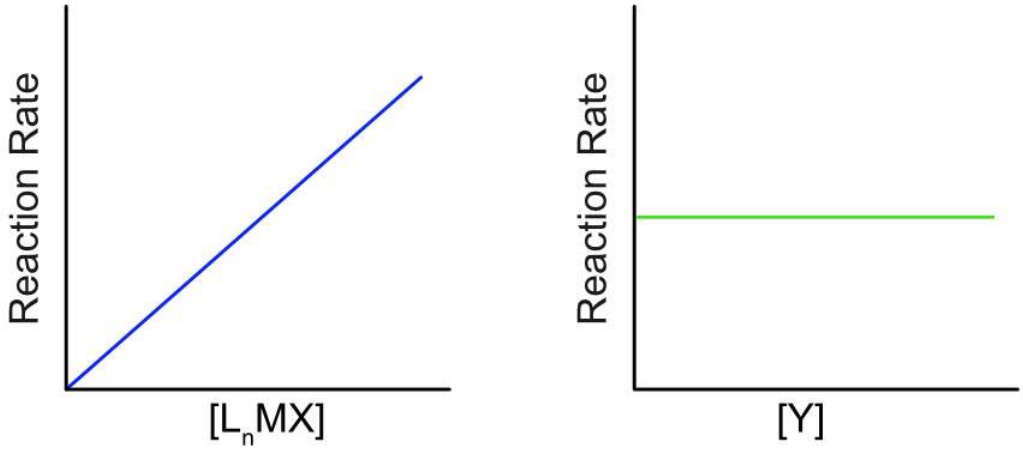


Figure **10.3.4**: Dependence of dissociative reaction rate on concentration of the starting metal complex [ML_nX] and the incoming ligand [Y]. (CC BY-NC-SA; Catherine McCusker)

Stereochemistry

Dissociation of a ligand from an octahedral complex generates an unsaturated ML_5 intermediate. The five coordinate intermediate could adopt either a trigonal bipyramidal (TBP) geometry or a square pyramidal geometry (SP). Both steric and electronic factors combine to determine which geometry is most favorable. For example, with 6 d electrons an issue arises with the TBP geometry. With 6 d electrons, the TBP geometry has two unpaired electrons in degenerate orbitals. Unpaired electrons in degenerate orbitals lead to Jahn-Teller distortion. For a TBP geometry, distortion to a SP or a distorted TBP geometry removes the degeneracy, and so five-coordinate d6 complexes typically have square pyramidal or distorted TBP geometries.

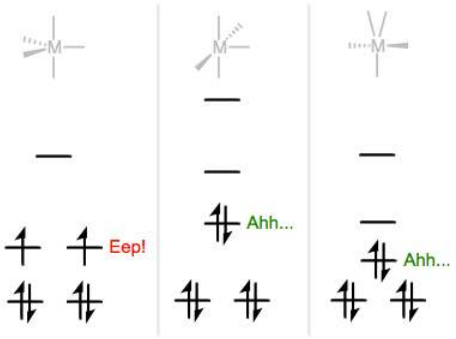


Figure **10.3.5**: TBP geometry (left) is electronically disfavored for d6 metals. Distorted TBP (right) and SP (center) geometries are favored.

When the intermediate adopts square pyramidal geometry, the incoming ligand can simply approach where the departing ligand left, resulting in retention of stereochemistry. Inversion is more likely when the intermediate is a distorted trigonal bipyramid.

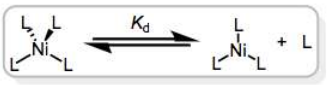
Factors That Favor Dissociative Substitution

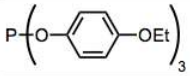
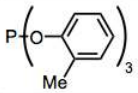
In general, introducing structural features that either stabilize the unsaturated intermediate or destabilize the starting complex can encourage dissociative substitution. Both of these strategies lower the activation barrier for the reaction.

Let's begin with features that stabilize the unsaturated intermediate. Electronically, the intermediate loves it when its d electron count is nicely matched to its crystal field orbitals. As you study inorganic chemistry, you'll learn that there are certain "natural" d electron counts for particular geometries that fit well with the metal-centered orbitals predicted by crystal field theory. Octahedral geometry is great for six d electrons, for example, and square planar geometry loves eight d electrons. Complexes with "natural" d electron counts—but bearing one extra ligand—are ripe for dissociative substitution. The classic examples are d^8 TBP complexes, which become d^8 square planar complexes (think Pt(II) and Pd(II)) upon dissociation. Similar factors actually can also stabilize the

starting complexes, making them less reactive in dissociative substitution reactions. Fro example, low spin d^6 octahedral complexes are particularly happy, and react most slowly in dissociative substitutions.

Destabilization of the starting complex is commonly accomplished by adding steric bulk to its ligands. Naturally, dissociation relieves steric congestion in the starting complex. Chelation has the opposite effect, and tends to steel the starting complex against dissociation.



L	Cone Angle	K_d
$P(OEt)_3$	109	$< 10^{-10}$
	128	$6 * 10^{-10}$
$P(Oi\text{-}Pr)_3$	130	$2.7 * 10^{-5}$
	141	$4 * 10^{-2}$
PPh_3	145	huge

As steric bulk on the ligand increases, dissociation becomes more favorable.

Interchange Substitution

Real life chemical reactions don't always fall neatly into one of the categories above. In some cases the M-X bond can break and the M-Y bond can form simultaneously. An interchange reaction is a concerted reaction without an intermediate. The transition state is a species where the bond to Y is partially formed and the bond to X is partially broken as seen in Figure **10.3.6**. If the new M-Y bond forms faster than the M-X bond breaks tat is an associative interchange (IA) reaction and if the M-X bond breaks faster than the new M-Y bond forms that is a dissociative interchange reaction (ID)

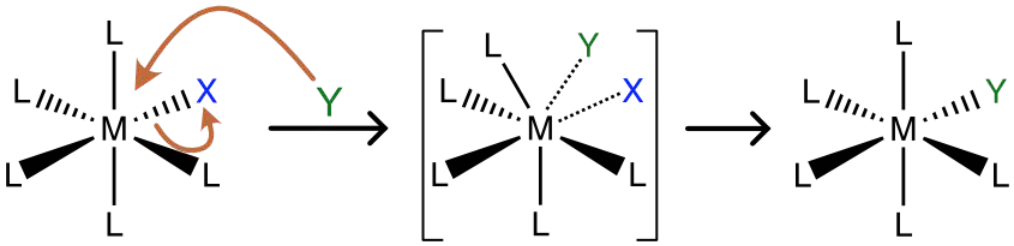


Figure **10.3.6**: A general scheme for an interchange ligand substitution reaction. Species in brackets is the transition state, not an intermediate. (CC BY-NC-SA; Catherine McCusker)

Contributors and Attributions

- Dr. Michael Evans (Georgia Tech)
- Modified by Catherine McCusker (East Tennessee State University)

This page titled 10.3: Ligand Substitution Mechanisms is shared under a CC BY-NC-SA 4.0 license and was authored, remixed, and/or curated by Michael Evans.

- **Current page** by Michael Evans is licensed CC BY-NC-SA 4.0.
- **4.2: Associative Ligand Substitution** by Michael Evans is licensed CC BY-NC-SA 4.0.
- **4.3: Dissociative Ligand Substitution Reactions** by Michael Evans is licensed CC BY-NC-SA 4.0.
- **4.4: Ligand substitution** by Michael Evans is licensed CC BY-NC-SA 4.0.

10.4: The Trans Effect

The trans effect is an ancient but venerable observation. First noted by Chernyaev in 1926, the trans effect and its conceptual siblings (the trans influence, cis influence, and cis effect) are easy enough to comprehend. That is, it's simple enough to know what they are. To understand why they are, on the other hand, is much more difficult.

Definitions & Examples

Let's begin with definitions: what is the trans effect? There's some confusion on this point, so we need to be careful. The trans effect proper, which is often called the kinetic trans effect, refers to the observation that certain ligands increase the rate of ligand substitution when positioned trans to the departing ligand. The key word in that last sentence is "rate"—the trans effect proper is a kinetic effect. The trans influence refers to the impact of a ligand on the length of the bond trans to it in the ground state of a complex. The key phrase there is "ground state"—this is a thermodynamic effect, so it's sometimes called the thermodynamic trans effect. Adding to the insanity, cis effects and cis influences have also been observed. Evidently, ligands may also influence the kinetics or thermodynamics of their cis neighbors. All of these phenomena are independent of the metal center, but do depend profoundly on the geometry of the metal (more on that shortly).

Kinetic trans and cis effects are shown in the figure below. In both cases, we see that X1 exhibits a stronger effect than X2. The geometries shown are those for which each effect is most commonly observed. The metals and oxidation states shown are prototypical.

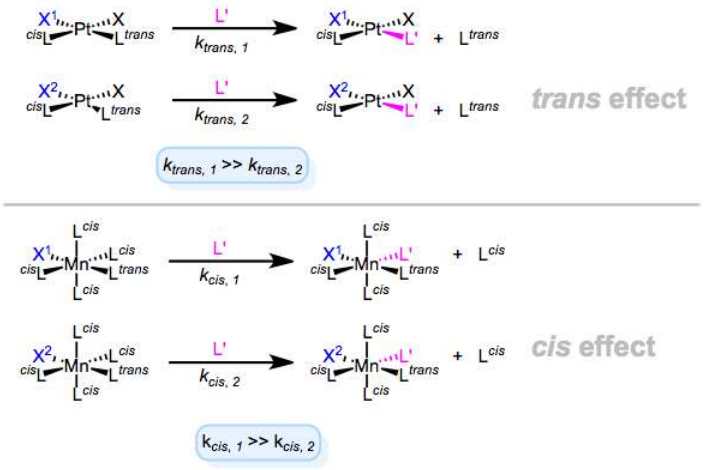


Figure 1: *The kinetic trans and cis effects in action. X^1 is the stronger (trans/cis)-effect ligand in these examples.*

On to the influences, which are simpler to illustrate since they're concerned with ground states, not reactions. The lengthened bonds below are exaggerated.

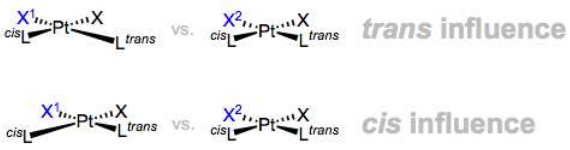


Figure 2: *The trans and cis influences in action. Note the elongated bond lengths.*

And there we have it folks, the thermodynamic and kinetic cis/trans effects. It's worth keeping in mind that the kinetic trans effect is most common for d8 square planar complexes, and the kinetic cis effect is most common for d6 octahedral complexes (particularly when the departing L is CO). But a lingering question remains: what makes for a strong trans effect ligand?

Origins of Effects & Influences

The trans effect and its cousins are all electronic, not steric effects. So, the electronic properties of the ligand dictate the strength of its trans effect. Let's finally dig into the trans effect series:

(weak) F^-, HO^-, H_2O <NH_3 < py < Cl^- < Br– < I–, SCN^-, NO_2^-, $SC(NH_2)_2$, Ph^- < SO_3^{2-} < PR_3 < AsR_3, SR_2, H_3C^- < H^-, NO, CO, NC^-, C_2H_4 (strong)

What's the electronic progression here? It's clear that electronegativity decreases across the series: F^- < Cl^- < Br^- < I^- < H_3C^-. From a bonding perspective, we can say that ligands with strong trans effects are strong σ-donors (or σ-bases). Yet σ-donation doesn't tell the whole story. What about ethylene and carbon monoxide, which both appear at the top of the heap? Neither of these ligands are strong σ-donors, but their π systems do interact with the metal center through backbonding. Consider the following sub-series: S=C=N– < PR_3 < CO. Backbonding increases across this series, along with the strength of the trans effect. Strong backbonders—better known as π-acceptors or π-acids—exhibit strong trans effects.

Strong trans effect = strong σ-donor + strong π-acceptor

Wonderful! Using these ideas we can identify ligands with strong trans effects. But we can dive deeper down the rabbit hole: why does this particular combination of electronic factors lead to a strong trans effect? To understand this, we need to know the mechanism of the ligand substitution reaction that's sped up by strong trans effect ligands. For 16-electron Pt(II) complexes, associative substitution is par for the course. The incoming ligand binds to the metal first, forming an 18-electron complex (yay!), which jettisons a ligand to yield a new 16-electron product. The mechanism in all its glory is shown in the figure below.

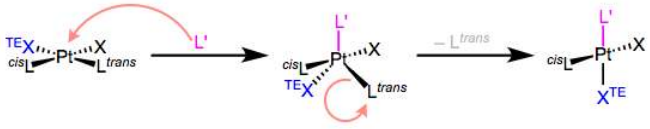


Figure 3: *The mechanism of associative ligand substitution of Pt(II) complexes.*

Some very important points about this mechanism:

- The incoming ligand always sits at an equatorial site in the trigonal bipyramidal intermediate. More on this another day, but I think of this result as governed by the principle of least motion. Consider the molecular gymnastics that would have to happen to place the incoming ligand in an axial position.
- Two ligands in the square plane are "pushed down" and become the other two equatorial ligands.
- Owing to microscopic reversibility, the leaving group must be one of the equatorial ligands.

The third point reveals that once L' has "pushed down" XTE and Ltrans, Ltrans has no choice but to leave (assuming XTE stays put). Thus, the trans effect has nothing to do with the second step of the mechanism, which is not rate determining anyway. The key is the first step—in particular, the "pushing down" event. Apparently, ligands with strong trans effects like to be pushed down. They like to occupy the equatorial plane of the TBP intermediate. Now here's the kicker: the equatorial sites of the TBP geometry are more π basic than the axial sites. The equatorial plane is just the xy-plane of the metal center, and the d orbitals in that plane (when occupied) are great electron sources for π-acidic ligands. Thus, π-acidic ligands want to occupy those equatorial sites, to receive the benefits of strong backbonding! Boom; strong π-acids encourage loss of the ligand trans to themselves.



Figure 4: *The equatorial sites of TBP metals are rich in electrons that can π bond.*

What about those pesky σ donors? Well, we can imagine that in a square planar complex, a ligand and its trans partner are competing for donation into the same d orbital. Strong σ donation from a ligand should thus weaken the bond trans to it. Although this is the thermodynamic trans effect (trans influence) in action, the resulting destabilization of the ground state relative to the transition state is a kinetic effect. On the whole, the barrier to substitution of the trans ligand goes down as σ-donating strength goes up.

This idea of "competition for the metal center" is a nice heuristic to use when thinking about the trans and cis influences. The type of metallic orbital involved in M–L bonding determines the strength of L's trans and cis influences on neighboring ligands that also need that metallic orbital for bonding. For example: both influences are large if the metal's s orbital is a significant contributor to

M–L bonding, since it's non-directional; the trans influence is much greater than the cis influence when metallic p orbitals are primarily involved in M–L. For a deeper explanation of these ideas, see this paper.

Summing up

Perhaps the most valuable lesson from a study of the trans effect is that many concepts from organometallic chemistry involve more than meets the eye. Geometric effects and influences are real icebergs, in the sense that the observations and trends are easy to grasp, but difficult to explain. We had to dig all the way into the mechanism of associative ligand substitution before a satisfactory explanation emerged!

Contributors

Dr. Michael Evans (Georgia Tech)

10.4: The Trans Effect is shared under a CC BY-NC-SA 4.0 license and was authored, remixed, and/or curated by LibreTexts.

10.5: Electron Transfer Reactions

Test Tube Experiments

Easy chemical or biological reactions performed in test tubes are sometimes called test tube experiments. Solutions in test tubes are mixed at room temperature in air and the mixture is shaken to observe a color change or formation of precipitates and the results of the reactions are speculated on. University professors occasionally attempt these sorts of experiments. Although easy, these simple experiments show only the effects of visible light absorption and solubility. However, since even great discoveries can be born from such experiments, they should not be dismissed.

Henry Taube wrote that he found a hint of the inner-sphere electron transfer mechanism from test tube experiments. He mixed Cr^{2+} (aq) and I_2 in a test tube in order to clarify the oxidation of Cr^{2+}(aq) and observed the change of color to the one characteristic of $[Cr(H_2O)_6]^{3+}$ via green. The green color is due to $[(H_2O)_5CrI]^{2+}$ which is unstable and changes to $[Cr(H_2O)_6]^{3+}$ + I^-. He assumed that this was due to the formation of a Cr-I bond before Cr(II) was oxidized by I_2. Subsequently, he performed another test tube experiment using $[(NH_3)_5CoCl]^{2+}$ as an oxidant and found that Cr^{2+}(aq) was converted into $[Cr(H_2O)_6]^{3+}$ via green $[(H_2O)_5CrCl]_{2+}$. This reaction established the inner-sphere electron transfer mechanism in which a Co-Cl-Cr bridge forms between Co^{3+} and Cr^{2+} and led to the Nobel Prize in a later year.

Redox reactions

The oxidation number of the central metal in a transition-metal compound can vary in a few steps from low to high. Namely, the oxidation state of a compound is changeable by redox reactions. As a consequence of this, the bond distance and the bond angle between the metal and coordinating elements, or between metals, change, and at times the whole structure of a complex can be distorted remarkably or the compound may even decompose. The reactions of a metal compound with various reducing or oxidizing agents are also very important from the viewpoint of synthetic chemistry. Especially, reduction reactions are used in the preparation of organometallic compounds, such as metal carbonyls or cluster compounds.

Meanwhile, the study of electron transfer between complexes, especially the redox reactions of transition metal complexes, has developed. Taube won the Nobel Prize (1983) for the study of electron transfer reactions in transition metal complexes, classifying such reactions into two mechanisms. The mechanism of electron transfer in which a bridging ligand is shared between two metals is called the **inner-sphere mechanism**, and the one involving a direct transfer of electrons between two metals without a bridging ligand is called the **outer-sphere mechanism**.

Inner Sphere Electron Transfer

In some cases, electron transfers occur much more quickly in the presence of certain ligands. For example, compare the rate constants for the following two electron transfer reactions, involving almost exactly the same complexes:

$$Co(NH_3)_6{}^{3+} + Cr^{2+} \longrightarrow Co^{2+} + Cr^{3+} + 6\,NH_3 \;\; k = 10^{-4} M^{-1} s^{-1}$$

$$Co(NH_3)_5Cl^{2+} + Cr^{2+} \longrightarrow Co^{2+} + CrCl^{2+} + 6\,NH_3 \;\; k = 6 \times 10^{5} M^{-1} s^{-1}$$

(Note: aqua ligands are omitted for simplicity. Ions, unless noted otherwise, are aqua complexes.)

Notice two things: first, when there is a chloride ligand involved, the reaction is much faster. Second, after the reaction, the chloride ligand has been transferred to the chromium ion. Possibly, those two events are part of the same phenomenon.

Similar rate enhancements have been reported for reactions in which other halide ligands are involved in the coordination sphere of one of the metals.

In the 1960's, Henry Taube of Stanford University proposed that halides (and other ligands) may promote electron transfer via bridging effects. What he meant was that the chloride ion could use one of its additional lone pairs to bind to the chromium ion. It would then be bound to both metals at the same time, forming a bridge between them. Perhaps the chloride could act as a conduit for electron transfer. The chloride might then remain attached to the chromium, to which it had already formed a bond, leaving the cobalt behind.

Electron transfers that occur via ligands shared by the two metals undergoing oxidation and reduction are termed "inner sphere" electron transfers. Taube was awarded the Nobel Prize in chemistry in 1983; the award was based on his work on the mechanism of electron transfer reactions.

Exercise 10.5.1

Take another look at the two electron transfer reactions involving the cobalt and chromium ion, above.

a. What geometry is adopted by these complexes?
b. Are these species high spin or low spin?
c. Draw d orbital splitting diagrams for each complex.
d. Explain why electron transfer is accompanied by loss of the ammonia ligands from the cobalt complex.
e. The chloride is lost from the cobalt complex after electron transfer. Why does it remain on the chromium?

Answer a

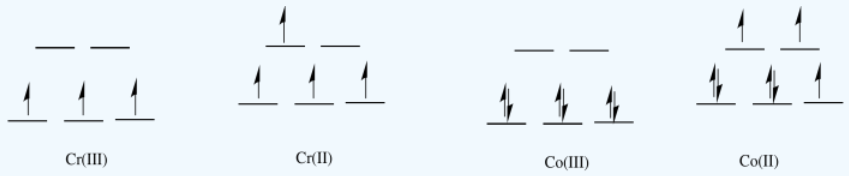
a) octahedral

Answer b

b) In the first row, 2^+ complexes are almost always high spin. However, 3^+ complexes are sometimes low spin.

Answer c

c)



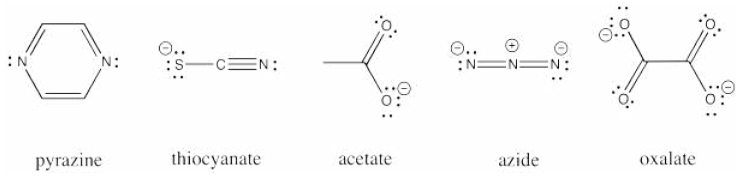
Answer d

d) The Co(II) complex is high spin and labile. The ligands are easily replaced by water.

Answer e

e) The Cr(III) complex is only d^3; it is inert.

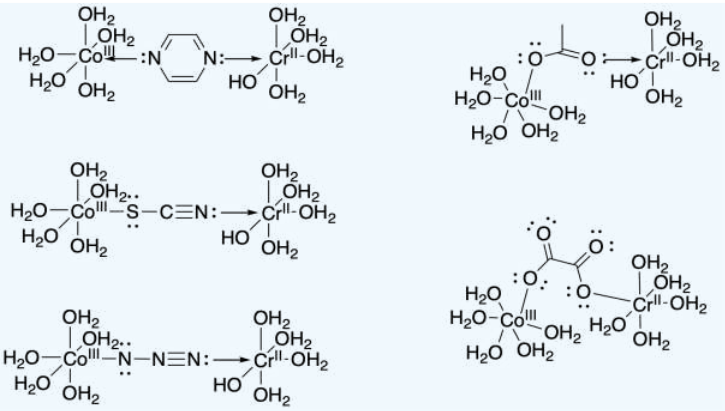
Other ligands can be involved in inner sphere electron transfers. These ligands include carboxylates, oxalate, azide, thiocyanate, and pyrazine ligands. All of these ligands have additional lone pairs with which to bind a second metal ion.



Exercise 10.5.2

Draw an example of each of the ligands listed above bridging between a cobalt(III) and chromium(II) aqua complex.

Answer

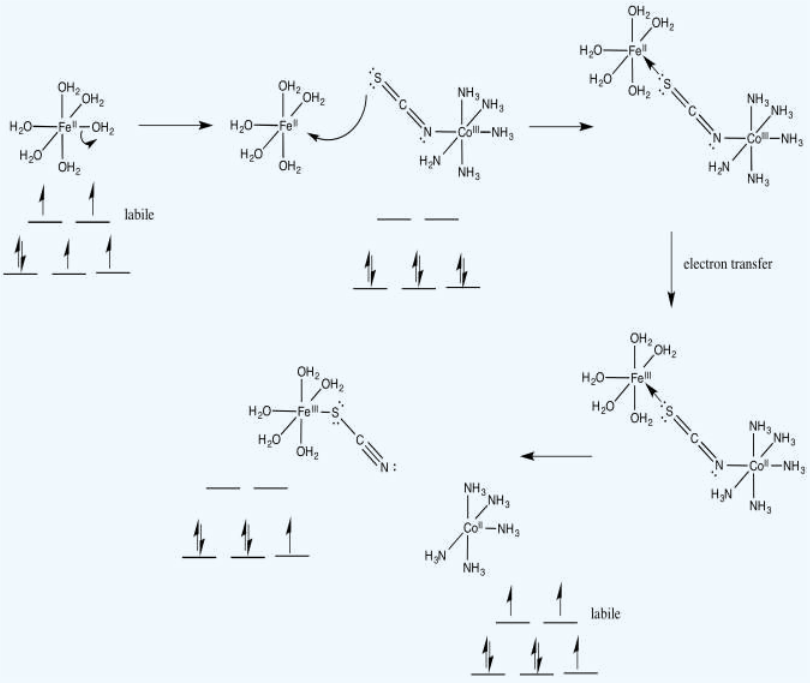


Exercise 10.5.3

Explain, with structures and d orbital splitting diagrams, how the products are formed in the following reaction, in aqueous solution.

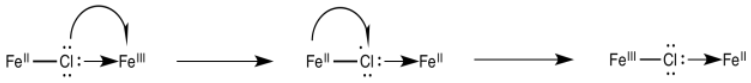
$$Fe(OH_2)_6^{2+} + (SCN)Co(NH_3)_5^{2+} \longrightarrow (NCS)Fe(OH_2)_5^{2+} + Co(OH_2)_6^{2+} + 5\,NH_3$$

Answer



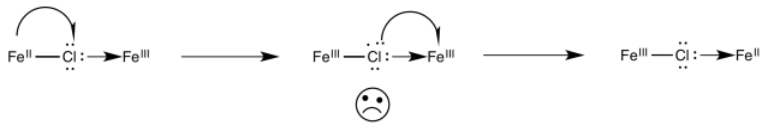
How does the electron travel over the bridge?

Once the bridge is in place, the electron transfer may take place via either of two mechanisms. Suppose the bridging ligand is a chloride. The first step might actually involve an electron transfer from chlorine to the metal; that is, the chloride could donate one electron from one of its idle lone pairs. This electron could subsequently be replaced by an electron transfer from metal to chlorine.



Sometimes, we talk about the place where an electron *used to be*, describing it as a "hole". In this mechanism, the electron donated from the bridging chloride ligand leaves behind a hole. The hole is then filled with an electron donated from the other metal.

Alternatively, an electron might first be transferred from metal to chlorine, which subsequently passes an electron along to the other metal. In the case of chlorine, this idea may be unsatisfactory, because chlorine already has a full octet. Nevertheless, some of the other bridging ligands may have low-lying unoccupied molecular orbitals that could be populated by this extra electron, temporarily.

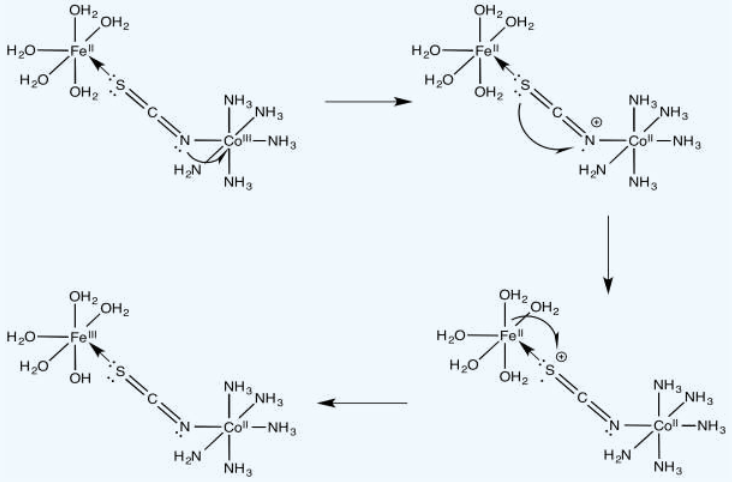


Exercise 10.5.4

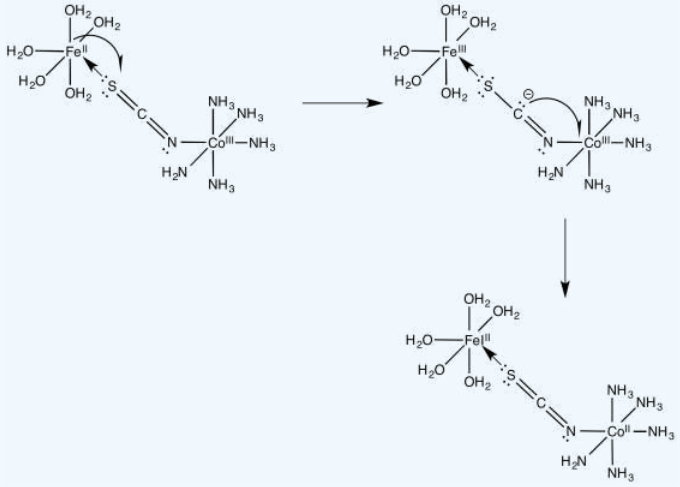
For the iron / cobalt electron transfer in problem Exercise **10.5.3** (RO9.3.), show

a. an electron transfer mechanism via a hole migration along the bridge
b. an electron transfer mechanism via an electron migration along the bridge

Answer a



Answer b



Exercise 10.5.5

One of the many contributions to the barrier for electron transfer between metal ions is internal electronic reorganization.

a) Draw d orbital splitting diagrams for each of the following metal ions in an octahedral environment.

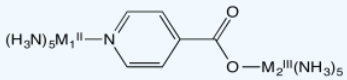
Ru(II) or Os(II)

Ru(III) or Os(III)

Co(II)

Co(III)

Flash photolysis is a method in which an electron can be moved instantly "uphill" from one metal to another (e.g. from M_2^{II} to M_1^{III}, below); the electron transfer rate can then be measured as the electron "drops" back from M_1^{II} to M_2^{III}.



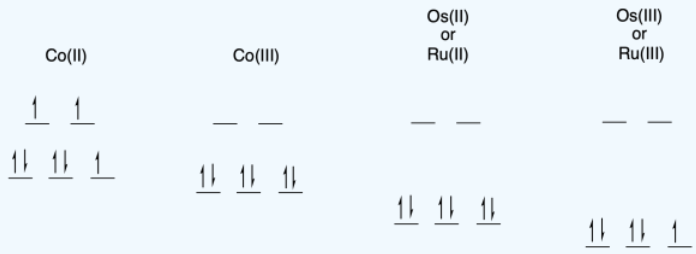
b) Explain the relative rates of electron transfer reaction in this system, as measured by flash photolysis in the table below.

M_1^{II}	M_2^{III}	k_{obs} s^{-1}
Os	Ru	$> 5 \times 10^9$
Os	Co	1.9×10^5

c) Does the reaction above probably occur via an inner sphere or by an outer sphere pathway? Why?

Answer a

a)



Answer b

b) The electron transfer between Os(II) and Ru(III) will not involve any electron reorganization because both are low spin to begin with. However, the electron transfer between Os(II) and Co(III) will result in cobalt changing from low spin to high spin. The need to move electrons between different d orbitals on the cobalt will add to the barrier, slowing down the reaction.

Answer c

c) The pathway is probably inner sphere because of the bridging ligand. Furthermore, the conjugation in the bridging ligand would help in conducting an electron from one end of the ligand to the other, either through an electron mechanism or a hole mechanism.

Exercise 10.5.6

Outer sphere electron transfer rates depend on the free energy change of the reaction (ΔG°) and the distance between oxidant and reductant (d) according to the relation

Rate constant = $k = Ae^{(-\Delta G)}e^{-d}$

a) What happens to the rate of the reaction as distance increases between reactants?

https://chem.libretexts.org/@go/page/326248

One potential problem in measuring rates of intramolecular electron transfer (i.e. *within* a molecule) is competition from intermolecular electron transfer (*between* molecules).

b) What would you do in the flash photolysis experiment above to discourage intermolecular electron transfer?

c) How could you confirm whether you were successful in discouraging intermolecular reaction?

Answer a

a) The rate decreases exponentially as distance increases.

Answer b

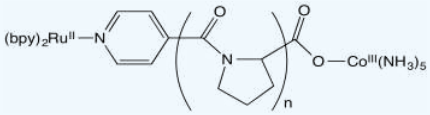
b) You might keep the concentration low in order to increase the distance between molecules, reducing the likely hood of an outer-sphere electron transfer.

Answer c

c) If you ran the experiment at a series of dilutions, intramolecular electron transfer would be unaffected but outer sphere electron transfer would not. If the rates were the same across a number of different concentrations, the reaction would probably be intramolecular.

Exercise 10.5.7

Stephan Isied and coworkers at Rutgers measured the following electron transfer rates between metal centers separated by a peptide. (*Chem Rev* **1992**, *92*, 381-394)



a. The proline repeating unit is crucial in ensuring a steady increase in distance between metal centers with increased repeat units, n. Why?
b. An inner sphere pathway in this case is expected to be somewhat slow because of the lack of conjugation in the polyproline bridge. Explain why.
c. Plot the data below, with log*k* on the y axis (range from 4-9) and d on the x axis (12-24 Angstroms).

n	d (Å)	k_{obs} (s^{-1})
1	12.2	5×10^8
2	14.8	1.6×10^7
3	18.1	2.3×10^5
4	21.3	5.1×10^4
5	24.1	1.8×10^4

d) A linear relationship is in agreement with Marcus theory; log*k* = - c x d. Is your plot linear?

Isied offers a number of possible explanations for the data, all of which involve two competing reaction pathways.

e) Suggest one explanation for the data.

Answer a

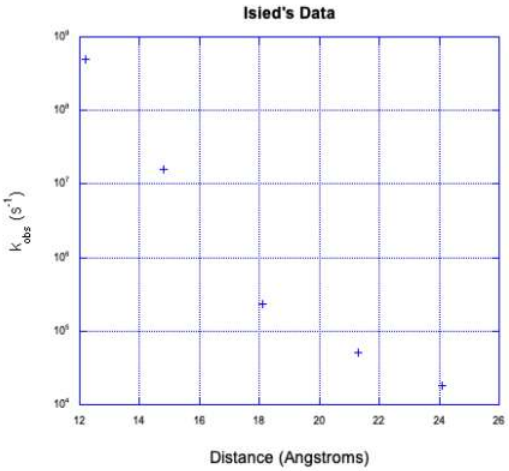
a) Rings are frequently used to introduce conformational rigidity (or decrease conformational flexibility), limiting the range of potential shapes a molecule could adopt. If the molecule can't wiggle around as much, then the distance between the ends of the molecule should be more constant.

Answer b

b) Although the ligand is bridging, it would be difficult to picture either an electron or hole mechanism of inner sphere electron transfer. There are few pi bonds or lone pairs to use as places to put electrons or temporarily remove electrons from, shuttling the electrons from place to place along the ligand. A conjugated system would be much more likely to carry out inner sphere electron transfer.

Answer c

c)



Answer d

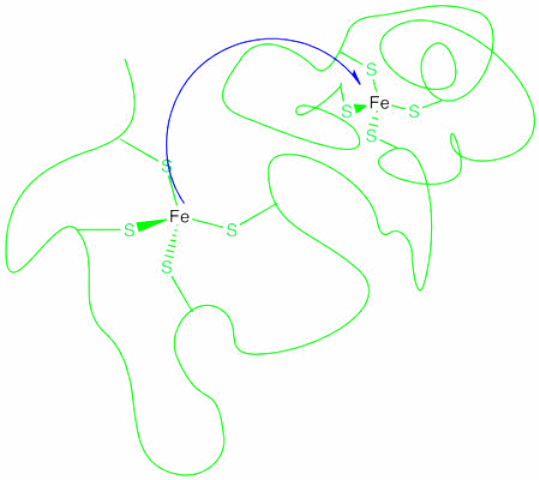
d) The data is not linear.

Answer e

e) The data appear to show two lines that cross. That's a classic symptom of two competing mechanisms. The faster mechanism, to the left, is probably an intramolecular electron transfer. The slower mechanism, to the right, may be an intermolecular electron transfer.

Outer Sphere Electron Transfer

Without a bridging ligand, how does an electron get from one metal to another? This might be a more difficult task than it seems. In biochemistry, an electron may need to be transferred a considerable distance. Often, when the transfer occurs between two metals, the metal ions may be constrained in particular binding sites within a protein, or even in two different proteins.



That means the electron must travel through space to reach its destination. Its ability to do so is generally limited to just a few Angstroms (remember, an Angstrom is roughly the distance of a bond). Still, it can react with something a few bond lengths away. Most things need to actually bump into a partner before they can react with it.

This long distance hop is called an outer sphere electron transfer. The two metals react without ever contacting each other, without getting into each others' coordination spheres. Of course, there are limitations to the distance involved, and the further away the metals, the less likely the reaction. But an outer sphere electron transfer seems a little magical.

Barrier to Reaction: A Qualitative Picture of Marcus Theory

So, what holds the electron back? What is the barrier to the reaction? Rudy Marcus at Caltech has developed a mathematical approach to understanding the kinetics of electron transfer, in work he did beginning in the late 1950's. We will take a very qualitative look at some of the ideas in what is referred to as "Marcus Theory". An electron is small and very fast. All those big, heavy atoms involved in the picture are lumbering and slow. The barrier to the reaction has little to do with the electron's ability to whiz around, although even that is limited by distance. Instead, it has everything to do with all of those things that are barely moving compared to the electron.

Imagine an iron(II) ion is passing an electron to an iron(III) ion. After the electron transfer, they have switched identities; the first has become an iron(III) and the second has become an iron(II) ion.

Nothing could be simpler. The trouble is, there are big differences between an iron(II) ion and an iron(III) ion. For example, in a coordination complex, they have very different bond distances. Why is that a problem? Because when the electron hops, the two iron atoms find themselves in sub-optimal coordination environments.

Exercise 10.5.1

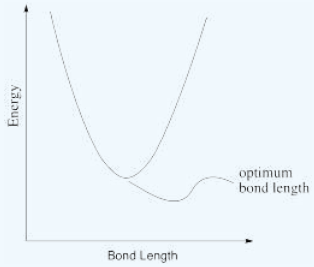
Suppose an electron is transferred from an Fe(II) to a Cu(II) ion. Describe how the bond lengths might change in each case, and why. Don't worry about what the specific ligands are.

Answer

The bonds to iron would contract because the increased charge on the iron would attract the ligand donor electrons more strongly. The bonds to copper would lengthen because of the lower charge on the copper.

Exercise 10.5.2

In reality, a bond length is not static. If there is a little energy around, the bond can lengthen and shorten a little bit, or vibrate. A typical graph of molecular energy vs. bond length is shown below.



a. Why do you think energy increases when the bond gets shorter than optimal?
b. Why do you think energy increases when the bond gets longer than optimal?
c. In the following drawings, energy is being added as we go from left to right. Describe what is happening to the bond length as available energy increases.

Answer a

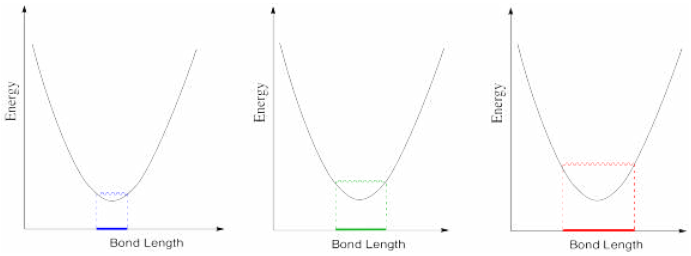
a) Most likely there are repulsive forces between ligands if the bonds get too short.

Answer b

b) Insufficient overlap between metal and ligand orbitals would weaken the bond and raise the energy.

Answer c

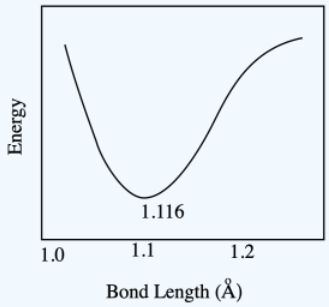
c) The range of possible bond lengths gets broader as energy is increased. The bond has more latitude, with both longer and shorter bonds allowed at higher energy.



Exercise 10.5.3

The optimum C-O bond length in a carbon dioxide molecule is 1.116 Å. Draw a graph of what happens to internal energy when this bond length varies between 1.10 Å and 1.20 Å. Don't worry about quantitative labels on the energy axis.

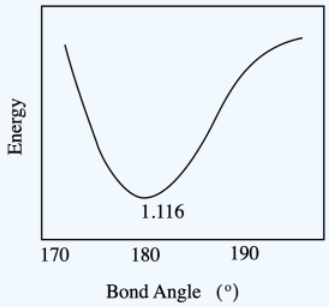
Answer



Exercise 10.5.4

The optimum O-C-O bond angle in a carbon dioxide molecule is 180 °. Draw a graph of what happens to internal energy when this bond angle varies between 170 ° and 190 °. Don't worry about quantitative labels on the energy axis.

Answer



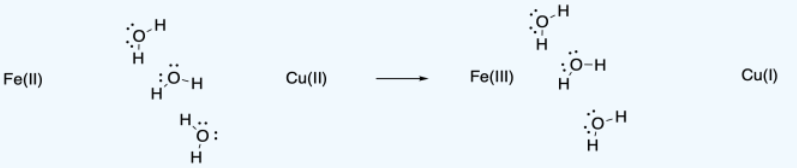
The barrier to electron transfer has to do with reorganizations of all those big atoms before the electron makes the jump. In terms of the coordination sphere, those reorganizations involve bond vibrations, and bond vibrations cost energy. Outside the coordination sphere, solvent molecules have to reorganize, too. Remember, ion stability is highly influenced by the surrounding medium.

Exercise 10.5.5

Draw a Fe(II) ion and a Cu(II) ion with three water molecules located somewhere in between them. Don't worry about the ligands on the iron or copper. Show how the water molecules might change position or orientation if an electron is transferred from iron to copper.

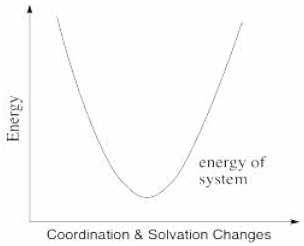
Answer

The water molecules may pivot toward the more highly charged Fe(III), or they may shift closer to it because of the attraction between the ion and the dipole of the water molecule.



Keep in mind that such adjustments would happen in non-polar solvents, too, although they would involve weaker IMFs such as ion - induced dipole interactions.

Thus, the energetic changes needed before electron transfer can occur involve a variety of changes, including bond lengths of several ligands, bond angles, solvent molecules, and so on. The whole system, involving both metals, has some optimum set of positions of minimum energy. Any deviations from those positions requires added energy. In the following energy diagram, the x axis no longer defines one particular parameter. Now it lumps all changes in the system onto one axis. This picture is a little more abstract than when we are just looking at one bond length or one bond angle, but the concept is similar: there is an optimum set of positions for the atoms in this system, and it would require an input of energy in order to move any of them move away from their optimum position.

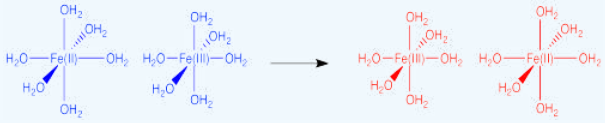


It is thought that these kinds of reorganizations -- involving solvent molecules, bond lengths, coordination geometry and so on -- actually occur prior to electron transfer. They happen via random motions of the molecules involved. However, once they have happened, there is nothing to hold the electron back. Its motion is so rapid that it can immediately find itself on the other atom before anything has a chance to move again.

Consequently, the barrier to electron transfer is just the amount of energy needed for all of those heavy atoms to get to some set of coordinates that would be accessible in the first state, before the electron is transferred, but that would also be accessible in the second state, after the electron is transfered.

Exercise 10.5.6

Describe some of the changes that contribute to the barrier to electron transfer in the following case.

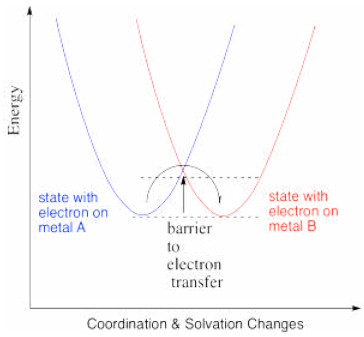


Answer

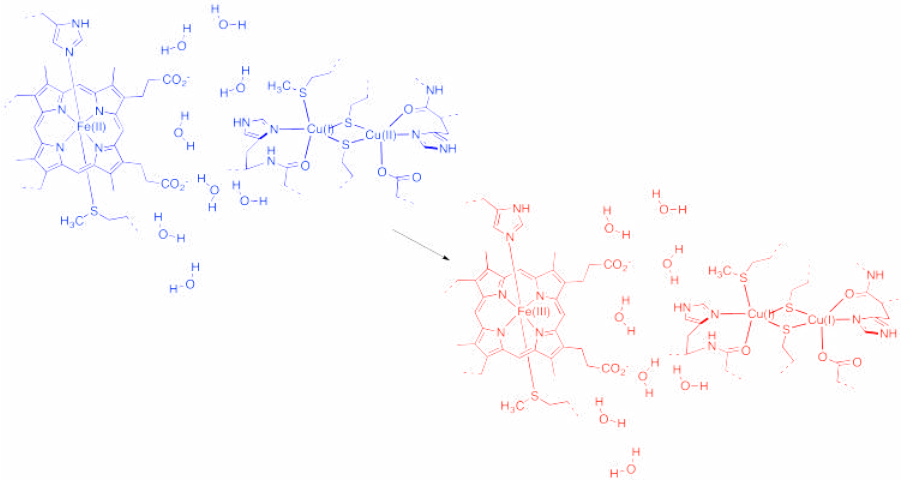
The reactants and products are very similar in this case. However, the Fe(III) complex has shorter bonds than the Fe(II) complex because of greater electrostatic interaction between the metal ion and the ligands. These changes in bond length needed in order to get ready to change from Fe(III) to Fe(II) (or the reverse) pose a major barrier to the reaction.

In the drawing below, an electron is transferred from one metal to another metal of the same kind, so the two are just switching oxidation states. For example, it could be an iron(II) and an iron(III), as pictured in the problem above. In the blue state, one iron has the extra electron, and in the red state it is the other iron that has the extra electron. The energy of the two states are the same,

and the reduction potential involved in this transfer is zero. However, there would be some atomic reorganizations needed to get the coordination and solvation environments adjusted to the electron transfer. The ligand atoms and solvent molecules have shifted in the change from one state to another, and so our energy surfaces have shifted along the x axis to reflect that reorganization.



That example isn't very interesting, because we don't form anything new on the product side. Instead, let's picture an electron transfer from one metal to a very different one. For example, maybe the electron is transferred from cytochrome c to the "copper A" center in cytochrome c oxidase, an important protein involved in respiratory electron transfer.



Exercise 10.5.7

In the drawing above, some water molecules are included between the two metal centres.

a. Explain what happens to the water molecules in order to allow electron transfer to occur, and why.
b. Suppose there were a different solvent, other than water, between the complexes. How might that affect the barrier to the reaction?

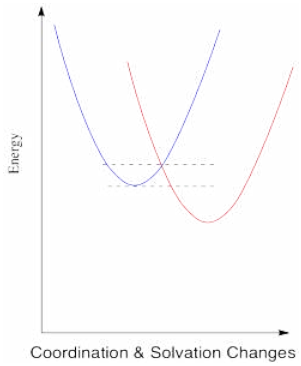
Answer a

a) The drawing is an oversimplification, but in general the water molecules are shown reorienting after the electron transfer because of ion-dipole interactions. In this case, the waters are shown orienting to present their negative ends to the more positive iron atom after the electron transfer. In reality, in a protein there are lots of other charges (including charges on the ligand) that may take part in additional ion-dipole interactions.

Answer b

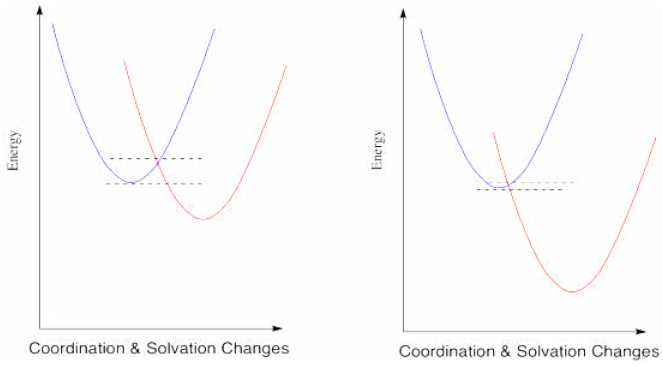
b) Because electron transfer is so fast, atomic and molecular reorganisations are actually thought to happen before the electron transfer. The water molecules would happen to shift into a position that would provide the greatest possible stabilisation for the ions and then the electron would be transferred. A less polar solvent than water would be less able to stabilize ions and the electron would be slower to transfer as a result. In addition, a less polar solvent than water would be a poor medium to transmit an electron, which is charged and therefore stabilized by interactions with polar solvents.

The energy diagram for the case involving two different metals is very similar, except that now there is a difference in energy between the two states. The reduction potential is no longer zero. We'll assume the reduction potential is positive, and so the free energy change is negative. Energy goes down upon electron transfer.



Compare this picture to the one for the degenerate case, when the electron is just transferred to a new metal of the same type. A positive reduction potential (or a negative free energy change) has the effect of sliding the energy surface for the red state downwards. As a result, the intersection point between the two surfaces also slides downwards. Since that is the point at which the electron can slide from one state to the other, the barrier to the reaction decreases.

What would happen if the reduction potential were even more positive? Let's see in the picture below.



The trend continues. According to this interpretation of the kinetics of electron transfer, the more exothermic the reaction, the lower its barrier will be. It isn't always the case that kinetics tracks along with thermodynamics, but this might be one of them.

But is all of this really true? We should take a look at some experimental data and see whether it truly works this way.

Oxidant	E°	k ($M^{-1}s^{-1}$) (margin of error shown in parentheses)
$Co(diene)(NH_3)_2^{3+}$	0.12	3.0(4)
$Co(diene)H_2O)NCS^{2+}$	0.38	11(1)
$Co(diene)(H_2O)_2^{3+}$	0.53	800(100)
Co(EDTA)	0.60	6000(1000)

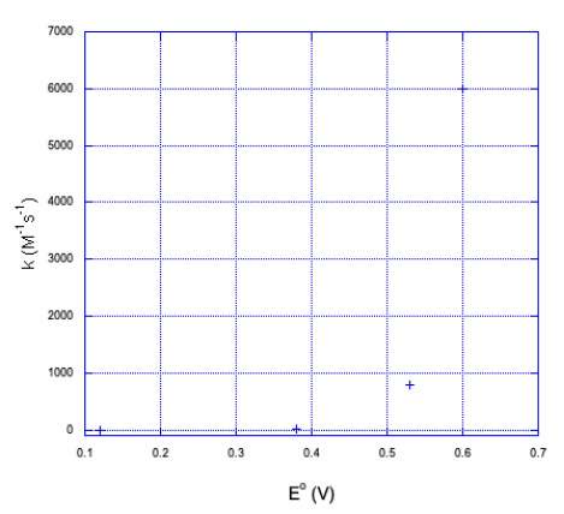
As the reduction potential becomes more positive, free energy gets more negative, and the rate of the reaction dramatically increases. So far, Marcus theory seems to get things right.

Exercise 10.5.8

a. Plot the data in the above table.
b. How would you describe the relationship? Is it linear? Is it exponential? Is it direct? Is it inverse?
c. Plot rate constant versus free energy change. How does this graph compare to the first one?

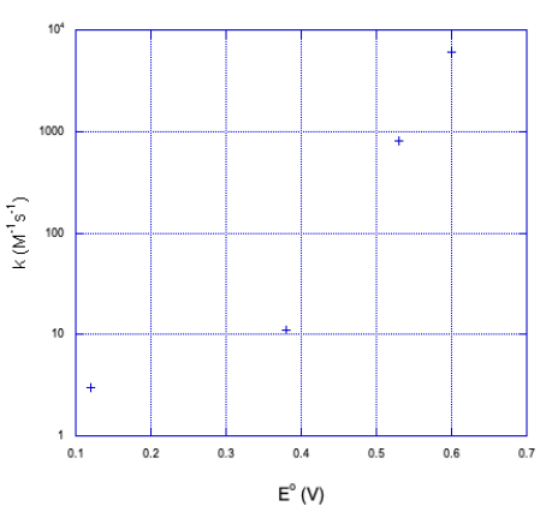
Answer a

a) Here is a plot of the data.



Answer b

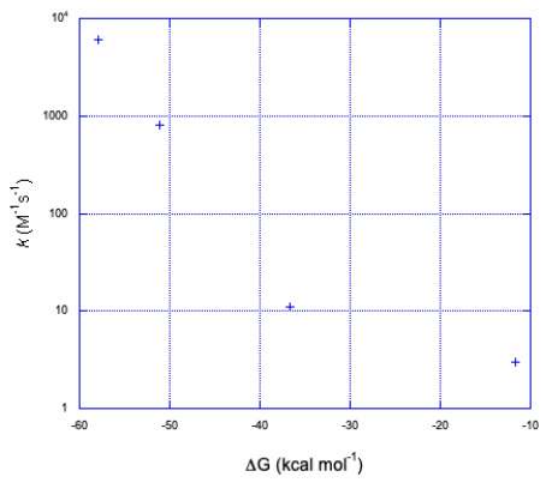
b) It doesn't look linear. If we plot the y axis on a log scale, things become a little more linear.



It looks closer to a logarithmic relationship than a linear one.

Answer c

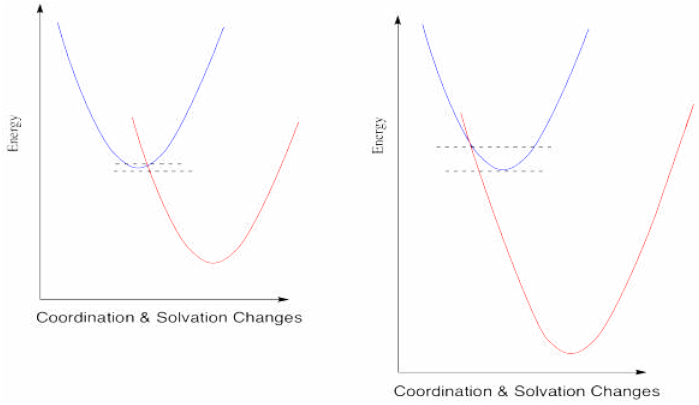
c) Assuming one electron transfer:



The graph takes the same form but in the opposite direction along the x axis.

Marcus Inverted Region

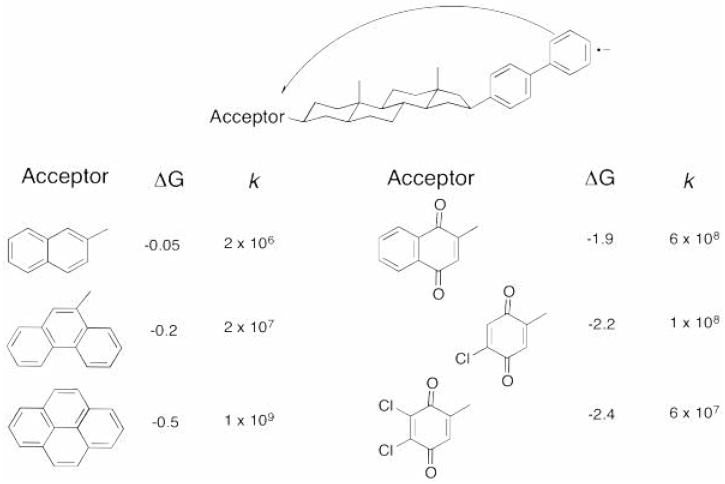
When you look a little closer at Marcus theory, though, things get a little strange. Suppose we make one more change and see what happens when the reduction potential becomes *even more* positive.



So, if Marcus is correct, at some point as the reduction potential continues to get more positive, reactions start to slow down again. They don't just reach a maximum rate and hold steady at that plateau; the barrier gets higher and higher and the reactions get slower and slower. If you feel a little skeptical about that, you're in good company.

Marcus always maintained that this phenomenon was a valid aspect of the theory, and not just some aberration that should be ignored. The fact that nobody had ever actually observed such a trend didn't bother him. The reason we didn't see this kind of thing, he said, was that we just hadn't developed technology that was good enough to measure these kind of rates accurately.

But technology did catch up. Just take a look at the following data (from Miller, *J. Am.Chem. Soc.* **1984**, *3047*).



Don't worry that there are no metals involved anymore. An electron transfer is an electron transfer. Here, an electron is sent from the aromatic substructure on the right to the substructure on the left. By varying the part on the left, we can adjust the reduction potential (or the free energy change, as reported here.

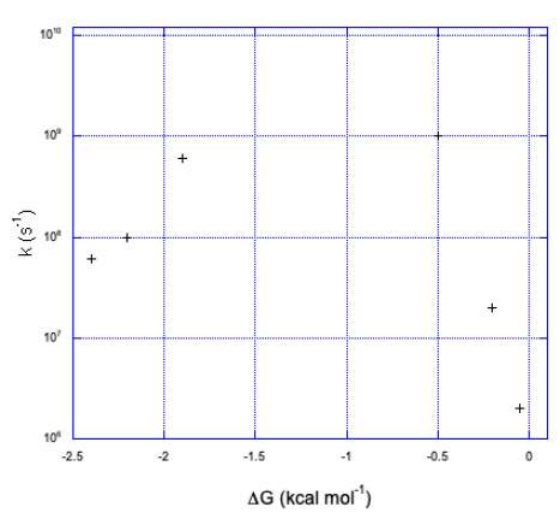
Exercise 10.5.9

a. Plot the data in the above table.

b. How would you describe the relationship?

Answer a

a)



Answer b

b) We can see two sides of an inverted curve. The reaction gets much faster as the free energy becomes more negative, but at some point the rate begins to decrease again.

As the reaction becomes more exergonic, the rate increases, but then it hits a maximum and decreases again. Data like this means that the "Marcus Inverted Region" is a real phenomenon. Are you convinced? So were other people. In 1992, Marcus was awarded the Nobel Prize in Chemistry for this work.

Exercise 10.5.10

Take a look at the donor/acceptor molecule used in Williams' study, above. a) Why do you suppose the free energy change is pretty small for the first three compounds in the table? b) Why does the free energy change continue to get bigger over the last three compounds in the table?

Answer

The acceptor compound becomes an anion when it accepts an electron. The first three compounds do not appear to be strongly electrophilic; they can accept electrons simply because of resonance stability of the resulting anion. The last three have electron withdrawing groups (chlorines and oxygens) that would stabilize the anion even further.

Exercise 10.5.11

The rates of electron transfer between cobalt complexes of the bidentate bipyridyl ligand, $Co(bipy)_3^{n+}$, are strongly dependent upon oxidation state in the redox pair. Electron transfer between Co(I)/Co(II) occurs with a rate constant of about 10^9 $M^{-1}s^{-1}$, whereas the reaction between Co(II)/Co(III) species proceeds with k = 18 $M^{-1}s^{-1}$.

a. What geometry is adopted by these complexes?
b. Are these species high spin or low spin?
c. Draw d orbital splitting diagrams for each complex.
d. Explain why electron transfer is so much more facile for the Co(I)/Co(II) pair than for the Co(II)/Co(III) pair.

Answer a

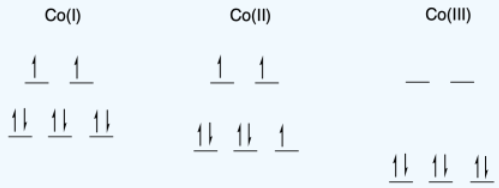
a) octahedral; bpy is a bidentate ligand.

Answer b

b) Co is first row; Co(I) and Co(II) have relatively low charge. Usually we would expect them to be high spin. Co(III) is at a cut-off point in the first row; it is just electronegative enough that it is usually low spin.

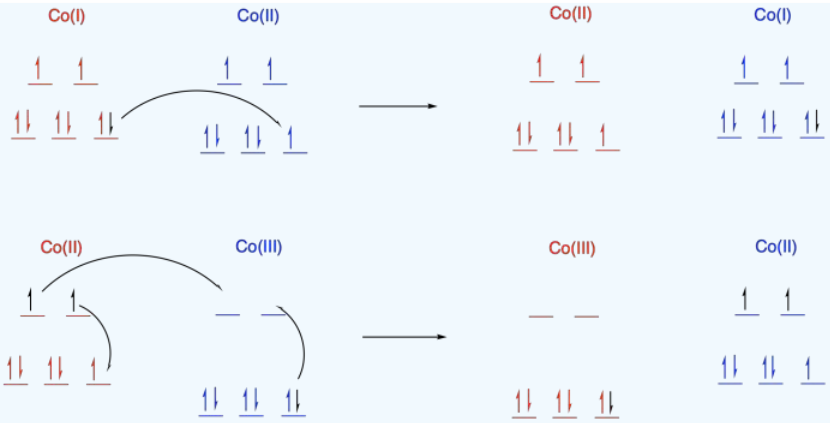
Answer c

c)



Answer d

d) In a transfer from Co(II) to Co(III), there is additional reorganization needed because the metal changes between high and low spin. Not only does one electron have to move from one metal to another metal, but additional electrons have to shuffle from one orbital to another on the same metal to accommodate the change. These reorganizations have a barrier, slowing the reaction.



Attribution

Chris P Schaller, Ph.D., (College of Saint Benedict / Saint John's University)

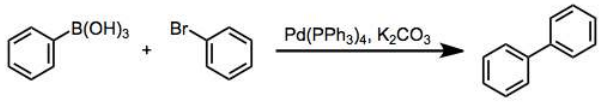
10.5: Electron Transfer Reactions is shared under a CC BY-NC-SA 4.0 license and was authored, remixed, and/or curated by LibreTexts.

CHAPTER OVERVIEW

11: Organometallic Chemistry

Organometallic chemistry is a subfield of inorganic chemistry involving the study of compounds containing, and reactions involving, metal-carbon bonds. The metal-carbon bond may be transient or temporary, but if one exists during a reaction or in a compound of interest, we're squarely in the domain of organometallic chemistry. In addition to M-C bond, bonds between metals and the other common elements of organic chemistry also appear in organometallic chemistry: metal-nitrogen, metal-oxygen, metal-halogen, and even metal-hydrogen bonds all play a role. Metals cover a vast swath of the periodic table and include the alkali metals, alkali earth metals, transition metals, the main group metals, and the lanthanides and actinides. We will focus most prominently on the transition metals in this chapter.

Why is the subject worth studying? Organometallic complexes are catalysts for a wide range of industrially important chemical reactions from polymers to pharmaceuticals. There's a reason the "organo" comes first in "organometallic chemistry"—These catalysts usually the aid in the creation of new bonds in organic compounds, building up complex products from simple starting materials. The fact is that you can do things with organometallic chemistry that you cannot do using straight-up organic chemistry. Case in point:



The venerable Suzuki reaction...unthinkable without palladium!

The establishment of a bond between two phenyl rings seems unthinkable to the pure organic chemist, but with a palladium catalyst it si a commonplace reaction. Bromobenzene looks like a potential electrophile at the bromine-bearing carbon, and if you're familiar with hydroboration you might see phenylboronic acid as a potential nucleophile at the boron-bearing carbon. Catalytic palladium makes it all happen. Organometallic chemistry is full of these mind-bending transformations, and can expand the synthetic toolbox of the organic chemist considerably.

Contributors and Attributions

- Dr. Michael Evans (Georgia Tech)

Learning Objectives

- Illustrate the orbital overlap involved in metal-ligand bonding for different classes of organometallic ligands
- Determine the metal electron count and use that to predict reactivity of the metal complex
- Recognize the different classes of reactions important to organometallic catalysis

Thumbnail image shows Wilkinson's catalyst (CC0; Benjah-bmm27 via Wikimedia Commons)

11.1: Organometallic Ligands
11.2: The 18 Electron Rule
11.3: Oxidative Addition
11.4: Reductive Elimination
11.5: Migratory Insertion- 1,2-Insertions
11.6: β-Elimination Reactions
11.7: Organometallic Catalysts

This page titled 11: Organometallic Chemistry is shared under a CC BY-NC-SA 4.0 license and was authored, remixed, and/or curated by Michael Evans.

11.1: Organometallic Ligands

There are some classes of ligands and modes of bonding that are important and in some cases unique to organometallic complexes and reactions. Before discussing reactions of organometallic complexes we will start with an overview of ligands common to organometallic complexes. In organometallic reactions, ligands can be either spectators, not chemically involved or changed during the reaction, or actors, chemically changed during the reaction. Similar to enzymes, a substrate will often bond to an organometallic catalyst as a ligands undergo a chemical transformation, and leave as a product.

Carbon Monoxide

Carbon monoxide is a neutral strong field ligand that we have discussed previously. We've seen that there are two bonding interactions at play in the metal carbonyl bond: a ligand-to-metal $n \rightarrow d_\sigma$ interaction (σ donation) and a metal-to-ligand $d_\pi \rightarrow \pi^*$ interaction (π accepting). The latter interaction is called backbonding because the metal donates electron density back to the ligand.

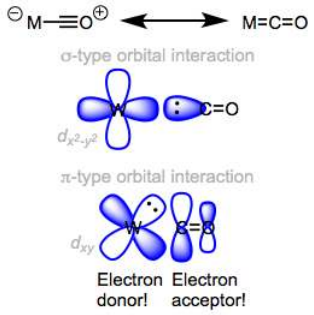


Figure **11.1.1**: Orbital interactions in M=C=O. (Copyright; Michael Evans)

CO is a fair σ-donor (or σ-base) and a good π-acceptor (or π-acid). The properties of ligated CO depend profoundly upon the identity of the metal center. More specifically, the electronic properties of the metal center dictate the importance of backbonding in metal carbonyl complexes. Most bluntly, *more electron-rich metal centers are better at backbonding to CO.* Why is it important to ascertain the strength of backbonding?

Backbonding and CO vibrational frequency

Infrared spectroscopy has famously been used to empirically support the idea of backbonding. The table below arranges some metal carbonyl complexes in "periodic" order and provides the frequency corresponding to the C=O stretching mode. Notice that without exception, every complexed CO has a stretching frequency lower than that of free CO. Backbonding is to blame! When a metal donates electrons into a π* antibonding MO on CO, the C-O bond order is lowered and the bond strength is weakened. According to Hooke's law, assuming all other things are equal, when the force constant (bond strength) decreases the vibrational frequency also decreases. Complexes with the strongest metal-CO backbonding will have the lowest frequency CO bond vibration(s).

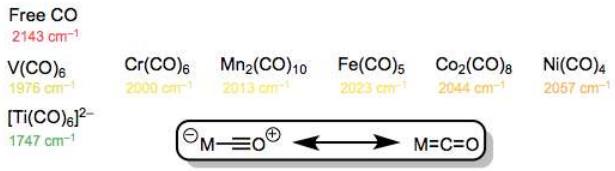


Figure **11.1.2**: CO stretching frequencies in metal-carbonyl complexes. (Copyright; Michael Evans)

The figure above depicts a clear increase in frequency (an increase in C–O bond order) as we move left to right across the periodic table. This finding may seem odd if we consider that the number of *d* electrons in the neutral metal increases as we move left to right. Shouldn't metal centers with more *d* electrons be better at backbonding (and more "electron rich")? What's going on here? Recall the periodic trend in *orbital energy*. As we move left to right, the *d* orbital energies decrease and the energies of the d_π and π* orbitals separate. As a result, the backbonding orbital interaction becomes worse (remember that strong orbital interactions require well-matched orbital energies) as we move toward the more electronegative late transition metals. We can draw an analogy

to enamines and enols from organic chemistry. The more electronegative oxygen atom in the enol is a worse electron donor than the enamine's nitrogen atom.

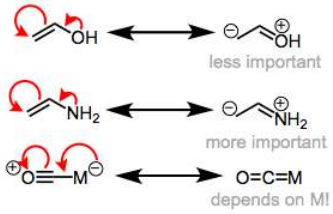


Figure **11.1.3**: The importance of backbonding depends on the electronegativity of the metal and its electron density. (Copyright; Michael Evans)

Of course, the contribution of other ligands on the metal center to backbonding cannot be forgotten, either. Logically, electron-donating ligands will tend to make the backbond stronger (they make the metal a better electron donor), while electron-withdrawing ligands will worsen backbonding. Adding electron-rich phosphine ligands to a metal center, for instance, *decreases* the CO stretching frequency due to *improved* backbonding.

CO as a bridging ligand

Carbonyl ligands are famously able to bridge multiple metal centers. Bonding in bridged carbonyl complexes may be either "traditional" or delocalized, depending on the structure of the complex and the bridging mode. The variety of bridging modes stems from the different electron donors and acceptors present on the CO ligand (and the possibility of delocalized bonding). Known bridging modes are shown in the figure below.

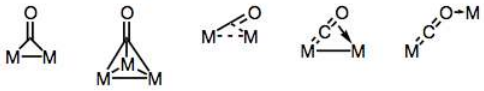
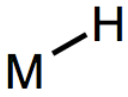


Figure **11.1.4**: Building bridges with carbonyl ligands. (Copyright; Michael Evans)

Metal Hydrides

Metal hydrides occupy an important place in transition metal organometallic chemistry as the M−H bonds can undergo insertion reactions with a variety of unsaturated organic substrates yielding numerous organometallic compounds with M−C bonds. Not only the metal hydrides are needed as synthetic reagents for preparing the transition metal organometallic compounds but they also are required for important hydride insertion steps in many catalytic processes. The first transition metal hydride compound was reported by W. Heiber in 1931 when he synthesized $Fe(CO)_4H_2$. Though he claimed that the $Fe(CO)_4H_2$ contained Fe−H bond, it was not accepted until 1950s, when the concept of normal covalent M−H bond was widely recognized.



Spectroscopic identification

The metal hydride moieties are easily detectable in ^{1}H NMR as they appear upfield of TMS in the region between 0 to -60 ppm, where no other H resonances appear. The hydride moieties usually couple with metal centers possessing nuclear spins. Similarly, the hydride moieties also couple with the adjacent metal bound phosphine ligands, if present in the complex, exhibiting characteristic *cis* (J = 15 − 30 Hz) and *trans* (J = 90 − 150 Hz) coupling constants. In the IR spectroscopy, the M−H frequencies appear between (1500 − 2200) cm^{-1} but their intensities are mostly weak. Crystallographic detection of metal hydride moiety is difficult as hydrogen atoms in general are poor scatterer of X−rays. Located adjacent to a metal atom in a M−H bond, the detection of hydrogen atom thus becomes challenging and as a consequence the X−ray crystallographic method systematically underestimates the M−H internuclear distance by ~ 0.1 Å. However, better data could be obtained by performing the X−ray diffraction studies at a low temperature in which the thermal motion of the atoms are significantly reduced. In light of these facts, the neutron diffraction becomes a powerful method for detection of the metal hydride moieties as hydrogen scatters neutrons more

effectively and hence the M−H bond distances can be measured more accurately. A limitation of neutron diffraction method is that large sized crystals are required for the study.

Bridging hydrides

Bridging hydrides are an intriguing class of ligands. A question to ponder: how can a ligand associated with only two electrons possibly bridge two metal centers? How can two electrons hold three atoms together? Enter the magic of three-center, two-electron bonding. We can envision the M–H sigma bond as an electron donor itself! With this in mind, we can imagine that hydrides are able to bind end-on to one metal and side-on to another. Consistent with the idea that bridging is the result of “end-on + side-on” bonding, bond angles of bridging hydrides are never 180°.

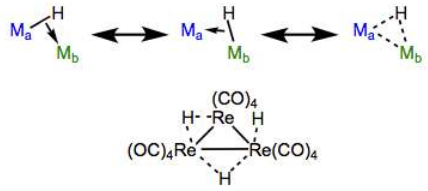
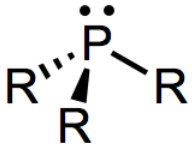


Figure **11.1.5**: Resonance forms of bridging hydrides, with an example. Sigma complexes like these show up in other contexts

Phosphines

Phosphines are most notable for their remarkable electronic and steric tunability and their “innocence”—they tend to avoid participating directly in reactions, but have the ability to profoundly modulate the electronic properties of the metal center to which they’re bound. Furthermore, because the energy barrier to inversion is quite high, “chiral-at-phosphorus” ligands can be isolated in enantioenriched form and introduced to metal centers, bringing asymmetry just about as close to the metal as it can get in chiral complexes. The one stable isotope of P (^{31}P) is NMR active so ^{31}P NMR is often used to cahrecterize complexes and reactions involving phosphine ligands . Soft phosphines match up very well with the soft low-valent transition metals. Electron-poor phosphines are even good π-acids.



Bonding

Like CO, phosphines are neutral σ donors and π acceptors that formally contribute two electrons to the metal center. Unlike CO, most phosphines are not small enough for more than four to bond to a single metal center (and for large R, the number is even smaller). Steric hindrance becomes a problem when five or more PR_3 ligands try to make their way into the space around the metal. Bridging by phosphines is extremely rare, but ligands containing multiple phosphine donors such as diphenylphosphinoethane metal center are common. For entropic reasons, chelating ligands like these bind to a single metal center at multiple points if possible, instead of attaching to two different metal centers (the aptly named chelate effect). An important characteristic of chelating phosphines is bite angle, defined as the predominant P–M–P angle in known complexes of the ligand. When the preferred bite angle of the ligand doesn't match the ideal bond angles of the geometry (i.e. 90° for octahedral) that introduces strain, and potentially reactivity into the complex.

The predominant orbital interaction contributing to phosphine binding is the one we expect, a lone pair on phosphorus donating to an empty metal d orbital. The electronic nature of the R groups influences the electron-donating ability of the phosphorus atom. For instance, alkylphosphines, which possess P–Csp^3 bonds, tend to be better electron donors than arylphosphines, which possess P–Csp^2 bonds. The rationale here is the greater electronegativity of the sp^2 hybrid orbital versus the sp3 hybrid, which causes the phosphorus atom to hold more tightly to its lone pair when bound to an sp^2 carbon. The same idea applies when electron-withdrawing and -donating groups are incorporated into R: the electron density on P is low when R contains electron-withdrawing groups and high when R contains electron-donating groups.

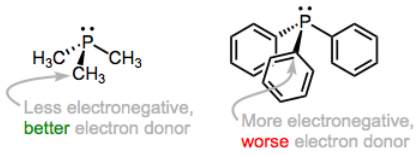


Figure **11.1.6**: As we add electronegative R groups, the phosphorus atom (and the metal to which it's bound) become more electron poor.

Like CO, phosphines participate in backbonding to a certain degree; however, the phenomenon here is of a fundamentally different nature than CO backbonding. For one thing, phosphines lack a π* orbital. In the days of yore, chemists attributed backbonding in phosphine complexes to an interaction between a metallic dπ orbital and an empty 3d orbital on phosphorus. However, this idea has elegantly been proven bogus, and a much more organic-friendly explanation has taken its place (no d orbitals on P required). In an illuminating series of experiments, M–P and P–R bond lengths were measured via crystallography for several redox pairs of complexes.

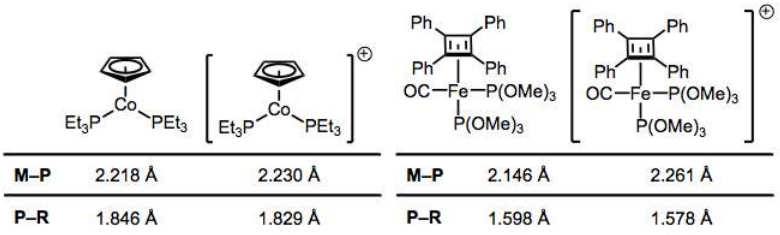


Figure **11.1.7**: Upon oxidation, M–P bond lengths increase and and P–R bond lengths decrease.

Oxidation decreases the ability of the metal to backbond, because it removes electron density from the metal. This explains the increases in M–P bond length—just imagine a decrease the M–P bond order due to decreased backbonding. And the decrease in P–R bond length? It's important to see that invoking only the phosphorus 3d orbitals would not explain changes in the P–R bond lengths, as the 3d atomic orbitals are most definitely localized on phosphorus. Instead, we must invoke the participation of σ*P–R orbitals in phosphine backbonding to account for the P–R length decreases. The figure below depicts one of the interactions involved in M–P backbonding, a dπ → σ* interaction (an orthogonal dπ → σ* interaction also plays a role). As with CO, a resonance structure depicting an M=P double bond is a useful heuristic! Naturally, R groups that are better able to stabilize negative charge—that is, electron-withdrawing groups—facilitate backbonding in phosphines. Electron-rich metals help too.

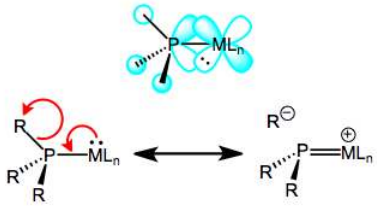


Figure **11.1.8**: Backbonding in phosphines, a sigma-bond-breaking affair.

Cone Angle

The steric and electronic properties of phosphines vary enormously. Tolman devised some intriguing parameters that characterize the steric and electronic properties of this class of ligands. To address sterics, he developed the idea of cone angle—the apex angle of a cone formed by a point 2.28 Å from the phosphorus atom (an idealized M–P bond length), and the outermost edges of atoms in the R groups, when the R groups are folded back as much as possible. Wider cone angles, Tolman reasoned, indicate greater steric congestion around the phosphorus atom. To address electronics, Tolman used the CO stretching frequency (νCO) of mixed phosphine-carbonyl complexes. Specifically, he used Ni(CO)3L complexes, where L is a tertiary phosphine, as his standard.

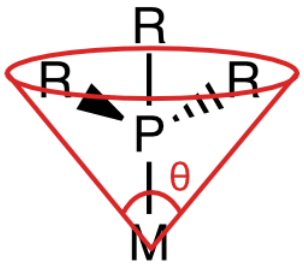
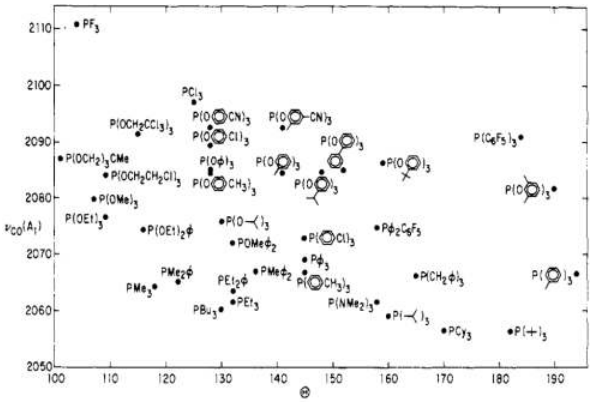


Figure **11.1.9**: Illustration of the cone angle in phosphines. (CC BY-NC-SA; Catherine McCusker)

Tolman's logic went as follows: more strongly electron-donating phosphines are associated with more electron-rich metals, which are better at CO backbonding (due fundamentally to higher orbital energies). Better CO backbonding corresponds to a lower νCO due to decreased C–O bond order. Thus, better donor ligands should be associated with lower νCO values (and vice versa for electron-withdrawing ligands). Was he correct? Exhibit A…



Tolman's map of the steric and electronic properties of phosphine ligands.

Notice the trifluorophosphine stuck in the "very small, very withdrawing" corner, and its utter opposite, the gargantuan tri(tert-butyl)phosphine in the "extremely bulky, very donating" corner.

σ Complexes

General Properties

Previously our discussion of metal-ligand σ bonding was limited to ligand lone pairs acting as donors. Ligands can also use a filled σ bonding molecular orbital to donate to a metal as shown in Figure **11.1.10**. This binding mode results in side-on η^2 bonding. If the backbonding interaction is too strong the single L-L ligands can become two L^- ligands by breaking the L-L sigma bond.

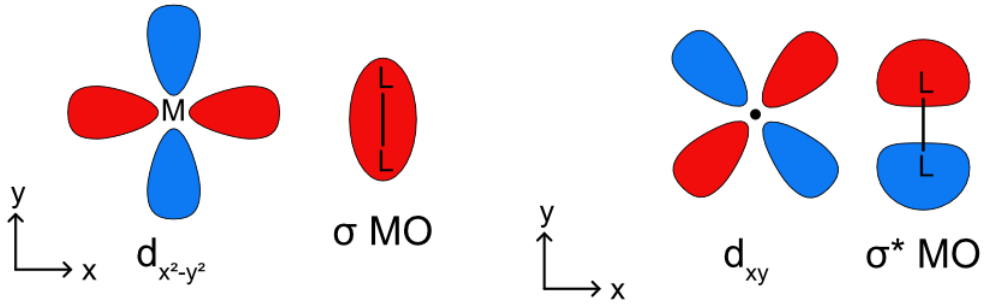


Figure **11.1.10**: Sigma bonding (left) and pi backbonding (right) orbital interaction in metal σ complexes (CC BY-NC-SA; Catherine McCusker)

The first thing to realize about σ complexes is that they are highly sensitive to steric bulk. Any old σ bond won't do; hydrogen at one end of the binding bond or the other (or both) is necessary. The best studied σ complexes involve dihydrogen (H2), so let's start there.

Dihydrogen complexes

Mildly backbonding metals may bind dihydrogen "side on." Like side-on binding in π complexes, there are two important orbital interactions at play here: σH–H → dσ and dπ → σ*H–H. Dihydrogen complexes can "tautomerize" to $(H)_2$ isomers through oxidative addition of the H–H bond to the metal. We should expect more electron-rich metal centers to favor the X2 isomer, since these should donate more strongly into the σ*H–H orbital. This idea was masterfully demonstrated in a study by Morris, in which he showed that H_2 complexes of π-basic metal centers show all the signs of dihydride complexes, rather than hydrogen complexes. More generally, metal centers in σ complexes need a good balance of π basicity and σ acidity (I like to call this the "Goldilocks effect"). Because of the need for balance, σ complexes are most common for centrally located metals (groups 6-9).

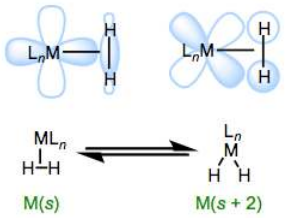


Figure **11.1.11**: Orbital interactions and L-X_2 equilibrium in σ complexes.

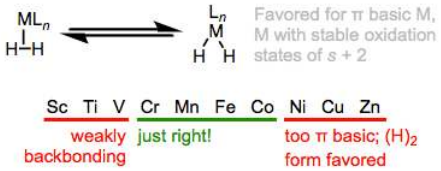
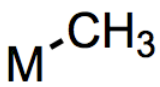


Figure **11.1.12**: Oxidative addition of H_2 is important for electron-rich, π-basic metal centers. Groups 6-9 hit the "Goldilocks" spot.

Metal Alkyls



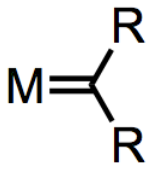
Alkyl or aryl transition metal compounds have M-C single bonds. In spite of many attempts over most of the course of chemical history, their isolation was unsuccessful and it was long considered that all M-C bonds were essentially unstable. Stable alkyl complexes began to be prepared gradually only from the 1950s. $Cp_2ZrCl(Pr)$,WMe_6, $CpFeMe(CO)_2$, $CoMe(py)(dmg)_2$, (dmg = dimethylglyoximato), $IrCl(X)(Et)(CO)(PPh_3)_2$, $NiEt_2(bipy)$, $PtCl(Et)(PEt_3)_2$ are some representative compounds. Among various synthetic processes so far developed, the reactions of compounds containing M-halogen bonds with main-group metal-alkyl compounds, such as a Grignard reagent or an organolithium compound, are common synthetic routes. Especially vitamin B_{12}, of which Dorothy Hodgkin (1964 Nobel Prize) determined the structure, is known to have a very stable Co-C bond. Metal alkyl compounds which have only alkyl ligand, such as WMe_6, are called homoleptic alkyls.

It is gradually accepted that a major cause of the instability of alkyl complexes is the low activation energy of their decomposition rather than a low M-C bond energy. The most general decomposition path is β elimination. Namely, the bonding interaction of a hydrocarbon ligand with the central transition metal tends to result in the formation of a metal hydride and an olefin. Such an interaction is called an **agostic interaction**. Although an alkyl and an aryl ligand are 1-electron ligands, they are regarded as anions when the oxidation number of the metal is counted. The hydride ligand, H, resembles the alkyl ligand in this aspect.

Carbenes

In this section we'll investigate two classes of carbenes, which are characterized by a metal-carbon double bond. Fischer carbenes and Shrock carbenes are usually actor ligands, but they may be either nucleophilic or electrophilic, depending on the nature of the

R groups and metal. In addition, these ligands present some interesting synthetic problems: because free carbenes are quite unstable, ligand substitution reactons can't be used for metal carbene synthesis.



Fisher vs Schrock carbenes

Metal carbenes all possess a metal-carbon double bond. What's interesting for us about this double bond is that there are multiple ways to deconstruct it to determine the metal's oxidation state and number of d electrons. We could give one pair of electrons to the metal center and one to the ligand. This procedure nicely illustrates why compounds containing M=C bonds are called "metal carbenoids"—the deconstructed ligand is a neutral carbenoid. Alternatively, we could give both pairs of electrons to the ligand and think of it as a dianionic ligand. The appropriate procedure depends on the ligand's substituents and the electronic nature of the metal. The figure below summarizes the two deconstruction procedures.

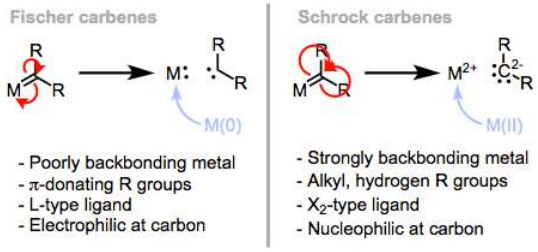
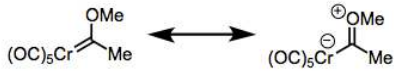


Figure **11.1.13**: The proper method of deconstruction depends on the electronic nature of the ligand and metal.

When the metal possesses π-acidic ligands and the R groups are π-basic, the complex is best described as an L-type Fischer carbene and the oxidation state of the metal is unaffected by the carbene ligand. When the ligands are "neutral" (R = H, alkyl) and the metal is a good backbonder—that is, in the absence of π-acidic ligands and electronegative late metals—the complex is best described as an anionic X_2-type Schrock carbene. Notice that the oxidation state of the metal depends on our deconstruction method. In organometallic complexes it isn't uncommon for the oxidation state of the metal and ligand to be ambiguous.

Deconstruction reveals the typical behavior of the methylene carbon in each class of complex. The methylene carbon of Schrock carbenes, on which electron density is piled through backbonding, is nucleophilic. On the other hand, the methylene carbon of Fischer carbons is electrophilic, because backbonding is weak and does not compensate for σ-donation from the ligand to the metal. To spot a Fischer carbene, be on the lookout for reasonable zwitterionic resonance structures like the one at right below.



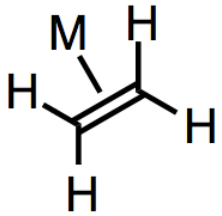
Thanks to the pi-accepting CO ligands, the metal handles the negative charge well. This is a Fischer carbene.

The clever reader may notice that we haven't mentioned π-acidic R groups, such as carbonyls. Complexes of this type are best described as Fischer carbenes as well, as the ligand is still electrophilic. However, complexes of this type are difficult to handle and crazy reactive (see below) without a π-basic substituent to hold them in check. Take care when diagnosing the behavior of metal carbenes. In these complexes, there is often a subtle interplay between the R groups on the carbene and other ligands on the metal. In practice, many carbenes are intermediate between the Fischer and Schrock ideals.

π Systems

In contrast to neutral spectator ligands, π systems most often play an important role in the reactivity of the organometallic complexes of which they are a part (since they act in reactions, they're called "actors"). π systems do useful chemistry, not just with the metal center, but also with other ligands and external reagents. Thus, in addition to thinking about how π systems affect the

steric and electronic properties of the metal center, we need to start considering the metal's effect on the ligand and how we might expect the ligand to behave as an active participant in reactions. To the extent that structure determines reactivity—a commonly repeated, and extremely powerful maxim in organic chemistry—we can think about possibilities for chemical change without knowing the elementary steps of organometallic chemistry in detail yet.



General Properties

Similar to σ complexes, the π bonding orbitals of alkenes, alkynes, carbonyls, and other unsaturated compounds may overlap with dσ orbitals on metal centers. This is the classic ligand HOMO → metal LUMO interaction that we've seen many times. Because of this electron donation from the π system to the metal center, coordinated π systems often act electrophilic, even if the starting alkene was nucleophilic. The π → dσ orbital interaction is central to the structure and reactivity of π-system complexes. π systems are also often subject to important backbonding interactions. We'll focus on alkenes here, but these same ideas apply to carbonyls, alkynes, and other unsaturated ligands bound through their π clouds. For alkene ligands, the relative importance of "normal" bonding and backbonding is nicely captured by the relative importance of the two resonance structures in Figure **11.1.14**.

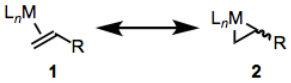


Figure **11.1.14**: Resonance forms of alkene ligands. In 1 backbonding is weak and in 2 the backbonding is strong.

Complexes of weakly backbonding metals, such as the electronegative late metals, are best represented by the traditional dative resonance structure **1**. But complexes of strong backbonders, such as electropositive Ti(II), are often best drawn in the metallacyclopropane form **2**. Bond lengths and angles in the alkene change substantially upon coordination to a strongly backbonding metal. We see an elongation of the C=C bond (consistent with decreased bond order) and some pyramidalization of the alkene carbons (consistent with a change in hybridization from sp^2 to sp^3). A complete orbital picture of sigma bonding and pi backbonding in alkenes is shown in Figure **11.1.15**.

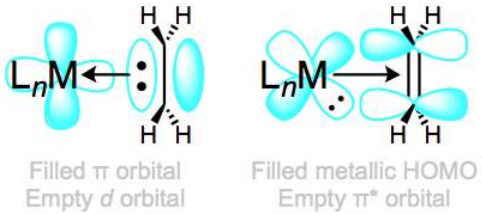
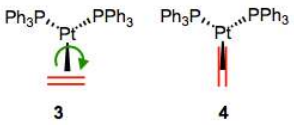


Figure **11.1.15**: Normal sigma bonding and pi backbonding in alkene complexes.

Here's an interesting question with stereochemical implications: what is the orientation of the alkene relative to the other ligands? From what we've discussed so far, we can surmise that one face of the alkene must point toward the metal center. Put differently, the bonding axis must be normal to the plane of the alkene. However, this restriction says nothing about rotation about the bonding axis, which spins the alkene ligand like a pinwheel. Is a particular orientation preferred, or can we think about the alkene as a circular smudge over time? The figure below depicts two possible orientations of the alkene ligand in a trigonal planar complex. Other orientations make less sense because they would involve inefficient orbital overlap with the metal's orthogonal d orbitals. Which one is favored?

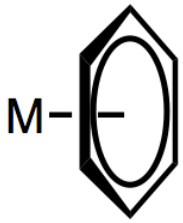


Two limiting cases for alkene orientation in a trigonal planar complex.

First of all, we need to notice that these two complexes are diastereomeric. They have different energies as a result, so one must be favored over the other. Steric considerations suggest that complex **4** ought to be more stable (in most complexes, steric factors dictate alkene orientation). To dig a little deeper, let's consider any electronic factors that may influence the preferred geometry. We've already seen that electronic factors can overcome steric considerations when it comes to complex geometry. To begin, we need to consider the crystal field orbitals of the complex as a whole. Verify on your own that in this d^{10}, Pt(0) complex, the crystal-field HOMOs are the d_{xy} and \(d-{x^2–y^2\) orbitals. Where are these orbitals located in space? In the xy-plane! Only the alkene in **3** can engage in efficient backbonding with the metal center. In cases when the metal is electron rich and/or the alkene is electron poor, complexes like **3** can sometimes be favored in spite of sterics.

Arenes

Arenes or aromatic ligands are neutral ligands that may serve either as actors or spectators. Arenes commonly bind to metals through more than two atoms, although η^2-arene ligands are known. Structurally, most η^6-arenes tend to remain planar after binding to metals. Both sigma bonding and pi backbonding are possible for arene ligands; however, arenes are stronger sigma donors than CO and backbonding is less important for these ligands. The reactivity of arenes changes dramatically upon metal binding, along lines that we would expect for strongly electron-donating ligands. After coordinating to a transition metal, the arene usually becomes a better electrophile (particularly when the metal is electron poor). Thus, metal coordination can enable otherwise difficult nucleophilic aromatic substitution reactions.



General Properties

The coordination of an aromatic compound to a metal center through its aromatic π MOs removes electron density from the ring. π → dσ (sigma bonding) and dπ → π* (backbonding) orbital interactions are possible for arene ligands, with the former being much more important, typically. To simplify drawings, you often see chemists draw arenes involving a circle and single central line to represent the π → dσ orbital interaction. Despite the single line these are not simple 2 electron donors. For instance, η^6-arenes are best describes as six-electron donors.

Multiple coordination modes are possible for arene ligands. When all six atoms of a benzene ring are bound to the metal (η^6-mode), the ring is flat and C–C bond lengths are slightly longer than those in free benzene. The ring is bent and non-aromatic in η^4-mode, so that the four atoms bound to the metal are coplanar while the other π bond is out of the plane. Even η^2-arene ligands bound through one double bond are known. Coordination of one π bond results in dearomatization and makes η^2-benzene behave more like butadiene, and furan act more like a vinyl ether. With naphthalene as ligand, there are multiple η^2 isomers that could form; the isomer observed is the one that retains aromaticity in the free portion of the ligand. In fact, this result is general for polycyclic aromatic hydrocarbons: binding maximizes aromaticity in the free portion of the ligand. Arene ligands are usually hydrocarbons, not heterocycles. Why? Aromatic heterocycles, such as pyridine, more commonly bind using their basic lone pairs. That said, a few heterocycles form important π complexes. Thiophene is perhaps the most heavily studied, as the desulfurization of thiophene from fossil fuels is an industrially useful process.

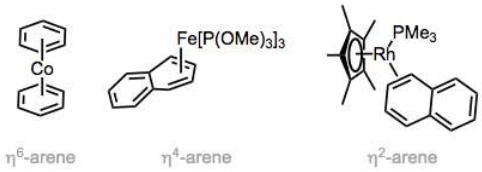
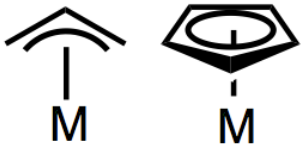


Figure **11.1.16**: Arene ligands exhibit multiple coordination modes.

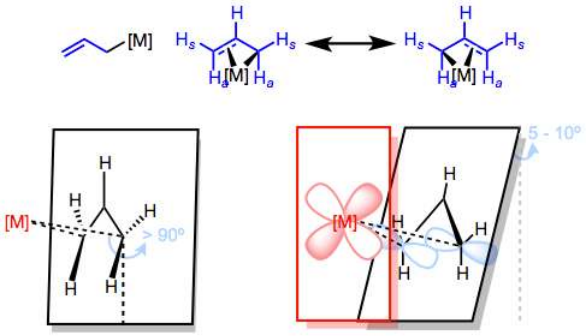
Odd Numbered π Systems

Odd-numbered π systems—most notably, the allyl and cyclopentadienyl ligands—are formally monoanionic ligands which donate n+1 electrons (i.e. η^5 cyclopentadienyl ligand is a 6 electron donor). To illustrate the plurality of equally important resonance structures for this class of ligands, we often just draw a curved line from one end of the π system to the other. Yet, even this form is not perfect, as it obscures the possibility that the datively bound atoms may dissociate from the metal center, forming σ-allyl or ring-slipped ligands. What do the odd-numbered π systems really look like, and how do they really behave?



Metal Allyls

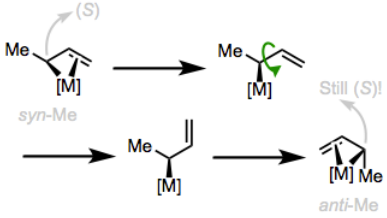
Allyls are often actor ligands, most famously in allylic substitution reactions. The allyl ligand is an interesting beast because it may bind to metals in two ways. When its double bond does not become involved in binding to the metal, allyl is a simple anionic ligand bound covalently through one carbon—basically, a monodentate alkyl! Alternatively, allyl can act as a bidentate LX-type ligand, bound to the metal through all three conjugated atoms. The LX or "trihapto" form can be represented using one of two resonance forms, or (more common) the "aromatic" form seen in the illustration above.



Can we use FMO theory to explain the wonky geometry of the allyl ligand?

The lower half of the figure above illustrates the slightly weird character of the geometry of allyl ligands. In a previous post on even-numbered π systems, we investigated the orientation of the ligand with respect to the metal and came to some logical conclusions by invoking FMO theory and backbonding. A similar treatment of the allyl ligand leads us to similar conclusions: the plane of the allyl ligand should be parallel to the xy-plane of the metal center and normal to the z-axis. In reality, the allyl plane is slightly canted to optimize orbital overlap—but we can see at the right of the figure above that π2–dxy orbital overlap is key. Also note the rotation of the anti hydrogens (anti to the central C–H, that is) toward the metal center to improve orbital overlap.

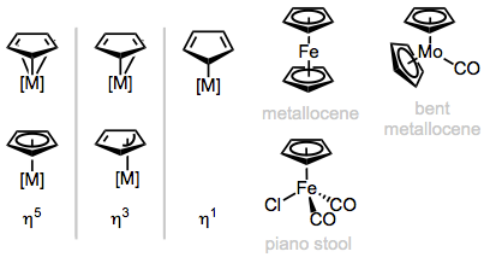
Exchange of the syn and anti substituents can occur through σ,π-isomerization followed by bond rotation and formation of the isomerized trihapto form. Notice that the configuration of the stereocenter bearing the methyl group is unaffected by the isomerization! It should be noted that 1,3-disubstituted allyl complexes almost exclusively adopt a syn,syn configuration without danger of isomerization.



The methylene and central C–H simply change places!

Metal Cyclopentadienyls

Upon deconstruction, the cyclopentadienyl (Cp) ligand yields the aromatic cyclopentadienyl anion, an L2X-type ligand. Cp is normally an η^5-ligand, but η^3 (LX) and η^1 (X) forms are known in cases where the other ligands on the metal center are tightly bound. η^1-Cyclopentadienyl ligands can sometimes be fluxional—the metal has the ability to "jump" from atom to atom. Variations on the Cp lignad include Cp* (C_5Me_5) and the monomethyl version (C_5H_4Me). A single Cp may bond alongside other ligands (in "half-sandwich" or "piano-stool" complexes), or paired up with a second Cp ligand in metallocenes. The piano-stool and bent metallocene complexes are most interesting for us, since these have potential for open coordination sites—metallocenes tend to be relatively stable and boring.



Binding modes of Cp and general classes of Cp complexes.

Contributors and Attributions

- Dr. Michael Evans (Georgia Tech)
- Modified by Catherine McCusker (East Tennessee State University)

This page titled 11.1: Organometallic Ligands is shared under a CC BY-NC-SA 4.0 license and was authored, remixed, and/or curated by Michael Evans.

- **2: Organometallic Ligands** by Michael Evans is licensed CC BY-NC-SA 4.0.
- **Current page** by Michael Evans is licensed CC BY-NC-SA 4.0.
- **2.2: Carbon Monoxide** by Michael Evans has no license indicated.
- **2.6: Metal Hydrides** by Michael Evans is licensed CC BY-NC-SA 4.0.
- **2.9: Phosphines** by Michael Evans is licensed CC BY-NC-SA 4.0.
- **2.3: σ Complexes** by Michael Evans is licensed CC BY-NC-SA 4.0.
- **2.5: Metal Alkyls** by Michael Evans is licensed CC BY-NC-SA 4.0.
- **2.1: Carbenes** by Michael Evans is licensed CC BY-NC-SA 4.0.
- **2.10: π Systems** by Michael Evans is licensed CC BY-NC-SA 4.0.
- **2.8: Odd-numbered π Systems** by Michael Evans is licensed CC BY-NC-SA 4.0.

SECTION OVERVIEW

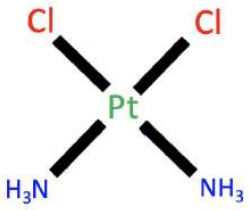
11.2: The 18 Electron Rule

Electron Counting In Transition Metal Complexes

In this chapter we will learn how to count valence electrons in coordination compounds. Electron counting is important because the number of electrons in a complex can tell us a lot about the stability and reactivity in a coordination compound. In addition, it allows us to predict and understand structures to a certain extent. Electron counting sounds trivial, but it is not as trivial as it seems, actually there are even two different methods for electron counting. Each method leads to the same result. Which method you prefer is “personal taste”, but each method is about equally common in the literature, so you need to know both of them.

The Neutral Atom Method

The first method is called the “neutral atom method”. As the name suggests, we will break up the complex into neutral fragments, and count the electrons that contribute to the bonding in each of the fragments. The neutral atom method is carried out according to the following three steps. First, we count the number of the valence electron of the metal. We consider the metal as neutral atom. The number valence electrons is the same as the group number of the transition metal in the periodic table. For transition metals the group number varies from 3 to 12. In the second step, we account for the ionic charge of the complex, if the complex is not neutral. This will reduce the number of electrons for a complex cation, and increase the number of valence electrons for a complex anion. In the third step, we need to determine how many electrons are contributed by each ligand. This is the most complicated step. To determine the number of electrons must cleave each metal-ligand bond so that a ligand fragment results that is neutral. We then count the number of electrons at the ligand that contributed to the bond. The number of electrons contributed by each ligand is then summed up. This is sum is then added to the number of electrons determined by the previous steps. This is gives the overall number of valence electrons.



	Number of e's
Pt	10
charge	0
2 Cl	2 · 1 = 2
2 N	2 · 2 = 4
Total	= 16

Figure 6.1.1 Example of neutral atom method

Let us apply these rules by an example, the cis-platinum complex. We first need to count the number of electrons of the metal. The metal is platinum which is located in group 10 of the periodic table. Therefore, a neutral platinum atom has ten valence electrons.

Next, we look at the charge of the complex. In this case, there is no charge, and therefore no electrons are added or subtracted.

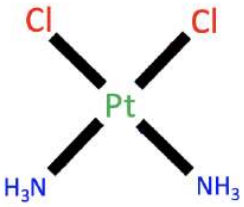
Lastly, we count the electrons of the ligands. There are two types of ligands, the chloro-ligands and the ammine ligands. Now, our task is to cleave the Pt-ligand bond so that neutral ligand fragments result. We can see that for the chloro-ligands we must cleave the Pt-Cl bond, homoleptically, meaning in the middle, assigning one electron to the Pt and one electron to Cl, because doing so creates a neutral chlorine atom. The fact that we cleaved the bond homoleptically, means that the chloro ligand contributed one electron. Because we have two chloro ligands, there are overall two electrons.

Now, let us think about how many electrons the ammine ligands contribute. In this case we need to cleave the metal-ligand bond heteroleptically to produce a neutral ligand fragment. Both bonding electrons are assigned to the ligand. This produces a neutral NH3 molecule. This means that each ammine ligand contributes two electrons. Overall, that makes four electrons, because we have two ammine ligands.

Finally, we need to sum up the electrons from all three steps. That is ten electrons from Pt, zero electrons due to charge, two electrons from the chloro ligands, and four electrons from the ammine ligands equaling 16 valence electrons total. This is the final result.

"Oxidation State" Method

The oxidation state method is also comprised of three steps. The first step is the same as in the neutral atom method. We determine the number of electrons of the neutral metal which the same as its group number in the periodic table. The next step is different though. It requires the determination of the oxidation state of the metal. How can we determine it? First, we cleave the metal-ligand bonds heteroleptically so that all bonding electrons are assigned to the ligands. Then we determine what is the charge of the ligands? Ligands can either be neutral of negatively charged. We determine the overall number of charges at the ligands. The difference between that number and the charge of the complex is the oxidation state of the metal. We either add or subtract electrons depending on the oxidation state of the metal. If the oxidation state is positive we subtract electrons, if it is negative, which is rare, then we add electrons. The third step counts the number of the electrons contributed by the ligands. Because we cleaved all bonds homoleptically, all bonding electrons are considered to be contributed by the ligands, and we count them accordingly. Finally, we sum up the electrons of all three steps which gives the total number of electrons.



	Number of electrons
Pd	10
Oxid. state	-(+2)
2 Cl^-	$+2 \cdot 2 = 4$
2 N	$+2 \cdot 2 = 4$
Total	**= 16**

Figure 6.1.2 Example of oxidation state method

Let us apply the method to the previous example cis-platinum. Applying the first step gives us 10 valence electrons for the platinum.

Next, we need to determine the oxidation state of Pt. To do so, we must now cleave all metal-ligands heteroleptically, so that all bonding electrons are assigned to the ligand. By the way, this is equivalent to saying that we treat all the bonds as dative bonds with all electrons coming from the ligands as the donors. When we do this for the chloro ligands we see that this created chloride anions with a 1- charge. Cleaving the Pt-N bonds heteroleptically leads to neutral NH_3 molecules. Therefore the overall number of charges at the ligands is 2x(-1)+2x0=-2. The charge at the complex is zero, therefore the oxidation state of Pt is 0-(-2)=+2. We must therefore subtract two electrons from the 10 electrons of the platinum.

Now we must determine the number electrons coming from the ligands. Because all bonds are considered as dative bonds, the chloro ligands contribute two electrons each, and the ammine ligands contribute two electrons each. That makes overall four electrons.

In sum, 10 electrons from the neutral Pt atom minus two electrons due to the +2 oxidation state of Pt plus 2x2=4 electrons from Cl plus 2x2=4 electrons from NH_3 gives 16 electrons total. We can see that we have arrived at the same results as in the case of the oxidation state method.

We can discuss the advantages and disadvantages of both methods, also. They neutral atom method has the advantage that we do not have to think about charges at ligands and oxidation states. However, we have to think about how to cleave bonds to create neutral fragments. We may need ot cleave bonds in an way that is not reflecting the donor-acceptor nature of a coordination compound. The oxidation method does account for the donor-acceptor nature of a coordination compound because the bonds are considered dative bonds, and the electrons are assigned to the ligands and metal accordingly. We not not need to think how to cleave bonds, because we cleave the bonds always heteroleptically. However, it requires us to think about charges at the ligands to determine oxidation states which is an additional, non-trivial step.

Counting Electrons: Ligand Contributions

The most difficult step in electron counting is mostly the determination of the number of electrons a ligand provides. Therefore, let us practice this by a few example.

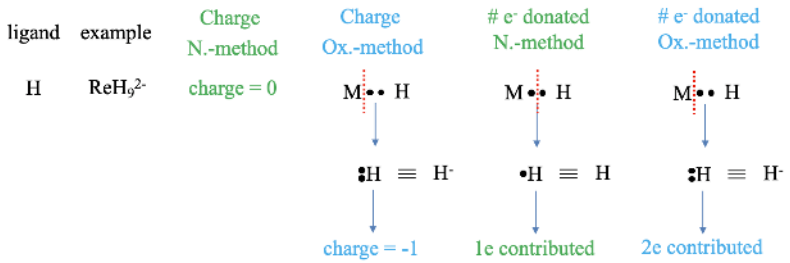


Figure 6.1.3 Example of counting electrons with a hydrido ligand

Let us first look at an hydrido ligand which for example occurs in the nonohydridorhentate(2-) complex. What is the charge of the ligand in the two methods? In the neutral atom method the charge is always zero, this is a no-brainer. In the case of the oxidation statement method, we need to treat the bond as a dative bond, and that means that we must cleave the bond heteroleptically, so that both bonding electrons can be assigned to the ligand. An H atom with two electrons is a hydride anion with a -1 charge. Next, let us think about the number of electrons donated. In the neutral atom method we need to produce neutral ligand fragments. To do so we must cleave the M-H bond homoleptically, because this will create a neutral hydrogen atom. How many electron will it contribute. It will contribute one electron, because we cleaved the bond homoleptically assigning only one of the two bonding electrons to H. In the oxidation state method, the hydrido ligand contributes two electrons because the bond was considered dative and therefore cleaved heteroleptically. Both bonding electrons were assigned to the ligand, therefore the ligand contributes two electrons.

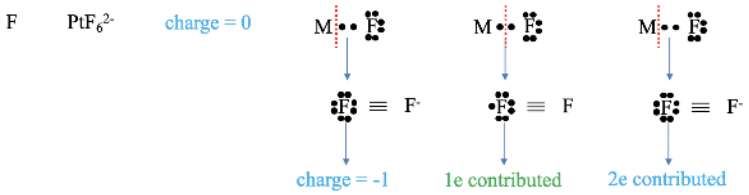


Figure 6.1.4 Example of counting electrons with a halogenide ligand

Next, let us consider a halogenide ligand. What is the charge at the ligand. For the neutral atom method, the answer is trivial, the charge is always zero. In the oxidation state method both bonding electrons in the M-L bond get assigned to the ligand. This gives the ligand a -1 charge. What is the number of electrons contributed? In the neutral atom method we need to think again how to cleave the M-L bond to create a neutral ligand fragment. We need to see that we must cleave the bond homoleptically to produce that fragment. Cleaving the bond homolopetically means that that ligand has contributed one electron. In the oxidation state method, we cleave the bond always heteroleptically so that all bonding electrons are assigned to the ligand. Thus, the ligand contributes two electrons.

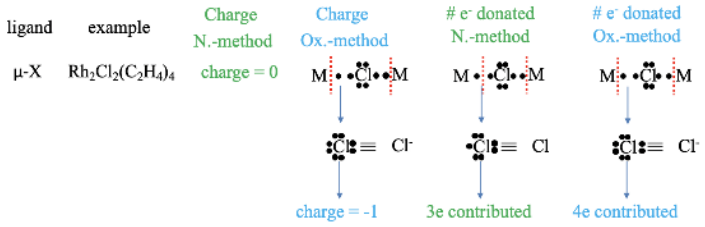


Figure 6.1.5 Example of counting electrons with a bridging halogenide ligand

A halogenide anion as a ligand cannot only be terminal, but bridging. An example is the μ-dichloro bis(tetraethylene rhodium(I)) complex in which two chloro-ligands bridge two rhodium atoms. What is the charge in the neutral atom method. Of course, it is zero. What is the charge in the oxidation state method? We can see that if we consider both metal-ligand bonds dative bonds, and cleave the bonds heteroleptically, that the Cl atom is surrounded by eight unshared electrons, which give it a -1 charge. How, many electrons are contributed in the neutral atom method? To answer this question, we need to decide if we have to cleave the bonds homo- or heteroleptically to produce a neutral Cl atom. Can you see it? The answer is: We must cleave one bond homoleptically, and the other one heteroleptically. How many electrons are then contributed by the chloro ligan? It is the two electrons from the heteroleptically cleaved bond, and one electron from the homoleptically cleaved bond. So overall it is three electrons. What about

the oxidation state method? In this case both bonds very cleaved heteroleptically, and this means that overall four electrons have been contributed.

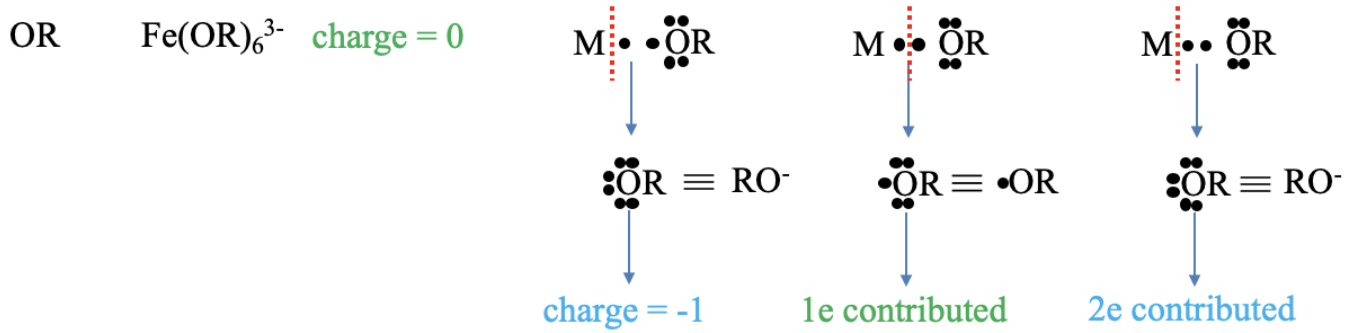


Figure 6.1.6 Example of counting electrons with an OR ligand

What are the charges and electrons contributed by an alkoxy ligand? An example for a complex with such as ligand is pentaphenoxy ferrate (3-). The charge according to the neutral atom method is zero. In the oxidation state method we cleave the bonds heteroleptically, and our ligand becomes an alkoxide anion. This anion has a 1- charge. How many electrons does the ligand contribute? To get a neutral fragment we must cleave the bond homoleptically. This actually produces an alkoxy radical. This radical contributes its radical electron, thus there is one contributed electron. In the oxidation state method we treated the bond as a dative bond and cleaved the bond heteroleptically. Therefore two electrons are contributed according to the oxidation state method.

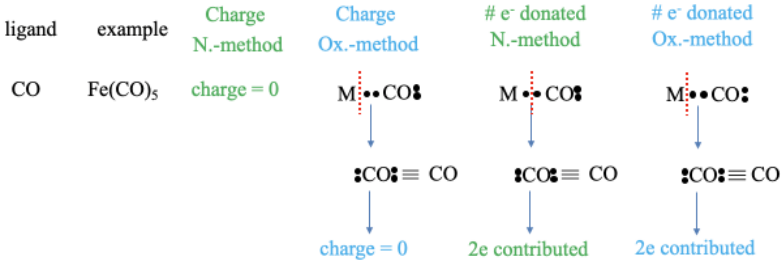


Figure 6.1.7 Example of counting electrons with a carbonyl ligand

Next, let us apply electron counting to the carbonyl ligand. For example four carbon monoxide molecules form an iron pentacarbonyl complex with iron. The charge at the ligand in the neutral atom method is zero. In the oxidation state method, we assign both bonding electrons to the ligand, and that produces a neutral carbon monoxide molecule. Note that the carbon atom is formally negatively charged, because it is surrounded by 5 electrons, but the oxygen atom is positively charged because it is surrounded by five electrons. So overall, the molecule is neutral. What is the number of electrons contributed in the neutral atom method? To produce a neutral ligand we must cleave the bond heteroleptically. This produces a neutral carbon monoxide molecule. Because we cleaved the bond heteroleptically, the ligand contributes two electrons. In the oxidation state method we always cleave the bonds heteroleptically, and thus two electrons come from the ligand.

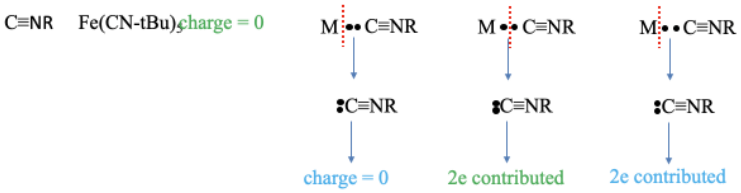


Figure 6.1.8 Example of counting electrons with

The last ligand we discuss here is the isonitrile ligand. An example is the pentakis-(tert-butyl isonitrile) iron molecule. The charge of the ligand is zero in the neutral atom method, but what is it in the oxidation state method? Let us see what happens as we assign both bonding electrons to the ligand. We we see that the carbon is now surrounded by five electrons. Three are in the carbon-nitrogen triple bond and they other two come from the electron lone pair at the carbon atom. This means that the carbon atom has a -1 charge. Now, let us look at the N atom. We see that it is surrounded by four electrons, three coming from the C-N triple bond, and one from the C-R bond. That means that the N atom has a +1 charge. Overall, the molecule is neutral and does not carry a

charge. What about the number of electrons contributed? We can see that we must cleave the bond heteroleptically to produce a neutral isoitrile, there are two electrons are contributed in the neutral atom method. The oxidation state method must cleave the bond heteroleptically, therefore, the number of electrons is also two.

18 Electron Rule

Electron counting is important in the context of an important rule in coordination chemistry: The 18 electron rule. The 18 electron rule states that for d-block elements *normally* complexes with 18 electrons in the shell ($ns^2(n-1)d^{10}np^6$ configuration) are most stable. If this number is not reached, the species is **coordinatively unsaturated** and tend to add more ligands. It also tends to be reduced because adding electrons brings the complex to or at least closer to 18 electrons. Coordinatively unsaturated complexes therefore tend to have a higher reactivity.

Definition: Coordinatively Unsaturated

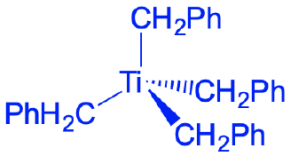
A species is coordinatively unsaturated when the 18 electrons are not reached in the ($ns^2(n-1)d^{10}np^6$ configuration) shell. They tend to add more ligands, and to be reduced. They are associated with higher reactivity.

If a species has more than 18 electrons it is coordinatively oversaturated and tends to lose ligands. It is usually easily oxidized. Both loss of ligands and oxidation reduces to the number of electrons to or at least closer to 18.

Definition: Coordinatively Oversaturated

A species is coordinatively oversaturated when it has more than 18 electrons in the shell ($ns^2(n-1)d^{10}np^6$ configuration) shell. They tend to lose ligands and are easily oxidized.

The 18 electron rule has many exceptions, and therefore needs to be applied with caution. In particular group 3, 4, and 10 complexes deviate often from the 18 electron rule.



Contribution metal:	4e
Oxidation state: +4	-4e
Electrons contributed by ligands:	4x2e=8e
Sum:	**8e**

Figure 6.1.9 Example of counting electrons in the tetrahedral tetrabenzyltitanium(0) complex

For illustration purposes, let count the number of electrons of the tetrahedral tetrabenzyltitanium(0) complex by the oxidation state method. We could also use the neutral atom method, which would give the same results. This complex is a group 4 complex because titanium is in group 4. How many electrons will the titanium contribute? Because number of electrons is always the same as the group number, it will contribute four electrons. Next, what is oxidation state of Ti? To determine it we must determine the charge at the ligands. To do that we cleave the bonds heteroleptically. This will give benzylate anions with -1 charge. There are four of these ions, and therefore there will be four negative charges overall. The complex is charge-neutral, and thus the oxidation state is +4 because -4+4=0. Therefore, we need to subtract four electrons. Because we cleaved the bond heteroleptically, each ligand contributed two electrons, giving overall eight electrons coming from the four ligands. This means that we have overall eight electrons, or an 8-electron complex. This is far, far away from 18 electrons. Nonetheless, the complex is quite stable, does not have a tendency to get reduced, or to add ligands. How can we explain this. The answer is that in order to achieve 18 electrons it would need to add five additional ligands if each ligand is considered a 2-electron donor. This would increase the coordination number to 9 which is too high to produce a stable complex. In order to reduce the complex to an 18 electron complex, 10 electrons would need to be added. This would produce a complex with a -10 charge which is way to high to be stable. The arguments are

generalizable for group 3 and group 4 complexes. Because these elements only have a few d electrons, the ligands would contribute a lot of electrons to produce an 18 electrons complex. This would require just too many ligands to add. The coordination numbers would get too high. If electrons are added instead to ligands, the negative charge at the complex would be to high to be stable based on electron-electron repulsion arguments.



Contribution metal:	10e
Charge:	0e
Electrons contributed by Cl ligands:	2x1e=2e
Electrons contributed by NH_3 ligands:	2x2e=4e
Sum:	**16e**

Figure 6.1.10 Example of counting electrons in the dichlorodiammine palladium complex

These arguments cannot be applied for group 10 elements, because these elements have many d electrons. The explanation in this case is that these elements like to make square planar complexes when in the common oxidation state +2. Square planar complexes prefer 16 instead of electrons. You can see that the square planar dichlorodiammine palladium complex shown is square planar and has sixteen electrons. There are 10 electrons coming from Pd. If we use the neutral atom method, no electrons need to be added or subtracted due to the charge at complex. The complex is charge-neutral. To assess how many electrons come from the ligands we need to cleave the bonds so that neutral ligands are produced. The Pd-Cl bonds need to be cleave homoleptically, the Pd-N bonds need to be cleave heteroleptically. Therefore, the two chloro ligands are 1e donors, and the two ammine ligands are 2e donors. This gives 10+4+2=16 electrons

---

This page titled 11.2: The 18 Electron Rule is shared under a CC BY-NC-SA 4.0 license and was authored, remixed, and/or curated by Kai Landskron.

11.3: Oxidative Addition

Overview

In the next few sections we will introduce reactions that are unique to organometallic complexes and play important roles in organometallic catalysis. The first reaction type is oxidative addition. As the name implies, the oxidative addition reaction involves increasing the coordination number of the metal complex by two and oxidizing the metal center by two electrons as shown in Figure **11.3.1**. The metal donates two electrons to break the A-B bond and form two new bonds, M-A and M-B.

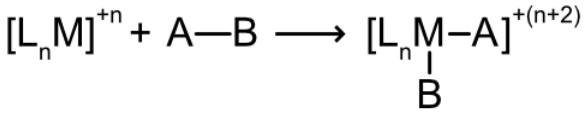


Figure **11.3.1**: General scheme for oxidative addition. (CC BY-NC-SA; Catherine McCusker)

How important are oxidative additions? Very. The addition of dihydrogen (H_2) is an important step in catalytic hydrogenation reactions. Organometallic C–H activations depend on oxidative additions of C–H bonds. In a fundamental sense, oxidative additions of organic compounds are commonly used to establish critical metal-carbon bonds. Non-polar oxidative additions get the ball rolling in all kinds of catalytic organometallic reactions. Here the mechanisms and important trends associated with oxidative additions are discussed.

Oxidative Additions of H_2

Electron-rich metal centers with open coordination sites (or the ability to form them) undergo oxidative additions with dihydrogen gas. The actual addition step is concerted, but before the addition step, some interesting gymnastics are going on. The status of the σ complex that forms prior to H–H insertion is an open question—for some reactions it is a transition state, others a discrete H2Fe(CO)4">intermediate. In either case, the two new hydride ligands end up cis to one another. Subsequent isomerization may occur to give a trans dihydride.

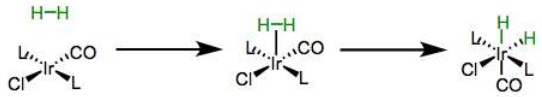


Figure **11.3.2**: Oxidative addition of dihydrogen to Vaska's complex. Note the cis arrangement of the hydride ligands.

Oxidative Additions of Silanes (H–Si)

Silanes bearing Si–H bonds may react with organometallic complexes in oxidative addition reactions. Spectroscopic experiments support the intermediacy of a silyl σ complex before insertion. Since the mechanism is concerted, oxidative addition occurs with retention of configuration at Si. The usual pair of forward bonding (σSi–H→dσ) and backbonding (dπ→σ*Si–H) orbital interactions are at play here. File this reaction away as a great method for the synthesis of silyl complexes.

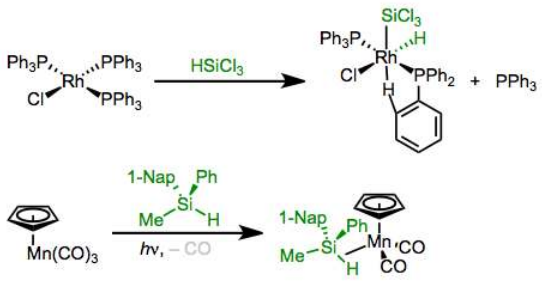


Figure **11.3.3**: Si–H bonds undergo oxidative addition to electron-rich metal complexes. Electron-poor complexes may stop at the σ complex stage

Needless to say, oxidative addition reactions of C–H bonds are highly prized among organometallic chemists. As simple as it is to make silyl complexes through oxidative addition, analogous reactions of C–H bonds that yield alkyl hydride complexes are harder to come by. The thermodynamics of C–H oxidative addition tell us whether it's favorable, and depend heavily on the nature of the organometallic complex. The sum of the bond energies of the new M–C and M–H bonds must exceed the sum of the energies of the C–H bond and any M–L bonds broken during the reaction. For many complexes, the balance is not in favor of oxidative addition. For example, the square planar Vaska's complex (L2(CO)IrCl; L = PPh3) seems like a great candidate for oxidative addition of methane—at least to the extent that the product will be six-coordinate and octahedral. However, thermodynamics is a problem:

$$104\ (C–H) – [60\ (Ir–H) + 35\ (Ir–Me)] + 9\ kcal/mol\ (entropy) = 18\ kcal/mol$$

18 kcal/mol is prohibitively high in energy, and playing with the temperature to adjust the entropy factor can't "save" the reaction.

More electron-rich complexes exhibit favorable thermodynamics for insertions of C–H bonds. The example below is so favorable (104 – [75 + 55] + 9 = –17 kcal/mol) that the product is a rock.

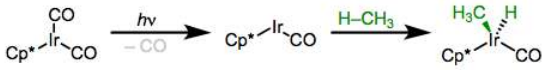


Figure **11.3.4**: This thermodynamically favorable C–H oxidative addition is helped by the electron-donating Cp* ligand.

Arenes undergo C–H oxidative addition faster (and more favorably) than alkanes for several reasons. It seems likely that an intermediate arene π complex and/or C–H σ complex precede insertion, and these complexes ought to be more stable than alkyl σ complexes. In addition, metal-aryl bonds tend to be stronger than metal-alkyl bonds.

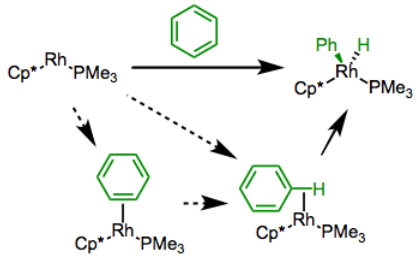


Figure **11.3.5**: Mechanistic possibilities for the oxidative addition of arene C–H bonds.

Contributors and Attributions

- Dr. Michael Evans (Georgia Tech)
- Modified by Catherine McCusker (East Tennessee University)

11.3: Oxidative Addition is shared under a CC BY-NC-SA 4.0 license and was authored, remixed, and/or curated by LibreTexts.

11.4: Reductive Elimination

Reductive elimination is the microscopic reverse of oxidative addition. It is literally oxidative addition run in reverse. Chemically, reductive elimination and oxidative addition share the same reaction coordinate. The only difference between their reaction coordinate diagrams relates to what we call “reactants” and “products.” Thus, their mechanisms depend on one another, and trends in the speed and extent of oxidative additions correspond to opposite trends in reductive eliminations. In this section, we’ll address reductive elimination in a general sense, as we did for oxidative addition.

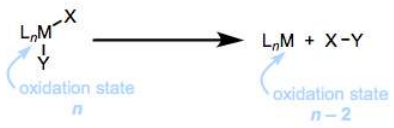


Figure **11.4.1**:A general reductive elimination scheme. The oxidation state of the metal decreases by two units, and open coordination sites become available.

During reductive elimination, the electrons in the M–X bond head toward ligand Y, and the electrons in M–Y head to the metal. The eliminating ligands are always anionic. On the whole, the oxidation state of the metal decreases by two units, two new open coordination sites become available, and an X–Y bond forms. What does the change in oxidation state suggest about changes in electron density at the metal? As suggested by the name “reductive,” the metal gains electrons. The ligands lose electrons as the new X–Y bond cannot possibly be polarized to both X and Y, as the original M–X and M–Y bonds were.

It’s been observed in a number of cases that a ligand dissociates from octahedral complexes before concerted reductive elimination occurs. Presumably, dissociation to form a distorted trigonal bipyramidal geometry brings the eliminating groups closer to one another to facilitate elimination. Square planar complexes may either take on an additional fifth ligand or lose a ligand to form an odd-coordinate complex before reductive elimination. Direct reductive elimination without dissociation or association is possible, too.

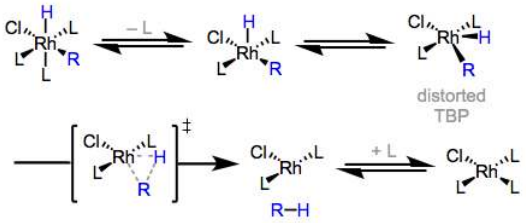


Figure **11.4.2**:Reductive elimination is faster from five-coordinate than six-coordinate complexes.

Reactivity trends in reductive elimination are opposite those of oxidative addition. More electron-rich ligands bearing electron-donating groups react more rapidly, since the ligands lose electron density as the reaction proceeds. More electron-poor metal centers—bearing π-acidic ligands and/or ligands with electron-withdrawing groups—react more rapidly, since the metal center gains electrons. Sterically bulky ancillary ligands promote reductive elimination since the release of X and Y can “ease” steric strain in the starting complex. Steric hindrance helps explain, for example, why coordination of a fifth ligand to a square planar complex promotes reductive elimination even though coordination increases electron density at the metal center. A second example: trends in rates of reductive eliminations of alkanes parallel the steric demands of the eliminating ligands: C–C > C–H > H–H.

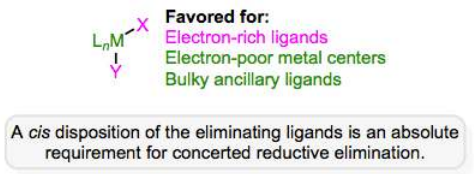


Figure **11.4.3**: Reactivity trends for reductive eliminations.

Mechanistic trends for reductive elimination actually parallel trends in mechanisms of oxidative addition, since these two reactions are the microscopic reverse of one another. Non-polar and moderately polar ligands react by concerted or radical mechanisms;

highly polarized ligands and/or very electrophilic metal complexes react by ionic (S_N2) mechanisms. The thermodynamics of reductive elimination must be favorable in order for it to occur! Most carbon–halogen reductive eliminations, for example, are thermodynamically unfavorable (this has turned out to be a good thing, especially for cross-coupling reactions).

Reductive elimination is an important step in many catalytic cycles—it usually comes near the "end" of catalytic mechanisms, just before product formation. For some catalytic cycles it's the turnover-limiting step, making it very important to consider. Hydrocyanation is a classic example; in the mechanism of this reaction, reductive elimination of C–CN is the slow step. Electron-poor alkyl ligands, derived from electron-poor olefins like unsaturated ketones, are bad enough at reductive elimination to prevent turnover altogether.

Contributors and Attributions

Dr. Michael Evans (Georgia Tech)

11.4: Reductive Elimination is shared under a CC BY-NC-SA 4.0 license and was authored, remixed, and/or curated by LibreTexts.

11.5: Migratory Insertion- 1,2-Insertions

Overview

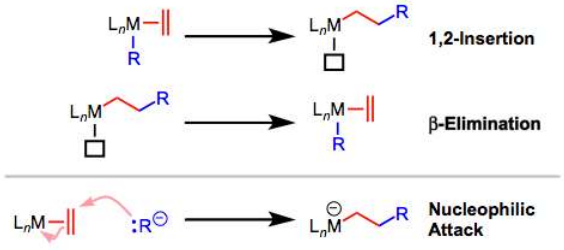


Figure **11.5.1**: 1,2-Insertion is dinstinct from nucleophilic/electrophilic attack on coordinated ligands.

Insertions of π systems into M-X bonds are appealing in the sense that they establish two new σ bonds in one step, in a stereocontrolled manner. 1,2-insertions generate a vacant site on the metal, which is usually filled by external ligand. For unsymmetrical alkenes, it's important to think about site selectivity: which atom of the alkene will end up bound to metal, and which to the other ligand? To make predictions about site selectivity we can appeal to the classic picture of the M–X bond as M+X–. Asymmetric, polarized π ligands contain one atom with excess partial charge; this atom hooks up with the complementary atom in the M–R bond during insertion. Resonance is our best friend here!

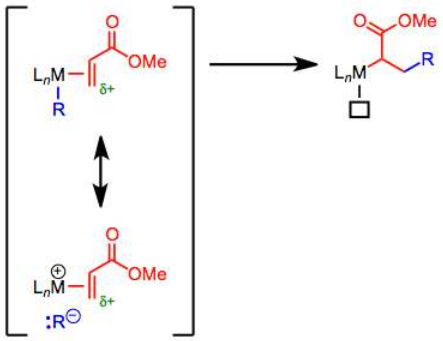


Figure **11.5.2**: The site selectivity of 1,2-insertion can be predicted using resonance forms and partial charges.

A nice study by Yu and Spencer illustrates these effects in homogeneous palladium- and rhodium-catalyzed hydrogenation reactions. Unactivated alkenes generally exhibit lower site selectivity than activated ones, although steric differences between the two ends of the double bond can promote selectivity.

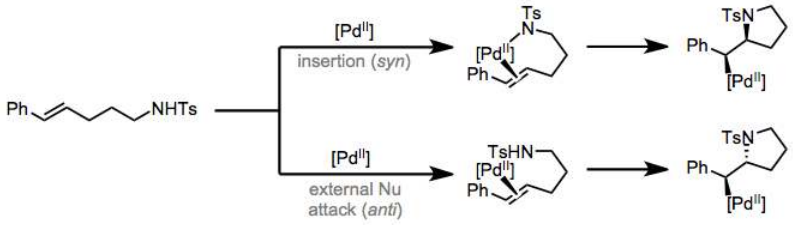
Reactivity Trends in 1,2-Insertions

The thermodynamics of 1,2-insertions of alkenes depend strongly on the alkene, but we can gain great insight by examining the structure of the product alkyl. Coordinated alkenes that give strong metal-alkyl bonds after migratory insertion tend to undergo the process. Hence, electron-withdrawing groups, such as carbonyls and fluorine atoms, tend to encourage migratory insertion—remember that alkyl complexes bearing these groups tend to have stable M–C bonds.

Insertions of alkenes into both M–H and M–R (R = alkyl) are favored thermodynamically, but the kinetics of M–R insertion are much slower. This observation reflects a pervasive trend in organometallic chemistry: M–H bonds react more rapidly than M–R bonds. The same is true of the reverse, β-elimination. Even in cases when both hydride and alkyl elimination are thermodynamically favored, β-hydride elimination is much faster. Although insertion into M–R is relatively slow, this elementary step is critical for olefin polymerizations that form polyalkenes (Ziegler-Natta polymerization). This reaction deserves a post all its own!

As the strength of the M–X bond increases, the likelihood that an L-type π ligand will insert into the bond goes down. Hence, while insertions into M–H and M–C are relatively common, insertions into M–N and M–O bonds are more rare. Lanthanides and palladium are known to promote insertion into M–N in some cases, but products with identical connectivity can come from external attack of nitrogen on a coordinated π ligand. The diastereoselectivity of these reactions provides mechanistic insight—

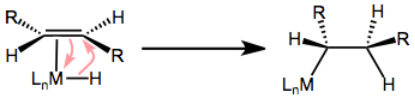
since migratory insertion is syn (see below), a syn relationship between Pd and N is to be expected in the products of migratory insertion. An anti relationship indicates external attack by nitrogen or oxygen.



The diastereoselectivity of formal insertions provides insight about their mechanisms.

Stereochemistry of 1,2-Insertions

1,2-Insertion may establish two stereocenters at once, so the stereochemistry of the process is critical! Furthermore, 1,2-insertions and β-eliminations are bound by important stereoelectronic requirements. An analogy can be made to the E2 elimination of organic chemistry, which also has strict stereoelectronic demands. For migratory insertion to proceed, the alkene and X-type ligand must be syncoplanar during insertion; as a consequence of this alignment, X and MLn end up on the same face of the alkene after insertion. In other words, insertions into alkenes take place in a syn fashion. Complexes that have difficulty achieving a coplanar arrangement of C=C and M–X undergo insertion very slowly, if at all.

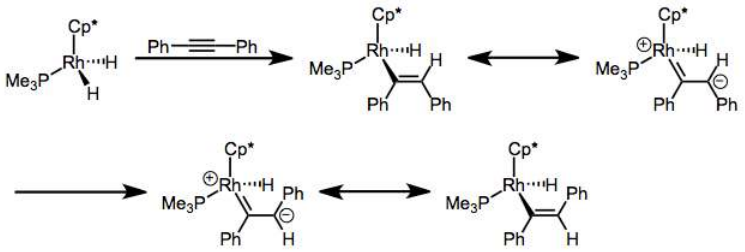


1,2-Insertions take place in a syn fashion. The metal and X end up bound to the same face of the alkene.

This observation has important implications for β-elimination, too—the eliminating X and the metal must have the ability to align syn.

Insertions of Other π Systems

To close this section, let's examine insertions into π ligands other than alkenes briefly. Insertions of alkynes into metal-hydride bonds are known, and are sometimes involved in reactions that I refer to collectively as "hydrostuffylation": hydrosilylation, hydroesterification, hydrogenation, and other net H–X additions across the π bond. Strangely, some insertions of alkynes yield trans products, even though cis products are to be expected from syn addition of M–X. The mechanisms of these processes involve initial syn addition followed by isomerization to the trans complex via an interesting resonance form. The cis complex is the kinetic product, but it isomerizes over time to the more thermodynamically stable trans complex.



Migratory insertions of alkynes into M–H produce alkenyl complexes, which have been known to isomerize.

The strongly donating Cp* ligand supports the legitimacy of the zwitterionic resonance form—and suggests that the C=C bond may be weaker than it first appears!

Polyenes can participate in migratory insertion, and insertions of polyenes are usually quite favored because stabilized π-allyl complexes result. In one mind-bending case, a coordinated arene inserts into an M–Me bond in a syn fashion!

Have you ever stopped to consider that the addition of methyllithium to an aldehyde is a formal insertion of the carbonyl group into the Li–Me bond? It's true! We can think of these as (very) early-metal "insertion" reactions. Despite this precedent, migratory insertion reactions of carbonyls and imines into late-metal hydride and alkyl bonds are surprisingly hard to come by. Rhodium is the most famous metal that can make this happen—rhodium has been used in complexes for arylation and vinylation, for example. Insertion of X=C into the M–R bond is usually followed by β-hydride elimination, which has the nifty effect of replacing H in aldehydes and aldimines with an aryl or vinyl group.

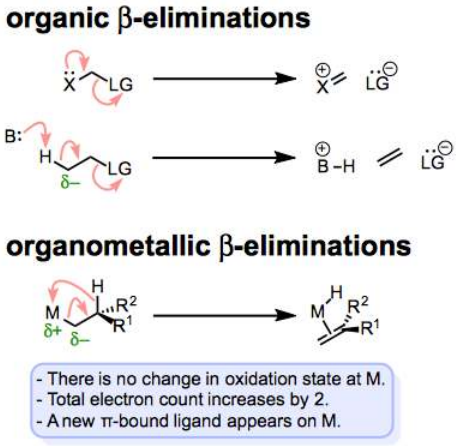
Contributors and Attributions

Dr. Michael Evans (Georgia Tech)

11.5: Migratory Insertion- 1,2-Insertions is shared under a CC BY-NC-SA 4.0 license and was authored, remixed, and/or curated by LibreTexts.

11.6: β-Elimination Reactions

In organic chemistry class, one learns that elimination reactions involve the cleavage of a σ bond and formation of a π bond. A nucleophilic pair of electrons (either from another bond or a lone pair) heads into a new π bond as a leaving group departs. This process is called β-elimination because the bond β to the nucleophilic pair of electrons breaks. Transition metal complexes can participate in their own version of β-elimination, and metal alkyl complexes famously do so. Almost by definition, metal alkyls contain a nucleophilic bond—the M–C bond! This bond can be so polarized toward carbon, in fact, that it can promote the elimination of some of the world's worst leaving groups, like –H and –CH3. Unlike the organic case, however, the leaving group is not lost completely in organometallic β-eliminations. As the metal donates electrons, it receives electrons from the departing leaving group. When the reaction is complete, the metal has picked up a new π-bound ligand and exchanged one X-type ligand for another.



Comparing organic and organometallic β-eliminations. A nucleophilic bond or lone pair promotes loss or migration of a leaving group.

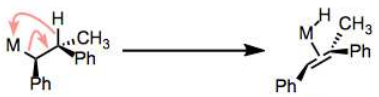
In this post, we'll flesh out the mechanism of β-elimination reactions by looking at the conditions required for their occurrence and their reactivity trends. Many of the trends associated with β-eliminations are the opposite of analogous trends in 1,2-insertion reactions. A future post will address other types of elimination reactions.

β-Hydride Elimination

The most famous and ubiquitous type of β-elimination is **β-hydride elimination**, which involves the formation of a π bond and an M–H bond. Metal alkyls that contain β-hydrogens experience rapid elimination of these hydrogens, provided a few other conditions are met.

The complex must have an open coordination site and an accessible, empty orbital on the metal center. The leaving group (–H) needs a place to land. Notice that after β-elimination, the metal has picked up one more ligand—it needs an empty spot for that ligand for elimination to occur. We can envision hydride "attacking" the empty orbital on the metal center as an important orbital interaction in this process.

The M–C_α and C_β–H bonds must have the ability to align in a syn coplanar arrangement. By "syn coplanar" we mean that all four atoms are in a plane and that the M–C_α and C_β–H bonds are on the same side of the C_α–C_β bond (a dihedral angle of 0°). You can see that conformation in the figure above. In the syn coplanar arrangement, the C–H bond departing from the ligand is optimally lined up with the empty orbital on the metal center. Hindered or cyclic complexes that cannot achieve this conformation do not undergo β-hydride elimination. The need for a syn coplanar conformation has important implications for eliminations that may establish diastereomeric olefins: β-elimination is stereospecific. One diastereomer leads to the (E)-olefin, and the other leads to the (Z)-olefin.



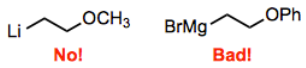
β-elimination is stereospecific. One diastereomer of reactant leads to the (Z)-olefin and the other to the (E)-olefin.

The complex must possess 16 or fewer total electrons. Examine the first figure one more time—notice that the total electron count of the complex increases by 2 during β-hydride elimination. Complexes with 18 total electrons don't undergo β-elimination because the product would end up with 20 total electrons. Of course, dissociation of a loose ligand can produce a 16-electron complex pretty easily, so watch out for ligand dissociation when considering the possibility of β-elimination in a complex. Ligand dissociation may be reversible, but β-Hydride elimination is almost always irreversible.

The metal must bear at least 2 d electrons. Now this seems a bit strange, as the metal has served as nothing but an empty bin for electrons in our discussion so far. Why would the metal center need electrons for β-hydride elimination to occur? The answer lies in an old friend: backbonding. The $\sigma_{C-H} \rightarrow M$ orbital interaction mentioned above is not enough to promote elimination on its own; an $M \rightarrow \sigma^*_{C-H}$ interaction is also required! I've said it before, and I'll say it again: backbonding is everywhere in organometallic chemistry. If you can understand and articulate it, you'll blow your instructor's mind.

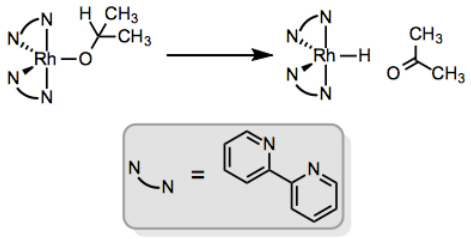
Other β-Elimination Reactions

The leaving group does not need to be hydrogen, of course, and a number of more electronegative groups come to mind as better candidates for leaving groups. β-Alkoxy and β-amino eliminations are usually thermodynamically favored thanks to the formation of strong M–O and M–N bonds, respectively. These reactions are so favored in β-alkoxyalkyl "complexes" of alkali and alkaline earth metals (R–Li, R–MgBr, etc.) that using these as σ-nucleophiles at carbon is untenable. Such compounds eliminate immediately upon their formation. I had an organic synthesis professor in undergrad who was obsessed with this—using a β-alkoxyalkyl lithium or β-alkoxyalkyl Grignard reagent in a synthesis was a recipe for red ink. β-Haloalkyls were naturally off limits too.



Watch out…these are not stable compounds!

The atom bound to the metal doesn't have to be carbon. β-Elimination of alkoxy ligands affords ketones or aldehydes bound at oxygen or through the C=O π bond (this step is important in many transfer hydrogenations, and an analogous process occurs in the Oppenauer oxidation). Amido ligands can undergo β-elimination to afford complexes of imines; however, this process tends to be slower than β-alkoxy elimination.



β-Elimination helps transfer the elements of dihydrogen from one organic compound to another.

Incidentally, I haven't seen any examples in which the β atom is not carbon, but would be interested if anyone knows of an example!

Applications of β-Eliminations

As with many concepts in organometallic chemistry, there are two ways to think about applications of β-elimination. One can take either the "inorganic" perspective, which focuses on the metal center, or the "organic" perspective, which focuses on the ligands.

With the metal center in focus, we can recognize that β-hydride elimination has the wonderful side effect of establishing an M–H bond—a feat generally difficult to achieve in a selective manner via oxidative addition of X–H. If the ligand from which the hydrogen came displaced something more electronegative, the whole process represents reduction at the metal center. For example, imagine rhodium(III) chloride is mixed with sodium isopropoxide, $NaOCH(CH_3)_2$. The isopropoxide easily displaces chloride, and

subsequent β-hydride elimination affords a rhodium hydride, formally reduced with respect to the chloride starting material. See p. 236 of this review for more.

With the ligand in focus, we see that the organic ligand is oxidized in the course of β-hydride elimination. Notice that the metal is reduced and the ligand oxidized! A π bond replaces a σ bond in the ligand, and if the conditions are right, this represents a bona fide oxidation (as opposed to a mere elimination). For example, oxidative addition into a C–H bond followed by β-hydride elimination at a C–H bond next door sets up an alkene where two adjacent C–H bonds existed before, an oxidation process. These dehydrogenation reactions are incredibly appealing in a theoretical sense, but still at an early stage when it comes to scope and practicality.

Summary

We already encountered β-hydride elimination in an earlier series of posts on metal alkyl complexes, where we noted that it's a very common decomposition pathway for metal alkyls. β-Hydride elimination isn't all bad, however, as it can be an important step in catalytic reactions that result in the oxidation of organic substrates (dehydrogenations and transfer hydrogenations) and in reactions that reduce metal halides to metal hydrides. The general idea of β-elimination involves the transfer of a leaving group from a ligand to the metal center with simultaneous formation of a π bond in the ligand. β-Elimination requires an open coordination site and at least two d electrons on the metal center, and eliminations of chiral complexes are stereospecific. The leaving group is commonly hydrogen, but need not be—the more electronegative the leaving group, the more favorable the elimination. Stronger π bonds in the product also encourage β-elimination, so eliminations that form carbonyl compounds or imines are common.

In the next post, we'll explore other types of organometallic elimination reactions, which establish π bonds at different positions in metal alkyl or other complexes. α-Eliminations, for example, establish metal-carbon, -oxygen, or -nitrogen multiple bonds, which are generally difficult to forge through other means

Dr. Michael Evans (Georgia Tech)

11.6: β-Elimination Reactions is shared under a CC BY-NC-SA 4.0 license and was authored, remixed, and/or curated by LibreTexts.

11.7: Organometallic Catalysts

Overview

The different types of organometallic reactions discussed in the previous sections can be combined together into catalytic cycles to produce valuable chemicals or perform otherwise difficult chemical reactions. While the organometallic catalyst will undergo a number of transformations over the course of the cycle, it will return to its original active state at the end of the reaction. By definition catalysts are reactive, because of this the metal complex added to a reaction is at times a more stable precatalyst which must undergo a reaction such as ligand dissociation to form the active catalyst.

Hydrogenation Catalysis

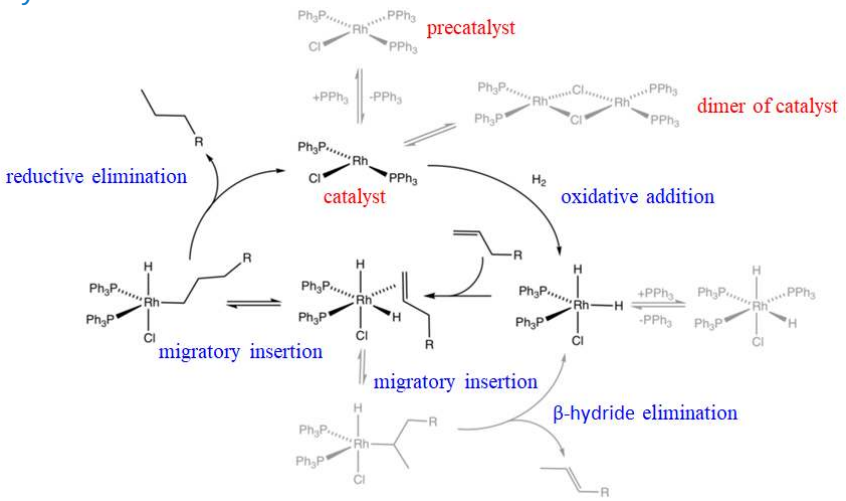


Figure 11.7.1: Mechanism of the Wilkinson hydrogenation catalyst (CC BY-SA; Smokefoot via Wikimedia Commons)

Migratory insertions play an important role in catalysis.For example a Rh-catalyst called Wilkinson's catalyst is an effective hydrogenation catalyst for olefins. The mechanism of the hydrogenation involves a combination of oxidative additions, olefin migratory (1,2) insertions, and reductive eliminations as shown in Figure 11.7.1. Wilkinson's catalyst is the square planar chloridotris(triphenylphosphine)rhodium(I) complex. This molecule is actually a precatalyst that becomes the active catalyst when it loses a triphenylphosphine ligand producing chloridobis(triphenylphosphine)rhodium(I). The loss of this ligand is a reversible reaction, and thus the catalyst is in chemical equilibrium with the precatalyst. The active catalyst is also in chemical equilibrium with its dimer. The chloridobis(triphenylphosphine)rhodium(I) catalyst can undergo an oxidative addition in the presence of hydrogen to form a trigonal bipyramidal chloridodihydridobis(triphenylphosphine)rhodium(III) complex. This species is in chemical equilibrium with an octahedral chlorodihydridotris(triphenylphosphine)rhodium(III) species that can form due to the presence of free triphenylphosphine ligands in the system. The trigonal bipyramidal species can then add an olefin ligand that binds side-on to the Rh. Because the olefin is in cis-position to the hydride ligand it can undergo a 1,2 insertion. The Rh-C bond can either form with the first or the second carbon in the carbon chain of the olefin, giving a linear and a branched alkyl complex, respectively. The branched complex can undergo a β-hydride elimination thereby reforming the trigonal bipyramidal Rh-complex, and an olefin. This reaction is a side-reaction because the branched alkyl complex is sterically more crowded than the linear complex. The linear alkyl Rh complex can undergo a reductive elimination to form the linear alkane and the $RhCl(PPh_3)_2$ catalyst. This completes the catalytic cycle, and a new cycle can start.

Ziegler-Natta Polymerization

Another example of an organometallic catalytic reaction is the Ziegler-Natta olefin polymerization. This reaction is of high industrial importance for the production of polymers like polyethylene. There are both heterogeneous and homogeneous Ziegler-Natta catalysts. The mechanism for the homogeneous catalysts is generally well understood. Homogeneous catalysts are typically metallocene catalysts.

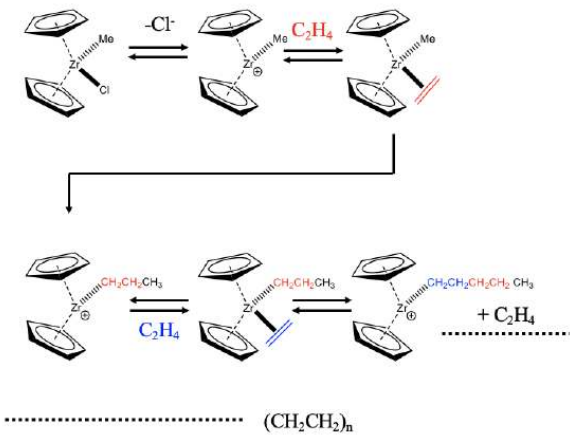


Figure **11.7.2**: Mechanism for Zirconium-based Ziegler-Natta catalysis (Attribution: A. Vedernikov, U Maryland (modified).)

An example of a zirconium-based catalyst is shown in Figure **11.7.2**. The catalyst is a coordinatively unsaturated complex cation with two cyclopentadienyl rings and a methyl group. The catalyst is formed from its precatalyst, a neutral molecule with an additional chloride ligand. The catalyst oxidatively adds an olefin like an ethylene molecule to the coordinatively unsaturated site. This step is followed an 1,2b insertion step that produces a propyl group. The migratory insertion leads to the formation of a vacant site, that can be reoccupied by another ethylene molecule. This molecule can insert into the propyl chain thereby prolonging the propyl chain to a pentyl chain. The olefin insertion step generates another vacant site that can be reoccupied by a new ethylene molecule. Repeating the catalytic cycle many times eventually leads to polyethylene.

Catalytic Olefin Hydroformylation

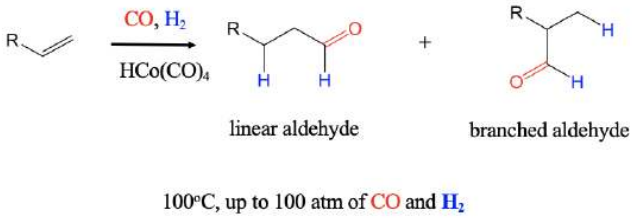


Figure **11.7.3**: Scheme for catalytic olefin hydroformylation

A further important industrial reaction is the catalytic hydroformylation reaction, also known as oxo-process. It was discovered in 1938 by Otto Roelen at BASF. In the hydroformylation reaction an H atom and a formyl group are added to an alkene to form aldehydes. The reaction can produce both branched an linear aldehydes from terminal alkenes, CO, and H_2 using a carbonyl hydrides such as $HCo(CO)_4$ as a catalyst. The reaction is performed at about 100°C at a pressure of up to 100 atm.

Mechanism

How does the hydroformylation work mechanistically?

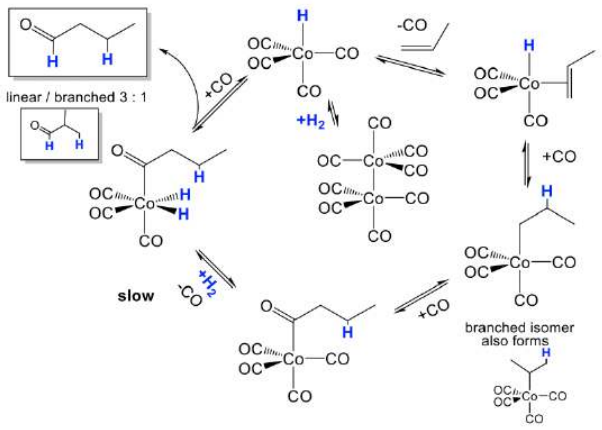


Figure **11.7.4**: Mechanism of the catalytic olefin hydroformylation by $HCo(CO)_4$ (Attribution: A. Vedernikov, U Maryland (modified).)

The mechanism is illustrated for the hydroformylation of propene in Figure **11.7.4**. The actual catalyst $HCo(CO)_4$ is first formed from its precatalyst $Co_2(CO)_8$ in the presence of H_2 in a dinuclear oxidative addition reaction. The catalyst can undergo a substitution reaction in which a CO ligand is replaced by the olefin that binds side-on to the cobalt. This species can then undergo a migratory 1,2 olefin insertion reaction. This leads to a mixture of linear and branched alkyl groups attached to the Co. A new CO ligand can add to the vacant site. The alkyl group can then insert into a carbonyl group in another migratory insertion step, and the vacant site can be reoccupied by a new CO molecule. Then, H_2 is added in an oxidative addition. This is the slowest and rate-limiting step in the catalytic cycle. From the addition product the aldehyde can then be eliminated in a reductive elimination reaction. Addition of CO regenerates the catalyst, and the catalytic cycle can begin again.

Hydrocarbonylations

After the hydroformylation, a number of other hydrocarbonylations were developed, and industrially deployed.

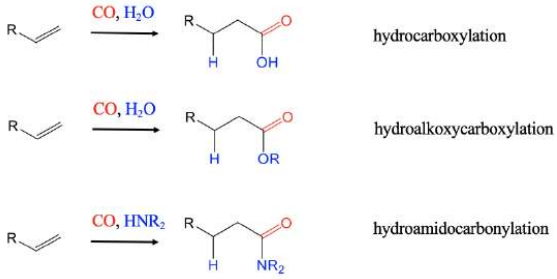


Figure **11.7.5**: Hydrocarbonylation reactions

When hydrogen is replaced by H_2O hydrocarboxylations of alkenes lead to carboxylic acids Figure **11.7.5**. With an alcohol instead of H_2 hydroalkoxycarbonylcations lead to esters. The employment of amines instead of H_2 leads to amides in hydroamidocarbonylation reactions.

Monsanto Acetic Acid Process

Another carbonylation reaction involving an organometallic catalyst is the Monsanto acetic acid process. It has been introduced by Monsanto in the 1970s for the industrial production of acetic acid from methanol. The reaction involves dual catalysis with HI and $[RhI_2(CO)_2]^-$ as a co-catalysts. How does this reaction work?

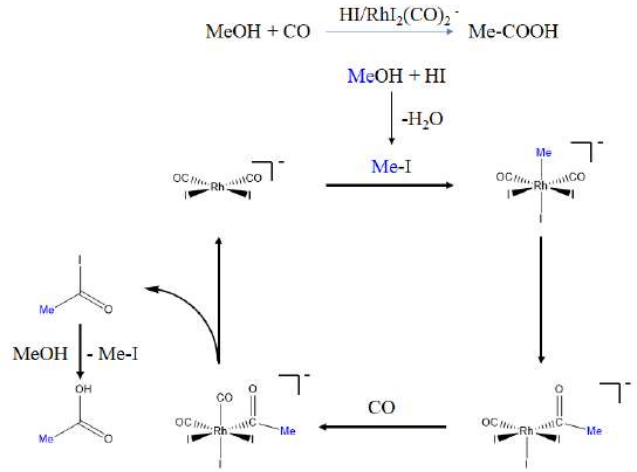


Figure 11.7.6: The catalytic cycle in the Monsanto acetic acid process

In the first step methanol reacts with HI to form methyl iodide. The methyl iodide then reacts with the Rh-catalyst in an oxidative addition reaction in which a methyl and an iodo group are added in trans-fashion to the square-planar Rh-complex to give an octahedral complex. The octahedral complex then undergoes a migratory insertion reaction with CO producing an acyl group and a vacant site. A CO molecule can then add to the vacant site. The acetyl iodide can then be eliminated in a reductive elimination to reform the Rh-catalyst thereby closing the catalytic cycle. The acetyl iodide can then react with methanol to form new methyl iodide and acetic acid. The methyl iodide can start a new catalytic cycle with the Rh-catalyst.

Olefin Metathesis

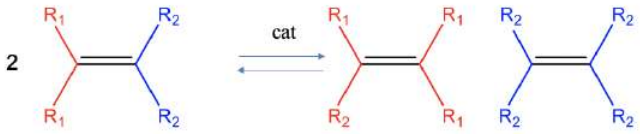


Figure 11.7.7: Scheme for olefin metathesis

Olefin metathesis is a reaction which allows to cut and rearrange C=C double bonds in olefins to make new olefins Figure 11.7.7. Formally, the carbon-carbon bond of the reactant is cleaved homoleptically and the two carbene fragments are combined in a different way. This reaction is typically an equilibrium reaction, and neither the reactants nor the products are clearly favored. This reaction is catalyzed by molybdenum arylamido carbene complexes or ruthenium carbene complexes.

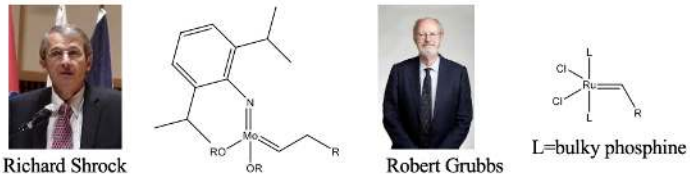


Figure 11.7.8: Shrock catalyst (left) (CC BY-SA; Materialscientist via Wikimedia Commons) and Grubbs catalyst (right) (CC BY-SA; The Royal Society via Wikimedia Commons)

The former are called Shrock catalysts, and the latter Grubbs catalysts named after their discoverers Richard Shrock and Robert Grubbs who received the Nobel prize for Chemistry in 2005 (Figure 11.7.8). The Schrock catalysts are more active, but also very sensitive to air and water. The Grubbs catalysts, while less active, are less sensitive to air and water.

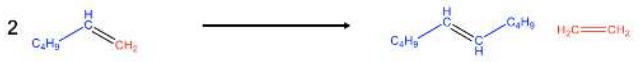


Figure 11.7.9: Scheme for regular metathesis

Olefin metathesis often allows for simpler preparation of olefins compared to other methods. Olefin metathesis is particularly powerful when one olefin product is gaseous because then it can be quite easily removed from the chemical equilibrium by

purging. This drives the chemical equilibrium to the right side. An example is the preparation of 5-decene from 1-hexene. Cleavage of the C=C double bond in the hexene leads to C_5 and C_1 carbene fragments (Figure **11.7.9**). The two C_1 fragments can combine to form ethylene and the two C_5 fragments combine to 5-decene. The ethylene is volatile and can be purged from the reaction system thereby driving the chemical reaction to the right side.

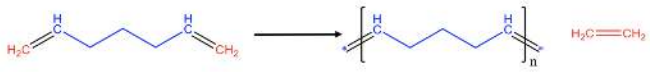


Figure **11.7.10**: Acylic diene metathesis (ADMET)

The same principles can also be applied to produce polymers from dienes with two terminal C=C double bonds at the chain ends. This is called acylic diene metathesis (ADMET), Figure **11.7.10**. For instance the cleavage of the two terminal double bonds in a diene with seven C atoms leads to C_1 and C_5 fragments. The C_1 fragments can combine to form ethylene, and the C_5 fragments can combine to make an unsaturated polymer of the type $[CH(CH_2)_3CH]_n$. Again, the reaction can be driven to the right side by removing the gaseous ethylene from the reaction mixture through purging.

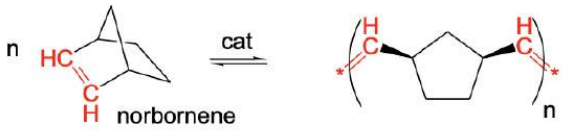


Figure **11.7.11**: Ring-opening metathesis polymerization (ROMP)

Another variation of olefin metathesis is ring-opening metathesis polymerization (ROMP). It allows to make polymers from strained cycloolefins, for example norbornene. The reaction driving force is the relief of the strain. Because the strain is removed in the polymer, the chemical equilibrium lies far on the right side. The reaction product in norbornene is a polymer with 5-membered rings that are interconnected by ethylene -CH=CH- units (Figure **11.7.11**).

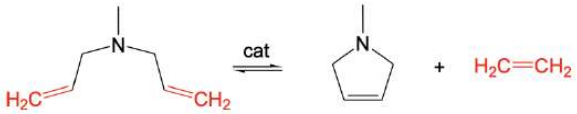


Figure **11.7.12**: Ring-closing metathesis (RCM)

The opposite of ROMP is ring-closure metathesis (RCM). RCM allows for the preparation of unstrained rings with C=C double bonds from dienes with C=C double bonds that are five or six carbon atoms apart. This distance is suitable to produce unstrained rings. In the shown example a five-membered ring with a C=C double bond is formed from a diene with terminal C=C double bonds that are five atoms apart.

Mechanism

What is the mechanism of olefin metathesis?

https://chem.libretexts.org/@go/page/326268

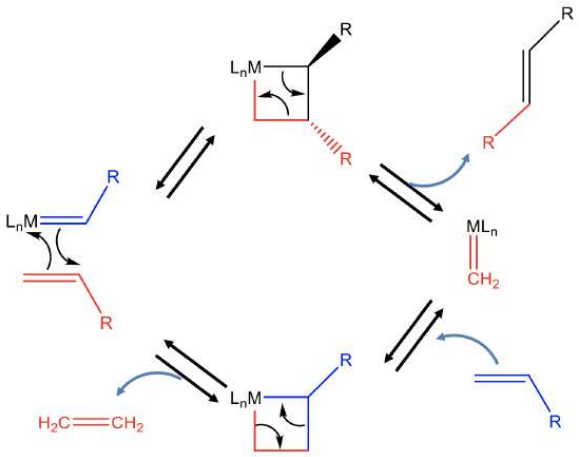


Figure **11.7.13**: The mechanism of olefin metathesis

In the first step, the alkene adds to the the carbene fragment of the catalyst in a 2+2 cycloaddition reaction to produce an unstable intermediate with a highly strained four-membered ring (Figure **11.7.13**). This four membered ring can open to produce the first new alkene product R-CH=CH-R and a metal carbene species. This metal carbene can react with another reactant olefin to form another highly stained 4-ring intermediate via a 2+2 cycloaddition reaction. This ring can then reopen again to produce the second alkene metathesis product, in this case ethylene, and the original catalyst. The regenerated catalyst can then start a new catalytic cycle.

Carbon-Carbon Cross Coupling Reactions

The palladium catalyzed cross-coupling reactions are a class of highly successful reactions with applications in the organic synthesis to have emerged recently. The reactions carry out a coupling of the aryl, vinyl or alkyl halide substrates with different organometallic nucleophiles and as such encompasses a family of C−C cross-coupling reactions that are dependent on the nature of nucleophiles like that of the B based ones in the Suzuki-Miyuara coupling, the Sn based ones in the Stille coupling, the Si based ones in the Hiyama coupling, the Zn based ones in the Negishi coupling and the Mg based ones in the Kumada coupling reactions (Figure **11.7.14**).

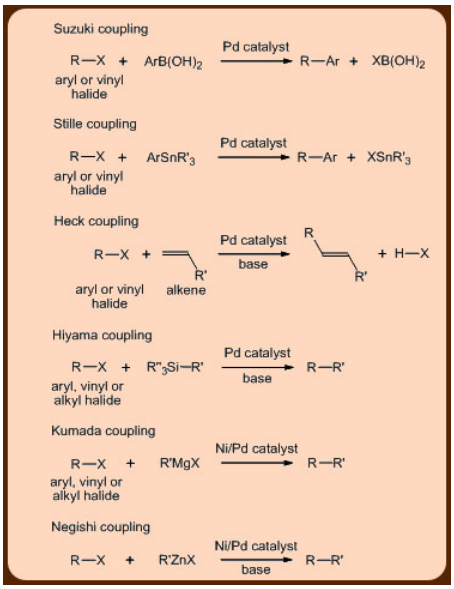


Figure **11.7.14**: Various types of the palladium mediated C−C cross-coupling reactions.

An unique feature of these reactions is the exclusive formation of the cross-coupled product without the accompaniment of any homo-coupled product. Another interesting feature of these coupling reactions is that they proceed *via* a common mechanism involving three steps that include the oxidative addition, the transmetallation and the reductive elimination reactions (Figure **11.7.15** and **11.7.16**).

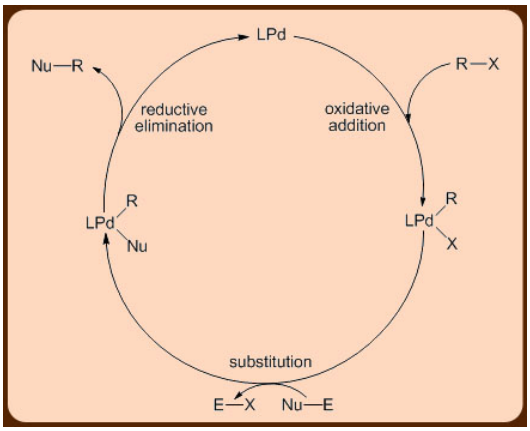


Figure **11.7.15**: A general catalytic cycle for the palladium mediated C−C cross-coupling reactions.

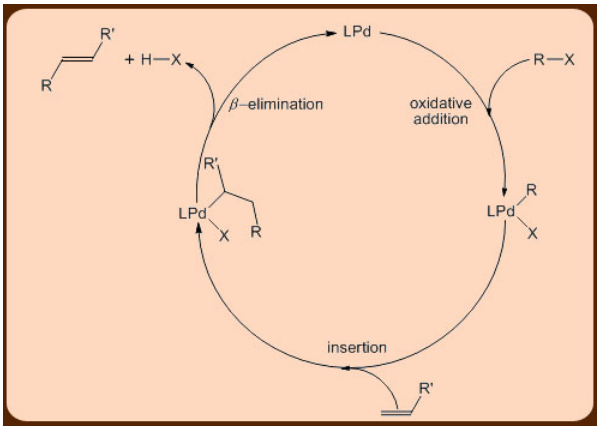


Figure **11.7.16**: A catalytic cycle for the palladium mediated Heck coupling reaction.

Summary

Organometallic complexes play a pivotal role in several successful homogeneous catalysis reactions like that of the hydroformylation and the C−C cross-coupling reactions. These reactions are important because of the fact that both of the hydroformylation and the C−C cross-coupling reactions give more value added products compared to the starting reactants. The palladium catalyzed C−C cross-coupling reactions are a class of highly successful reactions that have permanently impacted the area of organic synthesis in a profound way to an extent that the 2010 Nobel prize has been conferred on one of these reactions thereby recognizing the importance of the C−C cross-coupling recations.

Contributors and Attributions

- http://nptel.ac.in/courses/104101006/31
- Dr. Kai Landskron (Lehigh University). If you like this textbook, please consider to make a donation to support the author's research at Lehigh University: Click Here to Donate.

11.7: Organometallic Catalysts is shared under a CC BY-NC-SA 4.0 license and was authored, remixed, and/or curated by LibreTexts.

- **12.2: Organometallic Catalysts** by Kai Landskron is licensed CC BY 4.0.
- **Current page** is licensed CC BY-NC-SA 4.0.
- **25.5F: C−C cross-coupling reactions** is licensed CC BY-NC-SA 4.0.

CHAPTER OVERVIEW

12: Bioinorganic Chemistry

Metals play a wide range of important roles in biological systems. This chapter will give an overview of the roles metals can play in biochemical reactions and highlight a few metal containing proteins in greater detail.

Learning Objectives

- Observe the different roles metals can play in biological systems
- Apply inorganic chemistry principles (MO theory, CFT, HSAB, etc.) to metalloproteins

Thumbnail images is the structure of Cytochrome C (CC BY-SA; Vossman via Wikimedia Commons)

12.1: Biological Significance of Metals

12.2: Introduction to Amino Acids and Proteins

12.3: Biological Dioxygen Transport and Storage

12.4: Biological Metal Storage

12.5: Zinc as Lewis Acid and Template

12.6: Electron Transfer

12: Bioinorganic Chemistry is shared under a CC BY-NC-SA 4.0 license and was authored, remixed, and/or curated by LibreTexts.

12.1: Biological Significance of Metals

Overview

The transition metals are among the least abundant metal ions in the sea water from which contemporary organisms are thought to have evolved (Table **12.1.1**).[1-5] For many of the metals, the concentration in human blood plasma greatly exceeds that in sea water. Such data indicate the importance of mechanisms for accumulation, storage, and transport of transition metals in living organisms.

Table **12.1.1**: Concentrations of transition metals and zinc in sea water and human plasma.*Data from References 1 - 5 and 12

Element	Sea Water (M) x 10^8	Human Plasma (M) x 10^8
Fe	0.005 - 2	2230
Zn	8.0	1720
Cu	1.0	1650
Mo	10.0	1000
Co	0.7	0.0025
Cr	0.4	5.5
V	4.0	17.7
Mn	0.7	10.9
Ni	0.5	4.4

The metals are generally found either bound directly to proteins or in cofactors such as porphyrins or cobalamins, or in clusters that are in turn bound by the protein; the ligands are usually O, N, S, or C. Proteins with which transition metals and zinc are most commonly associated catalyze the intramolecular or intermolecular rearrangement of electrons. Although the redox properties of the metals are important in many of the reactions, in others the metal appears to contribute to the structure of the active state, e.g., zinc in the Cu-Zn dismutases and some of the iron in the photosynthetic reaction center. Sometimes equivalent reactions are catalyzed by proteins with different metal centers; the metal binding sites and proteins have evolved separately for each type of metal center.

Iron

Iron is the most common transition metal in biology.[6,7] Its use has created a dependence that has survived the appearance of dioxygen in the atmosphere ca. 2.5 billion years ago, and the concomitant conversion of ferrous ion to ferric ion and insoluble rust. All plants, animals, and bacteria use iron, except for a lactobacillus that appears to maintain high concentrations of manganese instead of iron. The processes and reactions in which iron participates are crucial to the survival of terrestrial organisms, and include ribonucleotide reduction (DNA synthesis), energy production (respiration), energy conversion (photosynthesis), nitrogen reduction, oxygen transport (respiration, muscle contraction), and oxygenation (e.g., steroid synthesis, solubilization and detoxification of aromatic compounds). Among the transition metals used in living organisms, iron is the most abundant in the environment. Whether this fact alone explains the biological predominance of iron or whether specific features of iron chemistry contribute is not clear.

Many of the other transition metals participate in reactions equivalent to those involving iron, and can sometimes substitute for iron, albeit less effectively, in natural Fe-proteins. Additional biological reactions are unique to nonferrous transition metals.

Zinc

Zinc is relatively abundant in biological materials.[8,9] The major location of zinc in the body is metallothionein, which also binds copper, chromium, mercury, and other metals. Among the other well-characterized zinc proteins are the Cu-Zn superoxide dismutases (other forms have Fe or Mn), carbonic anhydrase (an abundant protein in red blood cells responsible for maintaining the

pH of the blood), alcohol dehydrogenase, and a variety of hydrolases involved in the metabolism of sugars, proteins, and nucleic acids. Zinc is a common element in nucleic-acid polymerases and transcription factors, where its role is considered to be structural rather than catalytic. Interestingly, zinc enhances the stereoselectivity of the polymerization of nucleotides under reaction conditions designed to simulate the environment for prebiotic reactions. Recently a group of nucleic-acid binding proteins, with a repeated sequence containing the amino acids cysteine and histidine, were shown to bind as many as eleven zinc atoms necessary for protein function (transcribing DNA to RNA).[10] Zinc plays a structural role, forming the peptide into multiple domains or "zinc fingers" by means of coordination to cysteine and histidine. A survey of the sequences of many nucleic-acid binding proteins shows that many of them have the common motif required to form zinc fingers. Other zinc-finger proteins called steroid receptors bind both steroids such as progesterone and the progesterone gene DNA. Much of the zinc in animals and plants has no known function, but it may be maintaining the structures of proteins that activate and deactivate genes.[11]

Copper

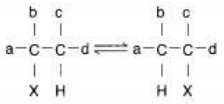
Copper and iron proteins participate in many of the same biological reactions:

1. reversible binding of dioxygen, e.g., hemocyanin (Cu), hemerythrin (Fe), and hemoglobin (Fe);
2. activation of dioxygen, e.g., dopamine hydroxylase (Cu) (important in the synthesis of the hormone epinephrine), tyrosinases (Cu), and catechol dioxygenases (Fe);
3. electron transfer, e.g., plastocyanins (Cu), ferredoxins, and c-type cytochromes (Fe);
4. dismutation of superoxide by Cu or Fe as the redox-active metal (superoxide dismutases).

The two metal ions also function in concert in proteins such as cytochrome oxidase, which catalyzes the transfer of four electrons to dioxygen to form water during respiration. Whether any types of biological reactions are unique to copper proteins is not clear. However, use of stored iron is reduced by copper deficiency, which suggests that iron metabolism may depend on copper proteins, such as the serum protein ceruloplasmin, which can function as a ferroxidase, and the cellular protein ascorbic acid oxidase, which also is a ferrireductase.

Cobalt

Cobalt is found in vitamin B_{12} , its only apparent biological site.[12] The vitamin is a cyano complex, but a methyl or methylene group replaces CN in native enzymes. Vitamin-B_{12} deficiency causes the severe disease of pernicious anemia in humans, which indicates the critical role of cobalt. The most common type of reaction in which cobalamin enzymes participate results in the reciprocal exchange of hydrogen atoms if they are on adjacent carbon atoms, yet not with hydrogen in solvent water:



(An important exception is the ribonucleotide reductase from some bacteria and lower plants, which converts ribonucleotides to the DNA precursors, deoxyribonucleotides, a reaction in which a sugar -OH is replaced by -H. Note that ribonucleotide reductases catalyzing the same reaction in higher organisms and viruses are proteins with an oxo-bridged dimeric iron center.) The cobalt in vitamin B_{12} is coordinated to five N atoms, four contributed by a tetrapyrrole (corrin); the sixth ligand is C, provided either by C5 of deoxyadenosine in enzymes such as methylmalonyl-CoA mutase (fatty acid metabolism) or by a methyl group in the enzyme that synthesizes the amino acid methionine in bacteria.

Nickel

Nickel is a component of a hydrolase (urease), of hydrogenase, of CO dehydrogenase, and of S-methyl CoM reductase, which catalyzes the terminal step in methane production by methanogenic bacteria. All the Ni-proteins known to date are from plants or bacteria.[13,14] However, about 50 years elapsed between the crystallization of jack-bean urease in 1925 and the identification of the nickel component in the plant protein. Thus it is premature to exclude the possibility of Ni-proteins in animals. Despite the small number of characterized Ni-proteins, it is clear that many different environments exist, from apparently direct coordination to protein ligands (urease) to the tetrapyrrole F430 in methylreductase and the multiple metal sites of Ni and Fe-S in a hydrogenase

from the bacterium *Desulfovibrio gigas*. Specific environments for nickel are also indicated for nucleic acids (or nucleic acid-binding proteins), since nickel activates the gene for hydrogenase.[15]

Manganese

Manganese plays a critical role in oxygen evolution catalyzed by the proteins of the photosynthetic reaction center. The superoxide dismutase of bacteria and mitochondria, as well as pyruvate carboxylase in mammals, are also manganese proteins.[16,17] How the multiple manganese atoms of the photosynthetic reaction center participate in the removal of four electrons and protons from water is the subject of intense investigation by spectroscopists, synthetic inorganic chemists, and molecular biologists.[17]

Vanadium and Chromium

Vanadium and chromium have several features in common, from a bioinorganic viewpoint.[18a] First, both metals are present in only small amounts in most organisms. Second, the biological roles of each remain largely unknown.[18] Finally, each has served as a probe to characterize the sites of other metals, such as iron and zinc. Vanadium is required for normal health, and could act *in vivo* either as a metal cation or as a phosphate analogue, depending on the oxidation state, V(lV) or V(V), respectively. Vanadium in a sea squirt (tunicate), a primitive vertebrate, is concentrated in blood cells, apparently as the major cellular transition metal, but whether it participates in the transport of dioxygen (as iron and copper do) is not known. In proteins, vanadium is a cofactor in an algal bromoperoxidase and in certain prokaryotic nitrogenases. Chromium imbalance affects sugar metabolism and has been associated with the glucose tolerance factor in animals. But little is known about the structure of the factor or of any other specific chromium complexes from plants, animals, or bacteria.

Molybdenum

Molybdenum proteins catalyze the reduction of nitrogen and nitrate, as well as the oxidation of aldehydes, purines, and sulfite.[19] Few Mo-proteins are known compared to those involving other transition metals. Nitrogenases, which also contain iron, have been the focus of intense investigations by bioinorganic chemists and biologists; the iron is found in a cluster with molybdenum (the iron-molybdenum cofactor, or FeMoCo) and in an iron-sulfur center. Interestingly, certain bacteria (*Azotobacter*) have alternative nitrogenases, which are produced when molybdenum is deficient and which contain vanadium and iron or only iron. All other known Mo-proteins are also Fe-proteins with iron centers, such as tetrapyrroles (heme and chlorins), Fe-sulfur clusters, and, apparently, non-heme/non-sulfur iron. Some Mo-proteins contain additional cofactors such as the Havins, e.g., in xanthine oxidase and aldehyde oxidase. The number of redox centers in some Mo-proteins exceeds the number of electrons transferred; reasons for this are unknown currently.

References

1. (a) J. H. Martin and R. M. Gordon, *Deep Sea Research* **35** (1988), 177; (b) F. Egami, *J. Mol. Evol.* **4** (1974), 113.
2. J. F. Sullivan *et al.*, *J. Nutr.* **109** (1979), 1432.
3. M. D. McNeely *et al.*, *Clin. Chem.* **17** (1971), 1123
4. A. R. Byrne and L. Kosta, *Sci. Total Env.* **10** (1978), 17
5. A. S. Prasad, *Trace Elements and Iron in Human Metabolism*, Plenum Medical Book Company, 1978.
6. E. C. Theil, *Adv. Inorg. Biochem.* **5** (1983), 1.
7. E. C. Theil and P. Aisen, in D. van der Helm, J. Neilands, and G. Winkelmann, eds., *Iron Transport in Microbes, Plants, and Animals*, VCH, 1987, p. 421.
8. C. F. Mills, ed., *Zinc in Human Biology*, Springer-Verlag, 1989.
9. B. L. Vallee and D. S. Auld, *Biochemistry* **29** (1990), 5647.
10. J. Miller, A. D. McLachlan, and A. Klug, *EMBO J.* **4** (1985), 1609.
11. J. M. Berg, *J. Biol. Chem.* **265** (1990), 6513.
12. C. Sennett, L. E. G. Rosenberg, and I. S. Millman, *Annu. Rev. Biochem.* **50** (1981), 1053.
13. J. J. G. Moura *et al.*, in A. V. Xavier, ed., *Frontiers in Biochemistry*, VCH, 1986, p. 1.
14. C. T. Walsh and W. H. Orme-Johnson, *Biochemistry* **26** (1987), 4901.
15. H. Kim and R. J. Maier, *J. Biol. Chem.* **265** (1990), 18729.
16. Reference 5, p. 5.
17. V. L. Schramm and F. C. Wedler, eds., *Manganese in Metabolism and Enzyme Function*, Academic Press, 1986.

18. (a) D. W. Boyd and K. Kustin, *Adv. Inorg. Biochem.* **6** (1984), 312; (b) R. C. Bruening *et al.*, *J. Nat. Products* **49** (1986), 193.
19. T. G. Spiro, ed., *Molybdenum Biochemistry*, Wiley, 1985.

12.1: Biological Significance of Metals is shared under a CC BY-NC-SA 4.0 license and was authored, remixed, and/or curated by LibreTexts.

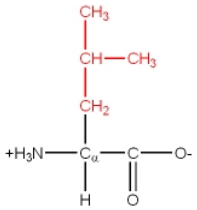
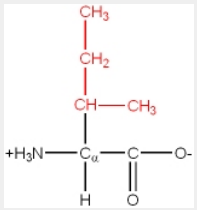
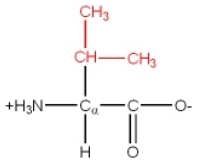
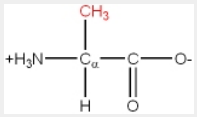
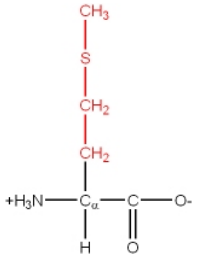
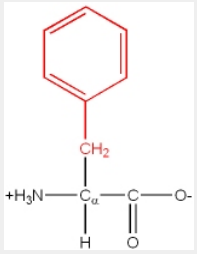
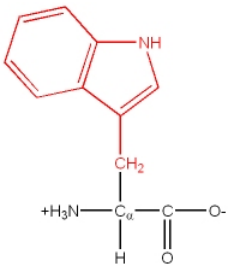
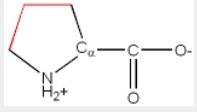
12.2: Introduction to Amino Acids and Proteins

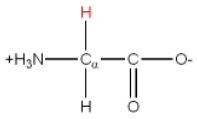
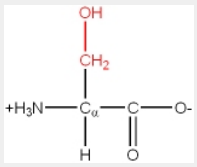
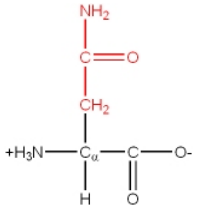
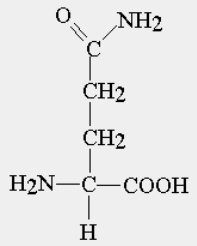
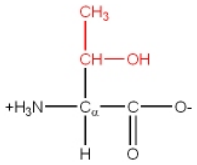
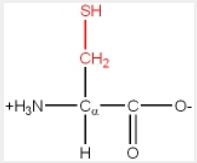
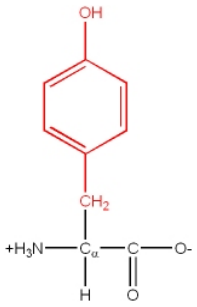
Common amino acids

There are 20 common amino acids. They are composed of C, H, O, N and S atoms. They are structurally and chemically different, and also differ in size and volume. Some are branched structures, some are linear, some have ring structures. One of the 20 common amino acids is actually an imino acid. A typical grouping of their chemical nature is as follows:

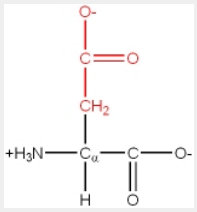
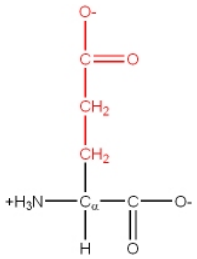
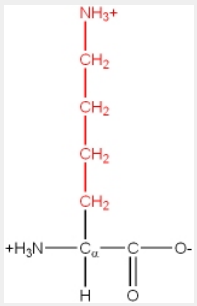
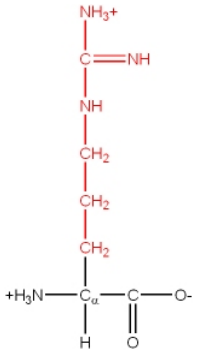
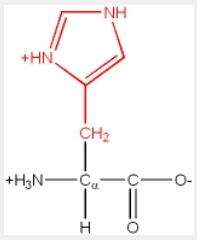
- Nonpolar (hydrocarbons and one sulfur-containing amino acid). Dispersion forces and hydrophobic effects predominate in their interactions. They cannot H-bond with water and these side chains have a characteristic hydrophobic effect in water.
- Polar uncharged. Contain functional groups that can H-bond with water and other amino acids. Include C, H, O, N and S atoms.
- Acidic. Contain a carboxylic acid functional group with a negative charge at neutral pH. Can H-bond with water, can form ionic interactions, and can also serve as nucleophiles or participate in acid-base chemistry.
- Basic. Nitrogen containing bases (e.g. guanidino, imidazole or amino groups) with a net positive charge at neutral pH. Can serve as proton donors in chemical reactions, and form ionic interactions.

The amino acids have a name, as well as a three letter or single letter mnemonic code:

Type	Name	R-group Structure
Nonpolar	Leucine Leu, L	
	Isoleucine Ile, I	
	Valine Val, V	
	Alanine Ala, A	
	Methionine Met, M	
	Phenylalanine Phe, F	
	Tryptophan Trp, W	
	Proline Pro, P	

Type	Name	R-group Structure
	Glycine Gly, G (note: sometimes included in polar group)	
Polar, uncharged	Serine Ser, S	
	Asparagine Asn, N	
	Glutamine Gln, Q	 glutamine
	Threonine Thr, T	
	Cysteine Cys, C	
	Tyrosine Tyr, Y	

https://chem.libretexts.org/@go/page/326272

Type	Name	R-group Structure
Acidic	Aspartic acid Asp, D	
	Glutamic acid Glu, E	
Basic	Lysine Lys, K	
	Arginine Arg, R	
	Histidine His, H	

Uncommon amino acids

In addition to the 20 common amino acids, there are several uncommon ones found:

- Hydroxylysine and hydroxyproline. These are found in the protein collagen. Collagen is a fibrous protein made up of three polypeptides that form a stable assembly, but only if the proline and lysine residues are hydroxylated. (requires vitamin C for reduction of these amino acids to hydroxy form)
- Thyroxine, an iodinated derivative of tyrosine, found in thyroglobulin (produced by thyroid gland; requires iodine in diet)

- g-carboxyglutamic acid (i.e. glutamic acid with two carboxyl groups) found in certain blood clotting enzymes (requires vitamin K for production)
- N-methyl arginine and n-acetyl lysine. Found in some DNA binding proteins known as histones

Amino acid derivatives not found in proteins

Some amino acids are made that are not intended for incorporation into proteins, rather they have important functionalities on their own

- Serotonin (derivative of tryptophan) and g-amino butyric acid (a derivative of glutamic acid) are both neurotransmitters
- Histamine (derivative of histidine) involved in allergic response
- Adrenaline (derivative of tyrosine) a hormone
- Various antibiotics are amino acid derivatives (penicillin)

Contributors and Attributions

- Mike Blaber (Florida State University)

Thumbnail: 3D model of L-tryptophan. (Public Domain; Benjah-bmm27).

This page titled 12.2: Introduction to Amino Acids and Proteins is shared under a CC BY-NC-SA 4.0 license and was authored, remixed, and/or curated by Tim Soderberg via source content that was edited to the style and standards of the LibreTexts platform.

- **Nomenclature of Amino acids** is licensed CC BY-NC-SA 4.0.

12.3: Biological Dioxygen Transport and Storage

Oxygen Transport

Most organisms require molecular oxygen in order to survive. The oxygen is used in a host of biochemical transformations, although most is consumed in the reaction that is the terminal (or primary) step of oxidative phosphorylation to form ATP.

$$O_2 + 4H^+ + 4e^- \rightarrow 2H_2O \tag{12.3.1}$$

The transportation of oxygen from the air or water to the cells of an organism is vital. In the three chemically distinct dioxygen carrier proteins that have evolved and are found today, the dioxygen binding site in the protein, the active site, is an iron or copper complex. For hemoglobins, the most widely distributed family of dioxygen carriers, the active site has long been known to consist of an iron porphyrin (heme) group embedded in the protein. Almost all hemoglobins share the basic structure illustrated in Figure 4.2. Hemocyanin and hemerythrin, the other two biological dioxygen carriers, feature pairs of copper atoms and iron atoms, respectively, at the active sites.* Some basic properties of these metalloproteins are summarized in Table **12.3.1**.

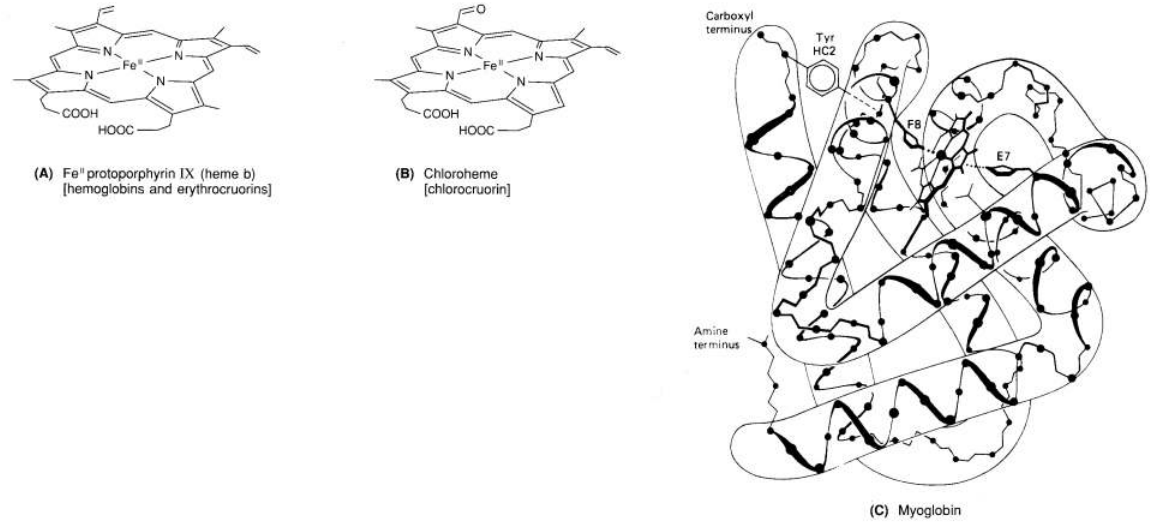


Figure **12.3.1**: Heme groups used in hemoglobin: (A) Protoporphyrin IX (heme b), (hemoglobins and erythrocruorins); (B) Chloroheme (chlorocruorin); (C) The encapsulation of the heme molecule in myoglobin.[11a] Reproduced with permission from M. F. Perutz, Nature **228** (1970), 726-737.

Table **12.3.1**: General Features of Dioxygen-carrier Proteins

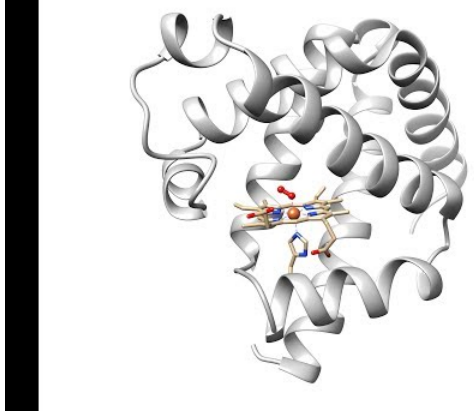
Metalloprotein	Active Site of deoxy	Color Change deoxy → oxy	MW (Dalton)	# Subunits	Average MW Subunit (Dalton)
Hemoglobins					
Vertebrate					
Human A	heme Fe^{II}	purple → red	64,000	4	16,000
Invertebrate					
Erythrocruroin (*Lumbricus terrestris*, earthworm)	heme Fe^{II}	purple → red	up to 3.3×10^6	192	17,000
Chlorocruorn *(Eudistylia vancouveri*, feather duster worm*)*	chloroheme Fe^{II}	purple → green	3.1×10^6	192	15,000
Hemocyanins					
Mollusk (*Helix pomatia*-**α**, edible snail)	$Cu^1 \ldots Cu1$	colorless → blue	-9×10^6	160	52,700
Arthropod *(Cancer magister*, crab)	$Cu^1 \ldots Cu1$	colorless → blue	-9×10^5	12	76,600
Hemerythrins *(Phascolopsis* syn. *golfingia gouldii)*	$Fe^{II} \ldots Fe^{II}$	colorless → burgundy	108,000	8	13,500

* The use of the prefix *hem-* is confusing. In this context *hem* connotes blood. Thus, since hemocyanin and hemerythrin lack a heme group [an iron(II) porphyrin], they are nonheme metalloproteins.

In many organisms an additional dioxygen-binding protein, which stores dioxygen, is located in tissues that are subject to sudden and high dioxygen demand, such as muscles. These dioxygen-storage proteins are prefixed *myo-* (from the Greek root *mys* for muscle). Thus for the dioxygen-transport protein hemerythrin there exists a chemically similar dioxygen-storage protein myohemerythrin. For the hemoglobin family the corresponding storage protein is called myoglobin. Interestingly, some organisms that use hemocyanin as the dioxygen-*transport* protein use myoglobin as the dioxygen-*storage* protein.

Introduction to Myoglobin and Hemoglobin

Myoglobin: O_2 storage



The respiratory system is an organ system in the body that functions in gas exchange with the environment. Exchange of gases like carbon dioxide (CO_2) and dioxygen (O_2) are essential for sustaining life forms. O_2 is necessary in aerobic metabolism for oxidative phosphorylation (synthesis of ATP) at the electron transport chain (ETC).[2] ATP is the energy source needed for muscular

contraction in mammals. ATP synthesis requires oxygen as an electron acceptor in the ETC, therefore oxygen must be readily available for use in metabolically active muscles. Since muscles need large quantities of O_2, it is transported by proteins in the blood and stored in muscle tissue. One of these proteins is myoglobin. Myoglobin is a hemoprotein found in the skeletal muscle of mammals that functions in oxygen storage and diffusion. The heme in myoglobin can reversibly bind a O_2 molecule to regulate the transportation of O_2 from red blood cells to mitochondria when skeletal muscles are metabolically active.

Structure of Myoglobin

The structure of myoglobin (Figure **12.3.2**) is similar to the structure of one of the β subunits of hemoglobin. Myoglobin and hemoglobin are both part of the globin family; a family of heme-containing globular polypeptides with eight α-helices in their protein fold. Myoglobin contains only one subunit of globin, while hemoglobin has four subunits.

The iron-containing heme group allows myoglobin to reversibly bind to O_2 (Figure **12.3.2**). Heme is a large, aromatic porphyrin ring with four pyrrole nitrogens bound to an Fe(II) ion at the center (Figure **12.3.2***C*).[2,3] The nitrogens from the porphyrin ring and a histidine serve as ligands for the Fe(II) metal center. The heme Fe is bound to the myoglobin polypeptide through the proximal histidine residue. The iron ion has six coordination sites: four equitorial sites are occupied by pyrole nitrogens of heme, and one axial site is occupied by a proximal histidine residue. The remaining axial coordination site is available for binding a O_2 molecule (Figure **12.3.2***A* – *C*).

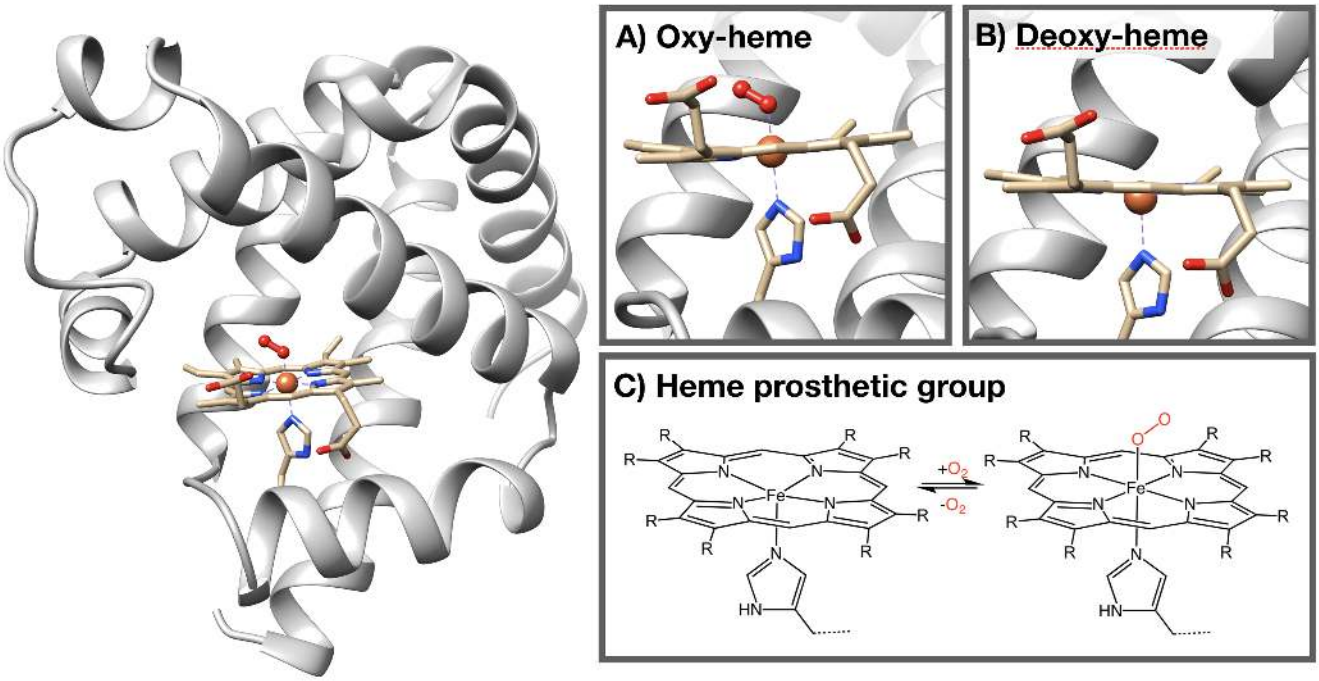


Figure **12.3.2**: Structure of myoglobin. This is a ribbon depiction of mammalian myoglobin protein (grey, PDB code 1a6m). The heme group, shown in stick depiction (tan) with Fe shown as an orange sphere, bound to a O_2 molecule (red ball-and-stick). Inset A shows enlarged view of the O_2-bound heme. Inset B illustrates the de-oxygenated heme (PDB code 1a6n). The proximal histidine imidazole bound to Fe is shown toward the bottom of insets A and B. Inset C shows reversible binding of O_2 to the skeletal structure of the heme prosthetic group. This group consists of four central nitrogen donor atoms bound to iron (II) (attribution: Smokefoot, Mboxygenation, CC BY-SA 4.0). The porphyrin ring contains four pyrrole nitrogens bound to a ferrous (Fe(II)) ion center. There are six coordination sites in the Fe(II) ion; four are occupied by the pyrrole nitrogens, one is occupied by a proximal histidine, and the final site has the ability to reversibly bond to an O_2 molecule.

Reversible binding of oxygen

Now let's move on to the function of myoglobin: oxygen storage. Myoglobin can reversibly bind a dioxygen molecule to regulate the transportation of oxygen from red blood cells to mitochondria when skeletal muscles are metabolically active. This binding occurs at the iron center of the heme group. Although the 18-electron rule was a rule developed for organometallic complexes and chemistry, we can apply it here to explain the O_2-binding behavior of myoglobin. In deoxymyoglobin, the total valence electron count around Fe is 16 electrons (See Fig. **12.3.2**, 10 electrons from ligands plus 6 electrons from Fe(II)). Under the 18-electron rule,

a predictable step for a 16-electron species is ligand addition. The binding of O_2 to Fe(II) is a ligand addition reaction. Once O_2 binds to the Fe(II) in myoglobin, the new valence electron count around Fe is 18 electron. A predictable step for an 18-electron species is a ligand dissociation reaction, as is the reaction of O_2 dissociation from the Fe center. The binding and dissociation of O_2 makes sense based on the 18-electron rule.

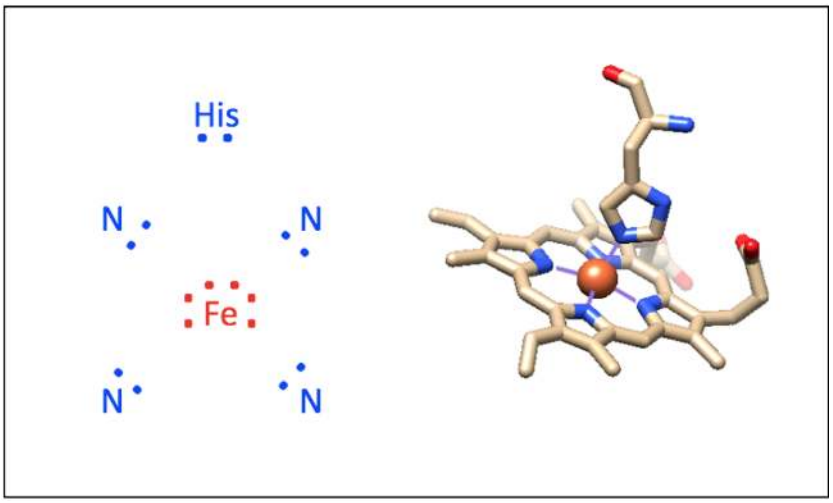


Figure **12.3.3**: The electron count of deoxygenated heme Fe is 16 electrons. A total of 10 electrons are donated from the ligands (8 from pyrrole nitrogens of the porphyrin ring and 2 from the imidaziole nitrogen of the proximal histidine); 6 electrons are present from the 6 d electrons of Fe(II). Thus, the deoxy-heme complex is available for another ligand to bind; this case in the form of oxygen. The image was created using PDB code 1a6n and UCSF Chimera.

Iron oxidation state

The oxidation state of Fe in oxy-myoglobin is a highly debated topic because data is inconclusive and seemingly contradictory. Data from infrared (IR) spectroscopy and magnetic measurements have lead scientists to propose two different modes of oxygen binding to the iron ion. In one model (Figure **12.3.4** left), Fe(II) simply binds to O_2. A second model predicts that electrons are transfered from the Fe center to the dioxygen molecule to create Fe(III) bound to superoxide (Figure **12.3.4** right). Although many debate whether the iron, after binding to oxygen, remains iron (II) or becomes iron (III), it is difficult to assign an oxidation state to the bound iron or the oxygen. The actual molecular orbitals that result from the iron-oxygen interaction have both iron and O_2 character. It is therefore not quite correct to focus on the electrons "belong" to Fe or dioxygen. The two extremes, where one is that Fe becomes an iron superoxide by donating an electron from iron to the oxygen, and the other that Fe becomes an iron oxide by sharing the electrons are probably both incorrect. The molecular orbitals contain characteristics of both iron superoxide and iron oxide.

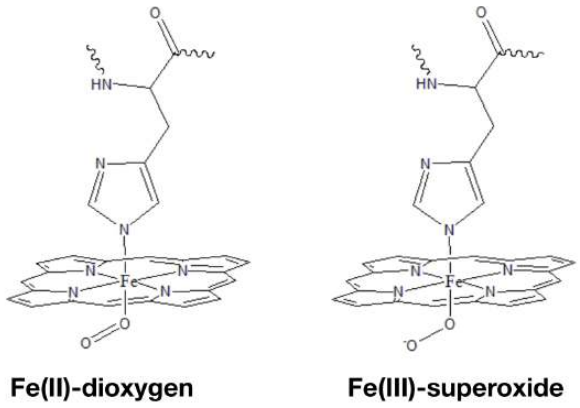


Figure **12.3.4**: The binding of oxygen to the metal iron ion center of heme, occupying the 6th binding site of heme. **Left:** illustrates the iron oxide binding of oxygen where there is no transfer of electrons from the oxygen to the iron ion. **Right:** illustrates the formation of the superoxide from the transfer of electrons from oxygen to iron.

Sources

1. Ordway, G. A. *Journal of Experimental Biology* 2004, *207*(20), 3441–3446.
2. Ahern, K.; Rajagopal, I.; Tan, T. *Biochemistry Free For All*; Creative Commons, 2017; Vol. 1.2.
3. Casiday, R.; Frey, R. Hemoglobin and the Heme Group: Metal Complexes in the Blood for Oxygen Transport Inorganic Synthesis Experiment
4. Penn State University. In *Chem 324: Bio-Inorganic Chemistry.*
5. Lippard, S.J., Berg, J.M. Principles of Bioinorganic Chemistry. University Science Books. 1994. 284-289.
6. Atkins, Overton, Rourke, Weller, Armstrong. Shriver and Atkins' Inorganic Chemistry. Oxford University Press. 2010. 738-79.
7. Richards, M. *Antioxidants and Redox Signaling* 2013. 2342-2351.
8. Mazumdra, S., Medhi, O.K., Mitra, S. *American Chemical Society*. 1990. 700-705.
9. Shriver, D., Atkins, P. Inorganic Chemistry, 5th ed.; W.H. Freeman and Company: New York, 2009; 739.
10. Vanholder, R., Sever, M.S., Erek, E., Lameire, N. 2000. Rhabdomyolysis. *Journal of the American Society of Nephrology* 11:1553-1561

Hemoglobin

Hemoglobin, a polypeptide found in red blood cells, allows dioxygen (O_2) to be transported within blood from the lungs to other tissues within the body. Hemoglobin is a polypeptide found in red blood cells. It allows for the transportation of O_2 from the lungs to other tissues within the body. This molecule also is also responsible for the color of blood.[1] Oxygenated blood is a bright red because hemoglobin absorbs green light of wavelengths 540-542 nm, and thus it results in a bright red colored solution.[2] Deoxygenated blood, however, is darker in color because it absorbs a more yellow/green color of wavelength 554 nm, and thus produces a darker color of red.

Hemoglobin is able to transport oxygen within the body due to its unique structure. Its structure consists of four globin subunits: two α and two β subunits. Each subunit contains a heme prosthetic group with an iron bound (Figure 1). Hemoglobin exists in high concentrations in the cytoplasm of red blood cells, so it needs to be very soluble in aqueous cytoplasm. This requirement is reflected in the protein's globular shape, and the fact that it is folded in such a way that hydrophilic residues are found on the surface of the protein exposed to water, while hydrophobic residues are found on the interior of the protein. This folding enables hemoglobin to have a stable fold in aqueous solution that also allows the protein to interact favorably with water and to be soluble in the water-filled cytoplasm of the cell.

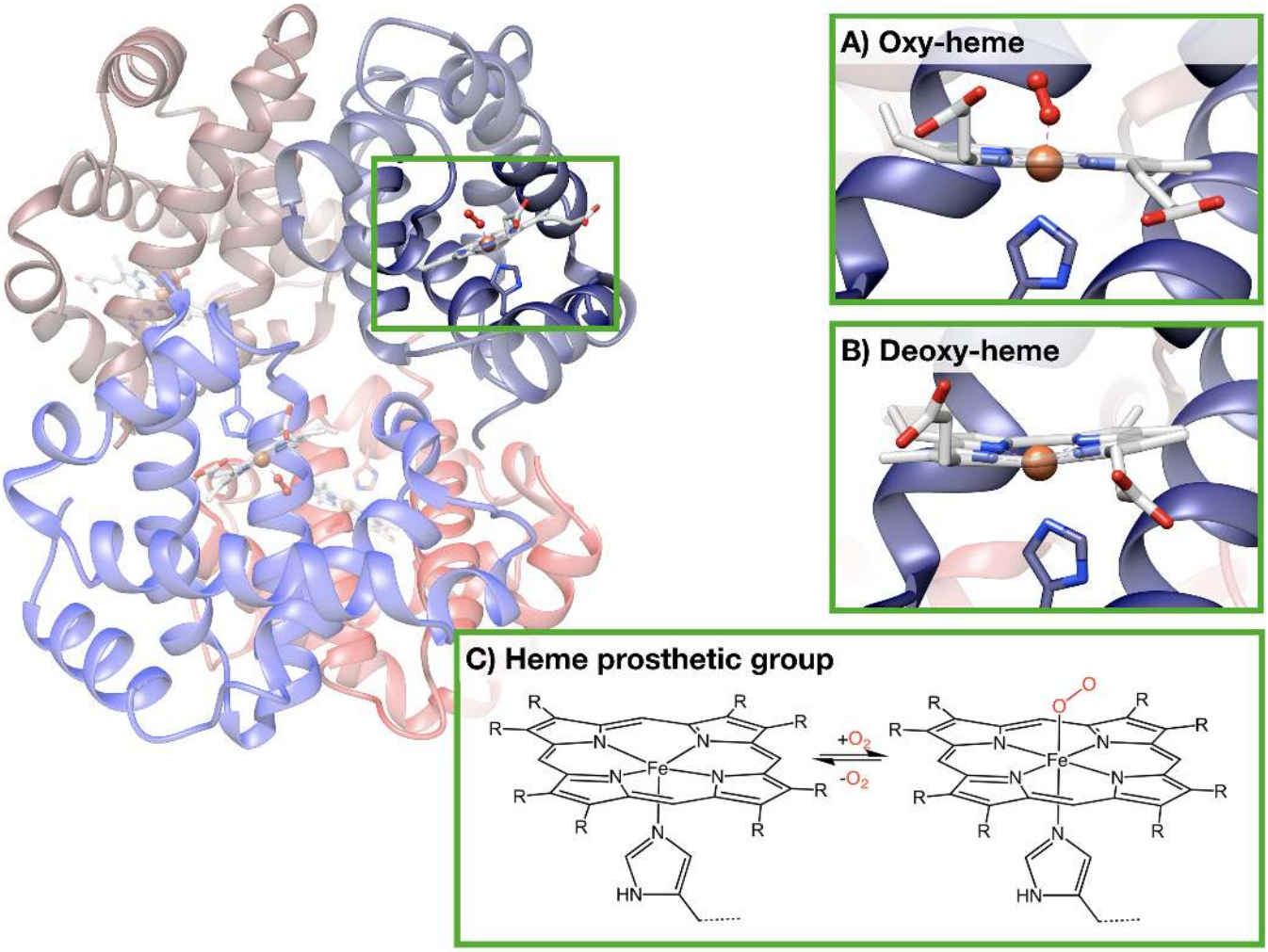


Figure **12.3.5**: On the left, the ribbon diagram of hemoglobin is displayed. Hemoglobin consists of four subunits: two α (blue) and two β subunits (red). A heme group (stick depiction) is located within each subunit, and within each heme an inorganic iron ion (orange) is located. **Inset A:** Oxy-hemoglobin has dioxygen (red) bound to the iron core of each heme group. The iron of the oxygenated hemoglobin is pulled into the porphyrin plane. **Inset B:** Deoxy-hemoglobin (no oxygen bound). The iron (II) ion lies 0.4 Å outside of the porphyrin plane. **Inset C:** Reversible binding of O_2 to the skeletal structure of the heme prosthetic group. This group consists of four central nitrogen donor atoms bound to iron (II) (attribution: Smokefoot, Mboxygenation, CC BY-SA 4.0). Iron (II) has two axial binding sites and, in hemoglobin, one is occupied by an imidazole N of the proximal histidine. The second axial coordination site has the ability to reversibly bond to an oxygen atom.

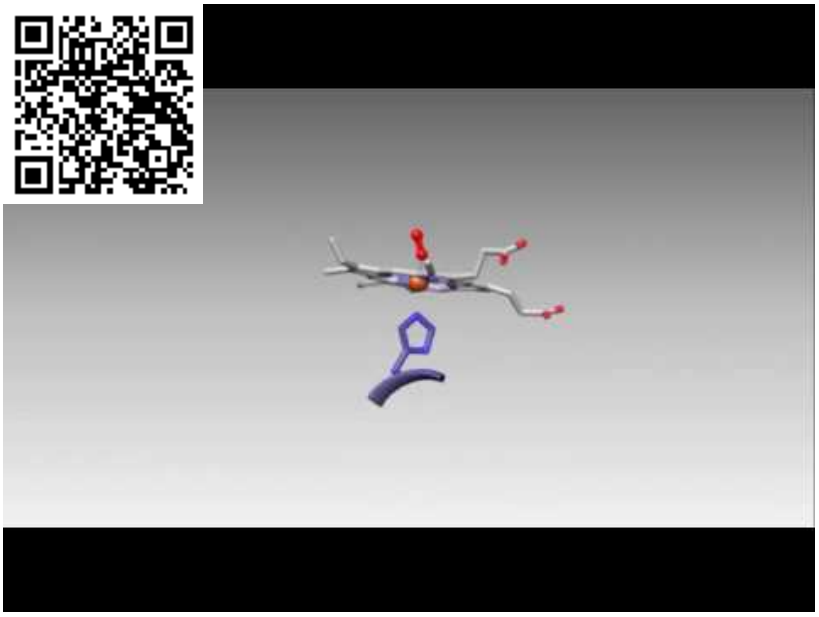
Cooperative binding of O_2

An important feature of hemoglobin is a cooperative binding of oxygen to each subunit due to conformational changes upon oxygen binding to the heme iron. Hemoglobin exists in both the T-state (tense state) and the R-state (relaxed). The T-state has lower affinity for dioxygen due to the tilting of the proximal histidine and steric hindrance of the O_2 coordination site. Steric hindrance makes it difficult for oxygen molecule to enter the site and bind to Fe. When an oxygen binds to one subunit of hemoglobin, the iron shifts into the plane of the porphoryn ring, and tugs on the proximal histidine.[3,9] This causes the proximal histidine ring to be pulled toward the plane of the prosthetic group, decreasing the tilt of the histidine, causing a shift in the tertiary structure of that subunit, and displacing residues that were providing steric hiderance of the oxygen binding site. These conformational changes in one subunit cause similar changes to the tertiary structures of adjacent subunits, in turn decreasing steric and electrostatic constraints in those adjacent units. The result is adoption of the R-state and a subsequent increase in oxygen affinity to the other subunits.

When the iron ion is bound to only five coordination sites the iron (II) lies 0.4 Å outside of the porphyrin ring.[3,9,12] When the oxygen binds to the iron core the iron becomes smaller as it becomes low-spin because electrons are pulled closer to the Fe core or

are transfered to the dioxygen molecule due to backbonding. The low spin iron and is able to fit in the plane of the porphyrin ring.[3,9]

The short video below illustrates conformational differences between fully oxygenated hemoglobin and deoxygenated hemoglobin. (Click here if the video does not load).



References

1. Casiday, R.; Frey, R. Washington University of St. Lous Chemistry. http://www.chemistry.wustl.edu/~edud...exinBlood.html (accessed 6 March).
2. Zijistra, W. G; Buursma, A.; Meeuwsen-van der Roest, W. P. Absorption Spectra of Human Fetal and Adult Oxyhemoglobin, De-Oxyhemoglobin, Carboxyhemoglobin, and Methemoglobin. Clin Chem [online] 1991, 37, 1633-1638.
3. Prahl, S. Oregon Medical Laser Center. https://omlc.org/spectra/hemoglobin/...uct/index.html (accessed 6 March).
4. Berg, J. M.; Tymoczko, J. L.; Stryer, L. *Biochemistry*, 5 ed., W. H Freeman and Company: New York, 2002; unknown.
5. Jensen, K. P.; Ryde, U.; How O2 Binds to Heme: Reasons for Rapid Binding and Spin

Inversion. *JBC* [online] **2004**, *279*, 14561-14569

6. http://chemed.chem.purdue.edu/genchem/topicreview/bp/1biochem/blood3.html iron (III) oxide also talks about cooperativity
7. http://nptel.ac.in/courses/104103069/module7/lec3/2.html iron (III) superoxide
8. https://www.ncbi.nlm.nih.gov/pmc/articles/PMC3230298/ Explains the oxygen dissociation curve
9. Shriver, D; Atkins, P. Inorganic Chemistry, 5th ed.; W.H. Freeman and Company: New York, 2009; 739.
10. Frausto da Silva J. J. R.; Williams R. J. P. The Biological Chemistry of the Elements: The Inorganic Chemistry of Life, 2nd ed.; Oxford University Press: Oxford, 2001; 370-373, 385-386.
11. Crabb, E.; Moore, E., Eds. Metals and Life; Royal Society of Chemistry: United Kingdom, 2010.
12. https://pubs.acs.org/doi/pdf/10.1021/cr00046a002 Low spin/high spin and cooperativity
13. Spin-Pairing Model of Dioxygen Binding and Its Application to Various Transition-Metal Systems as well as Hemoglobin Coopera

Hemocyanin

Hemocyanin is the oxygen transporter protein present in the hemolymph of arthropods and mollusks.[1] Hemolymph is the circulating fluid for these animals that is the invertebrate equivalent to vertebrate blood.[2] In hemocyanin, the active site contains two copper ions. Hemocyanin is a type-3 copper protein, meaning that it contains of two copper centers, each coordinated by three histidine residues, as seen in Figure **12.3.6** and Figure **12.3.7**. When deoxygenated (see Figure **12.3.6**, left), the copper exists in the colorless, reduced Cu(I) state. Molecular oxygen binds at the copper site and is reduced to peroxide (O_2^{2-}), Cu(I) is oxidized to

Cu(II), and a blue complex forms. This change in the oxidation state of copper is responsible for the blue color of oxygenated invertebrate hemolymph. The oxygen bound as peroxide bridges the two copper centers together in μ-η^2-η^2 fashion.[5]

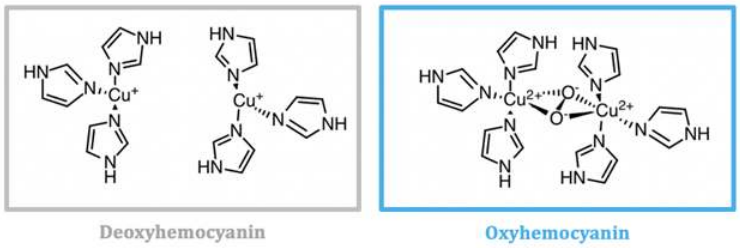


Figure **12.3.6**: Chemical Structure of Oxygen Binding Site of Hemocyanin. (Left) The deoxygenated form of the hemocyanin binding site. Each copper ion is bound to three histidine residues, however there is no oxygen bound to copper. In this state, copper is colorless and exists in the form of Cu(I). (Right) The oxygenated form of the hemocyanin binding site. Each copper is coordinated with three histidine residues, and molecular oxygen binds at the center to the copper ion as a peroxide, $\mathbf{O_2^{2-}}$, bridging the two copper centers together in a μ-η^2-η^2 fashion. Because copper is in the Cu(II) oxidation state, the oxygen-bound hemocyanin is a blue color.

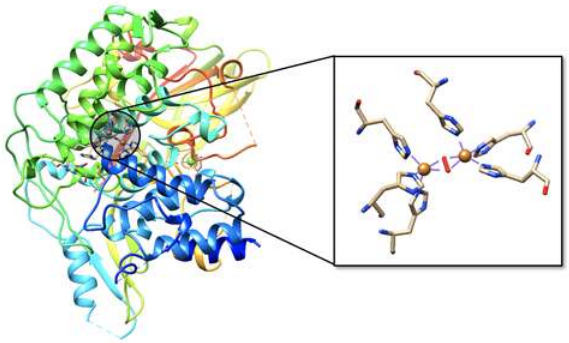


Figure **12.3.7**:[8] (Left) *Ribbon Structure of Arthropod Hemocyanin (PDB code 1NOL).* Image depicting the structure of arthropod hemocyanin (specifically from the horseshoe crab). The thin ribbons represent regions of the molecule that are unstructured. (Right) *Binding Site of Oxygen to Copper on Hemocyanin.* In the inset, three histidine residues (blue) can be seen coordinating with a copper (gold). The copper binds a molecular oxygen (red).

Mollusk and arthropod hemocyanins are structurally very different, however the active sites both contain two coppers at the center coordinated to three histidines. Arthropod hemocyanins have kidney-shaped subunits, each with an oxygen binding site, arranged into hexamers. Mollusk hemocyanin, on the other hand, is composed of about 10 subunits forming a hollow cylinder. Recently, there has been research into different therapeutic applications of hemocyanins. Studies suggest these metalloproteins have applications as viral and bacterial antigens, immune-stimulants for treatment of some cancers such as melanoma, and carrier molecules for vaccines.[9]

Note



The hemolymph of horseshoe crabs is incredibly valuable to pharmaceutical companies and biomedical researchers. It is the only known source of limulus amebocyte lysate, a substance which coagulates in the presence of bacterial endotoxin. This hemolymph extract is used to test medical devices, injectable drugs, and vaccines for bacterial contamination prior to distribution.

Learn more in this Chemistry World podcast

Image credit: CC BY; Amanda via Flickr

Structure

As seen in Figure **12.3.6** the active site of hemocyanin contains two copper ions, each bound to three histidine (His) residues. When the Cu(I) ions bind to oxygen they are oxidized to Cu(II). Cu(I) is a soft acid, Cu(II) is a borderline acid, and the imidazole ring of histidine is a borderline base. Because the copper ion alternates between a soft acid (Cu(I)) and a borderline acid (Cu(II)), it makes sense that it is bound to a borderline base. Borderline histidine is a better match for borderline Cu(II) than soft Cu(I), however His is still a better match for Cu(I) than a set of ligands that is harder. It is important to recognize, however, that there are other factors that affect metal ion selectivity, such as ionic size and ligand field stabilization energy, that must also be considered.

Hemocyanin exists in the hemolymph of invertebrates. Hemolymph is simply the invertebrate equivalent of blood that is present in vertebrates and is composed of water and organic and inorganic compounds. The inorganic metals present in hemolymph are sodium, chloride, calcium, magnesium, potassium, and manganese ions.[11,12] Na^+, Ca^{2+}, Mg^{2+}, K^+, and Mn^{2+} can all be seen as potential competitors for the copper at the active site due to the fact that they are all positively charged metal ions. They are all hard acids, indicating that they will likely not bind well with histidine, a borderline base. Based solely on HSAB, the histinines will prefer to bind to Cu(I)/Cu(II) because they are either soft/borderline acids. In addition to HSAB theory, it is also important to consider ionic size when determining if these competitors will bind in the site. These metal ions are larger than the copper ions, which may affect their ability to bind to the histidines in the pre-organized hemocyanin active site; the larger ions will not fit well into the pre-organized site, or if the site could accommodate the larger ion, it may change the protein structure to cause unfavorable steric interactions.

Kinetics and Thermodynamics

The stability of the complex is influenced by the energy of electrons in the d-orbital, as well as the geometry of the metal complexes. Because Cu(I) and Cu(II) have electrons at a higher energy, it makes them less stable and more likely to react. Additionally, Cu(II) is coordinated in a distorted tetrahedral geometry, but based on LFT, the square planar geometry is preferred. If Cu(II) was in the preferred geometry it would be more stable, and therefore reduction to Cu(I) and release of oxygen would be less favorable. Because Cu(II) is not fully stable in this environment, it allows for the cycling between the +1 and +2 oxidation states, and the transport of oxygen.

Lability is a desirable property for oxygen transport and storage proteins. The coordinated oxygen must be able to bind and unbind quickly and reversibly (carbon monoxide and cyanide gas are toxic because they will bind irreversibly with hemoglobin and displace oxygen). Cu(I) is a d^{10} metal and Cu(II) is a d^9 metal, so their higher-energy antibonding t_2 orbitals are occupied by electrons. When electrons occupy this higher-energy set of d-orbitals, the complex has a smaller CFSE and is more kinetically labile (has fast ligand substitutions reactions).

Redox Chemistry

The copper ions at the active site of hemocyanin cycle between Cu(I) and Cu(II) depending on whether or not oxygen is bound. Cu(I) is oxidized by oxygen when O_2 coordinates with the metal. For the copper oxidation half reaction, the reduction potential at pH = 7 is 0.153 V.[19] The one electron reduction of O_2 is difficult because it is spin forbidden.[20] The reduction potential of this reaction at pH = 7 is -0.33 V, which would make E_{rxn} for the one electron redox reaction -0.48 V, a non-spontaneous reaction. The two electron oxidation of O_2 to form H_2O_2 is much more favorable; the reduction potential of this reaction at pH = 7 is 0.281 V. This makes the overall which makes the overall E_{rxn} 0.128 V, which makes the binding of oxygen to hemocyanin spontaneous (Figure **12.3.8**).

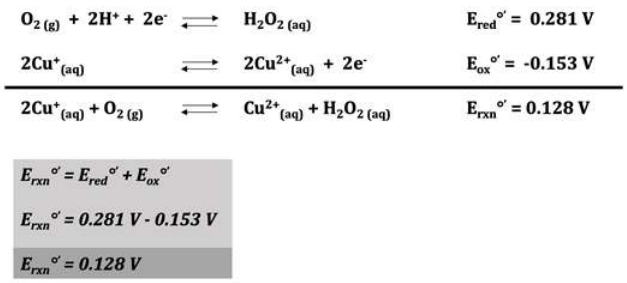


Figure **12.3.8**:[19] *Oxidation-Reduction Reactions for Hemocyanin.* The reduction half reaction can be seen on the first line. There are two electrons and two hydrogen ions involved in the reduction of oxygen, and the reduction potential of this reaction is 0.281 V at pH 7. On the following line, the oxidation half reaction can be seen where Cu(I) is oxidized to Cu(II) with an oxidation potential of -0.153 V at pH 7. The overall reaction appears on the third line. At pH 7, the redox potential of this reaction is 0.128 V.

Sources

1. Cook, J. D.; Penner-Hahn, J. E.; Stemmler, T. L. Structure and Dynamics of Metalloproteins in Live Cells. Methods in Cell Biology Methods in Nano Cell Biology 2008, 199–216.
2. Kanost, M. R. Hemolymph. Encyclopedia of Insects 2009, 446–449.
3. Christian, W. S.; Stefan, R. Functional morphology and diversity, Chapter 14: Circulatory System and Respiration; Oxford University Press: Oxford, 2013.
4. Hashim, O. H.; Adnan, N. A. Coenzyme, Cofactor and Prosthetic Group — Ambiguous Biochemical Jargon. Biochemical Education 1994, 22 (2), 93–94.
5. Kitajima, N.; Fujisawa, K.; Fujimoto, C.; Morooka, Y.; Hashimoto, S.; Kitagawa, T.; Toriumi, K.; Tatsumi, K.; Nakamura, A. A New Model for Dioxygen Binding in Hemocyanin. Synthesis, Characterization, and Molecular Structure of the .Mu.-.Eta.2:.Eta.2 Peroxo Dinuclear Copper(II) Complexes, [Cu(HB(3,5-R2pz)3)]2(O2) (R = Isopropyl and Ph). *Journal of the American Chemical Society* **1992**, *114* (4), 1277–1291.
6. IUPAC. Compendium of Chemical Terminology, 2nd ed. (the "Gold Book"). Compiled by A. D. McNaught and A. Wilkinson. Blackwell Scientific Publications, Oxford (1997). Online version (2019-) created by S. J. Chalk. ISBN 0-9678550-9-8. https://doi.org/10.1351/goldbook.
7. IUPAC. Compendium of Chemical Terminology, 2nd ed. (the "Gold Book"). Compiled by A. D. McNaught and A. Wilkinson. Blackwell Scientific Publications, Oxford (1997). Online version (2019-) created by S. J. Chalk. ISBN 0-9678550-9-8. https://doi.org/10.1351/goldbook.
8. Hazes, B.; Hol, W. Oxygenated Hemocyanin (Subunit Type Ii). **1996**.
9. Coates, C. J.; Decker, H. Immunological Properties of Oxygen-Transport Proteins: Hemoglobin, Hemocyanin and Hemerythrin. Cellular and Molecular Life Sciences 2016, 74 (2), 293–317.

10. Libretexts. 3.2.1: Hard and Soft Acid and Base Theory. https://chem.libretexts.org/Courses/Saint_Mary's_College,_Notre_Dame,_IN/CHEM_342:_Bio-inorganic_Chemistry/Readings/Week_3:_Metal-Ligand_Interactions_continued..../3.2:_The_identity_of_metal_ion_and_the_ligand_donor_atom(s)_affects_affinity/3.2.1:_Hard_and_Soft_Acid_and_Base_Theory (accessed Jan 28, 2020).
11. Pratoomchat, B.; Sawangwong, P.; Pakkong, P.; Machado, J. Organic and Inorganic Compound Variations in Haemolymph, Epidermal Tissue and Cuticle over the Molt Cycle in Scylla Serrata ž Decapoda/. 2002, 13.
12. Sowers, A. D.; Young, S. P.; Grosell, M.; Browdy, C. L.; Tomasso, J. R. Hemolymph Osmolality and Cation Concentrations in Litopenaeus Vannamei during Exposure to Artificial Sea Salt or a Mixed-Ion Solution: Relationship to Potassium Flux. Comparative Biochemistry and Physiology Part A: Molecular & Integrative Physiology 2006, 145 (2), 176–180. https://doi.org/10.1016/j.cbpa.2006.06.008.
13. Morris, R. H.; Lee, A.; Hadzovic, A. A Tour of Hemocyanin. https://sites.chem.utoronto.ca/chemistry/coursenotes/GTM/JM/hemocyanin/start.htm (accessed Mar 27, 2020).
14. Cirera, J.; Ruiz, E.; Alvarez, S. Stereochemistry and Spin State in Four-Coordinate Transition Metal Compounds. Inorganic Chemistry 2008, 47 (7), 2871–2889.
15. Sundberg, R. J.; Martin, R. B. Interactions of Histidine and Other Imidazole Derivatives with Transition Metal Ions in Chemical and Biological Systems. Chemical Reviews 1974, 74 (4), 471–517.
16. Nickerson, K. W.; Holde, K. E. V. A Comparison of Molluscan and Arthropod Hemocyanin—I. Circular Dichroism and Absorption Spectra. Comparative Biochemistry and Physiology Part B: Comparative Biochemistry 1971, 39 (4), 855–872.
17. Frieden, E.; Osaki, S.; Kobayashi, H. Copper Proteins And Oxygen: Correlations Between Structure And Function Of The Copper Oxidases. Journal of General Physiology 1965.
18. Tommerdahl, A. P.; Burnett, K. G.; Burnett, L. E. Respiratory Properties of Hemocyanin From Wild and Aquacultured Penaeid Shrimp and the Effects of Chronic Exposure to Hypoxia. The Biological Bulletin 2015, 228 (3), 242–252.
19. Lippard, S. J.; Berg, J. M. Principles of bioinorganic chemistry; University Science Books: Mill Valley, CA, 1994.
20. Solomon, E. I.; Heppner, D. E.; Johnston, E. M.; Ginsbach, J. W.; Cirera, J.; Qayyum, M.; Kieber-Emmons, M. T.; Kjaergaard, C. H.; Hadt, R. G.; Tian, L. Copper Active Sites in Biology. Chemical Reviews 2014, 114 (7), 3659–3853.

Contributed By:

This work was originally written by:

- ***Lydia Lorenc,*** *Spring 2018: Lydia is currently (as of 2018) a junior chemistry major at Saint Mary's College in Notre Dame, IN.*
- Margaret Benjamin, a chemistry major at Saint Mary's College, class of 2020.

This work was originally edited by Dr. Kathryn Haas, Assistant Professor and Madison Sendzik, Teaching and Research Assistant of Saint Mary's College.

12.3: Biological Dioxygen Transport and Storage is shared under a not declared license and was authored, remixed, and/or curated by LibreTexts.

12.4: Biological Metal Storage

Iron

Iron is widely used in a wide number of biological applications. Ferrous (Fe^{2+}) ion appears to have been the environmentally stable form during prebiotic times. The combination of the reactivity of ferrous ion and the relatively large amounts of iron used by cells may have necessitated the storage of ferrous ion; recent results suggest that ferrous ion may be stabilized inside ferritin long enough to be used in some types of cells. The ability of primitive organisms photosynthetically oxidize H_2O into dioxygen, probably produced the worst case of environmental pollution in terrestrial history. As a result, the composition of the atmosphere, the course of biological evolution, and the oxidation state of environmental iron all changed profoundly. Paleontologists and meteorologists estimate that there was a lag of about 200 - 300 million years between the first dioxygen production and the appearance of significant dioxygen concentrations in the atmosphere, because the dioxygen produced at first was consumed by the oxidation of ferrous ions in the oceans. The transition in the atmosphere, which occurred about 2.5 billion years ago, caused the bioavailability of iron to plummet and the need for iron storage to increase. Comparison of the solubility of Fe^{3+} at physiological conditions (about 10^{-18} M) to the iron content of cells (equivalent to 10^{-5} to 10^{-8} M) emphasizes the difficulty of acquiring sufficient iron.

Iron is stored mainly in the ferritins, a family of proteins composed of a protein coat and an iron core of hydrous ferric oxide [$Fe_2O_3(H_2O)_n$] with various amounts of phosphate.[6,7] As many as 4,500 iron atoms can be reversibly stored inside the protein coat in a complex that is soluble; iron concentrations equivalent to 0.25 M [about 10^{16}-fold more concentrated than Fe(III) ions] can be easily achieved *in vitro*. Ferritin is found in animals, plants, and even in bacteria; the role of the stored iron varies, and includes intracellular use for Fe-proteins or mineralization, long-term iron storage for other cells, and detoxification of excess iron. Iron regulates the synthesis of ferritin, with large amounts of ferritin associated with iron excess, small or undetectable amounts associated with iron deficiency.

Ferritin

Despite the importance of iron for life, excess iron can be toxic.[3] Unregulated free iron can catalyze the production of harmful reactive oxygen species (ROS) and free radicals, most commonly via Fenton chemistry. The Fenton reaction (below) is the reaction between iron(II) ions and hydrogen peroxide to produce the extremely reactive and harmful hydroxyl radical **($^{\bullet}OH$).**[1] ROS are generally strong oxidizing agents and can cause permanent cell damage, organ failure, and death

$$\mathbf{Fe^{2+} + H_2O_2 \rightarrow Fe^{3+} + OH^- + {}^{\bullet}OH}$$

Structurally, ferritin is a hollow cage and the sequestered iron is stored as an iron(III) mineral within the protein shell (Figure **12.4.1**).[2,3]

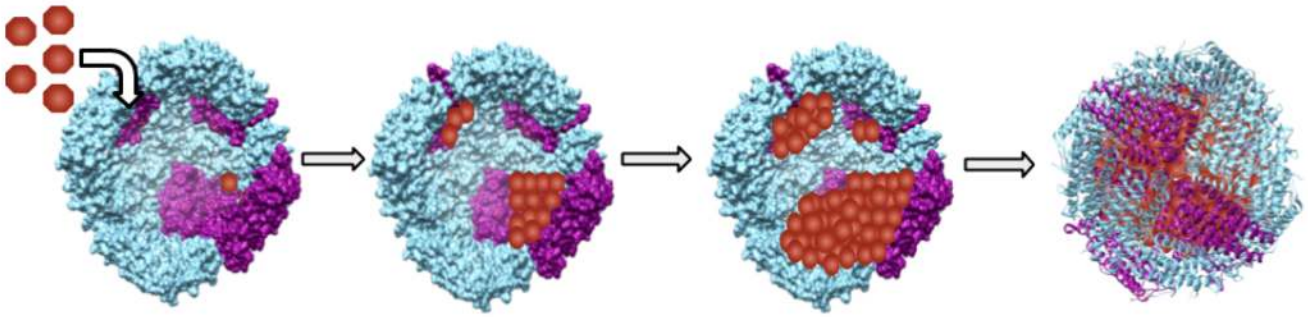


Figure 12.4.1: A cartoon diagram of sequestration of iron, which has been crystallized and is stored as an iron/oxy mineral in the hollow cage of ferritin. From left to right, the diagram depicts the cross section of the ferritin protein cage and the growing nucleation in the hollow center of ferritin. Each red shape represents some crystalline, mineral combination of iron, oxygen, and hydrogen (FeOOH core). Nucleation begins on the purple surfaces of ferritin, which will be discussed in detail later, but is otherwise random. The final image in the diagram on the far right is the spherical ribbon structure of full iron-containing ferritin protein with the cartoon depiction of iron/oxy mineral (red shapes) within the center. While this diagram depicts ferritin being filled to capacity with iron, in reality, ferritin can be filled as much or as little with iron, as needed. Thus, this figure can also be interpreted as different ferritin proteins in environments of different iron concentrations and so storing different amounts of iron.

Ferritin is made of subunits. Each subunit has four polypeptide α-helices or spirals.[2] Structures of ferritin differ based on the organism which produces it. Most ferritin is made of 24 of these subunits.[6] Human ferritin is a 24-subunit, 480 kDa, 12 nm globular protein with a hollow center cavity (cavity diameter of 8 nm).[2] One 24-subunit ferritin protein can store up to 4500 iron ions in its hollow center.[2] Ferritin is a very good space-saving model for the cell because of its high iron to protein ratio (4500 iron ions/8 nm cavity).[2,9] This iron to protein ratio is 200 times that of hemoglobin.[9] Up to 24% of ferritin's weight could be stored iron ions. Meanwhile, bacterial ferritin can be either a 12- or 24-subunit globular protein.[6] However, it is thought that the 12-subunit ferritin's may play an additional role in protecting DNA from oxidative damage, while the 24-subunit bacterial ferritin may control bacterial iron metabolism.[3]

The subunits of human ferritin are classified as the heavy subunit or "H-chain" and the light subunit or "L-chain" (Figure 12.4.2).[6] The two subunits, however, are not extremely different in molecular weight or amino acid sequence. The H-chain is made of 178 amino acids with a molecular weight of 21 kDa and the L-chain is made 171 amino acids and weighs 18 kDa.[4] The two types of subunits have ~53% protein sequence identity.[4] The designations of heavy and light are actually a modern recasting of designations that originally reflected the organs from which the two forms were isolated, "H" for heart and "L" for liver.[8]

The two types of subunits combine in different ratios to form the 24-subunit protein shell in humans (Figure 12.4.2).[6] This ratio is dependent on the tissue where the ferritin is synthesized.[6] The H subunit is responsible for catalyzing the oxidation of iron(II).[8] The L subunit hosts the site of nucleation and storage of iron.[8] The ratio of H:L will be higher in tissues where iron oxidation activity is high and iron detoxification is needed, such as the heart or the brain.[1,4] Tissues, like those in the spleen, are used more for storage and will have a lower H:L ratio. The human liver produces ferritin that is 50% H and 50% L.

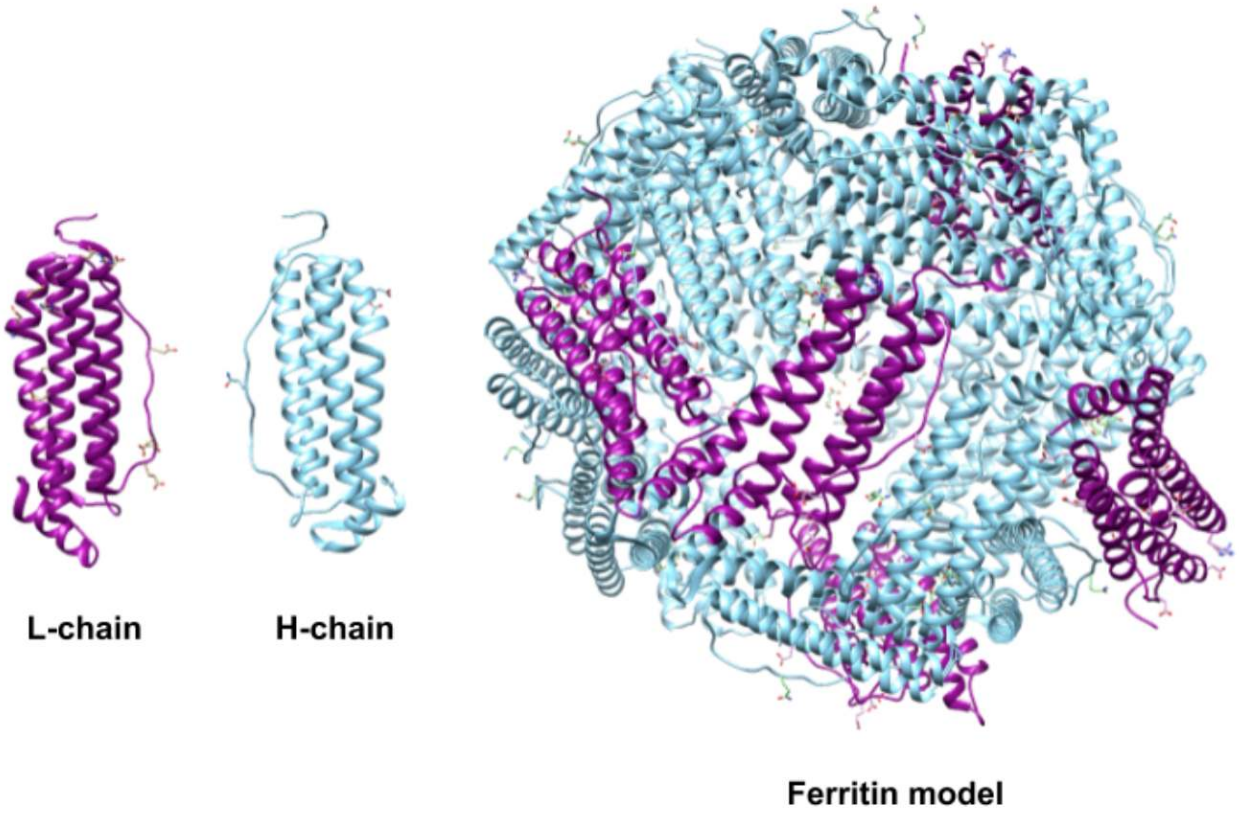


Figure 12.4.2: Light (L) (PDB 2FFX) and heavy (H) (PDB 2FHA) human ferritin subunit chains combine to form the human ferritin shell in specific ratios. The H:L ratio is dependent on the tissue where the protein is synthesized. The model seen here was created from the crystal structures of individual subunits, not a biologically obtained structure. However, it is approximately 30% L-type subunit and 70% H-type subunit and would be of a similar ratio to the ferritin found in the brain.[1]

Selectivity for Iron

Fe^{2+} ions are brought to ferritin for storage by the transport protein transferrin. The ions are believed to enter through one of the eight symmetric 3-fold channels or one of the six symmetric 4-fold channels formed by the subunits in the ferritin structure highlighted in Figure 12.4.3.[6]

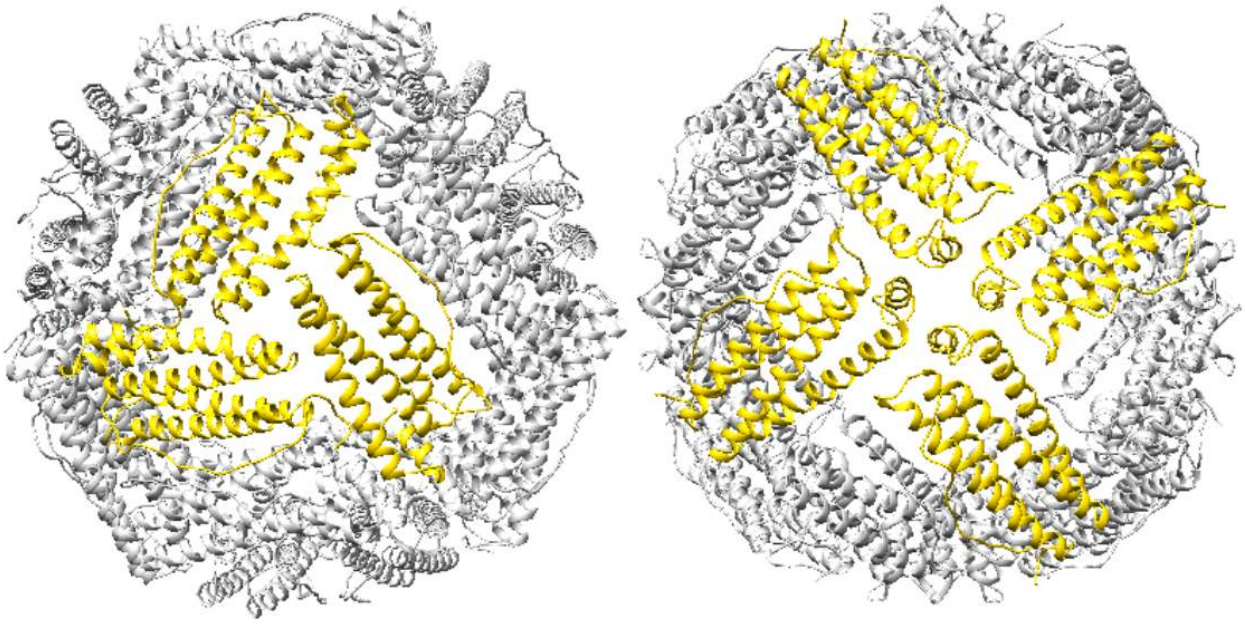


Figure 12.4.3. Symmetric channels of entry and exit in Ferritin (PDB: 1FHA). The 3-fold channel on the left appears eight times in the 24 subunit ferritin protein. The 3-fold channel is formed by three subunits. The 4-fold channel on the right appears six times in the 24 subunit ferritin protein. The 4-fold channel is formed by four subunits.

The 3-fold channels are lined with the polar side chains aspartate and glutamate and make the channel hydrophilic.[2] The hydrophilicity of the channel allows for the transport of water, metal cations, and hydrophilic molecules of an appropriate size into and and out of the ferritin center.[4] Most studies indicate that the 3-fold channel is the main channel for Fe^{2+} ions both into and out of the cell.[1,3] The 4-fold channels are lined with the non-polar side chain leucine and make the channel hydrophobic. It is widely thought that the 4-fold channels are involved with the diffusion of oxygen and hydrogen peroxide into and out of the ferritin center.[1]

Iron(II) ions are oxidized at the “ferroxidase site” on the H-chain subunits (Figure 12.4.4). After conversion to Fe^{3+}, the iron is stored as a crystalline iron/oxy mineral.[2] The mineral accumulates on the L-chain (Figure 12.4.5).[8]

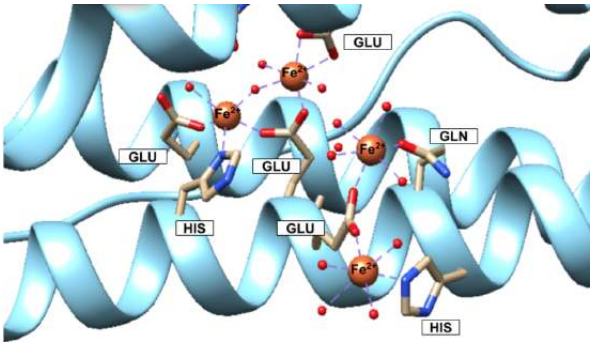


Figure 12.4.4: Human Ferritin H-chain (PDB 4YKH). Fe2+ ions are both shown traveling on their way to the ferroxidase site and at the ferroxidase site, to be covered in detail later. Fe2+ ions can be seen binding to water molecules, oxidizing agents and residues glutamic acid (Glu or GLU), glutamine (Gln or GLN), and histidine (His or HIS). The smaller red balls connecting to the Fe2+ ions via a purple dashed line are the oxidizing agents—oxygen molecules, hydrogen peroxide, or water molecules.

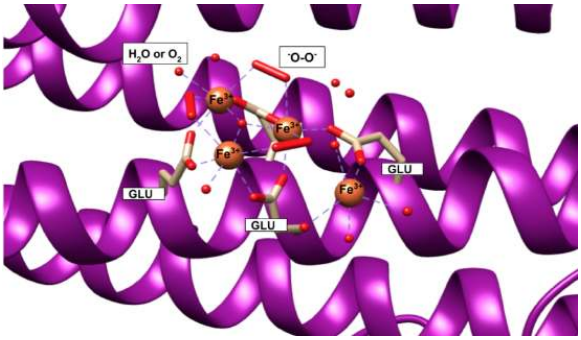


Figure 12.4.5: Human Ferritin L-chain (PDB 5LG8). Fe3+ ions can be seen binding to water and oxygen molecules (small red balls), peroxo groups (long red cylinders), and residues of glutamic acid (Glu or GLU) from the L-chain. Fe3+ is stored as an iron/oxy mineral on the L-chain. This is the beginning of nucleation within the ferritin cavity.

Figures 4 and 5 show iron(II) at the ferroxidase site and iron/oxy mineral at the nucleation site, according to the available crystal structures. The structure of the entire iron mineral core, however, is actually inconsistent throughout the whole mineral and differs even between identical ferritin shells. Traditionally, it was believed that the iron(III)/oxy mineral that makes up the core was similar to ferrihydrite and ideally structured as 20% tetrahedral and 80% octahedral; however, as more evidence has become available this model has been replaced by a “polyphasic” or heterogeneous model of the iron core that is thought to be more accurate.[2,4] According to the polyphasic model, the mineral structure is heterogeneous in its chemical content and geometric structure.[4] X-ray absorption fine structure (EXAFS) studies concluded that the iron core of ferritin was made of iron ions that are surrounded by six or seven oxygen atoms, surrounded by another shell of iron ions.[2] This inconsistency leads to the conclusion that the mineral is a heterogeneous, hydrated iron(III)/oxy.[3] In other words, the iron core itself is not packed regularly or in a pattern within ferritin.[6]

Selectivity of iron(II) by ferritin can be explained through hard-soft acid base (HSAB) theory. Ferritin binds an Fe^{2+} ion for oxidation. Fe^{2+} is categorized as a borderline acid. The binding sites on the H-chain are glutamic acid (Glu), histidine (His), and glutamine (Gln) residues (Figure 12.4.4).[6] Glu and Gln are categorized as hard bases, while His is categorized as borderline base. The oxidizing agents—oxygen molecules, hydrogen peroxide, or water molecules all have hard character. Fe^{2+} as a borderline acid binds well with the binding site of mixed hard and borderline character. The selection of Fe^{2+} in ferritin is further supported by experimental work where metals like zinc (which also exists in the body) were also shown to have binding abilities to ferritin.[5] But, zinc, although it is also borderline, has softer character than Fe^{2+} and so would not be as stable or favorable with the hard Glu and Gln ligands.[10]

Iron Mineralization

Iron(II) is oxidized at the ferroxidase site on the H-chain (sites A and B) by some oxidizing agent, most probably O_2 and H_2O_2.[1] Three reactions/models for Fe^{2+} oxidation and mineralization have been observed. There is a ferroxidation reaction or protein catalysis model (Reactions \PageIndex {1} -\PageIndex {4}), a mineralization reaction or crystal growth model (Reaction \PageIndex {5}), and a detoxification reaction of Fe^{2+} + H_2O_2 (Reaction \PageIndex {6}).[1] The ferroxidation reaction occurs at the ferroxidase site on the H-chain of ferritin. The ferroxidation reaction for the protein catalysis model of ferritin oxidation can be written as:

$$[2Fe^{2+} + O_2 + 4H_2O \rightarrow [Fe^{3+}-O-O-Fe^{3+}]^{2+} \quad (12.4.1)$$

$$Fe^{3+}-O-O-Fe^{3+}]^{2+}] \rightarrow [Fe_2O-(OH)_2]^{2+} \quad (12.4.2)$$

$$[Fe_2O-(OH)_2]^{2+} \rightarrow 2FeOOH_{core} + H_2O_2 + 4H^+ \quad (12.4.3)$$

$$\text{Net: } 2Fe^{2+} + O_2 + 4H_2O \rightarrow 2FeOOH_{core} + H_2O_2 + 4H^+ \quad (12.4.4)$$

The net mineralization reaction for the crystal growth model of ferritin oxidation is written as:

$$4Fe^{2+} + O_2 + 6H_2O \rightarrow 4FeOOH_{core} + 8H^+ \quad (12.4.5)$$

The most recently identified of the oxidation and mineralization reactions, the Fe^{2+} + H_2O_2 detoxification reaction is written as:

2 Fe^{2+} + H_2O_2 + 2 H_2O → 2 $FeOOH_{core}$ + 4 H^+ **(3.)**.[1]

Iron Release

When cells require iron, for enzyme synthesis, after blood loss, or during embryonic development, the iron stored in ferritin must be released rapidly, on demand, and under control.[8] Although, as with many aspects of ferritin function, the mechanism of iron release to the cell from ferritin is unknown. What is known inherently about the process is that over its course it must essentially reverse mineralization: the iron(III)/oxy mineral must be dissolved from its solid state to aqueous ions and the iron(III) ions must be reduced to iron(II).

Proposed models for ferritin iron release include (1) an equilibrium between the iron stored in ferritin and the iron in the cytoplasm of the cell, (2) ferritin protein degradation, (3) spontaneous, direct dissolution of iron(III) from the mineral core from scavenging by iron(III) binding proteins, and (4) the reduction of the iron(III) mineral which is then complexed iron(II) by a chelating agent and transported out of ferritin.[4,12] The last model (4) lacks confirmation, yet is considered by many to be the physiological mechanism. This model is the most efficient method and the presence of reducing agents under physiological conditions.[4]

Except the second model (2), the physiological relevance of all above models is still to be seen.[12] The ferritin degradation model (2) is the only mechanism to have been observed under physiological conditions. However, since this model would require iron release to be dependent of the turnover and synthesis of ferritin, another model is suspected to be necessary.[12]

However iron is released from ferritin, studies indicate that the physical exit of the iron from ferritin takes place via the 3-fold channels. One proposal for exit based on observations in bacterial ferritin is the localized folding/unfolding of ferritin.[4] The ferritin channels can be unfolded without affecting the overall function or structure of the protein. Unfolding the channels and thus, widening the opening, would allow for quick release of demineralized iron. The channels become highly disordered when this occurs to the effect that they do not appear in crystal structures.[8]

Much remains to be determined about human ferritin. Other functions of ferritin in the body, and the mechanisms for how Fe^{2+} enters and binds to ferritin, how Fe^{2+} is oxidized to Fe^{3+} for storage, and how iron is released remain undetermined, among others, are thought to be non-universal—even within the same organism.[3,6]

While much of the chemistry behind ferritin is, as of now, unexplained, ferritin is still an important protein for all life. Wherever iron is noted as an essential nutrient, ferritin must also be present for management and storage. The elucidation of ferritin can lead to advancements in iron metabolism and neurological disorders and new uses of ferritin chemistry in nanochemistry and catalytic industrial applications.[3,4]

Sources

[1] Bou-Abdallah, F. The Iron Redox and Hydrolysis Chemistry of the Ferritins. *Biochimica et Biophysica Acta (BBA) - General Subjects* **2010**, *1800* (8), 719–731.

[2] Crabb, E.; Moore, E. *Metals and life*; Royal Society of chemistry: Cambridge, **2010**.

[3] Theil, E. C.; Tosha, T.; Behera, R. K. Solving Biology's Iron Chemistry Problem with Ferritin Protein Nanocages. *Accounts of Chemical Research* **2016**, *49* (5), 784–791.

[4] Carmona, F.; Palacios, Ò.; Gálvez, N.; Cuesta, R.; Atrian, S.; Capdevila, M.; Domínguez-Vera, J. M. Ferritin Iron Uptake and Release in the Presence of Metals and Metalloproteins: Chemical Implications in the Brain. *Coordination Chemistry Reviews* **2013**, *257* (19–20), 2752–2764.

[5] Knovich, M. A.; Storey, J. A.; Coffman, L. G.; Torti, S. V. Ferritin for the Clinician. *Blood Rev* **2009**, *23* (3), 95–104.

[6] Bradley, J. M.; Le Brun, N. E.; Moore, G. R. Ferritins: Furnishing Proteins with Iron. *JBIC Journal of Biological Inorganic Chemistry* **2016**, *21* (1), 13–28.

[7] Watt, G. D.; Jacobs, D.; Frankel, R. B. Redox Reactivity of Bacterial and Mammalian Ferritin: Is Reductant Entry into the Ferritin Interior a Necessary Step for Iron Release? *Proceedings of the National Academy of Sciences* **1988**, *85* (20), 7457–7461.

[8] Bertini, I. *Biological Inorganic Chemistry: Structure and Reactivity*; University Science Books, **2007**.

[9] Chasteen, N. D.; Harrison, P. M. Mineralization in Ferritin: An Efficient Means of Iron Storage. *Journal of Structural Biology* **1999**, *126* (3), 182–194.

[10] Joshi, J. G.; Sczekan, S. R.; Fleming, J. T. Ferritin—A General Metal Detoxicant. *Biol Trace Elem Res* **1989**, *21* (1), 105.

[11] Bertini, I.; Lalli, D.; Mangani, S.; Pozzi, C.; Rosa, C.; Theil, E. C.; Turano, P. Structural Insights into the Ferroxidase Site of Ferritins from Higher Eukaryotes. *Journal of the American Chemical Society* **2012**, *134*(14), 6169–6176.

[12] Honarmand Ebrahimi, K.; Hagedoorn, P.-L.; Hagen, W. R. Unity in the Biochemistry of the Iron-Storage Proteins Ferritin and Bacterioferritin. *Chemical Reviews* **2015**, *115* (1), 295–326.

[13] H. Rodriguez, J.; Mccusker, J. Density Functional Theory of Spin-Coupled Models for Diiron-Oxo Proteins: Effects of Oxo and Hydroxo Bridging on Geometry, Electronic Structure, and Magnetism. *Journal of Chemical Physics* **2002**, *116*.

[14] Bertini, I., *Bioinorganic Chemistry*; Ed.; University Science Books: Mill Valley, Calif, **1994**.

Contributed By

*This work was originally written by **Anna Shadid,** Spring 2018: Anna is currently (as of 2018) a junior chemistry major at Saint Mary's College in Notre Dame, IN.*

This work was originally edited by Dr. Kathryn Haas, Associate Professor, and Madison Sendzik, Teaching and Research Assistant, of Saint Mary's College.

Zinc, Copper, Vanadium, Chromium, Molybdenum, Cobalt, Nickel, and Manganese

Ions of nonferrous transition metals require a much less complex biological storage system, because the solubilities are much higher ($\geq 10^{-8}$ M) than those for Fe^{3+}. As a result, the storage of nonferrous transition metals is less obvious, and information is more limited. In addition, investigations are more difficult than for iron, because the amounts in biological systems are so small. Essentially nothing is known yet about the storage of vanadium, chromium, molybdenum, cobalt, nickel, and manganese, with the possible exception of accumulations of vanadium in the blood cells of tunicates.

Zinc and copper, which are used in the highest concentrations of any of the non-ferrous transition metals, are specifically bound by the protein metallothionein. (see Figure **12.4.8**). Like the ferritins, the metallothioneins are a family of proteins, widespread in nature and regulated by the metals they bind. In contrast to ferritin, the amounts of metal stored in metallothioneins are smaller (up to twelve atoms per molecule) and the amount of protein in cells is less. Because the cellular concentrations of the metallothioneins are relatively low and the amount of metal needed is relatively small, it has been difficult to study the biological fate of copper and zinc in living organisms, and to discover the natural role of metallothioneins. However, the regulation of metallothionein synthesis by metals, hormones, and growth factors attests to the biological importance of the proteins. The unusual metal environments of metallothioneins have attracted the attention of bioinorganic chemists.

Metallothioneins, especially in higher animals, are small proteins rich in cysteine (20 per molecule) and devoid of the aromatic amino acids phenylalanine and tyrosine. The cysteine residues are distributed throughout the peptide chain. However, in the native form of the protein, the peptide chains fold to produce two clusters of -SH, which bind either three or four atoms of zinc, cadmium, cobalt, mercury, lead, or nickel. Copper binding is distinct from zinc, with 12 sites per molecule.

In summary, iron is stored in iron cores of a complicated protein. Ferritin, composed of a hollow protein coat, iron-protein interface, and an inorganic core, overcomes the problems of redox and hydrolysis by directing the formation of the quasi-stable mineral hydrous ferric oxide inside the protein coat. The outer surface of the protein is generally hydrophilic, making the complex highly soluble; equivalent concentrations of iron are ≤ 0.25 M. By contrast to iron, storage of zinc, copper, chromium, manganese, vanadium, and molybdenum is relatively simple, because solubility is high and abundance is lower. Little is known about the molecules that store these metals, with the possible exception of metallothionein, which binds small clusters of zinc or copper.

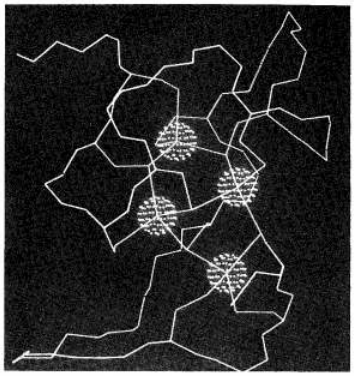


Figure **12.4.8**: - The three-dimensional structure of the a domain from rat cd_7 metallothionein-2, determined by NMR in solution, based on data in Reference 36b. The four metal atoms, bonded to the sulfur of cysteine side chains, are indicated as spherical collections of small dots. A recent description of the structure of the cd_5Zn_2 protein, determined from x-ray diffraction of crystals, agrees with the structure determined by NMR.

12.4: Biological Metal Storage is shared under a not declared license and was authored, remixed, and/or curated by LibreTexts.

12.5: Zinc as Lewis Acid and Template

Introduction

Unlike most other biologically important metals, zinc is not redox active and does not directly participate in catalytic reaction. In biological systems zinc is primarily found as Zn^{2+}, which is a d^{10} ion, making it unfavorable to either oxidize or reduce. Zinc ions do play important biochemical roles. They can act as Lewis acids, to indirectly catalyse reactions such as the hydration of carbon dioxide in carbonic anhydrase. They can also act as templates or scaffolds for protein tertiary structure.

Zinc in Carbonic Anhydrase

Chemical Reaction

Carbon-dioxide (CO_2) hydration and its mechanism in living systems are of fundamental importance for bioinorganic chemistry. In 1932 the existence of an enzyme catalyzing CO_2 hydration in red blood cells, carbonic anhydrase, was established. In 1939 the enzyme was recognized to contain zinc. Because CO_2 is both the starting point for photosynthesis and the endpoint of substrate oxidation, carbonic anhydrases are now known to be ubiquitous, occurring in animals, plants, bacteria, and fungi. Carbonic anhydrase is a classic example of a hydrolytic enzyme, one that catalyzes addition or removal of water to a substrate molecule. More specifically, it catalyzes the reversible conversion of carbon dioxide (CO_2) to bicarbonate (HCO_3^-).



Figure **12.5.1**: Reaction catalysed by carbonic anhydrase enzymes.

Although hydration of CO_2 is spontaneous in water at pH 7, the reaction is kinetically slow ($k = 10^{-1}\ s^{-1}$), too slow to convert all CO_2 produced in respiration. Only above pH 9 does the uncatalyzed reaction become fast, due to direct attack of OH^-, which is a much better nucleophile than H_2O ($k = 10^4\ M^{-1}\ s^{-1}$, in the presence of OH^-). Figure **12.5.2** compares nucleophilic attack of water versus hydroxide (OH-) on CO_2.



Figure **12.5.2**: Nucleophilic attack on carbon in carbon dioxide (CO_2) in the formation of bicarbonate (HCO_3^-). In the top panel, H_2O is the nucleophile. The bottom panel shows the reaction with hydroxide (OH^-) as the nucleophile. Since the OH^- is a stronger nucleophile, HCO_3^- formation is faster when OH^- is the nucleophile.

Between H_2O and OH^-, formation of HCO_3^- occurs faster when OH^- is the nucleophile. A faster reaction at higher pH, when more OH^- ions are present, suggests OH^- is involved in the rate determining step. However, realistically, the pH of human blood cannot be changed to speed up hydration of CO_2. Instead, humans use carbonic anhydrase to catalyse the reaction. When carbonic anhydrase is present, the reaction is sped up to a rate of $k = 10^6\ s^{-1}$.

The ubiquity of carbonic anhydrase in different organisms reflects the importance of these enzymes in sustaining life. The speed of catalyzed CO_2 hydration is essential to meet the needs of living cells. Some physiological carbonic anhydrase functions include pH regulation, electrolyte secretion, ion transport, and CO_2 homeostasis. In the digestive tract, carbonic anhydrases plays a role in the secretion of acid and keep saliva neutral by modulating pH. Among these functions, CA most notably plays a role in transport of CO_2 and HCO_3^- related to respiration. With low blood solubility, CO_2 must be converted to a more soluble form, HCO_3^-, for

transport throughout the body. Bicarbonate ions eventually reach the lungs, get converted back to CO_2, and exit the body through exhalation.

Medical research revolving around carbonic anhydrase focuses on the Zn-containing active site as a therapeutic target for various disease treatments; both carbonic anhydrase inhibitors and activators are incorporated in drug design. Carbonic anhydrase inhibitors are used as treatment for epilepsy, ulcers, cancer, obesity, and other neurological disorders. In the eye, carbonic anhydrase produces hydrogen ions that maintain optic pressure. However, too much pressure in the eye can damage the optic nerve and cause glaucoma. Carbonic anhydrase activity can create a concentration gradient that drives the transport of water to the optical nerve. When too much water is around the optical nerve, pressure around the nerve increases causing damage. Inhibition of carbonic anhydrase has become a key treatment of glaucoma.

Role of Zinc

The zinc ion is bound to the protein via three links to separate histidine residues in the chain, shown in pink in Figure **12.5.3**. The zinc is also attached to a hydroxide ion shown in the picture using red for the oxygen and white for the hydrogen.

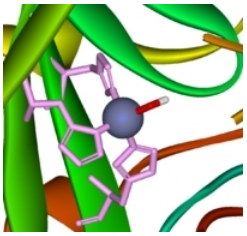
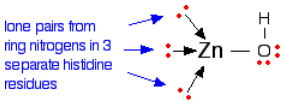


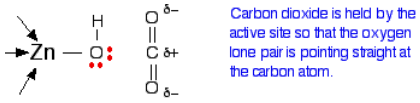
Figure **12.5.3**: Zinc active site of carbonic anhydrase showing the coordination of zinc (purple sphere) by three hisiadine residues (pink) and one hydroxide ion.

If you look at the model of the arrangement around the zinc ion in the picture above the arrangement of the four groups around the zinc is approximately tetrahedral.

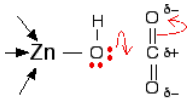


How does this catalyse the reaction between carbon dioxide and water?

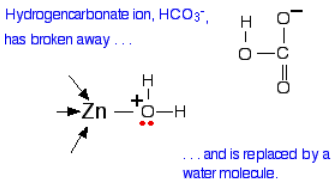
A carbon dioxide molecule is held by a nearby part of the active site so that one of the lone pairs on the oxygen is orientated towards the carbon atom of the carbon dioxide molecule. Binding the carbon dioxide in the enzyme also increases the existing polarity of the carbon-oxygen bonds.



If you have done any work on organic reaction mechanisms at all, then it is pretty obvious what is going to happen. The lone pair forms a bond with the carbon atom and part of one of the carbon-oxygen bonds breaks and leaves the oxygen atom with a negative charge on it. This results in a hydrogen carbonate ion coordinated to the zinc center.



The next step in the reaction is for the hydrogen carbonate to leave and be replaced with a water molecule from the cell solution.



All that now needs to happen to get the catalyst back to where it started is for the water to lose a hydrogen ion. This is transferred away from the zinc center and eventually out of the active site completely through the network of ordered, hydrogen bonded water molecules shown in Figure **12.5.4**. The carbonic anhydrase enzyme can do this sequence of reactions about a million times a second.

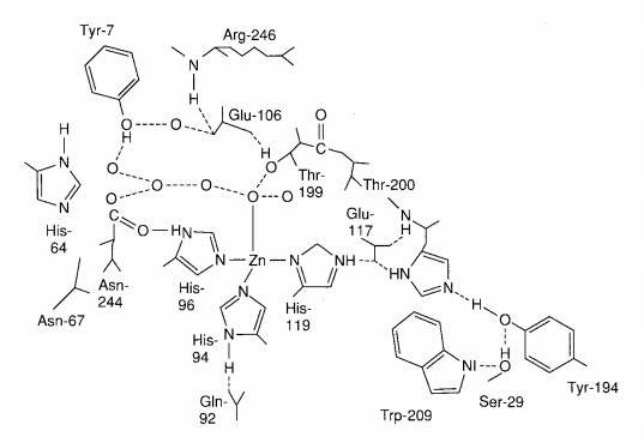


Figure **12.5.4**: Schematic representation of the active site of human carbonic anhydrase II. Hydrogen bonds (---) and ordered water molecules (o) are indicated.

Zinc as a Structural Template

Many proteins use Zn^{2+} as a structural scaffold for protein folding. These proteins employ "zinc finger" domains that bind to Zn through combinations of cysteine (Cys) and Histidine (His) side chains. Zinc binding to these domains stabilizes a specific protein fold that is critical to the protein's function. Over half of transcription factors have zinc finger domains that allow the proteins to recognize and bind to DNA. Many other proteins also have zinc-finger domains and these domains are important for a variety of functions including DNA-binding, RNA-binding, protein-protein interactions, and catalysis.

The human glioblastoma protein (GLI) family is a class of transcription factors that demonstrate sequence-specific DNA binding through "classic" Cys2His2 Zn-binding motifs. These proteins are essential during embryonic development. Dysfunction of these proteins are linked closely to glioblastoma and other aggressive cancers. The zinc finger domain of GLI1 is shown in this image (PDB 2gli),[2] where the protein surface is highlighted in yellow. GLI1 possesses five Cys2His2 zinc finger domains. When Zn is not bound to the protein, it does not have the appropriate structure to bind to recognize DNA.

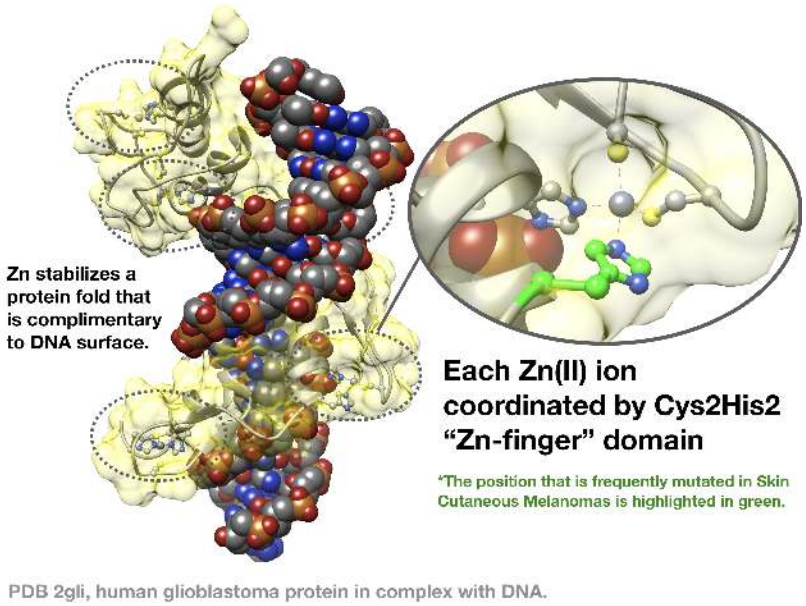


Figure **12.5.5**: The zinc finger domain of human glioblastoma protein GLI1 complexed with DNA. Inset shows the coordination of Zn^{2+} in the " zinc finger" domain.

The size and structure of the Zn^{2+} ion is critical to provide the correct protein fold for DNA binding. Thus, zinc fingers must bind specifically to Zn (as opposed to other biologically available metal ions). The zinc finger domains use principles of inorganic chemistry to control metal ion selectivity. While other metal ions, like Co^{2+}, Ni^{2+}, Fe^{2+}, and Mn^{2+}, can bind in the zinc finger sites, Zn^{2+} binds 1,000 to 100,000 times more strongly than any of these other metals.

Exercise 12.5.1

Apply HSAB theory to explain why there is such a strong selectivity for Zn^{2+} binding in a zinc finger site as opposed to other biologically available metals, including Co^{2+}, Ni^{2+}, Fe^{2+}, and Mn^{2+}.

Answer

The zinc binding site contains two borderline histadine ligands and two soft cystine ligands. The Zn^{2+} is a softer borderline Lewis acid compared to other biologically available metal ions, especially Fe^{2+}. This is because the size of transition metal cations don't vary much across the period, giving them all similar size to charge ratios and Zn^{2+}has the highest number of valence electrons, making it the most polarizable. Because the active site has two soft base donors and two borderline base donors, softer metals will preferentially bind in the active site.

Exercise 12.5.2

Cadmium (Cd^{2+}) and lead (Pb^{2+}) are toxic metal ions that bind more strongly than Zn^{2+} to zinc binding sites in proteins. Why do these toxic metals compete well with Zn^{2+}, while other metals like Co^{2+}, Ni^{2+}, Fe^{2+}, and Mn^{2+} don't?

Answer

As discussed in Exercise 1, the zinc finger binding site is biased towards coordinating softer metals. Both cadmium and lead ions are much softer than zinc and will have a stronger affinity than zinc for the zinc binding site. Under normal conditions this is not an issue because lead and cadmium are not present in significant concentrations.

Exercise 12.5.1

If a toxic metal, like Cd^{2+} would bind to the Zn^{2+} binding site, how and why might this affect the protein's ability to bind to DNA?.

Answer

The proper folding and structure of these proteins is dependent on zinc coordination in the zinc finger domains. If a larger metal ion, such as Cd^{2+} were to bind in place of Zn^{2+} this would change the size and/or geometry of the zinc finger domain and therefore the entire protein. The correct shape of the protein is essential for recognition and binding of DNA.

References

1. Inspired by Zinc Finger Proteins: A Bioinorganic Example of LFSE and HSAB, a problem set created by Elizabeth R. Jamieson, Smith College (ejamieso@smith.edu) and posted on VIPEr (www.ionicviper.org) on June 24, 2013. Copyright Elizabeth R. Jamieson 2013. This work is licensed under the Creative Commons Attribution-NonCommerical-ShareAlike 3.0 Unported License. To view a copy of this license visit http://creativecommons.org/about/license/.
2. Pavletich, N. P.; Pabo, C. O., Crystal Structure of a Five-Finger Gli-DNA Complex: New Perspectives on Zinc Fingers. *Science* **1993**, *261* (5129), 1701-7.
3. Munro, D.; Ghersi, D.; Singh, M., Two Critical Positions in Zinc Finger Domains Are Heavily Mutated in Three Human Cancer Types. *PLOS Computational Biology* **2018**, *14* (6), e1006290.

12.5: Zinc as Lewis Acid and Template is shared under a not declared license and was authored, remixed, and/or curated by LibreTexts.

12.6: Electron Transfer

Overview

Metalloproteins containing a single type of redox cofactor can be divided into two general classes: electron carriers and proteins involved in the transport or activation of small molecules. Some of the factors that seem to be characteristic of electron-transfer proteins (these proteins are sometimes called "electron transferases") are: (a) possession of a suitable cofactor to act as an electron sink (metal center with multiple stable oxidation states); (b) placement of the cofactor close enough to the protein surface to allow electrons to move in and out; (c) existence of a hydrophobic shell adjacent to, but not always entirely surrounding, the cofactor; (d) small structural changes accompanying electron transfer; and (e) an architecture that permits slight expansion or contraction in preferred directions upon electron transfer.

Metalloproteins that function as electron transferases typically place their metal coordination sites in a hydrophobic environment and may provide hydrogen bonds (in addition to ligands) to assist in stabilizing both the oxidized and the reduced forms of the cofactor. Metal-ligand bonds remain intact upon electron transfer to minimize inner-sphere reorganization energy. Many of the complex multisite metalloenzymes (e.g., cytochrome c oxidase, xanthine oxidase, the nitrogenase FeMo protein) contain redox centers that function as intramolecular electron transferases, shuttling electrons to/from other metal centers that bind exogenous ligands during enzymatic turnover.

There are three classes of metal containing electron transferases, each of which contains many members that exhibit important structural differences: blue copper proteins, iron-sulfur proteins, and cytochromes.

Blue Copper Proteins

Blue copper proteins were first isolated from bacteria in the 1950s and from plant tissues in the early 1960s. The intense blue color of these proteins is due to a strong absorption band at a wavelength of about 600 nm. Although simple Cu^{2+} complexes, such as $[Cu(H_2O)_6]^{2+}$ and $[Cu(NH_3)_4]^{2+}$, are also blue due to an absorption band at 600 nm, the intensity of the absorption band is about 100 times less than that of a blue copper protein. Moreover, the reduction potential for the Cu^{2+}/Cu^{+} couple in a blue copper protein is usually +0.3 to +0.5 V, considerably more positive than that of the aqueous Cu^{2+}/Cu^{+} couple (+0.15 V).

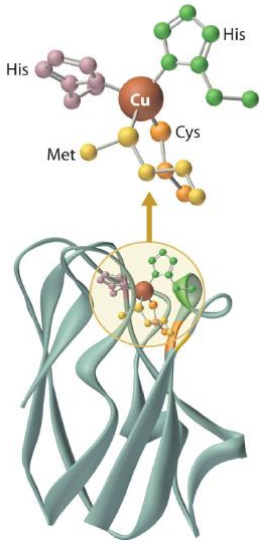


Figure **12.6.1**: A Blue Copper Protein. In both the oxidized and reduced forms of a blue copper protein, the copper is coordinated by four ligands (two histidine imidazole nitrogen atoms, a cysteine thiolate sulfur, and a thioether sulfur of a methionine) in a roughly tetrahedral arrangement.

The copper center in blue copper proteins has a distorted tetrahedral structure, in which the copper is bound to four amino acid side chains (Figure **12.6.3**). Although the most common structures for four-coordinate Cu^{2+} and Cu^{+} complexes are square planar and tetrahedral, respectively, the structures of the oxidized (Cu^{2+}) and reduced (Cu^{+}) forms of the protein are essentially identical. Thus

the protein forces the Cu^{2+} ion to adopt a higher-energy structure that is more suitable for Cu^{+}, which makes the Cu^{2+} form easier to reduce and raises its reduction potential.

Moreover, by forcing the oxidized and reduced forms of the metal complex to have essentially the same structure, the protein ensures that electron transfer to and from the copper site is rapid because only minimal structural reorganization of the metal center is required. Kinetics studies on simple metal complexes have shown that electron-transfer reactions tend to be slow when the structures of the oxidized and reduced forms of a metal complex are very different, and fast when they are similar. You will see that other metal centers used for biological electron-transfer reactions are also set up for minimal structural reorganization after electron transfer, which ensures the rapid transfer of electrons.

The blue copper proteins are characterized by intense S(Cys) → Cu chargetransfer absorption near 600 nm, an axial EPR spectrum displaying an unusually small hyperfine coupling constant, and a relatively high reduction potential.[4,8-10] With few exceptions (e.g., photosynthetic organisms), their precise roles in bacterial and plant physiology remain obscure. X-ray structures of several blue copper proteins indicate that the geometry of the copper site is approximately trigonal planar, as illustrated by the *Alcaligenes denitrificans* azurin structure (Figure 6.5).[11,12] In all these proteins, three ligands (one Cys, two His) bind tightly to the copper in a trigonal arrangement. Differences in interactions between the copper center and the axially disposed ligands may significantly contribute to variations in reduction potential that are observed[12] for the blue copper electron transferases. For example, $E^{\circ\prime}$ = 276 mV for *A. denitrificans* azurin, whereas that of *P. vulgaris* plastocyanin is 360 mV. In *A. denitrificans* azurin, the Cu-S(Met) bond is 0.2 Å longer than in poplar plastocyanin, and there is a carbonyl oxygen 3.1 Å from the copper center, compared with 3.8 Å in plastocyanin. These differences in bond lengths are expected to stabilize Cu^{II} in azurin to a greater extent than in plastocyanin, and result in a lower $E^{\circ\prime}$ value for azurin.

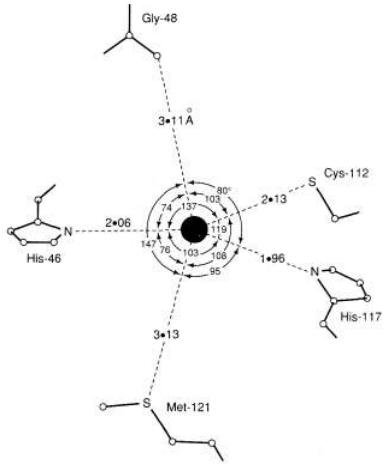


Figure 6.5 - Structure of the blue copper center in azurin.[11]

Iron Sulfur Proteins

Although all known bacteria, plants, and animals use iron–sulfur proteins to transfer electrons, the existence of these proteins was not recognized until the late 1950s. Iron–sulfur proteins transfer electrons over a wide range of reduction potentials, and their iron content can range from 1 to more than 12 Fe atoms per protein molecule. In addition, most iron–sulfur proteins contain stoichiometric amounts of sulfide (S^{2-}).

These properties are due to the presence of four different kinds of iron–sulfur units, which contain one, two, three, or four iron atoms per Fe–S complex (Figure **12.6.5**). In all cases, the Fe^{2+} and Fe^{3+} ions are coordinated to four sulfur ligands in a tetrahedral environment. Due to tetrahedral coordination by weak-field sulfur ligands, the iron is high spin in both the Fe^{3+} and Fe^{2+} oxidation states, which results in similar structures for the oxidized and reduced forms of the Fe–S complexes. Consequently, only small structural changes occur after oxidation or reduction of the Fe–S center, which results in rapid electron transfer.

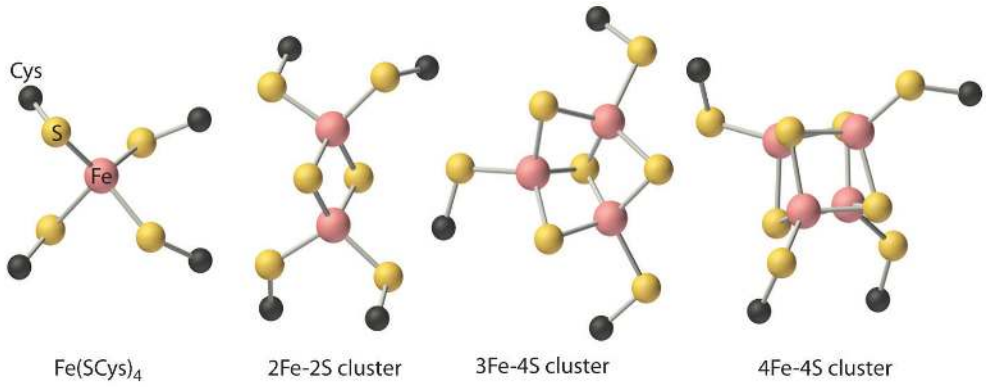


Figure **12.6.5**: Fe–S Centers in Proteins: Four kinds of iron–sulfur centers, containing one, two, three, and four iron atoms, respectively, are known in electron-transfer proteins. Although they differ in the number of sulfur atoms provided by cysteine thiolates versus sulfide, in all cases the iron is coordinated to four sulfur ligands in a roughly tetrahedral environment.

The iron-sulfur proteins play important roles[13,14] as electron carriers in virtually all living organisms, and participate in plant photosynthesis, nitrogen fixation, steroid metabolism, and oxidative phosphorylation, as well as many other processes (Chapter 7). The optical spectra of all iron-sulfur proteins are very broad and almost featureless, due to numerous overlapping charge-transfer transitions that impart red-brown-black colors to these proteins. On the other hand, the EPR spectra of iron-sulfur clusters are quite distinctive, and they are of great value in the study of the redox chemistry of these proteins.

The simplest iron-sulfur proteins, known as rubredoxins, are primarily found in anaerobic bacteria, where their function is unknown. Rubredoxins are small proteins (6 kDa) and contain iron ligated to four Cys sulfurs in a distorted tetrahedral arrangement. The $E^{\circ\prime}$ value for the $Fe^{III/II}$ couple in water is 770 mV; that of *C. pasteurianum* rubredoxin is -57 mV. The reduction potentials of iron-sulfur proteins are typically quite negative, indicating a stabilization of the oxidized form of the redox couple as a result of negatively charged sulfur ligands.

The [2Fe-2S] ferredoxins (10-20 kDa) are found in plant chloroplasts and mammalian tissue. The structure of *Spirulina platensis* ferredoxin[15] confirmed earlier suggestions, based on EPR and Mössbauer studies, that the iron atoms are present in a spin-coupled [2Fe-2S] cluster structure. One-electron reduction ($E^{\circ\prime}$ ~ -420 mV) of the protein results in a mixed-valence dimer (Equation 6.3):

$$[Fe_2S_2(SR)_4]^{2-} \underset{-e^-}{\overset{+e^-}{\rightleftharpoons}} [Fe_2S_2(SR)_4]^{3-} \tag{6.3}$$

$$Fd_{ox} \qquad Fd_{red} \tag{12.6.1}$$

$$2Fe(III) \qquad Fe(II) + Fe(III) \tag{12.6.2}$$

The additional electron in Fd_{red} is associated with only one of the iron sites, resulting in a so-called trapped-valence structure.[16] The $[Fe_2S_2(SR)_4]^{4-}$ cluster oxidation state, containing two ferrous ions, can be produced *in vitro* when strong reductants are used.

Four-iron clusters [4Fe-4S] are found in many strains of bacteria. In most of these bacterial iron-sulfur proteins, also termed ferredoxins, two such clusters are present in the protein. These proteins have reduction potentials in the -400 mV range and are rather small (6-10 kDa). Each of the clusters contains four iron centers and four sulfides at alternate comers of a distorted cube. Each iron is coordinated to three sulfides and one cysteine thiolate. The irons are strongly exchange-coupled, and the [4Fe-4S] cluster in bacterial ferredoxins is paramagnetic when reduced by one electron. The so-called "high-potential ironsulfur proteins" (HiPIPs) are found in photosynthetic bacteria, and exhibit anomalously high (~350 mV) reduction potentials. The *C. vinosum* HiPIP (10 kDa) structure demonstrates that HiPIPs are distinct from the [4Fe-4S] ferredoxins, and that the reduced HiPIP cluster structure is significantly distorted, as is also observed for the structure of the oxidized *P. aerogenes* ferredoxin. In addition, oxidized HiPIP is paramagnetic, whereas the reduced protein is EPR-silent.

This bewildering set of experimental observations can be rationalized in terms of a "three-state" hypothesis (i.e., $[4Fe\text{-}4S(SR)_4]^{n-}$ clusters exist in three physiological oxidation states).[17] This hypothesis nicely explains the differences in magnetic behavior and redox properties observed for these iron-sulfur proteins (Equation 6.4):

$$[4Fe-4S(SR)_4]^{-} \underset{-e^-}{\overset{+e^-}{\rightleftharpoons}} [4Fe-4S(SR)_4]^{2-} \underset{-e^-}{\overset{+e^-}{\rightleftharpoons}} [4Fe-4S(SR)_4]^{3-} \tag{6.4}$$

$$HiPIP_{ox} \qquad HiPIP_{red} \qquad Ferredoxin_{red} \tag{12.6.3}$$

$$Ferredoxing_{ox} \tag{12.6.4}$$

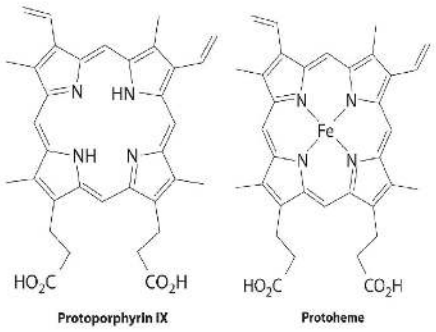
The bacterial ferredoxins and HiPIPs all possess tetracubane clusters containing thiolate ligands, yet the former utilize the -2/-3 cluster redox couple, whereas the latter utilize the -1/-2 cluster redox couple.

The protein environment thus exerts a powerful influence over the cluster reduction potentials. This observation applies to *all* classes of electron transferases—the factors that are critical determinants of cofactor reduction potentials are poorly understood at present but are thought[18] to include the low dielectric constants of protein interiors (~4 for proteins vs. ~78 for H_2O), electrostatic effects due to nearby charged amino-acid residues, hydrogen bonding, and geometric constraints imposed by the protein.

Cytochromes

The cytochromes (from the Greek cytos, meaning “cell”, and chroma, meaning “color”) were first identified in the 1920s by spectroscopic studies of cell extracts. Based on the wavelength of the maximum absorption in the visible spectrum, they were classified as cytochromes a (with the longest wavelength), cytochromes b (intermediate wavelength), and cytochromes c (shortest wavelength). It quickly became apparent that there was a correlation between their spectroscopic properties and other physical properties. For examples, cytochromes c are generally small, soluble proteins with a reduction potential of about +0.25 V, whereas cytochromes b are larger, less-soluble proteins with reduction potentials of about 0 V.

All cytochromes contain iron, and the iron atom in all cytochromes is coordinated by a planar array of four nitrogen atoms provided by a cyclic tetradentate ligand called a porphyrin. The iron–porphyrin unit is called a heme group. The structures of a typical porphyrin (protoporphyrin IX) and its iron complex (protoheme) are shown here. In addition to the four nitrogen atoms of the porphyrin, the iron in a cytochrome is usually bonded to two additional ligands provided by the protein, as shown in Figure **12.6.4**.



A cytochrome. Shown here is protoporphyrin IX and its iron complex, protoheme.

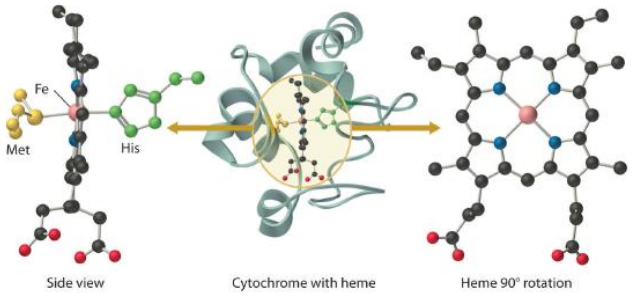


Figure **12.6.4**: A Cytochrome c. In a cytochrome c, the heme iron is coordinated to the nitrogen atom of a histidine imidazole and the sulfur atom of a methionine thioether, in addition to the four nitrogen atoms provided by the porphyrin.

In contrast to the blue copper proteins, two electron configurations are possible for both the oxidized and reduced forms of a cytochrome, and this has significant structural consequences. Thus Fe^{2+} is d^6 and can be either high spin (with four unpaired electrons) or low spin (with no unpaired electrons). Similarly, Fe^{3+} is d^5 and can also be high spin (with five unpaired electrons) or

low spin (with one unpaired electron). In low-spin heme complexes, both the Fe^{2+} and the Fe^{3+} ions are small enough to fit into the "hole" in the center of the porphyrin; hence the iron atom lies almost exactly in the plane of the four porphyrin nitrogen atoms in both cases. Because cytochromes b and c are low spin in both their oxidized and reduced forms, the structures of the oxidized and reduced cytochromes are essentially identical. Hence minimal structural changes occur after oxidation or reduction, which makes electron transfer to or from the heme very rapid.

> *Electron transfer reactions occur most rapidly when minimal structural changes occur during oxidation or reduction*

As a class, the cytochromes[19-22] are the most thoroughly characterized of the electron transferases. By definition, a cytochrome contains one or more heme cofactors. These proteins were among the first to be identified in cellular extracts because of their distinctive optical properties, particularly an intense absorption in the 410-430 nm region (called the Soret band). Cytochromes are typically classified on the basis of heme type. Figure 6.6 displays the three most commonly encountered types of heme: heme a possesses a long phytyl "tail" and is found in cytochrome c oxidase; heme b is found in b-type cytochromes and globins; heme c is covalently bound to c-type cytochromes via two thioether linkages. Cytochrome nomenclature presents a real challenge! Some cytochromes are designated according to the historical order of discovery, e.g., cytochrome c_2 in bacterial photosynthesis. Others are designated according to the λ_{max} of the α band in the absorption spectrum of the reduced protein (e.g., cytochrome c_{551}).

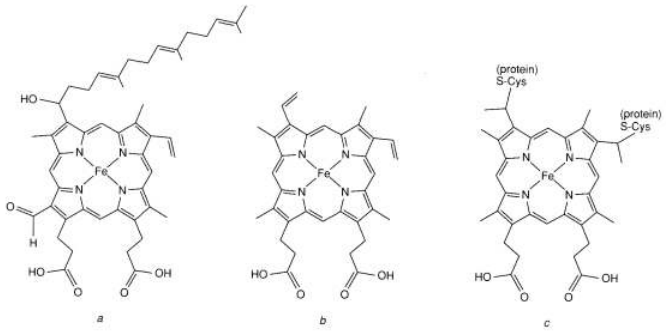


Figure 6.6 - Structures of hemes a, b, and c.

Cytochromes c are widespread in nature. Ambler[23] divided these electron carriers into three classes on structural grounds. The Class I cytochromes c contain axial His and Met ligands, with the heme located near the N-terrninus of the protein. These proteins are globular, as indicated by the ribbon drawing of tuna cytochrome c (Figure 6.7). X-ray structures of Class I cytochromes c from a variety of eukaryotes and prokaryotes clearly show an evolutionarily conserved "cytochrome fold," with the edge of the heme solvent-exposed. The reduction potentials of these cytochromes are quite positive (200 to 320 mV). Mammalian cytochrome c, because of its distinctive role in the mitochondrial electron-transfer chain, will be discussed later.

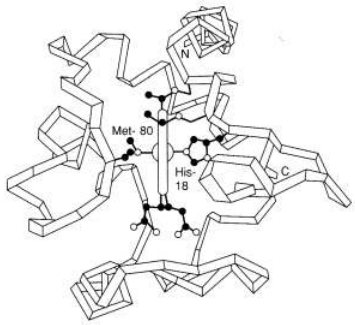


Figure 6. - Structure of tuna cytochrome c.

Class II cytochromes c ($E°' \sim -100$ mV) are found in photosynthetic bacteria, where they serve an unknown function. Unlike their Class I cousins, these c-type cytochromes are high-spin: the iron is five-coordinate, with an axial His ligand. These proteins, generally referred to as cytochromes c' , are four-α-helix bundles (Figure 6.8). The vacant axial coordination site is buried in the protein interior.

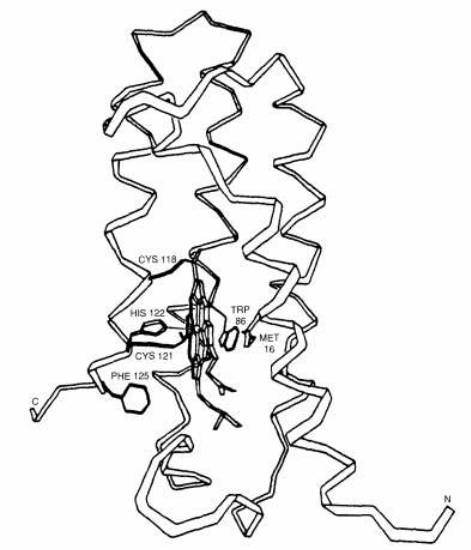


Figure 6.8 - Structure of cytochrome c'.

Finally, Class III cytochromes c, also called cytochromes c_3, contain four hemes, each ligated by two axial histidines. These proteins are found in a restricted class of sulfate-reducing bacteria and may be associated with the cytoplasmic membrane. The low molecular weights of cytochromes c_3 (~14. 7 kDa) require that the four hemes be much more exposed to the solvent than the hemes of other cytochromes (see Figure 6.9), which may be in part responsible for their unusually negative (-200 to -350 mV) reduction potentials. These proteins possess many aromatic residues and short heme-heme distances, two properties that could be responsible for their anomalously large solid-state electrical conductivity.[24]

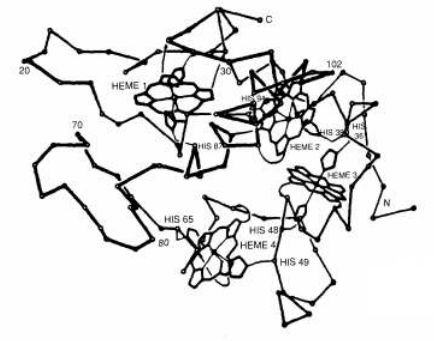


Figure 6.9 - Structure of cytochrome c_3.

12.6: Electron Transfer is shared under a not declared license and was authored, remixed, and/or curated by LibreTexts.

Index

A

A values
10.3: Ligand Substitution Mechanisms
active site
12.2: Introduction to Amino Acids and Proteins
amino acids
12.2: Introduction to Amino Acids and Proteins
ammonia ligands
10.1: Thermodynamic Stability of Metal Complexes
analogous complexes
10.1: Thermodynamic Stability of Metal Complexes
angular nodes
2.1: Quantum Numbers and Atomic Wavefunctions
antibonding molecular orbital
3.7A: Orbital Overlap
arenes
11.1: Organometallic Ligands
Associative Substitution
10.3: Ligand Substitution Mechanisms
atomic orbitals
2.1: Quantum Numbers and Atomic Wavefunctions
3.7A: Orbital Overlap
atomic radii
2.4: Periodic Properties of Atoms
atomization enthalpy
5.3: Lattice Enthalpies and Born Haber Cycles
Aufbau principle
2.3: Aufbau Principle
autoionization
6.2: Brønsted-Lowry Model

B

balance redox
7.1: Balancing Redox Reactions
band gap
5.5: Bonding in Metals and Semicondoctors
band theory
5.5: Bonding in Metals and Semicondoctors
bent
3.4: Valence-Shell Electron-Repulsion Theory
beryllium
3.3D: Limitation of Lewis Theory
bidentate
8.2: Nomenclature and Ligands
body centered cubic
5.1: Crystal Structures and Unit Cells
bond angle
3: Bonding Theories
3.4: Valence-Shell Electron-Repulsion Theory
bond order
3.7B: Homonuclear Diatomic Molecules
bonding molecular orbital
3.7A: Orbital Overlap
Bonding triangle
3.1: Types of Bonding
boron
3.3D: Limitation of Lewis Theory
bridging ligand
8.2: Nomenclature and Ligands
10.5: Electron Transfer Reactions
Bromobenzene
11: Organometallic Chemistry

C

carbene
11.1: Organometallic Ligands
carbon monoxide
11.1: Organometallic Ligands
carbonic anhydrase
12.5: Zinc as Lewis Acid and Template
character table
4.3: Introduction to Character Tables
Chelate complexes
10.1: Thermodynamic Stability of Metal Complexes
chelate effect
10.1: Thermodynamic Stability of Metal Complexes
Chelation
10.1: Thermodynamic Stability of Metal Complexes
chiral
4.4: Applications of Symmetry in Chemistry
complex ion
8: Coordination Chemistry- Structure and Isomers
compression
9.3: Jahn-Teller Distortions
conductors
5.5: Bonding in Metals and Semicondoctors
coordination complex
8: Coordination Chemistry- Structure and Isomers
coordination number
8.3: Coordination Numbers and Structures
copper
12.4: Biological Metal Storage
covalent bonding
3.1: Types of Bonding
crystal field splitting
9.1: Crystal Field Theory
9.2: Crystal Field Stabilization Energy
9.4: Factors That Affect Crystal Field Splitting
crystal field stabilization energy
9.2: Crystal Field Stabilization Energy
10.2: Trends in Kinetic Lability
crystal field theory
9.1: Crystal Field Theory
9.2: Crystal Field Stabilization Energy
crystal structure
5.1: Crystal Structures and Unit Cells
cubic closest packing
5.1: Crystal Structures and Unit Cells
cyclopentadienyl ligands
11.1: Organometallic Ligands

D

delta bond
3.7A: Orbital Overlap
diamagnatic
3.7B: Homonuclear Diatomic Molecules
diamagnetic
3.7: Molecular Orbital Theory
9.1: Crystal Field Theory
diatomic molecule
3.7B: Homonuclear Diatomic Molecules
dipole moment
3: Bonding Theories
3.4: Valence-Shell Electron-Repulsion Theory
3.5: Molecular Polarity
disproprotionation
7.3: Latimer Diagrams

E

effective nuclear charge
2.2: Shielding
electron affinity
2.4: Periodic Properties of Atoms
electronegativities
3.2: Electronegativity Values
Electronic Configurations
9.3: Jahn-Teller Distortions
electrophile
11: Organometallic Chemistry
elongation
9.3: Jahn-Teller Distortions
enzymes
12.2: Introduction to Amino Acids and Proteins
ethylenediamine ligands
10.1: Thermodynamic Stability of Metal Complexes
expanded valence
3.3C: Expanded Octets

F

ferritin
12.4: Biological Metal Storage
formal charge
3.3A: Formal Charge
frontier MOs
6.3: Lewis Concept and Frontier Orbitals
frontier orbitals
6.3: Lewis Concept and Frontier Orbitals
Frost diagrams
7.4: Frost Diagrams

G

group theory
4.2: Point Groups

H

Hapticity
8.2: Nomenclature and Ligands
hard acids
6.4: Hard and Soft Acids and Bases
hard base
6.4: Hard and Soft Acids and Bases
Hemocyanin
12.3: Biological Dioxygen Transport and Storage
hemoglobin
12.3: Biological Dioxygen Transport and Storage

Hexagonal Closest Packed
5.1: Crystal Structures and Unit Cells
high spin
9.1: Crystal Field Theory
9.2: Crystal Field Stabilization Energy
9.3: Jahn-Teller Distortions
9.4: Factors That Affect Crystal Field Splitting
history
1.3: History of Inorganic Chemistry
hybrid orbital
3.6: Valence Bond Theory
hybrid orbitals
3: Bonding Theories
hybridization
3.6: Valence Bond Theory
hydration
9.2: Crystal Field Stabilization Energy
hydride
11.1: Organometallic Ligands
hydroboration
11: Organometallic Chemistry
Hydrohalic Acids
6.2: Brønsted-Lowry Model
hypervalency
3.3: Lewis Electron-Dot Diagrams
3.3C: Expanded Octets
hypovalency
3.3: Lewis Electron-Dot Diagrams
3.3D: Limitation of Lewis Theory

I

improper rotation
4.1: Symmetry Operations and Elements
inductive effect
6.3: Lewis Concept and Frontier Orbitals
inert complex
10.2: Trends in Kinetic Lability
infrared active vibration
4.4: Applications of Symmetry in Chemistry
inner coordination sphere
8: Coordination Chemistry- Structure and Isomers
inner sphere
10.5: Electron Transfer Reactions
Inner sphere electron transfer
10.5: Electron Transfer Reactions
inorganic chemistry
1: Introduction to Inorganic Chemistry
1.1: What is Inorganic Chemistry?
insulator
5.5: Bonding in Metals and Semicondoctors
Interchange
10.3: Ligand Substitution Mechanisms
intermediate
10.2: Trends in Kinetic Lability
inversion center
4.1: Symmetry Operations and Elements
ionic bonding
3.1: Types of Bonding
Ionic Radii
2.4: Periodic Properties of Atoms
ionic solids
5: Structure and Energetics of Solids
ionization energy
2.4: Periodic Properties of Atoms
iron
12.4: Biological Metal Storage
Iron storage
12.4: Biological Metal Storage
irreducible representations
4.3: Introduction to Character Tables

L

labile complex
10.2: Trends in Kinetic Lability
Latimer diagrams
7.3: Latimer Diagrams
lattice enthalpy
5.3: Lattice Enthalpies and Born Haber Cycles
Lewis acid
6.3: Lewis Concept and Frontier Orbitals
Lewis structure
3: Bonding Theories
ligand
8: Coordination Chemistry- Structure and Isomers
ligand field theory
9.5: Ligand Field Theory
ligand substitution
10.3: Ligand Substitution Mechanisms
ligands
8.2: Nomenclature and Ligands
linear
3.4: Valence-Shell Electron-Repulsion Theory
low spin
9.1: Crystal Field Theory
9.2: Crystal Field Stabilization Energy
9.3: Jahn-Teller Distortions
9.4: Factors That Affect Crystal Field Splitting

M

Marcus Theory
10.5: Electron Transfer Reactions
metal
5: Structure and Energetics of Solids
metal alkyl complexes
11.1: Organometallic Ligands
metal complexes
10.1: Thermodynamic Stability of Metal Complexes
metallic bonding
3.1: Types of Bonding
metallothionein
12.4: Biological Metal Storage
Molecular orbital diagram
3.7B: Homonuclear Diatomic Molecules
molecular orbital theory
3: Bonding Theories
3.7: Molecular Orbital Theory
molecular orbitals
4.4: Applications of Symmetry in Chemistry
monodentate
8.2: Nomenclature and Ligands
10.1: Thermodynamic Stability of Metal Complexes
monodentate ligands
10.1: Thermodynamic Stability of Metal Complexes
Mullikan electronegativity
3.2B: Mulliken Electronegativity Values
Myoglobin
12.3: Biological Dioxygen Transport and Storage

N

Nomenclature of Inorganic Compounds
8.2: Nomenclature and Ligands

O

octahedral
3.4: Valence-Shell Electron-Repulsion Theory
9.1: Crystal Field Theory
Octahedral Complexes
8.3: Coordination Numbers and Structures
Octahedral Preference
9.2: Crystal Field Stabilization Energy
Octahedral Site Preference Energy
9.2: Crystal Field Stabilization Energy
orbital overlap
3.7A: Orbital Overlap
organometallic
11: Organometallic Chemistry
organometallic chemistry
11: Organometallic Chemistry
Organometallic Ligands
11.1: Organometallic Ligands
outer coordination sphere
8: Coordination Chemistry- Structure and Isomers
Outer Sphere Electron Transfer
10.5: Electron Transfer Reactions
Oxidative addition
11.3: Oxidative Addition
oxyacids
6.2: Brønsted-Lowry Model
Oxygen Binding
12.3: Biological Dioxygen Transport and Storage
oxygen transport
12.3: Biological Dioxygen Transport and Storage

P

paramagnetic
3.7: Molecular Orbital Theory
3.7B: Homonuclear Diatomic Molecules
9.1: Crystal Field Theory
Pauling Electronegativity
3.2A: Pauling Electronegativity Values
Peptide bond
12.2: Introduction to Amino Acids and Proteins
periodic trends
2.4: Periodic Properties of Atoms
philosopher's stone
1.3: History of Inorganic Chemistry
phosphines
11.1: Organometallic Ligands
pi acceptor
9.5: Ligand Field Theory
pi bond
3.7A: Orbital Overlap
pi donor
9.5: Ligand Field Theory

point groups
4.2: Point Groups
polar bond
3.5: Molecular Polarity
polar compound
3.5: Molecular Polarity
Polarizability
6.4: Hard and Soft Acids and Bases
Pourbaix diagrams
7.5: Pourbaix Diagrams
probability distribution function
2.1: Quantum Numbers and Atomic Wavefunctions
proper rotation
4.1: Symmetry Operations and Elements
proteins
12.2: Introduction to Amino Acids and Proteins

Q

quantum numbers
2.1: Quantum Numbers and Atomic Wavefunctions

R

radial distribution function
2.1: Quantum Numbers and Atomic Wavefunctions
radial nodes
2.1: Quantum Numbers and Atomic Wavefunctions
raman spectroscopy
4.4: Applications of Symmetry in Chemistry
reaction coordinate diagram
10.2: Trends in Kinetic Lability
redox
10.5: Electron Transfer Reactions
redox reaction
7.1: Balancing Redox Reactions
reflection symmetry
4.1: Symmetry Operations and Elements
resonance
3.3B: Resonance
resonance structures
3.3B: Resonance

S

Schrödinger equation
2.1: Quantum Numbers and Atomic Wavefunctions
seesaw
3.4: Valence-Shell Electron-Repulsion Theory
Selection rules
4.4: Applications of Symmetry in Chemistry
semiconductor
5.5: Bonding in Metals and Semicondoctors
shielding constant
2.2: Shielding
sigma donor
9.5: Ligand Field Theory
simple cubic structure
5.1: Crystal Structures and Unit Cells
Slater's rules
2.2: Shielding
soft acid
6.4: Hard and Soft Acids and Bases
soft bases
6.4: Hard and Soft Acids and Bases
sp hybrid orbital
3.6: Valence Bond Theory
sp2 hybrid orbital
3.6: Valence Bond Theory
sp3 hybrid orbital
3.6: Valence Bond Theory
spectrochemical series
9.4: Factors That Affect Crystal Field Splitting
spin pairing energy
9.1: Crystal Field Theory
9.2: Crystal Field Stabilization Energy
square planar
9.1: Crystal Field Theory
square pyramidal
3.4: Valence-Shell Electron-Repulsion Theory
steric effect
6.3: Lewis Concept and Frontier Orbitals
strong field
9.5: Ligand Field Theory
substitutions
10.3: Ligand Substitution Mechanisms
substrate
12.2: Introduction to Amino Acids and Proteins
Superacid
6.2: Brønsted-Lowry Model
Suzuki reaction
11: Organometallic Chemistry
symmetry
4.2: Point Groups
4.4: Applications of Symmetry in Chemistry
symmetry elements
4.1: Symmetry Operations and Elements
symmetry operations
4.1: Symmetry Operations and Elements

T

tetrahedral
3.4: Valence-Shell Electron-Repulsion Theory
9.1: Crystal Field Theory
Tetrahedral Complexes
8.3: Coordination Numbers and Structures
thermodynamically
10.1: Thermodynamic Stability of Metal Complexes
thermodynamically stable
10.1: Thermodynamic Stability of Metal Complexes
transition state
10.2: Trends in Kinetic Lability
tridentate
8.2: Nomenclature and Ligands
trigonal bipyramidal
3.4: Valence-Shell Electron-Repulsion Theory
trigonal planar
3.4: Valence-Shell Electron-Repulsion Theory
trigonal pyramidal
3.4: Valence-Shell Electron-Repulsion Theory
trimethylenediamine
10.1: Thermodynamic Stability of Metal Complexes

V

valence bond theory
3: Bonding Theories
3.6: Valence Bond Theory
valence shell electron pair repulsion theory
3.4: Valence-Shell Electron-Repulsion Theory
vanadium
12.4: Biological Metal Storage
VSEPR
3: Bonding Theories
3.4: Valence-Shell Electron-Repulsion Theory

W

weak field
9.5: Ligand Field Theory

Z

zinc
12.4: Biological Metal Storage

Glossary

Sample Word 1 | Sample Definition 1

https://chem.libretexts.org/@go/page/326134

Detailed Licensing

Overview

Title: CHEM 3110: Descriptive Inorganic Chemistry

Webpages: 92

Applicable Restrictions: Noncommercial

All licenses found:

- CC BY-NC-SA 4.0: 83.7% (77 pages)
- Undeclared: 13% (12 pages)
- CC BY-SA 4.0: 2.2% (2 pages)
- CC BY-NC 4.0: 1.1% (1 page)

By Page

- CHEM 3110: Descriptive Inorganic Chemistry - *CC BY-NC-SA 4.0*
  - Front Matter - *CC BY-NC-SA 4.0*
    - TitlePage - *CC BY-NC-SA 4.0*
    - InfoPage - *CC BY-NC-SA 4.0*
    - Table of Contents - *Undeclared*
    - Licensing - *Undeclared*
  - 1: Introduction to Inorganic Chemistry - *CC BY-NC-SA 4.0*
    - 1.1: What is Inorganic Chemistry? - *CC BY-NC-SA 4.0*
    - 1.2: Inorganic vs Organic Chemistry - *CC BY-NC-SA 4.0*
    - 1.3: History of Inorganic Chemistry - *CC BY-NC-SA 4.0*
  - 2: Atomic Theory - *CC BY-NC-SA 4.0*
    - 2.1: Quantum Numbers and Atomic Wavefunctions - *CC BY-NC-SA 4.0*
    - 2.2: Shielding - *CC BY-NC-SA 4.0*
    - 2.3: Aufbau Principle - *CC BY-NC-SA 4.0*
    - 2.4: Periodic Properties of Atoms - *CC BY-NC-SA 4.0*
  - 3: Bonding Theories - *CC BY-NC-SA 4.0*
    - 3.1: Types of Bonding - *CC BY-NC-SA 4.0*
    - 3.2: Electronegativity Values - *CC BY-NC-SA 4.0*
      - 3.2A: Pauling Electronegativity Values - *CC BY-NC-SA 4.0*
      - 3.2B: Mulliken Electronegativity Values - *CC BY-NC-SA 4.0*
      - 3.2C: Allred-Rochow Electronegativity Values - *CC BY-NC-SA 4.0*
    - 3.3: Lewis Electron-Dot Diagrams - *CC BY-NC-SA 4.0*
      - 3.3A: Formal Charge - *CC BY-NC-SA 4.0*
      - 3.3B: Resonance - *CC BY-NC-SA 4.0*
      - 3.3C: Expanded Octets - *CC BY-NC-SA 4.0*
      - 3.3D: Limitation of Lewis Theory - *CC BY-NC-SA 4.0*
    - 3.4: Valence-Shell Electron-Repulsion Theory - *CC BY-NC-SA 4.0*
    - 3.5: Molecular Polarity - *CC BY-NC-SA 4.0*
    - 3.6: Valence Bond Theory - *CC BY-NC-SA 4.0*
    - 3.7: Molecular Orbital Theory - *CC BY-NC-SA 4.0*
      - 3.7A: Orbital Overlap - *Undeclared*
      - 3.7B: Homonuclear Diatomic Molecules - *CC BY-NC-SA 4.0*
      - 3.7C: Heteronuclear Diatomic Molecules - *Undeclared*
  - 4: Molecular Symmetry and Point Groups - *Undeclared*
    - 4.1: Symmetry Operations and Elements - *CC BY-NC-SA 4.0*
    - 4.2: Point Groups - *CC BY-NC-SA 4.0*
    - 4.3: Introduction to Character Tables - *CC BY-NC-SA 4.0*
    - 4.4: Applications of Symmetry in Chemistry - *CC BY-NC-SA 4.0*
  - 5: Structure and Energetics of Solids - *Undeclared*
    - 5.1: Crystal Structures and Unit Cells - *CC BY-NC-SA 4.0*
    - 5.2: Energetics of Ionic Solids- Lattice Energy - *CC BY-NC-SA 4.0*
    - 5.3: Lattice Enthalpies and Born Haber Cycles - *CC BY-NC 4.0*
    - 5.4: Lattice Energy and Solubility - *CC BY-SA 4.0*
    - 5.5: Bonding in Metals and Semicondoctors - *CC BY-NC-SA 4.0*

- 5.6: Nanomaterials - *CC BY-SA 4.0*

- 6: Acid-Base and Donor-Acceptor Chemistry - *CC BY-NC-SA 4.0*
  - 6.1: Arrhenius Model - *CC BY-NC-SA 4.0*
  - 6.2: Brønsted-Lowry Model - *CC BY-NC-SA 4.0*
  - 6.3: Lewis Concept and Frontier Orbitals - *CC BY-NC-SA 4.0*
  - 6.4: Hard and Soft Acids and Bases - *CC BY-NC-SA 4.0*
- 7: Reduction and Oxidation Chemistry - *CC BY-NC-SA 4.0*
  - 7.1: Balancing Redox Reactions - *CC BY-NC-SA 4.0*
  - 7.2: Electrochemical Potentials - *CC BY-NC-SA 4.0*
  - 7.3: Latimer Diagrams - *CC BY-NC-SA 4.0*
  - 7.4: Frost Diagrams - *CC BY-NC-SA 4.0*
  - 7.5: Pourbaix Diagrams - *CC BY-NC-SA 4.0*
- 8: Coordination Chemistry- Structure and Isomers - *CC BY-NC-SA 4.0*
  - 8.1: History - *CC BY-NC-SA 4.0*
  - 8.2: Nomenclature and Ligands - *CC BY-NC-SA 4.0*
  - 8.3: Coordination Numbers and Structures - *CC BY-NC-SA 4.0*
  - 8.4: Isomerism - *CC BY-NC-SA 4.0*
- 9: Coordination Chemistry- Bonding - *CC BY-NC-SA 4.0*
  - 9.1: Crystal Field Theory - *CC BY-NC-SA 4.0*
  - 9.2: Crystal Field Stabilization Energy - *CC BY-NC-SA 4.0*
  - 9.3: Jahn-Teller Distortions - *CC BY-NC-SA 4.0*
  - 9.4: Factors That Affect Crystal Field Splitting - *CC BY-NC-SA 4.0*
  - 9.5: Ligand Field Theory - *CC BY-NC-SA 4.0*
- 10: Coordination Chemistry- Reactions and Mechanisms - *CC BY-NC-SA 4.0*
  - 10.1: Thermodynamic Stability of Metal Complexes - *CC BY-NC-SA 4.0*
  - 10.2: Trends in Kinetic Lability - *Undeclared*
  - 10.3: Ligand Substitution Mechanisms - *CC BY-NC-SA 4.0*
  - 10.4: The Trans Effect - *CC BY-NC-SA 4.0*
  - 10.5: Electron Transfer Reactions - *CC BY-NC-SA 4.0*
- 11: Organometallic Chemistry - *CC BY-NC-SA 4.0*
  - 11.1: Organometallic Ligands - *CC BY-NC-SA 4.0*
  - 11.2: The 18 Electron Rule - *CC BY-NC-SA 4.0*
  - 11.3: Oxidative Addition - *CC BY-NC-SA 4.0*
  - 11.4: Reductive Elimination - *CC BY-NC-SA 4.0*
  - 11.5: Migratory Insertion- 1,2-Insertions - *CC BY-NC-SA 4.0*
  - 11.6: β-Elimination Reactions - *CC BY-NC-SA 4.0*
  - 11.7: Organometallic Catalysts - *CC BY-NC-SA 4.0*
- 12: Bioinorganic Chemistry - *CC BY-NC-SA 4.0*
  - 12.1: Biological Significance of Metals - *CC BY-NC-SA 4.0*
  - 12.2: Introduction to Amino Acids and Proteins - *CC BY-NC-SA 4.0*
  - 12.3: Biological Dioxygen Transport and Storage - *Undeclared*
  - 12.4: Biological Metal Storage - *Undeclared*
  - 12.5: Zinc as Lewis Acid and Template - *Undeclared*
  - 12.6: Electron Transfer - *Undeclared*
- Back Matter - *CC BY-NC-SA 4.0*
  - Index - *CC BY-NC-SA 4.0*
  - Glossary - *CC BY-NC-SA 4.0*
  - Detailed Licensing - *Undeclared*